

Alma Mater Studiorum – Università di Bologna

DOTTORATO DI RICERCA IN
CHEMISTRY

Ciclo XXXII

Settore Concorsuale: 03/C1

Settore Scientifico Disciplinare: CHIM/06

TITOLO TESI

Ni(II) and Photocatalyzed Functionalization of Carbon-Carbon
Double Bonds

Presentata da: Yang Liu

Coordinatore Dottorato

Supervisore

Prof. Domenica Tonelli

Marco Bandini

Esame finale anno 2020

Acknowledgments

When it is close to the ending of my study in University of Bologna, in retrospect, I feel really lucky for things happened to me and the people I met in my life.

First, I would like to thank China Scholarship Council for providing me the scholarship (No. 201609120008) and the University of Bologna for financial support, so that I got the chance to study in UNIBO for three years. Meanwhile, I thank the Marco Polo programme for providing me a chance to study as an intern in EPFL for 3 months.

Second, I would give my most ardent and sincere appreciation to my supervisor Prof. Dr. Marco Bandini for his incessant and patient guidance in research field during the past three years. What I learned from him is not limited to the knowledge in organic chemistry, but also the way to do research, the taste and aesthetic of chemistry. I also appreciate his supportive attitude and effort he did towards helping me seek for further development in my career.

Next, I would like to thank Prof. Dr. Cramer who provided me an internship position in EPFL. During that period of time, not only my knowledge field was broadened but also acquaintance with many friends was made in Lausanne. In his group, I worked with Dr. Shouguo Wang, one of the most outstanding chemists I have ever seen. I acquired substantial amount of skills of doing chemistry from him. I think Prof. Dr. Pier G. Cozzi for his supporting knowledge on cobalt and his effort to help me look for postdoc position.

In UNIBO, I also made friends with quite many enthusiastic and talented students who not only gave me support on my research but also on my live. Among them, I would like to thank Dr. Assunda De Nisi, an experienced, keen and patient lady who helped commence my research when I was a freshman in this lab. I also feel lucky to get acquaintance with Mr. Alessandro Cerveri, an honest and gifted doctoral student who is keen to make a breakthrough in organic chemistry. I appreciate it that he helped me so much in the work on nickel chemistry. I hope that one day he can achieve outstanding feats in his career. Meanwhile, I want to thank Mr. Mario Daka for his irreplaceable work in the allenoate chemistry; also Mr. Simone Battaglioli and Mr. Marcos Alvarez for thier constant work on the photochemistry. I also would like to thank Mr. Lombardi Lorenzo, Dr. Michele Anselmi, Dr. Lucia Ferrazzano, Dr. Giulia Martelli and Mr. Dario Corbisiero for the favour they did in my research.

I am grateful to my friends including Dr. Juzeng An, Dr. Liang Wang and Dr. Bairang Wei for accompanying me for three years which is essential to an international student.

Last but not the least, I always appreciate the supports and love from my beloved parents, my sisters. And now, at the ending of my study abroad, this feeling becomes stronger and stronger.

Abstract

Homogenous nickel catalysis is gaining more and more attention of chemist due to a variety of oxidative states resulting from distribution of its external electron in 3d orbital and abundance in the earth crust. Due to difference in diameter and distribution of external electron, nickel complexes possess some unique activities that 4d, 5d noble metals can't achieve.

In this thesis, we described our work on nickel(II) catalyzed Suzuki coupling of electron perturbed allenes to synthesize stereochemically defined enamine and ester. The methodology showed excellent tolerance to variously substituted phenylboronic acids. Additionally, with allenamide, it can also proceed in cascade tricomponent versions with aldehyde wherein dimethylzinc was also compatible. Theoretical computation was conducted to reveal the nature of mechanism. This work realized an umpolung of nucleophilicity of allenamide, extending the reactivity of it.

As an expansion of previous work on nickel chemistry, we stretched our sight to photoredox reaction with initial idea of using organonickel as co-catalyst. So, we devoted to develop photocatalyzed synthesis of 1,3,4-trisubstituted pyrrole in a mild, oxidant-free way which was also documented in this thesis. Further work to disclose the mechanism were also done suggesting the azide were reduced through a new pathway.

Wacker oxidation is a quite useful transformation from alkene to ketone or aldehyde which always needs palladium catalyst system and theoretically at least one equivalent oxidant. Herein, we disclose a new way to realize Wacker Oxidation through a gentle photoredox process where noble metal, harsh condition, oxidant or other additives are not indispensable any more.

At last, the assistant work has been done to realize the Cp*Rh(III) catalyzed enantioselective C-H activation of acrylamide which is not further mentioned in this thesis. In this work, the activated acrylamide coupled with terminal allene affording an annulated 5-member lactam with excellent enantioselectivity. (DOI: 10.1002/anie.201909971)

Contents

Abstract	1
1 Nickel Catalyzed Functionalization of Allenes	1
1.1 Introduction	1
1.2 Literature survey: Progress in nickel catalyzed functionalization of allenes	2
1.2.1 Ni(0) initiated coupling reactions	2
1.2.2 Ni(II) initiated coupling reactions	11
1.2.3 Ni(II) initiated polymerization	12
1.2.4 Ni-catalyzed cycloaddition reactions	13
1.2.5 Ni(0) promoted/catalyzed CO ₂ fixation	16
1.3 Conclusions	18
Reference	20
2 Nickel Catalyzed Suzuki Coupling of Electronically Perturbed Allenes.....	22
2.1 Retrospect on metal catalyzed coupling of allenamide	22
2.2 Nickel catalyzed Suzuki coupling of allenamides.....	26
2.3 Precious work of metal catalyzed coupling of allenolate	39
2.4 Ni(II) Catalyzed Coupling of Allenolate with Boronic acids.....	45
2.5 Conclusions	49
Reference	51
3 Photocatalyzed Synthesis of 1,3,4-trisubstituted Pyrrole	52
3.1 Introduction: progress in visible-light introduced reaction of azide	52
3.2 Photocatalyzed Synthesis of the 1,3,4- Substituted Pyrrole.....	61
3.3 Conclusions	70
Reference	72
4 Photocatalyzed Wacker Oxidation of Trisubstituted Alkene	74
4.1 Introduction: Wacker Oxidation	74
4.2 Photocatalyzed Wacker Oxidation	86
4.2.1 Background of application of cobaloxime complexes.....	86
4.2.2 Photocatalyzed Wacker Oxidation of trisubstituted alkene	89
4.3 Conclusions	94
Reference	95
Supplementary materials	97
Ni(II) Catalyzed Suzuki Coupling of Electron Perturbed Allenes.....	97
Photocatalyzed Synthesis of 1,3,4- Trisubstituted Pyrrole.....	129
Photocatalyzed Wacker Oxidation of Trisubstituted Alkene	140
Reference	145
Spectra of Selected Compounds	146

1 Nickel Catalyzed Functionalization of Allenes

1.1 Introduction

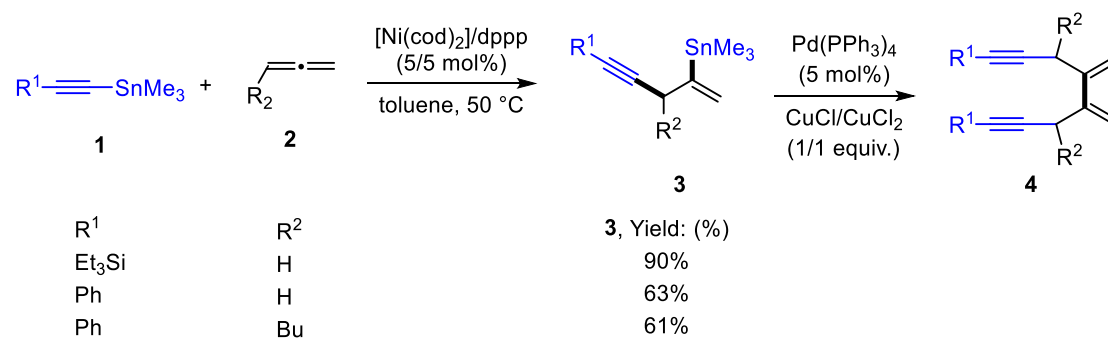
Homogenous nickel catalysis is facing a growing interest worldwide due to some key intrinsic chemical properties of the 3d-metal derivatives.¹ Beside the substantial abundance on Earth crust of nickel compounds in comparison with 4d- and 5d-late- transition metals (and consequently lower Prices),² the accessibility of a wide range of oxidative states and the remarkable catalytic fine-tunability based on ligand design³ make nickel catalysis a current hot-topic in the nowadays organic synthetic chemistry scenario. In this picture, cross-couplings, photocatalysis, asymmetric catalysis, functional-group transformations and total synthesis of nature product probably deserve a specific mention.⁴ In particular, redox cross-couplings applied to the formation of new C-C and C-X (heteroatom) bond based on multiple hybridization patterns,⁵ faced a dramatic change over the past decade, along with the development of more efficient, functional group tolerant and robust Ni-based catalytic species. Among the unfunctionalized hydrocarbons that benefited from the nickel catalysis advent, allenes and cumulene derivatives⁶ played a unprecedented role in opening direct access to chemical diversity and complexity starting from easy availability of starting materials. 1,2-Dienes represent an irreplaceable functional group in synthetic chemistry featuring a variety of reaction profiles and multiple coordination/activation modes operated by metal-based and metal-free agents. Their intrinsic electronic properties and reactivity can be adequately tuned by conjugating electron withdrawing groups (EWGs) or electron donating groups (EDGs) to the cumulenyl unit, dictating the overall site-selectivity of the transformations. The renaissance of nickel catalysis reinforced these aspects expanding dramatically the chemical portfolio accessible via allene modifications. C-C as well as C-X bond formation processes via cross-couplings and cycloadditions, represented prominent examples. Additionally, the high reducing potential of [Ni(0)] complexes provided a unique way to realize the activation of CO₂ and subsequent fixation into 1,2-diene compounds. Last but not the least, the asymmetric Ni-catalyst rules an irreplaceable frontier in asymmetric transformations of allenyl substrates, contributed substantially in opening new horizons in this research area.

All at once, in this chapter we wish to present a collection of the most representatives on homogenous Ni-catalysis and allene derivatives. Emphasis has been mainly addressed in highlighting scope, limitations but also rational mechanistic behind the experimental outcomes. This introduction is deliberately limited to a personal selection of protocols and we do not intend to provide a comprehensive and exhaustive (encyclopedic) coverage of all the examples present in the literature. Accordingly, the employment of Ni-catalysis for the synthesis of allenenes^[7] should be considered outside the scope of this introduction.

1.2 Literature survey: Progress in nickel catalyzed functionalization of allenenes

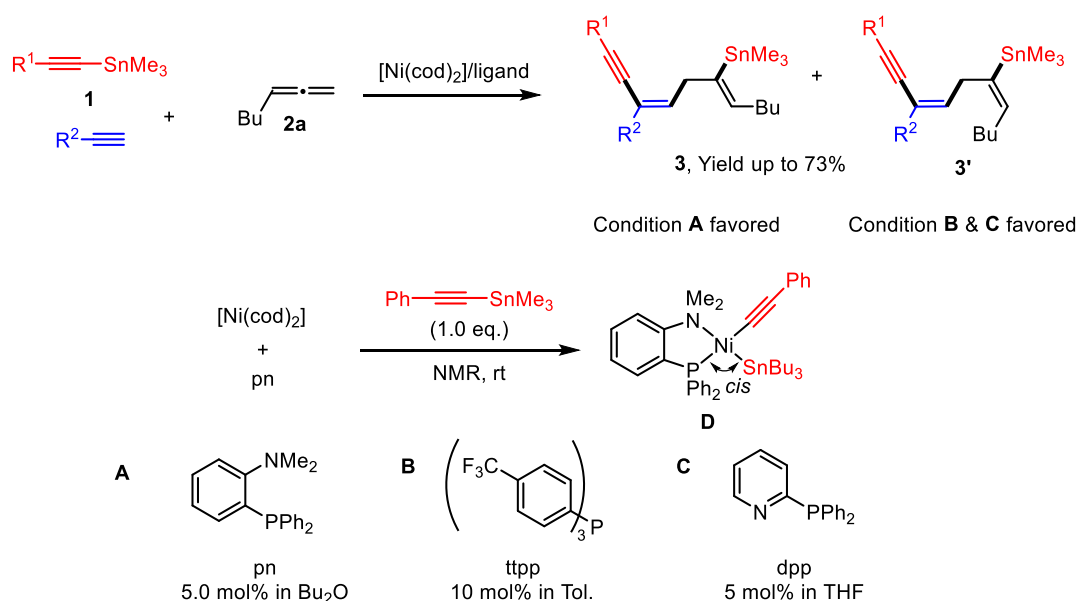
1.2.1 Ni(0) initiated coupling reactions

In 2002, Hiyama and coworkers pioneered the Ni catalyzed cross coupling by presenting the reaction involving alkynylstannanes (**1**) and 1,2-dienes (**2**) catalyzed by $[\text{Ni}(\text{cod})_2]/\text{dppp}$ complex (5 mol%, dppp = 1,3-bis(diphenylphosphino)propane).⁸ The resulting α -(alkynylmethyl)vinylstannanes **3** (only three examples were documented, yields up to 90%) underwent homocoupling with $[\text{Pd}(0)]$ catalysis to provide synthetically valuable dienediynes **4** (Scheme 1.1) which were used to synthesize polycyclic compounds containing linearly-fused six-membered rings.



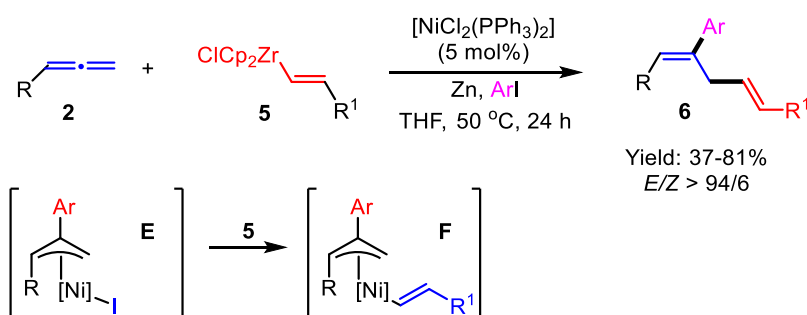
Scheme 1.1 $[\text{Ni}(0)]$ -catalyzed alkynyl-stannylation of allenenes.

Interestingly, a combinatorial tin reagent turned out to be adoptable in a $[\text{Ni}(\text{cod})_2]$ -catalyzed (5 mol%) three-component tandem carbostannylation reaction with different alkynyl compounds and the 1,2-heptadiene involved (**2a**, Scheme 1.2).⁹ The stereochemistry of the resulting vinylstannanes **3** was strongly affected by the ligand employed. In particular, while tris[*p*-trifluoromethylphenyl]phosphane (tpp) and 2-(diphenylphosphanyl)pyridine (dpp) mainly provided the *E*-product as the major compound, meanwhile the pn ([2-(dimethylamino)phenyl]diphenylphosphane) ligand mainly provided the *Z*-product. Detailed mechanistic insights were also provided by NMR spectroscopy. In particular, ³¹P NMR and ¹¹⁹Sn NMR analysis carried out on the stoichiometric mixture of $[\text{Ni}(\text{cod})_2]/$ trimethyl(phenylethynyl)tin revealed the formation of the organonickel intermediate **D** that could derive from the initial oxidative insertion of the $[\text{Ni}(0)]$ complex into the C-Sn bond.



Scheme 1.2 [Ni(0)]-catalyzed tandem carbostannylation of allenes.

A [Ni(0)]-catalyzed three-component assembly of allenes with ArI and arylzirconium species **5** was documented by Cheng (2003).¹⁰ The methodology offered a mild and convenient method for synthesis of 1,4-dienes **6** in good yields with valuable regio- (terminal) and *E*- stereoselectivity. The usage of *in situ*- generated [Ni(0)] catalyst ([NiCl₂(PPh₃)₂/Zn, 5 mol%/2.75 eq.) guaranteed functional group tolerance to all the reaction partners, with some limitations regarding *ortho*-functionalization. Stereochemically defined allyl-vinyl-Ni(II) intermediates **F** are assumed as active species in the catalytic cycle upon transmetalation with the organo-zirconium reagent. It is noteworthy to mention that under similar conditions, both [Pd(0)] and [Pd(II)]-catalyzed afforded the two-component coupling product (*i.e.* aryl iodide and organozirconium reagents), exclusively (Scheme 1.3).

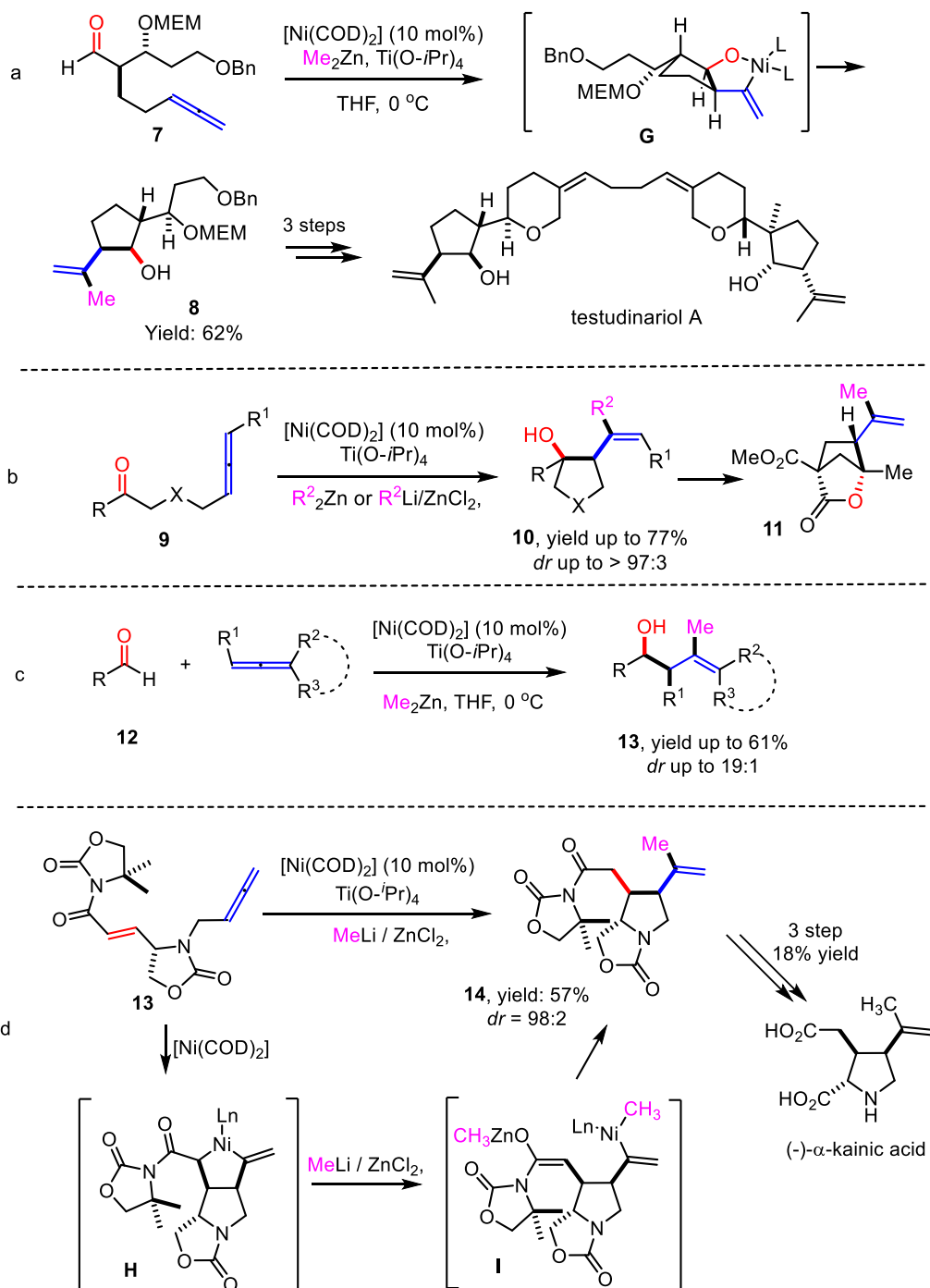


Scheme 1.3 [Ni]-catalyzed three-component manipulation of allenes

In 2002, Montgomery and co-workers utilized the [Ni(0)]-catalyzed intramolecular coupling of allenes and aldehydes in the total synthesis of (+)-Testudinariol A (Scheme 1.4a).^{11a} Under standard conditions (Me₂Zn, Ti(O-*i*-Pr)₄ and [Ni(COD)₂] 10 mol%), allene **7** could afford **8** in 62% yield and > 97:3 diastereoselectivity. This process was proposed to form oxidized metallacycle **G** through coordination of [Ni(0)] with aldehyde and adjacent allene. The subsequent dimethylzinc transmetalation to Ni, followed by reductive elimination resulted in the formation of **8**, a suitable

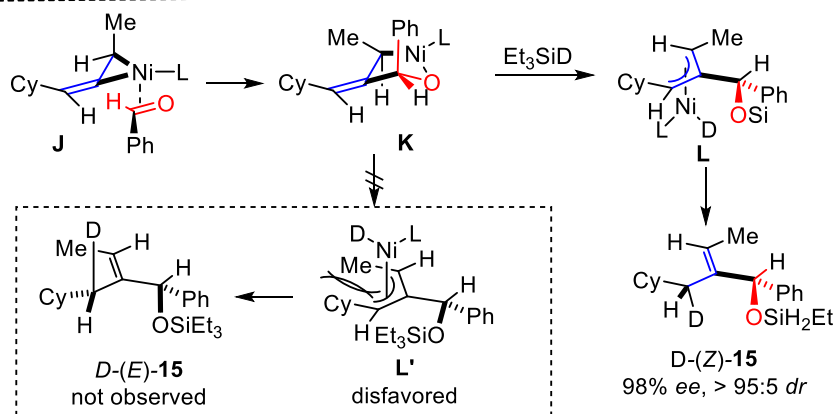
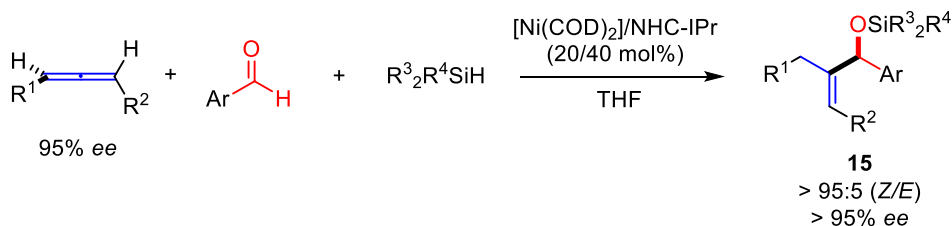
intermediate to (+)-testudinarior A.

In same year, their group extended this strategy to the preparation of homoallylic alcohols.^{11b} This protocol was applicable to mono-, 1,3-substituted allenes and different organozinc and ZnCl_2 were used. Almost simultaneously, Suk-Ku Kang group documented on a similar work wherein ketones (**9**) was also employed to provide tertiary alcohol (Scheme 1.4b).^{11c} In some cases, the hydroxyl group of adducts could undergo intramolecular lactonization provided bicycle lactone **11**. Although accompanied with a narrow reaction scope an intermolecular variant was also documented (Scheme 1.4c).^{11d} Finally, the synthetic potential of the methodology was empathized by the synthesis of (+)- α -allokainic acid via allene/alkene coupling of **13**.^{11e}



Scheme 1.4 [Ni]-catalyzed cascade coupling of allenes, carbonyl compounds and organozinc reagents

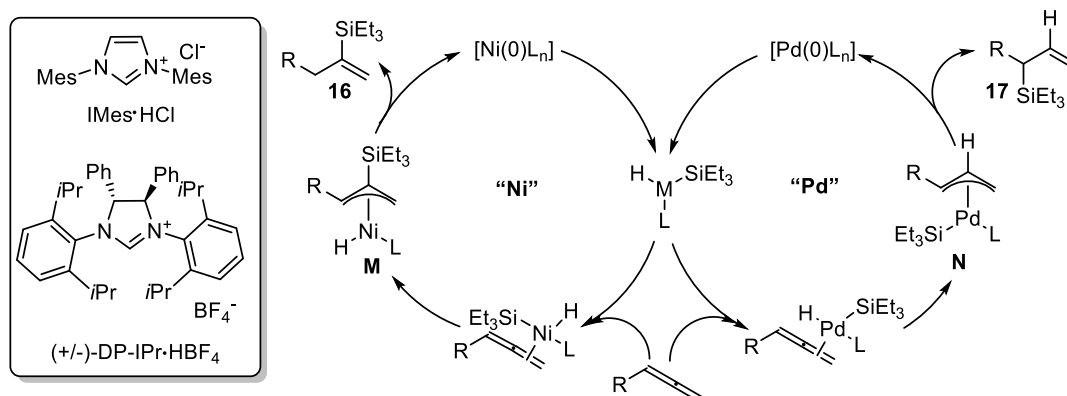
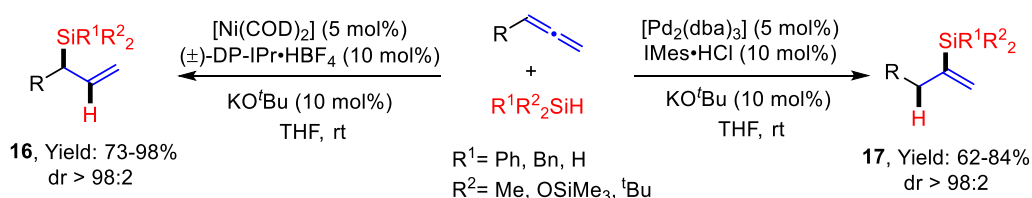
A remarkable breakthrough in the Ni-catalyzed modification of allenes was made by Jamison and colleagues with an enantiospecific [Ni(COD)₂]/NHC-IPr-catalyzed multicomponent coupling reaction of allenes with aldehyde, silanes to provide variously substituted allylic alcohols **15** in well stereochemically defined manner (Scheme 1.5).^{12a} Among several peculiarities of the method, it is worthy to mention that the electrophilic trapping of the central *C*_{sp}-atom of the allenyl framework is firstly documented. Additionally, this methodology provides *Z*-geometry product exclusively, in

**Scheme 1.5** Synthesis of allylic alcohols via Ni-catalyzed reductive

contrast to analogous reductive alkyne/aldehyde coupling; the addition generally happens to C=C bond of more steric hindrance (even in mono-substituted allene case), which partially accounts for *Z*-geometry of the product. Mechanistically, labeling experiments suggested that σ -bond metathesis between alkoxy-Ni intermediate **K** and Et₃SiD could afford the intermediate **L** instead of **L'**, in which case an unfavorable Me/*c*-Hex 1,3-interaction was presented. Further explorations showed that some phosphine-based ligands could also promote the reaction, however with somewhat erosion either on yield or enantioselectivity.^{12b} Finally, mono-substituted 1,2-dienes were also challenged in the three-component coupling by the research group. After some optimization, P(Cyp)₃ ligand (Cyp = cyclopentyl) was proved to be the best ligand for [Ni(COD)₂] affording disubstituted allylic alcohols **15** in moderate to acceptable yields (up to 75%).^{12c}

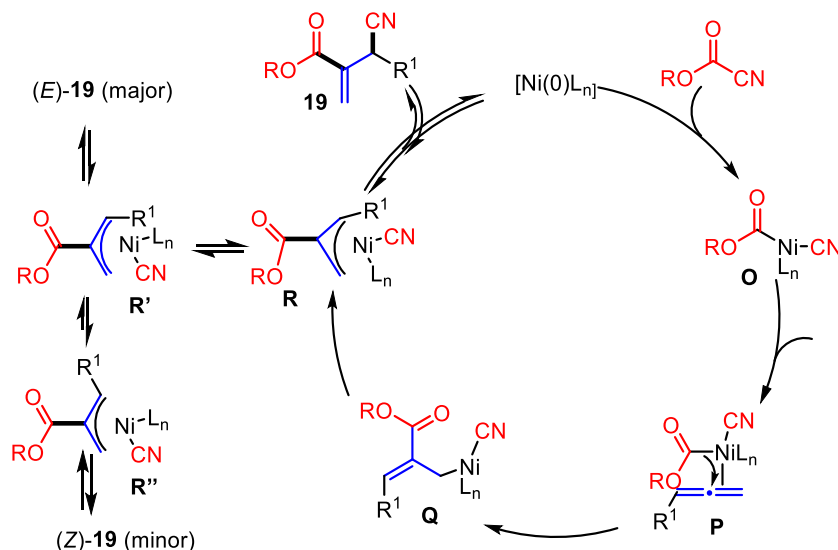
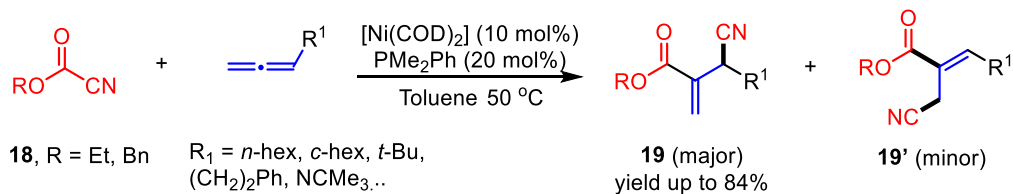
Concomitantly, the [Ni(0)]-catalyzed ([Ni(COD)₂]/DP-IPr-HBF₄, 10/10 mol%) regioselective hydrosilylation of allenes was described by Montgomery and coworkers furnishing a selective 2,3-addition machinery.^{13a} The ligand investigation demonstrated that, the larger the ligand size was, the higher the yield and regioselectivity in the nickel catalysis afforded. Interestingly, reverse selectivity was observed in the presence of [Pd₂dba₃]/IMes·HCl catalyst (5/10 mol%). Although the origin of the regioselectivity is still uncertain, mechanistic profiles involving a silylmatalation

pathway with nickel and hydrometalation with palladium were proposed respectively. In particular, upon the formation of the allylic metal intermediate via migratory insertion at the middle carbon atom, while the Ni complex preferentially transferred the silyl group to the allene (N), the Pd-intermediate promoted the hydrogen migration. After reductive elimination, the allylic metal intermediate **L** would deliver the corresponding products **16** and **17** (Scheme 1.6). Subsequently, the same team was able to expand the protocol to the stereoselective hydrosilylation of challenging 1,3-disubstituted allenes by using differently substituted carbene ligands.^{13b}



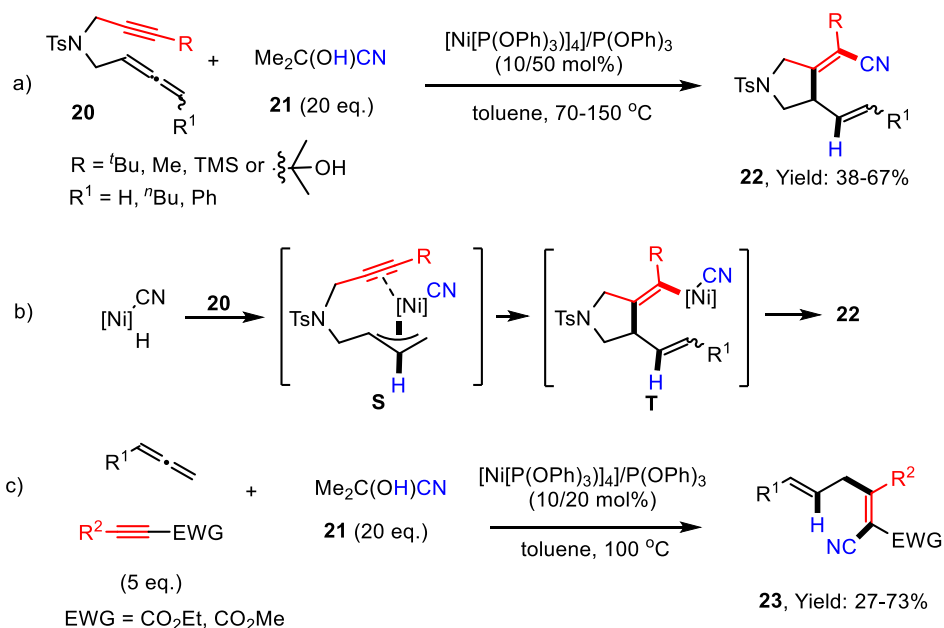
Scheme 1.6 [Ni(0)] vs [Pd(0)] catalyzed hydrosilylation of allenes

In 2006, Hiyama and Nakao documented a [Ni(0)]-catalyzed regioselective cyanoesterification of allenes.¹⁴ Under optimal conditions, ester- and cyano- group could be installed at the 2,3- carbon atoms of the allenyl moiety, respectively providing the kinetic adduct **19**; whereas when an excess of allene (1.2 eq. to **18**) was employed, the thermodynamic **19'** was isolated predominantly (Scheme 1.7). The reaction was proposed to initiate by oxidative insertion of [Ni(COD)₂]/PMe₂Ph into EtOC(O)-CN (**O**). The terminal carbon-carbon double bond could coordinate to nickel (**P**) due to its sterically less hinderance, followed by migration of the EtOC(O)-group to central carbon of allene (**P**→**Q**). This intermediate was stabilized by formation of π -allylnickel complex **R** that could deliver product **19** via reductive elimination. Formation of the regioisomer **19'** may result from coordination of the allene in an opposite mode with respect to **P**, followed by similar catalytic steps. Under thermodynamic conditions, isomerization of **19** might take place via a reversible oxidative addition triggered by [Ni(0)] that results in the allylnickel intermediates **R**, **R'** and **R''**, leading to the formation of *E*- or *Z*-**20**.



Scheme 1.7 [Ni(0)]-catalyzed cyanoesterification of allene.

Arai reported a tandem hydrocyanation/C-C bond forming process of alkynylallenes **20** in combination with hydrocyanic acid (produced in situ from acetonecyanohydrin AC, **21**) with [Ni(OPPh₃)₃] as catalyst (Scheme 1.8a).¹⁵ The reaction was proposed to involve the initial regioselective hydronicelation of the allenyl framework delivering the allyl-Ni intermediate **S** partially stabilized by a Lewis acid/base connected with the SO₂ moiety. The subsequent 5-*exo*-



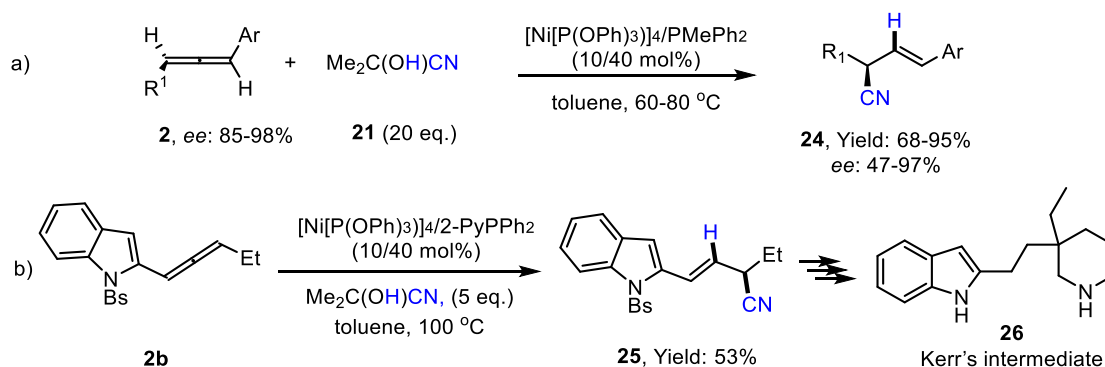
Scheme 1.8 [Ni(0)]-catalyzed tandem hydrocyanation/C-C bond forming cyclization of alkynyl-allenes

cyclization **T**, followed by reductive cyanation of the terminal alkynyl carbon, restored the catalytically active [Ni(0)] species (Scheme 1.8b).

Subsequently, the carbocyanation of allene/alkyne was extended to an intermolecular variant (Scheme 1.8c). The resulting three-component compound **24** was isolated in moderate to good yield, featuring the triple bond hydronickelation species as the main side-product. The employment of terminal bulky silyl group (*i.e.* TIPS, TBDPS) at the *C_{sp}* terminus turned out to be effective to diminish this side reaction.

Later on, the same team documented a similar strategy for the highly regio- and stereoselective systematic hydrocyanation of 1,3-disubstituted allenes.^{16a} Final outcome turned to be highly dependent on the substitution pattern of the allene. However, primary, secondary and tertiary alkyl groups as well as aromatic units were adequately tolerated on di- and trisubstituted allenes.

Additionally, the use of axially chiral allenes in the [Ni(0)]-catalyzed hydrocyanation process with acetone cyanohydrin delivered the corresponding carbonitriles **24** with only a slight erosion of chirality purity (Scheme 1.9a). Detailed mechanistic interpretations were provided for both reaction profiles and the recorded allene racemization in the absence of AC.^{16b} The synthetic utility of the protocol was further proved by the synthesis of the synthetic intermediate of (±)-quebrachamine **26**.^{16c} In particular, the regio- and stereoselective [Ni(0)]-catalyzed hydrocyanation of indolylallene **2b** delivered the cyanide compound **25** in 53% yield by means of 2-PyPPh₂ as the [Ni(0)] ligand. Subsequent chemical manipulations led to **26** in 11 steps and 18% overall yield.

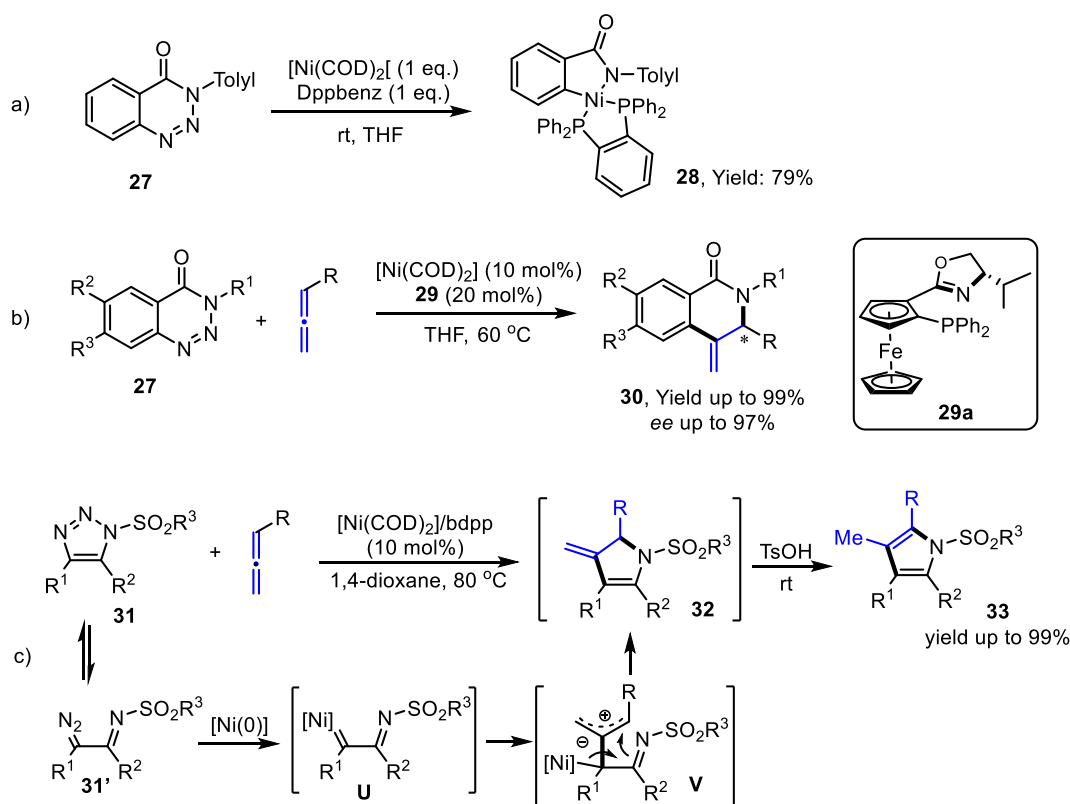


Scheme 1.9 Axial chirality transfer in the [Ni(0)]-catalyzed hydrocyanation of allenes.

In 2010, Murakami documented a Ni(0) catalyzed denitrogenative annulation of 1,2,3-benzotriazin-4(3*H*)-ones with allenes.^{17a} When *N*-tolyl-1,2,3-benzotriazin-4(3*H*)-one **27** was treated with stoichiometric amount of [Ni(0)] and 1,2-bis(diphenylphosphino)benzene (Dppbenz), the metal inserted into *N*-(tolyl) group, delivering the azanickelacycle **28** (yield: 79%) with extrusion of N₂ (Scheme 1.10a). Further examinations showed that this intermediate could undergo C-C and C-N bond forming reaction with allenes to provide annulated formal [4+2] product **30** in high yield and regioselectivity. The enantioselective profile of the transformation was also effectively manipulated with *ee* up to 97% by using (*S,S*)-*i*-Pr-FOXAP **29a** as the chiral ligand of nickel (Scheme 10b).

This denitrogenation coupling reaction was used to synthesize pyrrole in the presence of 1-sulfonyl-1,2,3-triazoles **31** and with *rac*-2,4-bis(diphenylphosphino)pentane (bdpp) as ligand (Scheme 10c).^{17b} In analogy to the previous work, the reaction intermediate **32** (confirmed by NMR) originated the final pyrroles **33** after transposition of C=C double bond in the presence of *p*-toluenesulfonic acid (yield up to 99%). Mechanistically, the α -amino nickel carbene intermediate **U**,

which was produced by insertion of $[\text{Ni}(0)]$ into α -diazo imine **31'** could take subsequent nucleophilic addition with the allene to furnish the zwitterionic intermediate **V**.

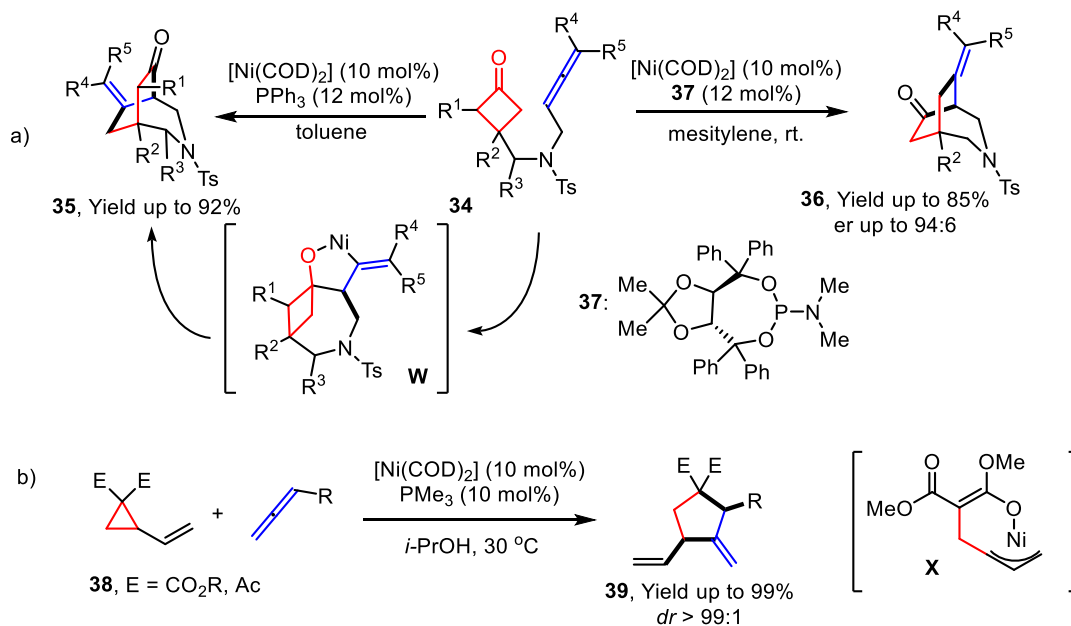


Scheme 1.10 $[\text{Ni}(0)]$ -catalyzed denitrogenative annulation of allenenes

In 2016, Dong developed a $[\text{Ni}(0)]$ -catalyzed intramolecular annulation of highly strained cyclobutanones **34** with allenes which furnished a [3,3,2]-bicyclic scaffold **35** (Scheme 1.11a).^{18a} The reaction was proposed to proceed through a process involving the five-membered metallacycle **W** between the carbonyl group and unsaturated unit, that could evolve to **35** via a β -carbon atom elimination/reductive elimination sequence.

The chemical outcome was proved to be extremely dependent on the allene-substitution pattern with the possibility to extend the protocol to an enantioselective variant taking advantage of TADDOL-derived phosphoramidite **37** as the chiral ligand (*er* value up to 94:6).

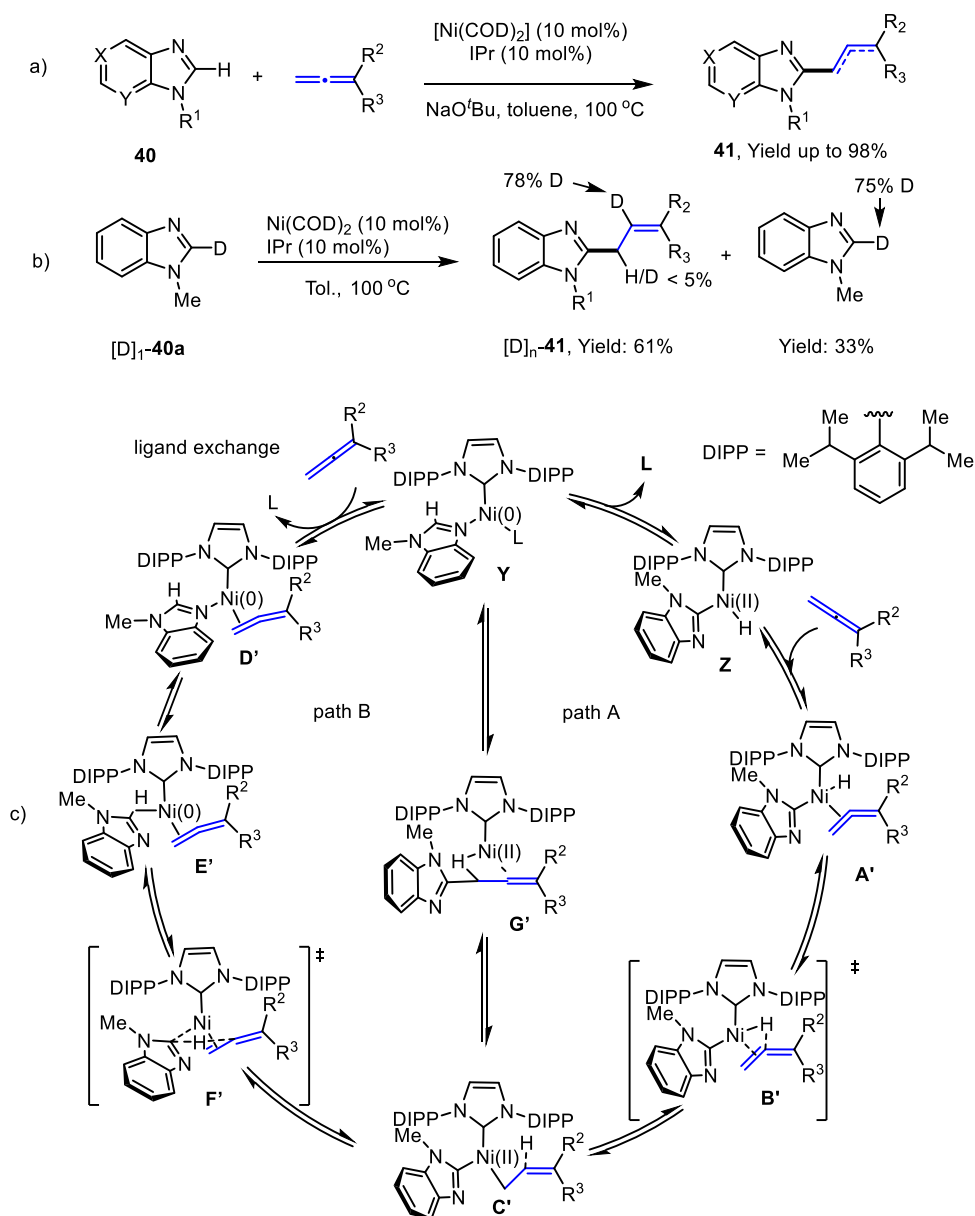
Always in relation to the $[\text{Ni}]$ -catalyzed ring-opening of strength-cycles, Matsubara documented an intermolecular [3+2] annulation of cyclopropane with allenes (Scheme 1.11 b).^{18b} The oxidative addition of the system $[\text{Ni}(0)]/\text{PMe}_3$ with **38**, was counted as key step on the entire protocol to obtain the allyl-Ni intermediate **V**. Optimization of the reaction conditions showed that protic solvents (i.e. *i*PrOH) were supportive for this [3+2] addition delivering the corresponding substituted cyclopentanes **39** in high yields and excellent diastereoselectivity (*dr* = 99:1).



Scheme 1.11 Nickel-catalyzed intramolecularly annulation of cyclobutanone and allenes.

[Ni(0)]-carbene complexes were also studied by Ackermann for the C-H bonds activation of heteroarene to couple with allenes (Scheme 1.12a).¹⁹ The substrate scope showed remarkable functional group and the use of stoichiometric amounts of base provided conjugated product **41** chemoselectively.

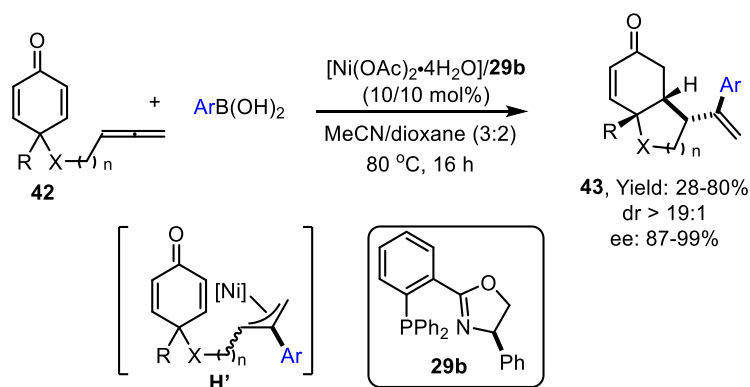
Mechanistic experiments revealed a kinetic isotope effect value of $k_H/k_D = 1.1$, which suggested that the C-H cleavage was not the turnover-limiting step (Scheme 1.12b). Based on that and previous evidences, a catalytic cycle depicted in Scheme 1.12c was proposed. The reaction cycle initiated with ligand exchange (**Y**) and subsequent C-H insertion, providing organo-Ni intermediate **Z** (path A, Scheme 1.12c). Subsequent coordination to allene (**A'**) followed by hydronickelation (**B'**) and reductive elimination could generate the organo-Ni adduct **G'**. Further exchange of ligand would furnish the active complex **Y**. An alternative regime (*i.e.* path B) was envisioned also starting from complex **Y** which could coordinate with allene (**D'**), underwent agnostic insertion (**E'**) and subsequent C-H insertion to give **C'**.



Scheme 1.12 [Ni(0)]-catalyzed C-H activation of heteroarenes and coupling with allenes

1.2.2 Ni(II) initiated coupling reactions

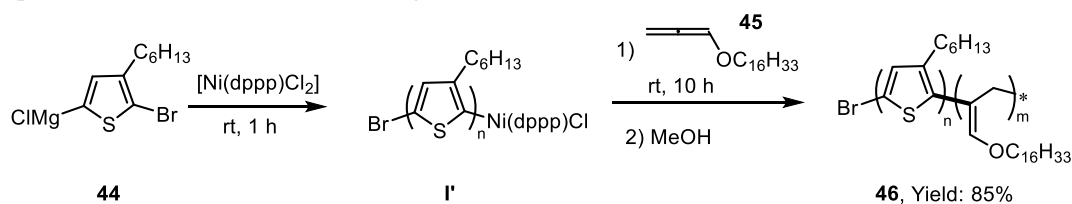
Very recently, Lam and co-workers described an enantioselective nickel catalyzed ($\text{Ni}(\text{OAc})_2 \cdot 4\text{H}_2\text{O}/\mathbf{29b}$) cascade coupling of allenes with boronic acids followed by intramolecular conjugated addition to cyclohexa-2,5-dienones **42** (Scheme 1.15).²⁰ Mechanistically, the present nickel-catalyzed arylation of allenes provides a transient allylnickel intermediate **H'** which undergoes 1,4-addition to cyclo-hexa-2,5-dienyl framework to give the 6,5-bicyclic hexahydroindol-5-ones and 6,6-bicyclic hexahydrobenzofuran-5-ones **43** (yield: 77%-80%) with three contiguous stereogenic centers. Chiral phosphinooxazoline ligand (Phox) **29b** ensured high diastereo- as well as enantioselectivity (*ee*: 90%-94%) in the final product.



Scheme 1.13 Synthesis of 6,5- and 6,6-bicyclic scaffolds **43** via cascade Ni-catalyzed arylation of allene/Michael-type condensation on cyclohexa-2,5-dienones **42**.

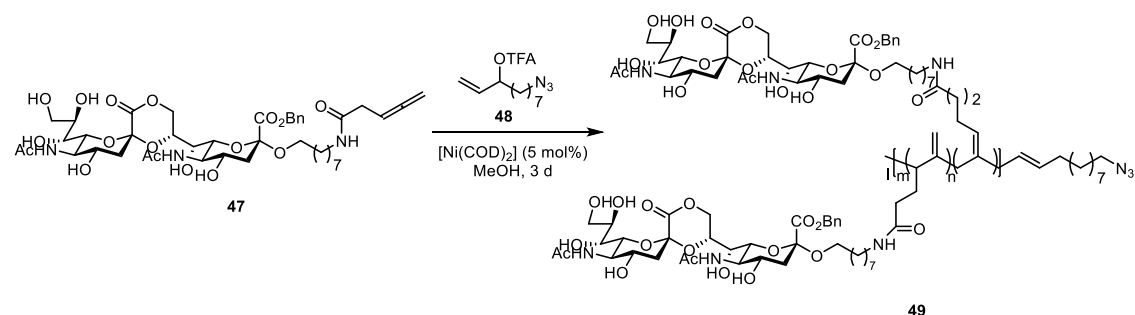
1.2.3 Ni(II) initiated polymerization

The Ni-catalyzed polymerization of allenol ether **45** was effectively developed by Wu and co-workers in the synthesis of functional materials such as poly(3-hexylthiophene)-block poly(hexadecyloxy allene) **46** (yield: 85%) featuring important electronic charge transport properties.²¹ In particular, $[\text{Ni}(\text{dppp})\text{Cl}_2]$ (M/C = 60:1) enabled the synthesis of the macro-compound via a sequential monomeric addition and high control in the chain extension (Scheme 1.14).²²



Scheme 1.14 Synthesis of π -conjugated copolymers via $[\text{Ni}(\text{II})]$ -initiated cross-coupling reactions.

π -Allyl nickel compound could be also used to prepare end-functionalized glycol-polymers which were difficult to assemble in a living way due to the presence of multiple functional groups and indolence towards polymerization.²³ When the substrate **47** was exposed to $[\text{Ni}(\text{COD})_2]$ (5 mol%) and alkene **48** in MeOH for 3 days (rt), the azido glycol-polymer **49** was isolated with complete consumption of the starting monomer (Scheme 1.15). When the amount of $[\text{Ni}(0)]$ was reduced to 2 mol%, the copolymer was still isolated in acceptable 86% yield.



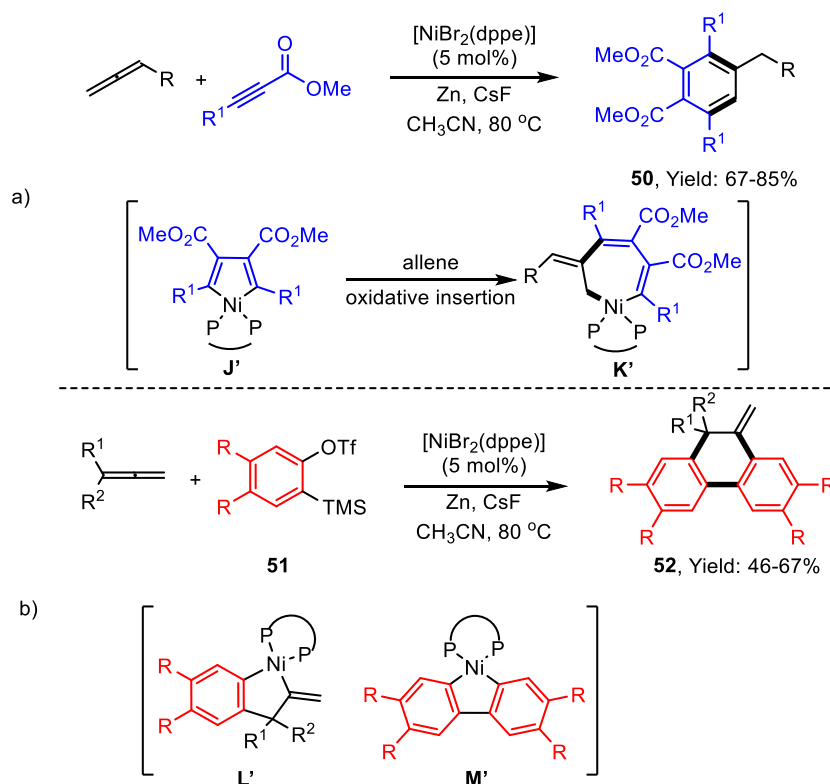
Scheme 1.15 $[\text{Ni}(0)]$ -catalyzed polymerization of allene containing $\alpha(2,8)$ disialic acid.

1.2.4 Ni-catalyzed cycloaddition reactions

Cumulenes have been frequently adopted in the realization of chemical diversity within cyclic and heterocyclic scaffolds via cycloaddition reactions.²⁴ In this section, we present a collection of cycloaddition reactions engaging Ni-catalyzed activation of allenes.

In 2002, Cheng and co-workers pioneered this field with $[\text{Ni}(\text{dppe})\text{Br}_2]$ catalyzed synthesis of fuse functionalized benzenes (yield up to 84%) through a [2+2+2]-cycloaddition involving allenes and propiolates (Scheme 1.16a).^{25a,b} The observed regioselectivity was supposed to arise from initial “head-to-head” oxidative cycloaddition of two propiolates with Ni to provide **J'**, followed by insertion of the allene into the C-Ni(II) bond, delivering a nickelacycloheptadiene **K'**.

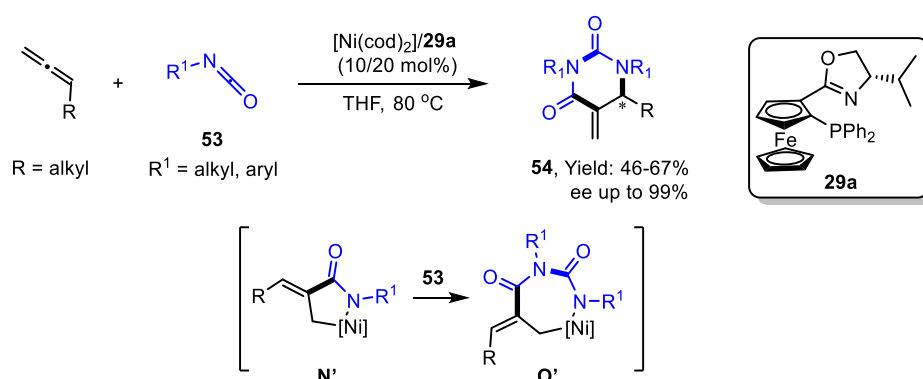
Shortly after, they extended the protocol to involve benzyne precursors **51** as the alkyne source, providing 10-methylene-9,10-dihydrophenanthroline skeleton **52** in moderate to good yields (Scheme 1.16b).^{25c} Also in this case, two different nickelacyclopentene species **L'** and **M'** were hypothesized as the organometallic intermediates. It is noteworthy that, the regioselectivity of allene in this pattern is different from the former one.



Scheme 1.16 $[\text{Ni}(\text{II})/\text{Zn}]$ promoted [2+2+2]-cycloadditions of allenes with propiolates and benzyne-precursors (dppe: 1,3-bis(diphenylphosphino)-ethane).

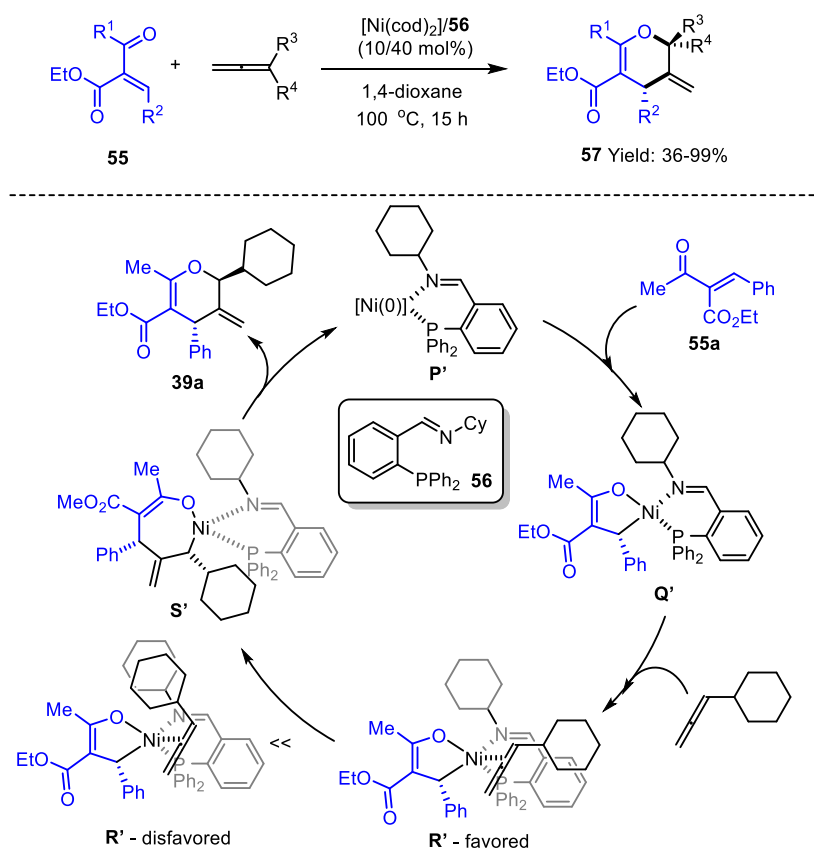
A very interesting $[\text{Ni}(\text{COD})_2]/\mathbf{29a}$ catalyzed enantioselective [2+2+2]-cycloaddition reaction was realized by Murakami in 2010. The transformation involves the use of monosubstituted allenes and isocyanates **53** (ratio = 1:2) and consents the isolation of dihydropyrimidine-2,4-diones **54** in enantiomerically enriched manner (*ee* up to 99%, Scheme 1.17).²⁶ From a mechanistic view point, the initial coupling of the heteropair (*i.e.* allene and isocyanate) with $[\text{Ni}(0)]$ would result into the

formation of azanickelacyclic adduct **O'** that could evolve into the final compound **54** after insertion of a second molecule of **53** and final recombination event.



Scheme 1.17 Enantioselective [Ni(0)]-catalyzed [2+2+2]-cycloaddition of allenes with isocyanates.

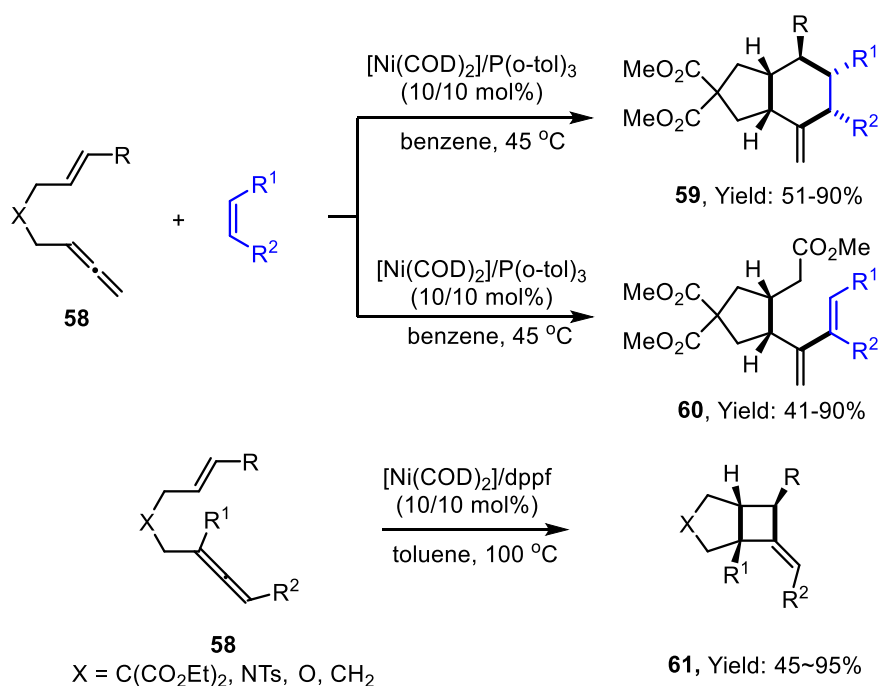
In 2011, Kurahashi and Matsubara reported a regioselective [4+2] cycloaddition of allene and enones **55** to provide multisubstituted dihydropyran **56** catalyzed by [Ni(COD)₂]/iminophosphine (10/40 mol%).²⁷ The methodology tolerates a variety of functional groups such as CN, AcO and R₃SiO at the allenyl site. However, moderate diastereoselectivity was recorded in the final product when asymmetrically disubstituted allenes were subjected to the cycloaddition process (1:1 to 9:1, Scheme 1.18). Mechanistic elucidations showed that the nickel complex **P'**, treated with the enone



Scheme 1.18 [Ni]-catalyzed [4+2]-cycloaddition between allenes and enones.

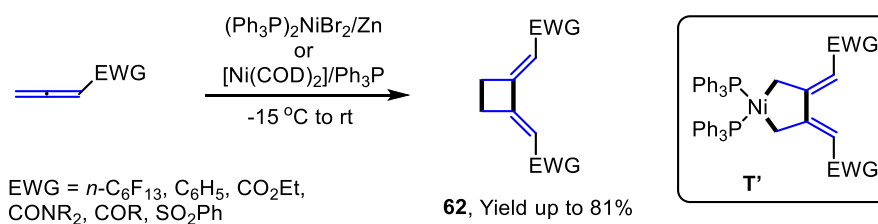
55 could provide the oxanickelacycle **Q'**, with a *trans*-arrangement of the oxygen and phosphorous atoms. Activation of the allenyl moiety by the metal (**R'**) and subsequent insertion into the C-Ni bond (**R'→S'**) would furnish the final product **56** upon reductive elimination.

An efficient and highly stereoselective Ni-catalyzed [2+2+2] cycloaddition of alkene tethered allene **58** and alkenes was reported by Alexanian and coworkers.^{28a} In their work, when P(*o*-tol)₃ was used as the ligand, a series of *cis*-fused carbocycles with up to five contiguous stereocenters were produced (Scheme 1.19a). The product could be tuned by the employment of PtBu₃ which provided diverse dienes **60** (Scheme 1.19b). Meanwhile, further studies demonstrated that a wide range of poly-carbocyclic [2+2]-cycloadducts **61** were obtained in good yields in the presence of [Ni(COD)₂]/dppf (10 mol%) as catalyst (100 °C). A good chirality relay was also obtained starting from enantiomerically pure substrates (Scheme 1.19c).^{28b}



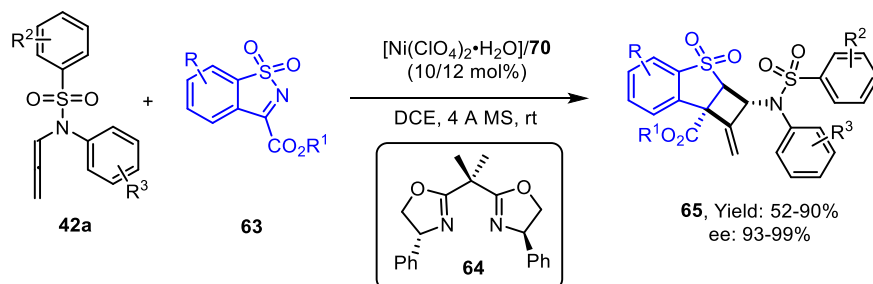
Scheme 1.19 Stereoselective Ni-catalyzed [2+2+2]- and [2+2]-cycloadditions of ene-allene

In 2000, Yamamoto reported a [Ni(0)] catalyzed (both Ni(COD)₂ or (Ph₃P)₂NiBr₂/Zn can be utilized) annulation of electron-deficient allenenes in a regio- and chemoselective pattern, providing a head-to-head cyclodimerized product **62** (Scheme 1.22).²⁹ The reaction was proved efficient with various electron-withdrawing groups. However keto-allenes or sulfonyl-allenes led to deterioration of outcome, probably due to the acidity of the α-protons. Based on some titled control experiments, the reaction was hypothesized to involve a five-member metallacycle **T'** and a subsequent reductive elimination.



Scheme 1.20 [Ni(0)]-catalyzed [2+2] dimerization of electron-deficient allene.

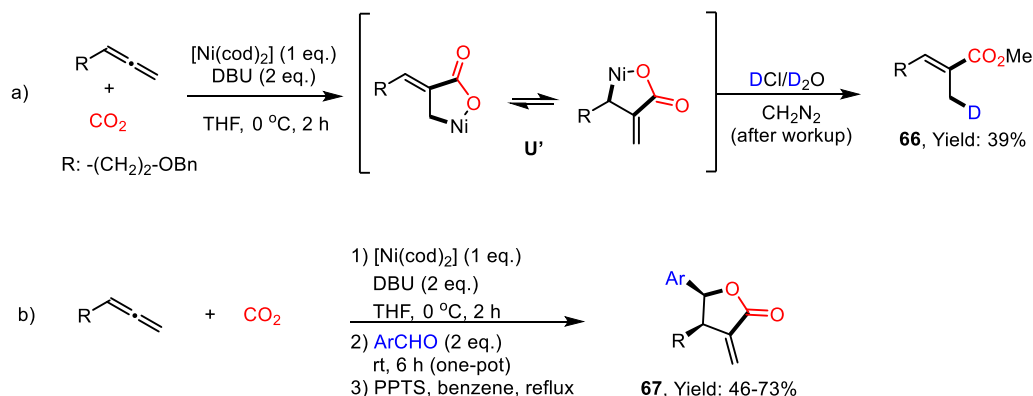
Very recently, Jia's group reported an enantioselective [2+2]-cycloaddition of allenamides with cyclic *N*-sulfonylketimines **63**.³⁰ In this work, Ni(ClO₄)₂ was hypothesized to activate the imine moiety towards the stepwise nucleophilic condensation together with the allenamides **42a**. Optimal reaction condition tolerated a variety of functional groups at C5 and C7 positions of the α -ketiminoesters including halides, OMe, CF₃, OCF₃. Additionally, *N*-allenyl pyrrolidinones and oxazolidinones could also work efficiently under optimal conditions, providing the corresponding aldehyde, directly. Last but not the least, the employment of isopropylidene bisoxazoline **64** as a ligand led to the production of the desired [2+2]-cycloadduct **65** in good yield very high enantiomeric excess (up to 99%, Scheme 1.23).



Scheme 1.21 Enantioselective [2+2] cycloaddition of allenamides catalyzed by [Ni(II)].

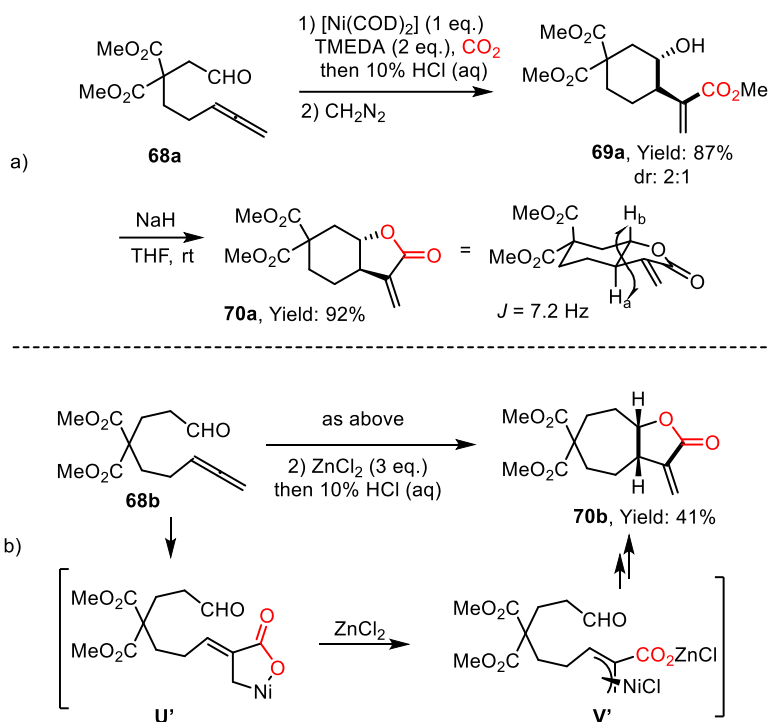
1.2.5 Ni(0) promoted/catalyzed CO₂ fixation

[Ni(0)] complexes are able to electrophilically activate CO₂ as a C(1)-synthon in organic transformations.^{31a} In particular, pioneered by the Aresta' complex [Ni(CO₂)(PCy₃)₂], several examples of oxidative fixation of CO₂ promoted by stoichiometric low-valent transition metals were presented.^{31b} In this context, Mori contributed substantially to the field by developing a [Ni(0)]-catalyzed cascade addition of CO₂ and aldehydes to terminal allenenes.^{32a} Accordingly, when terminal allenenes and CO₂ were exposed to stoichiometric amounts of [Ni(COD)₂], an oxidative cycloaddition was supposed to occur providing an oxanickelacycle intermediate **U'** that could be trapped by D⁺ (Scheme 1.22a).^{32b} The methodology evolved into a three-component variant wherein the *in situ* formed allyl-Ni species was electrophilically trapped by aromatic aldehydes. Acid work-up enabled the final isolation of the corresponding lactones **67** (Scheme 1.22b).



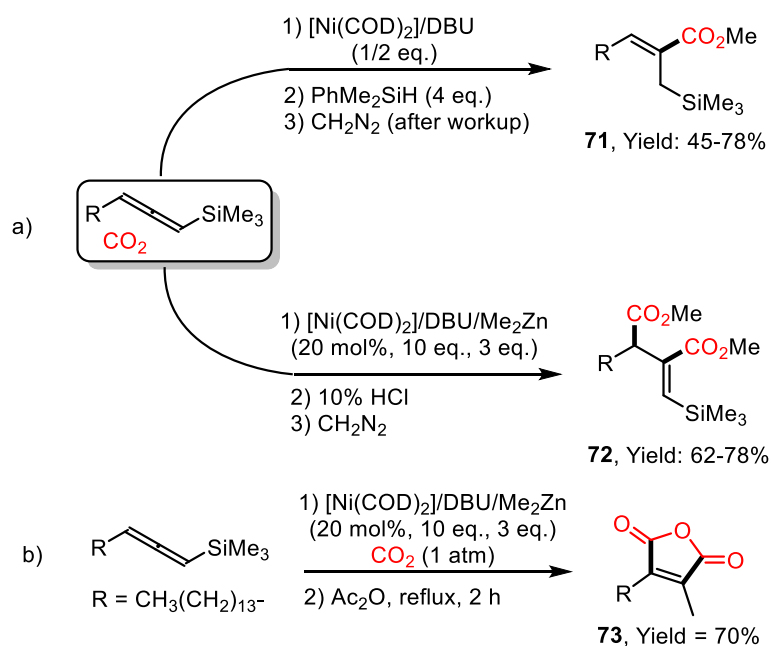
Scheme 1.22 [Ni(0)]-promoted site-specific carboxylation of allenenes with CO₂.

A high regioselective preparation of a terminal alkenyl- γ -hydroxy ester **69** was developed by the same team via an intramolecular [Ni(0)]-promoted cycloaddition of CO₂ to allenes **68**.³³ Treatment of **69a** with NaH led to ester **70a** via spontaneous lactonization. (Scheme 1.23a). Interestingly, the larger lactones (*i.e.* 7-member ring, **70b**) was also obtained by exploitation of stoichiometric amount of ZnCl₂ (3 eq.). ZnCl₂ was suggested to work not only as a Lewis acid but also as a *trans*-metalating reagent in order to form a more nucleophilic allylnickel species **V'** (Scheme 1.23b).



Scheme 1.23 Ni promoted intramolecular CO₂ condensation with allenes and aldehydes. Synthesis of functionalized lactones.

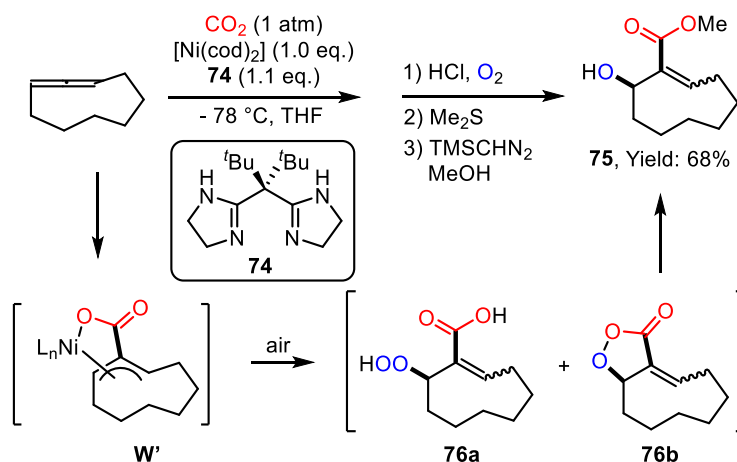
An Ni(0)-assisted fixation of atmospheric CO₂ into allenyl frameworks was also achieved with trimethylsilylallenes.^{34a} Key factor for the methodology relied on the use of phenyldimethylsilane which was supposed to convert the oxanickel cycle intermediates into allyl or vinyl silanes via a σ -bond metathesis process enabling the isolation of allylsilanes **71** in satisfying yields (up to 78%, Scheme 1.24a). Very interestingly, replacement of PhMe₂SiH by Me₂Zn (used as reducing agent of the metal) with the nickel loading dropped to 20 mol% could promote the double carboxylation event of the allenyl core at the C(2), C(3) positions. The exclusive formation of densely functionalized (*Z*)-vinylsilanes **72** prompted the authors to apply the methodology to the total synthesis of Chaetomelic acid **A** anhydride **73** (Scheme 1.24b).^{34b}



Scheme 1.24 Ni-assisted fixation of CO_2 with silylallenenes.

Similar efficiency also exhibited in the site-selective carboxylation of allenamides in the presence of $[\text{Ni}(\text{COD})_2]/\text{DBU}$ (1/4 eq.) and CO_2 (1 atm). Under optimal condition, stereochemically defined enamides were obtained in moderate to good yield (up to 91%).^{34c}

Finally, Iwasawa and co-workers disclosed that the allylnickel intermediate **W'**, generated via oxidative activation of 1,2-dienes and atmospheric CO_2 by $[\text{Ni}(\text{COD})_2]/\text{bis}(\text{amidine})$ ligand (**74**), can be adequately trapped by molecular oxygen during the acid workup of the carboxylation reaction.³⁵ The *in situ* formed peroxides **76a** or peroxy lactones **76b** were conveniently cleaved by Me_2S , providing the β -hydroxycarboxylic ester **75** in high yields (Scheme 1.25).



Scheme 1.25 Synthesis of β -hydroxy-carboxylic acids **75** via $[\text{Ni}(0)]$ -assisted fixation of CO_2 on allenenes

1.3 Conclusions

Homogenous nickel catalysis is becoming pervasive in organic synthesis with a particular impact

on the manipulation of unsaturated hydrocarbons. In this summary, we summarized the most recent efforts in this field encompassing the transformation of allenes and derivatives. The chemical diversity commonly guaranteed by the use of 1,2-dienes in organic synthesis is substantially amplified by the combination with [Ni]-catalysis, resulting into applications such as: total synthesis of bioactive compounds, the development of unprecedented and environmentally convenient methodologies and the realization of functional materials for organic electronic applications.

The field is extremely flourishing, and more is expected to come in the near future.

Our work emphasizes on development of the nickel(II) chemistry, especially on Ni(II) catalyzed coupling of electron-perturbed allenes and boronic acid. In addition to that, we exerted effort on application of Ni(II) on photochemistry, although at last it turned out to be not necessary. At last, we also made a little progress on photocatalyzed Wacker oxidation due to our huge interest in photochemistry.

Reference

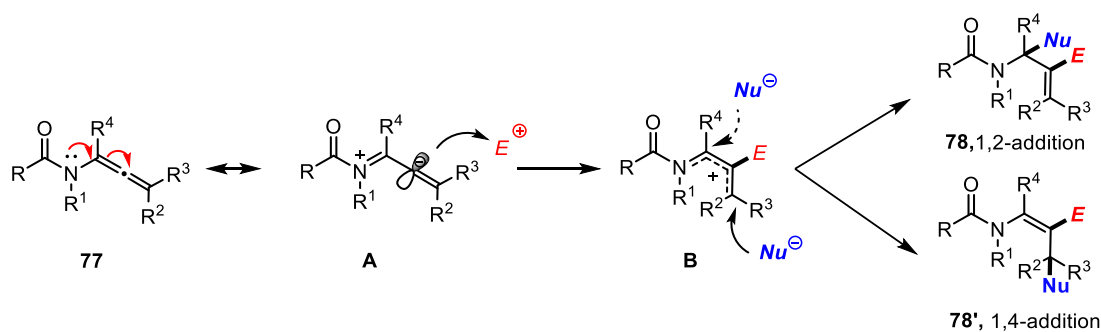
- ¹ (a) Y. Tamaru, in *Modern Organonickel Chemistry*, Ed.: Tamaru, Y., Wiley-VCH Verlag GmbH & Co. KGaA, Weinheim, **2005**; (b) S. Z. Tasker, E. A. Standley, T. F. Jamison, *Nature* **2014**, *509*, 299 – 309; (c) E. J. Tollefson, L. E. Hanna, E. R. Jarvo, *Acc. Chem. Res.* **2015**, *48*, 2344 – 2353; (d) J. Choi, G. C. Fu, *Science* **2017**, *356*, 152 – 160; (e) G. C. Fu, *ACS Cent. Sci.* **2017**, *3*, 692 – 700; (f) E. Richmond, J. Moran, *Synthesis* **2018**, *50*, 499 – 513.
- ² (a) D. Wong, D. Astruc, *Chem. Soc. Rev.* **2017**, *46*, 816 – 854; (b) J. E. Zweig, D. E. Kim, T. R. Newhouse, *Chem. Rev.* **2017**, *117*, 11680 – 11752.
- ³ E. C. Hansen, D. J. Pedro, A. C. Wotal, N. J. Gower, J. D. Nelson, S. Caron, D. J. Weix, *Nat. Chem.* **2016**, *8*, 1126 – 1130.
- ⁴ E. A. Standley, S. Z. Tasker, K. L. Jensen, T. F. Jamison, *Acc. Chem. Res.* **2015**, *48*, 1503 – 1514; (b) B. Tóth, O. Tischler, Z. Novák, *Tetrahedron Lett.* **2016**, *57*, 4505 – 4513.
- ⁵ (a) M. R. Netherton, G. C. Fu, *Adv. Synth. Catal.* **2004**, *346*, 1525 – 1532; (b) B. M. Rosen, K. W. Quasdorf, D. A. Wilson, N. Zhang, A. -M. Resmerita, N. K. Garg, V. Percec, *Chem. Rev.* **2011**, *111*, 1346 – 1416; (c) K. Muto, J. Yamaguchi, D. G. Musaev, K. Itami, *Nat. Commun.* **2015**, *6*, 7508; (d) Z. Li, L. Liu, *Chin. J. Catal.* **2015**, *36*, 3 – 14.
- ⁶ For selected reviews, see: (a) *Modern Allene Chemistry*, Eds.: N. Krause, A. S. K. Hashmi, Wiley-VCH, Weinheim, Germany, 2004, Vol. 1; (b) S. Ma, Palladium-Catalyzed Two- or Three-Component Cyclization of Functionalized Allenes. in *Palladium in Organic Synthesis*, Ed.: J. Tsuji, Springer, Berlin, 2005, p. 183; (c) L. Brandsma, N. A. Nedolya, *Synthesis* **2004**, 735 – 745; (d) S. Ma, *Chem. Rev.* **2005**, *105*, 2829 – 2872; (e) S. Ma, *Aldrichimica Acta* **2007**, *40*, 91 – 102; (f) H. Kim, L. J. J. Williams, *Curr. Opin. Drug Discovery Dev.* **2008**, *11*, 870 – 894; (g) M. Brasholz, H.-U. Reissig, R. Zimmer, *Acc. Chem. Res.* **2009**, *42*, 45 – 56; (h) S. Ma, *Acc. Chem. Res.* **2009**, *42*, 1679 – 1688; (i) C. Aubert, L. Fensterbank, P. Garcia, M. Malacria, A. Simonneau, *Chem. Rev.* **2011**, *111*, 1954 – 1993; (j) S. Yu, S. Ma, *Angew. Chem. Int. Ed.* **2012**, *51*, 3074 – 3112; (k) J. Ye, S. Ma, *Acc. Chem. Res.* **2014**, *47*, 989 – 1000; (l) W.-D. Chu, Y. Zhang, J. Wang, *Catal. Sci. Technol.* **2017**, *7*, 4570 – 4579.
- ⁷ Q. Li, H. Gau, *Synlett* **2012**, *23*, 747 – 750.
- ⁸ E. Shirakawa, Y. Nakao, T. Tsuchimoto, T. Hiyama, *Chem. Commun.*, **2002**, 1962 – 1963.
- ⁹ E. Shirakawa, Y. Yamamoto, Y. Nakao, S. Oda, T. Tsuchimoto, T. Hiyama, *Angew. Chem. Int. Ed.* **2004**, *43*, 3448 – 3451.
- ¹⁰ M. S. Wu, D. K. Rayabarapu, C. H. Cheng, *J. Am. Chem. Soc.* **2003**, *125*, 12426 – 12427.
- ¹¹ (a) K. K. D. Amarasing, J. Montgomery, *J. Am. Chem. Soc.* **2002**, *124*, 9366 – 9367; (b) J. Montgomery, M. Song, *Org. Lett.* **2002**, *4*, 4009 – 4011; (c) S.-K. Kang, S.-K. Yoon, *Chem. Commun.* **2002**, 2634 – 2635; (d) M. Song, J. Montgomery, *Tetrahedron* **2005**, *61*, 11440 – 11448; (e) M. V. Chevliakov, J. Montgomery, *J. Am. Chem. Soc.* **1999**, *121*, 11139 – 11143.
- ¹² (a) S. S. Ng, T. F. Jamison, *J. Am. Chem. Soc.* **2005**, *127*, 7320 – 7321; (b) S. S. Ng, T. F. Jamison, *Tetrahedron* **2005**, *61*, 11405 – 11417; (c) S. S. Ng, T. F. Jamison, *Tetrahedron* **2006**, *62*, 11350 – 11359.
- ¹³ (a) Z. D. Miller, W. Li, T. R. Belderrain, J. Montgomery, *J. Am. Chem. Soc.* **2013**, *135*, 15282 – 15285; (b) Z. D. Miller, R. Dorel, J. Montgomery, *Angew. Chem. Int. Ed.* **2015**, *54*, 9088 – 9091. For computational investigations on the Ni-catalyzed hydrosilylation of allenenes see: (c) H. Xie, L. Zhao, L. Yang, Q. Lei, W. Fang, C. Xiong, *J. Org. Chem.* **2014**, *79*, 4517 – 4527; (d) H. Xie, J. Kuang, L. Wang, Y. Li, L. Huang, T. Fan, Q. Lei, W. Fang, *Organometallics* **2017**, *36*, 3371 – 3381.
- ¹⁴ Y. Nakao, Y. Hirata, T. Hiyama, *J. Am. Chem. Soc.* **2006**, *128*, 7420 – 7421.
- ¹⁵ (a) S. Arai, Y. Amako, X. Yang, A. Nishida, *Angew. Chem. Int. Ed.* **2013**, *52*, 8147 – 8150; (b) X.

- Yang, S. Arai, A. Nishida, *Adv. Synth. Catal.* **2013**, 355, 2974 – 2981; (c) Y. Amako, H. Hori, S. Arai, A. Nishida, *J. Org. Chem.* **2013**, 78, 10763 – 10775.
- ¹⁶ (a) S. Arai, H. Hori, Y. Amako, A. Nishida, *Chem. Commun.* **2015**, 51, 7493 – 7496; (b) Y. Amako, S. Arai, A. Nishida, *Org. Biomol. Chem.* **2017**, 15, 1612 – 1617; (c) K. Matsumoto, S. Arai, A. Nishida, *Tetrahedron* **2018**, 74, 2865 – 2870.
- ¹⁷ (a) M. Yamauchi, M. Morimoto, T. Miura, M. Murakami, *J. Am. Chem. Soc.* **2010**, 132, 54 – 55; (b) T. Miura, K. Hiraga, T. Biyajima, T. Nakamuro, M. Murakami, *Org. Lett.* **2013**, 15, 3298 – 3301.
- ¹⁸ (a) X. Zhou, G. Dong, *Angew. Chem. Int. Ed.* **2016**, 55, 15091 – 15095; (b) R. Tombe, T. Iwamoto, T. Kurahashi, S. Matsubara, *Synlett* **2014**, 25, 2281 – 2284.
- ¹⁹ S. Nakanowatari, T. Muller, J. C. A. Oliveira, L. Ackermann, *Angew. Chem. Int. Ed.* **2017**, 56, 15891 – 15895.
- ²⁰ N. Nguyen, A. Incerti-Pradillos, L. Lewis, H. W. Lam, *Chem. Commun.* **2018**, 54, 5622 – 5625.
- ²¹ Z. Q. Wu, Y. Chen, Y. Wang, X. Y. He, Y. S. Ding, N. Liu, *Chem. Commun.* **2013**, 49, 8069 – 8071.
- ²² For a recent Ni-catalyzed stereoselective polymeration of allenes see: H. Zhu, S. Luo, Z. Wu, *Chin. Chem. Lett.* **2019**, 30, 153 – 156.
- ²³ H. Ohira, Y. Yasuda, I. Tomita, K. Kitajima, T. Takahashi, H. Satob, H. Tanaka, *Chem. Commun.* **2017**, 53, 553 – 556.
- ²⁴ A. Lledó, A. Pla-Quintana, A. Roglans, *Chem. Soc. Rev.* **2016**, 45, 2010 – 2023.
- ²⁵ (a) M. Shanmugasundaram, M.-S. Wu, C.-H. Cheng, *Org. Lett.* **2002**, 3, 4233 – 4236; (b) M. Shanmugasundaram, M.-S. Wu, M. Jeganmohan, C.-W. Huang, C.-H. Cheng, *J. Org. Chem.* **2002**, 67, 7724 – 7729; (c) J. C. Hsieh, D. K. Rayabarapu, C.-H. Cheng, *Chem. Commun.* **2004**, 532 – 533.
- ²⁶ T. Miura, M. Morimoto, M. Murakami, *J. Am. Chem. Soc.* **2010**, 132, 15836 – 15838.
- ²⁷ S. Sako, T. Kurahashi, S. Matsubara, *Chem. Commun.* **2011**, 47, 6150 – 6152.
- ²⁸ (a) N. N. Noucti, E. J. Alexanian, *Angew. Chem. Int. Ed.* **2013**, 52, 8424 – 8427; (b) N. N. Noucti, E. J. Alexanian, *Angew. Chem. Int. Ed.* **2015**, 54, 5447 – 5450.
- ²⁹ S. Saito, K. Hirayama, C. Kabuto, Y. Yamamoto, *J. Am. Chem. Soc.* **2000**, 122, 10776 – 10780.
- ³⁰ R. R. Liu, J. P. Hu, J. J. Hong, C. J. Lu, J. R. Gao, Y. X. Jia, *Chem. Sci.* **2017**, 8, 2811 – 2815.
- ³¹ (a) Q. Liu, L. Wu, R. Jackstell, M. Beller, *Nat. Commun.* **2015**, 6, 5933; (b) M. Aresta, C. F. Nobile, V. G. Albano, E. Forni, M. Manassero, *J. Chem. Soc., Chem. Commun.* **1975**, 636 – 637.
- ³² (a) M. Takimoto, M. Kawamura, M. Mori, *Org. Lett.* **2003**, 5, 2599 – 2601; (b) H. Hoberg, B. W. Oster, *J. Organomet. Chem.* **1984**, 266, 321 – 326.
- ³³ M. Takimoto, M. Kawamura, M. Mori, Y. Sato, *Synlett* **2011**, 1423 – 1426.
- ³⁴ (a) M. Takimoto, M. Kawamura, M. Mori, *Synthesis* **2004**, 791 – 795; (b) M. Takimoto, M. Kawamura, M. Mori, Y. Sato, *Synlett* **2005**, 2019 – 2022; (c) N. Sato, Y. Sugimura, Y. Sato, *Synlett* **2014**, 25, 736 – 740.
- ³⁵ M. Aoki, S. Izumi, M. Kaneko, K. Ukai, J. Takaya, N. Iwasawa, *Org. Lett.* **2007**, 9, 1251 – 1253.

2 Nickel Catalyzed Suzuki Coupling of Electronically Perturbed Allenes

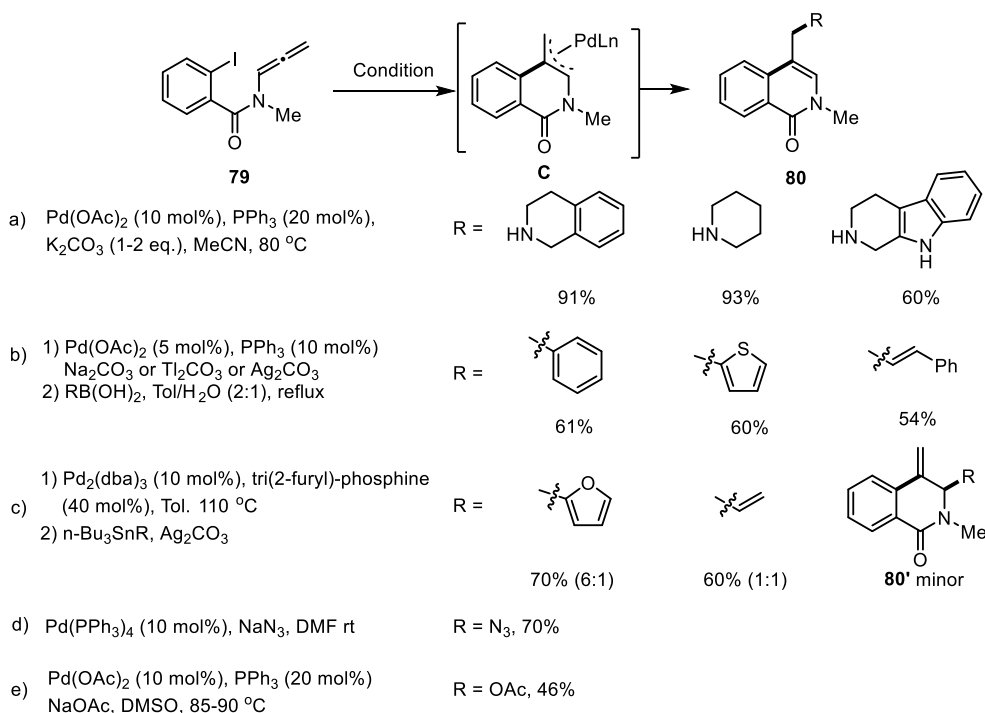
2.1 Retrospect on metal catalyzed coupling of allenamide

Due to the electron donating property of nitrogen atom, allenamide actually is electron-richly tuned allene. Particularly, β -carbon is more nucleophilic than rest site leading to the unicity on the reactivity (Scheme 2.1). Consequently, the theme of allenamide chemistry is to find different combinations of electrophile and nucleophile.¹ However, it is necessary to present the metal (palladium in particular) catalyzed cross coupling of allenamide which lead to similar product with our work: inserting one aryl group at β -carbon of allene moiety and introduction of another function group at α - or γ - position.



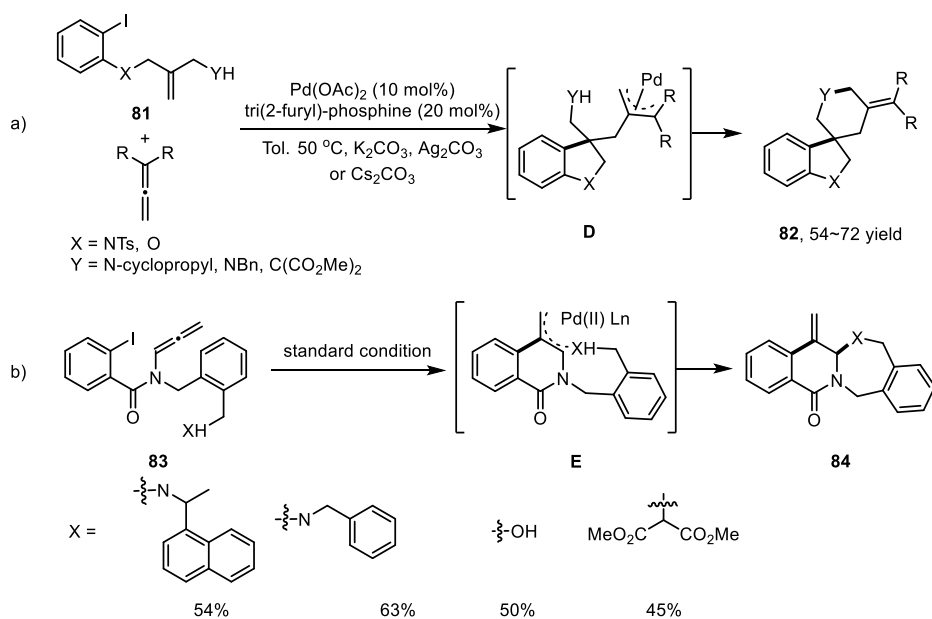
Scheme 2.1 Typical reaction protocol of allenamide

In 1995, Grigg opened new difunctionalization pattern of allenamide through a sequence of β -arylation carbopalladation and α - or γ -anion capture cascade process (Scheme 2.2). Oxidative addition of palladium(0) to aryl iodide was followed by insertion to β -carbon of allene providing an electrophilic (π -allyl)palladium intermediate which could be captured by a nucleophile (amines) at less hindered γ -position regioselectively. Amine (Scheme 2.2a),^{2a} boronic acid (Scheme 2.2b)^{2b}, organotin (Scheme 2.2c)^{2c}, azide (Scheme 2.2d)^{2d, 2e} and acetate (Scheme 2.2e)^{2f} were tolerated in this pattern with modification on source of palladium and ligand. It is noteworthy that, when disubstituted amine was used as nucleophile and Ag_2CO_3 as base, the attack site moved to α -allenenic carbon due to (π -allyl)palladium complex turned to be cationic in the presence of Ag_2CO_3 which favored α -attack. When organotin was used, a mixture of α - or γ -attack products were produced.



Scheme 2.2 Palladium catalyzed difunctionalization of the allenamide by Grigg.

Intramolecular anion capture was also adoptable to form polycyclic tetrahydropyrans, piperidines and isoquinolones with tri(2-furyl)-phosphine as ligand in moderate yield (Scheme 2.3).³ Both allenamide and allene were tolerated in this pattern divergently in two aspects: a) the allenamide provided *exo-dig* annulated product **84**, while the allene provided *exo-trig* spirocyclic product **82**; b) the *sp*² hybridized carbon palladium intermediate to couple with allene moiety was compatible

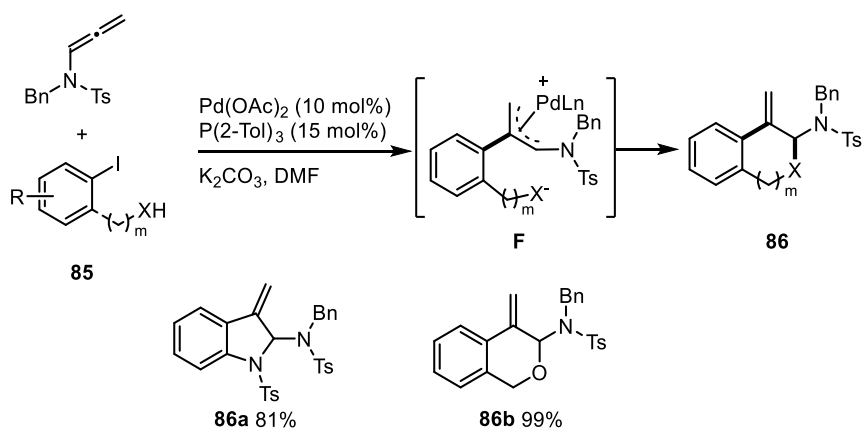


Scheme 2.3 The intramolecular anion capture pattern by Grigg

with allenamide, while *sp*³ one worked with allene. The intermolecular capture of *sp*³-

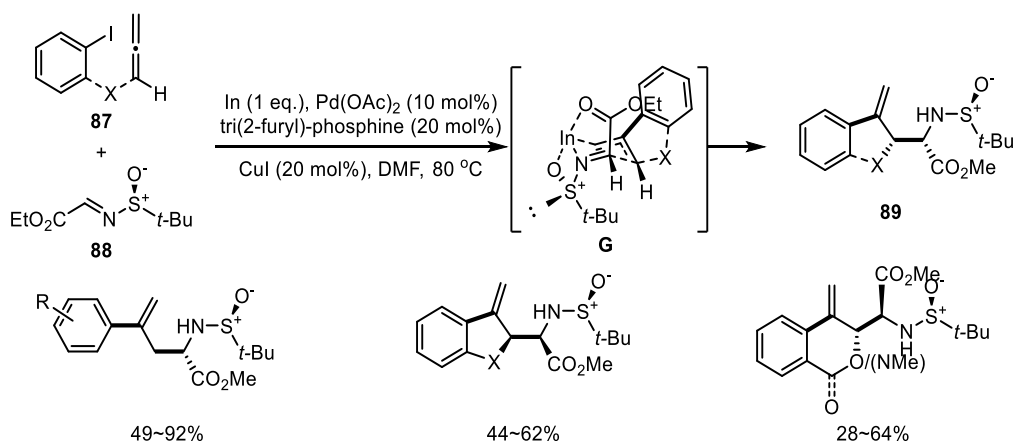
alkylpalladium intermediate could be firstly intermolecularly captured by nucleophilic allene to provide (π -allyl)palladium intermediate the less hindered end of which was subsequently intramolecularly captured by anion, providing an spirocyclic product (Scheme 2.3a).

In 2005, Sakamoto⁴ reported a palladium catalyzed [4+2] annulation of allenamide and aryl iodides (Scheme 2.4). After the intermolecular allylation of organopalladium, the electrophilic intermediate could be trapped by amino or hydroxyl group intramolecularly providing annulated product. The reaction offered 5- or 6-*exo*-trig product exclusively due to, according to author, the nitrogen stabilized the allyl cation which overcomes the repulsion which results in α - attack. In addition to allenamides, the allenethers also provided similar annulated product.



Scheme 2.4 The intramolecular [4+2] annulation of allenamide and phenyl iodide.

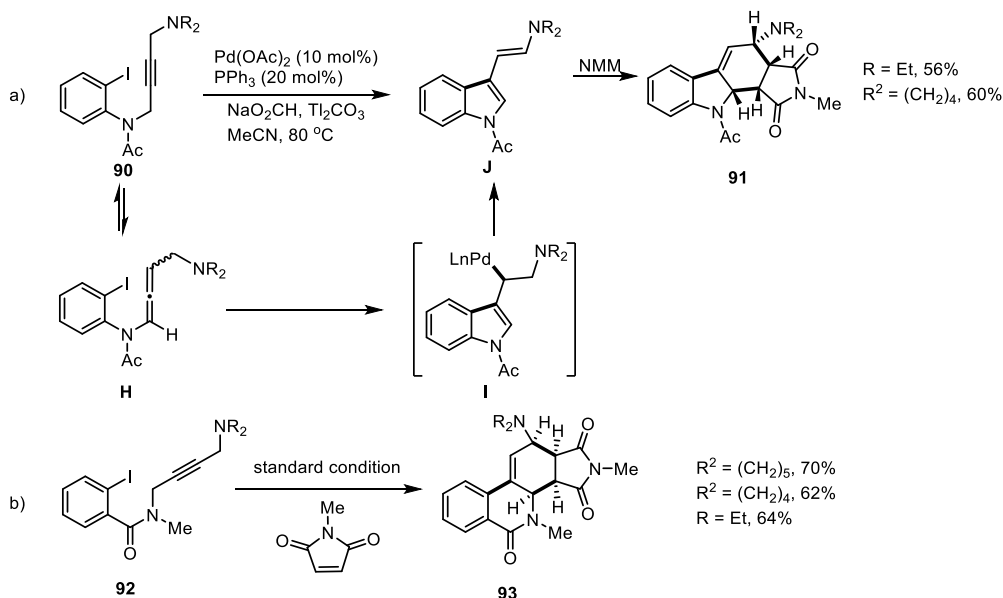
A tactical Pd/In catalyzed intro- and intermolecular cascade reaction was developed to synthesize α -amino acid was reported by Grigg.⁵ In this process, the generation of electrophilic (π -allyl)palladium species was followed by transmetalation to indium, providing an η^1 -allyl indium species. This nucleophilic intermediate could add to enantiopure *N*-sulfinyl- α -iminoester to provide product enantioselectively.



Scheme 2.5 Enantioselective preparation of amino acid via Pd/In catalytic system.

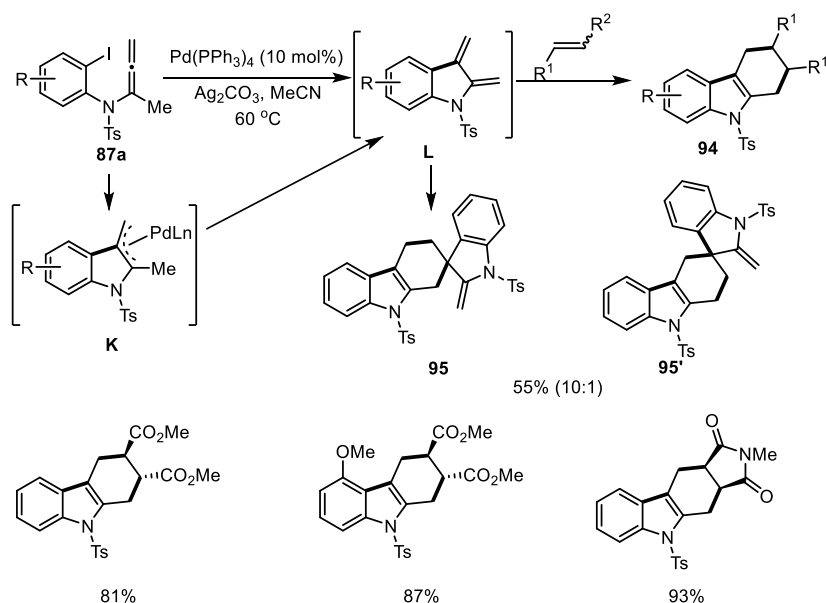
In 1996, Grigg reported a multicomponent [4+2] cyclization including palladium catalyzed coupling and endo-cycloaddition process (Scheme 2.6).⁶ The reaction started with Tl₂CO₃ assisted alkyne-

allene isomerization (**90**→**H**) followed by palladium catalyzed oxidative insertion to aryl iodide, regioselective 5- or 6-exo-dig cyclization and oxidative reductive elimination providing enaminoindoles (**J**) which was not separable. Then enaminoindole could be trapped by *N*-methylmaleimide (NMM) to deliver the Diels–Alder cycloaddition product **91** or **93**.



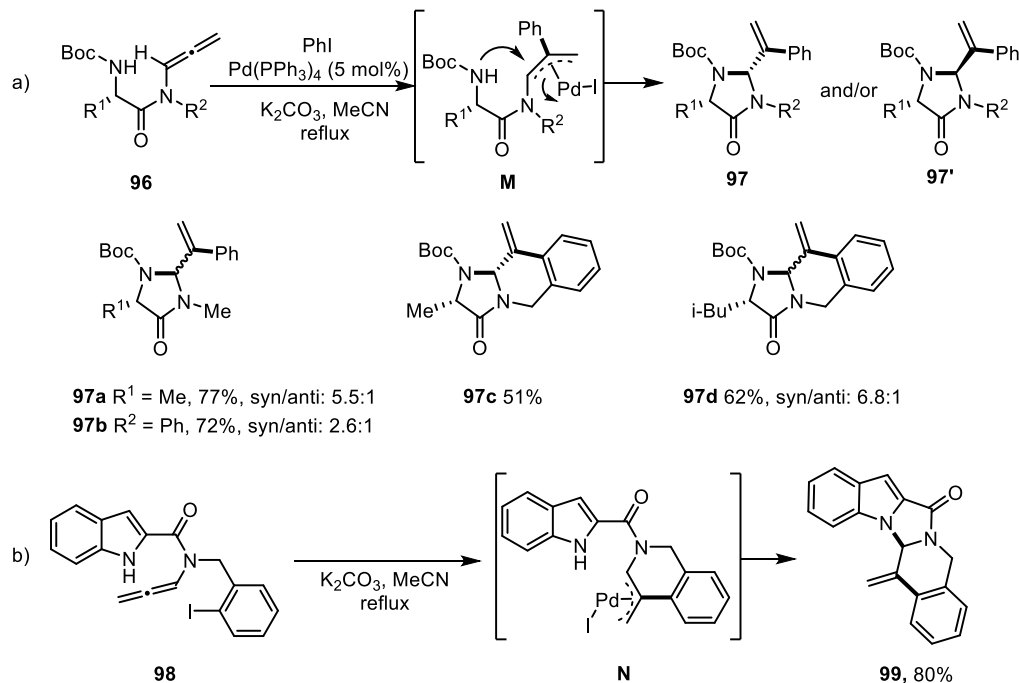
Scheme 2.6 Palladium catalyzed [4+2] cyclization initiated by alkyne/allene isomerization.

In 2008, Fuwa and Sasaki⁷ evolved the strategy to synthesize indole-2,3-quinodimethane **L** which underwent Diels–Alder cycloaddition offering tetrahydrocarbazoles **94** or relative compounds which could be used to synthesize *Aspidosperma* alkaloids (Scheme 2.7). The absence of external dienophile, a Diels–Alder cycloaddition homodimers **95** & **95'** could be formed with good regioselectivity.



Scheme 2.7 Synthesis of indole-2,3-quinodimethane and subsequent Diels–Alder process.

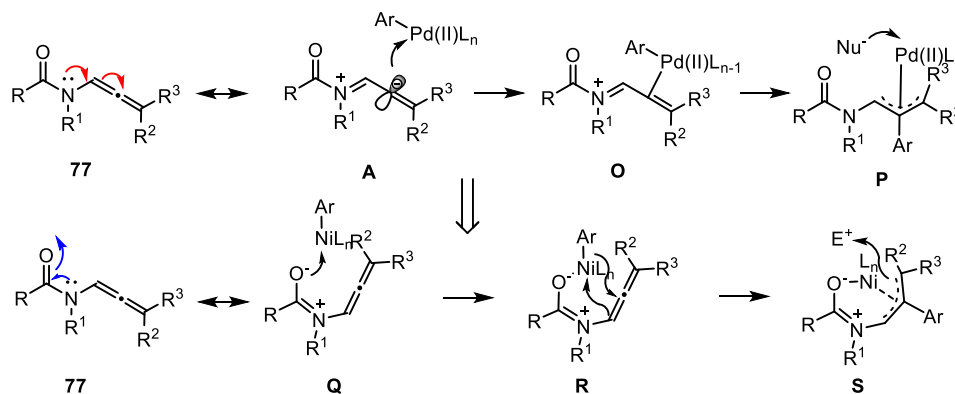
In 2009, Brogini⁸ reported palladium catalyzed β -arylation- α -amination of allenamide **96** through (π -allyl)palladation-5-*exo*-dig amination process to form enantiopure 2-vinylimidazolidin-4-ones **97** (Scheme 2.8). When the arylation worked in intramolecular way the methodology was able to synthesize fused-ring imidazolidinones such as **97c**, **97d**. Unprotected nitrogen of indole could also work as nucleophile to provide **99**.



Scheme 2.8 Palladium catalyzed β -arylation- α -amination of allenamide.

2.2 Nickel catalyzed Suzuki coupling of allenamides

Our work commenced with our hypothesis to realize the umpolung with an organometal intermediate. In contrast to former palladium catalyzed coupling, we need a metal that can happen transmetalation or oxidative addition easily, meanwhile, the metal should possess substantial oxygen affinity so that the oxygen of carbonyl group can chelate to it (**77**→**S**), which also reduce the electron richness of allenyl moiety (Scheme 2.9).

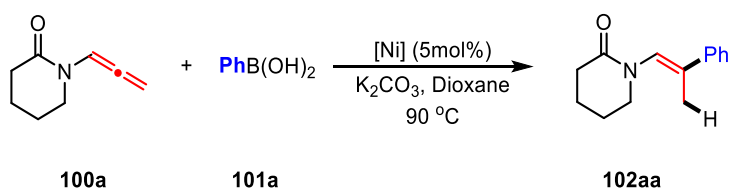


Scheme 2.9 The hypothesis of the umpolung of reactivity of allenamide.

We chose the 1-(propa-1,2-dien-1-yl)piperidin-2-one **100a** as the standard substrate because of easy accessibility and its substantial stability; tactical combination of phenylboronic acid **101a**/Ni(II) as organometal recourse at first; K₂CO₃ as base and dioxane as solvent which were widely used in the Suzuki coupling reaction.

Firstly, we examined some common nickel complexes including bis(triphenylphosphine)-NiCl₂ (Table 2.1, entry 1), bis(tricyclohexylphosphane)-NiCl₂ (Table 2.1, entry 2), bis(diphenylphosphino)-propane-NiCl₂ (dppp-NiCl₂) (Table 2.1, entry 3), 1,3-bis-(2,6-diisopropylphenyl)imidazolium-NiCl₂ (IPr-NiCl₂) (Table 2.1, entry 4), bipyridine-NiCl₂ (Table 2.1, entry 5) at 90 °C with dioxane as solvent. Luckily, we found that only bipyridine-NiCl₂ promoted the reaction to give product **102aa** in 71% yield while other complexes performed no apparent help on the formation of product.

Table 2.1. The elementary research on different nickel species.

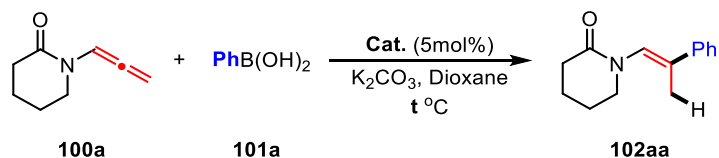


Entry ^[a]	[Ni]	Time	Yield of xx (%)
1	(PPh ₃) ₂ NiCl ₂	24	<10%
2	(PCy ₃) ₂ NiCl ₂	24	<10%
3	dpppNiCl ₂	24	<10%
4	IPr•HCl/NiCl ₂	1	No
5	BpyNiCl ₂	1	71

^[a] All the reactions were carried out under nitrogen atmosphere with dry 1,4-dioxane. **100a**:**101a**:**[Ni]**:base = 1:1.5:0.05:3 (0.2 mmol scale of **100a**). ^[b] Isolated yields after flash chromatography. In all cases, **102aa** was isolated with *E*:*Z* ratio > 95:5 by ¹H-NMR. ^[c] Complex formed *in situ* was utilized. dppp: 1,3-bis(diphenylphosphino)propane. NR: no reaction.

Given that the bipyridine-NiCl₂ gave the best result, we further tested other metals such as palladium, ruthenium. We found that tetrakis(triphenylphosphine)palladium(0) could not promote the reaction (Table 2.2, entry 1) when bipyridine was used as ligand, the reaction gave only 13% yield (Table 2.2, entry 2). Bipyridine-ruthenium chloride complex was also tested which turned out to be idle in the reaction (Table 2.2, entry 3). After confirmation of the uniqueness of Ni, we measured other nickel sources such as bis(cyclooctadiene)nickel(0) and nickel(II) trifluoromethanesulfonate. The reaction didn't proceed when Ni(0) was used maybe due to decomposition or polymerization of the allene (Table 2.2, entry 4). The Ni(OTf)₂ provided only 37% yield which was lower than NiCl₂ (Table 2.2, entry 5). We proposed that, the stronger acidity of counterion (TfO⁻) in contrast to Cl⁻ might result in more inclination of transmetalation, so we tried the reaction at room temperature. In fact, the reaction could not happen at lower temperature (Table 2.2, entry 6).

Table 2.2. Survey of effect of different metals and nickel resource.



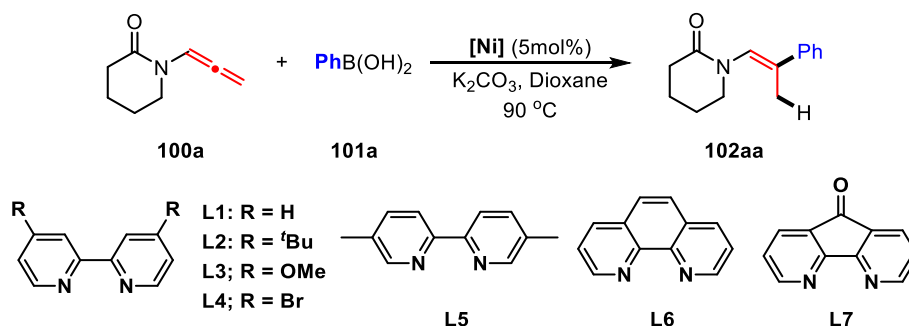
Run ^[a]	Cat.	T (°C)	Yield 102aa (%)
1	Pd(PPh ₃) ₄	90	NR
2	bpy-PdCl ₂	90	13%
3	bpy-RuCl ₂	90	NR
4	bpy-Ni(cod) ₂	90	NR
5	bpy-Ni(OTf) ₂	90	37%
6	bpy-Ni(OTf) ₂	20	NR
7	bpyNiCl ₂	90	71

^[a] All the reactions were carried out under nitrogen atmosphere with dry 1,4-dioxane. **100a**:**101a**:**cat.**:**base** = 1:1.5:0.05:3 (0.2 mmol scale of **100a**). ^[b] Isolated yields after flash chromatography. In all cases, **102aa** was isolated with *E*:*Z* ratio > 95:5 by ¹H-NMR. NR: no reaction.

Up to now, we have confirmed the crucial role of Ni(II) in the coupling reaction. Next, we needed to measure the parameter of the ligand in detail which always determined fatality of reaction. We selected several bipyridine type ligand as candidate due to its outstanding performance in the previous examination.

Firstly, we examined the ligand with substitutions at 4,4'- positions which were used widely in nickel chemistry. We found that if tert-butyl group was set at *para*-position, the activity of catalyst was reduced obviously (Table 2.3, entry 2), but when the electron donating group MeO- appeared at same position, the yield was elevated by 11% in contrast to bipyridine (Table 2.3, entry 3). Secondly, the ligand with electron-withdrawing group at *para*- position was also tested, which resulted in a significant drop of the yield (Table 2.3, entry 4). In addition to those ligand, we also tried the ligand with substitution at 5,5'-position (Table 2.3, entry 5) which cause no apparent change; 1,10-phenanthroline exhibit no catalytic activity (Table 2.3, entry 7); 4,5-diazafluoren-9-one also caused a significant drop of the yield (Table 2.3, entry 8). We proposed that, due to the angle of two pyridine in 4,5-diazafluoren-9-one was too small, the activity declined; in 1,10-phenanthroline case, the angle was zero, so the catalyst exhibited no significant activity in this reaction. In a sharp contrast, the activity of 4,4'-MeObpyridine was so high that even reaction time was shorten to 0.5 hr, the reaction completed. But, when the catalyst was prepared in situ, the activity was reduced significantly to give only 40% yield.

Table 2.3. Survey of bipyridine type ligand

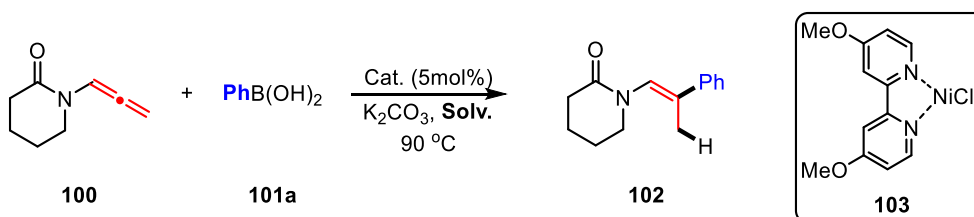


Entry ^[a]	[Ni]	t (h)	Yield (%)
1	L1NiCl ₂ •2H ₂ O	1	71
2	L2NiCl ₂ •2H ₂ O	8	60
3	L3NiCl ₂ •2H ₂ O	1	82
4	L4NiCl ₂ •2H ₂ O	1	56
5	L5NiCl ₂ •2H ₂ O	1	65
6	L6NiCl ₂ •2H ₂ O	1	< 10
7	L3NiCl ₂ •2H ₂ O	0.5	82
8	L7NiCl ₂ •2H ₂ O	0.5	22
9	L3/NiCl ₂ (in situ)	0.5	40%

^[a] All the reactions were carried out under nitrogen atmosphere with dry 1,4-dioxane. **100a:101a:[Ni]:K₂CO₃** = 1:1.5:0.05:3 (0.2 mmol scale of **100**). ^[b] Isolated yields after flash chromatography. In all cases, **101** was isolated with *E:Z* ratio > 95:5 by ¹H-NMR. NR: no reaction.

Next, we checked the influence of the solvent. The acetonitrile could almost kill the reaction (Table 2.4, entry 1); meanwhile the *N,N*-dimethylformamide stopped the reaction totally (Table 2.4, entry 2). Then we tested the ether solution and found that diethyl ether could give 36% yield (Table 2.4, entry 3) which was similar with tetrahydrofuran (Table 2.4, entry 4). To our astonishment, dimethoxyethane, a powerful solvent in Suzuki coupling, also prevented the reaction entirely (Table 2.4, entry 5).

Table 2.4. Survey of solvents



Entry ^[a]	Solvent	T (°C)/t (h)	Yield (%)
1	ACN	Reflux/3	< 10
2	DMF	Reflux/3	0
3	Et ₂ O	Reflux/3	36
4	THF	Reflux/3	34
5	DME	Reflux/3	0
6	1,4-dioxane	90/0.5	82

^[a] All the reactions were carried out under nitrogen atmosphere with dry 1,4-dioxane. **100a:101a:103:K₂CO₃** = 1:1.5:0.05:3 (0.2 mmol scale of **100a**). ^[b] Isolated yields after flash chromatography. In all cases, **102aa** was isolated with *E:Z* ratio > 95:5 by ¹H-NMR. NR: no reaction.

Afterwards, we measured other base to get higher yield. Firstly, we examined some common bases used in Suzuki coupling such as lithium carbonate (Table 2.5, entry 1), sodium carbonate (Table 2.5, entry 2) and cesium carbonate (Table 2.5, entry 4). In comparison to potassium carbonate, only sodium carbonate could provide relatively lower yield, while others didn't work in the reaction. Also, acetic base of weaker acidity was also tested, which show no promotion towards the reaction

(Table 2.5, entry 5 & 6). Potassium phosphate (Table 2.5, entry 7) and cesium fluoride (Table 2.5, entry 9) promoted the reaction to some extent but not so much as potassium carbonate. Compared with cesium fluoride, potassium fluoride didn't work in the reaction at all (Table 2.5, entry 8). Stronger base such as sodium tert-butyrate also gave trace product (Table 2.5, entry 10). So, the exploration of base showed no others could act even as efficient as potassium carbonate.

Table 2.5. Survey of bases.

Entry ^[a]	Base	Yield (%)
1	Li ₂ CO ₃	trace
2	Na ₂ CO ₃	52
3	K ₂ CO ₃	84
4	Cs ₂ CO ₃	trace
5	NaOAc	trace
6	KOAc	trace
7	K ₃ PO ₄	40
8	KF·2H ₂ O	trace
9	CsF	25
10	NaO ^t Bu	trace

^[a] All the reactions were carried out under nitrogen atmosphere with dry 1,4-dioxane. **100a**:**101a**:**103**:base = 1:1.5:0.05:3 (0.2 mmol scale of **100a**). ^[b] Isolated yields after flash chromatography. In all cases, **102aa** was isolated with *E*:*Z* ratio > 95:5 by ¹H-NMR. NR: no reaction.

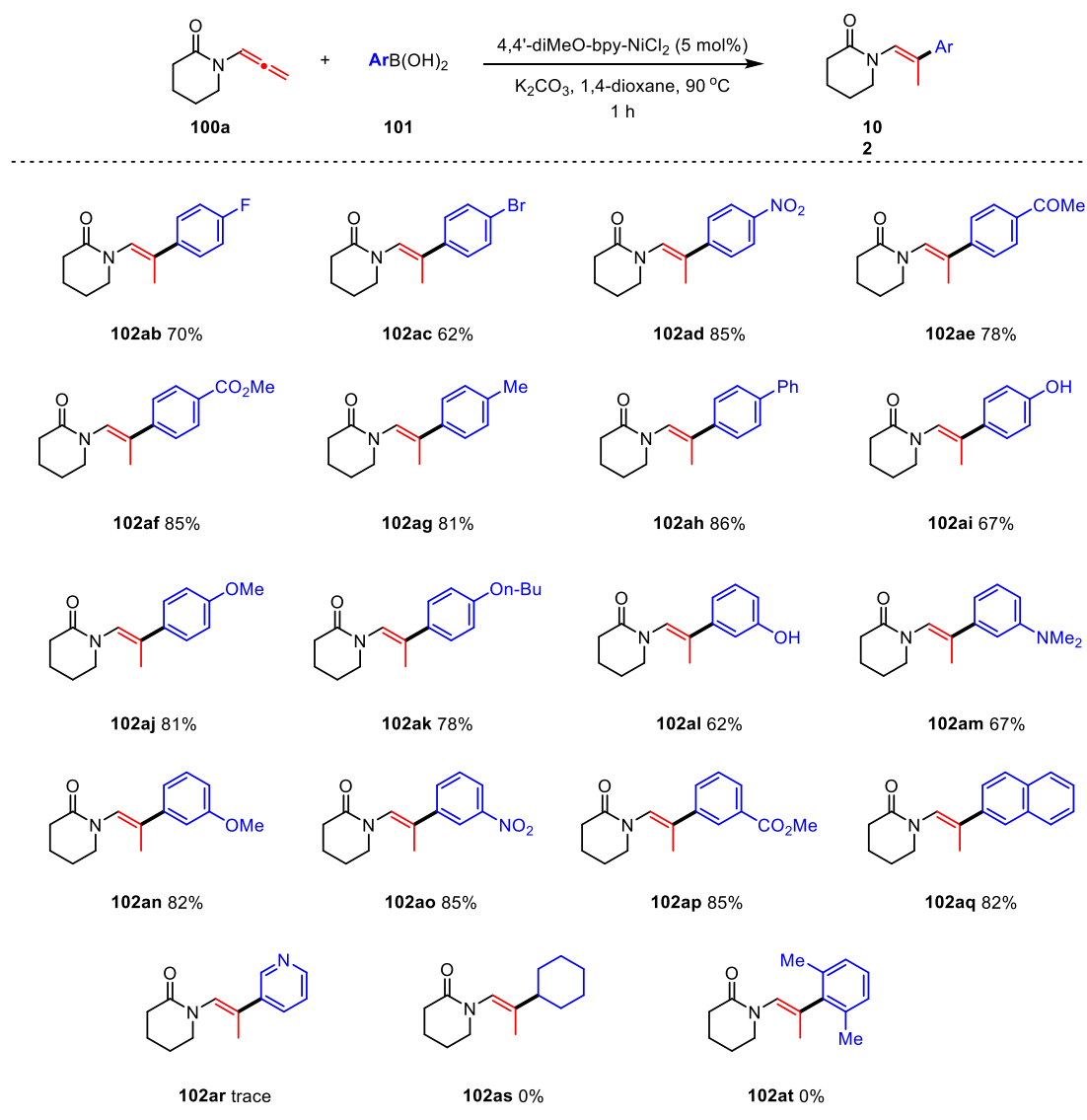
Up to now, according to all the parameter we had screened, the best condition of the reaction had been established: 1,4-dimethoxypyridine/nickel chloride (5 mol%) as catalyst, potassium carbonate (3.0 eq.) as base, 1,4-dioxane as solvent, conducted at 90 °C for 1 hour the reaction could afford product of *E*- configuration exclusively in 82% yield. So, the exploration entered next stage to extend the scope of the substrate to examine the utility of this methodology.

Encouraged by the result we had gotten, we examined the scope of the phenylboronic acid with 1-(propa-1,2-dien-1-yl)piperidin-2-one **100a** as substrate under standard condition (Scheme 2.10). Firstly, we tested the challenging phenylboronic acid with electron withdrawing substitution at *para*-position. The halogen with faint electron withdrawing property in *para*-position led to significant drop of the yield. To our surprise, rather than causing a decrease of the yield the stronger electron withdrawing group (-NO₂, -Ac, CO₂Me) gave slightly higher yield. The electron donating group (-Me, -Ph, -OH, -OMe, -On-Bu) at *para*- position showed no significant effect on the result. Only the 4-OH-phenylboronic acid gave a relatively lower yield probably due to the chelation of hydroxy group to the nickel.

So, we could draw a preliminary conclusion that the factor cause change of the richness of the phenyl would not influence the reaction significantly. Furthermore, we predicted that both electron-

withdrawing and electron-donating group at meta- position would not affect the result so much either. The outcome was consistent with our prediction. Both electron-rich (-OH, -NMe₂, -OMe) and electron-deficient (-NO₂, -CO₂Me) meta- substituted phenylboronic acid worked very well providing good yield up to 85%. In addition to the aforementioned phenylboronic acid, the naphthalen-2-ylboronic acid also offered good yield.

The phenylboronic acid with ortho- substitution such as 2,6-dimethylphenylboronic acid however, failed in the reaction, maybe because of the repulsion arising from the two methyl groups. Besides, when pyridin-3-ylboronic acid was used, the reaction produced only trace of product. We speculated the unsatisfying yield resulted from the chelation of nitrogen atom to nickel. The cyclohexylboronic acid failed in the reaction either, due to the failure of transmetalation between cyclohexyl group and nickel.

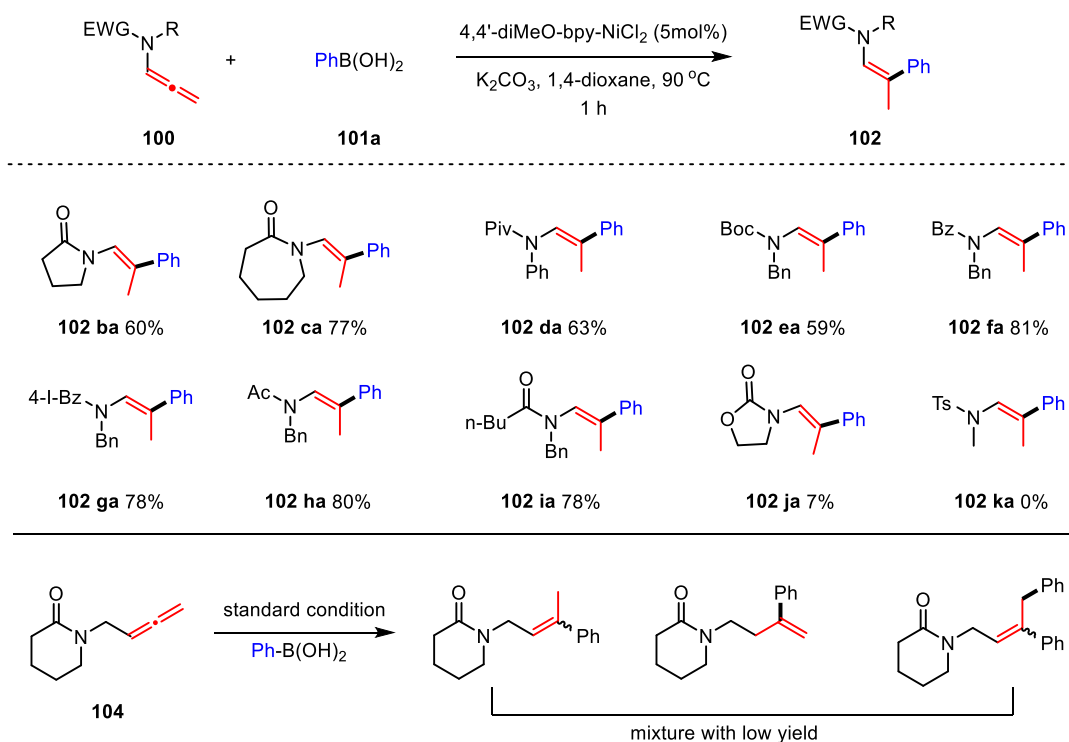


[a] All the reactions were carried out under nitrogen atmosphere with dry 1,4-dioxane, **100a**:**101**:**103**:K₂CO₃ = 1:1.5:0.05:3 (0.2 mmol scale of **100a**, 90 °C, 1 hr). [b] Isolated yields after flash chromatography. In all cases, **102** was isolated with *E:Z* ratio > 95:5 by ¹H-NMR.

Scheme 2.10 The scope of the boronic acid of coupling with allenamide.

Next, we explored the scope of the allenamide with phenylboronic acid as standard substrate

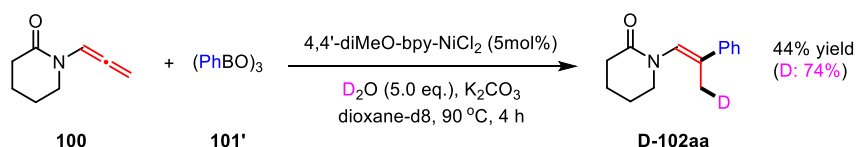
(Scheme 2.11). We examined the size of the lactam ring which turned out to be not significant factor. Both 5- and 7-member ring lactams provided moderate yield. Then we tested the substitution of the nitrogen atom. As we can see, all the carbonyl amide including pivaloyl, tert-butoxycarbonyl, benzoyl, acetyl and butyl amide worked normally providing moderate to good yield. It is noteworthy that the 4-iodobenzoyl amide also offered average yield which eliminated the possibility of formation of Ni(0) intermediate during the reaction process. In contrast to the good results mentioned above, the 3-(propa-1,2-dien-1-yl)oxazolidin-2-one gave product in only 7% yield due to its decomposition under standard condition. Either in sharp contrast, a widely used sulfonyl allenamide either did not react even the system was heated to reflux due to its strong stability. 1-(buta-2,3-dien-1-yl)piperidin-2-one was further used to extend the scope of allene. Under standard conditions, a mixture of mono- and di-substituted was produced in pretty low yield.



^[a] All the reactions were carried out under nitrogen atmosphere with dry 1,4-dioxane, **100**:**101a**:**[Ni]**:**K₂CO₃** = 1:1.5:0.05:3 (0.2 mmol scale of **100**), 90 °C, 1 hr. ^[b] Isolated yields after flash chromatography. In all cases, **102** was isolated with *E*:*Z* ratio > 95:5 by ¹H-NMR.

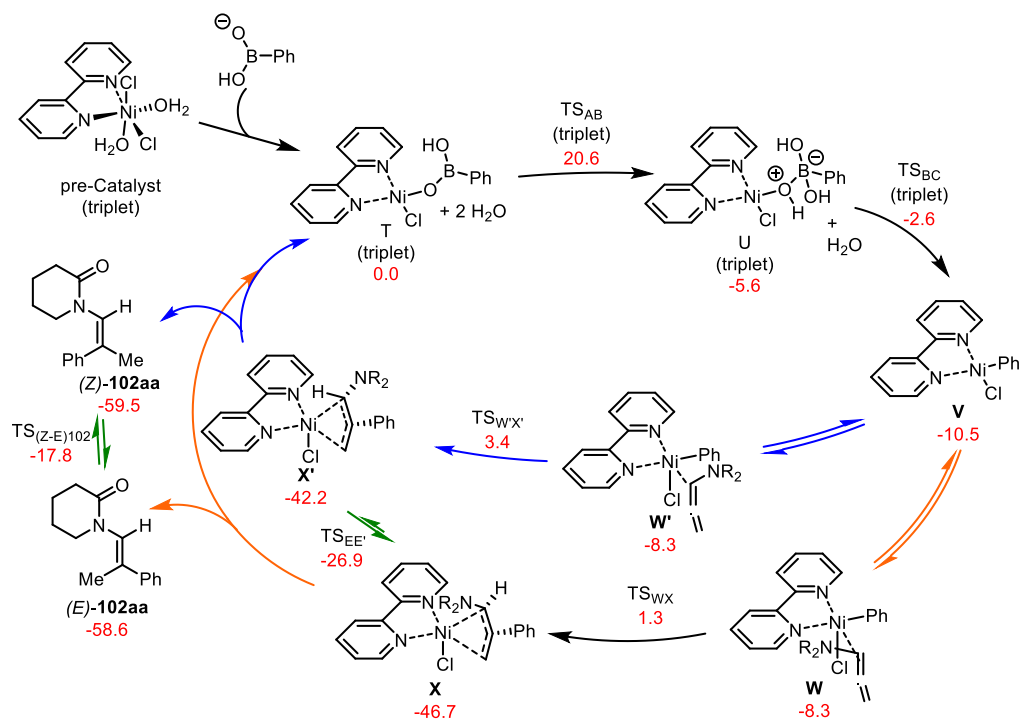
Scheme 2.11 The scope of allenamide in the coupling with phenylboronic acid.

Although the wide applicability of the reaction seemed to have been confirmed, there was another puzzle to be solved: the source of the proton which captured the proposed nucleophile—the allyl nickel complex **S**. A quick analysis of the reagents we used in the reaction indicated that the proton came from boronic acid. Therefore, we used a combination of 2,4,6-triphenyl-1,3,5,2,4,6-trioxatriborinane **101'** and 5 equivalents of D₂O to produce the deuterated boronic acid in situ. The reaction finished in 4 hours and furnished the γ -deuterated product in 44% yield with 74% deuteration. The α -deuterated product was not observed.



Scheme 2.12 Deuterium labeled reaction to determine the recourse of the proton.

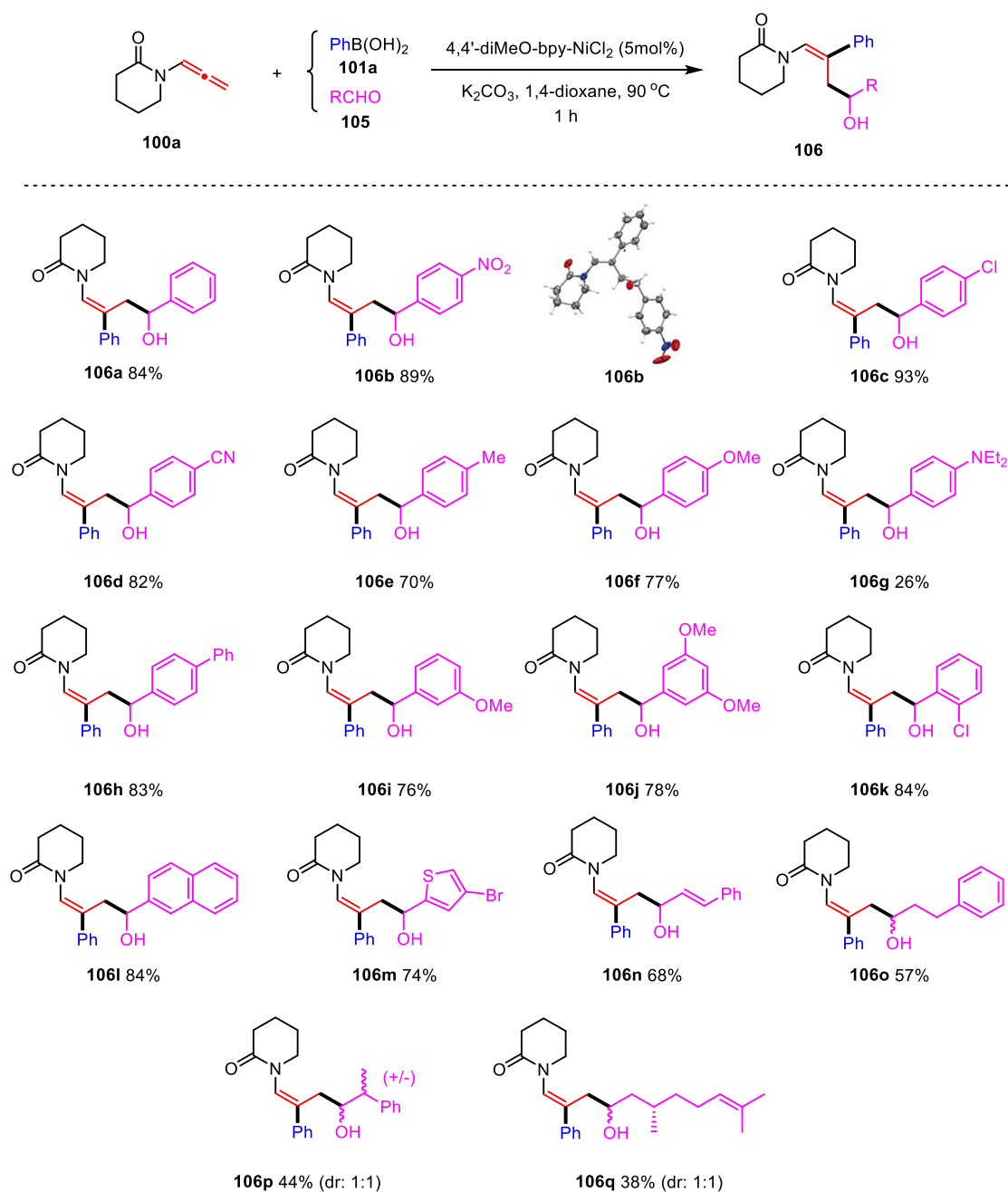
To get more insight into mechanism, we performed theoretical computation. In combination with computational investigation, the elementary pattern of mechanism dawns. The initial stage of the mechanism occurs on the triplet surface. First, the phenylboronic acid, deprotonated with the aid of potassium carbonate, displaces a chlorine ligand. Two water molecules of the complex would leave the metal coordination sphere and provided the square-planar structure **T**. Addition of one of aforementioned water units to a boron center and subsequent protonation of the oxygen binding to nickel furnishes Ni-attached phenylborate **U**. A four-center transmetallation then affords a phenyl nickel complex **V**, which is the first structure in the reaction pathway with a singlet ground state. The triplet to singlet surface switching process is symmetry forbidden and therefore the observed activation energy for this step is likely higher than 3 kcal/mol shown in the Scheme 2.13. This energy barrier is supposed to be too small compared to the previous step (20.6 kcal/mol) to affect the overall kinetics of the mechanism. The remaining steps of the mechanism, up to the formation of the final products, will proceed on the singlet spin state. Once transmetallation has taken place, the allenamide can occupy an empty coordination site of nickel. Two orientations of the nitrogen and its substituents in the allenamide are possible (one with N towards the phenyl group, **W'**, and the other with N towards the bipyridine system, **W**), both are accidentally degenerate (-8.3 kcal/mol). Given the low energy difference between the phenylnickel complex **V** and complexes **W** and **W'** (2.2 kcal/mol) we assume that the allenamide ligand is relatively labile. Under these conditions, the geometry determining step would be the formation of the C–C bond via allenamide insertion from **W** and **W'**. This step is slightly more favorable for **W**, with an insertion transition state energy of 2.1 kcal/mol lower in contrast to TS_{W'X}. Applying a Maxwell-Boltzmann distribution this energy difference should lead to a roughly 90:10 ratio of *E/Z* products under the thermal conditions used to run the reaction (90 °C). Interestingly, however, once the insertion product has formed (**X** and **X'**) an accessible transition state (15.3 kcal/mol from **X'**) allows the *Z-E* isomerization process, hence transforming the possible minor amounts of **X'** into the more stable **X**. The 4.5 kcal/mol difference in stability between these two complexes ensures that the isomerization runs essentially in the **X'** → **X** direction. Both effects combined are compatible with the complete stereoselectivity observed in the laboratory favoring the formation of enamide (*E*)-**102aa** upon allyl protonation of **X** and ligand detachment.



Scheme 2.13 The computational study on the mechanism.

Given that the proton acted as electrophile and captured the allylnickel intermediate, other proper electrophiles were supposed to be able to replace the proton. So, we examined other generally used electrophiles such as methyl acrylate, methyl phenyl ketone, allyl diethyl phosphate, benzaldehyde, select-fluoro and so on. At last, only benzaldehyde worked and gave γ -substituted product in 84% yield with excellent regio- and *E* stereoselectivity.

Encouraged by this exiting result, we further tested the utility of this protocol with more aldehydes (Scheme 2.14). Firstly, we examined para- substituted benzaldehyde with electron withdrawing group. Except for paracyano- group gave similar yield with benzaldehyde, both nitro- and chloro- group gave better yield. Afterwards, we also tested the effect of electron donating group on the para-



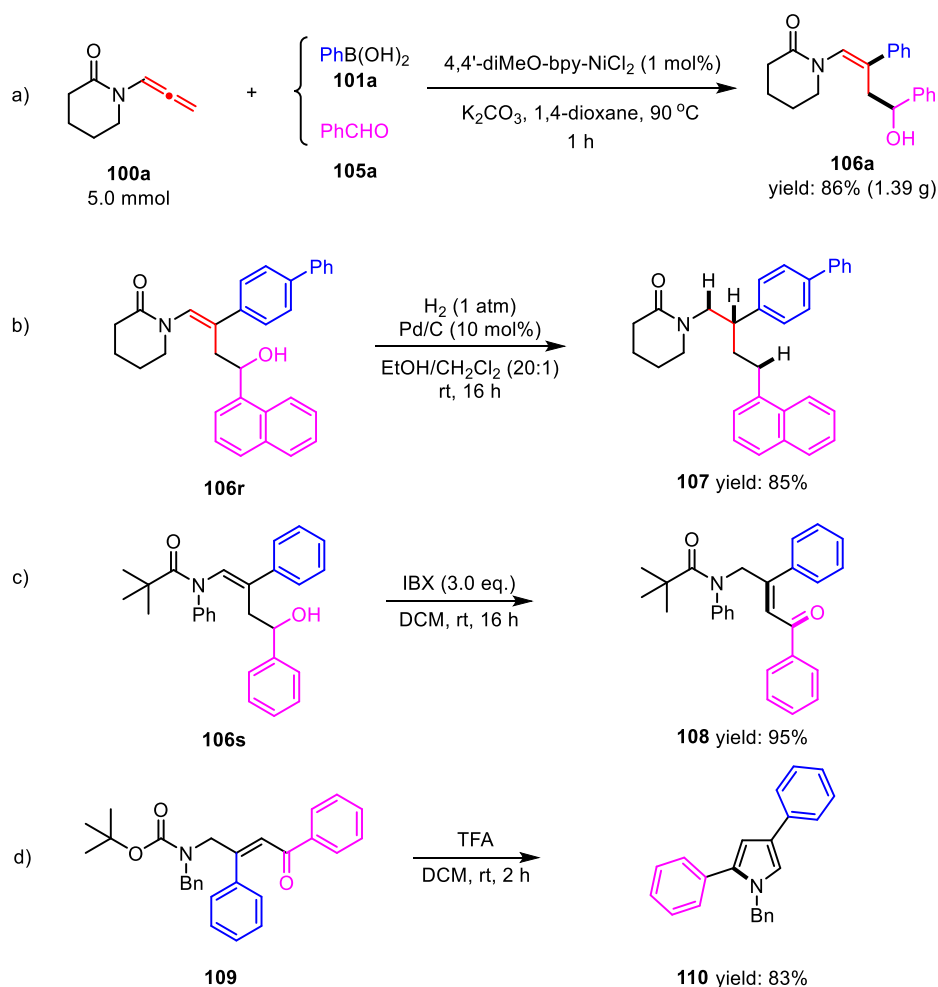
^[a] All the reactions were carried out under nitrogen atmosphere with dry 1,4-dioxane, **100a**:**101a**:**105**:**[Ni]**:K₂CO₃ = 1:1.5:2:0.05:3 (0.2 mmol scale of **100a**), 90 °C, 1 hr. ^[b] Isolated yields after flash chromatography. In all cases, **106** was isolated with *E*:*Z* ratio > 95:5 by ¹H-NMR.

Scheme 2.14 The scope of the aldehyde in the tricomponent reaction

position to the carbonyl group. The *N,N*-dimethylamino group cause a sharp drop of the yield to 26%. Meanwhile the methyl group, phenyl group and methoxy group did not show too much difference in contrast to hydrogen, providing good yield. From these results, a positive correlation seemed to exist between the reactivity of the aldehyde and the electron abundance of the benzyl carbon. Next, we examined the meta- mono-substituted and di-substituted benzaldehyde which provided good yield. As we anticipated before, the benzaldehyde with chloro- group at ortho-position provided product in 84% yield in spite of the repulsion exerted by chloro- group. 2-Naphthaldehyde and 4-bromothiophene-2-carbaldehyde also worked and gave good yield. To our surprise, the aliphatic aldehyde such as cinnamaldehyde and 3-phenylpropanal also provided the

product in moderate yield. When chiral center appeared in the aldehyde, the reaction would provide the product in medium yield with diastereomers ratio to be 1:1.

Afterwards, a gram-scale reaction was carried out to further test the applicability of the methodology. Even though the loading of catalyst was reduced to be 1 mol%, the reaction provided slightly higher yield than the standard reaction (Scheme 2.15a). Then we did the hydrogenation of the product **106r** under the simplest condition and found that not only the carbon-carbon double bond was reduced, but also the hydroxy group deriving from aldehyde was also removed (Scheme 2.15b). The reaction produced a multi-substituted amide in 85% yield. The hydroxy group is always a totipotent functional group in transformation. When we used IBX (2-Iodoxybenzoic acid) to oxidize the hydroxy group of **106s**, an α,β -unsaturated ketone **108** was produced in pretty high yield (95%) with the migration of carbon-carbon double bond (Scheme 2.15c). We found this product was a potential substrate to synthesize pyrrole, so we prepared **109** so that the Boc- group could be easily removed. As designed, when exposed to trifluoroacetic acid (TFA), it got rid of Boc- group, subsequently, the *in situ* produced amine reacted with the ketone and offered an annulated 1,2,4-trisubstituted pyrrole **110** in 83% yield (Scheme 2.15d).

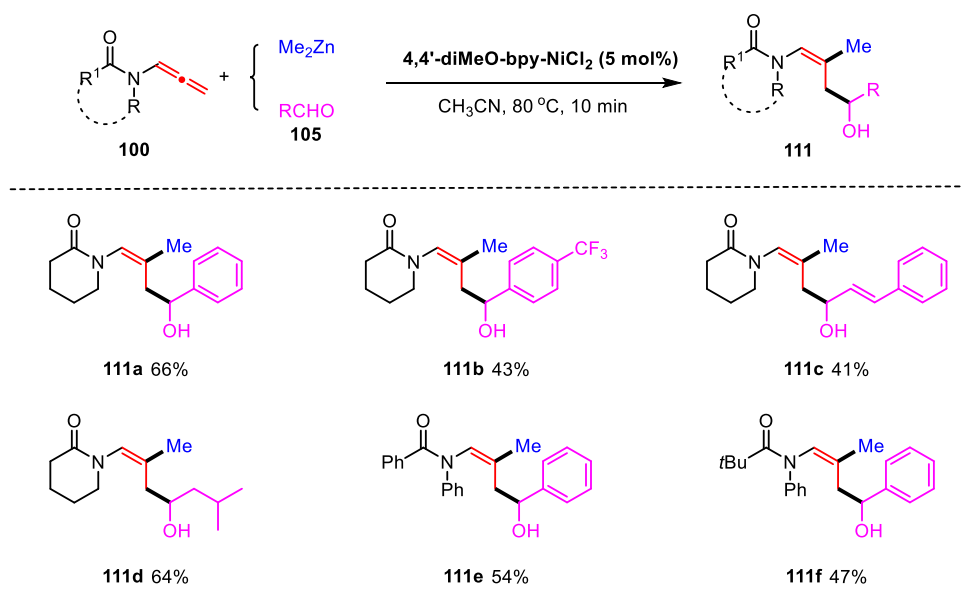


Scheme 2.15 The application of the tricomponent coupling product.

To develop methodology of wide substrate scope is always a target of chemist. Since we had successfully affected coupling of sp^2 hybrid carbon (phenyl boronic acid) with sp^2 hybrid carbon

(allenamide), we wondered if this methodology could be adapted in more challenging sp^3 - sp^2 coupling. After a series of investigation of nucleophile including dimethylzinc, diethylzinc, methylmagnesium bromide and so on in tricomponent reaction protocol, we found that only dimethylzinc could give coupling product **111** moderate yield while others caused decomposition of the allenamide providing very low or even 0% yield. Due to high reactivity of organozinc, the reaction completed in 10 min at 80 °C with acetonitrile as solvent. This reaction can't give the corresponding two component product without aldehyde as third reactant. We did not spend too much attention on the scope of the substrate because we only wanted to demonstrate practicability of this methodology.

With 1-(propa-1,2-dien-1-yl)piperidin-2-one **100** as substrate, both aryl, aliphatic and α,β -unsaturated aldehyde could provide amido-alcohols with high regioselectivity in moderate yield (Scheme 2.16). In addition to cyclic allenamide, benzamido and pivalamido allene also worked in similar efficiency.



Scheme 2.16 The three-component coupling with dimethylzinc as nucleophile.

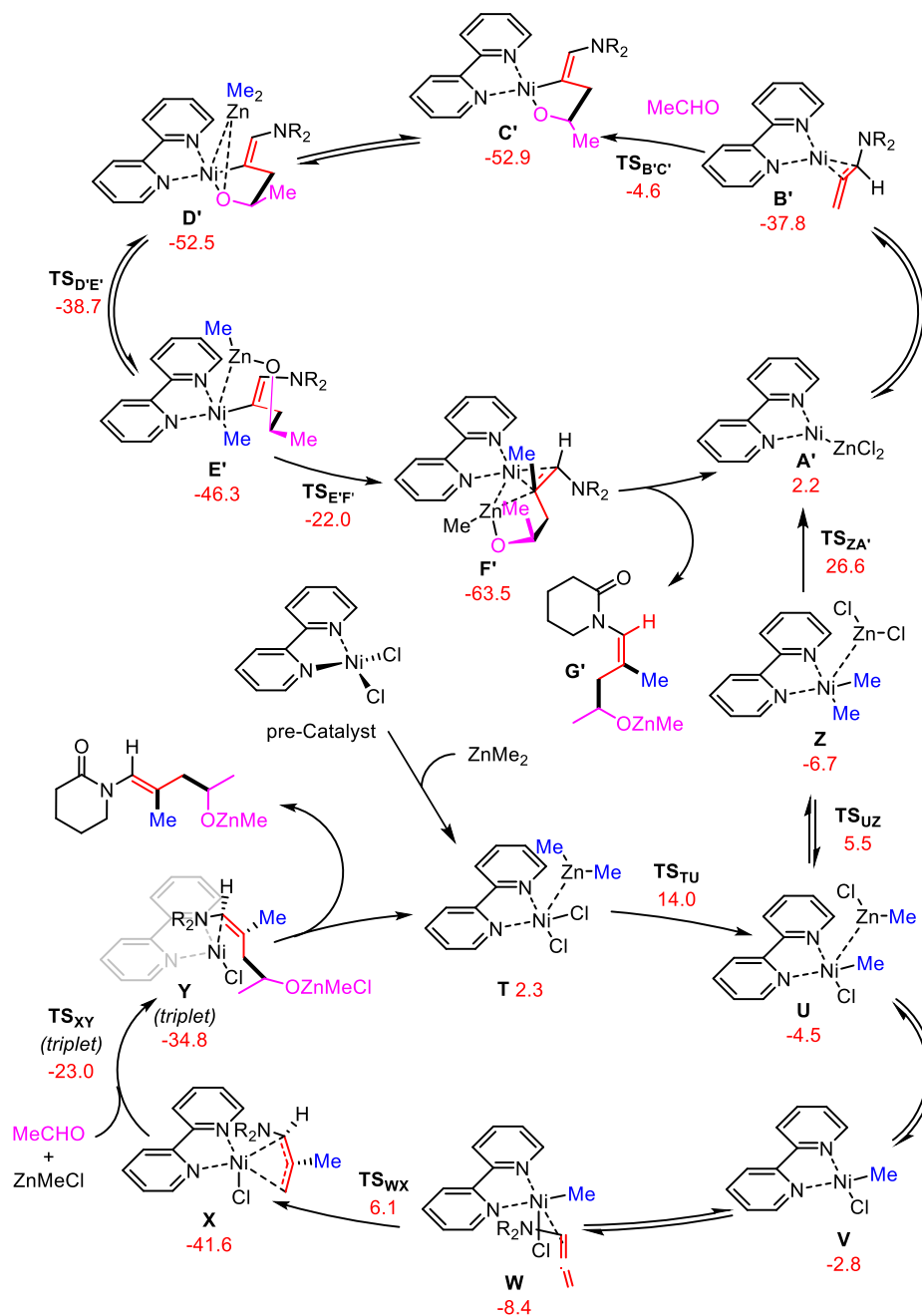
According to the reaction condition (the lower temperature & shorter reacting time), organozinc reagent was supposed to be more reactive than boronic acid. An analogous mechanism to the boronic acid reaction was computed (Scheme 2.17). The reduced energy requirement for this mechanism in contrast to the boronic acid (14.0 vs. 20.6 kcal mol⁻¹) was in line with reaction phenomenon. However, differences in terms of the spin state of the systems were found in the reaction cycle. In ZnMe₂ coupling process, in the steps before the electrophilic attack by aldehyde (TS_{XY}, occurred in triplet spin state), the nickel was always in singlet spin state which might due to the reduced Lewis acid abilities of zinc versus borane reagents. The less nucleophilicity of aldehyde activated by dimethylzinc would need radical character to realize C-C bond formation. However, according to the energy barrier (18.6 kcal·mol⁻¹), this is not the determining step; alternatively, spin-orbit couplings could play the key role in the kinetics in the catalytic cycle.

One distinct difference between zinc and borane reagents was observed during the reaction: the system turned dark in few seconds after addition of ZnMe₂ (by contrast, there was no obvious color

change in the borane chemistry) which means that the reaction went through a redox process. Hence, we endeavored to explore a new explanation of this chemistry.

The theoretical computation of new mechanism was based on assumption that ZnMe_2 played two roles during the reaction: a) reducing the $[\text{Ni(II)}]$ pre-catalyst to a $[\text{Ni(0)}]$ compound; b) acting as methyl group provider in the coupling. This redox mechanism is described in Scheme 2.17 (top) and divided with the aforementioned cycle by the simple ligand exchange and reductive elimination steps ($\text{U} \rightarrow \text{A}'$).

It seems that the $[\text{Ni(0)}]$ possesses strong ability to activate the C-C double bond of allenamide with extrusion of an ZnCl_2 ($-40 \text{ kcal mol}^{-1}$), the resulting reactive complex of which could be attacked by aldehyde easily providing an five-member ring intermediate C' . Then, another unit of ZnMe_2 tends to liberate the Ni-O bond followed by metathesis between nickel and zinc. There is a substantial inclination for the exchange of oxygen and methyl ion ($-38.7 \text{ kcal}\cdot\text{mol}^{-1}$). After the interchange furnishes six-member intermediate E' , the reductive elimination seems to be inevitable to provide the final product through: 1) the role of allenamide and nickel switches from σ - donor to π -donor; 2) one methyl group migrates from Ni to center carbon of allene moiety; 3) the Zn-Ni interaction switches from perpendicular to parallel to plane; 4) Zn establishes a new weak connection with the C-C π -bond. Finally, the $[\text{Ni(0)}]$ complex would be released by the product and restart a new cycle.



Scheme 2.17 Computed reaction mechanisms for the ZnMe₂-mediated organonickel insertion onto N-allenyl amides. Non redox cycle (bottom) and Ni(0)/Ni(II) redox cycle (top) linked via a reductive elimination step highlighted in green. Gibbs free energies are given in kcal mol⁻¹ and are computed relative to the pre-catalyst + ZnMe₂.

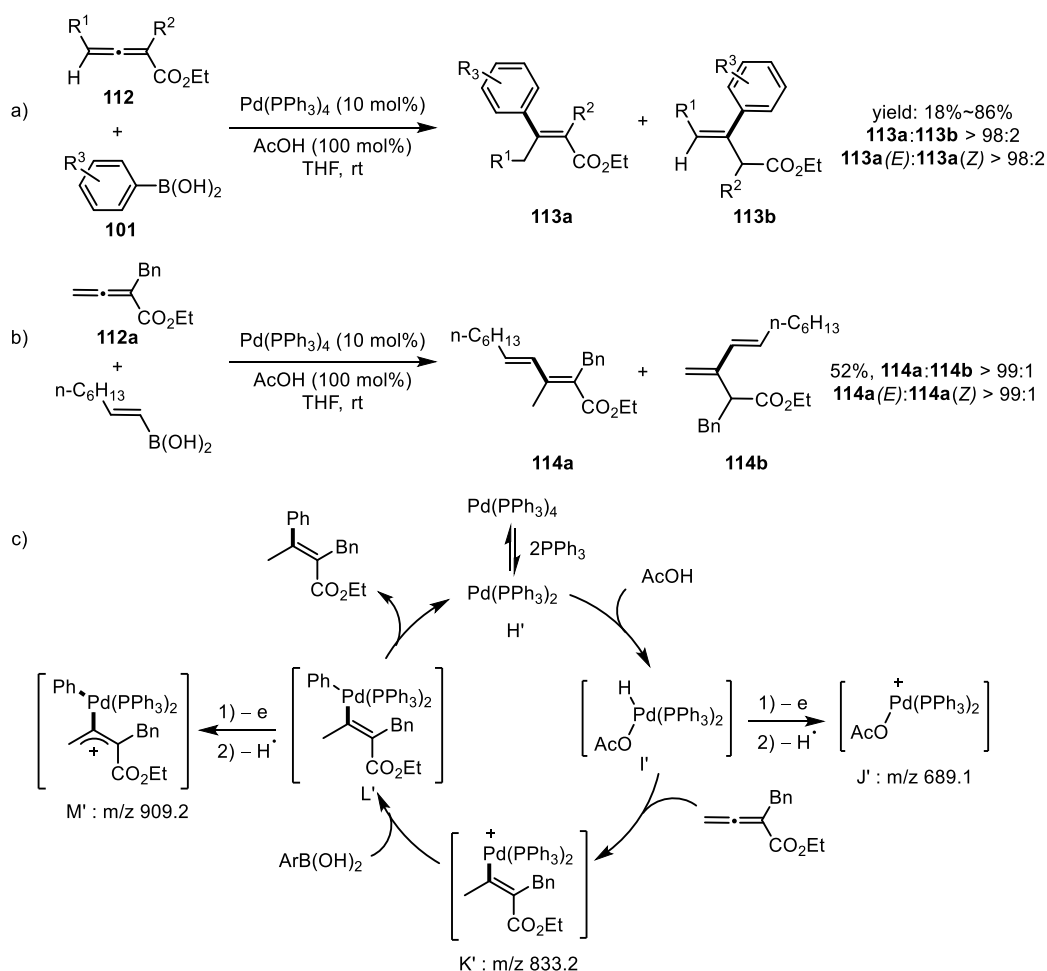
2.3 Precious work of metal catalyzed coupling of allenolate

The α,β -addition of allenolates is one of the most convenient methods to prepare the β,γ -unsaturated ester which is not easily reached using other methods.

In 2003, Ma group first reported an intermolecular palladium(0) catalyzed coupling of allenolate **112** with aryl boronic acid (Scheme 2.18a).^{9a} In the presence of 100 mol% or 20 mol% of acetic acid, the reaction could provide thermodynamically stable conjugated product in irregular yields. This methodology offered good regio- and stereoselectivity: almost no unconjugated and Z- product was

observed. In addition to aryl boronic acid, the vinyl boronic acid could also work with allenamide in moderate yield. (Scheme 2.18b)

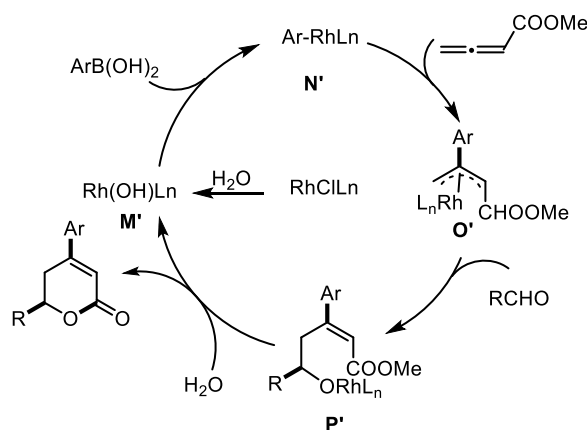
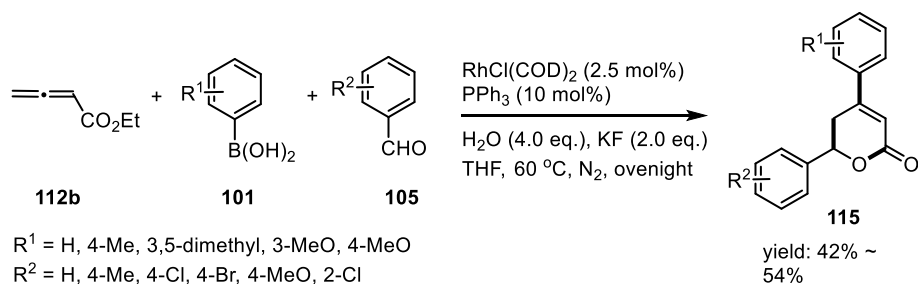
Using the ESI-FTMS technology, they also presented a proposed mechanism (Scheme 2.18c).^{9b} The reaction started with extrusion of two molecule PPh₃ providing an Pd(PPh₃)₂ species **H'**. In five minutes of reaction, the oxidative addition of Pd(PPh₃)₂ to AcOH would happen and afford [Pd(II)](**I'**) which could be detected in the form **J'** after loss of one electron and an hydrogen radical. As the reaction proceed constantly, the major cationic intermediates in the reaction system changed dramatically. The β,γ - addition product **K'** of Pd-H to allenamide was detected. Then the aryl group of boronic acid would transfer to palladium providing intermediate **L**. The existence of **L** was confirmed by the appearance of signal of cation **M** which came from the extrusion of an electron and a hydrogen radical during the ESI process. At last, after the reductive elimination, the **L'** produced final product and actual catalyst.



Scheme 2.18 Palladium catalyzed coupling of allenamide with boronic acid and the exploration of the mechanism with ESI-FTMS technology.

When these two compounds were exposed to rhodium(I)/triphenylphosphine, the resulting π -allyl rhodium intermediate could be further captured by the aldehyde (Scheme 2.19).¹⁰ Since the resulting intermediate was an δ -hydroxy ester, it could lactonize automatically providing an α,β -unsaturated lactone **115** in moderate yield. In this reaction, KF was turned out to be very unique base whereas other fluoride salt such as NaF, CsF and so on gave very poor performance. Water was

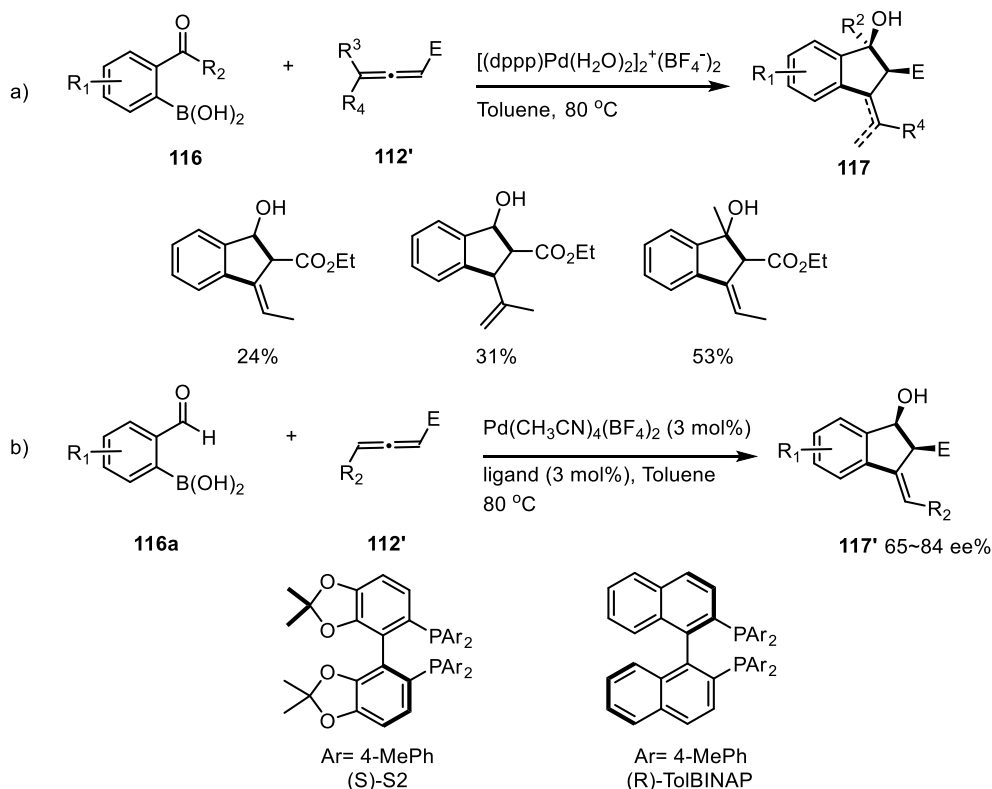
also vital in this reaction without which the reaction could not take place. A plausible mechanism was also given, in the presence of water, a hydroxy group could replace the chloride and provide a rhodium complex **M**. Then an aryl group could transfer from boronic acid to [Rh] to provide intermediate **N'**. Then carborhodination of allenyl moiety would provide an allyl rhodium intermediate **O'** which could be presently captured by aryl aldehyde affording an homoallylic alkoxyrhodium intermediate **P'**. Subsequently, the δ -hydroxy group attacked the ester group with a substitution by H₂O to give the final product.



Scheme 2.19 Rhodium catalyzed three-component coupling of allenamide with boronic acid

Intramolecular capture of allyl-metal intermediate with aldehyde could be realized when palladium was used (Scheme 2.20).¹¹ At presence of $[(\text{dppp})\text{Pd}(\text{H}_2\text{O})_2]^{2+}(\text{BF}_4^-)_2$ and 2-formylarylboronic acids **116**, the reaction proceeded smoothly and completed in 15 mins, providing a diastereo- and enantioselective [3+2] product **117** & **117'** in high yield. Both cationic property of palladium species and bisphosphine type ligands were vital to this methodology; meanwhile, in contrast to BF_4^- , the counterion TfO^- would promote the formation of conjugated product. It was presumed that the *in situ* generated HOTf and HBF_4 influenced the formation of C-C double bond whereas the additional TfOH could not turn unconjugated product to conjugated one.

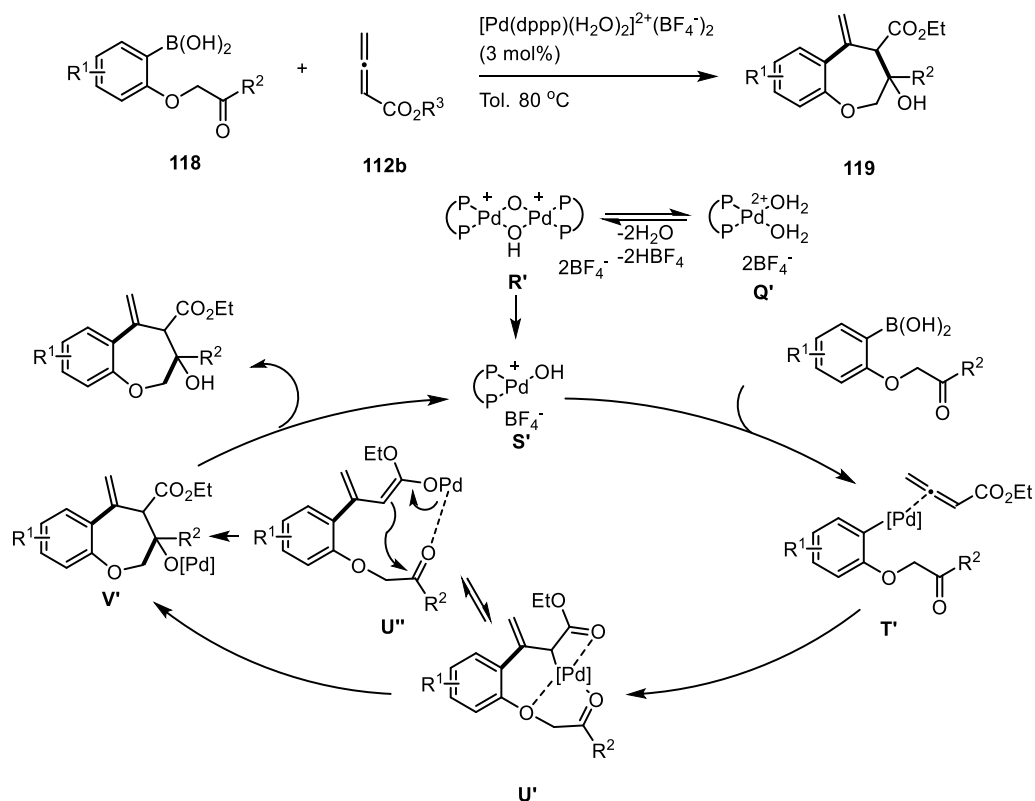
This reaction showed wide tolerance to 2-formylarylboronic acids and unsubstituted allenolate giving good yield, however when substitutions were introduced to γ - or α -position the yield was reduced dramatically or inhibited the reaction. The 2-acetylphenylboronic acid also worked affording low yield. The enantioselective version was explored where two ligands surfaced: (*S*)-*S*2 and (*R*)-TolBINAP. However, these two ligands could only work on unsubstituted allenolate providing moderate enantioselectivity. The introduction of methyl group at γ -position would disable the catalysis.



Scheme 2.20 Palladium catalyzed enantioselective cascade [3+2] cyclization.

Afterwards, the scope was extended to be 2-acylmethoxyarylboronic acids to perform [5+2] annulation, wherein 1-benzoxepine derivatives were synthesized conveniently (Scheme 2.21).¹² The asymmetric version was also explored with bis-phosphine type ligand such as (2*S*,4*S*)-bis-(diphenylphosphinyl)pentane, however enantioselectivity was poor. The substrate of allenoate was restricted to unsubstituted ones; the alkoxy group of arylboronic acid was limited to 2-oxopropoxyl group, other substitution such as 2-oxo-2-phenylethoxyl group caused a drop of yield; meanwhile other substitutions such as alkyl made the boronic acid inert in the reaction.

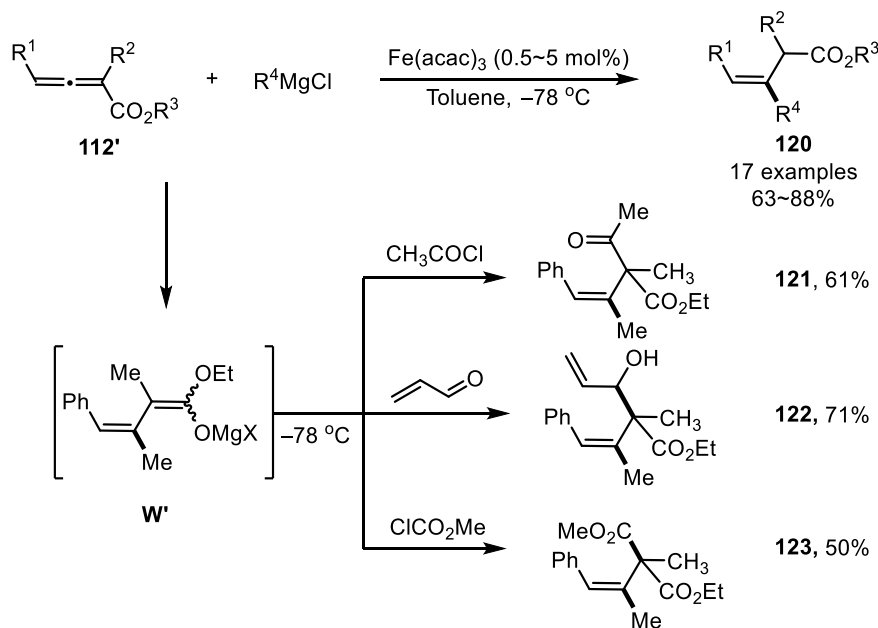
The mechanism was also proposed, the active catalyst **S'** was generated *in situ*, which facilitated the transmetalation. Then allene moiety would be activated and inserted by the palladium providing the η^1 -palladium intermediate **U'**. The oxygen-palladium linkage was supposed to be crucial in the reaction which could explain the failure of non-alkoxy substrates in the reaction. Meanwhile, the cationic palladium could also activate the carbonyl group and lead to the addition of η^1 -palladium to it providing the intermediate **V'**. The more stable η^3 -palladium addition product was not found due to the orthogonal orbitals of allene caused the difficulty to form η^3 -palladium intermediate. The protonation of **V'** afforded the final product and species **S'** to restart a new reaction cycle.



Scheme 2.21 Palladium catalyzed [2+5] cyclization by Lu.

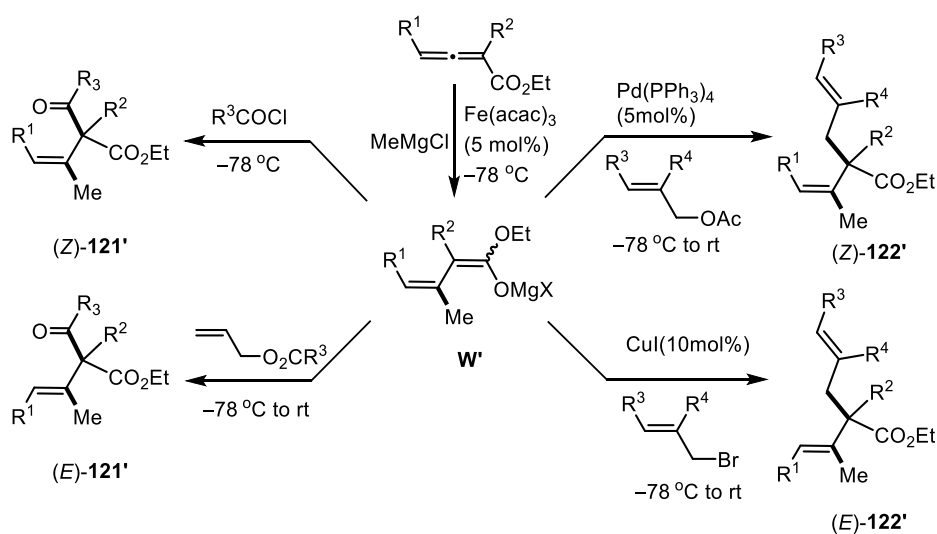
In addition to boronic acid, lithium dialkylcuprate or dialkenylcuprate also can couple or add to the simple allenoate or functional allenoate with good regio- and stereoselectivity. However, this addition always needs stoichiometric cuprate.¹³

In 2007, Ma reported iron catalyzed α,β -conjugated addition of Grignard reagent addition to allenoate with good regio- and stereoselectivity (Scheme 2.22).^{14a} The $\text{Fe}(\text{acac})_2$ showed substantial efficiency in this reaction, even the loading of catalyst was reduced to 0.5 mol% in the standard reaction, it could also provide good yield (73%). This methodology gave moderate to good yield with different Grignard reagents (including primary, secondary alkyl, phenyl and vinyl magnesium salt) and substituted allenoates. The active reagent was supposed to be iron-magnesium complex $[(\text{R}^4)_m\text{Fe}(\text{MgX})_n]$ which could add to the allenoate providing a 1,3-dienolate species, which could be quenched by proton. This could be testified to substantial extent by the formation of **121**, **122**, **123** which resulted from capture by acetic chloride, acrylaldehyde and methyl carbonochloridate. The excellent stereoselectivity (R^1 trans to R^4) was proposed to arise from the steric hindrance between the group at γ -carbon and the active reagent.



Scheme 2.22 Iron catalyzed coupling of Grignard reagent and allenolate.

Later on, the cascade α -allylation and acylation was systematically studied by them (Scheme 2.23).^{14b} As aforementioned, when the proposed intermediate **W'** was exposed to carbonyl chloride, it would take place α -carbonylation providing an (*Z*)-**121'** compound with high stereoselectivity. Interestingly, when they wanted to do α -allylation using allylic ester, an α -carbonylation product (*E*)-**121'** was produced exclusively. Same discrepancy on the stereoselectivity also exists during α -allylation. When the intermediate **W'** was dealt with Pd(PPh₃)₄ at presence of allylic ester, the reaction provided target product without deviation on configuration of the carbon-carbon double bond. In a sharp contrast, when CuI was used as catalyst and allylic bromide as allyl group provider, they afforded (*E*)-**122'** allylation product.

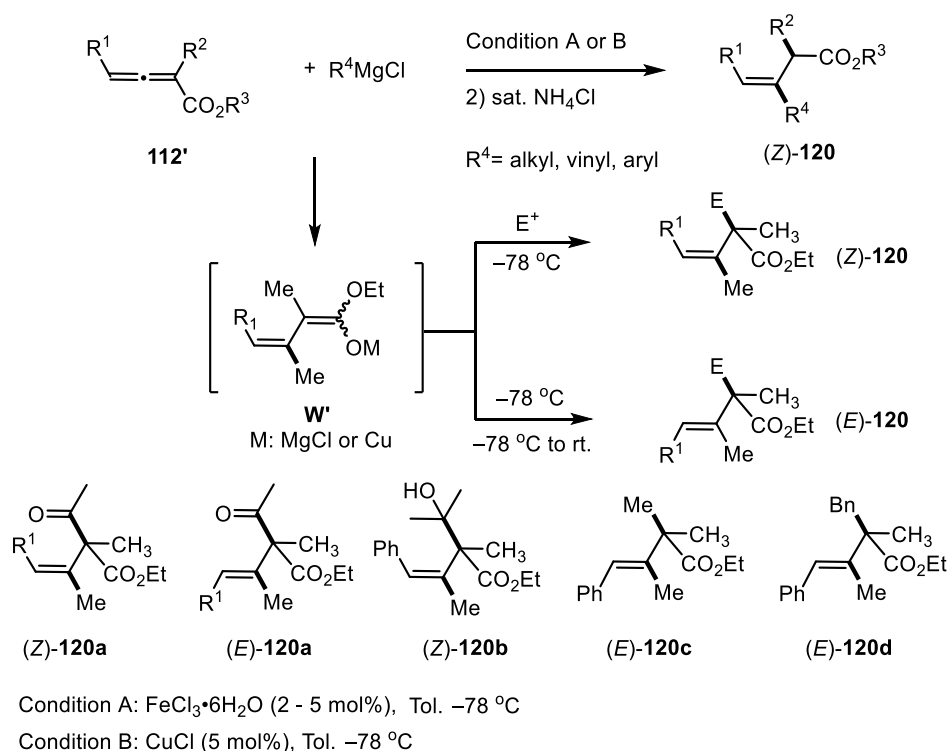


Scheme 2.23. Study of electrophilic capture of coupling of Grignard reagent and allenolate

According to authors, when allylic ester or bromide were used, the double bond and carbonyl

oxygen might coordinate to the metal (Mg^{2+} or Cu^+) which increased the repulsion between the metal and the substituted group on γ -carbon (R^1) arising the conversion of 1,3-(*Z*)-dienoate to 1,3-(*E*)-dienoate. Naturally, after carbonylation and allylation, they furnished *E* product. On the other hand, when the intermediate **W'** reacted with carbonyl chloride or allylic ester/ $\text{Pd}(\text{PPh}_3)_4$, the carbonylation and allylation happened too fast to allow the occurrence of the conversion at -78°C . This speculation was further confirmed by the phenomenon of providing a mixture of *Z*- and *E*-product when the latter stage was performed at room temperature.

Their later work proved the inorganic salt both $\text{FeCl}_3\cdot 6\text{H}_2\text{O}$ and CuCl were more efficient catalyst in this reaction profile (Scheme 2.24).^{14c-d} Especially, they tolerated wider scope of the Grignard reagent including primary, secondary, tertiary alkyl and phenyl, vinyl magnesium salt. In addition to that, when CuCl was used as catalyst, tri-substituted allenoate (methyl 4-methyl-2-phenylpenta-2,3-dienoate) could also give product in satisfying yield. Without exception, the conjugated addition intermediate could be further captured by other electrophile besides proton such as: acetyl chloride (condition A, (*Z*)-**120a**), allylic ester (condition A&B, (*E*)-**120a**), acetone (condition B, (*Z*)-**120b**), methyl *p*-toluenesulfonate (condition B, (*E*)-**120c**), benzyl bromide (condition B, (*E*)-**120d**) providing moderate yield.



Scheme 2.24 The application of $\text{FeCl}_3\cdot 6\text{H}_2\text{O}$ and CuCl in the coupling of Grignard reagent and allenoate.

2.4 Ni(II) Catalyzed Coupling of Allenoate with Boronic acids

Taking into consideration of the convenience of storage and stability of boronic acid and the advantage of safety, Suzuki coupling of boronic acid with allenoate is still attractive and meaningful, although the coupling of Grignard reagent with allenoate has been developed very well. Up to now, the reported catalyst used in Suzuki coupling of boronic acid with allenoate are rhodium and

palladium. Thus, to develop a non-noble and non-toxic metal catalyst is still valuable. Encouraged by the success of nickel catalyzed Suzuki coupling of allenamides, we applied the protocol to the coupling of allenates. To our surprise, the best conditions for the allenamide provided unconjugated Z-product with very good stereoselectivity in 65% yield (Table 2.6, entry 4). Then we detailedly examined the effect of different bipyridine type ligand under combination with nickel salt. Without any substitution on the bipyridine, the reaction gave 52% yield with slightly better stereoselectivity (Entry 1) which means that the electron donating group at 4,4'- position could promote the reaction. This was proven by catalyst of the 4,4'-di-tertbutylbipyridine with which the reaction afforded 82% yield (Table 2.6, entry 2). However, to our delight, when 4,4'-dibromobipyridine was used, the reaction gave 95% yield (Table 2.6, entry 3). When the bromine was replaced by methoxycarbonyl group, it worked even better than the one with electron donating group such as ^tBu- and MeO- (Table 2.6, entry 5). The efficiency of 5,5'-dimethylpyridine was similar with the dimethoxy one (Table 2.6, entry 6). In contrast to methoxycarbonyl group at 4,4'-position, when the carbonyl group connecting 3,3'-position was present, the reaction was inhibited (Table 2.6, entry 7). The complex of 1,10-phenanthroline/NiCl₂ also worked, but gave moderate yield (Table 2.6, entry 8).

Table 2.6 Survey of effect of the bipyridyl type ligand.

	Cat.1: R ¹ = R ² = H Cat.2: R ¹ = H, R ² = ^t Bu Cat.3: R ¹ = H, R ² = Br Cat.4: R ¹ = H, R ² = OMe Cat.5: R ¹ = H, R ² = CO ₂ Me Cat.6: R ¹ = Me, R ² = H		
--	--	--	--

Entry ^[a]	[Ni]	Yield (%)	E/Z
1	Cat.1	52	13:1
2	Cat.2	82	10:1
3	Cat.3	95	11:1
4	Cat.4	65	9:1
5	Cat.5	90	7:1
6	Cat.6	82	13:1
7	Cat.7	Traces	-
8	Cat.8	73	11:1

^[a] All the reactions were carried out under nitrogen atmosphere with dry 1,4-dioxane, **124a**:**101a**:**[Ni]**:K₂CO₃ = 1:1.5:0.05:3 (0.2 mmol scale of **121a**), 90 °C, 5 hr. ^[b] Isolated yields after flash chromatography.

To get better result, other dimensions such as different metals, temperature and bases need to be tried. The complex of triphenylphosphine/NiCl₂ was tested which gave isomerized product of allenate B at 90 °C (Table 2.7, entry 1). The widely used nitrene/NiCl₂ did not work in the reaction (Table 2.7, entry 2). Copper has been proven to be an efficient metal in boronic acid participated coupling the most famous work of which is Chan-Lam coupling. So bpy/Cu(II) was used in the

reaction which provided moderate yield. Tetrakis(triphenylphosphine)palladium which was used by Ma⁹ was also tested by us which turned out that the acetic acid was necessary (in their work) without which the reaction only gave conjugated product in 34% yield (Table 2.7, entry 4).

Next, we measured the influence of the temperature and base. Higher or lower temperature were proved to be detrimental to the reaction causing a little drop of the yield. (Table 2.7, entry 5&6). The effect of the base was similar with the case with allenamide: Na₂CO₃ caused slight fall of the yield (Table 2.7, entry 7), meanwhile the cesium carbonate did not work in the reaction (Table 2.7, entry 8).

Table 2.7. The effect of metal species, temperature and bases.

L1

L2

112a'

126

Entry ^[a]	Cat.	Base	T (°C)	Yield (%)	E/Z
1	[Ni(PPh ₃) ₂ Cl ₂]	K ₂ CO ₃	90	50 (126)	-
2	L2/NiCl ₂	K ₂ CO ₃	90	trace	-
3	L1/CuCl ₂	K ₂ CO ₃	90	53	11:1
4	[Pd(PPh ₃) ₄]	-	rt	34 (112a')	11:1
5	Cat.3	K ₂ CO ₃	60	trace	-
6	Cat.3	K ₂ CO ₃	110	82	5:1
7	Cat.3	Na ₂ CO ₃	90	85	10:1
8	Cat.3	Cs ₂ CO ₃	90	trace	-

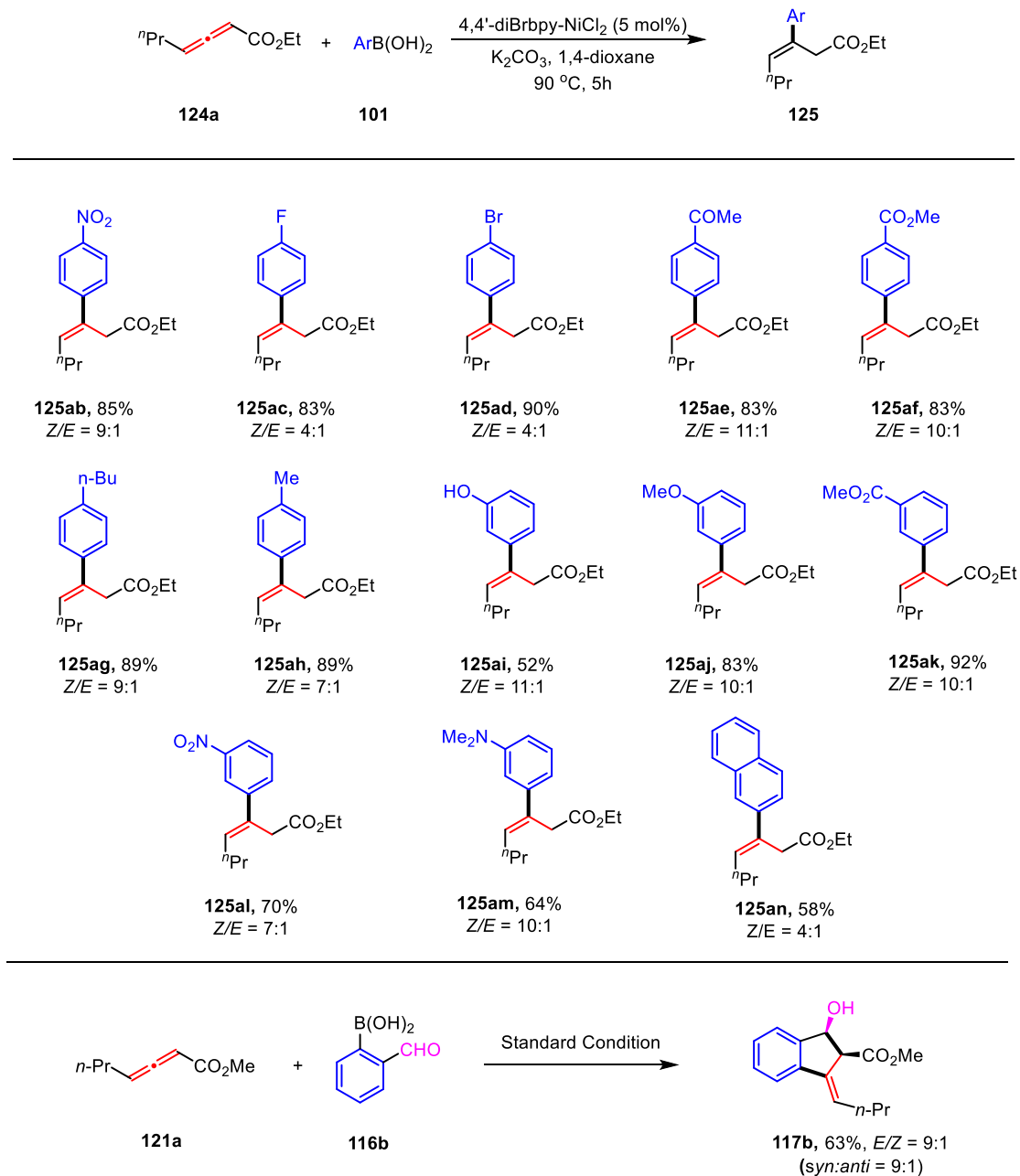
^[a] All the reactions were carried out under nitrogen atmosphere with dry 1,4-dioxane, **124a**:**101a**:**cat.**:**base** = 1:1.5:0.05:3 (0.2 mmol scale of **121a**), 90 °C, 5 hr. ^[b] Isolated yields after flash chromatography.

Optimal conditions involved: the ratio of allenoate and boronic acid 1:1.5; the loading of 4,4'-dibromobipyridine 5 mol%; 2 equivalents of K₂CO₃ the reaction was conducted in dioxane (0.2 M) at 90 °C for 5 hours. Next, we demonstrated the utility of this methodology over various boronic acid and electron-deficient allenenes.

First, we extend the scope of the boronic acid which turned out to be limited to substituted phenyl ones; aliphatic boronic acid such as *c*HexB(OH)₂ was proved ineffective in the catalytic process (Scheme 2.25). Remarkably, the protocol was not perturbed by a variety of boronic acids in spite of the electronic property and the position of the substitution. EWGs including NO₂, Br, COMe, CO₂Me, F and EDGs including OH, Me, OⁿBu, NMe₂, OMe were tolerated providing the corresponding β,γ -unsaturated esters in very high yields (up to 92%) and from moderate to very high *E*:*Z* ratio. However, there were still some trends between these results, such as: 1) generally, the electron withdrawing group cause more drop of the yield in contrast to electron donating ones;

2) halogens (*i.e.* Br and F) cause more loss of the stereoselectivity (4:1) than other substitutions (the worst one was 7:1); 3) in comparison, the substitution on para- position was more effective than on meta- position.

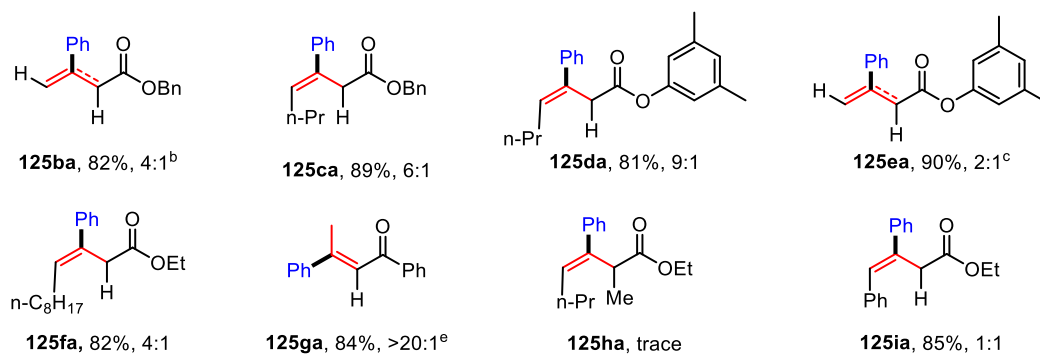
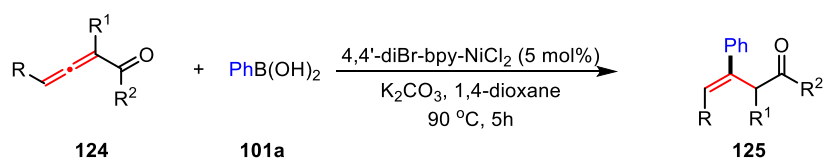
Then we used 2-formyl phenyl boronic acid¹⁰ which also afforded unconjugated annulated [3+2] in 63% yield with diastereoselectivity to be 9:1.



Scheme 2.25 The scope of the boronic acid in the coupling with allenolate.

Next, we studied the application on electron-deficient allenenes including allenolate and allenylketone (Scheme 2.26). Because of the difficulty in preparing the allenolate, we chose several typical ones to study. Generally speaking, this reaction protocol worked efficiently on the unsubstituted and mono-substituted allenolate. The α,γ -disubstituted allenolate (**121h**) afforded trace product under standard condition. The substitution on the γ -positions exhibit substantial power in controlling the regioselectivity. γ -Unsubstituted allenolate (**121e** & **121g**) provided a mixture of unconjugated and

conjugated product in 4:1 and 2:1 ratio although the yields were satisfying. The long linear chain ($n\text{C}_8\text{H}_{17}$) on γ position would lead *E*- superiority to descend from 11:1 ($n\text{Pr}$) to 4:1; furthermore, the phenyl group (**121i**) would exacerbate the ratio to be 1:1. By contrast, the protocol showed relatively satisfying tolerance to the substitution on the carboxylic oxygen (Bn and 3,5-dimethylphenyl), furnishing decent yield (89% and 81%) and stereoselectivity (6:1 and 9:1).



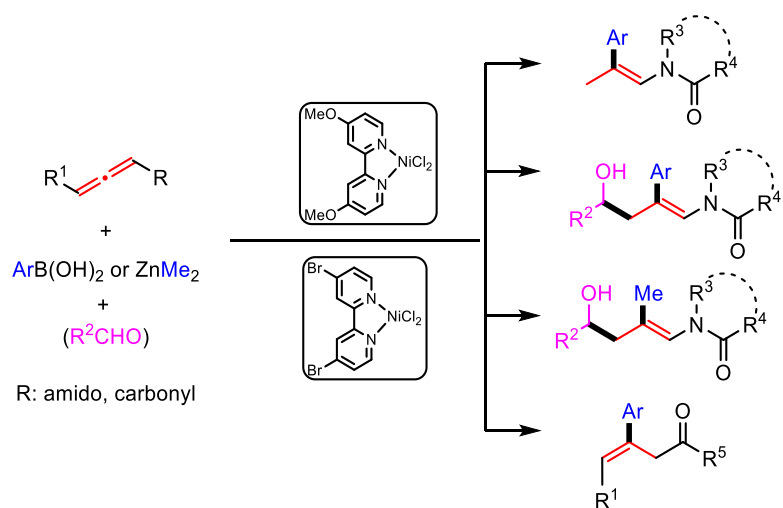
^{a)} All the reactions were carried out under nitrogen in reagent grade 1,4-dioxane. The yields are isolated yield after flash chromatography. The *E/Z* ratio were determined by ¹H-NMR and/or GC-MS on the reaction crude. ^{b)} β,γ -/ α,β -conjugated compound is represented, reaction at 40 °C. ^{c)} β,γ -/ α,β - conjugated compound is represented. ^{d)} The (*E*)- α,β -unsaturated isomer was obtained exclusively (reaction at 40 °C).

Scheme 2.26 The scope of the electron deficient allenenes.

2.5 Conclusions

We developed a new nickel(II) catalyzed Suzuki coupling of allenamide and allenolate, as a consequence, a series of stereo- and regio- defined enamides (which is pervasive motif in bioactive molecules as well as in naturally occurring compounds)¹⁵ and β,γ -unsaturated ester were more prone to be synthesized in a practically meaningful yield. In the coupling of the allenamide, a nucleophilic nickel intermediate was foreseen, trapped and used in further three component variation to provide an δ -hydroxy functionalized stereo- and regio- defined enamides. Besides, the nucleophilic coupling partners was also extended to dimethylzinc with slight change on reaction condition, so that two-fold sp^3 - sp^2 carbon-carbon bond building was realized.

The mechanism was explored using a series of practical as well as computational experiment.



Reference

- ¹ a) T. Lu, Z. Lu, Z. Ma, Y. Zhang, R. P. Hsung, *Chem. Rev.* **2013**, *113*, 4862 – 4904. (b) E. Manoni, M. Bandini, *Eur. J. Org. Chem.* **2016**, 3135 – 3142.
- ² a) R. Grigg, V. Sridharan, L. Xu, *J. Chem. Soc., Chem. Commun.* **1995**, 1903 – 1904; b) R. Grigg, J. M. Sansano, V. Santhakumar, V. Sridharan, R. Thangavelanthum, M. Thornton-Pett, D. Wilson, *Tetrahedron* **1997**, *53*, 11803 – 11826; c) P. Fretwell, R. Grigg, J. M. Sansano, V. Sridharan, S. Sukirthalingam, D. Wilson, J. Redpath, *Tetrahedron* **2000**, *56*, 7525 – 7539; d) M. Gardiner, R. Grigg, V. Sridharan, N. Vicker, *Tetrahedron Lett.* **1998**, *39*, 435 – 438; e) M. Gardiner, R. Grigg, M. Kordes, V. Sridharan, N. Vicker, *Tetrahedron* **2001**, *57*, 7729 – 7735; f) S. Husinec, M. Petkovic, V. Savic, M. Simic, *Synthesis* **2012**, *44*, 399 – 408.
- ³ R. Grigg, I. Köppen, M. Rasparini, V. Sridharan, *Chem. Commun.* **2001**, 964 – 965.
- ⁴ K. Inamoto, A. Yamamoto, K. Ohsawa, K. Hiroya, T. Sakamoto, *Chem. Pharm. Bull.* **2005**, *53*, 1502 – 1507.
- ⁵ R. Grigg, S. McCaffrey, V. Sridharan, C. W. G. Fishwick, C. Kilner, S. Korn, K. Bailey, J. Blacker, *Tetrahedron*, **2006**, *62*, 12159 – 12171.
- ⁶ R. Grigg, V. Loganathan, V. Sridharan, P. Stevenson, S. Sukirthalingam, T. Worakun, *Tetrahedron* **1996**, *52*, 11479 – 11502.
- ⁷ H. Fuwa, T. Tako, M. Ebine, M. Sasaki, *Chem. Lett.* **2008**, *37*, 904 – 905.
- ⁸ a) E. M. Beccalli, G. Broggini, F. Clerici, S. Galli, C. Kammerer, M. Rigamonti, S. Sottocornola, *Org. Lett.* **2009**, *11*, 1563 – 1566; b) E. M. Beccalli, A. Bernasconi, E. Borsini, G. Broggini, M. Rigamonti, G. Zecchi, *J. Org. Chem.* **2010**, *75*, 6923 – 6932.
- ⁹ a) S. Ma, N. Jiao, L. Ye, *Chem. Eur. J.* **2003**, *9*, 6049 – 6056; b) R. Qian, H. Guo, Y. Liao, Y. Guo, S. Ma, *Angew. Chem. Int. Ed.* **2005**, *44*, 4771 – 4774.
- ¹⁰ T. Bai, S. Ma, G. Jia, *Tetrahedron* **2007**, *63*, 6210 – 6215.
- ¹¹ X. Yu, X. Lu, *Org. Lett.* **2009**, *11*, 4366 – 4369.
- ¹² X. Yu, X. Lu, *J. Org. Chem.* **2011**, *76*, 6350 – 6355.
- ¹³ (a) J. G. Knight, S. W. Ainge, C. A. Baxter, T. P. Eastman, S. J. Harwood, *J. Chem. Soc. Perkin Trans.* **2000**, *1*, 3188 – 3190; (b) T. A. Bryson, D. C. Smith, S. A. Krueger, *Tetrahedron Lett.* **1977**, 525 – 528. (c) N. Waizumi, T. Itoh, T. Fukuyama, *Tetrahedron Lett.* **1998**, *39*, 6015 – 6018; (d) R. K. Dieter, K. Lu, *Tetrahedron Lett.* **1999**, *40*, 4011 – 4104; (e) R. K. Dieter, K. Lu, S. E. Velu, *J. Org. Chem.* **2000**, *65*, 8715 – 8724.
- ¹⁴ a) Z. Lu, G. Chai, S. Ma, *J. Am. Chem. Soc.* **2007**, *129*, 14546 – 14547; b) Z. Lu, G. Chai, X. Zhang, S. Ma, *Org. Lett.* **2008**, *10*, 3517 – 3520; c) G. Chai, Z. Lu, C. Fu, S. Ma, *Adv. Synth. Catal.* **2009**, *351*, 1946 – 1954; (d) J. He, Z. Lu, G. Chai, C. Fu, S. Ma, *Tetrahedron* **2012**, *68*, 2719 – 2724.
- ¹⁵ (a) L. A. McDonald, J. C. Swersey, C. M. Ireland, A. R. Carroll, J. C. Coll, B. F. Bowden, C. R. Fairchild, L. Cornell, *Tetrahedron*, **1995**, *51*, 5237 – 5244; (b) Y. Sugie, K. A. Dekker, H. Hirai, T. Ichiba, M. Ishiguro, Y. Shioni, A. Sugiura, L. Brennan, J. Duignan, L. H. Huang, J. Sutcliffe, Y. Kojima, *J. Antibiot.*, **2001**, *54*, 1060 – 1065; (c) L. Yet, *Chem. Rev.*, **2003**, *103*, 4283 – 4306; (d) N. Tan, J. Zhou, *J. Chem. Rev.*, **2006**, *106*, 840 – 895; (e) Y. Kuranaga, Y. Sesoko, M. Inoue, *Nat. Prod. Rep.*, **2014**, *31*, 514 – 532.

3 Photocatalyzed Synthesis of 1,3,4-trisubstituted Pyrrole

3.1 Introduction: progress in visible-light introduced reaction of azide

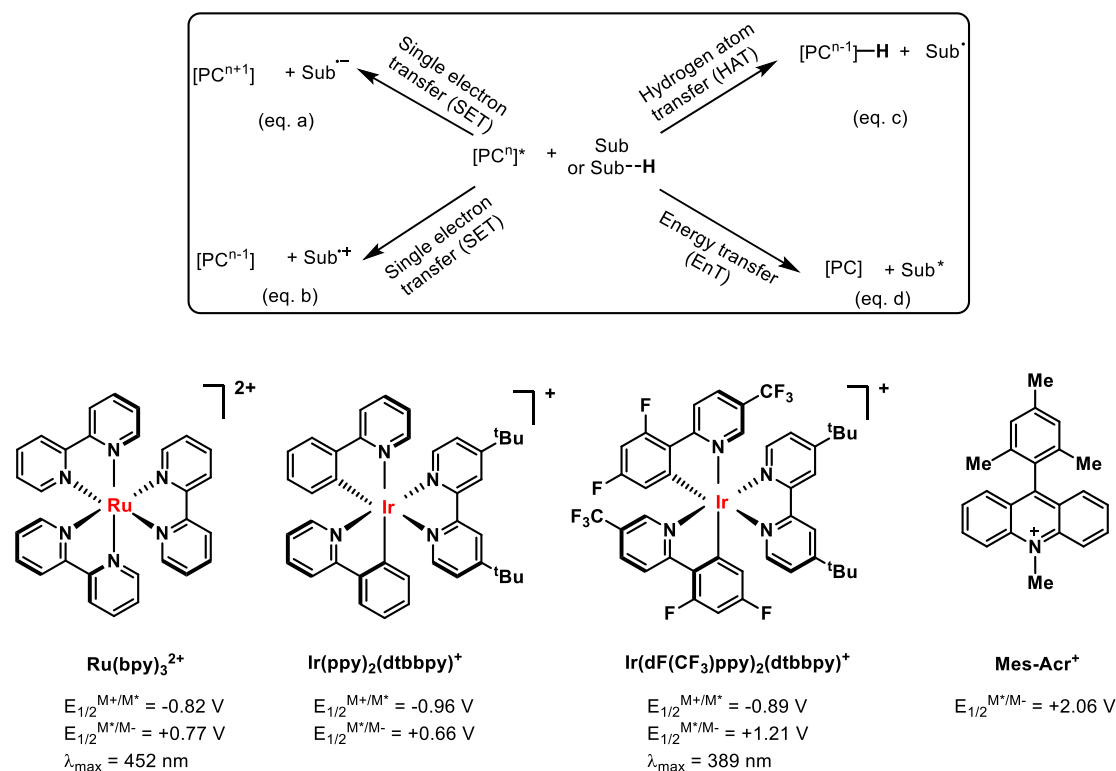
Over the past centuries, organic chemistry has grown to be a fully developed and comprehensive subject. It is difficult to find a new reaction without the participation of a catalyst. In this context, to explore new catalyst has become an ‘straw for a drowning man’. In the past decades, the metal-based and non-metal based organocatalyst has been developed completely in theoretical and industrially practical aspects. These catalysts not only solved the problem of enantio-, regio- and chemoselectivity but also brought the possibility of building nuovo bond.

As a historic branch of organic chemistry, the photochemistry although provided more and unique possibilities to the reaction, the light used in its infancy was ultraviolet (UV) the high-energy photon of which was indistinguishably detrimental to organic compounds, the development of it was sluggish. By contrast, the photosensitizer could absorb photon of long wavelength light (not harmful to general organic compound) more efficiently and transfer it to be chemical energy that caused the transform of the molecule. The reactivities of radical anion or radical, diradical caused by the energy transfer, proton atom or electron shifting are generally different from activating intermediates produced by traditional ways. Meanwhile if the unique active compounds introduced though photochemical pathway are further manipulated with traditional ways, a more complex and novel transformation could be produced. An intriguing version was dual-catalyst profile, in which case the photogenerated intermediate could participate in another independent catalytic cycle. This strategy has enjoyed huge growth in past ten years.¹

According to the interaction between the photocatalyst and the substrate, photocatalysis could be approximately categorized into three classes. The most common interaction is single electron transfer (SET) which is based on the electronic propensity of photoexcited catalyst. Photoexcited catalyst is usually a stronger oxidant or reductant than its ground state analogue. Consequently, the substrate is activated by losing one electron or getting one electron to give a radical ion (Scheme 3.1 a & b). Depending on the nature of the substrate, the intermediate could go through a variety of two-fold new bonds construction or bond cleavage to give further reacting intermediates. Sometimes, the electron is used so efficiently that no extra reductant or oxidant are needed in the reaction, although there are electron exchanges, which is called ‘photoredox’. And deviation of this mode recently emerged *i.e.* ligand-to-metal charge transfer (LMCT), the substrate chelates to excited photocatalyst and is deprived of one electron delivering a reactive radical.

In some cases, instead of by a sequence of electron and matter exchanges between catalyst and substrate, the radical intermediate can also be produced by direct hydrogen atom transfer (HAT) from substrate to photoexcited catalyst (Scheme 3.1c). This activation protocol is applicable to the photoexcited aromatic ketones and recently reported polyoxometalates as photocatalyst.² A sharp difference between single electron transfer (SET) and hydrogen atom transfer (HAT) is on the thermodynamic parameters which determine the practicability of process. For the SET process, the redox potential of excited-state photocatalyst and substrate mainly control the reaction; whereas, for the HAT process, the strength of the C-H bond of the substrate and the ability of photoexcited catalyst to abstract hydrogen atom.

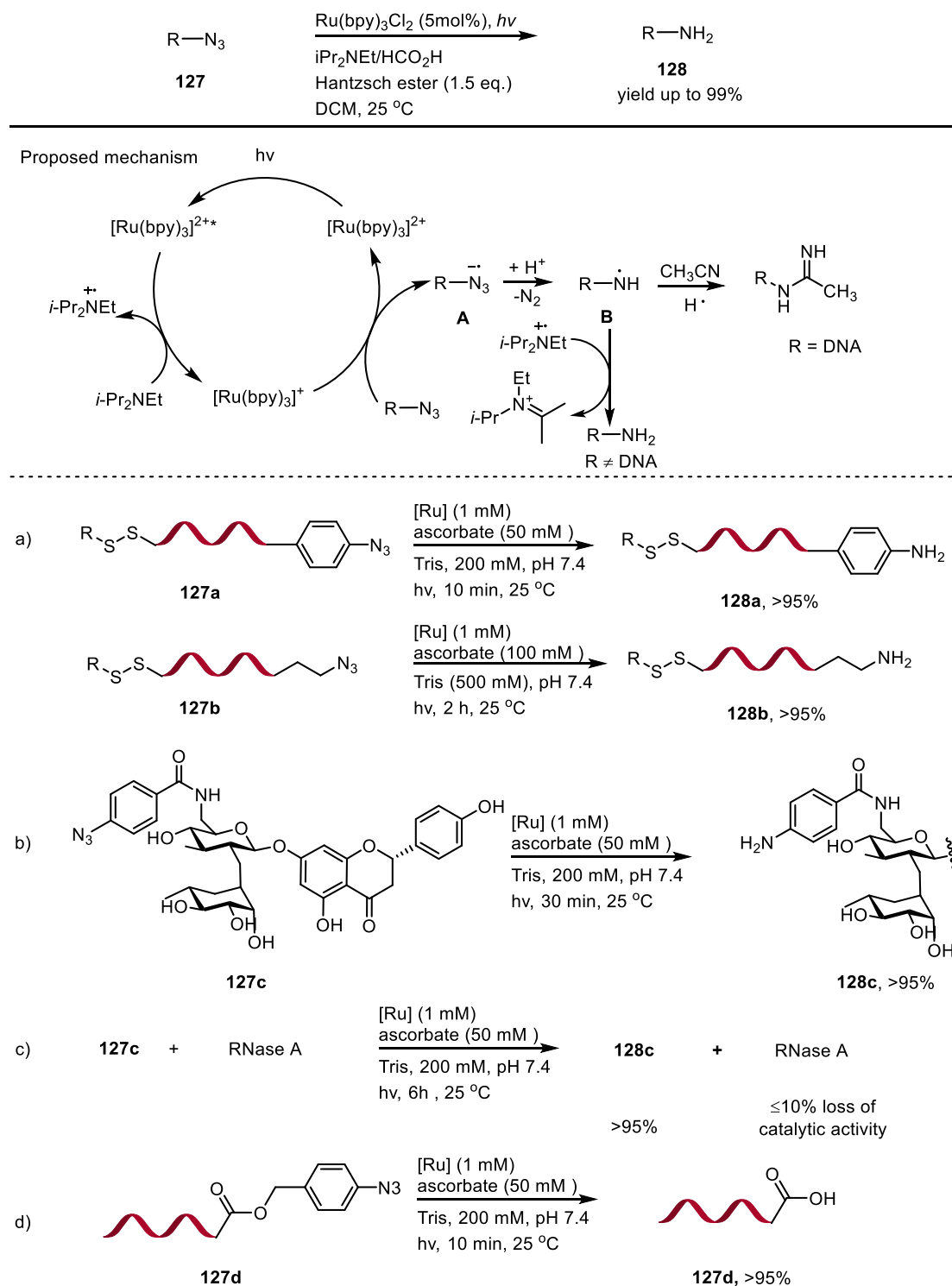
Third, there are also some molecules of redox potential mismatched with the photoexcited catalyst. In this case, the excited photocatalyst at triplet state could activate the ground-state substrate through energy transfer (EnT).³ This energy transfer may happen in different modes among which the most famous one is the Dexter energy transfer (Scheme 3.1d). The photocatalyst could be excited into low-lying state after absorbing the light which after an intersystem crossing (ISC) event could transform to be excited states. Then energy transfer from triplet photocatalyst to substrate would afford ground state photocatalyst and excited substrate analogue. In this context, to guarantee the energy transfer thermodynamically feasible, the energy of the triplet photocatalyst must be higher than the substrate; the triplet photocatalyst should go through fast intersystem crossing process. We also list the photocatalyst that we will mention in the summary of visible light catalyzed transformation of azide.



Scheme 3.1 The reaction profile of photocatalysis and several relevant photocatalysts.

In 2011, David Liu discovered Ru(bpy)₃Cl₂ catalyzed reduction of azide under blue light using DNA-encoded reaction-discovery system.⁴ Although traditional reduction methods of the azide such as using metal-hydride, thiols and Staudinger condition were widely used, the limitation cannot be neglected. In addition of providing excellent yields, this method turned out to be compatible with functional group containing acidic proton, such as unsubstituted indoles, acids and alcohols which may not be tolerated by metal-hydride; alkenes, alkynes and aryl halide which are sensitive to hydrogenation conditions. The reaction was proposed to launch with the excitation of the photosensitizer under blue light, which could subsequently be reduced by single electron transfer. The Ru(I) would further lose one electron to azide leading to the formation of an azido radical anion. After extrusion of one molecule of nitrogen and protonation, the radical anion could provide an amino radical. After that, the radical would capture a hydrogen radical from solvent producing an

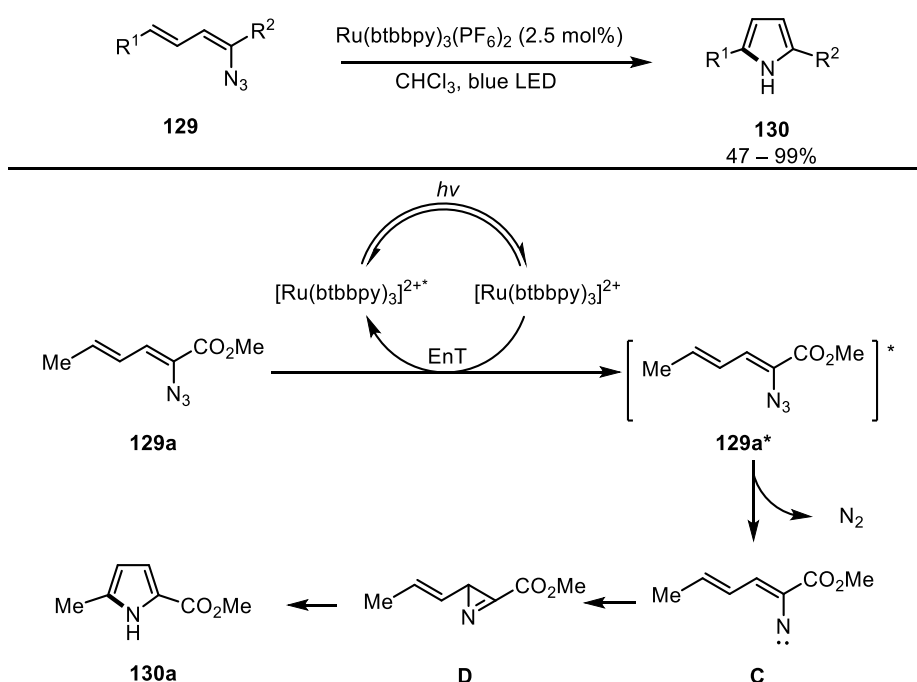
amine.

**Scheme 3.2** Photocatalyzed reduction of azide and its application by Liu.

Given remarkable chemoselectivity, they extended the reaction to biological application. When ascorbate was used as hydrogen donor, the reaction proceeded efficiently in buffers. In the buffer of tris(hydroxymethyl)aminomethane (Tris), the phenyl and aliphatic azide tethered with DNA oligonucleotide was reduced in 10 minutes with the disulfide-bond untouched (Scheme 3.2a). Then

the compatibility with oligosaccharide was tested using an azide-containing variant of naringin. The reduction finished within 30 minutes under standard condition (Scheme 3.2b). The outstanding chemoselectivity was further examined at the presence of RNase A, the reduction of **127c** could proceed steadily providing more than 95% yield with less than 10% loss of catalytic reactivity of RNase A (Scheme 3.2c). The highly efficient photouncaging of 4-azidobenzyl ester of DNA oligonucleotide-linked carboxylic acids was also achieved through 1,6-elimination in 10 minutes under standard aqueous reduction conditions (Scheme 3.2d).

In 2014, Yoon reported a rearrangement of vinyl nitrenes enabled by $\text{Ru}(\text{dtbbpy})_3(\text{PF}_6)_2$ mediated energy transfer from visible light to organic molecules. (Scheme 3.3)⁵ In contrast to high-energy UV light, visible light had better functional group tolerance and avoided side photodecomposition (caused by sensitivity of product to UV light) which might decrease the yield. This rearrangement provided a mild and highly efficient way to synthesize a variety of multi-substituted pyrrole and indole in moderate to nearly quantitative yield. The author proposed an azirine intermediate **D** to interpret the mechanism which was successfully isolated in the case the following ring expansion was slow. Since the azirines are highly reactive compound, the utility of it was further exploited, such as by addition of nucleophile or reacting with cyclopentadiene providing hetero-Diels–Alder cycloaddition product. According to the proposed mechanism, the photocatalyst would transform to its excited state of long lifespan which underwent an exergonic energy transfer to vinyl azide producing a triplet intermediate **129a***. After extrusion of one molecule of nitrogen (**129a** → **C**), vinyl nitrene **C** was produced and cyclized to form the azirine **D** which underwent ring expansion affording the final product **130**.

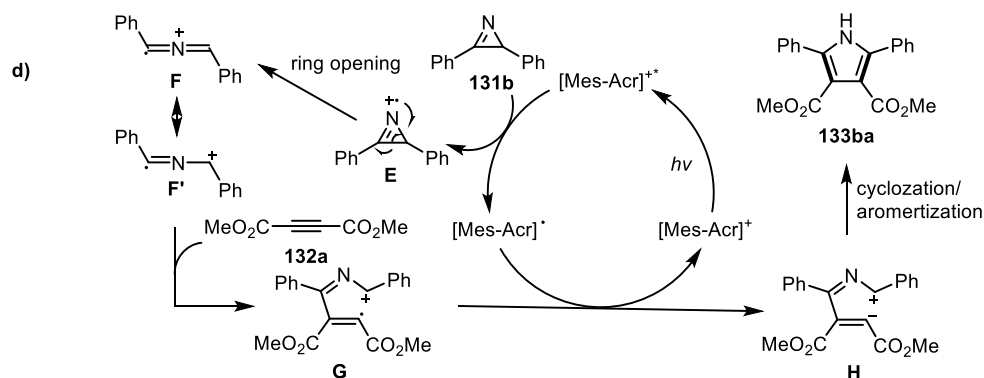
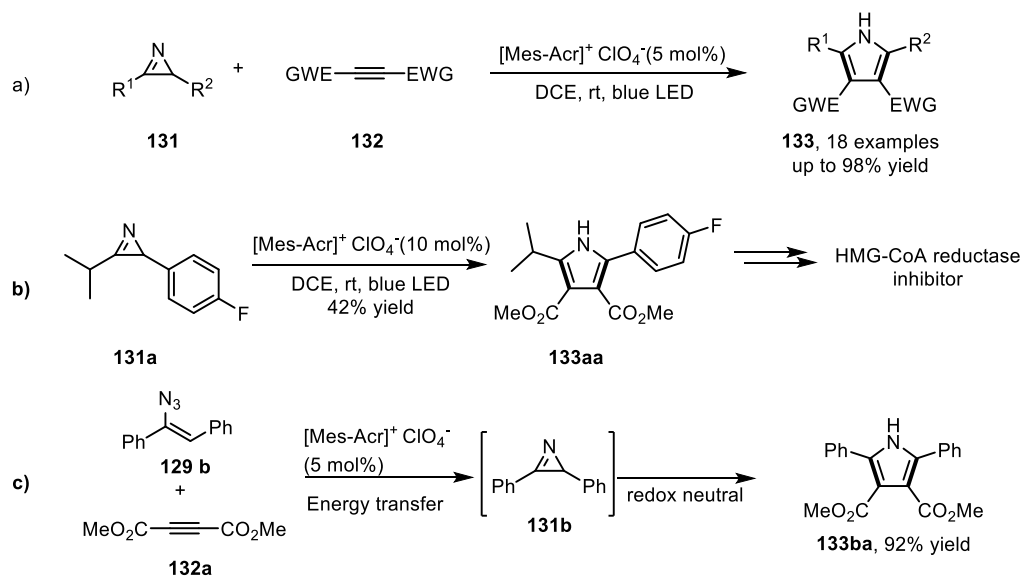


Scheme 3.3 Photocatalyzed preparation of pyrrole from vinyl azide through energy transfer

In same year, Xiao group documented a metal-free, visible-light introduced formal [3+2] annulation to synthesize highly functionalized pyrroles **133** (Scheme 3.4).⁶ Under mild conditions (7 W blue LED, rt), the azirine **131** was activated by excited 9-mesityl-10-methylacridinium perchlorate and

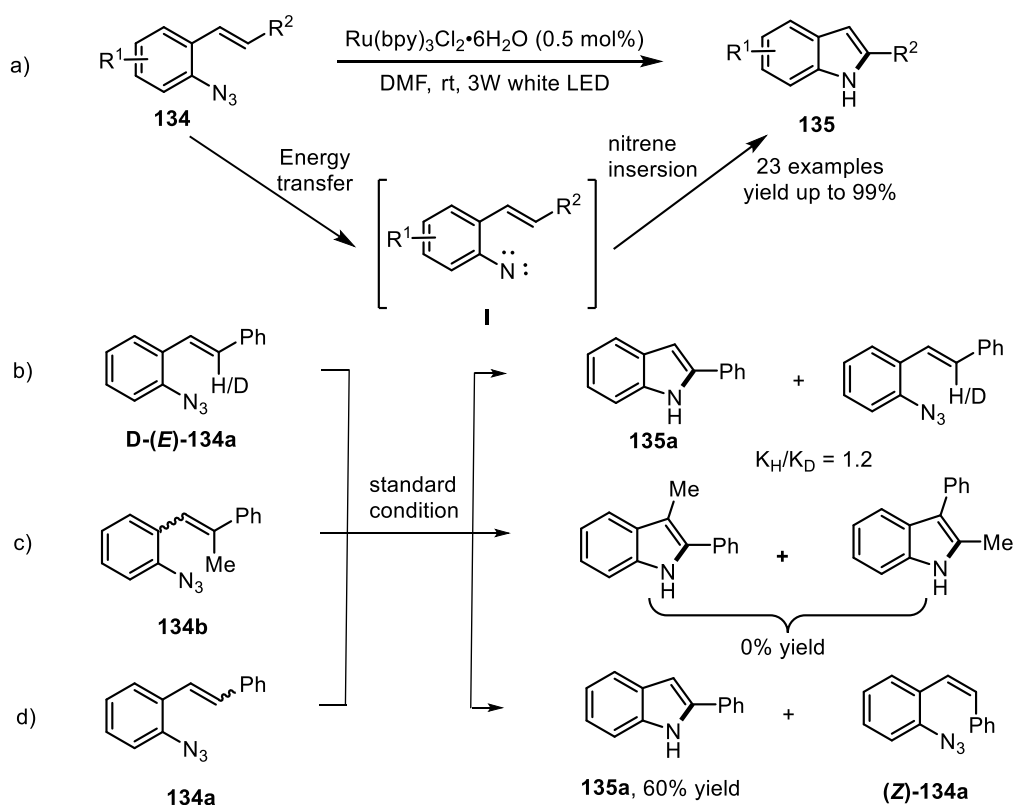
electron deficient alkyne underwent two fold C-C bond construction forming an *N*-free multi-substituted pyrrole in moderate to high yield (Scheme 3.4a). The protocol exhibited pleasing tolerance to the functional group of different electronic nature on the phenyl ring. However, due to the nature of the stability of the azirine, the substrate was limited to at least mono-phenyl substituted azirine. The utility of this concise manner was further demonstrated by the application on synthesize the core structure of HMG-CoA reductase inhibitor (Scheme 3.4b). As aforementioned, Yoon reported the azirine intermediate in his photocatalyzed annulation of vinyl azide. The authors also tried the azide as azirine *in situ* provider which turned out to be an ideal substrate to afford **133ba** in 90% yield. By contrast, the Ru catalyst used by Yoon did not work in this protocol (Scheme 3.4c).⁵

They proposed that, the excited photocatalyst firstly deprive one electron from the nitrogen of azirine delivering a radical cation and a reduced photocatalyst which was theoretically feasible according to the oxidation potential of the reactants. Then, ring opening happened to the azirine radical cation **E** affording a linear radical cation **F** in tautomerism with **F'**. The radical moiety of **F'** could be captured by the active alkyne supplying an 1,5-radical cation **G** which subsequently underwent a sequence of reduction by the reduced photocatalyst, annulation and aromatization and provided the final product.



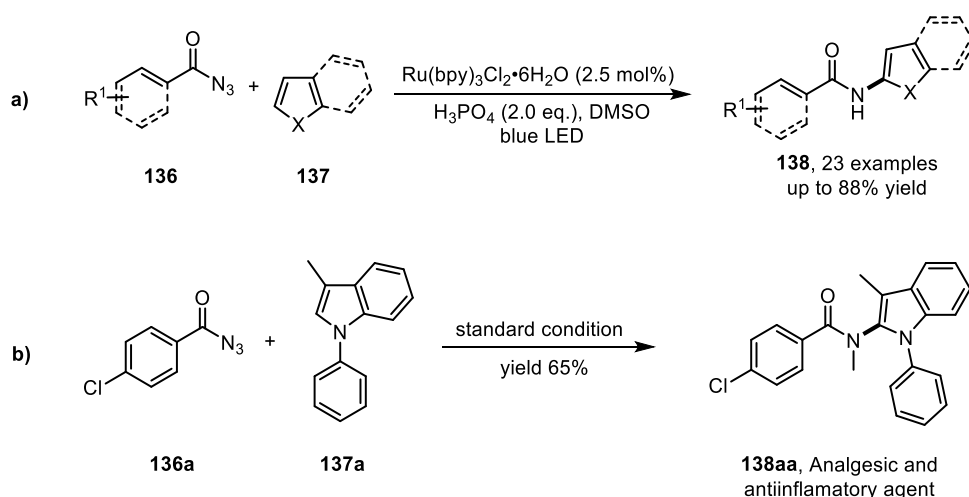
Scheme 3.4 Photocatalyzed preparation of pyrrole from azirine

In same year, Xiao also reported an efficient visible light introduced the synthesis of 2-substituted indole **135** from styryl azides **134** in the presence of $\text{Ru}(\text{bpy})_3\text{Cl}_2$ (Scheme 3.5).⁷ Under 3W white LED, with 0.5 mol% loading of photocatalyst, the reaction was proposed to undergo mild energy transfer and expel one molecule of nitrogen providing an reactive nitrene **I**. Subsequently the nitrene intermediate took place a concerted insertion to γ -C-H and provided the final product in moderate to high yield. The proposed nitrene intermediate was supported by the value of kinetic isotope effect (KIE) of the reaction confirmed to be $K_{\text{H}}/K_{\text{D}} = 1.2$ (Scheme 3.5b); the failure of the γ -disubstituted styryl azides **134b** under standard condition (Scheme 3.5c); and the sluggish reactivity of the (*Z*)-**134a** azide (Scheme 3.5d).



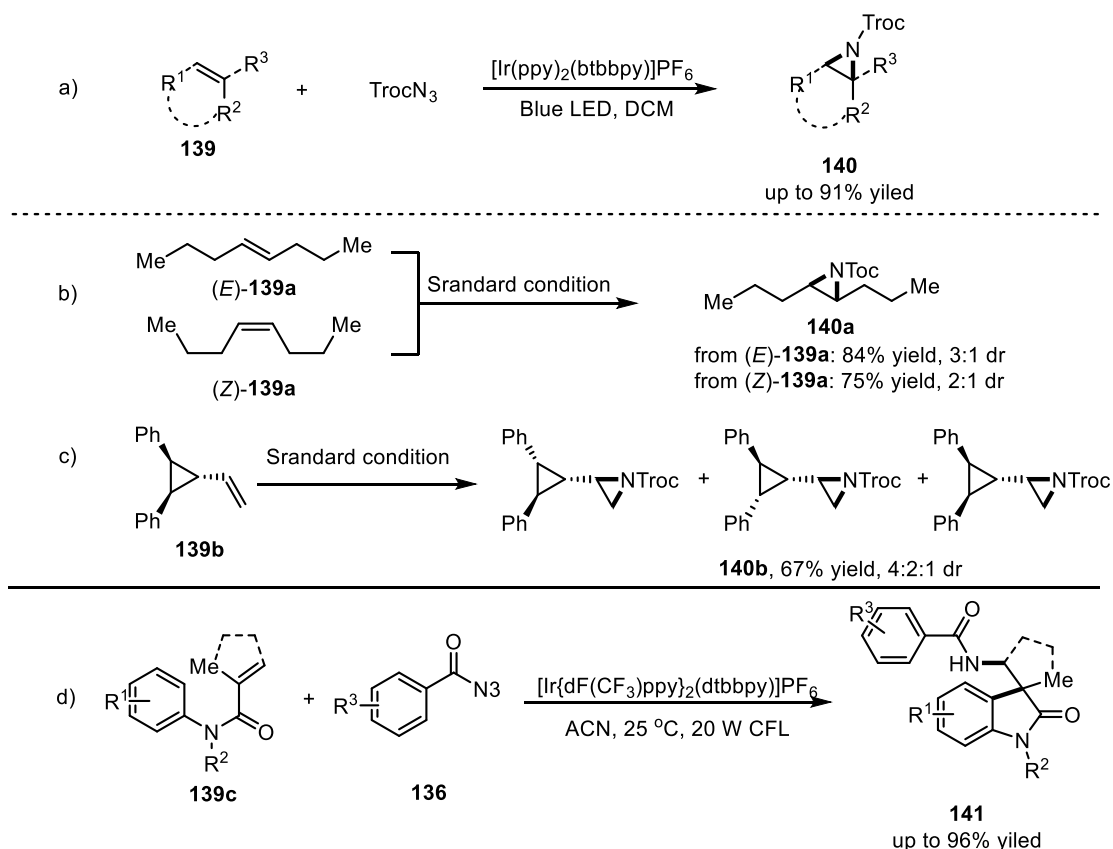
Scheme 3.5 Photocatalyzed preparation of pyrrole from azirine

Simultaneously, König made the use of energy transfer strategy to realize the C-H amination of electron-rich heteroarenes **137** with aryl acyl azides **136** (Scheme 3.6).⁸ In contrast to traditional metal catalyzed method, this strategy features low cost, mild condition, no reliance to directing group, wide functional group tolerance and ability of late-stage amination of complicated compound. The research on the scope of the azide indicated that this amination worked on the aryl acyl azide, other azides such as alkyl, phenyl azide turned out to be sluggish in this protocol. This result was in accordance with the energy analysis: the available energy of triplet $\text{Ru}(\text{bpy})_3^{2+}$ was 46 kcal/mol which was not sufficient for the phenyl azide (68 kcal/mol). The potential value was further illustrated by the successful application on the synthesis of the medically valuable amide **138aa**

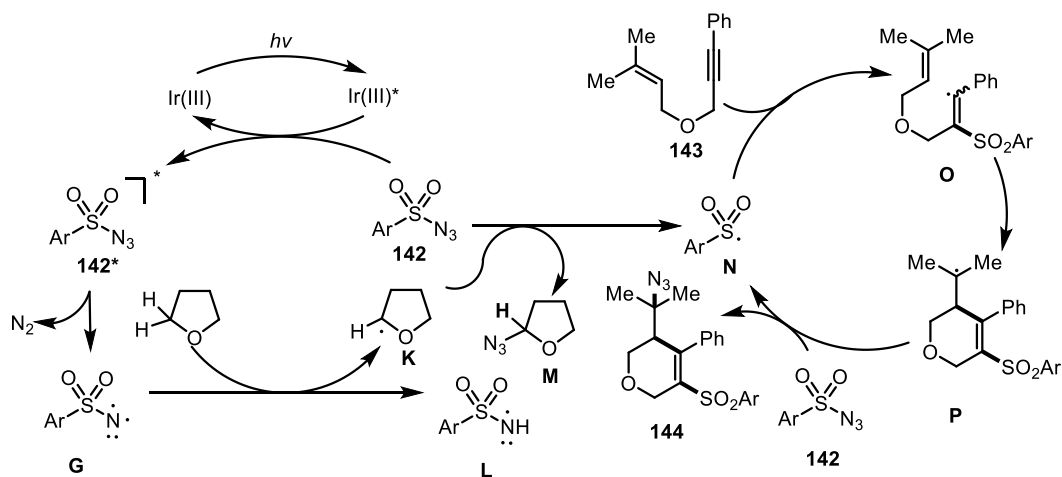
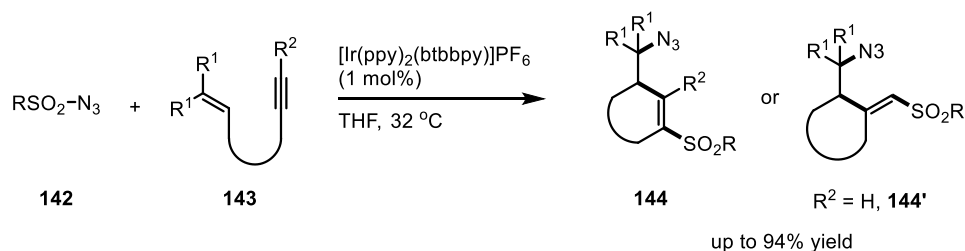


Scheme 3.6 Photocatalyzed regioselective amination of electron-rich heteroarenes.

In 2016, Yoon reported a mild olefin aziridination through photocatalyst introduced spin-selective photogeneration of triplet nitrene from the azidoformates.⁹ Because of the high reactivity of free nitrene, the challenge to realize photocatalyzed aziridination utilizing nitrene derived from azide is to selectively produce triplet nitrene (Scheme 3.7a). In contrast to acyl azide aforementioned, the azidoformate is less prone to be reduced which cut down the possibility of other photo-introduced reaction. So, it is reasonable that, the $\text{Ru}(\text{bpy})_3^{2+}$ ($E_T = 46.5$ kcal/mol) used in the former case did not promote the reaction, on the other hand, the derivatives of $[\text{Ir}(\text{bpy})_2(\text{dtbbpy})]\text{PF}_6$ of high potential ($E_T = 49.2$ kcal/mol) promoted reaction. The scope of the alkene turned out to be pretty wide such as both terminal and internal alkene, aliphatic and aryl alkene were all efficient substrates. One trait of the triplet nitrene process is the cyclization goes through a stepwise fashion involving a relatively slow intersystem crossing and sequent ring closure. In this direction, *E*-**139a** and *Z*-**139a** internal alkene were tested in the reaction, both of which gave mixture of *trans*- & *cis*- product (Scheme 3.7b); exposure of cyclopropyl alkene to standard condition also cultivated a mixture, consistent with the proposed existence of reversible radical intermediate (Scheme 3.7c).

**Scheme 3.7** Photocatalyzed aziridination of alkene.

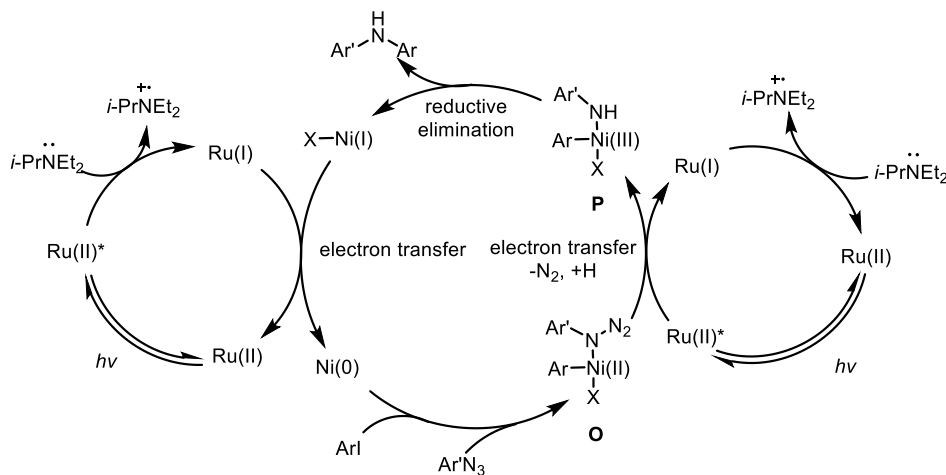
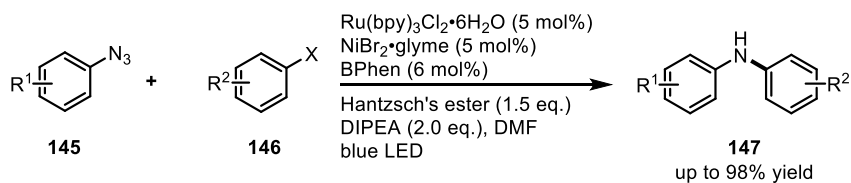
In 2017, photocatalyzed introduction of triplet sulfonyl nitrene was documented by Lam and co-workers with $[\text{Ir}(\text{ppy})_2(\text{btbbpy})]\text{PF}_6$ as photosensitizer which was used to realize azidosulfonylative cyclization of enyne providing functionalized heterocycle (Scheme 3.8).¹⁰ This methodology tolerated sulfonyl azides containing various aryl or alkyl substituents, a variety of the aryl substituent of the alkyne affording moderate to excellent yield. In the case of the terminal alkyne, the reaction produced exocyclic alkenylsulfone. It was noteworthy that the solvent THF played a unique and crucial role in this reaction. In addition to that, the photoexcited $[\text{Ir}]$ ($E^{*\text{III/IV}} = -0.96$ V vs. SCE) was insufficiently to reduce para-toluenesulfonyl azide ($E_{1/2}^{\text{red}} = -1.22$ V vs. SCE). In this context, they proposed an THF participating mechanism. The energy transfer from the photoexcited $[\text{Ir}]$ to azide led to excited $\mathbf{142}^*$. After expelling an equivalent of nitrogen, $\mathbf{142}^*$ could provide a triplet nitrene \mathbf{G} which grabbed a hydrogen atom from THF resulting in a tetrahydrofuran-2-yl radical \mathbf{K} . \mathbf{K} could abstract an azido group from sulfonyl azide delivering a sulfonyl radical \mathbf{N} . The sulfonyl radical took a sequence of addition to alkyne, ring closure and azidation providing the final product and another sulfonyl radical \mathbf{N} .



Scheme 3.8 Photocatalyzed sulfonylation/azidation/annulation.

Inspired by Liu's work, Konev and Johannes developed photoredox-mediated Ru/Ni dual catalysis strategy to prepare diaryl amine (Scheme 3.9).¹¹ The reaction was supposed to start with photocatalyzed reduction of Ni(II) to Ni(0), so that Ni(0) could oxidatively insert into the aryl-halide bond. With the aid of the Aryl-Ni(II) intermediate, photoexcited [Ru]* would reduce the azide through single-electron-transfer process expelling one equivalent nitrogen and providing an Ni(III) intermediate. After the reductive elimination, the final product was produced releasing an Ni(I) catalyst. This reaction turned out to be robust to a wide array of arenes and the substitution patterns of the azide and the aryl electrophiles, such as electron rich, neutral phenyl ring, azidopyrazole, pyridines and so on.

Some preliminary study was conducted to elucidate the mechanism. Interestingly, the corresponding anilines which was possible reduction product of azides were used in the control experiment which gave similar yield but at slower speed. This means the aniline produced *in situ* from azide could be oxidized by the photocatalyst and continued the rest transformation. The α -allylphenyl azide was used in the coupling, instead of the cyclization aziridine product or subsequent product, coupling product diaryl amine was found exclusively, which ruled out the possibility of nitrene intermediate.

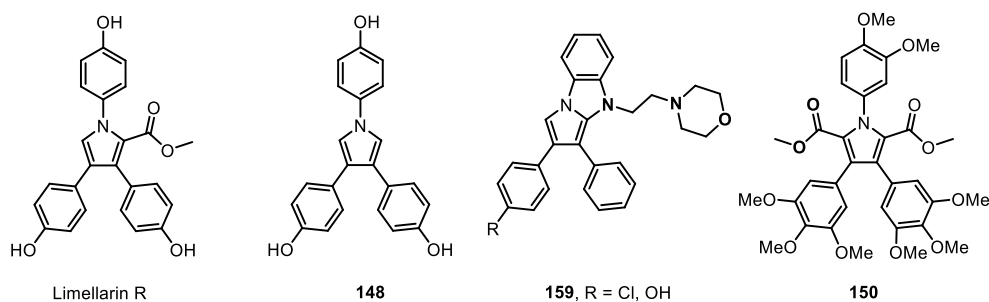


Scheme 3.9 Photocatalyzed coupling of azide and heteroarene.

3.2 Photocatalyzed Synthesis of the 1,3,4- Substituted Pyrrole

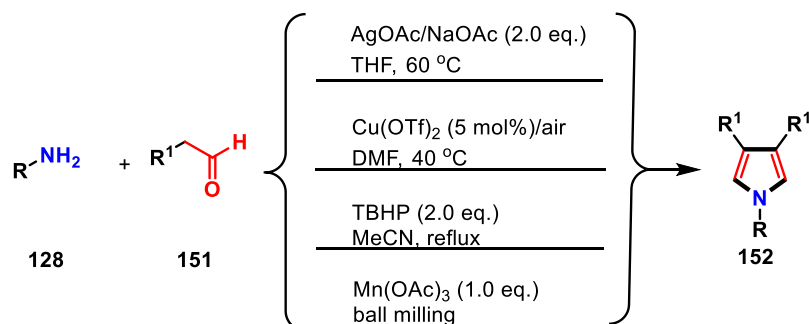
The pyrrole is one of the most important heterocycles which appears in many natural product, advanced material,¹² dyes, bioactive molecules which possess an array of antitumor, anti-inflammatory, and antibiotic activities¹³. Hence, many chemical ways to synthesize pyrrole has been developed, such as Paal–Knorr, Huisgen, and Hantzsch processes. But the exploration towards this direction never ceased, a variety of approaches through transition metal catalyzed 'hydrogen auto-transfer' reactions¹⁴, C-H bond functionalization,¹⁵ [3+2] annulation¹⁶, [2+2+1] coupling¹⁷ and others¹⁸. However, almost all of these traditional methods need complex starting material. Thus, the simpler way to synthesize pyrrole from commercially available substrate is still a challenge.

One of the most important pyrrole analogues are 1,3,4-substituted pyrroles which appear as natural compound or have pharmacetic activities.(Scheme 3.10) For example, the Limellarin R was isolated with its analogues from an Australian marine sponge, *Dendrilla cactus*¹⁹; 4,4',4''-(1H-pyrrole-1,3,4-triyl)triphenol **148** was reported to exhibit estrogenic activity in MCF-7 cell proliferation assay²⁰; compound **149** and its analogues showed ability to inhibit the ascorbate-dependent lipid peroxidation; compound **150** and its analogues exhibit a clear trend in MDR reversal activity when tested in combination with vinblastine or doxorubicin against HCT116/VM46.



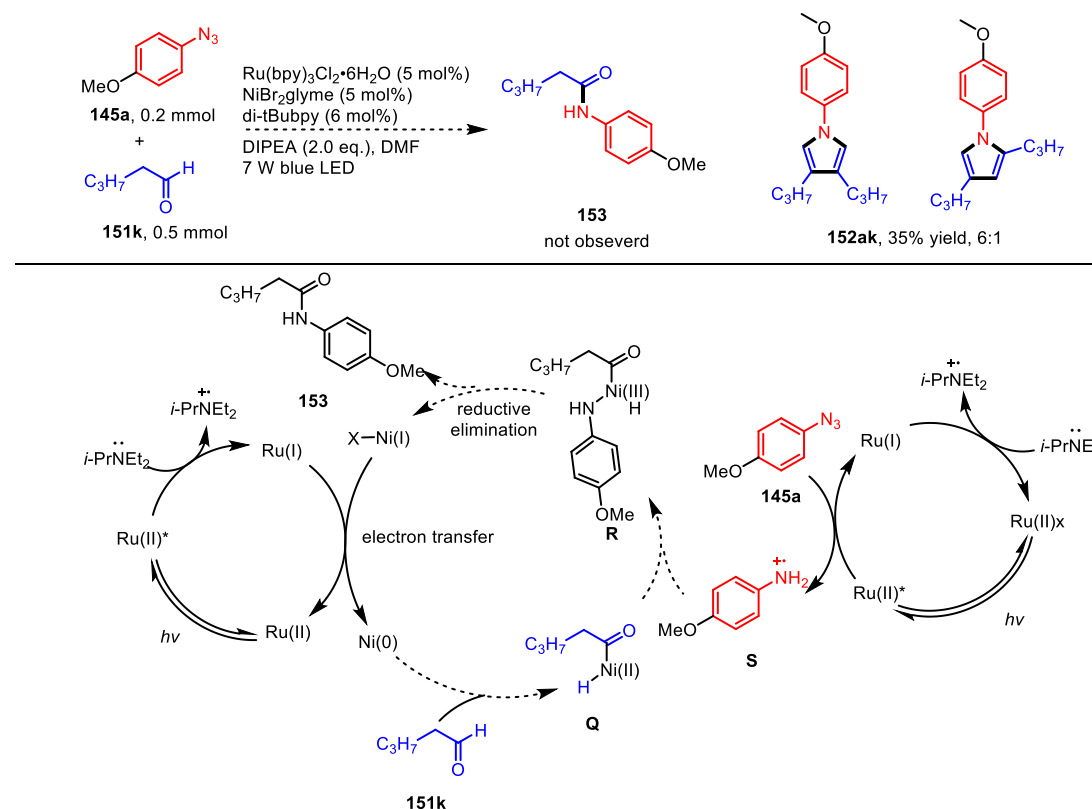
Scheme 3.10 Typical compound containing 1,3,4-trisubstituted pyrrole structure.

In this context, recently, several groups documented their achievement of the synthesis of 1,3,4-substituted pyrrole from simplest starting material: aldehyde **151** and aniline analogues **128**.²⁰ Although these reactions are conducted under mild, metal-free or boil-milling conditions, at least one equivalent of oxidant is mandatory for all these reactions.



Scheme 3.11 Synthesis of pyrrole from aldehyde and aniline.

As reported by Johannes and co-workers,¹² Ni(0) was proposed under the reductive conditions, meanwhile Ni(0) was used in the C-H functionalization of the aldehyde by Dong.²¹ In this context, at the beginning of our research, we planned to use the *in situ* generated Ni(0) to realize the C-H activation of the aldehyde group to afford Ni(II) intermediate **Q** (Scheme 3.12). At the same time, the anilino radical cation **S** could be produced by reduction of azide. Consequently, there might be



Scheme 3.12 Initial design of amination of aldehyde.

some chances for the Ni(II) intermediate to be captured by the amino radical, which after reductive elimination could give an amide **153**. But when we conducted the reaction under ideal condition: the ratio of aldehyde and azide was 1:2.5, 5 mol% of Ru(bpy)₃Cl₂·H₂O, 5 mol% of NiBr₂·glyme, 6 mol% of di-*t*Bubpy as ligand, 2 equivalent of diisopropylethylamine as reductant and dimethylformamide as solvent, left the reaction under 7 W blue LED for 24 hours. The reaction gave the pyrrole **152ak** as product exclusively in 30% yield with regioselectivity to be 6:1.

Although the product was not the target one, taking into consideration of importance of the pyrrole and the easy availability of starting material, we judged this reaction was valuable to be further explored.

First, the control experiments were performed without acetic acid (Table 3.1, entry 2) and blue light (Table 3.1, entry 3), which demonstrated the necessity of acid and light. We suspected that the azide was reduced to aniline first before taking part in further transformation, so we conducted reaction with aniline instead of the azide. The reaction did not take place when aniline was used, so we could tell that the azide participated in the reaction before it was reduced to aniline (Table 3.1, entry 4). Then we tried Co(II) to replace the Ni(II) which gave only 16% yield (Table 3.1, entry 5). Other ligands such as 1,10-phenanthroline was not as efficient as *tert*-butylbipyridine (Table 3.1, entry 8). Since [Ir{dF(CF₃)ppy}₂(dtbbpy)]PF₆ was also used in the aforementioned energy transfer, we also tried it in this chemistry which turned out to be invalid. Up to now, the necessity of Ru(II) and di-*tert*-butylbipyridine has been confirmed.

Table 3.1 Control experiments on the synthesis of pyrrole.

Entry ^a	Conditions	Yield (%) 152al ^b	152ak: 152al' ^c
1	standard	35	85:15
2	no AcOH	0	--
3	no hv	0	--
4	no Ru	Trace	--
5	Aniline instead of azide	0	--
6	[Ir{dF(CF ₃)ppy} ₂ (dtbbpy)]PF ₆ instead of Ru	Trace	--
7	CoCl ₂ ·6H ₂ O instead of NiCl ₂	16	--
8	1,10-phenanthroline instead of di ^t Bubpy	16	87:13

^a All the reactions were carried out under nitrogen atmosphere with dry DMF. **145a:1511:cat.:[Ni]:dtBubpy:DIPEA:AcOH** = 1:2.5:0.01:0.05:0.06:2:2, (0.2 mmol scale of **145a**). ^b After flash chromatography. ^c Determined via GC-MS on the reaction crude.

Next, we examined the effect of solvent towards the reaction. Taking into consideration that proton was involved in photocatalyzed reduction, we tried methanol as solvent which turned out to almost inhibit the reaction (Table 3.2, entry 1). Afterwards the non-protonic chloroform was either

confirmed to be not supportable to the reaction (Table 3.2, entry 2). The non-protonic, polar DMSO used by König in his amination of heteroaryl compound provided a little lower yield (Table 3.2, entry 3). Ether type solvent used by Lam in his cascade azidosulfonylative cyclization also reduced the yield to 19% (Table 3.2, entry 4). Another promising solvent acetonitrile also gave similar yield (Table 3.2, entry 5). Since the optimal condition was similar to the Liu's work, we speculated that this reaction might be applicable to biological molecules, so we tried the mixed solvent of DMF/H₂O (10:1). It is surprising that at the presence of water, the reaction could also provide 20% yield (Table 3.2, entry 6).

Table 3.2 The effect of the solvent to the reaction.

Reaction conditions:
 Ru(bpy)₃Cl₂·6H₂O (1 mol%)
 NiBr₂·glyme (5 mol%)
 4,4'-di-tBubpy (6 mol%)
 DIPEA/AcOH (2.0 eq.), Solv.
 7 W blue LED

Entry ^a	Conditions	Yield (%) 152al ^b
1	MeOH	trace
2	CHCl ₃	-
3	DMSO	31
4	THF	19
5	ACN	29
6	DMF/H ₂ O = 10:1	20
7	DMF	35

^a All the reactions were carried out under nitrogen atmosphere with dry solvent (0.2M). **145a:1511:cat.:[Ni]:dtBuppy:DIPEA:AcOH** = 1:2.5:0.01:0.05:0.06:2:2, (0.2 mmol scale of **145a**). ^b After flash chromatography.

We proposed that the formation of the pyrrole was related to the tautomerism of aldehyde to enol form, so we used the phenylacetaldehyde as substrate. As predicted, under standard condition, the phenylacetaldehyde gave 42% yield (Table 3.3, entry 1). We suspected that the weakness of the light might result in the low transformation efficiency, so 23 W bulb was used which turned out to be too strong for the reaction (Table 3.3, entry 2). The control experiment was conducted to confirm the roles of Ni(II), DIPEA and 4,4'-di-tertbutylbipyridine. With none of them, the reaction gave only 24% yield (Table 3.3, entry 3), meanwhile, to our surprise with only the presence of diisopropylethylamine (DIPEA) and 4,4'-di-tertbutylbipyridine, the reaction afforded 68% yield (Table 3.3, entry 4.). So, the Ni(II) was confirmed to be not necessary for the process. Then the [Ru(4,4'-(^tBu)₂bpy)₃](PF₆)₂ was used to replace the original photocatalyst, which was demonstrated to be more efficient to provide 73% yield (Table 3.3, entry 5). To our astonishment, at the absence of DIPEA, the reaction even furnished higher yield to be 74% (Table 3.3, entry 6).

This outcome reflected that during the reaction process, the photoexcited ruthenium complex did not grab the electron from the DIPEA. And according to the reaction with replacement of azide with amine (Table 3.3, entry 7), there was no reaction took place. Therefore, we could tell that, the azide either went through the energy transfer process or was reduced by photoexcited catalyst.

As we know from the entry 2 that stronger light might cause loss of the yield, we tried the fainter light (1 W) which was proved to be not sufficient (Table 3.3, entry 8). We also tried the [Ir] without presence of DIPEA which gave slightly lower yield (Table 3.3, entry 9). Since the beginning of this project, we had used the degassed solvent, so we tried the undegassed solvent which nearly stopped the reaction (Table 3.3, entry 10).

Table 3.3 The effect of the solvent to the reaction.

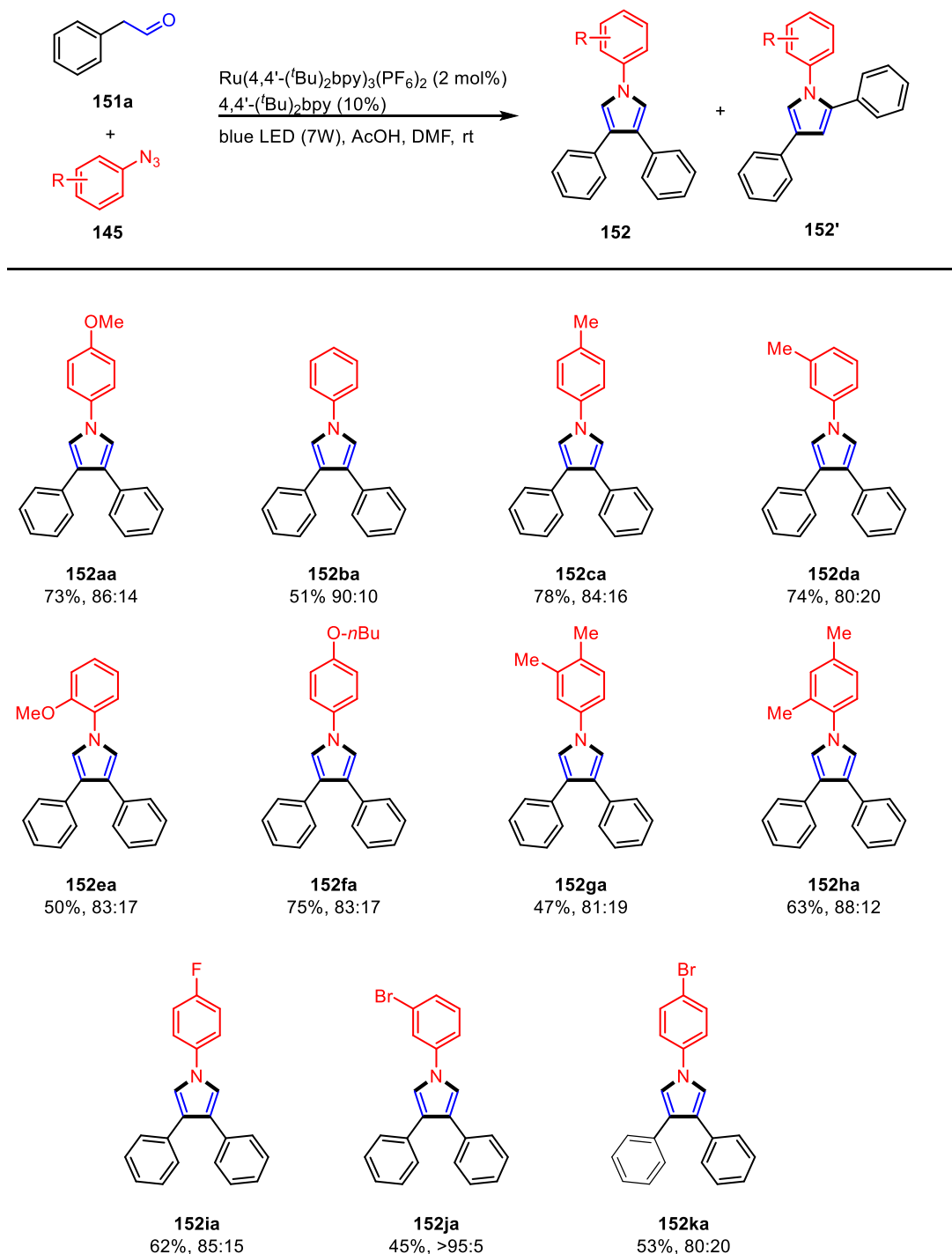
Entry ^a	Conditions	Yield (%) 152aa ^b	152aa : 152aa' ^c
1	[Ru(4,4'- <i>t</i> Bu) ₂ bpy) ₃]Cl ₂ (1 mol%) NiBr ₂ ·glyme (5 mol%) DIPEA (2 equiv)	42	88:12
2	[Ru(4,4'- <i>t</i> Bu) ₂ bpy) ₃]Cl ₂ (1 mol%) NiBr ₂ ·glyme (5 mol%), DIPEA (2 equiv), 23 W blue-LED	35	ND
3	[Ru(4,4'- <i>t</i> Bu) ₂ bpy) ₃]Cl ₂ (1 mol%) No 4,4'- <i>t</i> Bu) ₂ bpy, No DIPEA	24	87/13
4	[Ru(4,4'- <i>t</i> Bu) ₂ bpy) ₃]Cl ₂ (2 mol%) DIPEA (2 equiv)	68	90:10
5	[Ru(4,4'- <i>t</i> Bu) ₂ bpy) ₃](PF ₆) ₂ (2 mol%) DIPEA (2 equiv)	73	89:11
6	[Ru(4,4'- <i>t</i> Bu) ₂ bpy) ₃](PF ₆) ₂ (2 mol%) No DIPEA	74	86:14
7	<i>p</i> -anisidine instead of azide	0	--
8	[Ru(4,4'- <i>t</i> Bu) ₂ bpy) ₃](PF ₆) ₂ (1 mol%) Blue LED (1 W)	62	85/15
9	[Ir{dF(CF ₃)ppy} ₂ (dtbbpy)]PF ₆ (2 mol%) [Ru(4,4'- <i>t</i> Bu) ₂ bpy) ₃](PF ₆) ₂ (1 mol%)	67	84:16
10	Not degassed solvent	trace	--

^a All the reactions were carried out under nitrogen atmosphere with dry DMF (0.2M). **145a**:**151k**:dtbbpy:AcOH = 1:2.5: 0.06:2, (0.2 mmol scale of **145a**). ^b After flash chromatography. ^c Determined via GC-MS on the reaction crude. ND: not determined.

Up to now, the optimal condition has been established: [Ru(4,4'-*t*Bu)₂bpy)₃](PF₆)₂ (2 mol%), 4,4'-*t*Bu)₂bpy (10 mol%), AcOH (2 eq.), degassed DMF (0.12 M) as solvent, blue LED (7W), reaction time is 48 h.

Next, we tested the practicality of this protocol with a variety of substituted phenyl azide. (Scheme 3.13) First, followed the standard electron rich substituted phenyl azide, we tested the electron neutral phenyl azide which gave 50% yield without the group stabilizing the amino intermediate deriving from azide (**152ba**). Other electron-donating groups at the *para*-position such as methyl

and butoxy group were approved to be beneficial to the reactivity of the azide providing even higher yield (**152ca** & **152fa**). The electron donating groups at meta- and ortho- position were also tolerated in this protocol which afforded products in moderate yield (**152da** & **152ea**). The di-methyl substituted phenyl azide was also examined which gave only moderate yield (**152ga** & **152fa**). In



All the reactions were carried out under nitrogen atmosphere with dry solvent (0.2M). **145:151a:[Ru]:ditBupy:AcOH** = 1:2.5:0.02:0.10:2, (0.2 mmol scale of **145**). All the yield was gotten after flash chromatography.

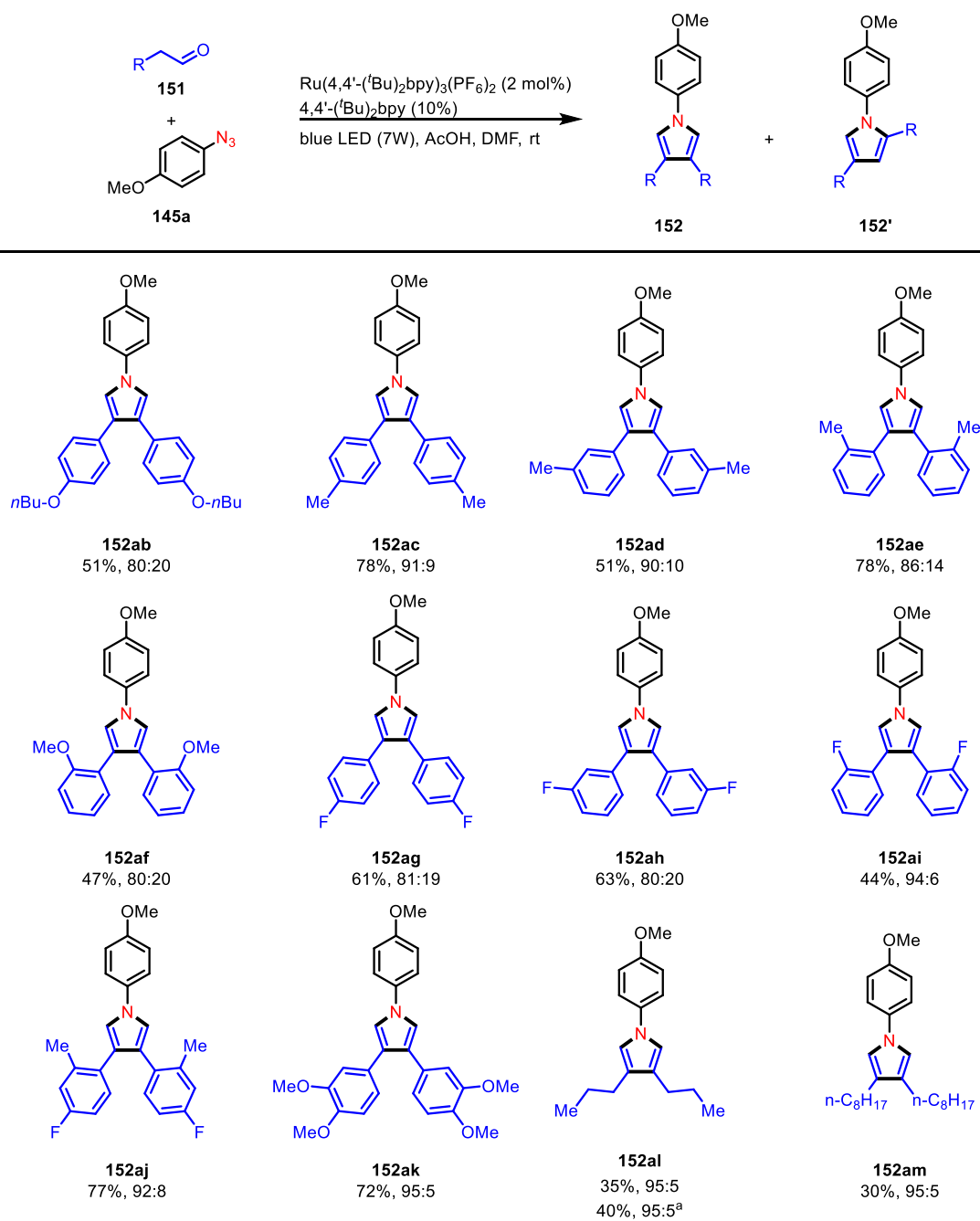
Scheme 3.13 The scope of the azide of photocatalyzed synthesis of pyrrole

most case, the halide was sensitive to the radical intermediate to some extent, therefore it was

reasonable that the para- and meta-bromophenyl azide gave lower yield (**152ja** & **152ka**). Generally speaking, the fluoride possesses more compatibility with the radical environment. Hence, the reaction condition seemed friendly to parafluorophenyl azide giving 62% yield (**152ia**).

This reaction also faces limitations to other azides such as benzoyl and sulfonyl azides which stayed untouched under standard condition.

As usual, we explored the scope of aldehyde of the protocol. The electron donating groups at para-, meta- and ortho- position were all tolerated in this reaction delivering moderate to good yield with regioselectivity of better than 4:1. This reaction also exhibited no limitation to the electron deficient

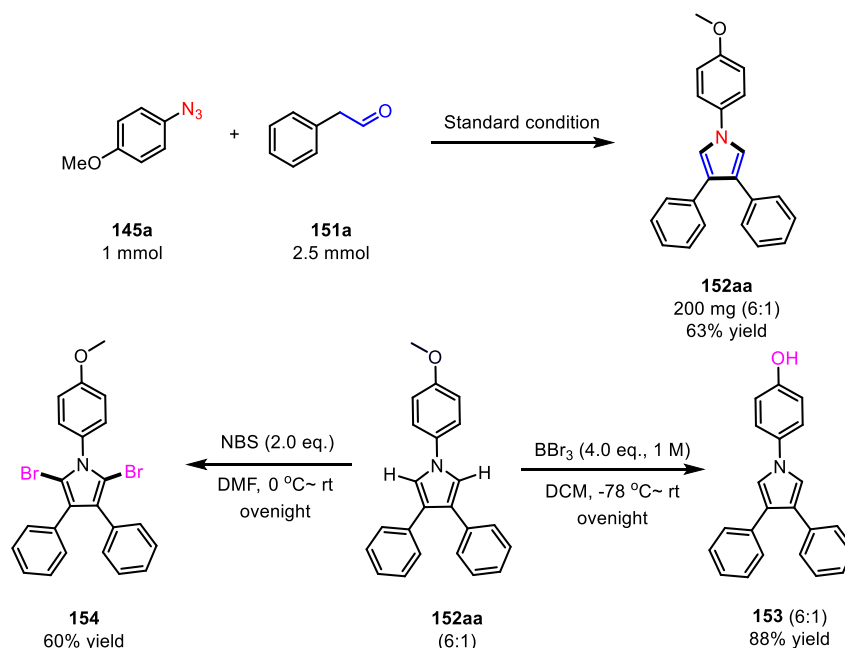


All the reactions were carried out under nitrogen atmosphere with dry DMF. **145a:151:[Ru]:dtBubpy:AcOH** = 1:2.5:0.02:0.10:2, (0.2 mmol scale of **145a**). All the yields were gotten after flash chromatography.

Scheme 3.14 The scope of aldehyde.

aryl ring of the aldehyde affording moderate yield. Interestingly, the aryl ring with two functional groups showed distinctly higher regioselectivity with good yield than other monosubstituted phenylacetaldehyde. To our surprise, the linear aldehyde with long aliphatic chain turned out to be efficient substrate of this protocol delivering product in more than 30% yield with excellent regioselectivity (>95:5).

To further explain the utility of this methodology, we did the scale-up reaction under standard condition in 1 mmol scale which provided the product in 63% yield with regioselectivity of 6:1. In addition to that, when the standard product was exposed to 2 equivalent *N*-bromosuccinimide (NBS), 1,3,4-triphenyl-2,5-dibromopyrrole was produced in 60% yield as single product. Besides, the methyl group of the standard product could be removed efficiently in 80% yield when exposed to boron tribromide at low temperature (Scheme 3.15)²².



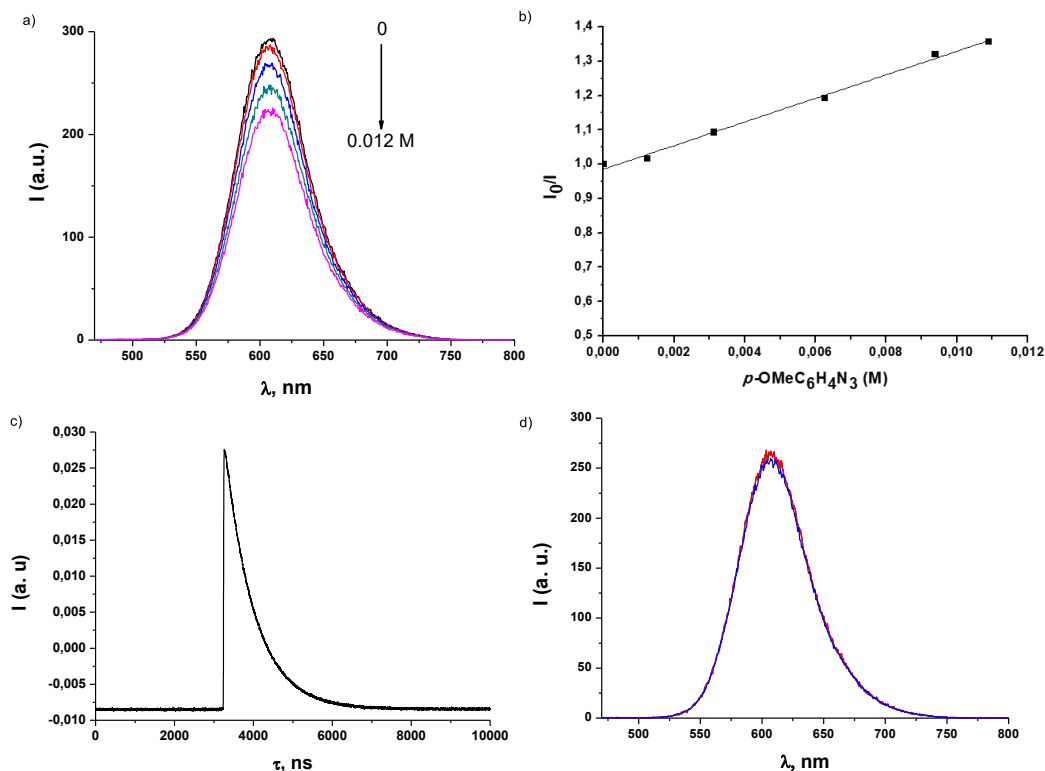
Scheme 3.15. The scale-up reaction and applications of the product **152aa**.

As aforementioned, there were two possible mechanistic pathways, a) the reaction went through an energy transfer process; b) the azide was reduced through single electron transfer (SET) by the photoexcited Ru(II) in which case some radical intermediates were supposed to be produced.

To shed light on the mechanism of the reaction, our co-worker conducted the elementary experiment. The photophysics of [Ru(4,4'-*t*Bu)₂bpy)₃](PF₆)₂ was investigated in acetonitrile, and an oxygen sensitive emission centered at 608 nm was found (Scheme 3.16). Interestingly, the emission of the complex resulted efficiently quenched by *p*-MeOC₆H₄N₃ whereas the presence of phenyl acetaldehyde and CH₃COOH was found ineffective (figure ST2). The emission lifetime (τ) of the complex in Ar-saturated acetonitrile was measured by means of Laser Flash Photolysis experiments and quantified in 745 ns. On the basis of these results and on the Stern Volmer equation:

$$[I]/[I_0] = 1 + K_q \tau [Q]$$

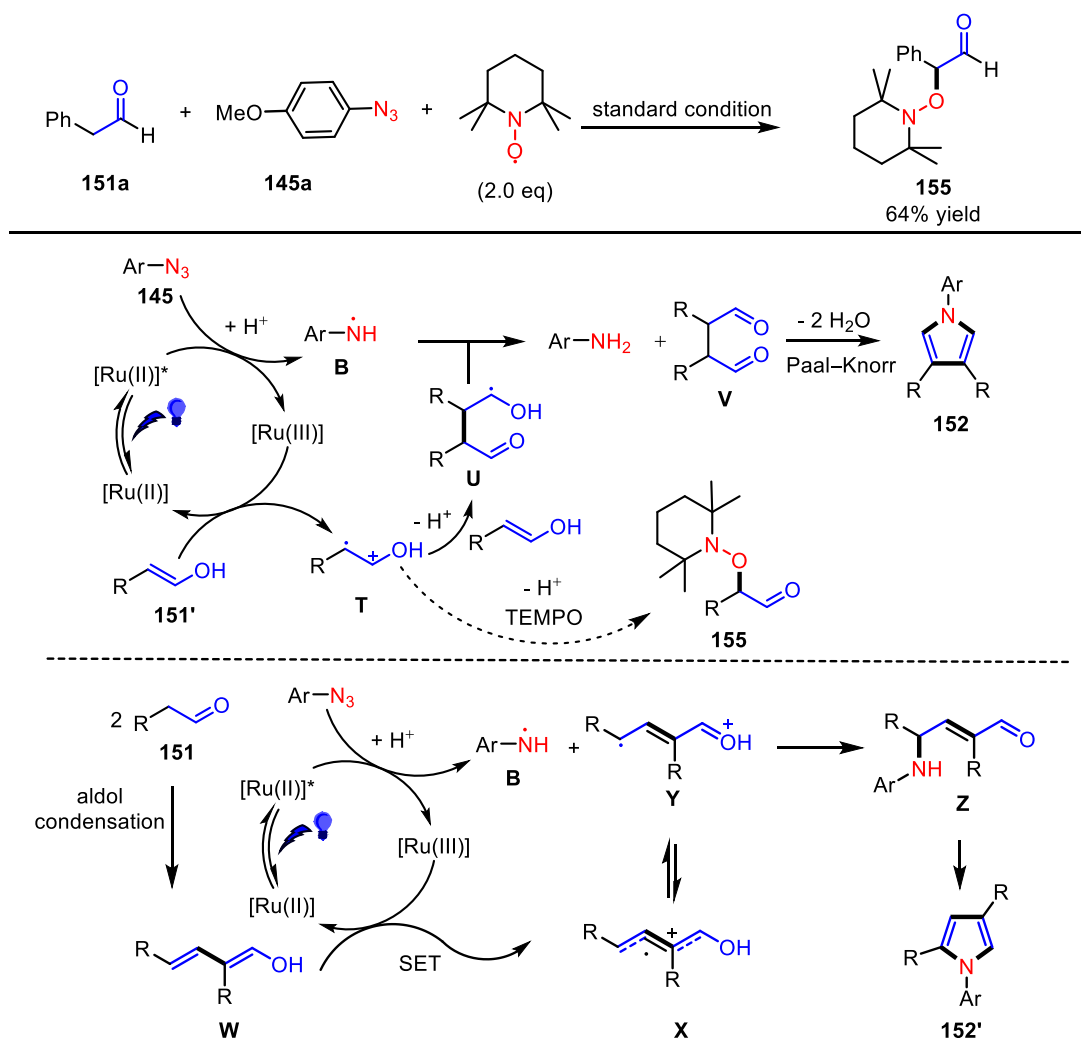
4.6 x 10⁷ s⁻¹ M⁻¹ value for K_q was obtained.



Scheme 3.16 a) Quenching experiments carried out on an Ar-saturated solution of $[\text{Ru}(\text{dbtbbpy})_3(\text{PF}_6)_2]$ 2×10^{-5} M in MeCN with increasing concentration of $p\text{-MeOC}_6\text{H}_4\text{N}_3$. b) measured Stern-Volmer. c) Time resolved emission of a solution of an Ar-saturated solution of $[\text{Ru}(4,4'\text{-}(t\text{Bu})_2\text{bpy})_3](\text{PF}_6)_2 \times 10^{-5}$ M in MeCN recorded at 630 nm. The lifetime of the emission was quantified in 745 ns. d) Emission of an Ar-saturated solution of $[\text{Ru}(4,4'\text{-}(t\text{Bu})_2\text{bpy})_3](\text{PF}_6)_2 \times 10^{-5}$ M in i) neat MeCN (blue line) and ii) in MeCN in the presence of CH_3COOH 0.1 M and phenyl acetaldehyde 0.02 M (red line).

On the other hand, we used the TEMPO to capture the proposed radical intermediate of SET pathway under standard condition, which gave the product **155** in 64% yield. (Scheme 3.17) Taking all the evidences into account, we propose the possible mechanism to be as follows. The ground state Ru(II) complex could be excited by the photon to triplet state ($\text{Ru}(\text{II})^*/\text{Ru}(\text{III}) = -1.20$ V vs SCE) which could transfer one electron to azide ($E = -0.39$ V vs SCE for $p\text{-NO}_2\text{-phenylazide}$) to deliver an anilino radical **B** after protonation and Ru(III) complex. Then, the Ru(III) deprives one electron from the enol **151'** (tautomer of aldehyde) to give a ground state Ru(II) complex and an radical cation **T**. The radical cation would couple with another equivalent enol forming radical intermediate **U**. The preformed anilino radical **B** could deprive the electron from radical **U** providing an aniline and 1,4-dicarbonyl compound **V**. Under acidic condition, the aniline and aldehyde **V** take place Paal-Knorr reaction affording final product.

On the other hand, because of the high propensity of aldol reaction, the condensation of aldehyde would happen easily under catalysis of acetic acid providing dienol compound **W**. Afterwards, the Ru(III) grab one electron from **W** giving the radical cation **X** which is in equilibrium with **Y** which we propose is more stable than other tautomers. Subsequently, the anilino radical could couple with **Y** affording unsaturated γ -aminobutaldehyde **Z**. At last, **Z** condensed and annulated easily to provide the byproduct **152'**. Since the reactivity of aliphatic linear aldehyde is not as high as 2-phenylacetaldehyde, the regioselectivity of former one is supposed to be better than the later one which is consistent to the result of our experiment.



Scheme 3.17 Capture of proposed radical intermediate and proposed mechanism.

3.3 Conclusions

In summary, we developed an unprecedented photocatalyzed synthesis of 1,3,4-trisubstituted symmetric pyrrole from commercially available starting materials (aldehyde and azide) in good regioselectivity and moderate to good yield. This methodology features a pretty mild reaction condition (2 mol% [Ru(II)] photocatalyst, 7 W blue-LED irradiation, 2 equivalent acetic acid, 10 mol% 4,4'-(tBu)₂bpy and room temperature) without demand of any oxidant such as Mn(III), O₂, or TBHP and is potentially applicable to biological molecules. The utility of the reaction is further demonstrated by the transformation of 2,5-dibromination and liberalization of the phenolic hydroxyl group of substitution on nitrogen. From mechanism respect, this reaction protocol features an photoredox process; in combination with optical experiment, our work drops a hint on that the aryl azide could be reduced through depriving one electron from photoexcited Ru(II)* which is supplementary to the oxidation of Ru(I) process.



Reference

- ¹ K. L. Skubi, T. R. Blum, T. P. Yoon, *Chem. Rev.* **2016**, *116*, 10035 – 10074.
- ² a) M. D. Tzirakis, I. N. Lykakis, M. Orfanopoulos, *Chem. Soc. Rev.* **2009**, *38*, 2609–2621. b) J.G. West, D. Huang, E. J. Sorensen, *Nat. Comoun.* **2015**, *1* – 7.
- ³ Q. Zhou, Y. Zou, L. Lu, W. Xiao, *Angew. Chem. Int. Ed.* **2018**, *57*, 2 – 21.
- ⁴ Y. Chen, A. S. Kamlet, J. B. Steinman, D. R. Liu, *Nat. Chem.* **2011**, *3*, 146 – 153.
- ⁵ E. P. Farney, T. P. Yoon, *Angew. Chem. Int. Ed.* **2014**, *53*, 793 – 797.
- ⁶ J. Xuan, X.-D. Xia, T.-T. Zeng, Z.-J. Feng, J.-R. Chen, L.-Q. Lu, W.-J. Xiao, *Angew. Chem. Int. Ed.* **2014**, *53*, 5653 – 5656.
- ⁷ X.-D. Xia, J. Xuan, Q. Wang, L.-Q. Lu, J.-R. Chen, W.-J. Xiao, *Adv. Synth. Catal.* **2014**, *356*, 2807 – 2812
- ⁸ E. Brachet, T. Ghosh, I. Ghosh and B. König, *Chem. Sci.*, **2015**, *6*, 987.
- ⁹ S. O. Scholz, E. P. Farney, S. Kim, D. M. Bates, T. P. Yoon, *Angew. Chem. Int. Ed.* **2016**, *55*, 2239 – 2242; *Angew. Chem.* **2016**, *128*, 2279 – 2282.
- ¹⁰ S. Zhu, A. Pathigoolla, G. Lowe, D. A. Walsh, M. Cooper, W. Lewis, H. W. Lam, *Chem. Eur. J.* **2017**, *23*, 17598 – 17604.
- ¹¹ M. O. Konev, T. A. McTeague, J. W. Johannes, *ACS Catal.* **2018**, *8*, 9120 – 9124.
- ¹² A. Loudelt, K. Burgess, *Chem. Rev.* **2007**, *107*, 4891 – 4932.
- ¹³ (a) J. M. Muchowski, *Adv. Med. Chem.* **1992**, *1*, 109. (b) P. Cozzi, N. Mongelli, *Curr. Pharm. Des.* **1998**, *4*, 181. c) C. T. Walsh, S. Garneau-Tsodikova, A. R. Howard-Jones, *Nat. Prod. Rep.*, **2006**, *23*, 517; (d) I. S. Young, P. D. Thornton, A. Thompson, *Nat. Prod. Rep.*, **2010**, *27*, 1801; (e) H. Fan, J. Peng, M. T. Hamann, J.-F. Hu, *Chem. Rev.*, **2008**, *108*, 264.
- ¹⁴ a) M. Zhang, H. Neumann, M. Beller, *Angew. Chem., Int. Ed.*, **2013**, *52*, 597 – 601; b) S. Michlik, R. Kempe, *Nat. Chem.*, **2013**, *5*, 140 – 144.
- ¹⁵ a) M. P. Huestis, L. Chan, D. R. Stuart, K. Fagnou, *Angew. Chem. Int. Ed.*, **2011**, *50*, 1338 – 1341; b) S. Rakshit, F. W. Patureau, F. Glorius, *J. Am. Chem. Soc.*, **2010**, *132*, 9585 – 9587.
- ¹⁶ a) D. J. Cyr, B. A. Arndtsen, *J. Am. Chem. Soc.*, **2007**, *129*, 12366 – 12367; b) Y. Lu, B. A. Arndtsen, *Angew. Chem., Int. Ed.*, **2008**, *47*, 5430 – 5433; c) E. Lourdasamy, L. Yao, C.-M. Park, *Angew. Chem., Int. Ed.*, **2010**, *49*, 7963 – 7967; d) D. K. Tiwari, J. Pogula, B. Sridhar, D. K. Tiwari, P. R. Likhar, *Chem. Commun.* **2015**, 13646 – 13469.
- ¹⁷ a) Z. W. Gilbert, R. J. Hue, I. A. Tonks, *Nat. Chem.* **2016**, *8*, 63 – 68; b) K. Kawakita, E. P. Beaumier, Y. Kakiuchi, H. Tsurugi, I. A. Tonks, K. Mashima, *J. Am. Chem. Soc.* **2019**, *141*, 4194 – 4198.
- ¹⁸ a) L. Wang, L. Ackermann, *Org. Lett.*, **2013**, *15*, 176 – 179; b) A. Mizuno, H. Kusama, N. Iwasawa, *Angew. Chem., Int. Ed.*, **2009**, *48*, 8318 – 8320; c) M. Farahi, M. Davoodi, M. Tahmasebi, *Tetrahedron Lett.* **2016**, *57*, 1582 – 1584; d) X. Wu, K. Li, S. Wang, C. Liu, A. Lei, *Org. Lett.* **2016**, *18*, 56 – 59; e) Y. Zheng, Y. Wang, Z. Zhou, *Chem. Commun.* **2015**, 16652 – 16255; f) X. Feng, Q. Wang, W. Lin, G. Dou, Z. Huang, D. Shi, *Org. Lett.* **2013**, *15*, 2542 – 2545; g) S. Pusch, D. Kowalczyk, T. Opatz, *J. Org. Chem.* **2016**, *81*, 4170 – 4178; h) X. Qi, H. Xiang, Y. Yang, C. Yang, *RSC Adv.* **2015**, *5*, 98549 – 98552; i) Z. W. Gilbert, R. J. Hue, I. A. Tonks, *Nat. Chem.* **2016**, *8*, 63 – 68; j) A. Keeley, S. McCauley, P. Evans, *Tetrahedron* **2016**, *72*, 2552 – 2559; k) C. Wang, K. Huang, J. Wang, H. Wang, L. Liu, W. Chang, J. Li, *Adv. Synth. Catal.* **2015**, *357*, 2795 – 2802; l) J. Zheng, L. Huang, Z. Li, W. Wu, J. Li, H. Jiang, *Chem. Commun.* **2015**, 5894 – 5897.
- ¹⁹ a) S. Urban, L. Hobbs, J. N. A. Hooper, R. J. Capon, *Aust. J. Chem.*, **1995**, *48*, 1491 – 1494; b) K. Ohta, F. Taguchi, Y. Endo, *Heterocycles*, **2012**, *86*, 165 – 170; c) V. A. Anisimova, A. A. Spasov, I. A. Bocharova, O. V. Ostrovskii, T. I. Panchenko, G. P. Dudchenko, *J. Pharm. Chem.*, **1996**, *30*,

22 – 26; d) D. R. Soenen, I. Hwang, M. P. Hedrick, D. L. Boger, *Bioorg. Med. Chem. Lett.* **2003**, *13*, 1777 – 1781.

²⁰ (a) Q. Li, A. Fan, Z. Lu, Y. Cui, W. Lin, Y. Jia, *Org. Lett.* **2010**, *12*, 4066 – 4069; (b) H. Huang, L. Tang, J. Cai, G.-J. Deng, *RSC Adv.* **2016**, *6*, 7011 – 7014; (c) Y. Gao, C. Hu, J.-P. Wan, C. Wen, *Tetrahedron Lett.* **2016**, *57*, 4854 – 4857; (d) J.-C. Zheng, H. Xu, Z. Zhang, *Tetrahedron Lett.* **2017**, *58*, 674 – 678; (e) D. Tzankova, S. Vladimirova, L. Peikova, M. Gerogieva, *J. Chem. Tech. Met.* **2018**, *53*, 451 – 464.

²¹ A. M. Whittaker, V. M. Dong, *Angew. Chem. Int. Ed.* **2015**, *54*, 1312 – 1315.

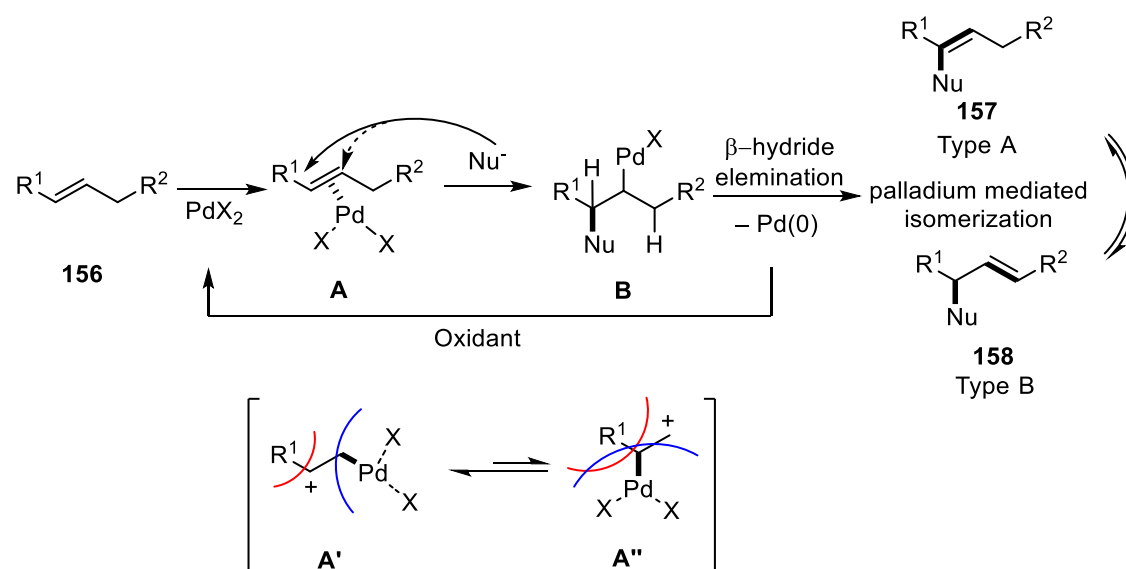
²² a) K. Tomoshige, T. Takeo, T. Yoko, U. Yosuke, *Tetrahedron*, **2001**, *57*, 9073 – 9085; b) T. Xu, R. Lu, X. Liu, X. Zheng, X. Qiu, Y. Zhao, *Org. Lett.*, **2007**, *9*, 797 – 800.

4 Photocatalyzed Wacker Oxidation of Trisubstituted Alkene

4.1 Introduction: Wacker Oxidation

Since the alkene is one of the most abundant resources on the earth, which is the cornerstone of modern chemical industry. As starting material, it has been transformed to be quite a number of building blocks to be further used. Therefore, the oxidation reaction to introduce the heteroatom into alkene is one type of the most useful and important reactions that have been developed. One of the most important metal catalyzed oxidation of olefin is Wacker oxidation (Scheme 1), which not only showcases the practical utility of huge economic merit, but also is a milestone which opened a new field of palladium chemistry.

The mechanism of Wacker oxidation has been studied for more than 60 years. This Wacker-type oxidation depends on the strong palladium– π -orbital interaction **A**, which increases the propensity of carbon-carbon double bond to be attacked by water which ends up with the hydroxypalladation intermediate **B**. (Scheme 4.1) The intermediate goes through β -hydrogen elimination providing the final product **157** or **157'** which in some cases followed by palladium-mediated isomerization (**157** \leftrightarrow **157'**) and a palladium(0) complex which could be oxidized to palladium(II) to restart a new reaction cycle.¹ The controversial part of the mechanism is the hydroxypalladation step since both *syn*- and *anti*- pathway were all supported by different reactions.² But it is more believed that the pathway is a condition-depending process, such as the lower concentration of Cl^- would favor the *syn*- hydroxypalladation.



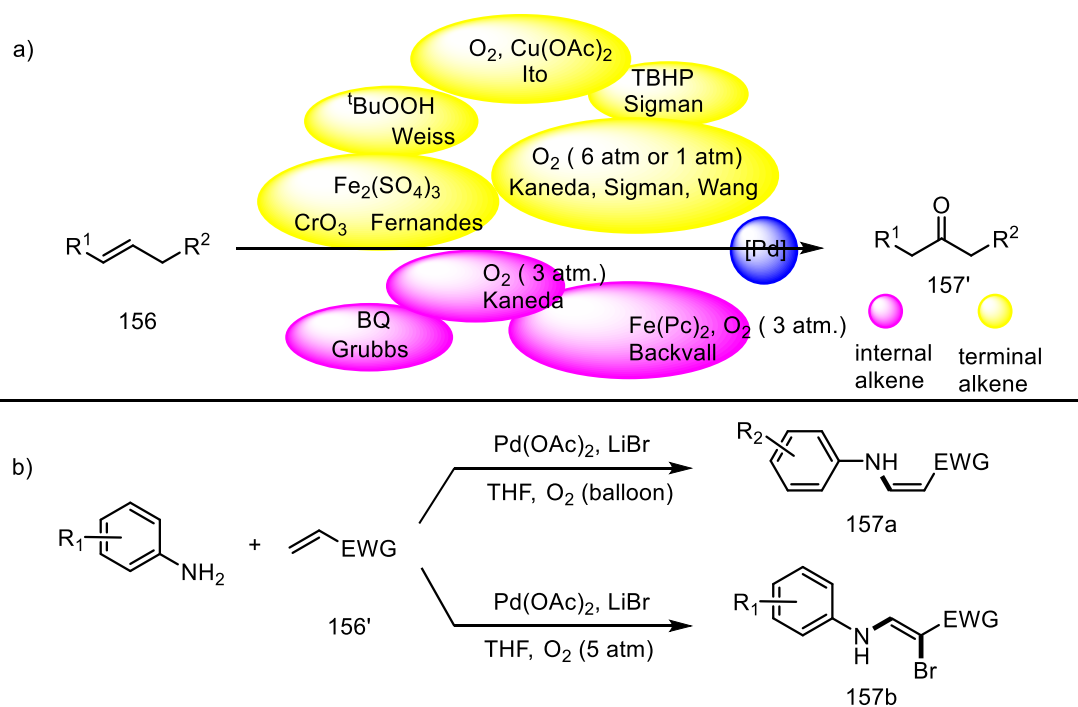
Scheme 4.1 Pathway of Wacker oxidation and regioselectivity.

Another aspect of the reaction has been studied thoroughly is on the regioselectivity. In most cases, the terminal alkene would provide methyl ketone exclusively which followed the Markovnikov's role (Scheme 4.1). This regioselectivity was rationalized by that the cationic center formed at more substituted carbon during the hydroxy-palladation could be further stabilized by the substitution.

Meanwhile, the less repulsion when the bulky palladium hinged to less hindered carbon also promoted this regioselectivity ($A' \leftrightarrow A''$). In addition to that, the subsequently developed ligand could inverse the regioselectivity with the aldehyde as exclusive product.³ Other factors, such as the directing group, could also lead to the formation of aldehyde;⁴ the usage of bulky solvent *tert*-butyl alcohol also favored the formation of anti-Markovnikov product⁵. The role of the bulky alcohol served as not only solvent but also the oxygen nucleophile provider which inclines to attack at less hindered carbon atom of the alkene.

The practical Wacker oxidation in laboratory needed high loading of the catalyst and stoichiometric quantities of copper salt which is not desirable.⁶ (Scheme 4.2 a) Therefore, other oxidant are developed to promote the turnover of the catalyst, such as *tert*-butyl hydroperoxide (tBuOOH)⁷, metal salt ($\text{Fe}_2(\text{SO}_4)_3$, CrO_3)⁸. (Scheme 4.2 a) The usage of molecule oxygen was first reported by Kaneda under high pressure, wherein the atmospheric oxygen was harnessed directly with sparteine as ligand or at the presence of trifluoroacetic acid (TFA).⁹ (Scheme 4.2 a)

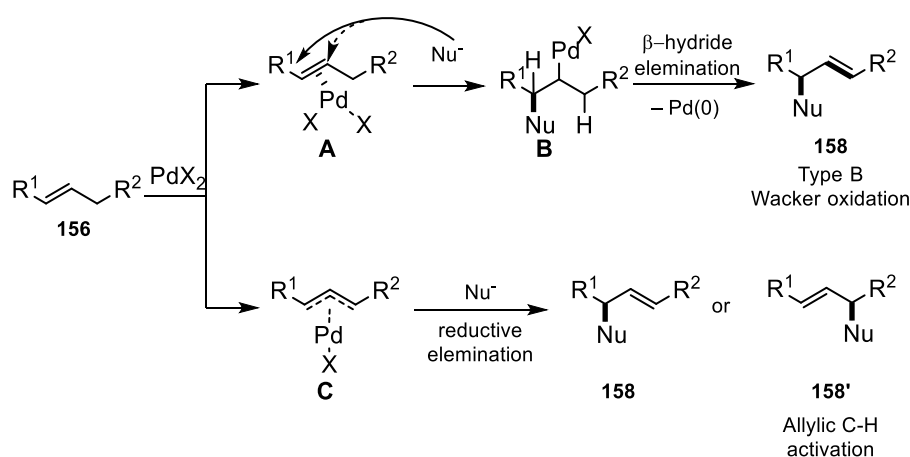
The traditional Wacker oxidation condition was not desirably adaptable to internal alkene because of low yield. In the past several years, a substantial progress has been made by chemists. Bäckvall found an BQ/ $\text{Fe}(\text{pc})$ catalyst system (pc = phthalocyanine) to make use of molecule oxygen as oxidant to realize non-terminal Wacker oxidation. Kaneda developed mixed solvent (DMF- H_2O) to facilitate oxidation. Grubbs developed a cationic palladium strategy. And the Quinox ligand was also used by Sigman in this kind of reaction (Scheme 4.2 a).¹⁰



Scheme 4.2 Development of traditional Wacker oxidation.

Instead of oxygen, the nitrogen could also be used as nucleophile which is called ‘aza-Wacker’ oxidation. It was found by Wang group that in the presence of $\text{Pd}(\text{OAc})_2$, O_2 and excess of Br^- , the acrylate or other electron-deficient alkene and anilines could provide *Z*-enamines **157a** (Scheme 4.2b).¹¹ Meanwhile, a slight change upon pressure of O_2 could exert effect on formation of the α -brominated *Z*-enamines **157b**.

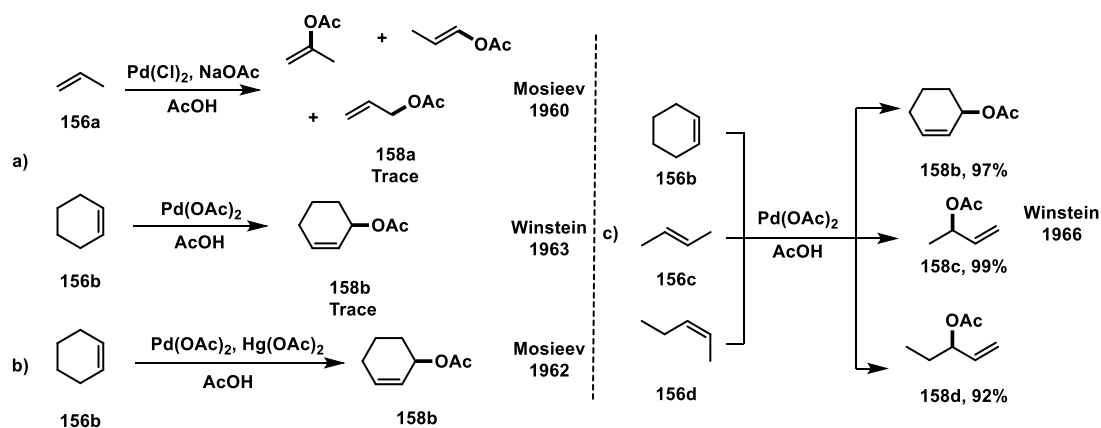
As aforementioned, after the oxy-palladation of the Wacker oxidation process, there are two possible β -hydrogen elimination pathways, a retro elimination to afford the enol ether/aldehyde (Scheme 4.3 Type A), or the other one aloof from oxygen to provide allylic alcohol or ester or allylic amine (when the nucleophilic atom was nitrogen, Scheme 4.3 Type B). Allylic alcohol and amine are ubiquitous moieties in the natural product, medicines, additionally, they have a wide range of application in synthetic chemistry the most typical of which are Sharpless asymmetric epoxidation¹² and Tsuji-Trost reaction¹³. In this context, the allylic oxidation has been studied as hot spot for years. The traditional methods to realize the allylic oxidation encounter several drawbacks including toxicity, environment problems and incompatibility with other functional groups.¹⁴ By contrast, the palladium(II) catalyzed allylic oxidation is milder and can be better tolerated by other groups. However, the mechanism is far from certainty, it may result from the Wacker oxidation (Type B), or allylic C-H functionalization wherein allyl-palladium intermediate **C** was formed (Scheme 4.2).



Scheme 4.3 Allylic oxidation catalyzed by palladium.

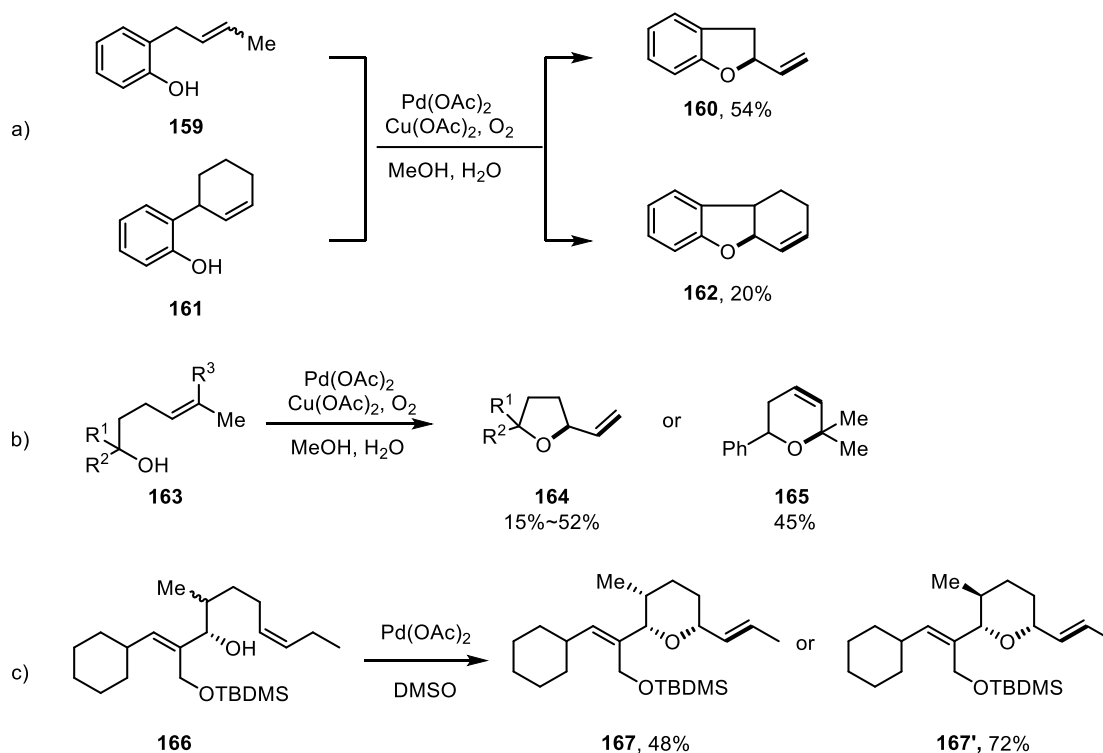
Herein, I would like to introduce the progress of preparation of allyl alcohol or amine through Wacker-type oxidation or similar process.

The type B Wacker oxidation was first reported in 1960s in Mosieev and Winstern's work as side product **158a**, **158b** (Scheme 4.4a).¹⁵ Soon after, Mosieev documented that with Hg(OAc)₂ as additive and carboxylic acid as solvent, the reaction provided the allylic ester **158b** as sole product (Scheme 4.4b). Then Winstern demonstrated the conversion of several internal alkene to



Scheme 4.4 The infancy of type B Wacker oxidation.

allylic ester **158b**, **158c**, **158d** in high yield (Scheme 4.5c).¹⁶ However, the mechanism was obscure, both Wacker oxidation and allylic C-H activation pathway could account for the formation of them. In 1975, Hosokawa and co-workers disclosed the palladium catalyzed intramolecular cyclization of 2-allyl-phenol **160**, **162** in moderate yield (Scheme 4.5a).^{17a} Afterwards, the preparation of 2-vinyltetrahydrofuran **164** and dihydropyran **165** through palladium(II) catalyzed cyclization of γ,δ -



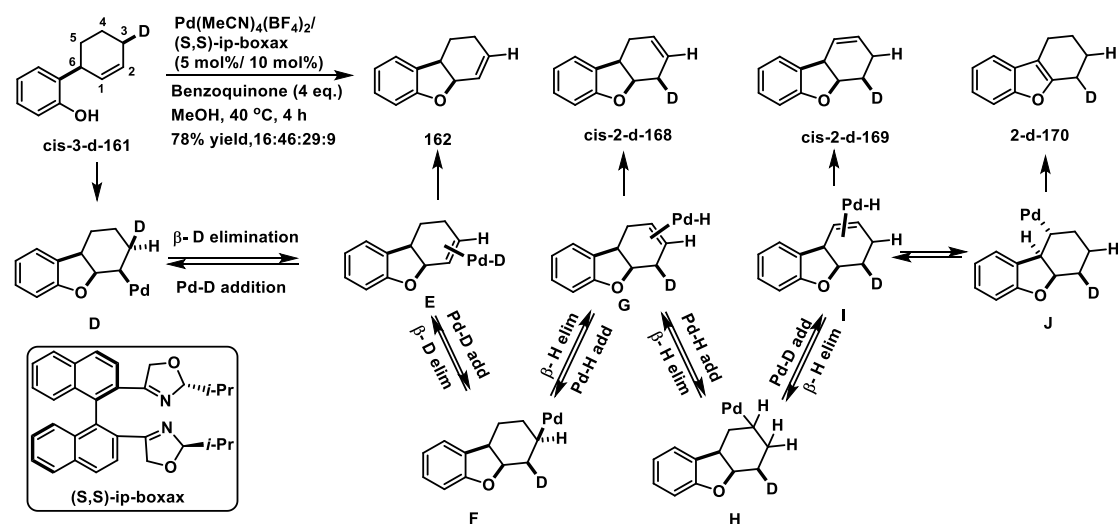
Scheme 4.5 Type B Wacker oxidation to construct tetrahydrofuran, di-/tetrahydropyran.

unsaturated alcohol **163** was reported. In the presence of Cu(II)-O₂ as oxidant, the reaction proceeded smoothly to provide the product in low to moderate yield. The vinyl group took *anti*-configuration to the group at C-1 when obvious steric difference existed between R¹ and R² (Scheme 4.5b).^{17b} Stoichiometric amount of palladium acetate was also used to synthesize pyran in complicated compounds **167** & **167'** was reported by Semmelhack (Scheme 4.5c).¹⁸ In this cyclization, the solvent DMSO was proved to be non-ignorable factor which effected the regioselectivity of the double bond.

Afterwards, using deuterated substrate (*cis*-3-d-**161** and *trans*-3-d-**161**) respectively, Hayashi studied the stereochemistry of the oxypalladation in Wacker-Type oxidative cyclization (Scheme 4.6).¹⁹ Take the *cis*- substrate as example: the reaction was conducted with Pd(MeCN)₄(BF₄)₂/(*S,S*)-ip-boxax (1:2) as catalyst, and benzoquinone (4 equivalent) as the oxidant in methanol at 40 °C which gave four regioisomeric analogues with ratio of 16/46/29/9 in 78% yield totally. The absence of the deuterium at C(3) position of **162**, *cis*-2-d-**168**, *cis*-2-d-**169**, 2-d-**170** and the appearance on C-2 position of *cis*-2-d-**168** and *cis*-2-d-**169**, demonstrated that the oxypalladation proceed through *syn*- mode. Only through *syn*- oxy-palladation, the intermediate **D** could be produced which after *syn*- β -H-elimination could provide alkene **E**. After the dissociation of palladium-deuterium from alkene, **162** containing no deuterium was produced. Then the palladium-

deuteration of C-C double bond could afford an intermediate **F** which after *syn*- β -H-elimination could provide alkene **G**. The dissociation of palladium-deuterium from alkene of alkene **G**, 2-deuterated **168** was produced. It is not difficult to understand that after a sequence of similar transformation, *cis*-2-d-**169** and 2-d-**170** could be formed.

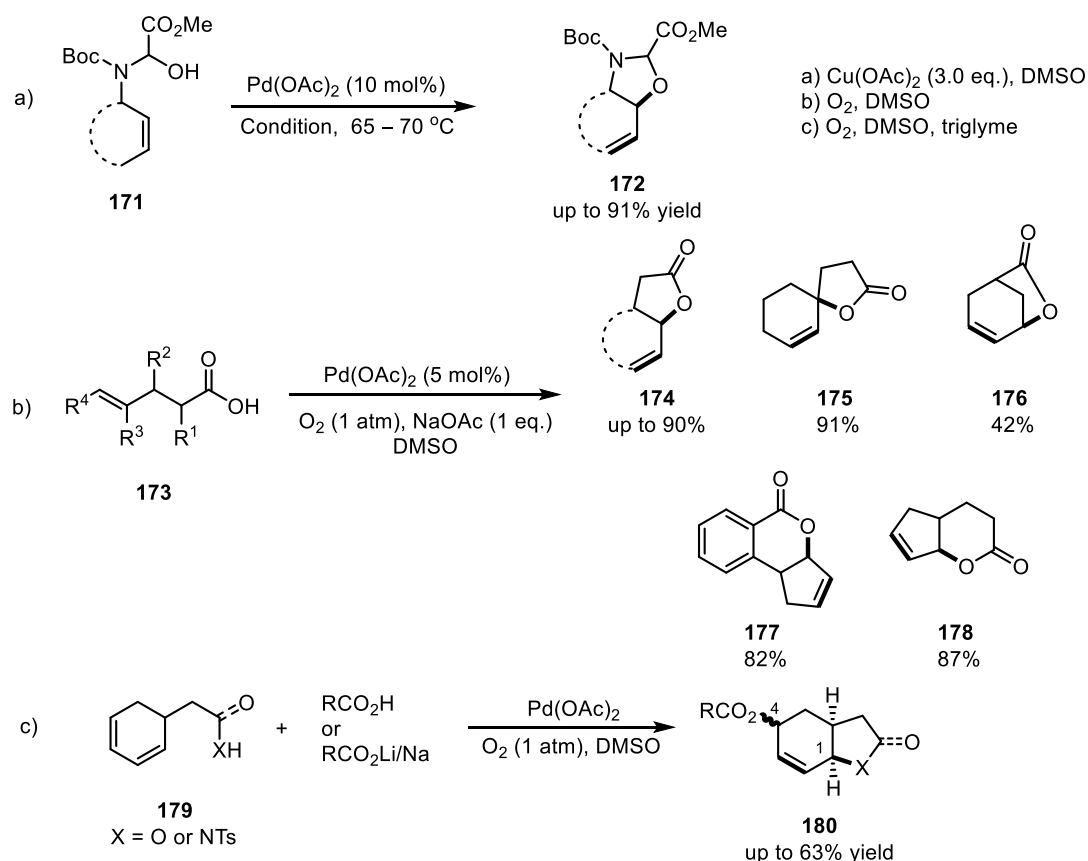
On the other hand, the *cis*-3-d-**161** was also used in the survey of the condition developed by Hegedus to synthesize nonaromatic nitrogen heterocycles using cyclization of *o*-olefinic tosamides: PdCl₂(MeCN)₂ (10 mol %), benzoquinone (1 eq.), Na₂CO₃ (2 eq.), and LiCl (2 eq.) in THF under reflux. The experiment disclosed that in the presence of chloride ion, the oxypalladation took *anti*-fashion.



Scheme 4.6 Deuterium labeling experiment to detect the stereochemistry of oxy-palladation.

Another catalytic system was developed by Hiemstra to synthesize *N*-Boc-1-aminoalk-3-en-2-ol **171** with Wacker oxidation as key step.²⁰ Both stoichiometric amount of Cu(OAc)₂ and molecule oxygen could be used as oxidant only if DMSO was used as solvent. During the reaction process, it did not turn black, but yellow, so the author suspected that the reacting catalyst was another species. Latter research demonstrated that, the role of the DMSO was far more than being solvent, which in fact turned out to be also a ligand; meanwhile the catalytic species was not simply the Pd(OAc)₂, but the giant palladium clusters of 26 ± 4 Å in size stabilized by DMSO (Scheme 4.7a&b).

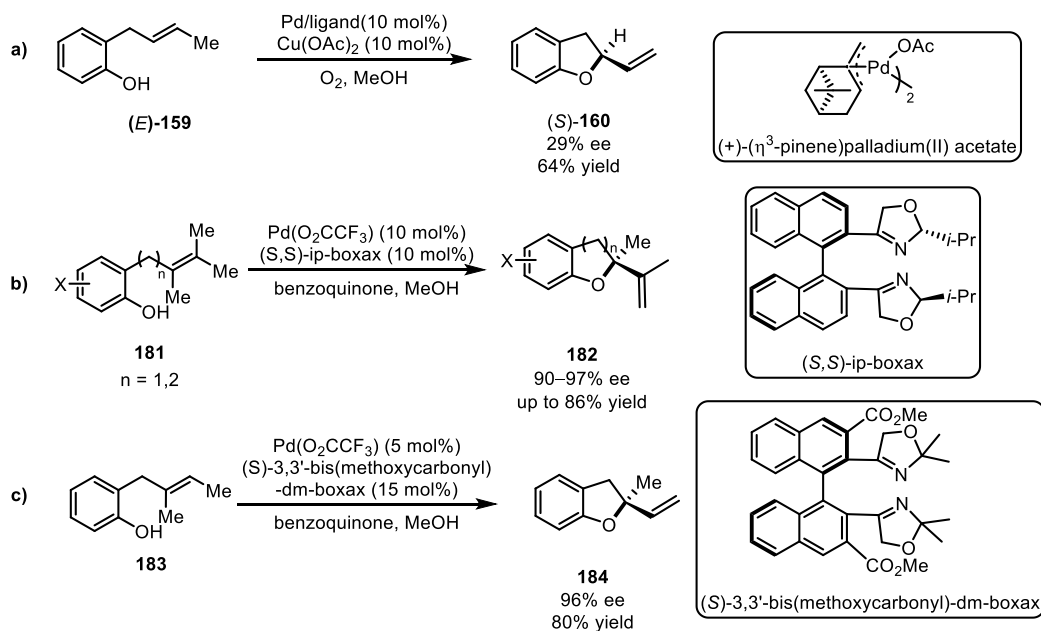
A similar catalytic system (at presence of 1 eq. NaOAc) was used by Larock to synthesize a series of unsaturated lactones **174** - **178** from corresponding acids. When the 1,3-diene compound **179** exposed to the O₂-DMSO system with another carboxylic compound, it provided 1,4-addition product **180** (Scheme 4.7c). If the substrate was unsaturated acid and the other nucleophile was carboxylic acid, the reaction tended to give 1,4-*cis*- addition product mainly, when the nucleophile was salt, 1,4-*trans* product was more preferable. If the substrate **179** was an alcohol, the reaction gave a mixture of *cis*- and *trans*- **180**.



Scheme 4.7 Utilizing O_2 as an oxidant with DMSO as solvent.

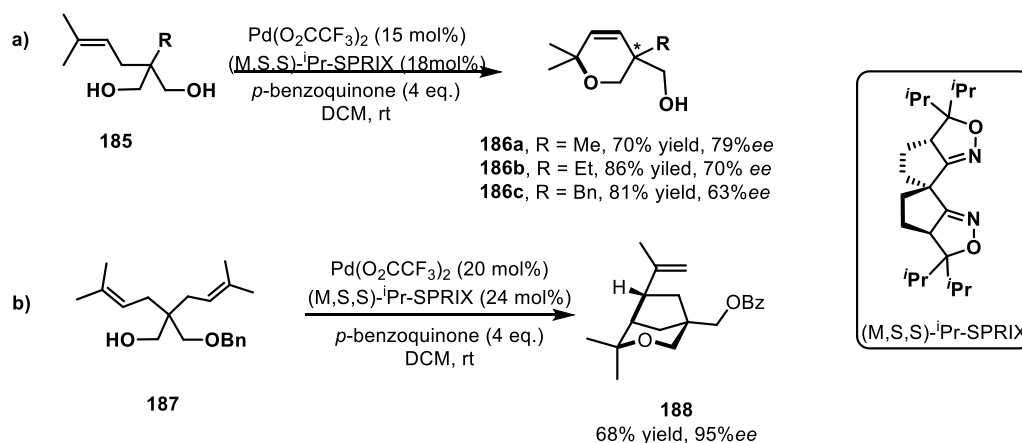
The catalytic asymmetric intramolecular Wacker oxidation was pioneered by Hosokawa and co-workers using (+)-(η^3 -pinene)palladium(II) acetate (10 mol%) as catalyst and Cu(II)-O_2 as oxidant (Scheme 4.8a).²¹ However, the enantioselectivity was not satisfying (up to 29% *ee*). It was not until 1997 that a practical breakthrough was made by Hayashi and co-workers.²² With the Pd(II)/(S,S) -ip-boxax as catalyst and benzoquinone as oxidant, the reaction proceeded smoothly providing unsaturated benzofuran or chromane type product **182** with excellent enantioselectivity and moderate to good yield (Scheme 4.8b). The loading of more than 1 equivalent benzoquinone and the species of counterion (CF_3CO_2^- , BF_4^-) of the palladium were found to be essential for the enantioselectivity, for example replacement of trifluoroacetate by chloride caused a drop of the enantioselective purity to 44% *ee*.

This type B Wacker oxidation turned out to be highly dependent on substitution of alkene. When the trisubstituted alkene **183** was used, the Pd(II)/(S,S) -ip-boxax could provide the product with very poor enantioselectivity. Further research showed that, if 3,3'-position of the backbone was sterically and electronically tuned properly by introduction of ester group, the reaction could provide the product **184** in satisfying yield with excellent enantioselectivity.



Scheme 4.8 Catalytic asymmetric intramolecular Wacker oxidation.

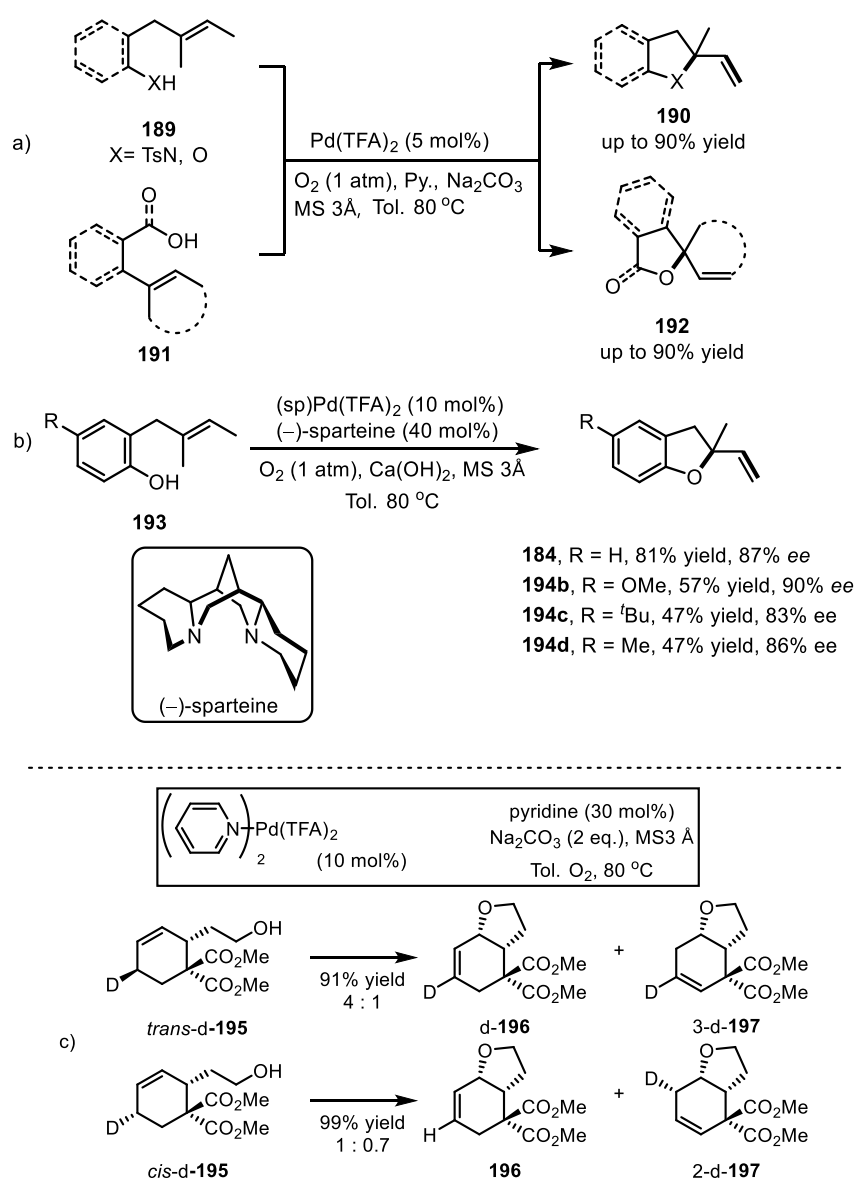
In 2001, Sasai used the novel *spiro*-bis(isoxazoline) ligand they designed in the Wacker type oxidation of γ,δ -unsaturated alcohol **185** which gave enantioselective pure dihydropyran **186** in up to 79% *ee* (Scheme 4.9a).²³ The 6-*endo* regioselectivity was proposed to attribute to the stability of the intermediary carbocation in the reaction process. It is noteworthy that, asymmetric catalysts aforementioned *i.e.* Pd(OCOCF₃)₂-(S,S)-ip-boxax and [(3,2,10- η^3 -pinene)-PdOAc]₂ could not promote the reaction. The reaction system not only showed the kinetic preference upon the hydroxy group, but also upon the alkene moiety (Scheme 4.9b). In the latter case, the catalyst not only showed higher enantioselectivity up to 95% *ee*, but also provided a fused ring compound after a sequence of C-O and C-C bond construction.



Scheme 4.9 Wacker oxidation through kinetic resolution process.

The ideal oxidant for oxidation reaction is always the oxygen, so that the byproduct is water. So, Stoltz documented the aerobic Wacker cyclization using O₂ as oxidant, and palladium trifluoroacetate (Pd(O₂CCF₃)₂) as catalyst at the presence of pyridine, sodium carbonate and

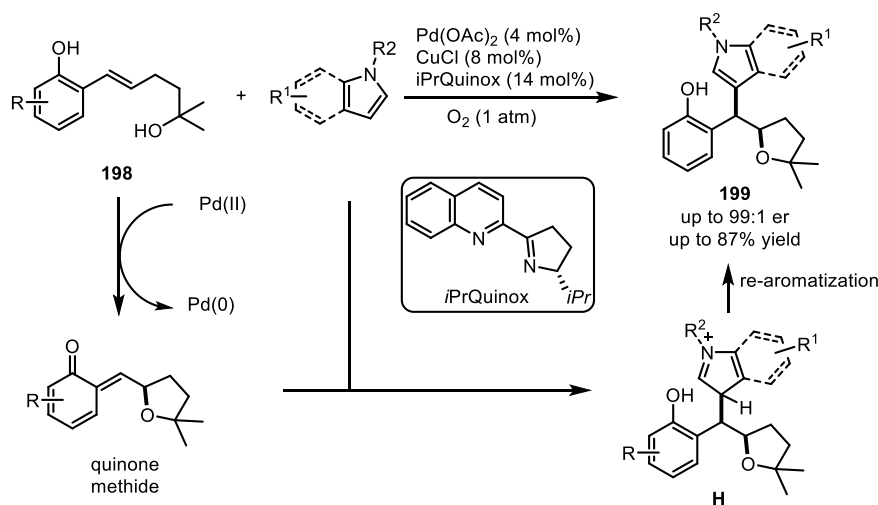
molecule sieves (3Å) in nonpolar solvent (toluene).²⁴ The strategy was applied to *ortho*-allylphenol or allylanilamide **189** to give unsaturated 2-vinylbenzofuran or spirocyclic ring product **190** in moderate to good yield. Afterwards, the scope was extended to γ,δ -unsaturated primary alcohol and carboxylic acid **191** (Scheme 4.10a). Then the bidentate ligand (–)-sparteine was tested for the enantioselective version of the phenol type substrate **193**, which gave up to 90% *ee* (Scheme 4.10b). A deuterium-labelling reaction similar to Hayashi's work was also conducted to get insight into the stereochemistry of oxy-palladation step with pyridine/Pd(O₂CCF₃)₂ as catalyst. According to the composition of the product, the cyclization of alcohol was suggested to proceed through *syn*-oxy-palladation fashion despite of the ligands being monodentate (pyridine), bidentate (bipyridyl) or the resource of the palladium. However, the oxy-palladation of the carboxylic acid tended to proceed through *anti*- fashion (Scheme 4.10c).



Scheme 4.10 Wacker oxidation using molecular O₂ as catalyst and deuterium labeling reaction.

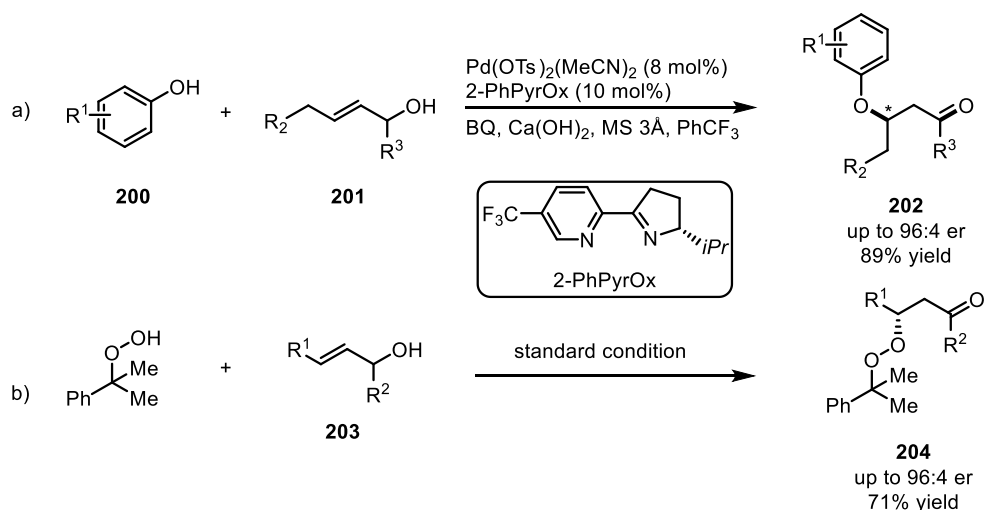
In 2010, Sigman and co-workers developed a palladium catalyzed asymmetric di-functionalization

of alkene with Wacker oxidation as an initial step with *i*PrQuinox as ligand (Scheme 4.11).²⁵ In the presence of the catalyst and O₂-Cu(I) as oxidant, an enantioselective Wacker oxidative oxypalladation took place which after extrusion of Pd(0) instead of β-hydride elimination gave an unsaturated conjugated ketone. The excess of nucleophile could adopt diastereoselective conjugated addition to provide the intermediate **H** which after re-aromatization could give **199** with high enantioselectivity and diastereoselectivity. This methodology showcased excellent tolerance to the substitution on the phenol ring, meanwhile, the electro-withdrawing ones generally gave higher yield. The utility of the methodology was further examined by the transformation of product to analogues of Communesin class natural products and the bio-activity of them turned out to be even more efficient in killing the tumor cell.



Scheme 4.11 Wacker oxidation using molecular O₂ as catalyst and deuterium labeling reaction.

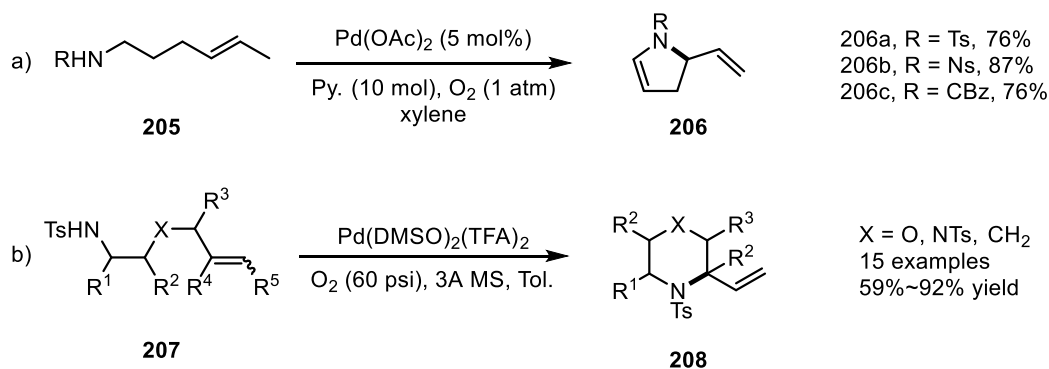
The enantioselective intermolecular type II Wacker oxidation of allylic alcohol **201** using a chiral pyridine oxazoline-ligated palladium catalyst was disclosed by Sigman and co-workers.²⁶ After a proposed *syn*- migratory insertion of the alkene into the Pd–O bond, the β-hydride elimination orienting to the hydroxyl group was proposed due to the difference between the acidity of 1-H of hydroxyl group and phenoxyl group. This reaction could tolerate a variety of substitution of the phenyl ring of phenol and Ts-, NC-, PhthN-, Cl- group at the chain of alcohol giving moderate yield with excellent enantioselectivity (Scheme 4.12a). In addition to that, the cumene hydroperoxide could also be used as nucleophile with O–O bond untouched in the product **204** to give 71% yield and good enantioselectivity (Scheme 4.12b).



Scheme 4.12 Enantioselective intermolecular type II Wacker oxidation.

Instead of the oxygen, the nitrogen could also be used as nucleophile in similar pathway to provide the allylic amine, which is called aza-Wacker Oxidation which appeared latter than the oxygen one. Since Kočovský and Bäckvall have gave the review,² herein I would like to give a brief introduction of this kind of reaction.

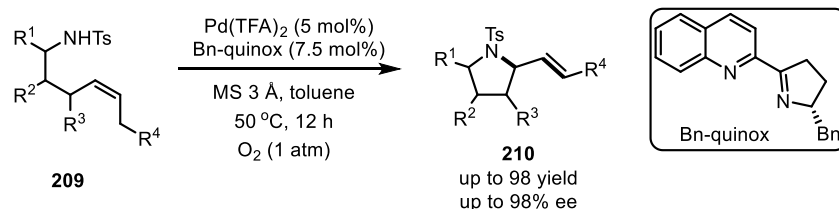
In 2002, Stahl and coworkers reported an efficient intramolecular aza-Wacker oxidation to prepare the substituted 2-vinylpyrrolidine **206** using dioxygen as oxidant (Scheme 4.13a).^{27a} In their catalyst system, the pyridine was used as ligand which was used by Stoltz in the study of Wacker oxidation as we aforementioned.²⁴ It is noteworthy that, this methodology showed superiority of turnover number to 250-300. A similar transformation to synthesize six-membered nitrogen heterocycles **208** from O, NTs, or methylene tethered alkene and amide **207** was achieved using Pd(DMSO)₂(TFA)₂ as catalyst and 60 psi of O₂ as oxidant (Scheme 4.13a).^{27b}



Scheme 4.13 Intramolecular aza-Wacker oxidation developed by Stahl.

An enantioselective version of palladium catalyzed aerobic oxidative amination of alkene was documented by Stahl and coworkers with Bn-quinox as ligand (Scheme 4.14).²⁸ This methodology showed excellent ability to control enantioselectivity which could tolerate different substitutions on various position to give up to 98% *ee*. When the enantioselective pure substrate was used as substrate, the racemic pyrox ligand could also provide good diastereoselectivity. The initiation of the reaction was found to begin with the chelation of amide to the palladium, which was followed by

the insertion of the alkene to amino-palladium bond. This insertion step was disclosed to be favored kinetically and thermodynamically with electron-rich amidates according to electronic-effect studies. The deuterium labelling reaction was conducted to shade light on the stereochemistry of amino-palladation (AP) step. The analysis of product revealed that the pyrox ligand played an vital role in taking the *trans*-AP pathway with Pd(TFA)₂ as palladium(II) source; otherwise, the reaction took *cis*-AP pathway.

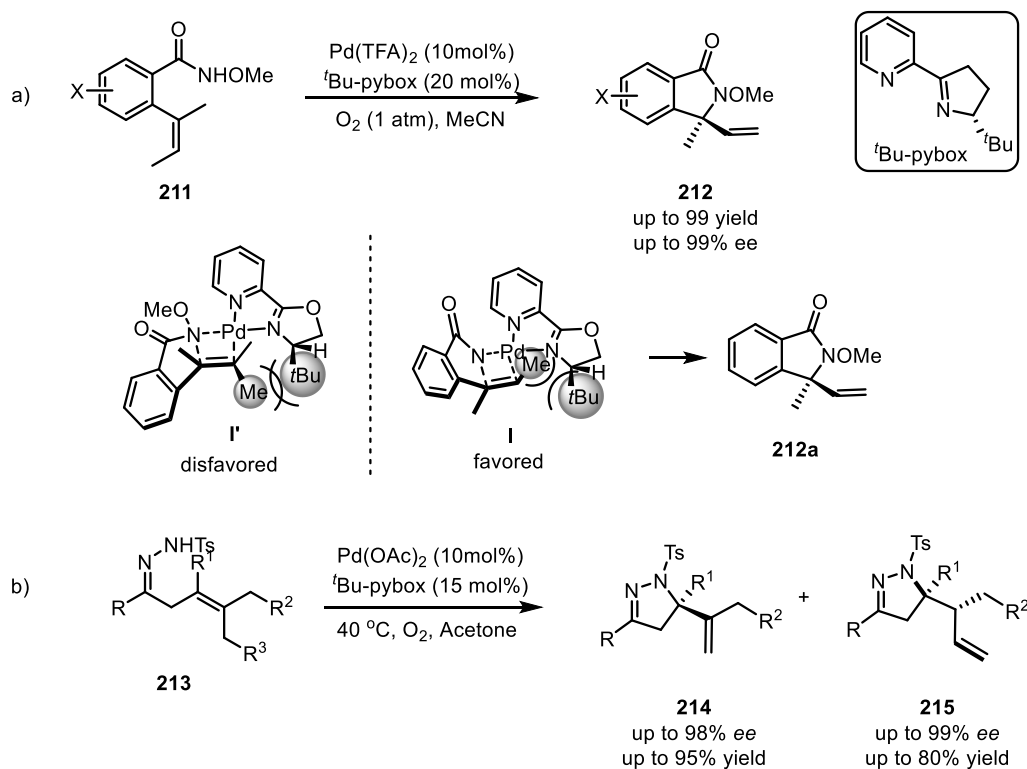


Entry	Pd	ligand	Yield	ee[%]	<i>trans</i> -AP/ <i>cis</i> -AP
1	Pd(TFA) ₂	(S)-X	90	96	>9:1
2	Pd(OAc) ₂	(S)-X	48	20	1:9
3	Pd(TFA) ₂	none	55	0	1:9
4	Pd(OAc) ₂	none	15	0	<1:9

Scheme 4.14 Enantioselective intramolecular aza-Wacker oxidation by Stahl.

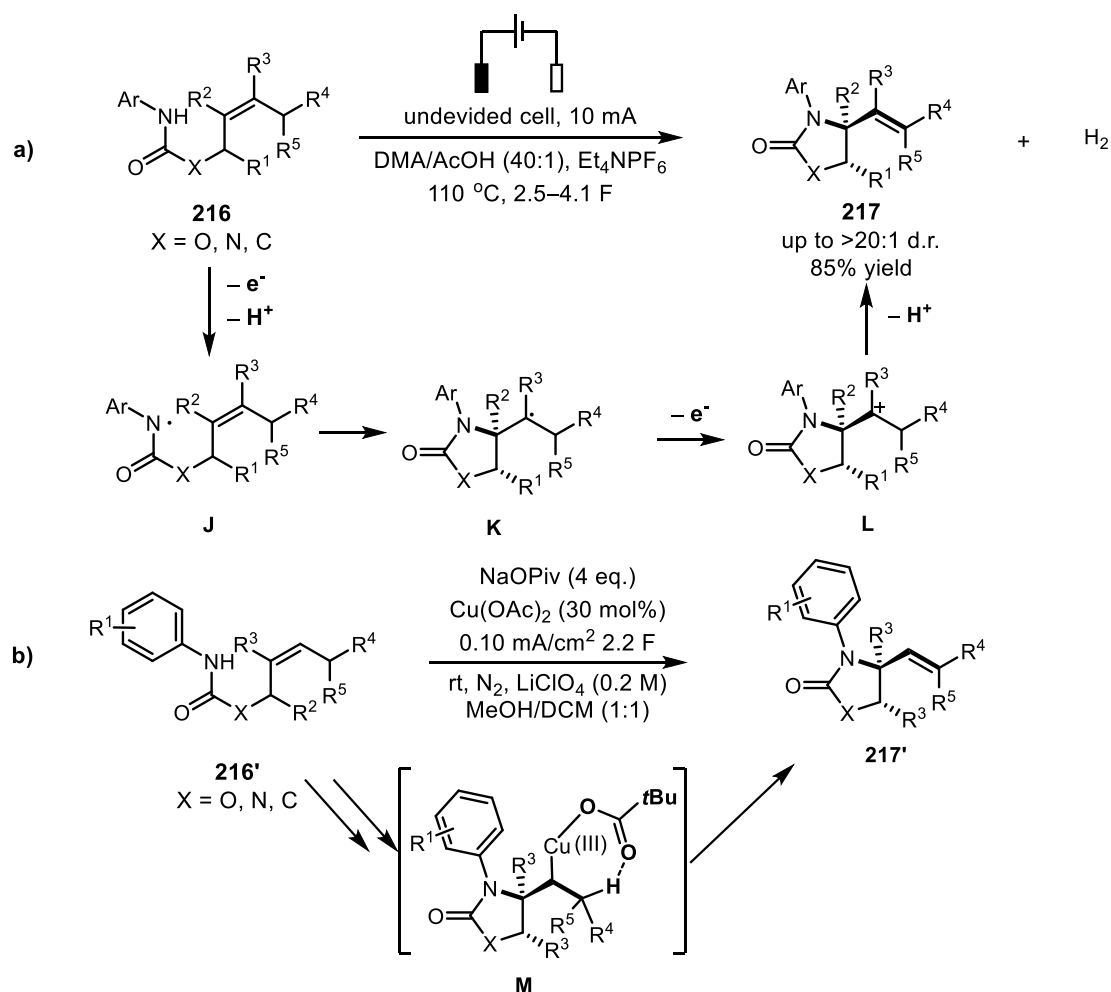
At almost same time, Zhang exploited the *t*Bu-pybox as ligand to construct the tetrasubstituted carbon stereocenters of isoindolinone **212** (Scheme 4.15).²⁹ According to Stahl and co-workers' model, the alkene took *trans*- direction to the pyridine moiety, meanwhile the terminal methyl group of the olefin oriented far away from the *tert*-butyl group which was favored transition state (**I**) leading to the formation of final optical product.

With Pd(OAc)₂ as palladium resource, this powerful ligand could also be used to realize the cyclization of N-Ts hydrazine-tethered tetrasubstituted olefins **213** to afford pyrazolines **214**, **215** with a tetrasubstituted stereogenic carbon center; when methylene group appeared as terminal of the alkene **213**, it could give cyclized product **215** with two vicinal stereocenters after olefin migration. The successive experiment showed that this reaction took *syn*- amino-palladation fashion.



Scheme 4.15 Enantioselective intramolecular aza-Wacker oxidation by Zhang.

Recently, Xu developed an electrochemical method to realize the oxidative amination of tri- and tetrasubstituted alkenes **216**, in a metal- and reagent-free way (Scheme 4.16a).^{30a} The anodic activation of the amide could lead to generation of a nitrogen-centered radical (NCR, **J**) which underwent an intramolecular cyclization to give a carbon radical intermediate **K**. After loss of an electron, a cationic intermediate **L** could be produced followed by deprotonation to give a variety of 5-membered *N*-heterocycles **217** in good diastereoselectivity. Since a carbon cation was produced, the substitution on the carbon of alkene closer to nitrogen was mandatory. To avoid the harsh condition, Hu group developed the Cu(II) assisted β -hydride elimination of aza-Wacker oxidation. Besides, the scope of the olefin was extended to di-substituted alkene **216'** (Scheme 4.16b).^{30b}



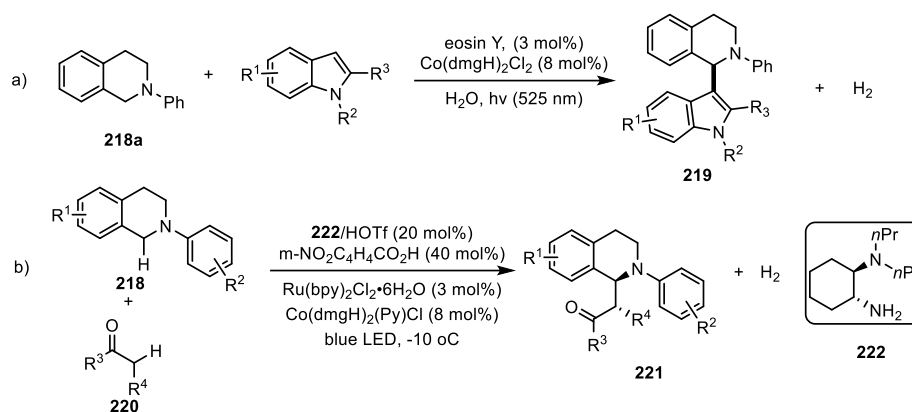
Scheme 4.16 Formal aza-Wacker oxidation through an electrochemical way.

1.2 Photocatalyzed Wacker Oxidation

4.2.1 Background of application of cobaloxime complexes

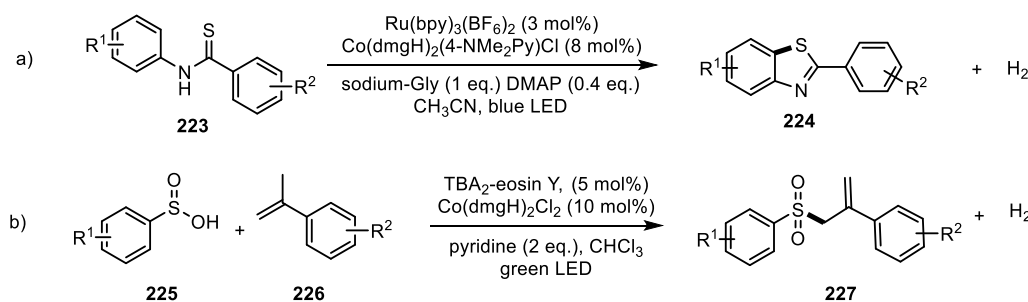
Before documenting our work herein, a brief summary of relevant photochemistry concerning cobaloxime is necessary to be mentioned.

In 2014, Wu group published photocatalyzed cross-coupling hydrogen evolution (CCHE) reaction to achieve the coupling of a varieties of isoquinolines **218** and indoles with hydrogen as sole byproduct (Scheme 4.17).^{31a} Eosin Y was proposed to deprive the electron from amine at excited state to produce an amino radical cation. Meanwhile the reduced eosin Y could transfer one electron to the [Co(III)] which could subsequently oxidize the nitrogen radical cation to give an imine and [Co(I)]. The [Co(I)] was proposed to be oxidized by the proton to engage in a new reaction cycle. The same notion was adapted to the asymmetric dehydrogenative coupling of the isoquinolines **218** with ketone **220** in a synergistic multiple catalysis system.^[31b]



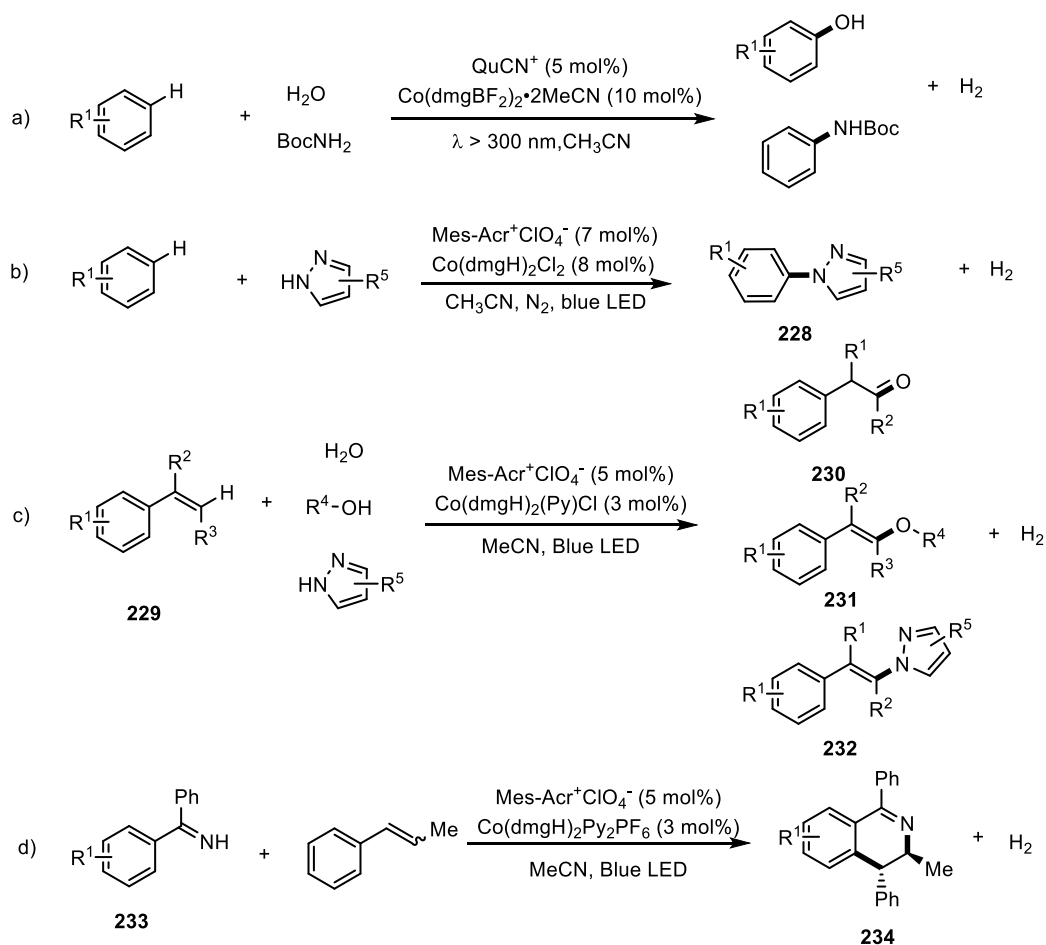
Scheme 4.17 Photocatalyzed cross-coupling hydrogen evolution.

In 2015, Lei documented the dual photocatalyzed intramolecular constriction of C-S bond (Scheme 4.18a).^{32a} In their study, the thiocarbonyl group was proposed to be activated by the photoexcited Ru(II)* to give a thio radical which could cyclize with the phenyl ring. The resulting phenyl radical could lose one electron to give a cation which could further lose one proton delivering the final product **224**. The similar reaction profile could be applicable to the coupling of sulfonic acid **225** and phenyl substituted alkene **226** to construct the intermolecular C-S bond to provide **227** (Scheme 4.18b).^{32b}



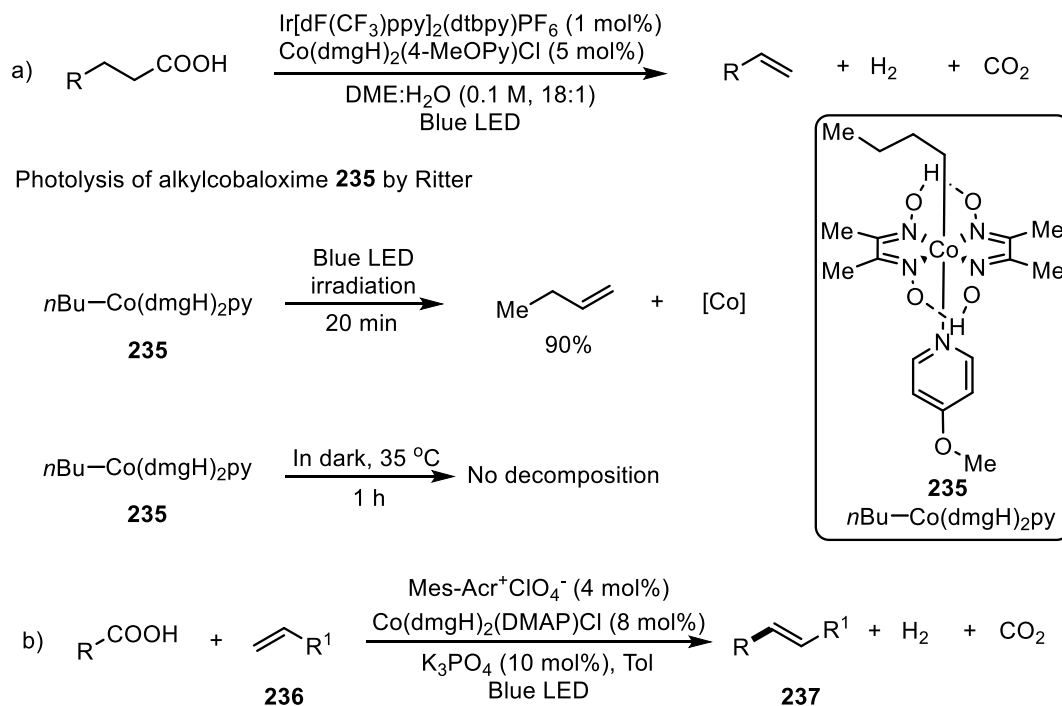
Scheme 4.18 Dual photocatalyzed intramolecular construction of C-S bond.

Instead of activating the heteroatom, there is another way to produce a reacting intermediate which is activation of the π -system in which case a photocatalyst of high reductive potential is mandatory. In 2016, Wu and Tung used the quinolinium salt to activate the phenyl group realizing the C-H amination and hydroxylation of benzene to give substituted phenol and aniline (Scheme 4.19a).³³ Lately, utilizing the acridinium salt as photocatalyst, Lei achieved the amination of benzene with 1H-pyrazole as resource of the nitrogen delivering **228** (Scheme 4.19b). The styrene derivatives **229** was oxidized using a combination of acridinium salt and cobaloxime complex to give a Wacker oxidation product **230** - **232** (Scheme 4.19c). The oxidized styrene was further used in the synthesis of 3,4-dihydroisoquinolines **234** through [4+2] imine/alkene annulation (Scheme 4.19d).



Scheme 4.19 Photocatalyzed functionalization of π - system.

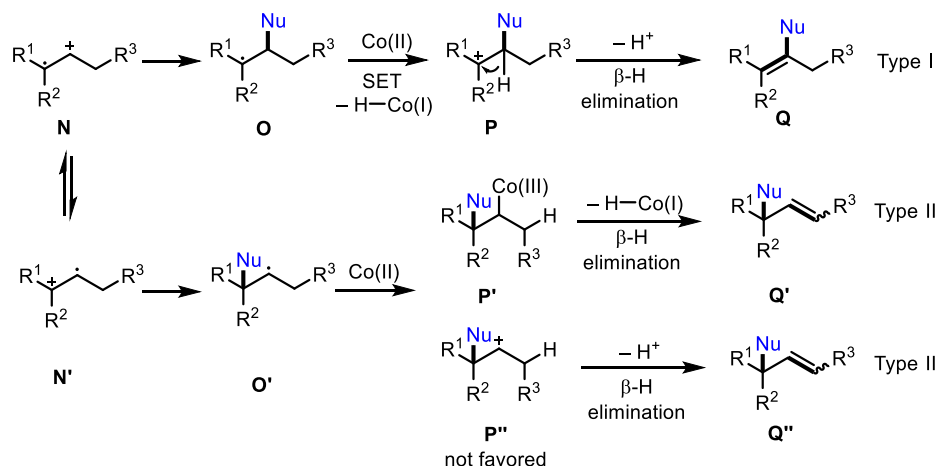
In 2018, Ritter and co-workers reported the photocatalyzed dehydrogenative decarboxylation of carboxylic acid to furnish the alkene. Meanwhile the photolysis of the alkyl cobaloxime **235** to give an alkene and Co(I)-H compound was also disclosed which was quite meaningful to our work (Scheme 4.20a).^{34a} The proposed photocatalyzed decarboxylative intermediate could be further captured by the styrene derivatives **236**, which after the photolysis of the alkyl cobaloxime intermediate providing the coupling product **237** (Scheme 4.20b).^{34b}



Scheme 4.20 Photocatalyzed dehydrogenative decarboxylation and decarboxylative coupling.

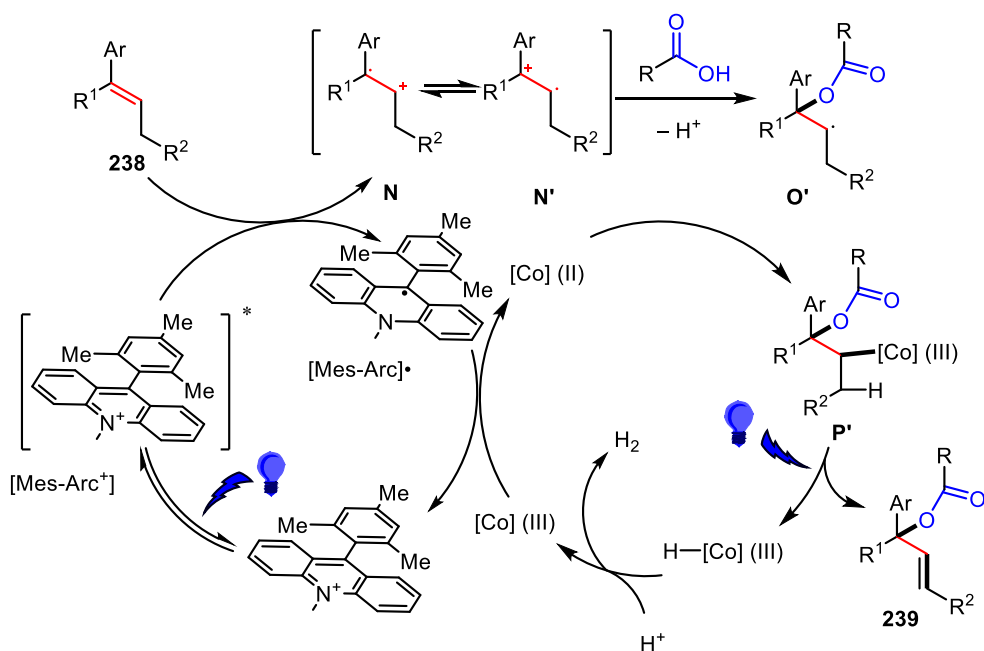
4.2.2 Photocatalyzed Wacker Oxidation of trisubstituted alkene

According to the published work, generally cobaloxime works in two possible pathway: a) Co(III) could deprive two electrons from reduced photocatalyst and the radical intermediate respectively providing ground state photocatalyst and a carbon cation (Scheme 4.21, type I); b) the Co(III) was reduced to Co(II) by single electron transfer (SET) from reduced photocatalyst, which could couple with radical intermediate to afford the organo-Co(III) compound and subsequently adopt photolysis to provide an alkene and Co(I)-H compound (Scheme 4.21, type II). The second pathway has been testified by Ritter with experiment indirectly. Although the gross roles of cobaloxime are same, there would be a slight difference in the reaction process as shown in Scheme 4.21. In Lei, Wu and Tung's work, the first pathway was proposed, the radical cation intermediate **A** was produced after SET which could capture a nucleophile to give a radical **B**. Then the Co(II) deprived one electron from the radical to give intermediate cation **C**. The precondition of this pathway is supposed to need substitution to stabilize the carbon cation, therefore intermediate **C''** is not favored thermodynamically. On the other hand, if the photolysis goes through the second pathway (**C'**→**D'**), no other substitution is need; on the contrary, more substitution would cause more steric hindrance which could block the formation of C-Co bond (**C'**). In summary, if the reaction proceeds in the way **A**→**D'**, the reaction gave type I Wacker oxidation product which is ketone. On the other hand, it could give a type II Wacker oxidation product *i.e.* allylic alcohol or ester, amine.



Scheme 4.21 Photocatalyzed Wacker oxidation of different pathway

In this context, we proposed a new pathway to realize type II Wacker oxidation to prepare allyl ester (Scheme 4.22). Under blue LED, the Mes-Acr⁺ could grab one photon and get to excited state which could deprive one electron from the alkene generating a radical cation intermediate and reduced photocatalyst [Mes-Acr]•. Then single electron transfer from [Mes-Acr]• to [Co(III)] could produce a [Co(II)]; meanwhile the radical cation could capture one nucleophile to produce a radical O'. The coupling product of [Co(II)] and O' proposed by Ritter could happen providing an [Co(III)] P' which under blue LED could adopt photolysis to afford the alkene 239 and [Co]-H compound. In protic environment, the Co-H compound could react with proton to give the Co(III) to restart a new reaction cycle.

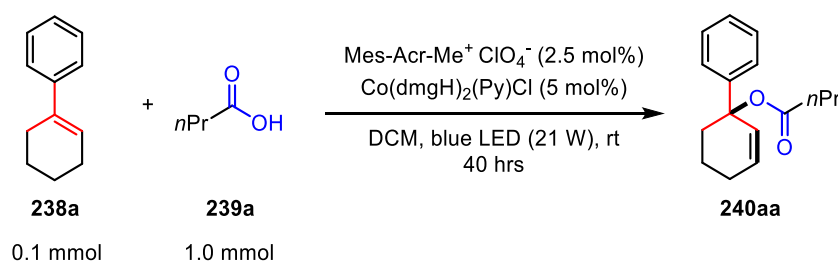


Scheme 4.22 Proposal to of photocatalyzed type II Wacker oxidation.

We launched our research with phenyl substituted alkene **238a** as substrate, butyric acid **239a** as nucleophile, and Mes-Acr-Me⁺ClO₄⁻ as photocatalyst, DCM as solvent. We chose Mes-Acr-

$\text{Me}^+\text{ClO}_4^-$ as the photocatalyst because of its excited-state reduction potential ($E_{\text{red}}^* = \text{Mes-Acr-Me}^{+\bullet}/\text{Mes-Acr-Me}^\bullet$) of +2.06 V vs SCE.³⁵ The reaction was left under blue LED at room temperature stirring for 40 hours. After elementary research on the substrate including 1,2-dihydronaphthalene, *trans*-beta-methylstyrene and some other phenyl-substituted alkenes, to our surprise, the 1-phenylcyclohexene produced an allylic ester **240aa** with 56% yield. Next, we tried the acridinium with other counterion, tetrafluoroborate gave even lower yield (Table 4.1, Entry 2). Other photocatalyst such as pyrylium (Table 4.1, Entry 3) and [Ir] (Table 4.1, Entry 4), they also failed to promote the reaction. Other cobaloxime with 1-methylimidazole, DMAP and chloride to replace the pyridine were also examined. The 1-methylimidazole and DMAP substituted [Co] gave lower yield, at the same time (Table 4.1, Entry 5 & 6), the $\text{Co}(\text{dmgH})_2\text{Cl}_2$ could barely catalyze the reaction (Table 4.1, Entry 7). We next tested the ratio of the acridinium salt and the [Co]. When the loading of acridinium salt was also increased to 5 mol%, the reaction gave 59% yield (Table 4.1, Entry 8). However, when the ratio was modified to 1:4, the yield decreased, when it was modified to 2:1, the reaction stopped. (Table 4.1, Entry 9 & 10) The screening of the concentration showed that both higher and lower concentrate caused erosion of the yield. And we suspected that maybe because of the product was also an alkene, the product was not stable under the standard condition. But the shorter reaction time only lead to incompleteness of the reaction.

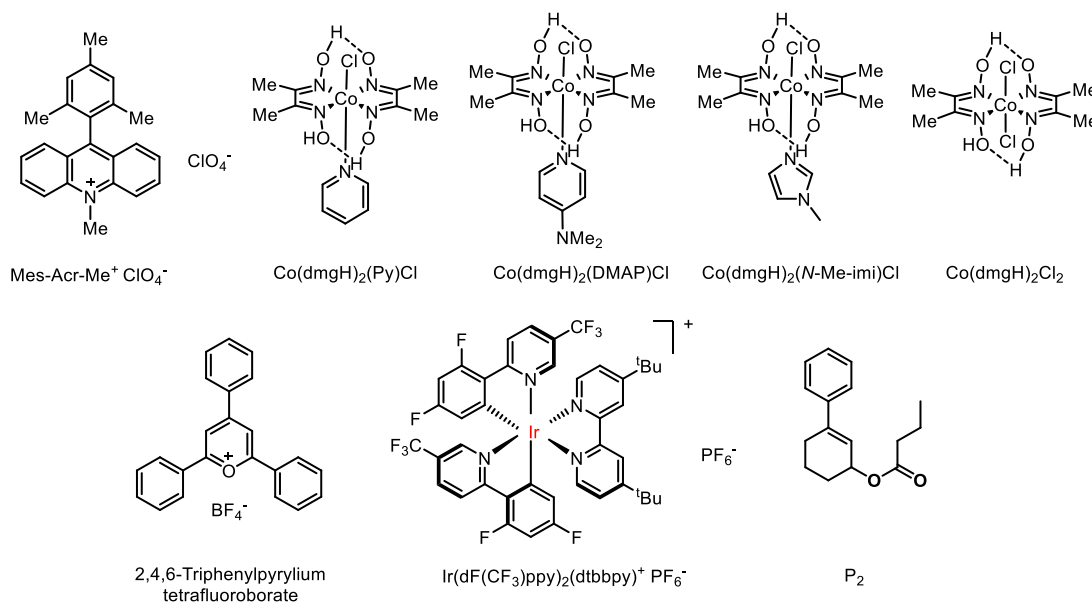
Table 4.1 Elementary survey of photocatalyzed type II Wacker oxidation



Entry ^a	Conditions	Yield (%) 240aa ^b	Note	
1	standard	56%	/	
2	Mes-Acr-Me ⁺ BF ₄ ⁻	52%	/	
3	Cat. 2,4,6-Triphenylpyrylium tetrafluoroborate	0	/	
4	Ir(dF(CF ₃)ppy) ₂ (dtbbpy) ⁺ PF ₆ ⁻	0	/	
5	Co(dmgh) ₂ (<i>N</i> -Me-imi)Cl	37	Trace of SM remained	
6	[Co] Co(dmgh) ₂ (DMAP)Cl	33	Trace of SM remained	
7 ^c	Co(dmgh) ₂ Cl ₂	Trace	Did not complete	
8	Cat. Ratio 1:1 (5%)	59	/	
9	Acridinium/[Co]	1:4 (2.5%:10%)	49	/
10		2:1 (2.5%:1.25%)	0	No reaction
11	Concentration 0.5 M	48	/	

12		0.2 M	44	/
13		0.025 M	17	Didn't complete
14	time	20 h	53	Didn't complete, P ₁ :P ₂ = 3:1

^a According to the NMR, the purity of 1-phenylcyclohexane is 93%; ^b After flash chromatography; ^c determined by GC-MS.



Afterwards, the effect of solvent was also examined. At the beginning, we chose the DCM as solvent in account of its wide utility in Nicewicz's work. We tried polar solvent (DMF) firstly which gave no product. (Table 4.2, Entry 1) Then both polar and nonpolar solvent containing phenyl ring were tested which give only 19% and 17% yield. (Table 4.2, Entry 3 & 2) Then the acetonitrile used by Lei and co-workers was also tested in which case the reaction provide product in 46% yield with some olefin substrate left. (Table 4.2, Entry 4 & 5) Therefore, we suspected that maybe the addition of DCM could promote that reaction. So, the mixed solvent of DCM/ACN (10:1) was tested resulting in lower yield. (Table 4.2, Entry 6). We also tried hexafluoroisopropanol as part of mixed solvent which gave no product. Other solvent such as ethyl estate and cyclohexane were screened giving trace of product.

Table 4. 2 Effect of the solvent

Entry ^a	Solv.	Yield (%) 240aa^b	Note
1	DMF	0	SM remained
2	Tol.	17	/

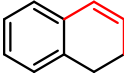
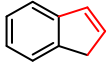
3	Chlorobenzene	19	Didn't complete
4	ACN	46	Didn't complete
5	ACN (degassed)	37	Didn't complete
6	DCM/ACN (10:1)	46	/
7 ^c	DCM/HFIP (1:1)	0	Unknown compounds
8 ^c	EtOAc	trace	/
9 ^c	Cyclohexane/DCM (5:1)	trace	/

^a According to the NMR, the purity of 1-phenylcyclohexene is 93%; ^b After flash chromatography; ^c determined by GC-MS.

Up to now, the optimal condition has been established. So, we examined the utility of this methodology with different phenyl substituted alkene. We first tried a variety of the 1-phenylcyclohexene with different substitution on the cyclohexene ring. To our surprise, tert-butyl group on the 4- position caused the promotion of yield to 71% (Table 4.3, entry 2), whereas the methyl and dimethyl substitution led to lower yield (Table 4.3, entry 3 & 4). Other common disubstituted alkene (one of the substituents was phenyl group) including β -methyl styrene, 1,2-dihydronaphthalene, 1H-indene did not work in the reaction (Table 4.3, entry 5 - 8).

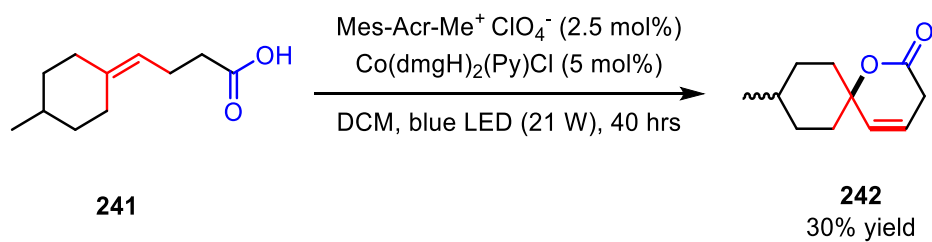
Table 4.3 Scope of the alkene

Entry	Olefin	Yield (%) 240^a
1	238a	63
2	238b	71
3	238c	51
4	238d	41
5	238e	0
6	238f	0

7		0
8		0

^a After flash chromatography.

According to our original design, we speculated that intramolecular version should work under this condition. To our delight, the compound **241** gave the spiro-lactone in 30% yield (Scheme 4.23).



Scheme 4.23 The intramolecular Wacker oxidation to afford lactone.

The successive work is on-going in our group.

4.3 Conclusions

We found a new photoredox way to realize the oxidation of alkene to afford an allylic ester featuring the independence to oxidant, mild condition and atom economy. The reaction could proceed through both inter- and intramolecular way. Further research is being carried on in our group.

Reference

- ¹ J. A. Keith, P. M. Henry, *Angew. Chem. Int. Ed.* **2009**, *48*, 9038 – 9049.
- ² P. Kočovský, J.–E. Bäckvall, *Chem. Eur. J.* **2015**, *21*, 36 – 56.
- ³ J. Smidt, W. Hafner, R. Jira, R. Sieber, J. Sedlmeier, A. Sabel, *Angew. Chem.* **1962**, *74*, 93 – 102.
- ⁴ For relevant review, see: J. Muzart, *Tetrahedron* **2007**, *63*, 7505 – 7521.
- ⁵ For relevant review, see: J. Dong, W. R. Browne, B. L. Feringa, *Angew. Chem. Int. Ed.* **2015**, *54*, 734 – 744.
- ⁶ a) J. Tsuji, H. Nagashima, H. Nemoto, *Org. Synth. Coll.* **1990**, *7*, 137 – 139; b) T. Kobayashi, Y. Kon, H. Abe, H. Ito, *Org. Lett.* **2014**, *16*, 6397 – 6399.
- ⁷ a) H. Mimoun, R. Charpentier, A. Mitschler, J. Fischer, R. Weiss, *J. Am. Chem. Soc.* **1980**, *102*, 1047 – 1054; b) C. N. Cornell, M. S. Sigman, *J. Am. Chem. Soc.* **2005**, *127*, 2796 – 2797; c) B. W. Michel, A. M. Camelio, C. N. Cornell, M. S. Sigman, *J. Am. Chem. Soc.* **2009**, *131*, 6076 – 6077.
- ⁸ a) R. A. Fernandes, D. A. Chaudhari, *J. Org. Chem.* **2014**, *79*, 5787 – 5793. b) R. A. Fernandes, V. Bethi, *Tetrahedron* **2014**, *70*, 4760 – 4767.
- ⁹ a) T. Mitsudome, T. Umetani, N. Nosaka, K. Mori, T. Mizugaki, K. Ebitani, K. Kaneda, *Angew. Chem. Int. Ed.* **2006**, *45*, 481 – 485; b) C. N. Cornell, M. S. Sigman, *Org. Lett.* **2006**, *8*, 4117 – 4120; c) For review article, see: K. M. Gligorich, M. S. Sigman, *Chem. Commun.* **2009**, 3854 – 3867; d) Y. Wang, Y. Gao, S. Mao, Y. Zhang, D. Guo, Z. Yan, S. Guo, Y. Wang, *Org. Lett.* **2014**, *16*, 1610 – 1613.
- ¹⁰ a) J. -E. Bäckvall, A. K. Awasthi, Z. D. Renko, *J. Am. Chem. Soc.* **1987**, *109*, 4750 – 4752; b) J. -E. Bäckvall, R. B. Hopkins, H. Grennberg, M. M. Mader, A. K. Awasthi, *J. Am. Chem. Soc.* **1990**, *112*, 5160 – 5166; c) T. Mitsudome, K. Mizumoto, T. Mizugaki, K. Jitsukawa, K. Kaneda, *Angew. Chem. Int. Ed.* **2010**, *49*, 1238 – 1240; d) B. Morandi, Z. K. Wickens, R. H. Grubbs, *Angew. Chem. Int. Ed.* **2013**, *52*, 2944 – 2948; e) B. Morandi, Z. K. Wickens, R. H. Grubbs, *Angew. Chem. Int. Ed.* **2013**, *52*, 9751 – 9754; f) M. M. Lerch, B. Morandi, Z. K. Wickens, R. H. Grubbs, *Angew. Chem. Int. Ed.* **2014**, *53*, 8654 – 8658; g) R. J. DeLuca, J. L. Edwards, L. D. Steffens, B. W. Michel, X. Qiao, C. Zhu, S. P. Cook, M. S. Sigman, *J. Org. Chem.* **2013**, *78*, 1682 – 1686.
- ¹¹ a) X. Ji, H. Huang, W. Wu, X. Li, H. Jiang, *J. Org. Chem.* **2013**, *78*, 11155 – 11162; b) X. Ji, H. Huang, W. Wu, H. Jiang, *J. Am. Chem. Soc.* **2013**, *135*, 5286 – 5289.
- ¹² For an typical review, see: R. A. Johnson, K. B. Sharpless. *In Catalytic Asymmetric Synthesis*; 2nd ed.; Ojima, I. Ed.; Wiley-CVH: New York, **2000**; 231 – 280.
- ¹³ For typical application review, see: B. M. Trost, M. L. Crawley, *Chem. Rev.* **2003**, *103*, 2921 – 2944.
- ¹⁴ For typical review, see: a) A. Nakamura, M. Nakada, *Synthesis* **2013**, *45*, 1421 – 1451; b) J. Eames, M. Watkinson, *Angew. Chem. Int. Ed.* **2001**, *40*, 3567 – 3571; c) N. Rabjohn, *Org. React.* **1976**, *24*, 261 – 309.
- ¹⁵ a) I. I. Moiseev, M. N. Vargaftik, J. K. Syrkin, *Dokl. Akad. Nauk SSSR*, **1960**, *133*, 377; b) C. B. Anderson, S. J. Winstein, *J. Org. Chem.* **1963**, *28*, 605 – 606; c) M. N. Vargaftik, I. I. Moiseev, *J. K. Syrkin, V. V. Yakshin, Izv. Akad. Nauk SSSR, Ser. Khim.* **1962**, 930.
- ¹⁶ W. Kitching, Z. Rappoport, S. Winstein, W. G. Young, *J. Am. Chem. Soc.* **1966**, *88*, 2054 – 2055.
- ¹⁷ a) T. Hosokawa, H. Ohkata, I. Moritani, *Bull. Chem. Soc. Japan*, **1975**, *48*, 1533 – 1536; b) T. Hosokawa, M. Hirata, S. Murahashi, A. Sonoda, *Tetrahedron Lett.*, **1976**, 1821 – 1824.
- ¹⁸ M. F. Semmelhack, C. R. Kim, W. Dobler, M. Meier, *Tetrahedron Lett.*, **1989**, *30*, 4925 – 4928.
- ¹⁹ T. Hayashi, K. Yamasaki, M. Mimura, Y. Uozumi, *J. Am. Chem. Soc.* **2004**, *126*, 3036 – 3037.
- ²⁰ a) R. A. T. M. V. Benthem, H. Hiemstra, W. N. Speckamp, *J. Org. Chem.* **1992**, *57*, 6083 – 6088; b) R. A. T. M. V. Benthem, H. Hiemstra, J. J. Michels, W. N. Speckamp, *J. Chem. Soc. Chem.*

- Commun.*, **1994**, 357 – 359; c) R. A. T. M. V. Benthem, H. Hiemstra, P. W. N. M. V. Leeuwen, J. W. Geus, W. N. Speckamp, *Angew. Chem. Int. Ed.* **1995**, *34*, 457 – 460; d) R. C. Larock, T. R. Hightower, *J. Org. Chem.* **1993**, *58*, 5298 – 5300; e) M. Rönn, P. G. Andersson, J.-E. Bäckvall, *Acta, Chemica Scandinavica*, **1997**, *51*, 773 – 777.
- ²¹ a) T. Hosokawa, T. Uno, S. Inui, S.-I. Murahashi, *J. Am. Chem. Soc.* **1981**, *103*, 2318 – 2323. (b) T. Hosokawa, C. Okuda, S.-I. Murahashi, *J. Org. Chem.* **1985**, *50*, 1282 – 1287.
- ²² a) Y. Uozumi, K. Kato, T. Hayashi, *J. Am. Chem. Soc.* **1997**, *119*, 5063 – 5064; b) Y. Uozumi, K. Kato, T. Hayashi, *J. Org. Chem.* **1998**, *63*, 5071 – 5075; c) Y. Uozumi, H. Kyota, K. Kato, M. Ogasawara, T. Hayashi, *J. Org. Chem.* **1999**, *64*, 1620 – 1625.
- ²³ M. A. Arai, M. Kuraishi, T. Arai, H. Sasai, *J. Am. Chem. Soc.* **2001**, *123*, 2907 – 2908.
- ²⁴ a) R. M. Trend, Y. K. Ramtohl, E. M. Ferreira, B. M. Stoltz, *Angew. Chem. Int. Ed.* **2003**, *42*, 2892 – 2895; b) R. M. Trend, Y. K. Ramtohl, B. M. Stoltz, *J. Am. Chem. Soc.* **2005**, *127*, 17778 – 17788.
- ²⁵ T. P. Pathak, K. M. Gligorich, B. E. Welm, M. S. Sigman, *J. Am. Chem. Soc.* **2010**, *132*, 7870 – 7871.
- ²⁶ N. J. Race, C. S. Schwalm, T. Nakamuro, M. S. Sigman, *J. Am. Chem. Soc.* **2016**, *138*, 15881 – 15884.
- ²⁷ a) S. R. Fix, J. L. Brice, S. S. Stahl, *Angew. Chem. Int. Ed.* **2002**, *41*, 164 – 166; b) Z. Lu, S. S. Stahl, *Org. Lett.* **2012**, *14*, 1234 – 1237; c) Liu, G.; Stahl, S. S. *J. Am. Chem. Soc.* **2007**, *129*, 6328 – 6335.
- ²⁸ a) R. I. McDonald, P. B. White, A. B. Weinstein, C. P. Tam, S. S. Stahl, *Org. Lett.*, **2011**, *13*, 2830 – 2833; b) P. B. White, S. S. Stahl, *J. Am. Chem. Soc.* **2011**, *133*, 18594 – 18597; c) A. B. Weinstein, S. S. Stahl, *Angew. Chem. Int. Ed.* **2012**, *51*, 11505 – 11509.
- ²⁹ a) G. Yang, C. Shen, W. Zhang, *Angew. Chem. Int. Ed.* **2012**, *51*, 9141 – 9145; b) X. Kou, Q. Shao, C. Ye, G. Yang, W. Zhang, *J. Am. Chem. Soc.* **2018**, *140*, 7587 – 7597.
- ³⁰ a) P. Xiong, H. Xu, H. Xu, *J. Am. Chem. Soc.* **2017**, *139*, 2956 – 2959; b) X. Yi, X. Hu, *Angew. Chem. Int. Ed.* **2019**, *58*, 4700 – 4704.
- ³¹ a) J. Zhong, Q. Meng, B. Liu, X. Li, X. Gao, T. Lei, C. Wu, Z. Li, C. Tung, L. Wu, *Org. Lett.* **2014**, *16*, 1988 – 1991; b) Q. Yang, L. Zhang, C. Ye, S. Luo, L. Wu, C. Tung, *Angew. Chem. Int. Ed.* **2017**, *56*, 3694 – 3698
- ³² G. Zhang, C. Liu, H. Yi, Q. Meng, C. Bian, H. Chen, J.-X. Jian, L.-Z. Wu, A. Lei, *J. Am. Chem. Soc.* **2015**, *137*, 9273 – 9280.
- ³³ (a) Y.-W. Zheng, B. Chen, P. Ye, K. Feng, W. Wang, Q.-Y. Meng, L.-Z. Wu, C.-H. Tung, *J. Am. Chem. Soc.* **2016**, *138*, 10080 – 10086; (b) L. Niu, H. Yi, S. Wang, T. Liu, J. Liu, A. Lei, *Nat. Commun.* **2017**, *8*, 14226; (c) G. Zhang, X. Hu, C. - W. Chiang, H. Yi, P. Pei, A. K. Singh, A. Lei, *J. Am. Chem. Soc.* **2016**, *138*, 12037 – 12040; (d) G. Zhang, L. Zhang, H. Yi, Y. Luo, X. Qi, C. Tung, L. Wu, A. Lei, *Chem. Commun.*, **2016**, *52*, 10407 – 10410; (e) X. Hu, G. Zhang, F. Bu, A. Lei, *Angew. Chem., Int. Ed.* **2018**, *57*, 1286 – 1290.
- ³⁴ a) X. Sun, J. Chen, T. Ritter, *Nat. Chem.* **2018**, *10*, 1229 – 1233; b) H. Cao, H. Jiang, H. Feng, J. Mun, C. Kwan, X. Liu, J. Wu, *J. Am. Chem. Soc.* **2018**, *140*, 16360 – 16367.
- ³⁵ K. A. Margrey, D. A. Nicewicz, *Acc. Chem. Res.* **2016**, *49*, 1997 – 2006.

Supplementary materials

Ni(II) Catalyzed Suzuki Coupling of Electron Perturbed Allenes

General Methods.

¹H-NMR spectra were recorded on Varian 400 (400 MHz) spectrometers. Chemical shifts are reported in ppm from TMS with the solvent resonance as the internal standard (deuteriochloroform: 7.24 ppm). Data are reported as follows: chemical shift, multiplicity (s = singlet, d = doublet, t = triplet, q = quartet, sext = sextet, sept = septet, p = pseudo, b = broad, m = multiplet), coupling constants (Hz). ¹³C-NMR spectra were recorded on a Varian 400 (100 MHz) spectrometers with complete proton decoupling. Chemical shifts are reported in ppm from TMS with the solvent as the internal standard (deuteriochloroform: 77.0 ppm). GC-MS spectra were taken by EI ionization at 70 eV on a Hewlett-Packard 5971 with GC injection. They are reported as: *m/z* (rel. intense). LC-electrospray ionization mass spectra were obtained with Agilent Technologies MSD1100 single-quadrupole mass spectrometer. Chromatographic purification was done with 240-400 mesh silica gel. Other anhydrous solvents were supplied by Sigma Aldrich in Sureseal® bottles and used without any further purification. Commercially available chemicals were purchased from Sigma Aldrich, Stream and TCI and used without any further purification. Analytical high performance liquid chromatography (HPLC) was performed on a liquid chromatograph equipped with a variable wave-length UV detector (deuterium lamp 190-600 nm), using a Daicel Chiracel™OD-H, (0.46 cm I.D. x 25 cm Daicel Inc). HPLC grade isopropanol and *n*-hexane were used as the eluting solvents. Melting points were determined with Bibby Stuart Scientific Melting Point Apparatus SMP 3 and are not corrected. Agilent Technologies LC/MSD Trap 1100 series (nebulizer: 15.0 PSI, dry Gas: 5.0 L/min, dry Temperature: 325 °C, capillary voltage positive scan: 4000 mA, capillary voltage negative scan: 3500 mA).

Crystallographic data collection and structure determination for [NiCl{(5,5')-Me₂-bpy}(H₂O)₃]Cl·4H₂O and 1-(2-([1,1'-biphenyl]-4-yl)-4-(naphthalen-2-yl)butyl)piperidin-2-one (+/-)-106r. The X-ray intensity data were measured on a Bruker Apex III CCD diffractometer. Cell dimensions and the orientation matrix were initially determined from a least-squares refinement on reflections measured in three sets of 20 exposures, collected in three different ω regions, and eventually refined against all data. A full sphere of reciprocal space was scanned by 0.3° ω steps. The software SMART¹ was used for collecting frames of data, indexing reflections and determination of lattice parameters. The collected frames were then processed for integration by the SAINT program.¹ and an empirical absorption correction was applied using SADABS.² The structures were solved by direct methods (SIR 97)³ and subsequent Fourier syntheses and refined by full-matrix least-squares on F² (SHELXTL)⁴ using anisotropic thermal parameters for all non-hydrogen atoms. In the asymmetric unit four water molecules are present. The aromatic, methylene, methino and methyl hydrogen atoms were placed in calculated positions and refined with isotropic thermal parameters $U(H) = 1.2 U_{eq}(C)$ or $U(H) = 1.5 U_{eq}(C)$ (methyl H), respectively and allowed to ride on their carrier carbons whereas the H atoms of the water molecules in [NiCl{(5, 5')-Me₂-bpy}(H₂O)₃]Cl·4H₂O were located in the Fourier map and refined isotropically [$U(H) = 1.2 U_{eq}(O)$].

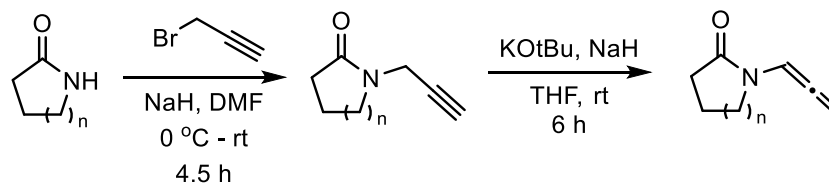
¹ SMART & SAINT Software Reference Manuals, version 5.051 (Windows NT Version), Bruker Analytical X-ray Instruments Inc.: Madison, WI, 1998.

² G.M. Sheldrick, SADABS, program for empirical absorption correction, University of Göttingen, Germany, 1996.

³ A. Altomare, M. C. Burla, M. Camalli, G. L. Cascarano, C. Giacovazzo, A. Guagliardi, A. G. Moliterni, G. R. Polidori, *J. Appl. Cryst.*, 1999, 32, 115 – 119.

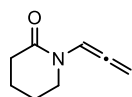
⁴ G. M. Sheldrick, SHELXTLplus (Windows NT Version) Structure Determination Package, Version 5.1. Bruker Analytical X-ray Instruments Inc.: Madison, WI, USA, 1998.

Crystal data and details of data collections for $[\text{NiCl}\{(5,5')\text{-Me}_2\text{-bpy}\}(\text{H}_2\text{O})_3]\text{Cl}\cdot 4\text{H}_2\text{O}$ and 1-(2-([1,1'-biphenyl]-4-yl)-4-(naphthalen-2-yl)butyl)piperidin-2-one are reported in Table S1.

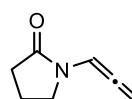
Synthesis of the Allenamides 100a-c (a: n = 2; b: n = 1; c: n = 3)


To a dry 2-necked-flask was added dry DMF (20 mL) and the desired lactame (10.0 mmol, 1.0 eq.) under nitrogen atmosphere. Then the mixture was cooled to 0 °C and NaH was added (12.0 mmol, 1.2 eq.). After 0.5 hr stirred at the same temperature, propargyl bromide (11.0 mmol, 1.1 eq. 80% purity) was added to the mixture dropwise at 0 °C. Then the reaction was warmed to room temperature and stirred for 4 hrs. TLC showed the lactame was consumed completely. Then the reaction was quenched with H₂O (40 mL) and extracted with ethyl acetate (40 mL × 3). Combined organic phase was dried over Na₂SO₄ and concentrated under vacuum. The residue was purified with silica gel column.

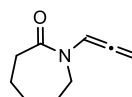
To a dry 2-necked flask dry THF (20 mL) was added followed by 1-(prop-2-yn-1-yl)-lactame (10.9 mmol, 1.0 eq.) under nitrogen atmosphere. Then NaH (18.6 mmol, 1.7 eq.) and *t*BuOK (3.3 mmol, 0.3 eq.) were added to the flask at room temperature. The resulting mixture was stirred for 6 hours. TLC showed 1-(prop-2-yn-1-yl)-lactame was completely consumed. The reaction was quenched with H₂O (20 mL) and extracted with ethyl acetate (40 mL × 3). Combined organic phase was dried over Na₂SO₄ and concentrated under vacuum. The residue was purified with silica gel column (*c*Hex:EtOAc = 1:1) to give **100a-c**.



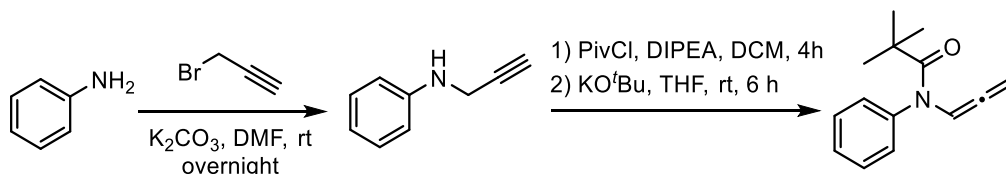
100a.¹ Yellow oil, *c*Hex:EtOAc = 1:1. Yield = 87%. ¹H NMR (400 MHz, CDCl₃) δ 7.61 (t, *J* = 6.5 Hz, 1H), 5.37 (d, *J* = 6.5 Hz, 2H), 3.31 (t, *J* = 5.8 Hz, 2H), 2.46 (t, *J* = 6.3 Hz, 2H), 1.91 – 1.77 (m, 4H). GC-MS (m/s): 137.



100b.² Yellow oil, *c*Hex:EtOAc = 1:1. Yield = 78%. ¹H NMR (400 MHz, CDCl₃) δ 7.08 (t, *J* = 6.4 Hz, 1H), 5.37 (d, *J* = 6.4 Hz, 2H), 3.45 – 3.36 (m, 2H), 2.47 (t, *J* = 8.1 Hz, 2H), 2.12 – 2.01 (m, 2H). ¹³C NMR (100 MHz, CDCl₃) δ 202.85, 173.06, 95.99, 86.70, 45.89, 31.35, 17.57. GC-MS (m/s): 123.



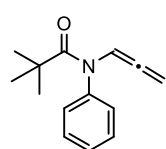
100c.¹ Colorless oil, *c*Hex:EtOAc = 1:1. Yield = 63%. ¹H NMR (400 MHz, CDCl₃) δ 7.45 (t, *J* = 6.4 Hz, 1H), 5.37 (d, *J* = 6.4 Hz, 2H), 3.52 – 3.44 (m, 2H), 2.65 – 2.55 (m, 2H), 1.77 – 1.62 (dd, *J* = 8.7, 6.7 Hz, 4H), 1.66 – 1.55 (m, 2H). ¹³C NMR (100 MHz, CDCl₃) δ 201.70, 174.00, 99.70, 87.46, 46.17, 37.34, 29.87, 27.79, 23.57. GC-MS (m/s): 151.

Synthesis of the allenamide **100d**

To a single-neck flask was added DMF (20 mL) and aniline 1.0 g (10.7 mmol, 1.0 eq.). Then the mixture was added potassium carbonate 1.8 g (12.8 mmol, 1.2 eq.), propargyl bromide 0.95 ml (10.7 mmol, 1.0 eq., 80% in toluene). The reaction was stirred overnight. TLC showed aniline was consumed completely. The reaction was quenched with H₂O (20 mL) and extracted with ethyl acetate (40 mL × 3). Combined organic phase was dried over Na₂SO₄ and concentrated under vacuum. The residue was purified with silica gel column (cHex:EtOAc = 10:1) to give *N*-(prop-2-yn-1-yl)aniline 1.0 g (yield 72%).

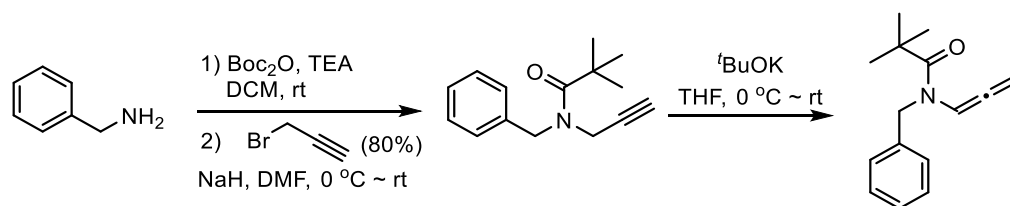
To a single-neck flask was charged with DCM. Then *N*-(prop-2-yn-1-yl)aniline 1.0 g (17.6 mmol, 1.0 eq.), DIPEA 1.5 g (11.5 mmol, 1.5 eq.) and pivaloyl chloride 1.0 g (8.4 mmol, 1.1 eq.) was added to flask. The resulting mixture was stirred for 4 hrs. TLC showed *N*-(prop-2-yn-1-yl)aniline was consumed completely. The reaction was quenched with H₂O (20 mL) and extracted with ethyl acetate (40 mL × 3). Combined organic phase was dried over Na₂SO₄ and concentrated under vacuum. The residue was purified with silica gel column (cHex:EtOAc = 10:1) to give *N*-phenyl-*N*-(prop-2-yn-1-yl)pivalamide 1.4 g (yield 85%).

To a single neck flask was charged with THF. Then *N*-phenyl-*N*-(prop-2-yn-1-yl)pivalamide 1.4 g (6.5 mmol, 1.0 eq.) and *t*BuOK 73 mg (0.65 mmol, 0.1 eq.) were added to flask. The resulting mixture was stirred for 6 hrs. TLC showed that the starting material was consumed completely. The reaction was quenched with H₂O (20 mL) and extracted with ethyl acetate (40 mL × 3). Combined organic phases were dried over Na₂SO₄ and concentrated under vacuum. The residue was purified with silica gel column (cHex:EtOAc = 5:1) to give **100d** 1.1 g (yield 79%).



100d.³ Pale yellow solid, mp = 79 - 81 °C. yield 80%. cHex:EtOAc = 10:1. ¹H NMR (400 MHz, CDCl₃) δ 7.68 (t, *J* = 6.4 Hz, 1H), 7.41 – 7.32 (m, 3H), 7.24 – 7.17 (m, 2H), 4.89 (d, *J* = 6.3 Hz, 2H), 1.07 (s, 9H). ¹³C NMR (100 MHz, CDCl₃) δ 202.86, 175.99, 140.62, 130.25, 128.72, 128.47, 104.29, 85.93, 41.30, 29.39. GC-MS (m/s): 215.

Synthesis of the Allenamide 100e



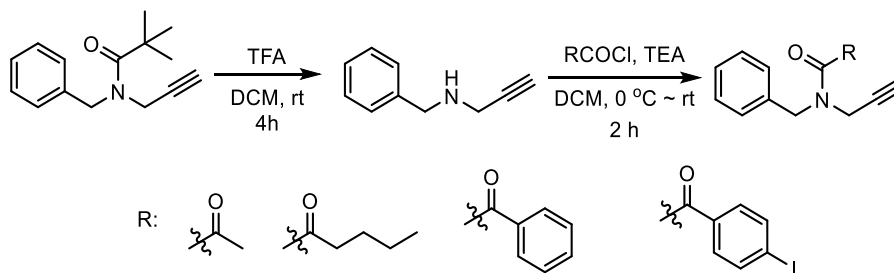
To a single-necked flask was charged with DCM 10 mL and cooled to 0 °C. Then triethylamine 3.4 g (34 mmol, 1.2 eq.), benzylamine 3.0 g (28 mmol, 1.0 eq.) and Boc₂O 6.7 (31 mmol, 1.1 eq.) were added into flask in a sequence. The resulting mixture was warmed to 20 °C and stirred for 5 h. Then the mixture was quenched with water and extracted with DCM for 3 times (3 × 20 mL). Combined organic phase was washed with water and dried over Na₂SO₄. After removing the solvent under vacuum, the residue was purified with silica gel flash chromatography (cHex:EtOAc = 5:1) to give product as yellow oil 5.0 g (yield 86%).

The BnNHBoc 4.1 g (19.8 mmol, 1.0 eq) was dissolved in DMF (40 mL) in a two-necked flask under N₂ atmosphere. To the cooled (0 °C) mixture was added NaH 0.95 g (23.7 mmol, 1.1 eq., 60%) and the resulting mixture was stirred at this temperature for 30 min when propargyl bromide 2.4 ml (21.9 mmol, 1.1 eq. 80% in toluene) was added. The reaction was warmed to 20 °C and stirred for 5 h. TLC showed that the amide was consumed completely. The reaction was quenched with KOH (2 M, 20 mL) and extracted with ethyl acetate (30 mL × 3). Combined organic phase was washed with brine (10 mL), dried over Na₂SO₄ and concentrated under reduced vacuum. The residue was purified with silica gel flash chromatography (cHex:EtOAc = 5:1) to give product as a bright yellow oil 4.3 g (yield 93%).

A single-necked flask was charged with THF and tert-butyl benzyl(prop-2-yn-1-yl)carbamate 140 mg (0.57 mmol, 1.0 eq.). The solution was cooled at 0 °C and added *t*BuOK 19 mg (0.17 mmol, 0.3 eq.) were added. The resulting mixture was warmed to 20 °C and stirred for 6 hrs. TLC showed starting material was completely consumed. The reaction was quenched with H₂O (20 mL) and extracted with ethyl acetate (40 mL × 3). Combined organic phases were dried over Na₂SO₄ and concentrated under vacuum. The residue was purified with silica gel column (cHex:EtOAc = 10:1) to give 1e as an yellow oil 119 mg (85 % yield).

100e. Colorless oil, ¹H NMR (400 MHz, CDCl₃) δ 7.35 – 7.15 (m, 5H), 7.02 (s, 1H), 5.28 (d, *J* = 14.2 Hz, 2H), 4.62 – 4.44 (m, 2H), 1.47 (m, 9H). ¹³C NMR (100 MHz, CDCl₃) δ 152.93, 128.38, 128.22, 127.56, 127.03, 126.88, 100.81, 87.56, 86.88, 81.23, 48.53, 47.83, 31.41, 30.18, 28.22. GC-MS (m/s): 189.

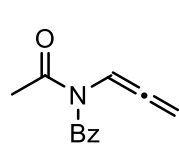
Synthesis of the Allenamide 100f-i precursors.



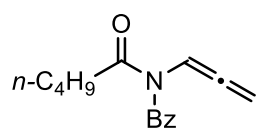
A single-necked flask was charged with DCM (60 mL) and cooled to 0 °C, then *tert*-butyl benzyl(prop-2-yn-1-yl)carbamate 2.87 g (11.3 mmol, 1.0 eq.) and TFA (11 mL) were added, successively. The resulting mixture was warmed to 20 °C, and stirred for 4 h. TLC showed starting material was completely consumed, then the mixture was quenched with saturated aqueous NaHCO₃ (50 mL) and extracted DCM (3 × 10 mL). Combined organic phases were washed with water and concentrated under vacuum. The residue was purified with silica gel flash chromatography to give *N*-benzyl-*N*-propargyl amine 1.55 g as yellow oil in 91% yield.

The *N*-benzyl-*N*-propargyl amine (2.7 mmol, 1.0 eq.) and triethylamine (1.1 eq.) were added to single-necked flask containing DCM (4 mL). Then, mixture was cooled to 0 °C and the desired chloride (1.1 eq.) was added to the mixture. The resulting mixture was warmed to 20 °C and stirred for 2 h. Then reaction was quenched with saturated aqueous NaHCO₃ and extracted DCM for 3 times. Combined organic phases were washed with water and concentrated to give product as yellow oil in 83 ~ 97% yield.

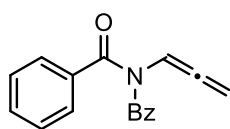
For the isomerization procedures: **100h**, **100i** see procedure for **100d**. For allenamides **100g** and **100f** see method described for **100a**.



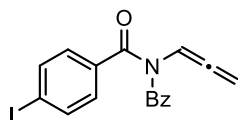
100h.⁴ Yellow oil, *c*Hex:EtOAc = 10:1, yield = 73%. ¹H NMR (400 MHz, CDCl₃, mixture of conformers *a* and *b*) δ 7.65 (t, *J* = 6.4 Hz, 1H_{*a*}), 7.32 (t, *J* = 7.4 Hz, 2H_{*a+b*}), 7.29 – 7.19 (m, 6H_{*a/b*}), 7.15 (d, *J* = 7.5 Hz, 2H_{*a/b*}), 6.69 (t, *J* = 6.2 Hz, 2H_{*b*}), 5.29 (d, *J* = 6.2 Hz, 2H_{*b*}), 5.25 (d, *J* = 6.4 Hz, 2H_{*a*}), 4.70 (s, 2H_{*b*}), 4.63 (s, 2H_{*a*}), 2.24 (s, 3H_{*b*}), 2.11 (s, 3H_{*a*}). GC-MS (*m/z*): 187.



100i. Yellow oil, yield = 68%. ¹H NMR (400 MHz, CDCl₃, mixture of conformers *a* and *b*) δ 7.69 (t, *J* = 6.4 Hz, 1H_{*a*}), 7.33 (dd, *J* = 14.3, 6.5 Hz, 2H_{*a/b*}), 7.29 – 7.20 (m, 6H_{*a/b*}), 7.17 (t, *J* = 7.4 Hz, 2H_{*a/b*}), 6.77 (t, *J* = 6.2 Hz, 1H_{*b*}), 5.30 (d, *J* = 6.2 Hz, 2H_{*b*}), 5.25 (d, *J* = 6.4 Hz, 2H_{*a*}), 4.72 (s, 2H_{*b*}), 4.65 (s, 2H_{*a*}), 2.49 (t, *J* = 7.2 Hz, 2H_{*b*}), 2.31 (t, *J* = 7.2 Hz, 2H_{*a*}), 1.74 – 1.56 (m, 4H_{*a/b*}), 1.48 – 1.35 (m, 4H_{*a/b*}), 0.95 (t, *J* = 7.4 Hz, 3H_{*b*}), 0.85 (t, *J* = 7.4 Hz, 3H_{*a*}). ¹³C NMR (100 MHz, CDCl₃) δ 202.46, 201.61, 172.02, 171.39, 137.95, 137.23, 128.89, 128.41, 128.04, 127.39, 127.11, 126.05, 100.53, 99.69, 87.50, 87.03, 49.25, 47.34, 33.64, 33.53, 27.27, 27.24, 22.65, 22.49, 13.99, 13.92. GC-MS (*m/z*): 229.

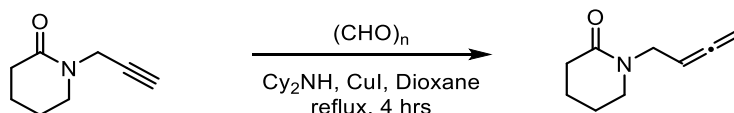


100g. Pale yellow solid, mp = 44 - 46 °C, yield = 78%. ¹H NMR (400 MHz, CDCl₃, mixture of conformers *a* and *b*) δ 7.73 – 7.27 (m, 20H_{*a/b*}), 7.12 (brs, 1H_{*a*}), 6.70 (brs, 1H_{*b*}), 5.27 (brs, 4H_{*a/b*}), 4.90 (brs, 3H_{*a+b*}), 4.67 (brs, 1H_{*a* or *b*}). ¹³C NMR (100 MHz, CDCl₃) δ 200.58, 169.59, 137.53, 135.01, 130.45, 128.58, 128.09, 127.25, 126.27, 102.57, 87.39, 47.75. GC-MS (m/s): 249.



100f. Pale yellow solid, mp = 77 - 80 °C, yield 54%. ¹H NMR (400 MHz, CDCl₃, mixture of conformers *a* and *b*) δ 7.78 – 7.28 (m, 18H_{*a/b*}), 7.12 (brs, 1H_{*a*}), 6.62 (brs, 1H_{*b*}), 5.28 (brs, 4H_{*a+b*}), 4.87 (brs, 3H_{*a+b*}), 4.64 (brs, 1H_{*a* or *b*}). ¹³C NMR (100 MHz, CDCl₃) δ 200.57, 168.53, 137.64, 137.18, 134.25, 129.68, 128.47, 128.00, 127.25, 125.99, 102.14, 99.23, 96.88, 87.49, 51.37, 47.81. GC-MS (m/s): 375.

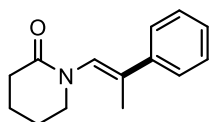
Synthesis of the allene 104



A dried Schlenk tube was charged with anhydrous dioxane (4 mL) and propargyl amide 206 mg (1.5 mmol, 1.0 eq.) under N₂. Then paraformaldehyde 109 mg (3.8 mmol, 2.5 eq.), dicyclohexylamine 489 mg (2.7 mmol, 1.8 eq.) and copper iodide 143 mg (0.75 mmol, 0.5 eq.) were added in a sequence and the mixture was refluxed for 4 hrs. TLC showed starting material was completely consumed, then the mixture was quenched with HCl (2M, 20 mL) and extracted with ethyl acetate 3 times. Combined organic phase was washed with saturated aqueous NaHCO₃ solution, brine, dried over Na₂SO₄ and then concentrated under vacuum. The residue was purified with silica gel flash chromatography to give 1-(buta-2,3-dien-1-yl)piperidin-2-one in 65% yield (147 mg). Yellow oil. *c*Hex:EtOAc = 1:1. ¹H NMR (400 MHz, CDCl₃) δ 5.05 (p, *J* = 6.5 Hz, 1H), 4.73 (dt, *J* = 6.6, 2.8 Hz, 2H), 3.95 – 3.88 (m, 2H), 3.24 (dd, *J* = 8.5, 3.6 Hz, 2H), 2.32 (t, *J* = 6.1 Hz, 2H), 1.78 – 1.67 (m, 4H). ¹³C NMR (101 MHz, CDCl₃) δ 209.12, 169.64, 86.23, 76.33, 47.41, 45.38, 32.31, 23.13, 21.38. GC-MS (m/s): 151.

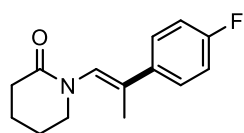
General procedure for the Ni-catalyzed bi-component cross-coupling reaction

To a dry Schlenk tube anhydrous 1,4-dioxane (1 mL) was added under nitrogen atmosphere, followed by [NiCl₂(**L3**)] (3.7 mg, 5 mol%), potassium carbonate (82.8 mg, 3.0 eq.), phenylboronic acid **101a** (36.9 mg, 1.5 eq.) and allenamide **100a** (27.4 mg, 1.0 eq.). Then the resulting mixture was poured into a pre-heated oil bath at 90 °C and stirred for 1 hour when TLC showed complete consumption of the allenamide. Then solvent was removed under vacuum and the residue purified with silica gel column flash-chromatography (*c*Hex:AcOEt 1:1). Pale yellow viscous oil. Yield = 82%, 36.4 mg.

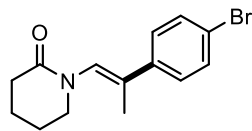


102aa. Yellow solid, mp = 51 - 53 °C, *c*Hex:EtOAc = 1:1. Yield = 82% (35.3 mg). ¹H NMR (400 MHz, CDCl₃) δ 7.44 – 7.38 (m, 2H), 7.33 – 7.27 (m, 2H), 7.27 – 7.21 (m, 1H), 6.48 (s, 1H), 3.48 – 3.40 (m, 2H), 2.48 (t, *J* = 3.5 Hz, 2H), 1.99 (d, *J*

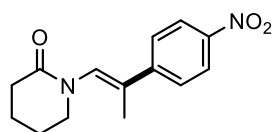
= 1.4 Hz, 3H), 1.88 – 1.85 (m, 4H). ^{13}C NMR (100 MHz, CDCl_3) δ 170.23, 140.71, 133.45, 128.36(2C), 127.56, 127.15, 126.25(2C), 50.08, 32.58, 23.37, 21.39, 16.30. LC-MS: 216.2 ($\text{M}+\text{H}^+$), 431.2 ($2\text{M}+\text{H}^+$), 453.2 ($2\text{M}+\text{Na}^+$). Anal. Calc. for ($\text{C}_{14}\text{H}_{17}\text{NO}$: 215.13): C, 78.10; H, 7.96; N, 6.51; found: C, 78.01, H, 7.80; N, 6.39.



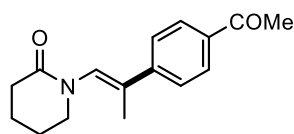
102ab. Yellow solid, mp = 103 - 105 °C, *c*Hex:EtOAc = 1:1. Yield = 70% (32.6 mg). ^1H NMR (400 MHz, CDCl_3) δ 7.41 – 7.36 (m, 2H), 7.01 (t, J = 8.7 Hz, 2H), 6.44 (s, 1H), 3.48 – 3.45 (m, 2H), 2.52 – 2.48 (s, 2H), 1.99 (d, J = 1.1 Hz, 3H), 1.90 – 1.87 (m, 4H). ^{13}C NMR (100 MHz, CDCl_3) δ 170.28, 163.66, 161.22, 136.76 (d, J = 3.3 Hz), 132.62, 127.84 (d, J = 7.9 Hz, 2C), 127.04, 115.20 (d, J = 21.4 Hz, 2C), 50.09, 32.57, 23.36, 21.37, 16.45. LC-MS: 234.0 ($\text{M}+\text{H}^+$), 489.0 ($2\text{M}+\text{Na}^+$). Anal. Calc. for ($\text{C}_{14}\text{H}_{16}\text{FNO}$: 233.12): C, 72.08; H, 6.91; N, 6.00; found: C, 72.00, H, 6.75; N, 5.85.



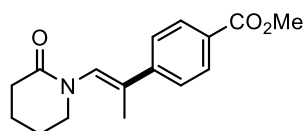
102ac. Yellow solid, mp = 104 - 106 °C, *c*Hex:EtOAc = 1:1. Yield = 62% (36.3 mg). ^1H NMR (400 MHz, CDCl_3) δ 7.45 – 7.41 (m, 2H), 7.30 – 7.27 (m, 2H), 6.49 (s, 1H), 3.47 – 3.45 (m, 2H), 2.52 – 2.46 (m, 2H), 1.98 (d, J = 1.3 Hz, 3H), 1.89 – 1.86 (m, 4H). ^{13}C NMR (100 MHz, CDCl_3) δ 170.29, 139.74, 132.25, 131.49(2C), 127.89(2C), 127.62, 121.49, 50.11, 32.60, 23.38, 21.38, 16.28. LC-MS: 294.0 ($\text{M}+\text{H}^+$), 296.0 ($\text{M}+\text{H}^+$). Anal. Calc. for ($\text{C}_{14}\text{H}_{16}\text{BrNO}$: 293.04): C, 57.16; H, 5.48; N, 4.76; found: C, 57.03, H, 5.32; N, 7.61.



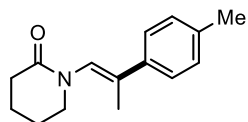
102ad. Yellow solid, mp = 146 - 148 °C, *c*Hex:EtOAc = 1:1. Yield = 89% (46.3 mg). ^1H NMR (400 MHz, CDCl_3) δ 8.19 – 8.14 (m, 2H), 7.57 – 7.52 (m, 2H), 6.68 (d, J = 1.0 Hz, 1H), 3.52 (t, J = 5.6 Hz, 2H), 2.52 (t, J = 5.6 Hz, 2H), 2.05 (d, J = 1.3 Hz, 3H), 1.95 – 1.86 (m, 4H). ^{13}C NMR (100 MHz, CDCl_3) δ 170.42, 147.61, 147.04, 130.58, 130.26, 126.84(2C), 123.74(2C), 50.15, 32.57, 23.34, 21.23, 16.33. LC-MS: 261.0 ($\text{M}+\text{H}^+$), 283.0 ($\text{M}+\text{Na}^+$). Anal. Calc. for ($\text{C}_{14}\text{H}_{16}\text{N}_2\text{O}_3$: 260.12): C, 64.60; H, 6.20; N, 10.76; found: C, 64.46, H, 6.02; N, 10.61.



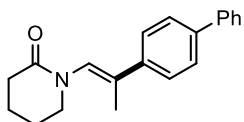
102ae. Yellow solid, mp = 65 - 67 °C, *c*Hex:EtOAc = 1:1. Yield = 78% (40.1 mg). ^1H NMR (400 MHz, CDCl_3) δ 7.93 – 7.86 (m, 2H), 7.52 – 7.46 (m, 2H), 6.62 (s, 1H), 3.49 (s, 2H), 2.58 (s, 3H), 2.50 (s, 2H), 2.02 (d, J = 1.3 Hz, 3H), 1.90-1.87 (m, 4H). ^{13}C NMR (100 MHz, CDCl_3) δ 197.72, 170.33, 145.59, 136.05, 131.88, 128.95, 128.52(2C), 126.28(2C), 50.10, 32.55, 26.69, 23.33, 21.28, 16.20. LC-MS: 258.0 ($\text{M}+\text{H}^+$), 259.0 ($\text{M}+\text{H}_2\text{O}$), 537.2 ($2\text{M}+\text{Na}^+$). Anal. Calc. for ($\text{C}_{16}\text{H}_{19}\text{NO}_2$: 257.14): C, 74.68; H, 7.44; N, 5.44; found: C, 74.51, H, 7.54; N, 5.21.



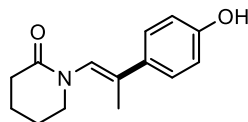
102af. Yellow solid, mp = 100 - 103 °C, *c*Hex:EtOAc = 1:1. Yield = 78% (42.6 mg). ^1H NMR (400 MHz, CDCl_3) δ 7.97 (d, J = 8.6 Hz, 2H), 7.47 (d, J = 8.7 Hz, 2H), 6.60 (s, 1H), 3.90 (s, 3H), 3.48 (s, 2H), 2.50 (s, 2H), 2.02 (d, J = 1.3 Hz, 3H), 1.91 – 1.84 (m, 4H). ^{13}C NMR (100 MHz, CDCl_3) δ 170.28, 166.98, 145.40, 132.01, 129.69(2C), 129.04, 128.82, 126.10(2C), 52.14, 50.08, 32.55, 23.34, 21.29, 16.21. LC-MS: 274.0 ($\text{M}+\text{H}^+$), 296.0 ($\text{M}+\text{Na}^+$), 312.0 ($\text{M}+\text{K}^+$). Anal. Calc. for ($\text{C}_{16}\text{H}_{19}\text{NO}_3$: 273.14): C, 70.31; H, 7.01; N, 5.12; found: C, 70.17, H, 6.93; N, 5.19.



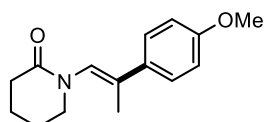
102ag. Yellow solid, mp: 70 - 72 °C, *c*Hex:EtOAc = 1:1. Yield = 81% (37.1 mg). ¹H NMR (400 MHz, CDCl₃) δ 7.32 (d, *J* = 8.1 Hz, 2H), 7.12 (d, *J* = 7.9 Hz, 2H), 6.47 (s, 1H), 3.46 (s, 2H), 2.50 (s, 3H), 2.34 (s, 3H), 1.99 (d, *J* = 1.2 Hz, 4H), 1.88 (m, 4H). ¹³C NMR (100 MHz, CDCl₃) δ 170.25, 137.80, 137.33, 133.44, 129.07(2C), 126.51, 126.13(2C), 50.12, 32.60, 23.40, 21.43, 21.21, 16.28. LC-MS: 230.2 (M+H⁺), 459.2 (2M+H⁺), 481.2 (2M+Na⁺). Anal. Calc. for (C₁₅H₁₉NO: 229.15): C, 78.56; H, 8.35; N, 6.11; found: C, 78.45, H, 8.21; N, 6.18.



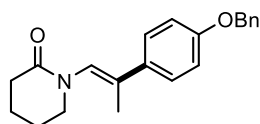
102ah. White solid, mp = 106 - 108 °C, *c*Hex:EtOAc = 1:1. Yield = 86% (50.1 mg). ¹H NMR (400 MHz, CDCl₃) δ 7.60 (dd, *J* = 8.0, 0.9 Hz, 2H), 7.54 (dd, *J* = 22.8, 8.6 Hz, 4H), 7.44 (t, *J* = 7.5 Hz, 2H), 7.34 (t, *J* = 7.3 Hz, 1H), 6.58 (s, 1H), 3.49 (s, 2H), 2.52 (s, 2H), 2.05 (d, *J* = 1.2 Hz, 2H), 1.92 - 1.87 (m, 4H). ¹³C NMR (100 MHz, CDCl₃) δ 170.28, 140.77, 140.34, 139.66, 132.85, 128.88(2C), 127.39, 127.22, 127.07(2C), 127.05(2C), 126.61(2C), 50.14, 32.60, 23.39, 21.40, 16.26. LC-MS: 292.0 (M+H⁺), 583.2 (2M+H⁺) 605.2 (2M+Na⁺). Anal. Calc. for (C₂₀H₂₁NO: 291.16): C, 82.44; H, 7.26; N, 4.81; found: C, 82.35, H, 7.36; N, 4.75.



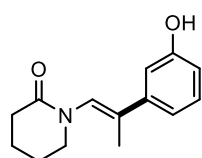
102ai. White solid, mp = 160 - 164 °C, *c*Hex:EtOAc = 1:1. Yield = 67% (31.0 mg). ¹H NMR (400 MHz, CDCl₃) δ 7.75 (s, 1H), 7.04 - 6.99 (m, 2H), 6.74 - 6.68 (m, 2H), 6.32 (s, 1H), 3.44 (s, 2H), 2.53 (s, 2H), 1.92 (t, *J* = 2.9 Hz, 3H), 1.88 (dt, *J* = 6.3, 3.1 Hz, 4H). ¹³C NMR (100 MHz, CDCl₃) δ 171.33, 156.51, 134.56, 131.07, 126.79(2C), 124.51, 115.42(2C), 50.12, 32.26, 23.05, 21.04, 15.56. LC-MS: 232.0 (M+H⁺), 485.2 (2M+Na⁺). Anal. Calc. for (C₁₄H₁₇NO₂: 231.13): C, 72.70; H, 7.41; N, 6.06; found: C, 72.55, H, 7.31; N, 5.89.



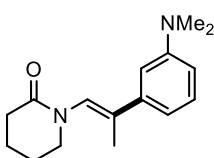
102aj. Yellow solid, mp = 70 - 72 °C, *c*Hex:EtOAc = 1:1. Yield = 81% (39.7 mg). ¹H NMR (400 MHz, CDCl₃) δ 7.38 - 7.34 (m, 1H), 6.88 - 6.83 (m, 2H), 6.42 (s, 1H), 3.80 (s, 3H), 3.46 - 3.43 (m, 2H), 2.51 - 2.47 (m, 2H), 1.98 (d, *J* = 1.2 Hz, 2H), 1.89 - 1.86 (m, 4H). ¹³C NMR (100 MHz, CDCl₃) δ 170.30, 137.74, 137.32, 133.52, 129.05(2C), 126.42, 126.10(2C), 50.10, 32.55, 23.35, 21.38, 21.18, 16.25. LC-MS: 246.2 (M+H⁺), 513.2 (2M+Na⁺). Anal. Calc. for (C₁₅H₁₉NO₂: 245.14): C, 73.44; H, 7.81; N, 5.71; found: C, 73.25, H, 7.25; N, 5.55.



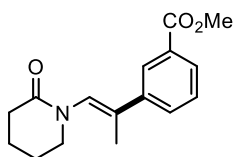
102ak. Yellow oil, *c*Hex:EtOAc = 1:1. Yield = 78% (44.8 mg). ¹H NMR (400 MHz, CDCl₃) δ 7.35 (d, *J* = 8.9 Hz, 2H), 6.85 (d, *J* = 8.8 Hz, 2H), 6.41 (s, 1H), 3.96 (t, *J* = 6.5 Hz, 2H), 3.45 (s, 2H), 2.50 (br, 2H), 1.98 (d, *J* = 1.2 Hz, 3H), 1.90 - 1.86 (m, 4H), 1.80 - 1.72 (m, 2H), 1.49 (dq, *J* = 14.7, 7.4 Hz, 2H), 0.98 (t, *J* = 7.4 Hz, 3H). ¹³C NMR (100 MHz, CDCl₃) δ 170.31, 158.86, 133.37, 132.84, 127.27(2C), 125.65, 114.35(2C), 67.83, 50.15, 32.56, 31.44, 23.37, 21.41, 19.36, 16.23, 13.97. LC-MS: 288.2 (M+H⁺), 575.2 (2M+H⁺), 597.2 (2M+Na⁺). Anal. Calc. for (C₁₈H₂₅NO₂: 287.19): C, 75.22; H, 8.77; N, 4.87; found: C, 75.08, H, 8.56; N, 4.65.



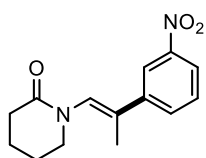
102al. White solid, mp = 104 - 106 °C, cHex:EtOAc = 1:1. Yield = 63% (29.1 mg). ¹H NMR (400 MHz, CDCl₃) δ 7.10 (t, *J* = 7.9 Hz, 1H), 6.89 – 6.87 (m, 1H), 6.85 (dd, *J* = 7.7, 0.8 Hz, 1H), 6.76 – 6.69 (m, 1H), 6.42 (s, 1H), 3.44 (s, 2H), 2.54 (s, 2H), 1.94 (d, *J* = 1.2 Hz, 3H), 1.90 – 1.87 (m, 4H). ¹³C NMR (100 MHz, CDCl₃) δ 171.18, 156.78, 141.58, 134.80, 129.25, 126.27, 117.63, 115.12, 113.48, 50.14, 32.32, 23.19, 21.18, 16.18. LC-MS: 232.0 (M+H⁺), 463.2 (2M+H⁺), 485.0 (2M+Na⁺). Anal. Calc. for (C₁₄H₁₇NO₂: 231.13): C, 72.70; H, 7.41; N, 6.06; found: C, 72.45, H, 7.25; N, 5.95.



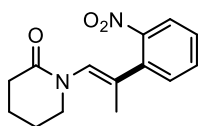
102am. Colorless oil, cHex:EtOAc = 1:2. Yield = 67% (34.6 mg). ¹H NMR (400 MHz, CDCl₃) δ 7.19 (t, *J* = 8.1 Hz, 1H), 6.80 – 6.76 (m, 2H), 6.69 – 6.65 (m, 1H), 6.47 (s, 1H), 3.47 (s, 2H), 2.95 (s, 6H), 2.50 (s, 2H), 2.00 (d, *J* = 0.7 Hz, 3H), 1.89– 1.86 (m, 4H). ¹³C NMR (100 MHz, CDCl₃) δ 170.16, 150.75, 141.78, 134.45, 128.98, 126.86, 115.11, 112.17, 110.84, 50.09, 40.89, 32.62, 23.41, 21.44, 16.61. LC-MS: 259.2 (M+H⁺), 297.2 (M+K⁺). Anal. Calc. for (C₁₆H₂₂N₂O: 258.17): C, 74.38; H, 8.58; N, 10.84; found: C, 74.21, H, 8.45; N, 10.69.



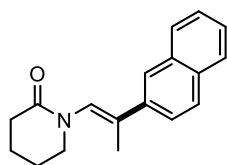
102an. Yellow oil, cHex:EtOAc = 1:1. Yield = 85% (46.4 mg). ¹H NMR (400 MHz, CDCl₃) δ 8.08 (t, *J* = 1.6 Hz, 1H), 7.94 – 7.91 (td, *J* = 7.8, 1.2 Hz, 1H), 7.61 (ddd, *J* = 7.8, 1.8, 1.2 Hz, 1H), 7.38 (t, *J* = 7.8 Hz, 1H), 6.55 (s, 1H), 3.91 (s, 3H), 3.48 (t, *J* = 5.9 Hz, 2H), 2.50 (t, *J* = 6.1 Hz, 2H), 2.03 (d, *J* = 1.3 Hz, 3H), 1.89–1.87 (m, 4H). ¹³C NMR (100 MHz, CDCl₃) δ 170.24, 167.14, 141.07, 132.39, 130.67, 130.30, 128.63, 128.47, 128.03, 127.39, 52.24, 50.10, 32.57, 23.36, 21.35, 16.32. LC-MS: 274.0 (M+H⁺), 296.0 (M+Na⁺), 312.0 (M+K⁺). Anal. Calc. for (C₁₆H₁₉NO₃: 273.14): C, 70.31; H, 7.01; N, 5.12; found: C, 70.41, H, 6.85; N, 5.11.



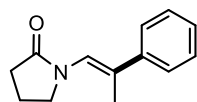
102ao. Yellow solid, mp = 108 - 110 °C, cHex:EtOAc = 1:1. Yield = 85% (44.2 mg). ¹H NMR (400 MHz, CDCl₃) δ 8.24 (t, *J* = 1.9 Hz, 1H), 8.11 – 8.07 (m, 1H), 7.75 – 7.72 (m, 1H), 7.47 (t, *J* = 8.0 Hz, 1H), 6.61 (s, 1H), 3.51 – 3.48 (m, 2H), 2.52 – 2.48 (m, 2H), 2.04 (d, *J* = 1.3 Hz, 3H), 1.91 – 1.87 (m, 4H). ¹³C NMR (100 MHz, CDCl₃) δ 170.33, 148.38, 142.60, 132.15, 130.77, 129.32, 122.25, 121.08, 50.13, 32.57, 23.33, 21.27, 16.34. LC-MS: 261.0 (M+H⁺), 283.0 (M+Na⁺), 521.0 (2M+H⁺), 543.0 (2M+Na⁺). Anal. Calc. for (C₁₄H₁₆N₂O₃: 260.12): C, 64.60; H, 6.20; N, 10.76; found: C, 64.51, H, 6.42; N, 10.50.



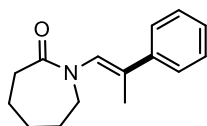
102ap. Yellow oil, cHex:EtOAc = 1:2. Yield = 38% (19.8 mg). ¹H NMR (401 MHz, CDCl₃) δ 7.88 (dd, *J* = 8.1, 1.2 Hz, 1H), 7.56 (td, *J* = 7.6, 1.3 Hz, 1H), 7.46 (dd, *J* = 7.7, 1.5 Hz, 1H), 7.44 – 7.38 (m, 1H), 6.20 (d, *J* = 0.9 Hz, 1H), 3.52 (t, *J* = 5.9 Hz, 2H), 2.47 (t, *J* = 6.1 Hz, 2H), 1.96 (d, *J* = 1.3 Hz, 3H), 1.88 – 1.85 (m, 4H). ¹³C NMR (101 MHz, CDCl₃) δ 170.82, 149.16, 137.73, 133.36, 131.85, 130.94, 128.65, 128.61, 124.61, 49.70, 32.76, 23.59, 21.58, 18.56. LC-MS: 261.1 (M+H⁺), 299.1 (M+K⁺). Anal. Calc. for (C₁₄H₁₆N₂O₃: 260.12): C, 64.60; H, 6.20; N, 10.76; found: C, 64.39, H, 6.15; N, 10.61.



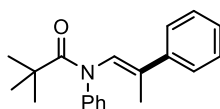
102aq. Yellow solid, mp = 83 - 85 °C, cHex:EtOAc = 1:1. Yield = 82% (43.5 mg). ¹H NMR (400 MHz, CDCl₃) δ 7.85 (d, *J* = 1.4 Hz, 1H), 7.83 – 7.77 (m, 3H), 7.60 (dd, *J* = 8.6, 1.9 Hz, 1H), 7.49 – 7.41 (m, 2H), 6.66 (s, 1H), 3.52 (t, *J* = 5.6 Hz, 2H), 2.54 (t, *J* = 6.4 Hz, 2H), 2.12 (d, *J* = 1.3 Hz, 3H), 1.91 (dt, *J* = 6.1, 3.0 Hz, 4H). ¹³C NMR (101 MHz, CDCl₃) δ 170.31, 138.01, 133.46, 133.20, 132.88, 128.19, 127.86, 127.67, 127.62, 126.26, 125.92, 125.05, 124.46, 50.17, 32.60, 23.39, 21.39, 16.35. LC-MS: 266.0 (M+H⁺), 304.0 (M+K⁺). Anal. Calc. for (C₁₆H₁₉NO₃: 265.15): C, 81.47; H, 7.22; N, 5.28; found: C, 81.31, H, 7.05; N, 5.15.



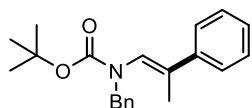
102ba. White solid, mp = 146 - 150 °C, cHex:EtOAc = 1:1. Yield = 60% (24.1 mg). ¹H NMR (400 MHz, CDCl₃) δ 7.42 – 7.37 (m, 2H), 7.34 – 7.28 (m, 2H), 7.26 – 7.21 (m, 1H), 6.60 (d, *J* = 1.1 Hz, 1H), 3.78 (t, *J* = 8.1 Hz, 2H), 2.47 (t, *J* = 8.1 Hz, 2H), 2.17 – 2.07 (m, 6H). ¹³C NMR (100 MHz, CDCl₃) δ 175.00, 141.85, 128.36(2C), 127.62, 127.17, 126.15(2C), 122.57, 49.30, 30.75, 19.08, 16.68. LC-MS: 202.0 (M+H⁺), 224.0 (M+Na⁺), 403.0 (2M+H⁺), 435.2 (2M+Na⁺). Anal. Calc. for (C₁₃H₁₅NO: 201.12): C, 77.58; H, 7.51; N, 6.98; found: C, 77.35, H, 7.41; N, 7.10.



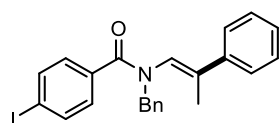
102ca. Yellow oil, cHex:EtOAc = 1:1. Yield = 77% (35.3 mg). ¹H NMR (400 MHz, CDCl₃) δ 7.43 – 7.37 (m, 2H), 7.31 – 7.29 (m, 2H), 7.26 – 7.20 (m, 1H), 6.58 (d, *J* = 1.3 Hz, 1H), 3.56 (d, *J* = 6.4 Hz, 2H), 2.62 (d, *J* = 8.6 Hz, 2H), 2.00 (d, *J* = 1.3 Hz, 3H), 1.77 (s, 6H). ¹³C NMR (100 MHz, CDCl₃) δ 176.13, 140.87, 131.31, 128.69, 128.35(2C), 127.39, 126.21(2C), 52.07, 37.64, 30.10, 28.98, 23.55, 16.61. LC-MS: 230.0 (M+H⁺). Anal. Calc. for (C₁₅H₁₉NO: 229.15)



102da. Yellow oil, cHex:EtOAc = 1:1. Yield = 63% (36.9 mg). ¹H NMR (400 MHz, CDCl₃) δ 7.44 – 7.39 (m, 2H), 7.39 – 7.30 (m, 5H), 7.29 – 7.25 (m, 2H), 7.23 – 7.19 (m, 1H), 6.85 (d, *J* = 1.3 Hz, 1H), 1.89 (d, *J* = 1.3 Hz, 3H), 1.33 (s, 9H). ¹³C NMR (100 MHz, CDCl₃) δ 178.71, 143.94, 140.44, 135.24, 128.70(2C), 128.47(2C), 128.29, 127.74, 127.10(2C), 126.00, 125.94(2C), 40.75, 28.16, 16.11. LC-MS: 294.2 (M+H⁺), 316.0 (M+Na⁺). Anal. Calc. for (C₂₀H₂₃NO: 293.18) C, 81.87; H, 7.90; N, 4.77; found: C, 81.73, H, 7.76; N, 4.61.

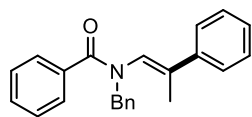


102ea. Yellow oil, cHex:EtOAc = 10:1. Yield = 59% (38.1 mg). ¹H NMR (400 MHz, CDCl₃) δ 7.34 – 7.22 (m, 10H), 6.16 (s, 1H), 4.61 (s, 2H), 1.93 (s, 3H), 1.47 (s, 9H). ¹³C NMR (100 MHz, CDCl₃) δ 141.37, 128.76, 128.53, 128.46, 128.40, 127.41, 127.33, 126.31, 29.86, 28.59, 28.54, 16.48. LC-MS: 268.0 (M-C₄H₉+2H⁺), 324.0 (M+H⁺), 346.0 (M+Na⁺). Anal. Calc. for (C₂₁H₂₅NO₂: 323.19): C, 77.98; H, 7.79; N, 4.33; found: C, 77.81, H, 7.85; N, 4.21.

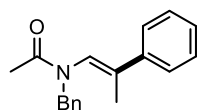


102fa. Colorless oil, cHex:EtOAc = 10:1. Yield = 78% (70.7 mg). ¹H NMR (400 MHz, CDCl₃) δ 7.66 (d, *J* = 8.2 Hz, 2H), 7.41 (d, *J* = 7.0 Hz, 2H), 7.34 (d, *J* = 8.4 Hz, 3H), 7.32 – 7.24 (m, 5H), 7.08 (d, *J* = 5.4 Hz, 2H), 6.24 (s, 1H), 4.85 (s, 2H), 1.50 (s, 2H). ¹³C NMR (100 MHz, CDCl₃) δ 169.64, 140.09, 136.97, 136.74, 135.99, 130.03, 129.13, 128.66, 128.57, 128.05, 127.77, 126.54, 126.06, 96.85,

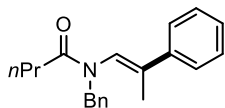
51.68, 16.18. LC-MS: 454 (M+H⁺), 476.0 (M+Na⁺), 928.8 (2M+Na⁺). Anal. Calc. for (C₂₃H₂₀INO: 453.06): C, 60.94; H, 4.45; N, 3.09; found: C, 60.75, H, 4.38; N, 3.11.



102ga. Yellow solid, mp = 83 - 85 °C, *c*Hex:EtOAc = 10:1. Yield = 81% (53.0 mg). ¹H NMR (400 MHz, CDCl₃) δ 7.61 (dd, *J* = 7.7, 1.6 Hz, 1H), 7.45 (d, *J* = 6.9 Hz, 1H), 7.38 – 7.28 (m, 3H), 7.27 – 7.18 (m, 2H), 6.26 (s, 1H), 4.90 (s, 1H), 1.52 (s, 2H). ¹³C NMR (100 MHz, CDCl₃) δ 170.55, 140.28, 136.87, 136.40, 130.09, 129.44, 128.92, 128.48, 128.32, 128.19, 127.69, 127.63, 127.52, 126.78, 125.97, 120.01, 115.41, 51.41, 16.10. LC-MS: 328.0 (M+H⁺), 350.0 (M+Na⁺), 677.2 (2M+Na⁺). Anal. Calc. for (C₂₃H₂₁NO: 327.16): C, 84.37; H, 6.46; N, 4.28; found: C, 84.25, H, 6.30; N, 4.10.



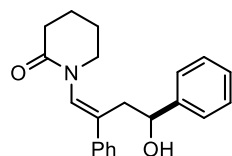
102ha. Yellow oil, *c*Hex:EtOAc = 5:1. Yield = 80% (42.4 mg). ¹H NMR (400 MHz, CDCl₃) δ 7.38 – 7.27 (m, 10H), 6.29 (d, *J* = 1.4 Hz, 1H), 4.72 (s, 2H), 2.09 (s, 3H), 1.83 (d, *J* = 1.4 Hz, 3H). ¹³C NMR (100 MHz, CDCl₃) δ 170.60, 139.86, 138.98, 137.23, 129.06(2C), 128.64(2C), 128.56(2C), 128.27, 127.54, 126.24, 126.15(2C), 50.71, 22.30, 15.77. LC-MS: 266 (M+H⁺), 288.0 (M+Na⁺). Anal. Calc. for (C₁₈H₁₉NO: 265.15): C, 81.47; H, 7.22; N, 5.28; found: C, 81.25, H, 7.111; N, 5.31.



102ia. White solid, mp = 145 - 50 °C, *c*Hex:EtOAc = 5:1. Yield = 81% (49.7 mg). ¹H NMR (400 MHz, CDCl₃) δ 7.37 – 7.22 (m, 10H), 6.28 (d, *J* = 1.4 Hz, 1H), 4.72 (s, 2H), 2.35 – 2.29 (m, 2H), 1.84 (d, *J* = 1.3 Hz, 3H), 1.65 (dt, *J* = 15.1, 7.5 Hz, 2H), 1.34 (dt, *J* = 14.6, 7.4 Hz, 2H), 0.90 (t, *J* = 7.3 Hz, 3H). ¹³C NMR (100 MHz, CDCl₃) δ 173.48, 139.96, 138.86, 137.46, 129.04(2C), 128.66(2C), 128.56(2C), 128.25, 127.49, 126.18(2C), 125.96, 50.83, 34.07, 27.47, 22.66, 15.82, 14.04. LC-MS: 308.2 (M+H⁺), 330.0 (M+Na⁺), 637.2 (2M+Na⁺). Anal. Calc. for (C₂₁H₂₅NO: 307.19): C, 82.04; H, 8.20; N, 4.56; found: C, 81.90, H, 8.15; N, 4.45.

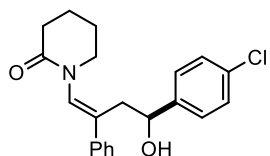
General procedure for the Ni-catalyzed tri-component cross-coupling reaction (example for (E)-106a).

To a dry Schlenk tube anhydrous 1,4-dioxane (1 mL) was added under nitrogen atmosphere, followed by 4,4'-diMeObpyNiCl₂ 3.7 mg (0.01 mmol, 5 mol%), potassium carbonate 82.8 mg (0.6 mmol, 3.0 eq.), phenylboronic acid **101a** 36.9 mg (0.3 mmol, 1.5 eq.), PhCHO 41 μL (0.4 mmol, 2.0 eq.) and **100a** 27.4 mg (0.2 mmol, 1.0 eq.). Then the resulting mixture was poured into a pre-heated oil bath at 90 °C and stirred for 1 hour when TLC showed complete consumption of the allenamide. Then solvent was removed under vacuum and the residue was purified with silica gel column flash-chromatography (*c*Hex:AcOEt 1:1) to give **106a** as white solid. Yield = 84%, 54.0 mg.

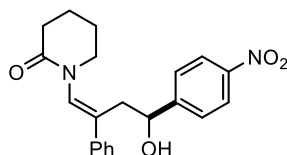


106a. White solid, mp = 145 - 150 °C, *c*Hex:EtOAc = 1:1. Yield = 84% (54.0 mg). ¹H NMR (400 MHz, CDCl₃) δ 7.51 – 7.47 (m, 2H), 7.43 – 7.37 (m, 2H), 7.37 – 7.29 (m, 5H), 7.25 – 7.19 (m, 1H), 5.99 (s, 1H), 4.63 (dd, *J* = 10.4, 4.0 Hz, 1H), 3.42 – 3.37 (m, 1H), 3.30 – 3.22 (m, 1H), 2.86 (ddd, *J* = 14.4, 4.0, 1.5 Hz, 1H), 2.74 (dd, *J* = 14.4, 10.4 Hz, 1H), 2.54 – 2.51 (m, 1H), 1.91 – 1.79 (m, 4H). ¹³C NMR (100 MHz, CDCl₃) δ 170.43, 146.12, 139.16, 138.77, 128.66(2C), 128.28(2C), 128.08, 128.04,

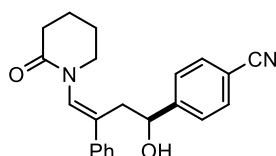
127.24(2C), 126.93, 125.52(2C), 70.77, 50.35, 40.57, 32.57, 22.95, 21.11. LC-MS: 304.0 (M-OH), 322.2 (M+H⁺), 665.2 (2M+Na⁺). Anal. Calc. for (C₂₁H₂₃NO₂: 321.17): C, 78.47; H, 7.21; N, 4.36; found: C, 78.31, H, 7.41; N, 4.15.



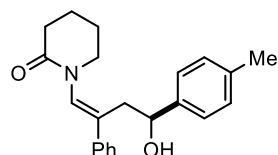
106b. Pink solid, mp = 162 - 165 °C, cHex:EtOAc = 1:1. Yield = 93% (66.0 mg). ¹H NMR (400 MHz, CDCl₃) δ 7.49 – 7.44 (m, 2H), 7.43 – 7.33 (m, 3H), 7.27 (s, 4H), 5.93 (s, 1H), 4.59 (dd, *J* = 10.6, 3.8 Hz, 1H), 3.43 – 3.37 (m, 1H), 3.34 – 3.20 (m, 1H), 2.81 (ddd, *J* = 14.3, 3.8, 1.4 Hz, 1H), 2.66 (dd, *J* = 14.4, 10.7 Hz, 1H), 2.53 (br, 1H), 1.94 – 1.76 (m, 4H). ¹³C NMR (100 MHz, CDCl₃) δ 170.45, 144.83, 139.17, 138.57, 132.46, 128.76(2C), 128.40(2C), 128.24, 128.01, 127.23(2C), 126.96(2C), 70.11, 50.44, 40.55, 32.62, 22.94, 21.12. LC-MS: 338.0 (M-OH), 356.0 (M+H⁺), 733.0 (2M+Na⁺). Anal. Calc. for (C₂₁H₂₂NCIO₂: 355.13): C, 70.88; H, 6.23; N, 3.94; found: C, 70.65, H, 6.11; N, 3.85.



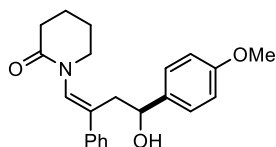
5c. White solid, mp = 176 - 178 °C, cHex:EtOAc = 1:1. Yield = 89% (65.1 mg). ¹H NMR (400 MHz, CDCl₃) δ 8.14 (d, *J* = 8.8 Hz, 2H), 7.50 (d, *J* = 8.5 Hz, 2H), 7.46 (dd, *J* = 8.0, 1.5 Hz, 2H), 7.42 – 7.33 (m, 3H), 5.91 (s, 1H), 4.70 (dd, *J* = 10.7, 3.8 Hz, 1H), 3.44 – 3.39 (m, 1H), 3.36 – 3.26 (m, 1H), 2.87 (ddd, *J* = 14.3, 3.8, 1.4 Hz, 1H), 2.65 (dd, *J* = 14.3, 10.7 Hz, 1H), 2.58-2.51 (m, 1H), 1.88-1.84 (m, Hz, 4H). ¹³C NMR (100 MHz, CDCl₃) δ 170.45, 154.06, 146.96, 138.79, 138.34, 128.82(2C), 128.38, 128.20, 127.24(2C), 126.35(2C), 123.62(2C), 70.05, 50.49, 40.20, 32.64, 22.87, 21.05. LC-MS: 367.0 (M+H⁺). Anal. Calc. for (C₂₁H₂₂N₂O₄: 366.16): C, 68.88; H, 6.05; N, 7.65; found: C, 68.71, H, 5.95; N, 7.55.



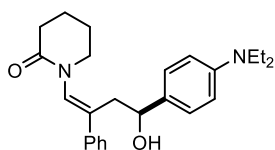
106d. Pink solid, mp = 189 - 190 °C, cHex:EtOAc = 1:1. Yield = 82% (56.7 mg). ¹H NMR (400 MHz, CDCl₃) δ 7.57 (d, *J* = 8.2 Hz, 2H), 7.44 (d, *J* = 7.8 Hz, 4H), 7.41 – 7.33 (m, 3H), 5.90 (s, 1H), 5.66 (s, 1H), 4.64 (d, *J* = 7.9 Hz, 1H), 3.46 – 3.34 (m, 2H), 3.31 – 3.28 (m, 1H), 2.84 (dd, *J* = 14.3, 2.7 Hz, 1H), 2.64 (dd, *J* = 14.3, 10.7 Hz, 1H), 2.52 (d, *J* = 3.1 Hz, 2H), 1.92 – 1.82 (m, 4H). ¹³C NMR (100 MHz, CDCl₃) δ 170.40, 151.90, 138.78, 138.38, 132.16(2C), 128.77(2C), 128.30, 128.15, 127.20(2C), 126.29(2C), 119.21, 110.50, 70.16, 50.44, 40.17, 32.61, 22.86, 21.03. LC-MS: 329.0 (M-OH), 347.0 (M+H⁺), 369.0 (M+Na⁺), 725.2 (2M+Na⁺). Anal. Calc. for (C₂₂H₂₂N₂O₂: 346.17): C, 76.28; H, 6.40; N, 8.09; found: C, 76.09, H, 6.21; N, 7.89.



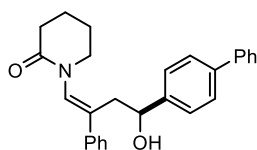
106e. Yellow solid, mp = 167 - 169 °C, cHex:EtOAc = 1:1. Yield = 70% (46.9 mg). ¹H NMR (400 MHz, CDCl₃) δ 7.50 – 7.46 (m, 2H), 7.42 – 7.38 (m, 2H), 7.36 – 7.33 (m, 1H), 7.24 (d, *J* = 8.0 Hz, 2H), 7.13 (d, *J* = 7.9 Hz, 2H), 5.98 (s, 1H), 4.60 (dd, *J* = 10.5, 3.8 Hz, 1H), 3.43 – 3.34 (m, 1H), 3.32 – 3.22 (m, 1H), 2.83 (ddd, *J* = 14.3, 3.9, 1.4 Hz, 1H), 2.72 (dd, *J* = 14.4, 10.6 Hz, 1H), 2.53 (br, 2H), 2.33 (s, 3H), 1.89 – 1.81 (m, 24H). ¹³C NMR (100 MHz, CDCl₃) δ 170.47, 143.22, 139.35, 138.74, 136.53, 129.01(2C), 128.71(2C), 128.13, 127.98, 127.26(2C), 125.45(2C), 70.58, 50.40, 40.65, 32.60, 22.99, 21.24, 21.16. LC-MS: 318.2 (M-OH), 693.2 (2M+Na⁺). Anal. Calc. for (C₂₂H₂₅NO₂: 335.19): C, 78.77; H, 7.51; N, 4.18; found: C, 78.51, H, 7.65; N, 4.25.



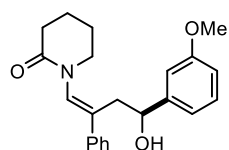
106f. Yellow solid, mp = 151 - 155 °C, *c*Hex:EtOAc = 1:1. Yield = 77% (54.1 mg). ¹H NMR (400 MHz, CDCl₃) δ 7.47 (dd, *J* = 8.1, 1.3 Hz, 2H), 7.39 (dd, *J* = 11.4, 4.4 Hz, 2H), 7.36 – 7.31 (m, 1H), 7.27 (s, 1H), 7.24 (s, 1H), 6.87 – 6.83 (m, 1H), 5.98 (s, 1H), 4.85 (s, 1H), 4.58 (dd, *J* = 10.0, 3.2 Hz, 1H), 3.79 (s, 1H), 3.42 – 3.36 (m, 1H), 3.32 – 3.24 (m, 1H), 2.82 (ddd, *J* = 14.3, 4.0, 1.3 Hz, 1H), 2.72 (dd, *J* = 14.4, 10.3 Hz, 1H), 2.53 (s, 2H), 1.86 (d, *J* = 3.5 Hz, 4H). ¹³C NMR (100 MHz, CDCl₃) δ 170.45, 158.61, 139.22, 138.75, 138.28, 128.67(2C), 128.09, 127.97, 127.22(2C), 126.66(2C), 113.67(2C), 70.35, 55.38, 50.38, 40.58, 32.59, 22.97, 21.14. LC-MS: 334.0 (M-OH), 725.2 (2M+Na⁺). Anal. Calc. for (C₂₂H₂₅NO₃: 351.18): C, 75.19; H, 7.17; N, 3.99; found: C, 75.06, H, 7.25; N, 4.15.



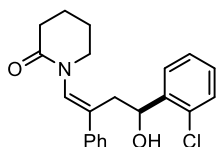
106g. Orange solid, mp: 77 - 80 °C, *c*Hex:EtOAc = 1:2. Yield = 26% (20.4 mg). ¹H NMR (400 MHz, CDCl₃) δ 7.49 – 7.45 (m, 2H), 7.40 – 7.38 (m, 2H), 7.35 – 7.30 (m, 1H), 7.17 (d, *J* = 8.6 Hz, 2H), 6.64 (d, *J* = 8.5 Hz, 2H), 6.05 (s, 1H), 4.59 – 4.51 (m, 1H), 4.27 (d, *J* = 4.8 Hz, 1H), 3.46 – 3.38 (m, 1H), 3.33 (q, *J* = 7.1 Hz, 4H), 3.30 – 3.23 (m, 1H), 2.83 – 2.78 (m, 2H), 2.53 (br, 2H), 1.86 (d, *J* = 3.5 Hz, 4H), 1.14 (t, *J* = 7.0 Hz, 6H). ¹³C NMR (100 MHz, CDCl₃) δ 170.50, 147.09, 139.15, 138.99, 132.60, 128.62, 128.04, 127.99, 127.26, 126.65, 111.78, 110.13, 70.64, 50.38, 44.53, 40.37, 32.60, 23.07, 21.22, 12.71. LC-MS: 375.2 (M-OH), 807.2 (2M+Na⁺). Anal. Calc. for (C₂₅H₃₂N₂O₂: 392.25): C, 76.49; H, 8.22; N, 7.14; found: C, 76.28, H, 8.03; N, 7.00.



106h. Pink solid, mp = 141 - 143 °C, *c*Hex:EtOAc = 1:1. Yield = 83% (65.9 mg). ¹H NMR (400 MHz, CDCl₃) δ 7.58 (d, *J* = 7.7 Hz, 2H), 7.55 (d, *J* = 8.0 Hz, 2H), 7.50 (d, *J* = 7.4 Hz, 2H), 7.42 (q, *J* = 7.4 Hz, 6H), 7.38 – 7.30 (m, 1H), 6.00 (s, 1H), 5.00 (s, 1H), 4.69 (dd, *J* = 10.3, 3.6 Hz, 1H), 3.46 – 3.38 (m, 1H), 3.31 – 3.28 (m, 1H), 2.90 (dd, *J* = 14.3, 3.3 Hz, 1H), 2.78 (dd, *J* = 14.3, 10.5 Hz, 1H), 2.55 (br, 2H), 1.87 (d, *J* = 3.5 Hz, 4H). ¹³C NMR (100 MHz, CDCl₃) δ 170.49, 145.30, 141.23, 139.94, 139.26, 138.77, 128.83(2C), 128.74(2C), 128.17, 128.10, 127.30(2C), 127.21(2C), 127.20, 127.13(2C), 126.00(2C), 70.58, 50.43, 40.59, 32.65, 23.01, 21.17. LC-MS: 380.0 (M-OH), 817.2 (2M+Na⁺). Anal. Calc. for (C₂₇H₂₇NO₂: 397.20): C, 81.58; H, 6.85; N, 3.52; found: C, 81.70, H, 6.64; N, 3.31.

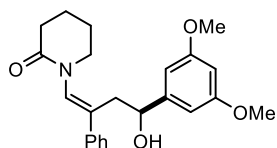


106i. Pink solid, mp = 175 - 178 °C, *c*Hex:EtOAc = 1:1. Yield = 76% (53.4 mg). ¹H NMR (400 MHz, CDCl₃) δ 7.48 (d, *J* = 7.6 Hz, 2H), 7.40 (t, *J* = 7.3 Hz, 2H), 7.37 – 7.32 (m, 1H), 7.23 (t, *J* = 7.9 Hz, 1H), 6.94 (d, *J* = 1.7 Hz, 1H), 6.91 (d, *J* = 7.7 Hz, 1H), 6.76 (dd, *J* = 8.1, 2.4 Hz, 1H), 5.97 (s, 1H), 4.98 (d, *J* = 5.6 Hz, 1H), 4.65 – 4.56 (m, 1H), 3.80 (s, 3H), 3.43 – 3.33 (m, 1H), 3.29 – 3.26 (m, 1H), 2.88 – 2.83 (m, 1H), 2.73 (dd, *J* = 14.4, 10.5 Hz, 1H), 2.53 (br, 2H), 1.91 – 1.82 (m, 4H). ¹³C NMR (100 MHz, CDCl₃) δ 170.45, 159.74, 148.01, 139.30, 138.70, 129.33(2C), 128.72, 128.16, 128.02, 127.26(2C), 117.86, 112.49, 111.07, 70.69, 55.37, 50.40, 40.47, 32.63, 22.99, 21.16. LC-MS: 334.2 (M-OH), 352.0 (M+H⁺), 725.2 (2M+Na⁺). Anal. Calc. for (C₂₂H₂₅NO₃: 351.18): C, 75.19; H, 7.17; N, 3.99; found: C, 75.31, H, 7.01; N, 4.20.

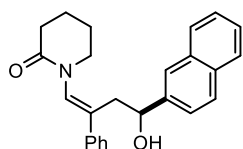


106j. Orange solid, mp = 146 - 148 °C, *c*Hex:EtOAc = 1:1. Yield = 84% (59.6 mg). ¹H NMR (400 MHz, CDCl₃) δ 7.66 (d, *J* = 7.8 Hz, 1H), 7.56 (dd, *J* = 8.1, 1.3 Hz, 2H), 7.42 – 7.34 (m, 2H), 7.37 – 7.33 (m, 1H), 7.27 (d, *J* = 7.6 Hz, 2H), 7.17

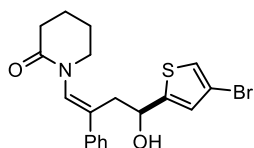
– 7.13 (m, 1H), 5.95 (s, 1H), 5.60 (d, $J = 6.5$ Hz, 1H), 5.00 – 4.92 (m, 1H), 3.47 – 3.38 (m, 1H), 3.30 – 3.28 (m, 1H), 3.13 (ddd, $J = 14.4, 3.5, 1.5$ Hz, 1H), 2.54 (s, 1H), 2.50 (dd, $J = 14.4, 10.9$ Hz, 2H), 1.90 – 1.82 (m, 4H). ^{13}C NMR (100 MHz, CDCl_3) δ 170.32, 143.81, 139.40, 138.18, 131.08, 129.03, 128.59(2C), 128.23, 127.93, 127.81, 127.53, 127.21, 127.17(2C), 67.88, 50.43, 37.50, 32.60, 22.87, 21.06. LC-MS: 338.0 (M-OH), 356.0 (M+H⁺), 733.0 (2M+Na⁺). Anal. Calc. for (C₂₁H₂₂NCIO₂: 355.13): C, 70.88; H, 6.23; N, 3.94; found: C, 71.02, H, 6.35; N, 3.70.



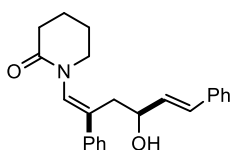
106k. Pink solid, mp = 103 - 106 °C, *c*Hex:EtOAc = 1:1. Yield = 78% (59.4 mg). ^1H NMR (400 MHz, CDCl_3) δ 7.46 – 7.43 (m, 2H), 7.39 – 7.35 (d, 2H), 7.34 – 7.30 (m, 1H), 6.50 (d, $J = 2.3$ Hz, 2H), 6.30 (t, $J = 2.3$ Hz, 1H), 5.95 (s, 1H), 4.99 (d, $J = 4.7$ Hz, 1H), 4.59 – 4.46 (m, 1H), 3.76 (s, 6H), 3.41 – 3.33 (m, 1H), 3.29 – 3.17 (m, 2H), 2.83 (ddd, $J = 14.3, 4.0, 1.4$ Hz, 1H), 2.71 (dd, $J = 14.4, 10.4$ Hz, 1H), 2.50 (br, 3H), 1.84 (d, $J = 3.4$ Hz, 4H). ^{13}C NMR (100 MHz, CDCl_3) δ 170.41, 160.78(2C), 148.88, 139.16, 138.66, 128.66(2C), 128.11, 127.98, 127.20(2C), 103.45(2C), 98.93, 70.76, 55.43, 50.35, 40.27, 32.58, 22.93, 21.10. LC-MS: 364.0 (M-OH), 382.0 (M+H⁺), 785.0 (2M+Na⁺). Anal. Calc. for (C₂₃H₂₇NO₄: 381.19): C, 72.42; H, 7.13; N, 3.67; found: C, 72.25, H, 7.30; N, 3.71.



106l. White solid, mp = 185 - 186 °C, *c*Hex:EtOAc = 1:1. Yield = 84% (62.3 mg). ^1H NMR (400 MHz, CDCl_3) δ 7.83 – 7.79 (m, 4H), 7.54 – 7.52 (m, 2H), 7.49 – 7.39 (m, 5H), 7.39 – 7.34 (m, 1H), 5.99 (s, 1H), 4.80 (dd, $J = 10.5, 3.7$ Hz, 1H), 3.43 – 3.37 (m, 1H), 3.30 – 3.25 (m, 1H), 2.95 (ddd, $J = 14.4, 3.7, 1.3$, 1H), 2.79 (dd, $J = 14.4, 10.6$ Hz, 1H), 2.57 – 2.54 (m, 2H), 1.90 – 1.81 (m, 4H). ^{13}C NMR (100 MHz, CDCl_3) δ 170.51, 143.62, 139.40, 138.77, 133.51, 132.80, 128.76(2C), 128.20, 128.06, 128.00, 127.73, 127.3(2C)2, 126.03, 125.56, 124.10, 123.94, 70.89, 50.42, 40.56, 32.64, 22.96, 21.14. LC-MS: 354.0 (M-OH), 765.2 (2M+Na⁺). Anal. Calc. for (C₂₅H₂₅NO₂: 371.19): C, 80.83; H, 6.78; N, 3.77; found: C, 80.71, H, 6.55; N, 3.60.

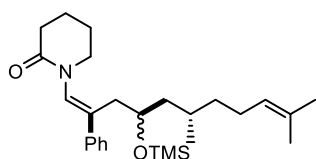


106m. White solid, mp = 169 - 171 °C, *c*Hex:EtOAc = 1:1. Yield = 73% (59.9 mg). ^1H NMR (400 MHz, CDCl_3) δ 7.44 (dd, $J = 8.1, 1.6$ Hz, 2H), 7.41 – 7.36 (m, 2H), 7.35 – 7.32 (m, 1H), 7.07 (d, $J = 1.4$ Hz, 1H), 6.82 – 6.78 (m, 1H), 5.92 (s, 1H), 4.78 (ddd, $J = 10.6, 3.8, 0.7$ Hz, 1H), 3.45 – 3.40 (m, 1H), 3.36 – 3.30 (m, 1H), 2.95 (ddd, $J = 14.3, 3.9, 1.5$ Hz, 1H), 2.82 (dd, $J = 14.3, 10.6$ Hz, 1H), 2.53 (t, $J = 5.4$ Hz, 2H), 1.93 – 1.84 (m, 4H). ^{13}C NMR (100 MHz, CDCl_3) δ 170.54, 152.48, 138.54, 138.24, 128.81(2C), 128.36, 128.19, 127.19(2C), 124.81, 121.12, 108.98, 66.86, 50.47, 40.00, 32.61, 22.94, 21.09. LC-MS: 348.0 (M-OH), 390.0 (M-OH). Anal. Calc. for (C₁₉H₂₀BrNO₂S: 405.05): C, 56.16; H, 4.96; N, 3.45; found: C, 56.29, H, 4.71; N, 3.33.

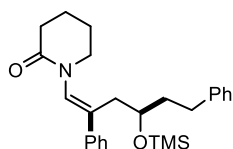


106n. Yellow solid, mp: 120-123 °C, *c*Hex:EtOAc = 1:1. Yield = 68% (47.2 mg). ^1H NMR (400 MHz, CDCl_3) δ 7.44 (dd, $J = 8.1, 1.4$ Hz, 2H), 7.39 – 7.35 (m, 2H), 7.33 (d, $J = 6.9$ Hz, 2H), 7.31 – 7.25 (m, 2H), 7.21 – 7.18 (m, 1H), 6.56 (d, $J = 15.9$ Hz, 1H), 6.22 (dd, $J = 15.8, 5.7$ Hz, 1H), 6.01 (s, 1H), 4.49 (s, 1H), 4.24 (s, 1H), 3.49 – 3.33 (m, 2H), 2.78 (ddd, $J = 14.2, 3.9, 1.3$ Hz, 1H), 2.67 (dd, $J = 14.2, 10.0$ Hz, 1H), 2.52 (br, 2H), 1.88 (d, $J = 5.4$ Hz, 4H). ^{13}C NMR (100 MHz, CDCl_3) δ 170.61, 138.96, 138.87, 137.17, 133.43, 128.87, 128.64(2C), 128.54(2C), 128.19, 128.08, 127.33, 127.28(2C), 126.49(2C), 69.36,

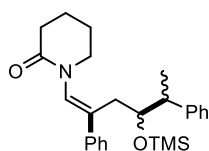
50.43, 38.09, 32.58, 23.00, 21.14. LC-MS: 330.0 (M-OH), 717.0 (2M+Na⁺). Anal. Calc. for (C₂₃H₂₅NO₂: 347.19): C, 79.51; H, 7.25; N, 4.03; found: C, 79.32, H, 7.35; N, 4.15.



106o. Yellow oil, cHex:EtOAc = 5:1. Yield = 39% (34.4 mg). ¹H NMR (400 MHz, CDCl₃, 1:1 mixture of diastereoisomers *a* and *b*) δ 7.37 – 7.23 (m, 10H_{*a+b*}), 6.43 (s, 1H_{*a*}), 6.40 (s, 1H_{*b*}), 5.08 – 5.00 (m, 2H_{*a+b*}), 3.77 – 3.60 (m, 4H_{*a+b*}), 3.51 – 3.43 (m, 2H_{*a+b*}), 2.72 – 2.54 (m, 4H_{*a+b*}), 2.47 (t, *J* = 6.4 Hz, 4H_{*a+b*}), 1.97 – 1.80 (m, 12H_{*a+b*}), 1.67 (brs, 6H_{*a+b*}), 1.58 (brs, 6H_{*a+b*}), 1.51 – 0.99 (m, 10H_{*a+b*}), 0.83 (d, *J* = 6.4 Hz, 3H_{*a*}), 0.68 (d, *J* = 6.5 Hz, 3H_{*b*}), -0.05 (s, 9H_{*a+b*}), -0.07 (s, 9H_{*a+b*}). ¹³C NMR (100 MHz, CDCl₃) δ 170.57, 170.51, 139.68, 136.67, 136.53, 131.27, 131.23, 128.97, 128.37(2C), 128.35(2C), 127.60, 127.58, 127.26(2C), 127.23(2C), 124.91, 124.84, 68.97, 68.69, 50.77, 50.71, 45.89, 45.40, 38.37, 37.81, 37.73, 37.25, 32.64, 29.37, 28.80, 25.86, 25.56, 25.40, 23.37, 21.40, 20.23, 19.41, 17.79, 17.78, 0.54, 0.49. LC-MS: 442.1 (M+H⁺), 4464.2 (M+Na⁺). Anal. Calc. for (C₂₇H₄₃NO₂Si: 441.31): C, 73.42; H, 9.61; N, 3.17; found: C, 73.33, H, 9.55; N, 3.26.



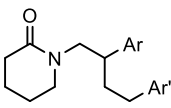
106p. Yellow oil, cHex:EtOAc = 5:1. Yield = 57% (50.0 mg). ¹H NMR (400 MHz, CDCl₃) δ 7.39 – 7.26 (m, 5H), 7.26 – 7.22 (m, 2H), 7.16 (t, *J* = 7.3 Hz, 1H), 7.10 (d, *J* = 7.9 Hz, 2H), 6.43 (s, 1H), 3.78 – 3.70 (m, 1H), 3.68 – 3.60 (m, 1H), 3.46 (dd, *J* = 7.6, 4.6 Hz, 1H), 2.78 – 2.53 (m, 4H), 2.48 (t, *J* = 5.2 Hz, 2H), 1.87 – 1.83 (m, 4H), 1.81 – 1.64 (m, 2H), -0.03 – -0.05 (m, 8H). ¹³C NMR (100 MHz, CDCl₃) δ 170.61, 142.16, 139.52, 136.44, 129.02, 128.42(2C), 128.41(2C), 128.39(2C), 127.63, 127.19(2C), 125.80, 69.98, 50.71, 39.03, 37.39, 32.60, 31.54, 23.32, 21.34, 0.43. LC-MS: 422.2 (M+H⁺), 444.2 (M+Na⁺). Anal. Calc. for (C₂₆H₃₅NO₂Si: 421.24): C, 74.06; H, 8.37; N, 3.32; found: C, 73.89, H, 8.25; N, 3.26.



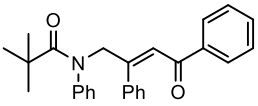
106q. Yellow oil, cHex:EtOAc = 5:1. Yield = 44% (37.0 mg). ¹H NMR (400 MHz, CDCl₃, 1:1 mixture of diastereoisomers *a* and *b*) δ 7.34 – 7.13 (m, 20H_{*a+b*}), 7.10 (brs, 1H_{*a*}), 7.08 (brs, 1H_{*b*}), 6.55 (s, 1H_{*b*}), 6.51 (s, 1H_{*a*}), 3.91 – 3.86 (m, 1H_{*b*}), 3.81 – 3.77 (m, 1H_{*a*}), 3.58 – 3.52 (m, 1H_{*a*}), 3.50 – 3.44 (m, 1H_{*b*}), 3.40 – 3.33 (m, 1H_{*a*}), 3.29 – 3.22 (m, 1H_{*b*}), 2.90 – 2.84 (m, 1H_{*b*}), 2.82 – 2.77 (m, 1H_{*a*}), 2.65 (d, *J* = 3.8 Hz, 1H_{*b*}), 2.61 (d, *J* = 3.8 Hz, 1H_{*a*}), 2.55 – 2.36 (m, 6H_{*a+b*}), 1.83 – 1.57 (m, 8H_{*a+b*}), 1.29 (d, *J* = 7.2 Hz, 3H_{*b*}), 1.25 (d, *J* = 7.1 Hz, 3H_{*a*}), -0.12 (s, 9H_{*b*}), -0.20 (s, 9H_{*a*}). ¹³C NMR (100 MHz, CDCl₃) δ 170.74, 170.63, 144.30, 143.19, 139.05, 135.50, 134.98, 129.14, 128.65, 128.24, 128.19, 128.11, 128.05, 127.99, 127.46, 127.29, 126.96, 126.87, 126.28, 126.18, 75.07, 74.76, 50.57, 45.51, 45.05, 34.54, 32.62, 32.37, 32.24, 23.06, 22.98, 21.12, 21.03, 15.40, 15.25. LC-MS: 441.8 (M+H⁺), 459.0 (M+H₂O), 463.8 (M+Na⁺). LC-MS: 422.2 (M+H⁺), 444.2 (M+Na⁺). Anal. Calc. for (C₂₆H₃₅NO₂Si: 421.24): C, 74.06; H, 8.37; N, 3.32; found: C, 73.65, H, 8.20; N, 3.21.

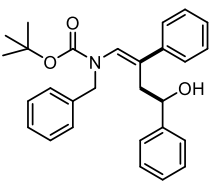
Hydrogenation of (+/-)-106r: The substrate 90 mg (0.20 mmol) was dissolved in EtOH (5 mL) and DCM (2 mL). Then Pd/C (10.6 mg, 0.01 mol, 10%) was added, the air in vessel was evacuated and recharged with H₂ (1 atm). TLC showed the reaction complete in 12 hours. The reaction solution was filtrated with silica gel pad and washed with EtOAc (20 mL). The solvent was removed under

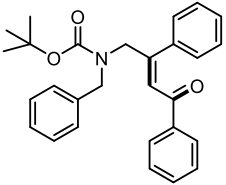
vacuum. Then the residue was purified with silica gel chromatography to give product 76.8 mg (85%) as solid.

 (+/-)-**106r** (Ar = pPh-C₆H₄, Ar' = 2-naphth). White solid. M.P.: 110.4 – 110.8°C. cHex:EtOAc = 1:1. Yield = 85% (76.8 mg). ¹H-NMR (400 MHz, CDCl₃) δ 7.82 – 7.78 (m, 1H), 7.76 (d, J = 8.4 Hz, 2H), 7.66 – 7.58 (m, 4H), 7.55 (s, 1H), 7.49 – 7.39 (m, 4H), 7.38 – 7.31 (m, 3H), 7.29 (dd, J = 8.4, 1.7 Hz, 1H), 4.09 – 3.99 (m, 1H), 3.16 (ddd, J = 26.7, 14.0, 7.0 Hz, 2H), 3.00 (ddd, J = 12.0, 7.1, 4.8 Hz, 1H), 2.77 – 2.60 (m, 3H), 2.34 (qt, J = 17.7, 6.5 Hz, 2H), 2.17 – 2.01 (m, 3H), 1.68 – 1.59 (m, 2H), 1.58 – 1.41 (m, 2H). ¹³C-NMR (100 MHz, CDCl₃) δ 170.11, 141.61, 140.73, 139.64, 139.51, 133.57, 131.95, 128.75, 128.51, 127.83, 127.56, 127.37, 127.25, 127.18, 127.13, 126.92, 126.35, 125.83, 125.06, 53.78, 49.05, 43.03, 34.79, 33.60, 32.20, 23.04, 21.05. LC-MS: 434.20 [M+H⁺]. MW: 433.24. Anal. Calcd for C₃₁H₃₁NO: C, 85.87; H, 7.21. Found: C, 85.61; H, 7.38.

Oxidation of (+/-)-106s: To a Schlenk tube was charged with a stirring bar and DCM (3 ml), then substrate (60 mg, 0.15 mmol) and IBX (126 mg, 0.45 mmol, 3.0 eq.) were added into the tube. Then the reaction was heated to reflux overnight. TLC showed the reaction completed. The mixture diluted with DCM (20 ml) and filtrated. The organic layer was concentrated under vacuum and purified with silica gel column to give a colorless oil in 95% yield.

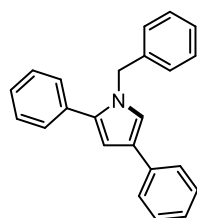
 **108**. White solid. cHex:EtOAc = 3:1. Yield = 95% (57 mg). M.P. = 113.0–114 °C. ¹H NMR (400 MHz, CDCl₃) δ 7.73 – 77.71 (m, 2H), 7.55 – 7.49 (m, 1H), 7.42 – 7.24 (m, 7H), 7.20 (t, J = 4.5 Hz, 4H), 7.14 – 7.09 (m, 1H), 7.03 (s, 1H), 4.00 (s, 2H), 1.26 (s, 9H). ¹³C NMR (100 MHz, CDCl₃) δ 195.55, 178.79, 143.23, 140.60, 136.68, 133.11, 131.45, 130.03, 129.12, 128.63, 128.53, 128.27, 128.04, 127.63, 126.89, 126.52, 41.21, 40.49, 28.78. LC-MS: 398.2 [M+H⁺], 817.2 [2M+Na⁺]. MW: 397.2. Anal. Calcd for C₂₇H₂₇NO₂: C, 81.51; H, 6.85. Found: C, 81.33; H, 6.71.

 **106t**. Colorless oil. cHex:EtOAc = 10:1. Yield = 89% (77 mg). ¹H NMR (400 MHz, CDCl₃) δ 7.46 – 7.19 (m, 15H), 6.07 (s, 1H), 4.61 (dd, J = 10.3, 3.8 Hz, 1H), 4.52 (br, 2H), 2.83 (br, 1H), 2.77 – 2.67 (m, 1H), 1.54 (s, 9H). ¹³C NMR (100 MHz, CDCl₃) δ 155.24, 139.26, 137.63, 128.63, 128.59, 128.34, 127.92, 127.53, 127.29, 125.65, 81.68, 71.15, 53.52, 40.47, 28.51. LC-MS: 356.0 [M-C₄H₉O]. MW: 429.23. Anal. Calcd for C₂₇H₂₉NO₃: C, 78.04; H, 7.03. Found: C, 77.85; H, 6.95.

 **109**. Colorless gel. cHex:EtOAc = 10:1. Yield = 89% (77 mg). ¹H NMR (400 MHz, CDCl₃) δ 7.84 (d, J = 7.4 Hz, 2H), 7.57 – 7.51 (m, 1H), 7.44 – 7.38 (m, 2H), 7.32 – 7.21 (m, 10H), 6.49 (s, 1H), 4.56 (s, 2H), 4.13 (s, 2H), 1.44 (s, 9H). ¹³C NMR (100 MHz, CDCl₃) δ 197.01, 140.09, 138.14, 136.90, 133.18, 128.63, 128.57, 128.50, 128.19, 127.56, 127.35, 126.61, 81.04, 52.77, 40.76, 28.40. LC-MS: 428.2 [M+H⁺], 877.2 [2M+Na⁺]. MW: 427.21. Anal. Calcd for C₂₇H₂₇NO₃: C, 78.42; H, 6.58. Found: C, 78.22; H, 6.41.

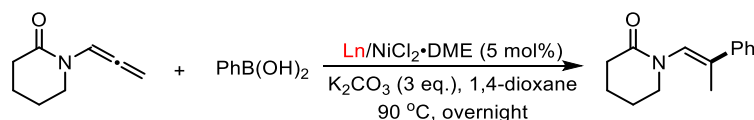
Decarboxylation/cyclization: synthesis of 110.

To a mixture of DCM and TFA (3 ml, 2:1) in flask was add **109** (55 mg). The mixture was stirred at room temperature for 4 hrs. TLC showed the reaction completed. Then 20 ml saturated aqueous NaHCO₃ was added into the flask. The mixture was extracted with DCM (3x 5 ml), the organic phase washed with brine and dried over NaSO₄. Then organic phase was concentrated under vacuum. The residue was purified with silica gel chromatography to give product as colorless gel.



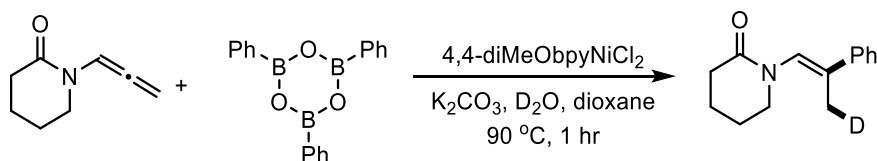
110. Colorless gel. *c*Hex:EtOAc = 10:1. Yield =83% (33 mg). ¹H NMR (400 MHz, CDCl₃) δ 7.56 (dd, *J* = 8.3, 1.1 Hz, 2H), 7.44 – 7.25 (m, 10H), 7.21 – 7.15 (m, 1H), 7.08 (dd, *J* = 11.4, 4.4 Hz, 3H), 6.61 (d, *J* = 2.0 Hz, 1H), 5.18 (s, 2H). ¹³C NMR (100 MHz, CDCl₃) δ 138.65, 136.17, 135.66, 133.11, 129.03, 128.87, 128.76, 128.59, 127.57, 127.39, 126.69, 125.66, 125.09, 124.98, 119.65, 107.03, 50.98. LC-MS: 310.2 [M+H⁺]. MW: 309.15. Anal. Calcd for C₂₃H₁₉N: C, 89.28; H, 6.19. Found: C, 89.07; H, 6.05.

Model reaction with the catalyst formed *in situ*

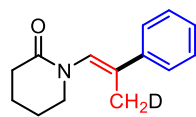


To a dry Schlenk tube was added dry dioxane (1 ml) under nitrogen. Then 4,4'-dimethoxybipyridine 2.2 mg (0.01 mmol, 5 mol%), NiCl₂·DME 2.0 mg (5 mol%), potassium carbonate 82.8 mg (0.6 mmol, 3.0 eq.), boronic acid 36.9 mg (0.3 mmol, 1.5 eq.) and allenamide 27.4 mg (0.2 mmol, 1.0 eq.) were added sequentially at room temperature under nitrogen atmosphere. Then the resulting mixture was heated to 90 °C and stirred overnight. TLC showed complete consumption of the allenamide **100a**. Then 1,4-dioxane was removed under vacuum and the residue was purified with silica gel column (*c*Hex:EtOAc = 1:1) to give product 17.2 mg (yield 40%).

Labeling experiment

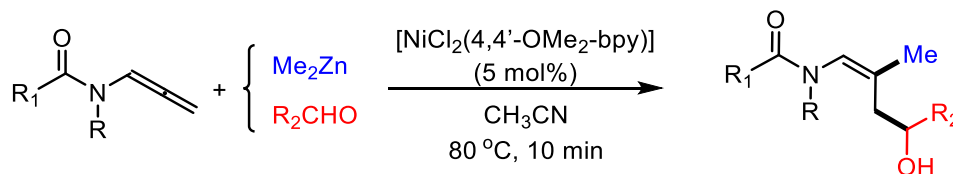


To a dry Schlenk tube was added dry 1,4-dioxane (1 mL) under nitrogen. Then catalyst 3.4 mg (0.01 mmol, 5 mol%), oven-dried potassium carbonate 82.8 mg (0.6 mmol, 3.0 eq.), (PhBO)₃⁵ 31.2 mg (0.1 mmol, 0.5 eq.), deuterium dioxide 20 mg (1.0 mmol, 5.0 eq) and allenamide **100a** 27.4 mg (0.2 mmol, 1.0 eq.) were added sequentially at room temperature under nitrogen atmosphere. Then the resulting mixture was heated to 90 °C and stirred overnight. TLC showed complete consumption of the allenamide. Then 1,4-dioxane was removed under vacuum and the residue was purified with silica gel column (*c*Hex:EtOAc = 1:1) giving product 17.5 mg (41%). Deuteration percentage: 73%.

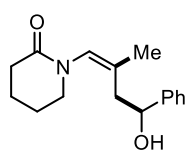


***d*-102aa+102aa** (73:27): Colorless oil, *c*Hex:EtOAc = 1:1. Yield = 41% (overall, 17.5 mg). ¹H NMR (400 MHz, CDCl₃, diagnostic signals) 6.50 (brs, 1H_{*d*-102aa+102aa}), 3.47 (s, 2H), 2.02 (d, *J* = 1.0 Hz, 3H_{102aa}), 2.00 – 1.98 (m, 2H_{*d*-102aa}). GC-MS (m/s): 216.

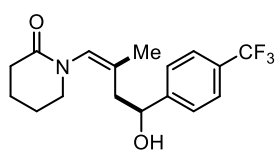
General procedure of tri-component reaction with organozinc reagent



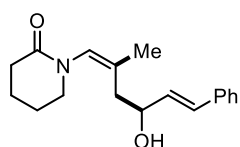
Under nitrogen atmosphere, a dry Schlenk tube was charged with stir bar and acetonitrile (1 mL). Then catalyst (3.4 mg, 0.01 mmol, 5 mol%), organozinc (0.4 mmol, 2.0 eq.), allenamide (0.2 mmol) and aldehyde (0.4 mmol, 2.0 eq.) were added sequentially at room temperature. Then the reaction was heated to 80 °C and kept stirring. TLC showed the reaction complete in 10 mins. The reaction was quenched with H₂O (3 mL) and extracted with EtOAc (3 × 5 mL). Then the organic phase was combined and washed with brine (5 mL). Then the residue was purified with silica gel chromatography to give corresponding product.



(+/-)-**111a** Yellow oil, *c*Hex:EtOAc = 1:1. Yield = 66% (34.2 mg). ¹H-NMR (400 MHz, CDCl₃) δ 7.40 – 7.28 (m, 4H), 7.22 (t, *J* = 6.6 Hz, 1H), 5.66 (s, 1H), 4.99 (s, 1H), 4.89 (dd, *J* = 10.7, 3.7 Hz, 1H), 3.35 – 3.24 (m, 1H), 3.16 (d, *J* = 12.0 Hz, 1H), 2.46 (s, 2H), 2.41 (d, *J* = 10.9 Hz, 1H), 2.20 (dd, *J* = 13.8, 3.2 Hz, 1H), 1.90 (s, 3H), 1.80 (d, *J* = 2.9 Hz, 4H). ¹³C-NMR (100 MHz, CDCl₃) δ 170.70, 146.31, 135.46, 128.34, 126.93, 125.67, 125.50, 70.48, 50.22, 42.10, 32.42, 22.95, 21.14, 19.49. LC-MS: 242.0 [M-OH], 260.2 [M+H⁺], 541.2 [2M+Na⁺]. Anal. Calcd for C₁₆H₂₁NO₂: C, 74.10; H, 8.16. Found: C, 74.25; H, 8.21.

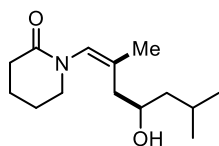


(+/-)-**111b** Yellow oil, *c*Hex:EtOAc = 1:1. Yield = 43% (28.2 mg). ¹H-NMR (400 MHz, CDCl₃) δ 7.57 (d, *J* = 8.2 Hz, 2H), 7.49 (d, *J* = 8.2 Hz, 2H), 5.63 (s, 1H), 5.47 (s, 1H), 4.94 (dd, *J* = 11.0, 4.0 Hz, 1H), 3.35 – 3.28 (m, 1H), 3.18 (dd, *J* = 7.0, 5.0 Hz, 1H), 2.45 (dd, *J* = 6.6, 4.1 Hz, 2H), 2.37 (dd, *J* = 13.8, 11.0 Hz, 1H), 2.20 (dd, *J* = 13.8, 3.6 Hz, 1H), 1.91 (d, *J* = 0.8 Hz, 3H), 1.86 – 1.75 (m, 4H). ¹³C-NMR (100 MHz, CDCl₃) δ 170.72, 150.65, 135.04, 125.84, 125.80, 125.36, 125.32, 125.28, 125.24, 69.92, 50.26, 41.88, 32.44, 22.90, 21.09, 19.39. LC-MS: 310.2 [M-OH], 328.2 [M+H⁺], 677.2 [2M+Na⁺]. Anal. Calcd for C₁₇H₂₀F₃NO₂: C, 62.38; H, 6.16. Found: C, 62.22; H, 6.01.

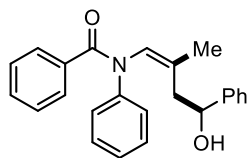


(+/-)-**111c** Yellow oil, *c*Hex:EtOAc = 1:1. Yield = 41% (23.4 mg). ¹H-NMR (400 MHz, CDCl₃) δ 7.38 (d, *J* = 7.5 Hz, 2H), 7.29 (t, *J* = 7.6 Hz, 2H), 7.21 (d, *J* = 7.4 Hz, 1H), 6.65 (d, *J* = 15.9 Hz, 1H), 6.24 (dd, *J* = 15.8, 5.6 Hz, 1H),

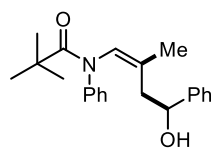
5.67 (s, 1H), 4.53 – 4.46 (m, 1H), 3.36 – 3.21 (m, 2H), 2.45 (d, $J = 5.4$ Hz, 2H), 2.35 (dd, $J = 13.6$, 10.4 Hz, 1H), 2.13 (dd, $J = 13.7$, 3.8 Hz, 1H), 1.86 (s, 3H), 1.81 (t, $J = 8.8$ Hz, 4H). ^{13}C -NMR (100 MHz, CDCl_3) δ 170.88, 137.22, 135.13, 133.62, 128.91, 128.58, 127.36, 126.52, 125.80, 68.91, 50.28, 39.56, 32.39, 31.03, 22.99, 21.14, 19.69. LC-MS: 268.2 [M-OH], 286.2 [M+H⁺], 571.2 [2M+H⁺]. Anal. Calcd for $\text{C}_{18}\text{H}_{23}\text{NO}_2$: C, 75.76; H, 8.12. Found: C, 75.61; H, 8.32.



(+/-)-**111d** (R = iBu). Colorless oil, cHex:EtOAc = 1:1. Yield = 64% (30.6 mg). ^1H -NMR (400 MHz, CDCl_3) δ 5.68 (s, 1H), 3.90 – 3.76 (m, 1H), 3.33 – 3.20 (m, 2H), 2.45 (d, $J = 3.2$ Hz, 2H), 2.15 (dd, $J = 13.5$, 10.2 Hz, 1H), 1.96 – 1.88 (m, 1H), 1.81 (d, $J = 3.5$ Hz, 4H), 1.78 (s, 3H), 1.42 (ddd, $J = 13.7$, 8.3, 5.6 Hz, 1H), 1.23 (s, 1H), 1.15 (ddd, $J = 13.1$, 8.3, 4.6 Hz, 1H), 0.89 (d, $J = 6.6$ Hz, 6H). ^{13}C -NMR (100 MHz, CDCl_3) δ 171.33, 136.04, 125.35, 66.32, 50.31, 48.06, 39.67, 32.31, 24.71, 23.39, 22.98, 22.36, 21.10, 19.91. LC-MS: 222.2 [M-OH], 240.2 [M+H⁺], 501.2 [2M+Na⁺]. Anal. Calcd for $\text{C}_{14}\text{H}_{25}\text{NO}_2$: C, 70.25; H, 10.53. Found: C, 70.02; H, 10.31.

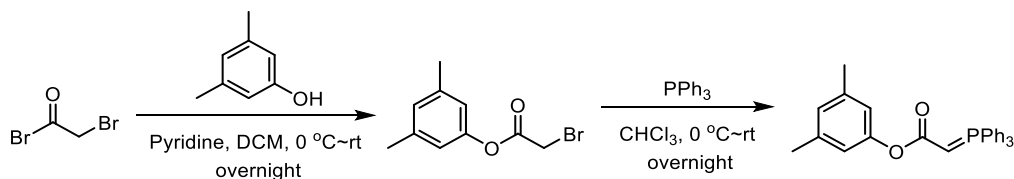


(+/-)-**111e**. Colorless oil, cHex:EtOAc = 1:1. Yield = 54% (40.0 mg). ^1H NMR (401 MHz, CDCl_3) δ 7.48 – 7.47 (m, 2H), 7.42 – 7.23 (m, 11H), 7.18 – 7.07 (m, 2H), 5.82 – 5.75 (m, 1H), 5.06 – 4.92 (m, 1H), 4.52 (s, 1H), 4.34 (d, $J = 14.0$ Hz, 1H), 2.25 – 2.14 (m, 1H), 1.91 – 1.68 (m, 2H), 1.56 (s, 2H). ^{13}C NMR (101 MHz, CDCl_3) δ 170.64, 144.23, 141.29, 137.31, 136.35, 134.48, 132.27, 132.17, 130.05, 129.02, 128.88, 128.74, 128.62, 128.39, 127.77, 127.08, 125.70, 125.67, 117.37, 71.29, 70.23, 51.67, 40.62, 28.11, 19.36. LC-MS: 372.2 [M+H⁺]. MW: 371.19. Anal. Calcd for $\text{C}_{25}\text{H}_{25}\text{NO}_2$: C, 70.25; H, 10.53. Found: C, 70.02; H, 10.31.



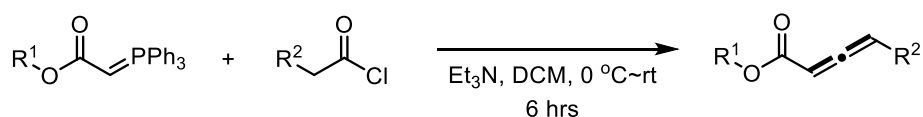
(+/-)-**111f**. Colorless oil, cHex:EtOAc = 1:1. Yield = 47% (16.0 mg). ^1H NMR (400 MHz, CDCl_3) δ 8.11 (d, $J = 7.7$ Hz, 1H), 7.47 (t, $J = 7.8$ Hz, 1H), 7.39 – 7.30 (m, 5H), 7.26 (dd, $J = 7.8$, 5.3 Hz, 1H), 7.20 (d, $J = 7.2$ Hz, 2H), 6.00 (s, 1H), 4.84 (dd, $J = 10.8$, 3.9 Hz, 2H), 2.70 (dd, $J = 13.9$, 10.8 Hz, 1H), 2.24 (dd, $J = 13.9$, 3.6 Hz, 2H) 1.86 (s, 3H), 1.12 (s, 9H). ^{13}C -NMR (100 MHz, CDCl_3) δ 179.51, 145.97, 143.52, 133.81, 129.35, 129.06, 128.69, 128.44, 127.77, 127.18, 125.55, 71.00, 42.07, 41.40, 29.33, 27.05, 19.62. LC-MS: 310.2 [M-OH], 338.2 [M+H⁺]. MW: 337.20. Anal. Calcd for $\text{C}_{22}\text{H}_{27}\text{NO}_2$: C, 78.30; H, 8.06. Found: C, 78.21; H, 8.00.

Synthesis of allenates 124b-f,h,i⁶

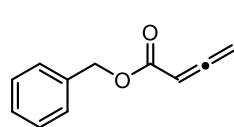


To a dry two-neck flask was charged with a stirring bar, 3,5-dimethylphenol (1.22g, 10 mmol), DCM (30 ml) and pyridine (1.77 ml, 22 mmol). Then the mixture was cooled to 0 °C, and 2-bromoacetic bromide (0.86 ml, 10 mmol) was added into the reaction slowly. Then the reaction was warmed to room temperature and stirred overnight. TLC showed the reaction completed. The reaction was washed with H₂O (20 ml) two times and the organic phase was dried over NaSO₄. Then solvent was removed and the residue was purified with flash silica gel chromatography (cHex/EtOAc = 10:1) to give product 3,5-dimethylphenyl 2-bromoacetate (2.1 g, 86%) as a colorless oil.

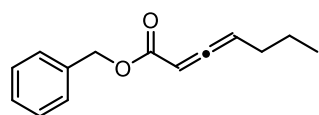
A dry two-neck flask was charged with triphenylphosphine (786 mg, 3.0 mmol) and CHCl₃ (10 ml). The solution was cooled to 0 °C and 3,5-dimethylphenyl 2-bromoacetate (729 mg, 3.0 mmol) was added. Then, the reaction was warmed to room temperature and stirred overnight. The mixture was washed with NaOH (2N, 2 x 20 ml) and the collected organic phase dried over Na₂SO₄. After removal of solvent under vacuum, pure product was obtained as a white solid (1.20 g, 95%) and used in the next step without further purification.



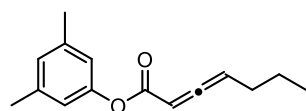
To a dry Schlenk tube with a stirring bar was charged with DCM (6 ml), ylide (2.0 mmol) and Et₃N (305 μL, 2.2 mmol). Then mixture was cooled to 0 °C in ice bath. Then a solution of acid chloride (2.2 mmol) in 2 ml DCM was added into the reaction drop-wise. The mixture was warmed to rt and stirred overnight. TLC showed the reaction completed. Most of solvent was removed under vacuum, and Et₂O (50 ml) was added into the flask. The mixture was stirred for 0.5 hr. Then the mixture was filtrated and the organic phase was concentrated under vacuum. The residue was purified with flash silica gel chromatography (cHex/EtOAc= 20:1) to give corresponding allenate as colorless oil in yield 50~85%. (CAUTION: longer reaction time may promote the isomerization of allenate into the corresponding alkyl ester).



124b. 296 mg, Yield = 85%. Colorless oil, R_f = 0.65 (cHex/EtOAc = 10:1). ¹H NMR (400 MHz, CDCl₃) δ 7.39 – 7.32 (m, 5H), 5.69 (t, *J* = 6.5 Hz, 1H), 5.24 (d, *J* = 6.5 Hz, 2H), 5.20 (s, 2H). ¹³C NMR (100 MHz, CDCl₃) δ 216.14, 165.66, 136.02, 128.67, 128.34, 128.26, 88.00, 79.54, 66.76. MS (70 eV): *m/z* (%) = 174 (100). Anal. Calcd for C₁₁H₁₀O₂: C, 75.84; H, 5.79. Found: C, 75.71; H, 5.61.

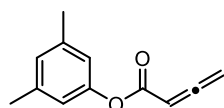


124c. 302 mg, Yield = 70%. Colorless oil, R_f = 0.70 (cHex/EtOAc = 10:1). ¹H NMR (400 MHz, CDCl₃) δ 7.37 (m, *J* = 4.3 Hz, 4H), 7.35 – 7.31 (m, 1H), 5.63 (m, *J* = 7.5, 3.9 Hz, 2H), 5.18 (d, *J* = 4.7 Hz, 2H), 2.15 – 2.09 (m, 2H), 1.55 – 1.44 (m, 2H), 0.94 (t, *J* = 7.4 Hz, 3H). ¹³C NMR (100 MHz, CDCl₃) δ 212.84, 166.23, 136.22, 128.62, 128.24, 128.21, 95.47, 88.11, 66.55, 29.64, 22.14, 13.62. MS (70 eV): *m/z* (%) = 216 (100). Anal. Calcd for C₁₄H₁₆O₂: C, 77.75; H, 7.46. Found: C, 77.61; H, 7.31.

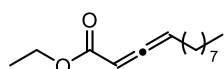


124d. 336 mg, Yield = 73%. Colorless oil, R_f = 0.70 (cHex/EtOAc = 10:1). ¹H NMR (400 MHz, CDCl₃) δ 6.86 (s, 1H), 6.75 (s, 2H), 5.75 (m, 1H), 5.70 (m, 1H), 2.32 (s, 6H), 2.17 (ddd, *J* = 14.4, 7.1, 3.0 Hz,

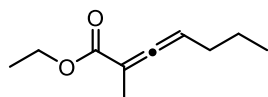
2H), 1.57 – 1.51 (m, 2H), 1.00 (t, $J = 7.4$ Hz, 3H). ^{13}C NMR (100 MHz, CDCl_3) δ 213.43, 165.02, 150.96, 139.28, 127.57, 119.28, 119.06, 95.66, 87.98, 29.61, 22.12, 21.34, 13.62. MS (70 eV): m/z (%) = 230 (100). Anal. Calcd for $\text{C}_{15}\text{H}_{18}\text{O}_2$: C, 78.23; H, 7.88. Found: C, 78.09; H, 7.71.



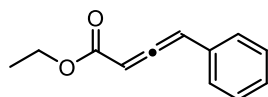
124e. 147 mg, Yield = 78%. Colorless oil, $R_f = 0.65$ (cHex/EtOAc = 10:1). ^1H NMR (400 MHz, CDCl_3) δ 6.87 (s, 1H), 6.75 (s, 2H), 5.84 – 5.79 (m, 1H), 5.34 – 5.29 (m, 2H), 2.35 – 2.30 (m, 6H). ^{13}C NMR (100 MHz, CDCl_3) δ 216.69, 164.49, 150.84, 139.39, 127.76, 119.26, 87.94, 79.81, 21.38. MS (70 eV): m/z (%) = 188 (100). Anal. Calcd for $\text{C}_{12}\text{H}_{12}\text{O}_2$: C, 76.57; H, 6.43. Found: C, 76.41; H, 6.61.



124f. 181 mg, Yield = 81%. Colorless oil, $R_f = 0.75$ (cHex/EtOAc = 10:1). ^1H NMR (400 MHz, CDCl_3) δ 6.00 – 5.90 (m, 2H), 4.55 (m, 2H), 2.48 (qd, $J = 7.1, 3.2$ Hz, 2H), 1.80 (dd, $J = 14.8, 7.4$ Hz, 2H), 1.68 (m, 2H), 1.63 (m, 11H), 1.24 (t, $J = 6.8$ Hz, 3H). ^{13}C NMR (100 MHz, CDCl_3) δ 212.44, 166.45, 95.53, 88.37, 60.85, 32.00, 29.47, 29.38, 29.08, 28.88, 27.65, 22.80, 14.40, 14.23. MS (70 eV): m/z (%) = 244 (100). Anal. Calcd for $\text{C}_{14}\text{H}_{24}\text{O}_2$: C, 74.95; H, 8.45. Found: C, 74.77; H, 8.35.

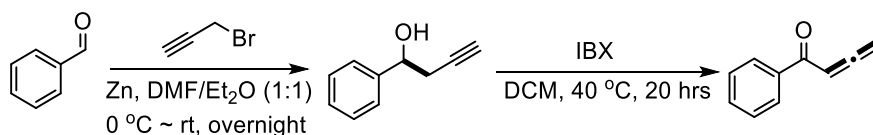


124h. 84 mg, Yield = 50%. Colorless oil, $R_f = 0.65$ (cHex/EtOAc = 10:1). ^1H NMR (400 MHz, CDCl_3) δ 5.47 – 5.38 (m, 1H), 4.22 – 4.13 (m, 2H), 2.07 (q, $J = 7.0$ Hz, 2H), 1.85 (d, $J = 2.9$ Hz, 3H), 1.54 – 1.38 (m, 2H), 1.26 (t, $J = 7.1$ Hz, 3H), 0.95 (t, $J = 7.4$ Hz, 3H). ^{13}C NMR (100 MHz, CDCl_3) δ 210.25, 168.22, 95.69, 93.67, 60.87, 30.16, 22.21, 15.37, 14.41, 13.60. MS (70 eV): m/z (%) = 168 (100). Anal. Calcd for $\text{C}_{10}\text{H}_{16}\text{O}_2$: C, 71.39; H, 9.59. Found: C, 71.30; H, 9.71.



124i. 248 mg, Yield = 66%. Colorless oil, $R_f = 0.55$ (cHex/EtOAc = 10:1). ^1H NMR (400 MHz, CDCl_3) δ 7.35 – 7.27 (m, 5H), 6.62 (d, $J = 6.4$ Hz, 1H), 6.02 (d, $J = 6.4$ Hz, 1H), 4.28 – 4.19 (m, 2H), 1.29 (t, $J = 7.1$ Hz, 3H). ^{13}C NMR (100 MHz, CDCl_3) δ 214.75, 165.24, 131.33, 128.99, 128.24, 127.65, 98.81, 92.09, 61.28, 14.39. MS (70 eV): m/z (%) = 188 (100). Anal. Calcd for $\text{C}_{12}\text{H}_{12}\text{O}_2$: C, 76.57; H, 6.43. Found: C, 76.41; H, 6.38.

Synthesis of the ketoallene 124g



A dry two-neck flask was charged with DMF/Et₂O (6 ml, 1:1), benzaldehyde (530 mg, 5 mmol) and zinc dust (630 mg, 10 mmol). The reaction was cooled to 0 °C and propargyl bromide (1.08 ml, 10 mmol, 80% in toluene) was added drop-wise. Then, the reaction was warmed to room temperature and stirred for 24 hr when TLC showed the complete reaction. The mixture was filtrated, the organic phase concentrated under vacuum and the residue was purified via flash silica gel chromatography (cHex/EtOAc = 5:1) to give 1-phenylbut-3-yn-1-ol (613 mg, 84%) as colorless oil.

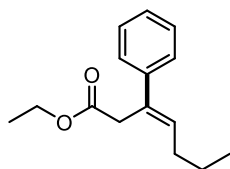
A dry single necked flask was charged with 6 mL of DCM, propargyl 1-phenylbut-3-yn-1-ol (292 mg, 2.0 mmol), followed by Ibx (6.0 mmol, 1.68 g). The reaction was stirred for 20 hr at rt. The

reaction was filtrated and the organic phase concentrated under vacuum. The residue was purified with flash silica gel chromatography (cHex/EtOAc= 20:1) to give allenoketone (225 mg, 78%) as colorless oil. $R_f = 0.80$ (cHex/EtOAc = 10:1)

$^1\text{H NMR}$ (400 MHz, CDCl_3) δ 7.93 – 7.86 (m, 2H), 7.58 – 7.53 (m, 1H), 7.48 – 7.42 (m, 2H), 6.44 (t, $J = 6.5$ Hz, 1H), 5.28 – 5.23 (m, 2H). $^{13}\text{C NMR}$ (100 MHz, CDCl_3) δ 217.20, 191.07, 137.59, 132.90, 128.79, 128.48, 93.37, 79.33. MS (70 eV): m/z (%) = 144 (100). Anal. Calcd for $\text{C}_{10}\text{H}_8\text{O}$: C, 83.31; H, 5.59. Found: C, 83.18; H, 5.40.

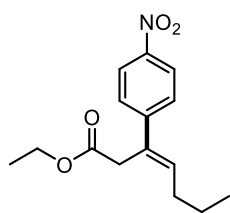
General procedure for the coupling of allenolate and boronic acid

A flame-dried Schlenk tube, filled with N_2 , was charged sequentially with reagent grade 1,4-dioxane (1 mL), [4,4'-dibromobpy-NiCl₂] (4.0 mg, 5 mol%), boronic acid (0.3 mmol, 1.5 equiv), allenolate **124a** (0.2 mmol, 1.0 equiv), and K_2CO_3 (55.2 mg, 0.4 mmol, 2.0 equiv). The reaction mixture was then heated at 90 °C for 5 h (complete consumption of the allenolate was monitored by TLC). Then the solvent was removed under vacuum and the residue purified via flash chromatography.



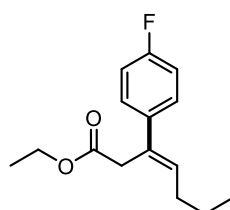
(*E*)-**125aa**: 44 mg, Yield = 95%. Colorless oil, $R_f = 0.73$ (cHex/EtOAc = 20:1), $E/Z = 11:1$. $^1\text{H NMR}$ (400 MHz, CDCl_3) δ 7.38 (m, 2H), 7.33 – 7.28 (m, 2H), 7.23 (m, 1H), 5.95 (t, $J = 7.3$ Hz, 1H), 4.10 (q, $J = 7.1$ Hz, 2H), 3.52 (s, 2H), 2.26 – 2.17 (m, 2H), 1.57 – 1.45 (m, 2H), 1.19 (t, $J = 7.1$ Hz, 3H), 0.97 (t, $J = 7.4$ Hz, 3H). $^{13}\text{C NMR}$ (100 MHz, CDCl_3) δ 171.61, 142.57, 132.76, 132.60, 128.38, 126.91, 126.09, 60.79, 36.22, 31.21, 22.75, 14.24, 14.04. IR (neat): 2961, 2934, 2874, 1960, 1713, 1463, 1249, 1154, 1039, 796 cm^{-1} . MS (70 eV): m/z (%) = 232 (100). Anal. Calcd for $\text{C}_{15}\text{H}_{20}\text{O}_2$: C, 77.55; H, 8.68. Found: C, 77.51; H, 8.45.

(*Z*)-**125aa** Diagnostic signal: $^1\text{H NMR}$ (400 MHz, CDCl_3) δ 5.62 (t, $J = 7.3$ Hz, 1H), 4.08 – 4.02 (q, $J = 7.1$ Hz, 2H), 3.34 (d, $J = 0.8$ Hz, 2H), 1.99 (q, $J = 7.4$ Hz, 2H), 1.41 – 1.34 (m, 2H), 1.14 (t, $J = 7.1$ Hz, 3H), 0.85 (t, $J = 7.4$ Hz, 3H). $^{13}\text{C NMR}$ (100 MHz, CDCl_3) δ 128.62, 128.14.



(*E*)-**125ab**. 47 mg, Yield = 85%. Colorless oil, $R_f = 0.45$ (cHex/EtOAc = 20:1), $E/Z = 9:1$. $^1\text{H NMR}$ (400 MHz, CDCl_3) δ 8.18 – 8.14 (m, 2H), 7.54 – 7.50 (m, 2H), 6.11 (t, $J = 7.3$ Hz, 1H), 4.11 (q, $J = 7.1$ Hz, 2H), 3.53 (s, 2H), 2.25 (q, $J = 7.4$ Hz, 2H), 1.58 – 1.48 (m, 2H), 1.20 (t, $J = 7.1$ Hz, 3H), 0.98 (t, $J = 7.4$ Hz, 3H). $^{13}\text{C NMR}$ (100 MHz, CDCl_3) δ 170.92, 149.10, 136.69, 131.45, 129.65, 126.76, 123.79, 61.12, 35.86, 31.38, 22.53, 14.25, 14.01. IR (neat): 2960, 2932, 2872, 1731, 1526, 1347, 1154, 1157, 736, 683 cm^{-1} . MS (70 eV): m/z (%) = 277 (100). Anal. Calcd for $\text{C}_{15}\text{H}_{19}\text{NO}_4$: C, 64.97; H, 6.91. Found: C, 64.81; H, 6.77.

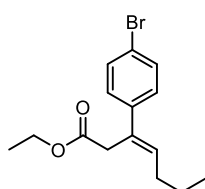
(*Z*)-**125ab** Diagnostic signal: $^1\text{H NMR}$ (400 MHz, CDCl_3) δ 5.74 (t, $J = 7.5$ Hz, 1H), 3.37 (d, $J = 0.8$ Hz, 2H), 1.96 (dd, $J = 14.8, 7.4$ Hz, 2H), 1.15 (t, $J = 7.1$ Hz, 3H), 0.85 (t, $J = 7.4$ Hz, 3H). $^{13}\text{C NMR}$ (100 MHz, CDCl_3) δ 146.74, 134.68, 123.55.



(*E*)-**125ac**. 42 mg, Yield = 83%. Colorless oil, $R_f = 0.70$ (cHex/EtOAc = 10:1), $E/Z = 4:1$. $^1\text{H NMR}$ (400 MHz, CDCl_3) δ 7.33 (m, 2H), 6.99 (m, 2H), 5.87 (t, $J = 7.3$ Hz, 1H), 4.10 (q, $J = 7.1$ Hz, 2H), 3.48 (s, 2H), 2.19 (q, $J = 7.3$ Hz, 2H), 1.51 (dt, $J = 14.8, 7.4$ Hz, 2H), 1.18 (t, $J = 7.1$ Hz, 3H), 0.97 (t, $J = 7.4$ Hz, 3H). $^{13}\text{C NMR}$ (100 MHz, CDCl_3) δ 171.42, 162.05 (d, $J = 244.0$).

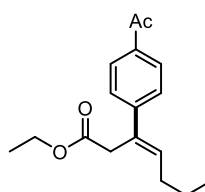
(Hz), 138.72 (d, $J = 3.0$ Hz), 132.72, 131.80, 127.70 (d, $J = 8.0$ Hz), 115.12 (d, $J = 22.0$ Hz), 60.83, 36.35, 31.17, 22.73, 14.23, 14.00. MS (70 eV): m/z (%) = 250 (100). Anal. Calcd for $C_{15}H_{19}FO_2$: C, 71.98; H, 7.65. Found: C, 71.69; H, 7.40.

(Z)-125ac Diagnostic signal: 1H NMR (400 MHz, $CDCl_3$) δ 5.62 (t, $J = 7.5$ Hz, 1H), 4.05 (q, $J = 7.1$ Hz, 2H), 3.31 (s, 2H), 1.95 (q, $J = 7.4$ Hz, 2H), 1.36 (dt, $J = 10.6, 5.4$ Hz, 2H), 1.17 – 1.13 (m, 3H), 0.84 (t, $J = 7.4$ Hz, 3H). ^{13}C NMR (100 MHz, $CDCl_3$) δ 171.66, 163.06, 132.25 (d, $J = 9.0$ Hz), 130.24 (d, $J = 8.0$ Hz), 115.16, 114.95.



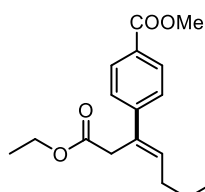
(E)-125ad. 56 mg, Yield = 90%. Colorless oil, $R_f = 0.75$ (cHex/EtOAc = 10:1), $E/Z = 4:1$. 1H NMR (400 MHz, $CDCl_3$) δ 7.43 – 7.39 (m, 2H), 7.26 – 7.22 (m, 2H), 5.93 (t, $J = 7.3$ Hz, 1H), 4.09 (q, $J = 7.1$ Hz, 2H), 3.47 (s, 2H), 2.19 (q, $J = 7.4$ Hz, 2H), 1.55 – 1.45 (m, 2H), 1.18 (t, $J = 7.1$ Hz, 3H), 0.96 (t, $J = 7.4$ Hz, 3H). ^{13}C NMR (100 MHz, $CDCl_3$) δ 171.33, 141.53, 133.40, 131.45, 131.36, 130.41, 127.81, 120.84, 60.90, 44.57, 36.07, 31.22, 22.67, 14.26, 14.02. MS (70 eV): m/z (%) = 310 (100). Anal. Calcd for $C_{15}H_{19}BrO_2$: C, 57.89; H, 6.15. Found: C, 57.55; H, 6.00.

(Z)-125ad Diagnostic signal: 1H NMR (400 MHz, $CDCl_3$) δ 5.63 (t, $J = 7.4$ Hz, 1H), 4.08 – 4.02 (q, $J = 7.1$ Hz, 2H), 3.31 (s, 2H), 1.95 (q, $J = 7.4$ Hz, 2H), 1.36 (dq, $J = 14.6, 7.4$ Hz, 2H), 1.17 – 1.13 (m, 3H), 0.84 (t, $J = 7.4$ Hz, 3H).



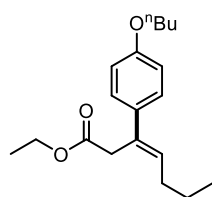
(E)-125ae. 45 mg, Yield = 83%. Colorless oil, $R_f = 0.35$ (cHex/EtOAc = 10:1), $E/Z = 11:1$. 1H NMR (400 MHz, $CDCl_3$) δ 7.91 – 7.87 (m, 2H), 7.48 – 7.43 (m, 2H), 6.06 (t, $J = 7.3$ Hz, 1H), 4.09 (q, $J = 7.1$ Hz, 2H), 3.52 (s, 2H), 2.58 (s, 3H), 2.23 (q, $J = 7.4$ Hz, 2H), 1.57 – 1.46 (m, 2H), 1.18 (t, $J = 7.1$ Hz, 3H), 0.97 (t, $J = 7.4$ Hz, 3H). ^{13}C NMR (100 MHz, $CDCl_3$) δ 197.73, 171.21, 147.22, 135.63, 135.01, 132.04, 128.61, 126.14, 60.94, 35.90, 31.30, 26.68, 22.62, 14.24, 14.01. MS (70 eV): m/z (%) = 274 (100). Anal. Calcd for $C_{17}H_{22}O_3$: C, 74.42; H, 8.08. Found: C, 74.25; H, 7.97.

(Z)-125ae Diagnostic signal: 1H NMR (400 MHz, $CDCl_3$) δ 5.68 (t, $J = 7.4$ Hz, 1H), 4.07 – 4.00 (m, 2H), 3.35 (s, 2H), 2.59 (s, 3H), 1.96 (dd, $J = 14.8, 7.4$ Hz, 2H), 1.37 (dd, $J = 14.8, 7.4$ Hz, 2H), 1.14 (t, $J = 7.1$ Hz, 3H), 0.84 (t, $J = 7.4$ Hz, 3H). ^{13}C NMR (100 MHz, $CDCl_3$) δ 128.92, 128.33.



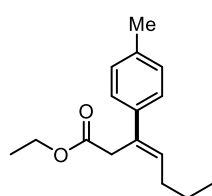
(E)-125af. 53 mg, Yield = 92%. Colorless oil, $R_f = 0.45$ (cHex/EtOAc = 10:1), $E/Z = 10:1$. 1H NMR (400 MHz, $CDCl_3$) δ 7.99 – 7.95 (m, 2H), 7.43 (d, $J = 8.6$ Hz, 2H), 6.05 (t, $J = 7.3$ Hz, 1H), 4.09 (q, $J = 7.1$ Hz, 2H), 3.90 (s, 3H), 3.52 (s, 2H), 2.22 (q, $J = 7.4$ Hz, 2H), 1.57 – 1.46 (m, 2H), 1.17 (t, $J = 7.1$ Hz, 3H), 1.13 (t, $J = 7.1$ Hz, 3H). ^{13}C NMR (100 MHz, $CDCl_3$) δ 171.23, 167.08, 147.06, 134.79, 132.10, 129.77, 128.53, 125.97, 60.91, 52.11, 35.95, 31.28, 22.62, 14.22, 14.01. MS (70 eV): m/z (%) = 290 (100). Anal. Calcd for $C_{17}H_{22}O_4$: C, 70.32; H, 7.64. Found: C, 70.21; H, 7.51.

(Z)-125af Diagnostic signal: 1H NMR (400 MHz, $CDCl_3$) δ 5.67 (t, $J = 7.4$ Hz, 1H), 4.07 – 4.00 (m, 2H), 3.90 (s, 3H), 3.34 (s, 1H), 1.95 (dd, $J = 14.8, 7.4$ Hz, 2H), 1.36 (dd, $J = 14.7, 7.4$ Hz, 2H), 0.83 (t, $J = 7.4$ Hz, 3H).



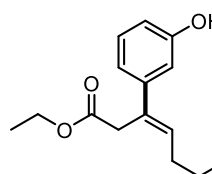
(E)-125ag. 54 mg, Yield = 89%. Colorless oil, $R_f = 0.70$ (cHex/EtOAc = 10:1), $E/Z = 9:1$. $^1\text{H NMR}$ (400 MHz, CDCl_3) δ 7.30 (d, $J = 8.8$ Hz, 2H), 6.83 (d, $J = 8.8$ Hz, 2H), 5.86 (t, $J = 7.3$ Hz, 1H), 4.10 (q, $J = 7.1$ Hz, 2H), 3.95 (t, $J = 6.5$ Hz, 2H), 3.48 (s, 2H), 2.19 (q, $J = 7.3$ Hz, 2H), 1.76 (m, 2H), 1.56 – 1.42 (m, 4H), 1.19 (t, $J = 7.1$ Hz, 3H), 0.99 – 0.95 (m, 6H). $^{13}\text{C NMR}$ (100 MHz, CDCl_3) δ 171.70, 158.32, 134.95, 132.06, 131.05, 127.11, 114.36, 67.82, 60.73, 36.29, 31.49, 31.18, 22.85, 19.39, 14.26, 14.03, 13.98. MS (70 eV): m/z (%) = 304 (100). Anal. Calcd for $\text{C}_{19}\text{H}_{28}\text{O}_3$: C, 74.96; H, 9.27. Found: C, 74.77; H, 9.15.

(Z)-125ag Diagnostic signal: $^1\text{H NMR}$ (400 MHz, CDCl_3) δ 5.60 – 5.54 (m, 1H), 4.05 (dd, $J = 14.3$, 7.1 Hz, 2H), 3.31 (s, 2H), 2.00 (dd, $J = 14.7$, 7.3 Hz, 2H), 0.85 (t, $J = 7.4$ Hz, 3H).



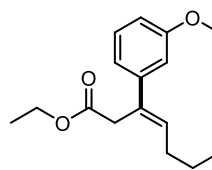
(E)-125ah. 44 mg, Yield = 89%. Colorless oil, $R_f = 0.70$ (cHex/EtOAc = 10:1), $E/Z = 7:1$. $^1\text{H NMR}$ (400 MHz, CDCl_3) δ 7.27 (t, $J = 5.5$ Hz, 2H), 7.11 (d, $J = 8.0$ Hz, 2H), 5.92 (t, $J = 7.3$ Hz, 1H), 4.10 (q, $J = 7.1$ Hz, 2H), 3.50 (s, 2H), 3.32 (s, 2H), 2.33 (s, 3H), 2.20 (q, $J = 7.3$ Hz, 2H), 1.55 – 1.45 (m, 2H), 1.19 (t, $J = 7.1$ Hz, 3H), 0.97 (t, $J = 7.4$ Hz, 3H). $^{13}\text{C NMR}$ (100 MHz, CDCl_3) δ 171.65, 139.72, 136.56, 132.44, 131.92, 129.07, 125.96, 60.74, 36.23, 31.18, 22.80, 21.15, 14.26, 14.03. MS (70 eV): m/z (%) = 246 (100). Anal. Calcd for $\text{C}_{16}\text{H}_{22}\text{O}_2$: C, 78.01; H, 9.00. Found: C, 77.87; H, 8.45.

(Z)-125ah Diagnostic signal: $^1\text{H NMR}$ (400 MHz, CDCl_3) δ 5.59 (t, $J = 7.3$ Hz, 1H), 4.08 – 4.03 (m, 2H), 3.32 (s, 2H), 2.34 (s, 2H), 1.99 (dd, $J = 14.7$, 7.4 Hz, 2H), 1.40 – 1.35 (m, 3H), 0.85 (t, $J = 7.4$ Hz, 3H). $^{13}\text{C NMR}$ (100 MHz, CDCl_3) δ 128.85, 128.48.



(E)-125ai. 26 mg, Yield = 52%. Colorless oil, $R_f = 0.40$ (cHex/EtOAc = 10:1), $E/Z = 11:1$. $^1\text{H NMR}$ (400 MHz, CDCl_3) δ 7.15 (t, $J = 7.9$ Hz, 1H), 6.93 (dd, $J = 7.8$, 0.6 Hz, 1H), 6.87 – 6.84 (m, 1H), 6.73 – 6.66 (m, 1H), 5.94 (t, $J = 7.3$ Hz, 1H), 5.34 (s, 1H), 4.11 (q, $J = 7.1$ Hz, 2H), 3.49 (s, 2H), 2.19 (q, $J = 7.3$ Hz, 2H), 1.55 – 1.44 (m, 2H), 1.19 (t, $J = 7.1$ Hz, 3H), 0.96 (t, $J = 7.4$ Hz, 3H). $^{13}\text{C NMR}$ (100 MHz, CDCl_3) δ 171.95, 155.78, 144.27, 133.01, 132.20, 129.55, 118.55, 113.99, 113.22, 60.99, 36.25, 31.17, 22.71, 14.23, 14.02. IR (neat): 3392, 2960, 2932, 2872, 1701, 1581, 1446, 1295, 1196, 1157, 1026, 783, 695 cm^{-1} . MS (70 eV): m/z (%) = 248 (100). Anal. Calcd for $\text{C}_{15}\text{H}_{20}\text{O}_3$: C, 72.55; H, 8.12. Found: C, 77.55; H, 8.12.

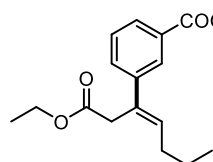
(Z)-125ai Diagnostic signal: $^1\text{H NMR}$ (400 MHz, CDCl_3) δ 5.59 (t, $J = 7.4$ Hz, 1H), 4.08 – 4.03 (q, $J = 7.1$ Hz, 2H), 3.32 (s, 2H), 1.98 (dd, $J = 14.7$, 7.4 Hz, 2H), 1.39 – 1.32 (m, 2H), 1.15 (t, $J = 7.1$ Hz, 3H), 0.84 (t, $J = 7.4$ Hz, 3H).



(E)-125aj. 44 mg, Yield = 83%. Colorless oil, $R_f = 0.65$ (cHex/EtOAc = 10:1), $E/Z = 100:9$. $^1\text{H NMR}$ (400 MHz, CDCl_3) δ 7.22 (t, $J = 7.9$ Hz, 1H), 6.99 – 6.95 (m, 1H), 6.95 – 6.92 (m, 1H), 6.78 (ddd, $J = 8.1$, 2.5, 0.7 Hz, 1H), 5.96 (t, $J = 7.3$ Hz, 1H), 4.11 (q, $J = 7.1$ Hz, 2H), 3.81 (s, 3H), 3.50 (s, 2H), 2.20 (q, $J = 7.3$ Hz, 2H), 1.56 – 1.45 (m, 2H), 1.19 (t, $J = 7.1$ Hz, 3H), 0.97 (t, $J = 7.4$ Hz, 3H). $^{13}\text{C NMR}$ (100 MHz, CDCl_3) δ 171.54, 159.69, 144.19, 132.92, 132.55, 129.31, 118.68, 112.33, 112.05, 60.79, 55.33, 36.32, 31.19, 22.73, 14.26, 14.02. IR (neat): 2958, 2932, 2871, 2835, 1731,

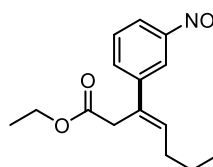
1598, 1149, 1034, 778, 695 cm^{-1} . MS (70 eV): m/z (%) = 262 (100). Anal. Calcd for $\text{C}_{16}\text{H}_{22}\text{O}_3$: C, 73.25; H, 8.45. Found: C, 73.02; H, 8.21.

(Z)-**125aj** Diagnostic signal: ^1H NMR (400 MHz, CDCl_3) δ 5.60 (t, $J = 7.3$ Hz, 1H), 4.06 (dd, $J = 14.3, 7.2$ Hz, 2H), 3.80 (s, 3H), 3.32 (d, $J = 0.7$ Hz, 2H), 2.00 (dd, $J = 14.7, 7.4$ Hz, 2H), 1.37 (dt, $J = 14.0, 7.1$ Hz, 2H), 1.16 (t, $J = 7.1$ Hz, 3H), 0.86 (t, $J = 7.4$ Hz, 3H). ^{13}C NMR (100 MHz, CDCl_3) δ 132.31, 129.14, 121.09, 114.34.



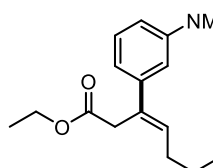
(E)-**125ak**. 54 mg, Yield = 93%. Colorless oil, $R_f = 0.70$ ($c\text{Hex}/\text{EtOAc} = 10:1$), $E/Z = 10:1$. ^1H NMR (400 MHz, CDCl_3) δ 8.05 (d, $J = 1.5$ Hz, 1H), 7.89 (dd, $J = 7.7, 1.1$ Hz, 1H), 7.59 – 7.54 (m, 1H), 7.37 (t, $J = 7.7$ Hz, 1H), 5.99 (t, $J = 7.3$ Hz, 1H), 4.09 (q, $J = 7.1$ Hz, 2H), 3.52 (s, 2H), 2.22 (q, $J = 7.4$ Hz, 2H), 1.57 – 1.45 (m, 2H), 1.18 (t, $J = 7.1$ Hz, 3H), 0.97 (t, $J = 7.4$ Hz, 3H). ^{13}C NMR (100 MHz, CDCl_3) δ 171.28, 167.26, 142.91, 133.86, 131.97, 130.66, 130.28, 128.46, 128.04, 127.31, 60.87, 52.21, 36.11, 31.23, 22.67, 14.22, 14.02. MS (70 eV): m/z (%) = 290(100). Anal. Calcd for $\text{C}_{17}\text{H}_{22}\text{O}_4$: C, 70.32; H, 7.64. Found: C, 77.45; H, 7.80.

(Z)-**125ak** Diagnostic signal: ^1H NMR (400 MHz, CDCl_3) δ 5.66 (t, $J = 7.3$ Hz, 1H), 4.06 – 4.00 (m, 2H), 3.35 (s, 2H), 1.94 (dd, $J = 14.7, 7.4$ Hz, 2H), 1.37 (td, $J = 14.8, 7.4$ Hz, 2H), 1.14 (t, $J = 7.2$ Hz, 3H), 0.84 (t, $J = 7.4$ Hz, 3H).



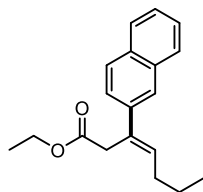
(E)-**125ai**. 39 mg, Yield = 70%. Colorless oil, $R_f = 0.40$ ($c\text{Hex}/\text{EtOAc} = 10:1$), $E/Z = 7:1$. ^1H NMR (400 MHz, CDCl_3) δ 8.24 (t, $J = 1.9$ Hz, 1H), 8.10 – 8.05 (m, 1H), 7.70 (ddd, $J = 7.8, 1.7, 1.0$ Hz, 1H), 7.47 (t, $J = 8.0$ Hz, 1H), 6.05 (t, $J = 7.3$ Hz, 1H), 4.11 (q, $J = 7.1$ Hz, 2H), 3.54 (s, 2H), 2.24 (q, $J = 7.4$ Hz, 2H), 1.58 – 1.47 (m, 2H), 1.23 – 1.18 (m, 3H), 1.15 (t, $J = 7.1$ Hz, 1H), 0.98 (t, $J = 7.4$ Hz, 3H). ^{13}C NMR (100 MHz, CDCl_3) δ 170.95, 148.50, 144.30, 135.52, 132.15, 131.05, 129.29, 121.73, 121.06, 61.10, 35.96, 31.27, 22.56, 14.23, 14.01. MS (70 eV): m/z (%) = 277 (100). Anal. Calcd for $\text{C}_{15}\text{H}_{19}\text{NO}_4$: C, 64.97; H, 6.91. Found: C, 64.85; H, 6.75.

(Z)-**125ai** Diagnostic signal: ^1H NMR (400 MHz, CDCl_3) δ 5.74 (t, $J = 7.4$ Hz, 1H), 4.06 (dd, $J = 15.2, 8.0$ Hz, 2H), 3.37 (s, 2H), 1.95 (dd, $J = 14.7, 7.4$ Hz, 2H), 1.39 (dd, $J = 15.5, 8.1$ Hz, 3H), 0.85 (t, $J = 7.4$ Hz, 3H). ^{13}C NMR (100 MHz, CDCl_3) δ 135.05, 134.54, 123.65, 122.03.



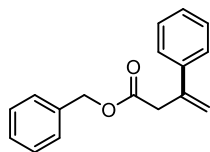
(E)-**125am**. 18 mg, Yield = 64%. Colorless oil, $R_f = 0.30$ ($c\text{Hex}/\text{EtOAc} = 10:1$), $E/Z = 10:1$. ^1H NMR (400 MHz, CDCl_3) δ 7.17 (t, $J = 7.9$ Hz, 1H), 6.79 – 6.74 (m, 2H), 6.64 (dd, $J = 8.3, 2.4$ Hz, 1H), 5.95 (t, $J = 7.3$ Hz, 1H), 4.11 (q, $J = 7.1$ Hz, 2H), 3.51 (s, 2H), 2.95 (s, 6H), 2.21 (q, $J = 7.3$ Hz, 2H), 1.56 – 1.46 (m, 2H), 1.20 (t, $J = 7.1$ Hz, 3H), 0.97 (t, $J = 7.4$ Hz, 3H). ^{13}C NMR (100 MHz, CDCl_3) δ 171.76, 150.80, 143.65, 133.34, 132.27, 128.97, 114.94, 111.58, 110.78, 60.72, 40.85, 36.59, 31.22, 22.79, 14.29, 14.05. MS (70 eV): m/z (%) = 275 (100). Anal. Calcd for $\text{C}_{17}\text{H}_{25}\text{NO}_2$: C, 72.84; H, 8.56. Found: C, 72.32; H, 8.32.

(Z)-**125am** Diagnostic signal: ^1H NMR (400 MHz, CDCl_3) δ 3.33 (s, 2H), 2.94 (s, 6H). ^{13}C NMR (100 MHz, CDCl_3) δ 131.63, 128.79, 117.10, 113.04, 111.29.



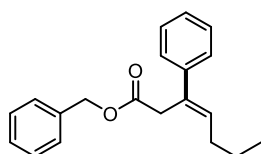
(E)-125an. 18 mg, Yield = 64%. Colorless oil, $R_f = 0.45$ (cHex/EtOAc = 10:1), $E/Z = 4:1$. $^1\text{H NMR}$ (400 MHz, CDCl_3) δ 7.82 – 7.77 (m, 3H), 7.72 – 7.64 (m, 1H), 7.60 – 7.53 (m, 1H), 7.50 – 7.40 (m, 2H), 6.11 (t, $J = 7.3$ Hz, 1H), 4.11 (q, $J = 7.1$ Hz, 2H), 3.63 (s, 2H), 2.28 (q, $J = 7.3$ Hz, 2H), 1.56 (dd, $J = 14.8, 7.4$ Hz, 2H), 1.19 (t, $J = 7.1$ Hz, 3H), 1.05 – 0.97 (m, 3H). $^{13}\text{C NMR}$ (100 MHz, CDCl_3) δ 171.60, 139.84, 133.37, 132.62, 128.69, 128.57, 128.22, 127.92, 127.61, 126.16, 125.70, 124.76, 124.59, 60.83, 36.27, 31.36, 22.81, 14.28, 14.08. MS (70 eV): m/z (%) = 282 (100). Anal. Calcd for $\text{C}_{19}\text{H}_{22}\text{O}_2$: C, 80.82; H, 7.85. Found: C, 80.59; H, 7.61.

(Z)-125an Diagnostic signal: $^1\text{H NMR}$ (400 MHz, CDCl_3) δ 5.71 (t, $J = 7.3$ Hz, 1H), 4.05 (q, $J = 7.1$ Hz, 2H), 3.44 (s, 2H), 2.03 (dd, $J = 14.7, 7.4$ Hz, 2H), 1.40 (m, $J = 14.8, 7.4$ Hz, 2H), 1.13 (t, $J = 7.1$ Hz, 3H), 0.85 (t, $J = 7.4$ Hz, 3H).



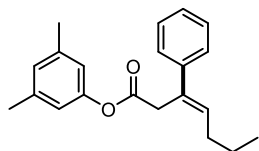
125ba. 41 mg, Yield = 82%. Colorless oil, $R_f = 0.55$ (cHex/EtOAc = 10:1), $E/Z = 4:1$. $^1\text{H NMR}$ (400 MHz, CDCl_3) δ 7.45 – 7.41 (m, 2H), 7.40 – 7.37 (m, 1H), 7.36 – 7.29 (m, 5H), 7.23 (m, 2H), 5.56 (s, 1H), 5.25 (s, 1H), 5.10 (s, 2H), 3.59 (s, 2H). $^{13}\text{C NMR}$ (100 MHz, CDCl_3) δ 180.67, 156.47, 140.89, 135.87, 128.59, 128.54, 128.25, 128.17, 127.93, 125.96, 116.55, 66.67, 41.42. MS (70 eV): m/z (%) = 252 (100).

125ba' Diagnostic signal: $^1\text{H NMR}$ (400 MHz, CDCl_3) δ 6.22 (d, $J = 1.2$ Hz, 1H), 5.22 (s, 2H), 2.62 (d, $J = 1.1$ Hz, 3H). $^{13}\text{C NMR}$ (100 MHz, CDCl_3) δ 171.24, 166.69, 142.21, 139.81, 136.41, 129.21, 128.69, 128.63, 128.36, 126.43, 116.87, 65.89, 27.04.



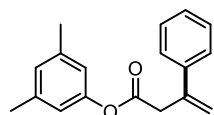
(E)-125ca. 52 mg, Yield = 89%. Colorless oil, $R_f = 0.60$ (cHex/EtOAc = 10:1), $E/Z = 6:1$. $^1\text{H NMR}$ (400 MHz, CDCl_3) δ 7.40 – 7.37 (m, 2H), 7.32 (m, 5H), 7.24 (m, 3H), 5.97 (t, $J = 7.3$ Hz, 1H), 5.10 (s, 2H), 3.60 (s, 2H), 2.21 (q, $J = 7.4$ Hz, 2H), 1.56 – 1.45 (m, 2H), 0.96 (t, $J = 7.4$ Hz, 3H). $^{13}\text{C NMR}$ (100 MHz, CDCl_3) δ 171.37, 142.46, 136.04, 132.93, 132.48, 128.57, 128.43, 128.19, 128.13, 126.97, 126.15, 66.57, 36.18, 31.23, 22.74, 14.01. MS (70 eV): m/z (%) = 294 (100). Anal. Calcd for $\text{C}_{20}\text{H}_{22}\text{O}_2$: C, 81.60; H, 7.53. Found: C, 81.38; H, 7.39.

(Z)-125ca Diagnostic signal: $^1\text{H NMR}$ (400 MHz, CDCl_3) δ 5.64 (t, $J = 7.3$ Hz, 1H), 5.05 (s, 2H), 3.42 (d, $J = 0.7$ Hz, 2H), 1.99 (q, $J = 7.4$ Hz, 2H), 1.37 (m, 2H), 0.85 (t, $J = 7.4$ Hz, 3H).



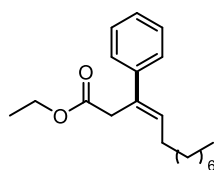
(E)-125da. 50 mg, Yield = 81%. Colorless oil, $R_f = 0.60$ (cHex/EtOAc = 10:1), $E/Z = 9:1$. $^1\text{H NMR}$ (400 MHz, CDCl_3) δ 7.47 – 7.46 (m, 2H), 7.36 – 7.34 (m, 2H), 7.29 – 7.25 (m, 1H), 6.83 (s, 1H), 6.57 (s, 2H), 6.03 (t, $J = 7.3$ Hz, 1H), 3.76 (s, 2H), 2.35 – 2.32 (m, 2H), 2.29 (s, 6H), 1.63 – 1.52 (m, 2H), 1.02 (t, $J = 7.4$ Hz, 3H). $^{13}\text{C NMR}$ (100 MHz, CDCl_3) δ 170.19, 150.85, 142.47, 139.26, 133.15, 132.43, 128.49, 127.57, 127.08, 126.29, 119.10, 36.45, 31.31, 22.78, 21.29, 14.04. MS (70 eV): m/z (%) = 308 (100). Anal. Calcd for $\text{C}_{21}\text{H}_{24}\text{O}_2$: C, 81.78; H, 7.84. Found: C, 81.66; H, 7.65.

(Z)-125da Diagnostic signal: Colorless oil, $R_f = 0.55$ (cHex/EtOAc = 20:1). $^1\text{H NMR}$ (400 MHz, CDCl_3) δ 5.04 (t, $J = 7.7$ Hz, 1H), 3.53 (s, 2H).



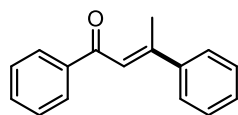
125ea. 48 mg, Yield = 90%. Colorless oil, $R_f = 0.55$ (cHex:AcOEt = 10:1), **125:125'** = 2:1. $^1\text{H NMR}$ (400 MHz, CDCl_3) δ 7.53 (m, 1H), 7.44 – 7.31 (m, 3H), 6.84 (d, $J = 0.6$ Hz, 1H), 6.79 (s, 1H), 6.57 (s, 2H), 5.62 (s, 1H), 5.37 (d, $J = 0.8$ Hz, 1H), 3.75 (d, $J = 0.9$ Hz, 2H), 2.28 (s, 6H). $^{13}\text{C NMR}$ (100 MHz, CDCl_3) δ 170.05, 150.75, 142.14, 139.30, 128.72, 128.61, 128.03, 127.66, 126.08, 119.06, 116.67, 41.58, 21.38. MS (70 eV): m/z (%) = 266 (100).

125'ea Diagnostic signal: $^1\text{H NMR}$ (400 MHz, CDCl_3) δ 6.89 (d, $J = 0.5$ Hz, 1H), 6.38 (d, $J = 1.2$ Hz, 1H), 2.66 (d, $J = 1.2$ Hz, 3H), 2.35 (s, 6H). $^{13}\text{C NMR}$ (100 MHz, CDCl_3) δ 165.47, 158.32, 150.72, 140.88, 139.92, 139.32, 129.46, 127.52, 126.52, 119.47, 116.36, 21.30, 18.33.

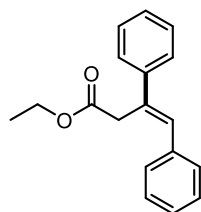


(E)-125fa. 51 mg, Yield = 84%. Colorless oil, $R_f = 0.75$ (cHex:AcOEt = 10:1), $E/Z = 7:1$. $^1\text{H NMR}$ (400 MHz, CDCl_3) δ 7.42 – 7.36 (m, 2H), 7.31 (t, $J = 7.7$ Hz, 2H), 7.24 – 7.20 (m, 1H), 5.95 (t, $J = 7.3$ Hz, 1H), 4.11 (q, $J = 7.1$ Hz, 2H), 3.51 (s, 2H), 2.23 (q, $J = 7.3$ Hz, 2H), 1.53 – 1.44 (m, 2H), 1.40 – 1.29 (m, 10H), 1.21 – 1.15 (t, $J = 7.1$ Hz, 3H), 0.90 (t, $J = 6.8$ Hz, 3H). $^{13}\text{C NMR}$ (100 MHz, CDCl_3) δ 171.58, 142.62, 132.99, 132.45, 128.37, 126.89, 126.11, 60.77, 36.25, 32.03, 29.66 (2C), 29.57, 29.56, 29.43, 29.21, 22.81, 14.24. IR (neat): 3023, 2956, 2853, 1734, 1463, 1151, 1033, 757, 696 cm^{-1} . MS (70 eV): m/z (%) = 302 (100). Anal. Calcd for $\text{C}_{20}\text{H}_{20}\text{O}_2$: C, 79.42; H, 10.00. Found: C, 79.21; H, 9.78.

(Z)-125fa Diagnostic signal: $^1\text{H NMR}$ (400 MHz, CDCl_3) δ 5.62 (t, $J = 7.3$ Hz, 1H), 4.05 (q, $J = 7.1$ Hz, 2H), 3.34 (s, 2H), 2.00 (q, $J = 7.3$ Hz, 2H).

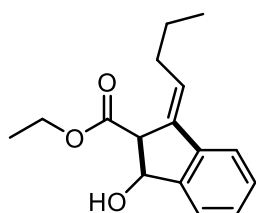


(E)-125ga'. 37 mg, Yield = 84%. Colorless oil, $R_f = 0.75$ (cHex:AcOEt = 10:1). $^1\text{H NMR}$ (400 MHz, CDCl_3) δ 8.03 – 7.97 (m, 2H), 7.60 – 7.53 (m, 3H), 7.48 (dd, $J = 8.1, 6.7$ Hz, 2H), 7.43 – 7.40 (m, 2H), 7.18 – 7.16 (m, 1H), 2.60 (d, $J = 1.2$ Hz, 3H). $^{13}\text{C NMR}$ (100 MHz, CDCl_3) δ 192.01, 155.20, 142.95, 139.53, 132.67, 129.26, 128.75, 128.69, 128.42, 126.64, 122.28, 19.04. MS (70 eV): m/z (%) = 222 (100). Anal. Calcd for $\text{C}_{16}\text{H}_{14}\text{O}_2$: C, 86.45; H, 6.35. Found: C, 86.29; H, 6.22.



(E)-125ia. 45 mg, Yield = 85%. Colorless oil, $R_f = 0.75$ (cHex:AcOEt = 10:1), $E/Z = 1:1$. $^1\text{H NMR}$ (400 MHz, CDCl_3) δ 7.52 – 7.49 (m, 1H), 7.40 – 7.21 (m, 9H), 7.03 (s, 1H), 4.09 (q, $J = 7.1$ Hz, 2H), 3.71 (s, 2H), 1.15 (t, $J = 7.1, 3\text{H}$). $^{13}\text{C NMR}$ (100 MHz, CDCl_3 , (E)+(Z)-125ia.) δ 171.61, 171.26, 141.88, 140.16, 137.59, 136.83, 135.42, 134.86, 131.34, 130.49, 129.29, 128.89, 128.81, 128.65, 128.58, 128.55, 128.01, 127.70, 127.45, 127.32, 126.88, 126.41, 60.91, 60.81, 45.99, 36.86, 14.24, 14.21. MS (70 eV): m/z (%) = 266 (100).

(Z)-125ia Diagnostic signal: $^1\text{H NMR}$ (400 MHz, CDCl_3) δ 6.59 (s, 1H), 3.50 (d, $J = 0.9$ Hz, 2H).



(E)-117b. 29 mg, Yield = 63%. Colorless oil, $R_f = 0.36$ (cHex:AcOEt = 10:1), $E/Z = 6:1$. $^1\text{H NMR}$ (400 MHz, CDCl_3) δ 7.46 (dd, $J = 5.0, 3.8$ Hz, 1H), 7.44 – 7.40 (m, 1H), 7.30 – 7.26 (m, 2H), 6.08 (td, $J = 7.6, 1.8$ Hz, 1H), 5.42 (dd, $J = 11.3, 7.5$ Hz, 1H), 4.23 – 4.20 (m, 1H), 4.17 (dd, $J = 14.3, 7.1$ Hz, 2H), 3.05 (d, $J = 11.4$ Hz, 1H), 2.29 – 2.20 (m, 2H),

1.53 – 1.43 (m, 2H), 1.26 (t, $J = 7.1$ Hz, 3H), 0.97 (t, $J = 7.4$ Hz, 3H). ^{13}C NMR (100 MHz, CDCl_3) δ 171.77, 144.98, 139.85, 136.54, 128.93, 128.49, 124.72, 124.56, 120.08, 74.93, 61.18, 53.03, 31.74, 22.73, 14.31, 14.06. MS (70 eV): m/z (%) = 260 (100). Anal. Calcd for $\text{C}_{16}\text{H}_{20}\text{O}_3$: C, 73.82; H, 7.74. Found: C, 73.65; H, 7.55.

(*Z*)-**117b** Diagnostic signal: ^1H NMR (400 MHz, CDCl_3) δ 5.79 (t, $J = 6.6$ Hz, 1H), 5.34 (dd, $J = 10.8$, 7.0 Hz, 1H), 3.97 (dd, $J = 7.0$, 1.2 Hz, 1H), 3.52 (d, $J = 10.8$ Hz, 1H), 2.44 (dd, $J = 14.7$, 7.4 Hz, 2H).

General procedure for the synthesis of complexes [Ni(H₂O)₂Cl₂L_n]

A variant of the previously reported protocol by Stanger⁷ was employed. Dry DMF was employed instead of THF with a reaction temperature of 90 °C and reaction time of 4 h. Then the solvent was removed under vacuum and the residue was washed with diethyl ether. At last the residue was dried under vacuum. [Ni(H₂O)₂Cl₂L_n] was got in 83~98% yield.

Crystallographic data collection and structure determination for 125aa, L₃NiCl₂ and 106c.

The X-ray intensity data were measured on a Bruker Apex III CCD diffractometer. Cell dimensions and the orientation matrix were initially determined from a least-squares refinement on reflections measured in three sets of 20 exposures, collected in three different ω regions, and eventually refined against all data. A full sphere of reciprocal space was scanned by 0.3° ω steps. The software SMART⁸ was used for collecting frames of data, indexing reflections and determination of lattice parameters. The collected frames⁴ were then processed for integration by the SAINT program, and an empirical absorption correction was applied using SADABS.⁹ The structures were solved by direct methods (SIR 97)¹⁰ and subsequent Fourier syntheses and refined by full-matrix least-squares on F² (SHELXTL)¹¹ using anisotropic thermal parameters for all non-hydrogen atoms. In the asymmetric unit of **102aa** two independent molecules are present that are conformers differing each other only for the orientation of the phenyl group with respect to the plane containing the C=C-CH₃ moiety. The aromatic, methylene and methyl hydrogen atoms were placed in calculated positions and refined with isotropic thermal parameters $U(H) = 1.2 U_{eq}(C)$ or $U(H) = 1.5 U_{eq}(C)$ (methyl H), respectively and allowed to ride on their carrier carbons whereas the H atoms of the water molecules in **L3Ni** and the hydroxy H atom in **106c** were located in the Fourier map and refined isotropically [$U(H) = 1.2 U_{eq}(O)$]. Crystal data and details of data collections for compounds **102aa-106c** are reported in Table Sx.

Crystallographic data have been deposited with the Cambridge Crystallographic Data Centre (CCDC) as supplementary publication numbers CCDC 1548725 (**102aa**), 1548726 ([**NiCl₂L3**]), 1548727 (**106c**). Copies of the data can be obtained free of charge via www.ccdc.cam.ac.uk/getstructures.

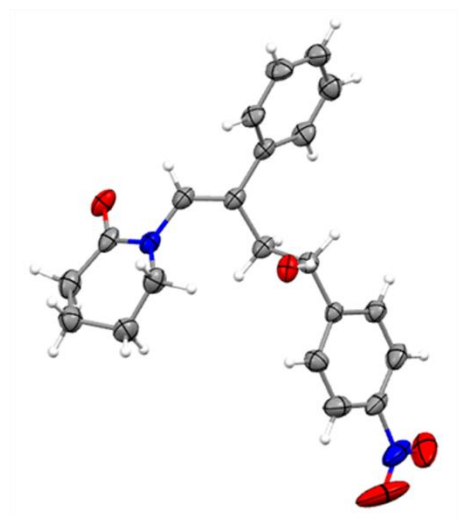
Table S1. Crystal data and structure refinement for compounds **102aa**, [**NiCl₂L3**] and **106c**.

Compound	102aa	[NiCl₂L3]	106c
Formula	C ₁₄ H ₁₇ NO	C ₁₂ H ₁₆ Cl ₂ N ₂ NiO ₄	C ₂₁ H ₂₂ N ₂ O ₄
Fw	215.28	381.88	366.40
T, K	296	296	296
λ , Å	0.71073	0.71073	0.71073
Crystal symmetry	Triclinic	Triclinic	Monoclinic
Space group	<i>P</i> -1	<i>P</i> -1	<i>P</i> 2 ₁ / <i>n</i>
<i>a</i> , Å	6.320(2)	7.193(2)	5.6474(14)
<i>b</i> , Å	11.047(4)	10.727(3)	15.192(4)
<i>c</i> , Å	16.999(6)	11.421(3)	21.790(5)
α	90.548(9)	108.743(4)	90
β	95.825(9)	107.602(5)	92.561(7)
γ	90.542(9)	102.591(5)	90
Cell volume, Å ³	1180.7(7)	745.4(4)	1867.6(8)
<i>Z</i>	4	2	4
<i>D</i> _c , Mg m ⁻³	1.211	1.702	1.303
μ (Mo-K α), mm ⁻¹	0.076	1.675	0.091
F(000)	464	392	776
Crystal size/ mm	0.25 x 0.23 x 0.20	0.20 x 0.07 x 0.05	0.30 x 0.28 x 0.25

θ limits, $^{\circ}$	1.204 - 24.741	2.057 - 24.685	1.635 - 28.298
Reflections collected	11115	7229	28668
Unique obs. Reflections	3857 [$R_{\text{int}} =$	2509 [$R_{\text{int}} = 0.1099]$	4602 [$R_{\text{int}} = 0.1286]$
$[F_o > 4\sigma(F_o)]$	0.0853]		
Goodness-of-fit-on F^2	1.137	1.080	1.005
$R_1 (F)^a$, $wR_2 (F^2)$ [$I > 2\sigma(I)$]	0.0971, 0.2356	0.0792, 0.1365	0.0855, 0.1672
Largest diff. peak and hole, e.	0.353 and -0.233	0.891 and -0.651	0.296 and -0.344

^a) $R_1 = \Sigma||F_o| - |F_c|| / \Sigma|F_o|$, ^b) $wR_2 = [\Sigma w(F_o^2 - F_c^2)^2 / \Sigma w(F_o^2)^2]^{1/2}$ where $w = 1 / [\sigma^2(F_o^2) + (aP)^2 + bP]$ where $P = (F_o^2 + F_c^2) / 3$.

Compound 106c



Photocatalyzed Synthesis of 1,3,4- Trisubstituted Pyrrole

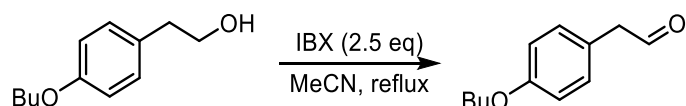
General Methods.

¹H-NMR spectra were recorded on Varian 400 (400 MHz) spectrometers. Chemical shifts are reported in ppm from TMS with the solvent resonance as the internal standard (deuteriochloroform: 7.24 ppm). Data are reported as follows: chemical shift, multiplicity (s = singlet, d = doublet, t = triplet, q = quartet, sext = sextet, sept = septet, p = pseudo, b = broad, m = multiplet), coupling constants (Hz). ¹³C-NMR spectra were recorded on a Varian 400 (100 MHz) spectrometers with complete proton decoupling. Chemical shifts are reported in ppm from TMS with the solvent as the internal standard (deuteriochloroform: 77.0 ppm).

GC-MS spectra were taken by EI ionization at 70 eV on a Hewlett-Packard 5971 with GC injection. They are reported as: *m/z* (rel. intense). LC-electrospray ionization mass spectra were obtained with Agilent Technologies MSD1100 single-quadrupole mass spectrometer.

Fluorescence spectra have been recorded by means of a Perkin Elmer LS-55 luminescence spectrometer. Lifetime emission of [Ru(dbbpy)₃(PF₆)₂] was measured by means of a nanosecond LFP apparatus (LP 920, Edinburgh Instruments) equipped with a Nd:YAG Laser (Spotlight 100, Optoprin, 7-8 ns, up to 100 mJ at 1064 nm). Samples were placed in a quartz cell (10 x 10 mm section). Analysis were performed at 532 nm.^[12]

Chromatographic purification was done with 240-400 mesh silica gel. Other anhydrous solvents were supplied by Sigma Aldrich in Sureseal® bottles and used without any further purification. Commercially available chemicals were purchased from Sigma Aldrich, Stream and TCI and used without any further purification. Melting points were determined with Bibby Stuart Scientific Melting Point Apparatus SMP 3 and are not corrected. Agilent Technologies LC/MSD Trap 1100 series (nebulizer: 15.0 PSI, dry Gas: 5.0 L/min, dry Temperature: 325 °C, capillary voltage positive scan: 4000 mA, capillary voltage negative scan: 3500 mA). Known compounds were prepared following the corresponding literatures (**145a-c**, **1i**),^[13] **145d**,^[14] **145h**,^[15] **145e,g**,^[16] **145f**,^[17] **145k**,^[18] **145j**,^[19] **151g**,^[20] **151c-f**,^[21] **151h**,^[22] **151i**,^[23] **151k**,^[24] Compound **145a**,^[25] **151j**, **151l-m** are commercially available and have been used as received.

Synthesis of aldehyde 151b

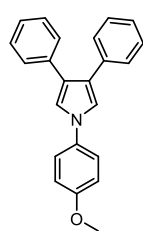
To an oven-dried Schlenk tube equipped with a magnetic stirring bar under N₂ were added in a sequence: acetonitrile, IBX and substrate. The mixture was refluxed overnight. TLC showed the starting material was consumed completely. The mixture was filtrated and washed with EtOAc twice (2 × 10 ml) after which the organic layer was concentrated under vacuum. The resulting mixture was purified with silica gel chromatography (cHex:EtOAc = 50:1 ~ 20:1).

151b. Colorless oil. ¹H NMR (400 MHz, CDCl₃) δ 9.70 (t, *J* = 2.4 Hz, 1H), 7.10 (d, *J* = 8.7 Hz, 2H), 6.88 (d, *J* = 8.7 Hz, 2H), 3.94 (t, *J* = 6.5 Hz, 2H), 3.59 (d, *J* = 2.4 Hz, 2H), 1.80 – 1.72 (m, 2H), 1.54 – 1.43 (m, 2H), 0.99 – 0.94 (m, 3H). ¹³C NMR (100 MHz, CDCl₃) δ 199.65, 158.52, 130.58, 123.42, 115.01, 67.71, 49.70, 31.27, 19.21, 13.80. **GC-MS:** 192 (100), 163 (25), 107 (15).

General procedure for the pyrrole synthesis.

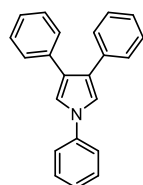
A 5 ml dry vial equipped with a stirring bar was charged with: [(di-^tBu)py]₃Ru(PF₆)₂] (4.8 mg, 2 mmol%), 4,4'-(^tBu)₂bpy (5.2 mg, 10 mol%), dry DMF (1 ml), azide (0.2 mmol), aldehyde (0.5 mmol, 2.5 equiv) and acetic acid (24 mg, 2.0 equiv). Then a stream of N₂ was blown into the vial for 30 s to remove the air. The reaction was stirred under 7 W blue LED irradiation, until TCL showed complete consumption of the azide. Therefore, DMF was removed under vacuum and the residue purified by silica gel chromatography.

The same procedure was also carried out for substrates **145a** and **151a** on 1 mmol scale of azide. Under optima conditions reported for the general procedure ([Ru]/ligand/CH₃CO₂H = 2 mol%/10 mol%/200 mol%), **152aa** was isolated in 63% yield (200 mg) after 48 h reaction time.



152aa.²⁶ White solid m.p.: 90 -95 °C. cHex:EtOAc: 100:1; yield = 73% (48 mg), **152:152'** = 87:13; ¹H NMR (400 MHz, cdcl₃) δ 7.42 – 7.38 (m, 2H), 7.35 – 7.31 (m, 5H), 7.29 – 7.28 (m, 2H), 7.27 (d, *J* = 1.7 Hz, 1H), 7.24 – 7.22 (m, 2H), 7.13 (s, 2H), 7.01 – 6.98 (m, 2H), 3.86 (s, 3H). ¹³C NMR (100 MHz, CDCl₃) δ 158.01, 135.58, 134.09, 128.62, 128.36, 126.04, 125.23, 122.00, 119.12, 114.92, 55.73. **GC-MS:** 325 (100), 310 (12), 191 (38); **Anal. Calc.** for (C₂₃H₁₉NO): 325.41): C, 84.89; H, 5.89; found: C, 84.71, H, 5.61.

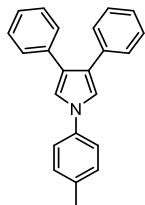
152aa' **Diagnostic signals:**²⁷ ¹H NMR (400 MHz, CDCl₃) δ 7.59 (dd, *J* = 8.3, 1.2 Hz, 2H), 7.14 (d, *J* = 9.0 Hz, 2H), 6.97 – 6.82 (m, 2H), 6.72 (d, *J* = 2.0 Hz, 1H), 3.81 (s, 3H). ¹³C NMR (100 MHz, CDCl₃) δ 128.65, 128.07, 126.40, 125.71, 121.06, 108.10.



152ba.²⁷ Light yellow solid m.p.: 97 - 101. cHex:EtOAc: 100:1; yield = 51% (30 mg), **152:152'** = 90:10; ¹H NMR (400 MHz, CDCl₃) δ 7.48 – 7.46 (d, *J* = 6.5 Hz, 3H), 7.35 – 7.30 (m, 7H), 7.29 – 7.26 (m, 3H), 7.25 – 7.21 (m, 4H); ¹³C NMR (100 MHz, CDCl₃) δ 140.21, 135.26, 129.63, 128.45, 128.20, 125.98, 125.81, 125.60, 120.13, 118.50; **GC-**

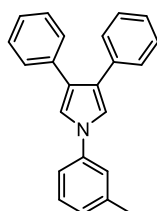
MS: 295 (100), 191 (34); **Anal. Calc.** for (C₂₂H₁₇N: 295.39): C, 89.46; H, 5.80; found: C, 89.23, H, 5.39.

152ba' Diagnostic signals:²⁸ **¹H NMR** (400 MHz, CDCl₃) δ 7.59 (d, *J* = 7.2 Hz, 2H), 6.74 (d, *J* = 2.0 Hz, 1H). **¹³C NMR** (100 MHz, CDCl₃) δ 129.02, 128.65, 128.28, 128.07, 126.75, 126.50, 125.08, 120.84, 108.71.



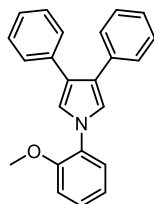
152ca.¹⁵ Yellow viscous oil. *c*Hex:EtOAc: 100:1; yield = 78% (48 mg), **152:152'** = 84:16; **¹H NMR** (400 MHz, CDCl₃) δ 7.38 (d, *J* = 8.3 Hz, 2H), 7.35 – 7.31 (m, 4H), 7.30 – 7.27 (m, 4H), 7.26 – 7.21 (m, 4H), 7.19 (d, *J* = 1.0 Hz, 2H), 2.41 (s, 3H). **¹³C NMR** (100 MHz, CDCl₃) δ 137.92, 135.63, 135.38, 130.15, 128.46, 128.20, 125.91, 125.46, 125.29, 125.08, 120.14, 118.61, 20.86. **GC-MS:** 309 (100), 191 (31), 91 (25); **Anal. Calc.** for (C₂₃H₁₉N: 309.41): C, 89.28; H, 6.19; found: C, 89.02, H, 5.97.

152ca' Diagnostic signals:¹⁶ **¹H NMR** (400 MHz, CDCl₃) δ 7.59 (d, *J* = 8.2 Hz, 2H), 7.12 (d, *J* = 7.2 Hz, 2H), 6.73 (d, *J* = 1.9 Hz, 1H), 2.36 (s, 3H). **¹³C NMR** (100 MHz, CDCl₃) δ 129.61, 128.65, 128.26, 128.06, 126.43, 125.74, 120.93, 108.45.



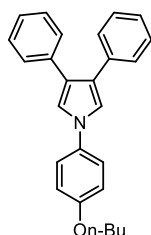
152da.¹⁵ Yellow viscous oil. *c*Hex:EtOAc: 100:1; yield = 74% (46 mg), **152:152'** = 80:20; **¹H NMR** (400 MHz, CDCl₃) δ 7.34 (m, 4H), 7.30 (m, 4H), 7.27 (m, 2H), 7.23 (m, 2H), 7.21 (s, 3H), 7.10 (d, *J* = 7.4 Hz, 1H), 2.44 (s, 3H). **¹³C NMR** (100 MHz, CDCl₃) 140.19, 139.65, 135.34, 129.42, 128.45, 128.18, 126.61, 125.93, 125.43, 125.07, 120.90, 118.57, 117.27, 21.49. **GC-MS:** 309 (42), 217 (32), 191 (37), 91 (100); **Anal. Calc.** for (C₂₃H₁₉N: 309.41): C, 89.25; H, 6.17; found: C, 89.05, H, 5.95.

152da' Diagnostic signal:¹⁶ **¹H NMR** (400 MHz, CDCl₃) δ 7.59 (d, *J* = 8.3 Hz, 2H), 6.95 (d, *J* = 7.6 Hz, 2H), 6.74 (d, *J* = 1.6 Hz, 1H), 2.33 (s, 3H). **¹³C NMR** (100 MHz, CDCl₃) δ 128.65, 128.03, 126.13, 108.57, 21.29.



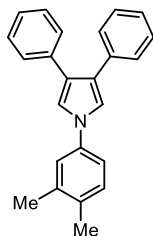
152ea.²⁸ Yellow viscous oil. *c*Hex:EtOAc: 100:1; yield = 50% (33 mg), **152:152'** = 83:17; **¹H NMR** (400 MHz, CDCl₃) δ 7.37 (dd, *J* = 7.7, 1.6 Hz, 1H), 7.32 (dt, *J* = 3.0, 1.8 Hz, 4H), 7.27 (dd, *J* = 8.5, 1.3 Hz, 4H), 7.21 – 7.15 (m, 3H), 7.13 (s, 2H), 7.07 – 7.02 (m, 2H), 3.88 (s, 3H). **¹³C NMR** (100 MHz, CDCl₃) δ 152.41, 135.63, 129.69, 128.53, 128.09, 127.50, 125.68, 125.24, 125.07, 124.04, 121.41, 121.03, 112.35, 77.30, 77.18, 76.98, 76.66, 55.84. **GC-MS:** 325 (100), 310 (14), 191 (36); **Anal. Calc.** for (C₂₃H₁₉NO: 325.41): C, 84.89; H, 5.89; found: C, 84.71, H, 5.61.

152ea' Diagnostic signals: **¹H NMR** (400 MHz, CDCl₃) δ 7.58 (dd, *J* = 8.3, 1.1 Hz, 2H), 6.98 – 6.86 (m, 4H), 6.74 (d, *J* = 1.9 Hz, 1H), 3.52 (s, 3H). **¹³C NMR** (100 MHz, CDCl₃) δ 128.81, 127.86, 127.30, 126.22, 125.53, 121.29, 120.72, 106.98, 55.45.



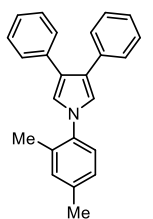
152fa. Yellow viscous oil. *c*Hex:EtOAc: 100:1; yield = 75% (55 mg), **152:152'** = 83:17; **¹H NMR** (400 MHz, CDCl₃) δ 7.39 – 7.36 (m, 2H), 7.34 – 7.31 (m, 3H), 7.29 – 7.27 (m, 3H), 7.25 (d, *J* = 5.2 Hz, 1H), 7.23 – 7.18 (m, 3H), 7.11 (s, 2H), 6.98 – 6.94 (m, 2H), 3.99 (t, *J* = 6.5 Hz, 2H), 1.83 – 1.75 (m, 2H), 1.56 – 1.46 (m, 2H), 1.00 (t, *J* = 7.4 Hz, 3H). **¹³C NMR** (100 MHz, CDCl₃) δ 157.41, 135.41, 133.69, 128.42, 128.15, 125.82, 124.97, 121.77, 118.93, 115.28, 68.05, 31.27, 19.20, 13.80. **GC-MS** (*m/z*): 367 (100), 191 (37), 57 (28); **Anal. Calc.** for (C₂₆H₂₅NO: 367.49): C, 84.97; H, 6.85; found: C, 84.74, H, 6.76.

Diagnostic signal of **152fa'**: $^1\text{H NMR}$ (400 MHz, CDCl_3) δ 7.59 (d, $J = 7.2$ Hz, 2H), 7.14 (s, 1H), 6.87-6.80 (m, 4H), 6.73 (d, $J = 2.0$ Hz, 1H), 3.95 – 3.88 (m, 2H), 0.99 (t, $J = 7.2$ Hz, 3H). $^{13}\text{C NMR}$ (100 MHz, CDCl_3) δ 157.93, 128.64, 128.05, 126.85, 126.37, 125.69, 121.08, 119.92, 115.73, 115.43, 114.71, 114.61, 114.71, 108.06, 67.95, 55.72, 31.29, 19.20, 13.81.



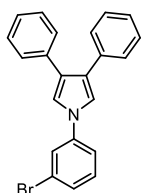
152ga. Yellow viscous oil. *c*Hex:EtOAc: 130:1; yield = 47% (30 mg), **152:152'** = 81:19; $^1\text{H NMR}$ (400 MHz, CDCl_3) δ 7.35 – 7.32 (m, 1H), 7.28 (dd, $J = 12.3, 4.3$ Hz, 1H), 7.21 (d, $J = 4.1$ Hz, 1H), 7.17 (s, 1H), 2.34 (s, 1H), 2.30 (s, 1H). $^{13}\text{C NMR}$ (100 MHz, CDCl_3) δ 138.19, 137.98, 135.43, 134.32, 130.57, 128.45, 128.17, 125.85, 125.13, 121.57, 118.66, 117.60, 19.97, 19.20 **GC-MS**: 323 (100), 217 (18), 191 (36); **Anal. Calc.** for ($\text{C}_{24}\text{H}_{21}\text{N}$: 323.44): C, 89.12; H, 6.54; found: C, 88.98, H, 6.47.

152ga' Diagnostic signals: $^1\text{H NMR}$ (400 MHz, CDCl_3) δ 7.58 (d, $J = 7.4$ Hz, 2H), 7.36 (d, $J = 7.7$ Hz, 2H), 7.05 (d, $J = 7.3$ Hz, 2H), 6.87 (dd, $J = 8.0, 2.0$ Hz, 2H), 6.72 (d, $J = 1.6$ Hz, 1H), 2.26 (s, 3H), 2.22 (s, 3H). $^{13}\text{C NMR}$ (100 MHz, CDCl_3) δ 129.96, 128.62, 127.99, 126.53, 125.66, 123.10, 120.99, 108.30, 19.75, 19.31.



152ha.²⁹ Yellow viscous oil. *c*Hex:EtOAc: 130:1; yield = 63% (41 mg), **152:152'** = 88:12; $^1\text{H NMR}$ (400 MHz, CDCl_3) δ 7.34 – 7.28 (m, 4H), 7.26 (t, $J = 4.4$ Hz, 3H), 7.24 (s, 1H), 7.22 – 7.17 (m, 3H), 7.12 (s, 1H), 7.07 (d, $J = 8.0$ Hz, 1H), 6.86 (s, 2H), 2.37 (s, 3H), 2.28 (s, 3H). $^{13}\text{C NMR}$ (100 MHz, CDCl_3) δ 137.65, 137.46, 135.67, 133.22, 131.77, 128.43, 128.14, 127.21, 126.22, 125.65, 124.93, 123.74, 121.58, 20.95, 17.93. **GC-MS**: 323 (100), 217 (20), 191 (33); **Anal. Calc.** for ($\text{C}_{24}\text{H}_{21}\text{N}$: 323.44): C, 89.12; H, 6.54; found: C, 89.01, H, 6.38.

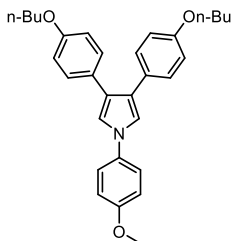
152ha' Diagnostic signals: $^1\text{H NMR}$ (400 MHz, CDCl_3) δ 7.58 (d, $J = 7.1$ Hz, 2H), 7.16 (d, $J = 1.4$ Hz, 1H), 7.15 (d, $J = 1.8$ Hz, 2H), 6.76 (d, $J = 2.0$ Hz, 1H), 2.34 (s, 3H), 1.90 (s, 3H).



152ka.¹⁵ Yellow viscous oil. *c*Hex:EtOAc: 120:1; yield = 53% (40 mg), **152:152'** = 80:20; $^1\text{H NMR}$ (400 MHz, CDCl_3) δ 7.56 (d, $J = 8.7$ Hz, 2H), 7.34 (d, $J = 8.7$ Hz, 2H), 7.29 (t, $J = 7.1$ Hz, 7H), 7.23 (dd, $J = 7.1, 3.8$ Hz, 3H), 7.15 (s, 2H). $^{13}\text{C NMR}$ (100 MHz, CDCl_3) δ 139.22, 134.97, 132.69, 132.18, 128.44, 128.25, 127.04, 126.16, 126.11, 125.13, 121.50, 118.89, 118.29. **GC-MS** (m/z): 373 (35), 216 (51), 189 (100), 155 (53); **Anal. Calc.**

for ($\text{C}_{22}\text{H}_{16}\text{BrN}$: 374.28): C, 70.60; H, 4.31; found: C, 70.51, H, 4.12.

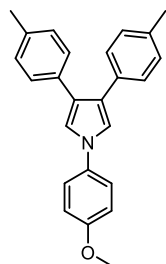
152ka' Diagnostic signals:²⁹ $^1\text{H NMR}$ (400 MHz, CDCl_3) δ 7.93 – 7.83 (m, 1H), 7.80 – 7.71 (m, 1H), 7.45 (d, $J = 8.7$ Hz, 2H), 7.11 – 7.02 (m, 2H), 6.77 – 6.69 (m, 1H). $^{13}\text{C NMR}$ (100 MHz, CDCl_3) δ 128.70, 128.35, 126.78, 109.19.



152ab. Yellow viscous oil. *c*Hex:EtOAc: 130:1; yield = 51% (47 mg), **152:152'** = 83:17 $^1\text{H NMR}$ (400 MHz, CDCl_3) δ 7.39 – 7.36 (m, 2H), 7.26 (s, 2H), 7.24 – 7.21 (m, 3H), 7.04 (s, 2H), 6.99 – 6.95 (m, 2H), 6.85 – 6.81 (m, 3H), 3.96 (t, $J = 6.5$ Hz, 4H), 3.85 (s, 3H), 1.81 – 1.73 (m, 4H), 1.54 – 1.46 (m, 4H), 0.98 (t, $J = 7.4, 6\text{H}$); $^{13}\text{C NMR}$ (100 MHz, CDCl_3) δ 157.74, 134.29, 130.98, 129.64, 128.03, 124.89, 121.85, 118.36, 114.91, 114.44, 67.82, 55.75, 31.61, 19.46, 14.03; **GC-**

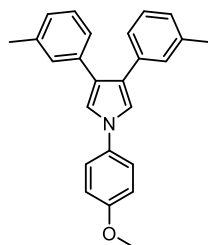
MS (m/z): 469 (89), 412 (17), 207(28), 57(100); **Anal. Calc.** for ($\text{C}_{31}\text{H}_{35}\text{NO}_3$: 469.63): C, 79.28; H, 7.51; found: C, 79.07, H, 7.35.

152ab' Diagnostic signal: $^1\text{H NMR}$ (401 MHz, CDCl_3) δ 7.10 (d, $J = 8.6$ Hz, 2H), 7.06 (d, $J = 8.6$ Hz, 1H), 6.78 – 6.75 (m, 2H), 6.69 (d, $J = 8.6$ Hz, 1H), 3.94 – 3.89 (m, 4H), 0.96 (t, $J = 7.6$ Hz, 6H). $^{13}\text{C NMR}$ (100 MHz, CDCl_3) δ 157.65, 127.42, 101.88



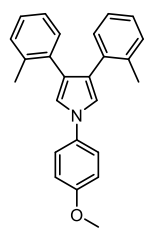
152ac. Yellow viscous oil. *c*Hex:EtOAc: 130:1; yield = 78% (55 mg), **152:152'** = 91:9; $^1\text{H NMR}$ (400 MHz, CDCl_3) δ 7.37 (d, $J = 8.9$ Hz, 2H), 7.20 (d, $J = 8.0$ Hz, 4H), 7.08 (d, $J = 8.7$ Hz, 6H), 6.96 (d, $J = 8.9$ Hz, 2H), 3.83 (s, 3H), 2.33 (s, 6H). $^{13}\text{C NMR}$ (100 MHz, CDCl_3) δ 157.71, 135.36, 134.00, 132.51, 130.27, 129.89, 129.31, 128.90, 128.29, 124.94, 121.74, 118.62, 114.70, 55.55, 21.12; **GC-MS:** 353 (100), 338 (10), 202 (19); **Anal. Calc.** for ($\text{C}_{25}\text{H}_{23}\text{ON}$: 353.47): C, 84.95; H, 6.56; found: C, 84.85, H, 6.42.

152ac' Diagnostic signals: $^1\text{H NMR}$ (400 MHz, CDCl_3) δ 7.74 (dd, $J = 23.8, 7.6$ Hz, 2H), 7.60 – 7.41 (m, 2H), 7.27 (d, $J = 7.5$ Hz, 2H), 7.14 (d, $J = 8.6$ Hz, 2H), 2.43 (s, 3H), 2.31 (s, 3H). $^{13}\text{C NMR}$ (100 MHz, CDCl_3) δ 132.11, 129.72, 129.09, 128.78, 128.17, 126.88, 126.33, 124.98, 120.46, 114.11, 55.43, 21.04, 21.01.



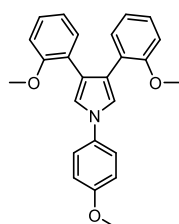
152ad. Yellow viscous oil. *c*Hex:EtOAc: 130:1; yield = 51% (35 mg), **152:152'** = 90:10; $^1\text{H NMR}$ (400 MHz, CDCl_3) δ 7.38 (d, $J = 8.9$ Hz, 2H), 7.20 – 7.12 (m, 4H), 7.09 (d, $J = 9.0$ Hz, 4H), 7.02 (d, $J = 7.3$ Hz, 2H), 6.97 (d, $J = 8.9$ Hz, 2H), 3.84 (s, 3H), 2.30 (s, 6H). $^{13}\text{C NMR}$ (100 MHz, CDCl_3) δ 157.77, 137.62, 135.34, 133.98, 129.01, 127.97, 126.59, 125.65, 125.11, 121.76, 118.83, 114.72, 55.56, 21.42; **GC-MS:** 353 (100), 338 (12), 202 (22); **Anal. Calc.** for ($\text{C}_{25}\text{H}_{23}\text{ON}$: 353.47): C, 84.92; H, 6.53; found: C, 84.77, H, 6.45.

152ad' Diagnostic signals: $^1\text{H NMR}$ (400 MHz, CDCl_3) δ 6.85 (d, $J = 8.9$ Hz, 2H), 6.70 (d, $J = 1.9$ Hz, 1H), 3.81 (s, 3H), 2.38 (s, 3H), 2.27 (s, 3H). $^{13}\text{C NMR}$ (100 MHz, CDCl_3) δ 132.69, 128.94, 128.52, 127.83, 127.13, 126.86, 126.46, 125.87, 125.34, 122.19, 120.96, 114.10, 55.45.



152ae. Yellow viscous oil. *c*Hex:EtOAc: 130:1; yield = 78% (55 mg), **152:152'** = 86:14; $^1\text{H NMR}$ (400 MHz, CDCl_3) δ 7.41 – 7.36 (m, 2H), 7.14 – 7.09 (m, 6H), 7.09 – 7.03 (m, 2H), 7.03 (s, 2H), 7.00 – 6.95 (m, 2H), 3.84 (s, 3H), 2.12 (s, 6H). $^{13}\text{C NMR}$ (100 MHz, CDCl_3) δ 157.58, 136.22, 135.44, 134.12, 130.75, 130.03, 126.30, 125.66, 125.30, 121.54, 118.51, 114.73, 113.96, 55.57, 20.51; **GC-MS:** 353 (100), 338 (14), 202 (24); **Anal. Calc.** for ($\text{C}_{25}\text{H}_{23}\text{ON}$: 353.47): C, 84.90; H, 6.52; found: C, 84.74, H, 6.41.

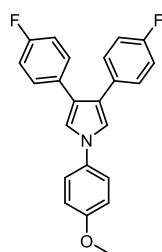
152ae' Diagnostic signals: $^1\text{H NMR}$ (400 MHz, CDCl_3) δ 7.49 (dd, $J = 7.6, 1.5$ Hz, 2H), 7.23 – 7.15 (m, 4H), 6.78 – 6.75 (m, 2H), 6.45 (d, $J = 2.0$ Hz, 1H), 3.76 (s, 3H), 2.53 (s, 3H), 2.08 (s, 3H). $^{13}\text{C NMR}$ (100 MHz, CDCl_3) δ 137.54, 131.36, 130.70, 129.99, 128.90, 127.56, 125.89, 125.85, 124.34, 120.91, 111.79, 55.36, 21.65, 20.35.



152af. Yellow viscous oil. *c*Hex:EtOAc: 60:1; yield = 47% (36 mg), **152:152'** = 87:13; $^1\text{H NMR}$ (400 MHz, CDCl_3) δ 7.38 (d, $J = 8.9$ Hz, 2H), 7.21 (s, 2H), 7.16 (ddd, $J = 15.4, 7.6, 1.5$ Hz, 4H), 6.98 – 6.93 (m, 2H), 6.87 – 6.80 (m, 4H), 3.83 (s, 3H), 3.47 (s, 6H). $^{13}\text{C NMR}$ (100 MHz, CDCl_3) δ 157.65, 156.60, 134.47, 130.66, 127.18, 125.90, 121.99, 121.92, 120.41, 119.53, 114.76, 110.90, 55.71, 55.16. **GC-MS:** 385 (100),

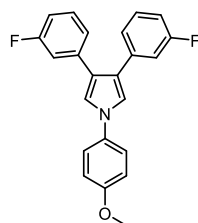
370 (6), 354 (9); **Anal. Calc.** for (C₂₅H₂₃O₃N: 385.46): C, 77.90; H, 6.01; found: C, 77.82, H, 5.94

152af' Diagnostic NMR signal: ¹H NMR (400 MHz, CDCl₃) δ 3.90 (s, 3H), 3.76 (s, 3H), 3.37 (s, 3H).



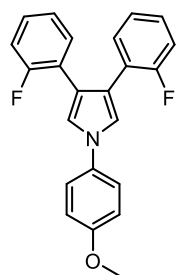
152ag. Light yellow solid. m.p.: 115 – 118 °C. *c*Hex:EtOAc: 120:1; yield = 44% (32 mg), **152:152'** = 81:19; ¹H NMR (400 MHz, CDCl₃) δ 7.38 – 7.34 (m, 2H), 7.24 (s, 2H), 7.24 – 7.19 (m, 4H), 7.05 (s, 2H), 6.97 (d, *J* = 8.6 Hz, 4H), 3.84 (s, 3H). ¹³C NMR (100 MHz, CDCl₃) δ 162.90, 160.47, 158.11, 133.92, 131.39, 131.36, 130.08, 130.00, 127.08, 124.18, 122.05, 118.95, 115.41, 115.20, 114.94, 55.74. ¹⁹F NMR (377 MHz, CDCl₃) δ -117.06 (dt, *J* = 8.8, 5.5 Hz). **GC-MS:** 361 (100), 346 (19), 227 (21); **Anal. Calc.** for (C₂₃H₁₇ONF₂: 361.39): C, 76.44; H, 4.74; found: C, 76.21, H, 4.63

152ag' Diagnostic NMR signal: ¹H NMR (400 MHz, CDCl₃) δ 7.50 (dd, *J* = 8.8, 5.4 Hz, 3H), 7.12 – 7.08 (m, 5H), 6.90 (d, *J* = 8.8 Hz, 2H), 6.85 (d, *J* = 8.9 Hz, 3H), 6.60 (d, *J* = 2.0 Hz, 1H), 3.81 (s, 3H). ¹³C NMR (100 MHz, CDCl₃) δ 158.46, 133.14, 126.48, 126.41, 120.64, 115.60, 115.38, 114.27, 107.85. ¹⁹F NMR (377 MHz, CDCl₃) δ -115.61 (dt, *J* = 8.8, 5.3 Hz), -117.46 (dt, *J* = 8.4, 5.1 Hz)



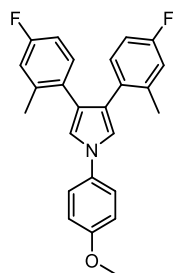
152ah. Yellow viscous oil. *c*Hex:EtOAc: 120:1; yield = 63% (45 mg), **152:152'** = 80:20; ¹H NMR (400 MHz, CDCl₃) δ 7.39 – 7.35 (m, 2H), 7.21 (dd, *J* = 7.9, 6.2 Hz, 2H), 7.09 (s, 2H), 7.05 (d, *J* = 7.7 Hz, 2H), 6.99 (ddd, *J* = 9.0, 5.3, 2.3 Hz, 4H), 6.89 (dtd, *J* = 12.4, 8.3, 4.3 Hz, 4H), 3.84 (s, 3H). ¹³C NMR (101 MHz, cdcl₃) δ 164.02, 161.59, 158.10, 137.34 (d, *J* = 8.2 Hz), 133.57, 129.65 (d, *J* = 8.6 Hz), 124.09 (d, *J* = 2.8 Hz), 126.89, 122.01, 119.44, 115.04 (d, *J* = 21.7 Hz), 114.80, 112.84 (d, *J* = 21.2 Hz), 55.57; ¹⁹F NMR (377 MHz, CDCl₃) δ -113.60 – -113.72 (m). **GC-MS:** 361 (100), 346 (17), 227 (23); **Anal. Calc.** for (C₂₃H₁₇ONF₂: 361.39): C, 76.42; H, 4.75; found: C, 76.24, H, 4.66.

152ah' Diagnostic signals: ¹H NMR (401 MHz, cdcl₃) δ 7.17 (d, *J* = 2.0 Hz, 2H), 7.13 (d, *J* = 8.9 Hz, 2H), 6.79 (d, *J* = 8.8 Hz, 1H), 6.70 (d, *J* = 2.0 Hz, 1H), 3.82 (s, 3H). ¹³C NMR (100 MHz, CDCl₃) δ 123.92 (d, *J* = 2.3 Hz), 121.95, 114.36, 108.54, 55.46. ¹⁹F NMR (377 MHz, CDCl₃) δ -113.19 (td, *J* = 9.2, 6.1 Hz).



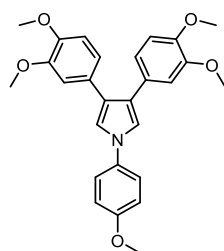
152ai. Colorless viscous oil. *c*Hex:EtOAc: 120:1; yield = 44% (32 mg), **152:152'** = 93:7; ¹H NMR (400 MHz, CDCl₃) δ 7.43 – 7.39 (m, 2H), 7.25 (s, 2H), 7.22 – 7.16 (m, 4H), 7.10 – 7.05 (m, 2H), 7.05 – 6.97 (m, 4H), 3.86 (s, 1H). ¹³C NMR (100 MHz, CDCl₃) δ 161.20 (s), 158.48 (d, *J* = 56.3 Hz), 134.01 (s), 131.20 (d, *J* = 3.7 Hz), 127.77 (d, *J* = 8.1 Hz), 123.89 (d, *J* = 3.6 Hz), 122.28 (s), 120.47 (d, *J* = 4.8 Hz), 118.64 (s), 115.82 (d, *J* = 22.7 Hz), 114.93 (s), 55.75 (s). ¹⁹F NMR (377 MHz, CDCl₃) δ -115.22 – -115.37 (m). **GC-MS:** 361 (100), 346 (18), 227 (22); **Anal. Calc.** for (C₂₃H₁₇ONF₂: 361.39): C, 76.41; H, 4.73; found: C, 76.25, H, 4.64.

152ai' Diagnostic signals: ¹H NMR (400 MHz, CDCl₃) δ 7.66 – 7.58 (m, 2H), 7.11 (d, *J* = 9.0 Hz, 2H), 6.82 (d, *J* = 8.8 Hz, 2H), 3.80 (s, 3H). ¹³C NMR (100 MHz, CDCl₃) δ 126.16, 123.31, 123.16, 114.08.



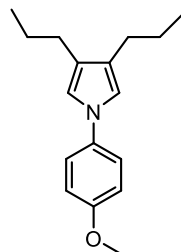
152aj. Colorless viscous oil. *c*Hex:EtOAc: 120:1; yield = 77% (60 mg), **152:152'** = 92:8; **¹H NMR** (400 MHz, CDCl₃) δ 7.36 (d, *J* = 8.8 Hz, 2H), 7.02 (dd, *J* = 8.4, 6.2 Hz, 2H), 6.97 (d, *J* = 7.0 Hz, 4H), 6.82 (dd, *J* = 9.8, 2.5 Hz, 2H), 6.74 (td, *J* = 8.4, 2.6 Hz, 2H), 3.84 (s, 3H), 2.09 (s, 6H). **¹³C NMR** (101 MHz, CDCl₃) δ 162.68, 160.26, 157.72, 138.49 (d, *J* = 7.7 Hz), 133.97, 132.01 (d, *J* = 8.1 Hz), 131.09 (d, *J* = 3.1 Hz), 125.75, 124.61, 121.60, 118.57, 116.52 (d, *J* = 20.8 Hz), 114.76, 112.12 (d, *J* = 20.8 Hz), 55.57, 20.56 (d, *J* = 1.5 Hz). **¹⁹F NMR** (377 MHz, CDCl₃) δ -117.23 (td, *J* = 9.0, 6.3 Hz). **GC-MS:** 389 (100), 374 (25), 255 (27); **Anal. Calc.** for (C₂₅H₂₁ONF₂: 389.45): C, 77.10; H, 5.44; found: C, 76.98, H, 5.23.

152aj' Diagnostic signals: **¹H NMR** (400 MHz, CDCl₃) δ 3.76 (s, 3H), 2.49 (s, 3H), 2.05 (s, 3H).



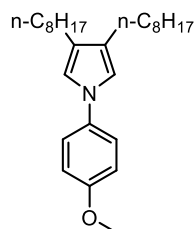
152ak. Yellow viscous oil. *c*Hex:EtOAc: 50:1; yield = 72% (64 mg), **152:152'** > 20:1; **¹H NMR** (400 MHz, CDCl₃) δ 7.38 (dd, *J* = 9.6, 2.8 Hz, 2H), 7.07 (s, 2H), 6.96 (dd, *J* = 2.0, 8.8 Hz, 2H), 6.89 (d, *J* = 1.9 Hz, 2H), 6.84 (d, *J* = 1.8 Hz, 2H), 6.83 (s, 1H), 6.81 (s, 1H), 3.88 (s, 6H), 3.85 (s, 3H), 3.70 (s, 6H). **¹³C NMR** (100 MHz, CDCl₃) δ 157.96, 148.64, 147.55, 134.13, 128.42, 124.93, 121.99, 120.75, 118.46, 114.91, 112.36, 111.31, 56.05, 55.83, 55.75. **GC-MS:** 445 (100), 430 (46), 311 (21); **Anal. Calc.** for (C₂₇H₂₇O₅N: 445.52): C, 72.79; H, 6.11; found: C, 72.68, H, 6.01.

152ak' Diagnostic signals: **¹H NMR** (400 MHz, CDCl₃) δ 7.14 (d, *J* = 8.9 Hz, 2H), 6.62 (d, *J* = 1.5 Hz, 1H), 6.60 (d, *J* = 1.9 Hz, 1H), 3.93 (s, 3H), 3.89 (s, 3H), 3.80 (s, 3H), 3.63 (s, 3H). **¹³C NMR** (100 MHz, CDCl₃) δ 122.29, 109.38, 51.20, 51.03, 50.74.



152al. Colorless viscous oil. *c*Hex:EtOAc: 150:1; yield = 30% (15 mg), **152:152'** = 94:6; **¹H NMR** (400 MHz, CDCl₃) δ 7.24 (d, *J* = 9.0 Hz, 2H), 6.89 (d, *J* = 9.0 Hz, 2H), 6.72 (s, 2H), 3.80 (s, 3H), 2.44 – 2.39 (m, 4H), 1.67 – 1.56 (m, 4H), 0.99 (t, *J* = 7.3 Hz, 6H). **¹³C NMR** (100 MHz, CDCl₃) δ 156.89, 134.72, 124.91, 121.07, 116.45, 114.50, 55.51, 27.58, 23.49, 14.25; **GC-MS:** 257 (32), 228 (100), 200 (7); **Anal. Calc.** for (C₁₇H₂₃ON: 257.38): C, 79.33; H, 9.01; found: C, 79.15, H, 8.94.

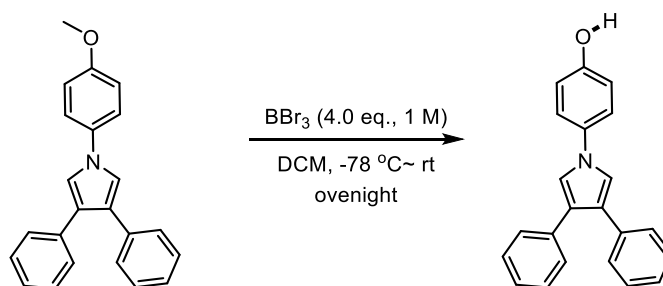
152al' Diagnostic signals: **¹H NMR** (400 MHz, CDCl₃) δ 7.18 (d, *J* = 8.9 Hz, 1H), 3.83 (s, 1H), 0.86 (t, *J* = 7.3 Hz, 3H). **¹³C NMR** (100 MHz, CDCl₃) δ 127.25, 113.99.



152am. Colorless viscous oil. *c*Hex:EtOAc: 150:1; yield = 30% (24 mg), **152:152'** = 92:8; **¹H NMR** (400 MHz, CDCl₃) δ 7.24 (d, *J* = 8.8 Hz, 2H), 6.89 (d, *J* = 8.9 Hz, 2H), 6.72 (s, 2H), 3.80 (s, 3H), 2.45 – 2.39 (m, 4H), 1.60 – 1.51 (m, 4H), 1.40-1.20 (m, 20H), 0.87 (t, *J* = 7.0 Hz, 6H). **¹³C NMR** (100 MHz, CDCl₃) δ 156.86, 134.72, 125.12, 121.06, 116.35, 114.49, 55.50, 31.91, 30.36, 29.74, 29.52, 29.30, 25.39, 22.67, 14.08. **GC-MS** (*m/z*): 397(57), 299 (63), 200 (100). **Anal. Calc.** for (C₂₇H₄₃NO: 397.65): C, 81.55; H, 10.90; found: C, 81.35, H, 10.73.

152am' Diagnostic signals: **¹H NMR** (400 MHz, CDCl₃) δ 7.18 (d, *J* = 8.8 Hz, 2H), 3.83 (s, 3H).

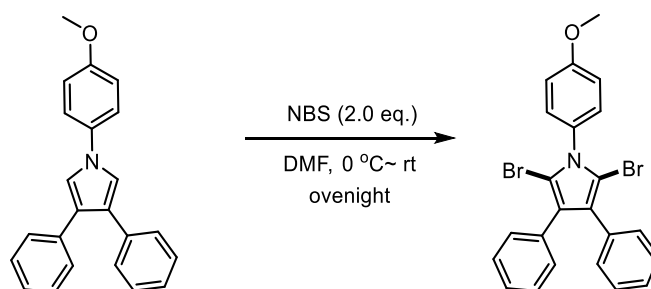
Chemical manipulations of 152aa



To a dry Schlenk tube was added the pyrrole **152aa** (42 mg, 0.13 mmol; **152aa**:**152'aa** 85:15) and DCM (2 ml), afterwards, the solution was cooled to -78 °C and added BBr_3 (4.0 eq, 1 M). Then the reaction was allowed to warm to room temperature and be stirred overnight. TLC showed the reaction completed. Water (5 ml) was added to quench the reaction and the mixture was extracted with ethyl acetate (3 × 10 ml). The collected organic phases were washed with brine (10 ml) and dried over Na_2SO_4 . After removal of the solvent under vacuum, the residue was purified via flash chromatography (*c*Hex/EtOAc = 5:1), providing 35 mg product **153aa** in 88% yield (**153aa**:**153'aa** = 85:15) as a grey foam.

153aa: $^1\text{H NMR}$ (400 MHz, CDCl_3) δ 7.37 – 7.27 (m, 9H), 7.25 – 7.18 (m, 3H), 7.11 (s, 2H), 6.93 – 6.90 (m, 2H), 4.92 (s, 3H). $^{13}\text{C NMR}$ (100 MHz, CDCl_3) δ 153.93, 135.55, 134.28, 128.62, 128.37, 126.06, 125.25, 122.23, 119.11, 116.40. **GC-MS** (*m/z*): 311(100). **Anal. Calc.** for ($\text{C}_{22}\text{H}_{17}\text{NO}$: 311.38): C, 84.86; H, 5.50; found: C, 84.66, H, 5.33.

153'aa Diagnostic signal: $^1\text{H NMR}$ (400 MHz, CDCl_3) δ 7.60 (dd, *J* = 8.2, 1.1 Hz, 2H), 6.81 – 6.78 (m, 2H), 5.07 (s, 1H). $^{13}\text{C NMR}$ (100 MHz, CDCl_3) δ 128.84, 128.25, 128.21, 127.31, 125.92, 125.23, 115.89.



To a dry Schlenk tube was added pyrrole **152aa** (42 mg, 0.13 mmol) and DMF (1 ml). The reaction was cooled to 0 °C and when a solution of NBS (46 mg, 2.0 eq.) in 1 ml DMF was added. Then the reaction was allowed to warm to room temperature and be stirred overnight. TLC showed the reaction completed. Water (5 ml) was added and after phases separation, the aqueous phase was extracted with EtOAc (3 × 10 ml), washed with brine (10 ml) and dried over Na_2SO_4 . After removal of solvent under vacuum, the residue was purified via flash chromatography column provide dibrominated compound **154aa** in 60% yield (38 mg) as a yellow solid.

154aa. mp: 189.8 ~ 191.5 °C. *c*Hex:EtOAc: 10:1. $^1\text{H NMR}$ (400 MHz, CDCl_3) δ 7.53 (dd, *J* = 7.9, 1.7 Hz, 4H), 7.41 – 7.35 (m, 8H), 7.04 – 6.99 (m, 2H), 3.85 (s, 3H). $^{13}\text{C NMR}$ (100 MHz, CDCl_3) δ 169.96, 159.16, 136.36, 130.16, 130.08, 128.73, 128.70, 127.76, 124.60, 114.56, 55.64. **GC-MS** (*m/z*): 397(57), 299 (63), 200 (100). **Anal. Calc.** for ($\text{C}_{23}\text{H}_{17}\text{Br}_2\text{NO}$: 483.20): C, 57.17; H, 3.55; found: C, 57.01, H, 3.41.

Crystallographic data collection and structure determination for 152aa and 152ag.

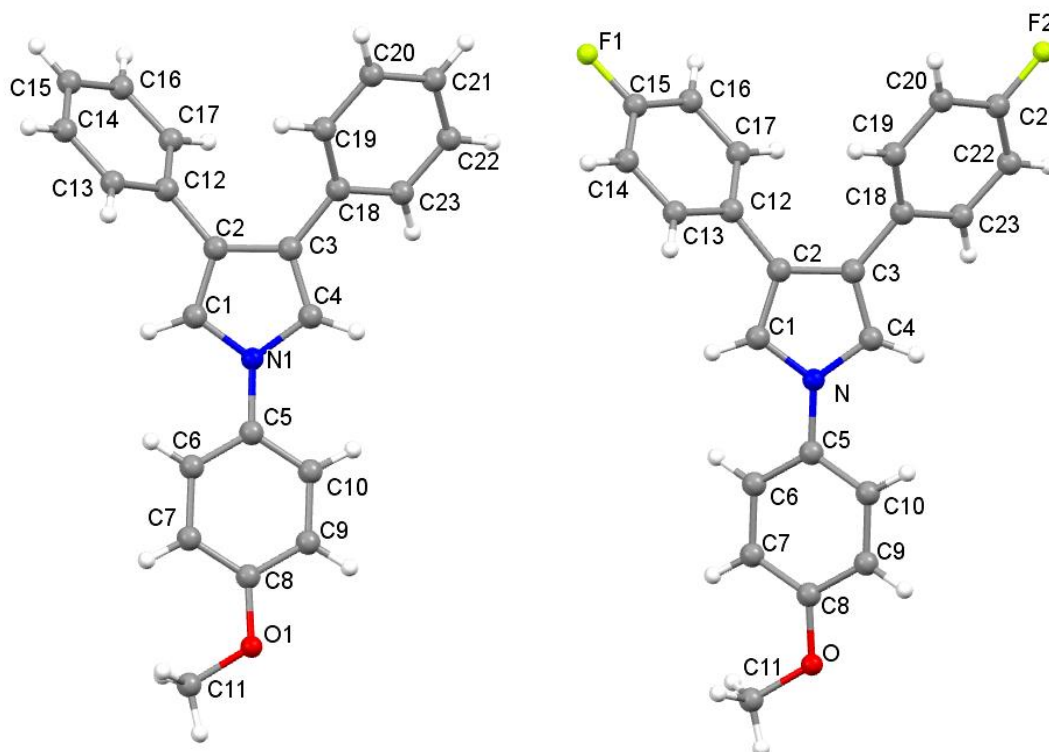
The X-ray intensity data were measured on a Bruker Apex III CCD diffractometer. Cell dimensions and the orientation matrix were initially determined from a least-squares refinement on reflections measured in three sets of 20 exposures, collected in three different ω regions, and eventually refined against all data. A full sphere of reciprocal space was scanned by 0.3° ω steps. The software SMART³⁰ was used for collecting frames of data, indexing reflections and determination of lattice parameters. The collected frames were then processed for integration by the SAINT program²⁰ and an empirical absorption correction was applied using SADABS.³¹ The structures were solved by direct methods (SIR 2014)³² and subsequent Fourier syntheses and refined by full-matrix least-squares on F^2 (SHELXTL)³³ using anisotropic thermal parameters for all non-hydrogen atoms. The aromatic and methyl hydrogen atoms were placed in calculated positions, refined with isotropic thermal parameters $U(H) = 1.2 U_{eq}(C)$ [and $U(H) = 1.5 U_{eq}(\text{methyl})$] and allowed to ride on their carrier carbons. Two independent molecules are present in the asymmetric unit of **152aa**. These two molecules differ in the orientations of the external aromatic rings with respect to the inner pyrrole plane. Crystal data and details of data collections for compounds **152aa** and **152ag** are reported in Table S1. Molecular drawings were generated using Mercury.³⁴

Crystallographic data have been deposited with the Cambridge Crystallographic Data Centre (CCDC) as supplementary publication numbers CCDC 1945119-1945120 (**152aa** and **152ag**, respectively). Copies of the data can be obtained free of charge via www.ccdc.cam.ac.uk/getstructures.

Table S1. Crystal data and structure refinement for compounds **152aa** and **152ag**.

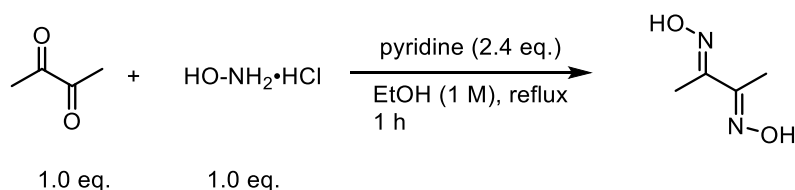
Compound	152aa	152ag
Formula	C ₂₃ H ₁₉ NO	C ₂₃ H ₁₇ F ₂ NO
Fw	325.39	361.38
T, K	296	296
λ , Å	0.71073	0.71073
Crystal symmetry	Monoclinic	Orthorhombic
Space group	<i>P2₁/c</i>	<i>Pbca</i>
<i>a</i> , Å	6.2137(9)	7.5997(12)
<i>b</i> , Å	71.053(9)	21.735(4)
<i>c</i> , Å	8.0096(10)	21.974(3)
α	90	90
β	93.280(5)	90
γ	90	90
Cell volume, Å ³	3530.5(8)	3629.7(10)
<i>Z</i>	8	8
<i>D_c</i> , Mg m ⁻³	1.224	1.323
$\mu(\text{Mo-K}\alpha)$, mm ⁻¹	0.074	0.095
<i>F</i> (000)	1376	1504
Crystal size/ mm	0.35 x 0.10 x 0.10	0.35 x 0.15 x 0.15
θ limits, °	1.720 - 25.215	2.636 - 25.181
Reflections collected	37088	27464
Unique obs. Reflections	6279 [R(int) = 0.1012]	3164 [R(int) = 0.0957]
[<i>F_o</i> > 4 σ (<i>F_o</i>)]		
Goodness-of-fit-on <i>F</i> ²	1.119	1.056

$R_1(F)^a$, $wR_2(F^2)$ [$I > 2\sigma(I)$]	0.1074, 0.1792	0.0785, 0.1982
Largest diff. peak and hole, e.	0.198 and -0.201	0.281 and -0.218

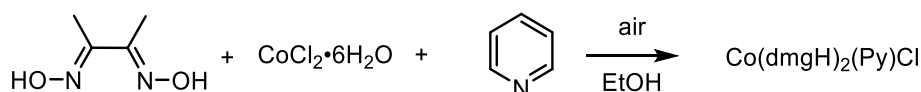
Figure S4

Crystal structure of one of the two conformers of **152aa** with the atom labelling scheme. Crystal structure of **152ag**

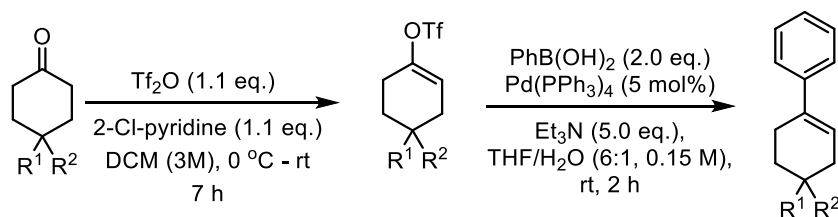
Photocatalyzed Wacker Oxidation of Trisubstituted Alkene

Preparation of Co(dmgh)₂(Py)Cl

To a flask was charged with stirring bar, ethanol (5 mol), biacetyl (430 mg, 5 mmol, 1.0 eq.), hydroxylammonium chloride (690 mg, 10 mmol, 2.0 eq.) and pyridine (960 mg, 12 mmol, 1.2 eq.). Then the reaction was refluxed for 1 hr. Then the solution was cooled down to room temp and pured into ice-water (20 ml). After a while, white precipitate was produced, filtrated and recrystallized in EtOH (the solid was dissolved in hot EtOH using the amount of EtOH as small as possible). The yield was 20%.



To an Erlenmeyer flask was charged with stirring bar, EtOH (20 ml), CoCl₂·6H₂O (474 mg, 2 mmol, 1.0 eq.), butane-2,3-dione dioxime (510 mg, 4.4 mmol, 2.2 eq.). Then the mixture was heated until CoCl₂·6H₂O was dissolved. After pyridine (320 mg, 4.0 mmol, 2.0 eq.) was added into the hot solution, the solution was cooled to 20 °C. Then air was blown into the solution for 30 mins. The reaction mixture is then allowed to stand for 60 minutes at 20 °C, during which period the product crystallizes out of the solution. The brown crystals are collected by filtration on a Buchner funnel, washed successively with 5-ml. portions of water, ethanol, and diethyl ether, and dried at room temperature in vacuum. Used in reaction without further purification.

Preparation of olefin 238b-d

238b. R¹ = H; R² = tBu

238c. R¹ = H; R² = Me

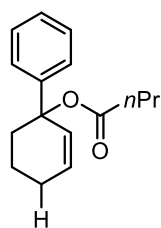
238d. R¹ = Me; R² = Me

Under N₂, to a dry Schlenk tube was charged with stirring bar, DCM (15 ml) and ketone (5 mmol, 1.0 eq.) at 0 °C, then 2-Cl-Pyridine (684 mg, 6.0 mmol, 1.2 eq) was added. The mixture was stirred for 10 min before Tf₂O (1.5 g, 5.5 mmol, 1.1 eq) was added at 0 °C. The resulting mixture was warmed to rt and stirred for 7 hrs. The reaction would turn dark red during the reaction. TLC monitoring the reaction showed the reaction completed. Then the solvent was removed under

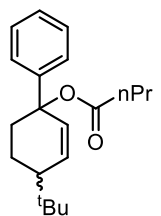
vacuum and the residue was purified with silica gel chromatographic column, Cy: EA (100:1). Under N₂, to a dry Schlenk tube was charged with stirring bar, THF (6 ml), distilled H₂O (1 ml) and Et₃N (505 mg, 5 mmol, 5.5 eq.) at room temp. Then PhB(OH)₂ (274 mg, 2.0 mmol, 2.0 eq.) and triflate (1.0 mmol, 1.0 eq.) was added. The reaction would turn black soon. Then reaction was stirred at room temp for 2 hrs. TLC showed the reaction completed. Then H₂O (10 ml) was added and the resulting mixture was extracted with EA (2 × 15 ml). then the organic phase was filtrated with Buchner filter with celite. The organic phase was dried over Na₂SO₄, then concentrated under vacuum. The residue was purified with silica gel chromatography, Cy (100%).

General procedure of photocatalysis

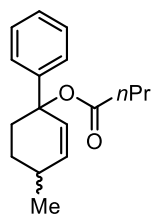
To a little vial charged with stirring bar was added Mes-Acr-Me⁺ClO₄⁻ (1.0 mg, 0.0025 mol, 2.5 mol%) and Co(III) (2.0 mg, 0.005 mol, 5 mol%) before solvent (DCM, 1 ml) was added. Then olefin (0.1 mmol) and carboxylic acid (1 mmol, 10 eq.) was added. Then the vial was charged with N₂ (blow with N₂ for 30s) and left in blue LED barrel (20 W) stirring for 40 hrs. TLC showed the reaction completed. Then the solvent was blow away and the residue was purified with silica gel chromatography, Cy:EA (100:2).



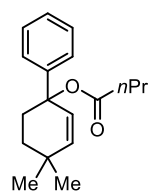
240aa, 63%. *c*Hex:EtOAc: 100:1. ¹H NMR (401 MHz, CDCl₃) δ 7.34 – 7.30 (m, 3H), 7.29 – 7.27 (m, 1H), 7.22 (m, 1H), 6.33 (dd, *J* = 4.6, 3.4 Hz, 1H), 5.96 (t, *J* = 3.9 Hz, 1H), 2.36 – 2.22 (m, 2H), 2.16 (td, *J* = 7.3, 2.9 Hz, 2H), 2.02 – 1.96 (m, 1H), 1.92 – 1.84 (m, 1H), 1.73 (dd, *J* = 10.3, 5.5 Hz, 2H), 1.52 (m 2H), 0.80 (t, *J* = 7.4 Hz, 1H). ¹³C NMR (101 MHz, CDCl₃) δ 173.51, 139.80, 135.89, 130.97, 128.45, 127.17, 125.77, 67.35, 36.71, 29.27, 26.04, 18.69, 17.82, 13.60.



240ba+240'ba (2:1), 71%. ¹H NMR (401 MHz, CDCl₃) δ 7.38 – 7.34 (m, 1H), 7.30 (m, 1H), 7.28 – 7.26 (m, 1H), 7.25 – 7.19 (m, 2H), 6.42 (dd, *J* = 5.7, 2.4 Hz, 0.6H, **240ba**), 6.11 – 6.07 (m, 0.6H, **240'ba**), 6.02 (s, 0.6H, **240ba**), 2.41 – 2.32 (m, 1H), 2.20 (m, 1H), 2.14 – 2.08 (m, 1H), 2.01 (m, 2H), 1.57 (m, 2H), 1.53 – 1.45 (m, 1H), 1.43 – 1.38 (m, 1H), 0.96 – 0.89 (m, 10H), 0.85 (dd, *J* = 9.3, 5.5 Hz, 2H). ¹³C NMR (101 MHz, CDCl₃) δ 173.54 (**240ca**), 139.60, 139.32, 138.23, 134.65, 131.49, 130.13, 128.53, 128.51, 128.22, 128.17, 127.26, 126.86, 126.13, 125.61, 71.12, 68.23, 42.99, 38.18, 36.82, 36.59, 32.38, 31.83, 31.03, 30.66, 27.94, 27.48, 27.28, 27.21, 18.88, 18.46, 13.65.

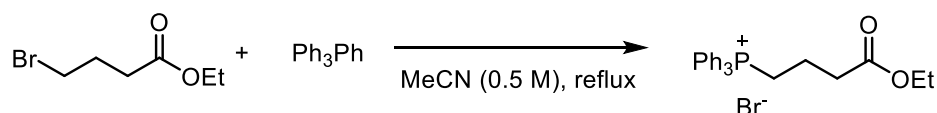


240ca+240'ca (2.4:1), 51%, colorless oil. ¹H NMR (401 MHz, CDCl₃) δ 7.37 – 7.33 (m, 1.5 H), 7.29 (m, 2H), 7.26 – 7.22 (m, 1.5H), 6.36 (dd, *J* = 5.5, 2.4 Hz, 0.8H, **240ca**), 6.11 – 6.08 (m, 0.6H, **240'ca**), 5.97 (d, *J* = 2.0 Hz, 0.8H, **240ca**), 2.39 (dt, *J* = 18.2, 5.0 Hz, 1H), 2.18 (td, *J* = 7.3, 2.6 Hz, 1H), 2.06 (dd, *J* = 14.0, 7.3 Hz, 1H), 2.01 – 1.96 (m, 1H), 1.83 (dd, *J* = 18.3, 10.5 Hz, 1H), 1.61 – 1.50 (m, 3H), 1.41 (dd, *J* = 14.8, 7.4 Hz, 1H), 1.03 (dd, *J* = 6.2, 4.4 Hz, 2H), 0.81 (t, *J* = 7.4 Hz, 2H), 0.76 (t, *J* = 7.4 Hz, 1H). ¹³C NMR (101 MHz, CDCl₃) δ 173.51 (**240ca**), 139.50, 135.04, 130.89, 129.70, 128.50, 128.25, 127.25, 126.93, 126.13, 125.72, 69.76, 67.87, 37.62, 37.58, 36.75, 36.59, 34.84, 34.38, 27.98, 23.58, 21.70, 21.53, 18.73, 18.51, 13.64, 13.56.

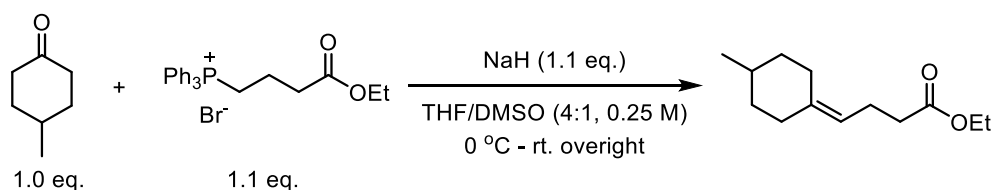


240da, 43%. *c*Hex:EtOAc: 100:1. $^1\text{H NMR}$ (401 MHz, CDCl_3) δ 7.29 (brs, 2H), 7.28 (brs, 2H), 7.22 (m, 1H), 6.14 (dd, $J = 5.8, 2.4$ Hz, 1H), 6.05 (t, $J = 5.6$ Hz, 1H), 2.17 – 2.11 (m, 1H), 2.10 – 2.06 (m, 2H), 2.05 – 1.99 (m, 1H), 1.95 (dd, $J = 13.4, 6.0$ Hz, 1H), 1.64 (dd, $J = 13.4, 6.7$ Hz, 1H), 1.48 – 1.41 (m, 2H), 1.05 (s, 3H), 1.04 (s, 3H), 0.77 (t, $J = 7.4$ Hz, 3H). $^{13}\text{C NMR}$ (101 MHz, CDCl_3) δ 173.60, 139.49, 135.76, 129.16, 128.34, 127.05, 126.02, 68.22, 41.89, 39.99, 36.65, 30.14, 29.63, 27.87, 18.54, 13.64.

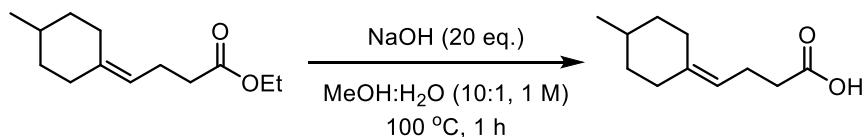
Preparation of acid **241**³⁵



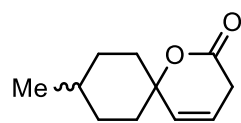
Under N_2 , to a 100 ml Schlenk tube was charged with stirring bar, ACN (25 ml), Ph_3P (3.14 g, 12 mmol, 1.0 eq.) and ethyl 4-bromobutanoate (2.34 g, 12 mmol, 1.0 eq.). Then reaction was refluxed for 5 days. NMR showed the reaction completed more than 93% (No H_2O in spectrum). Then ACN was removed under vacuum and the solid was dried under vacuum for 5 hrs. Used in next step directly.



Under N_2 , to a dry Schlenk tube was charged with stirring bar, THF (7ml), DMSO (1 ml) and (4-ethoxy-4-oxobutyl)triphenylphosphonium bromide (1.0 g, 2.2 mol, 1.1eq.). Then at 0 °C, NaH (88 mg, 2.2 mol, 1.1 eq., wt 60%) was added and the solution turned yellow. After stirred for 1 h, ketone or aldehyde (2.0 mol, 1.0 eq.) solution (in 1 ml THF) was added dropwise. Then the reaction was warmed to room temp and stirred overnight. TLC (R_f of starting material and product may be same) showed the reaction completed. Then 10 ml H_2O was added and the mixture was extracted with EA (2×15 ml). The organic layer was dried over Na_2SO_4 , concentrated under vacuum and purified with silica gel chromatography, Cy:EA (100:2).



To a Schlenk tube was charged with stirring bar, MeOH (9 ml), H_2O (1 ml), $\text{Na}(\text{OH})_2$ (800 mg, 20 mmol, 20.0 eq.), and ester (1.0 mmol, 1.0 eq.). The reaction was refluxed for 1 hr. TLC (Cy:EA = 2:1) showed the reaction complete. Then MeOH was removed under vacuum (if the water was also removed under vacuum, added NaOH (4N) solution 10 ml) and Et_2O (2×10 ml) was used to extract the impurity (Ph_3P and so on). Then HCl (2N) was added to acidify the solution. EA (2×15 ml) was used to extract the product. The organic layer was combined and dried over Na_2SO_4 , concentrated. The residue was purified with smallest column (Cy:EA = 6:1), the product comes down soon.

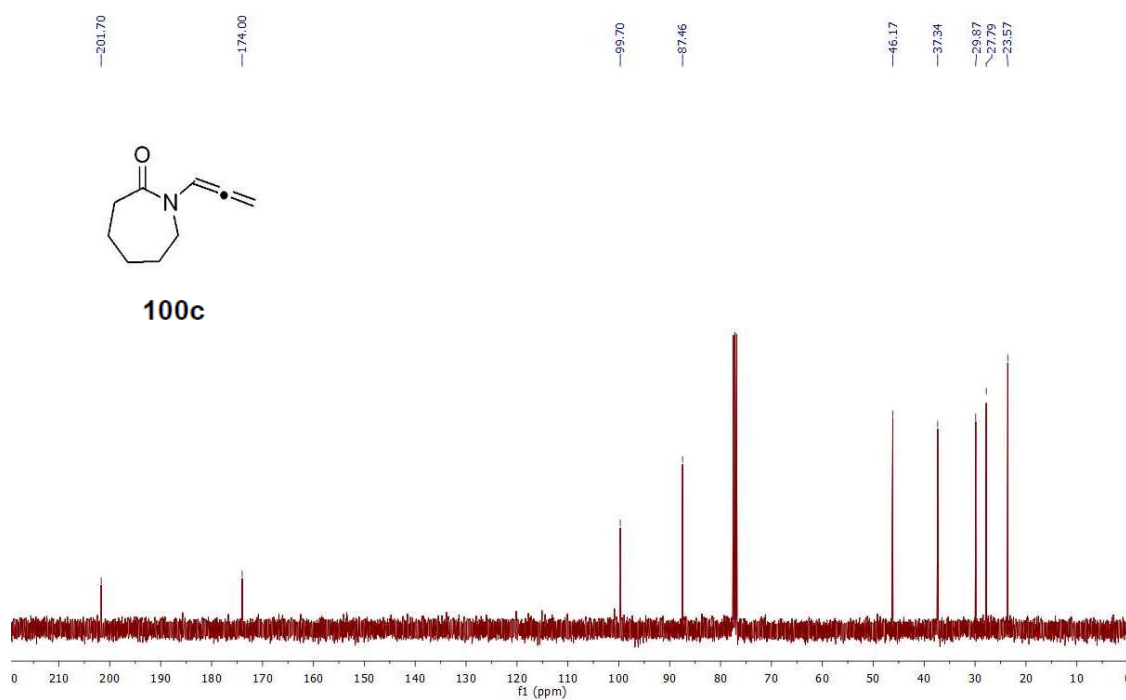
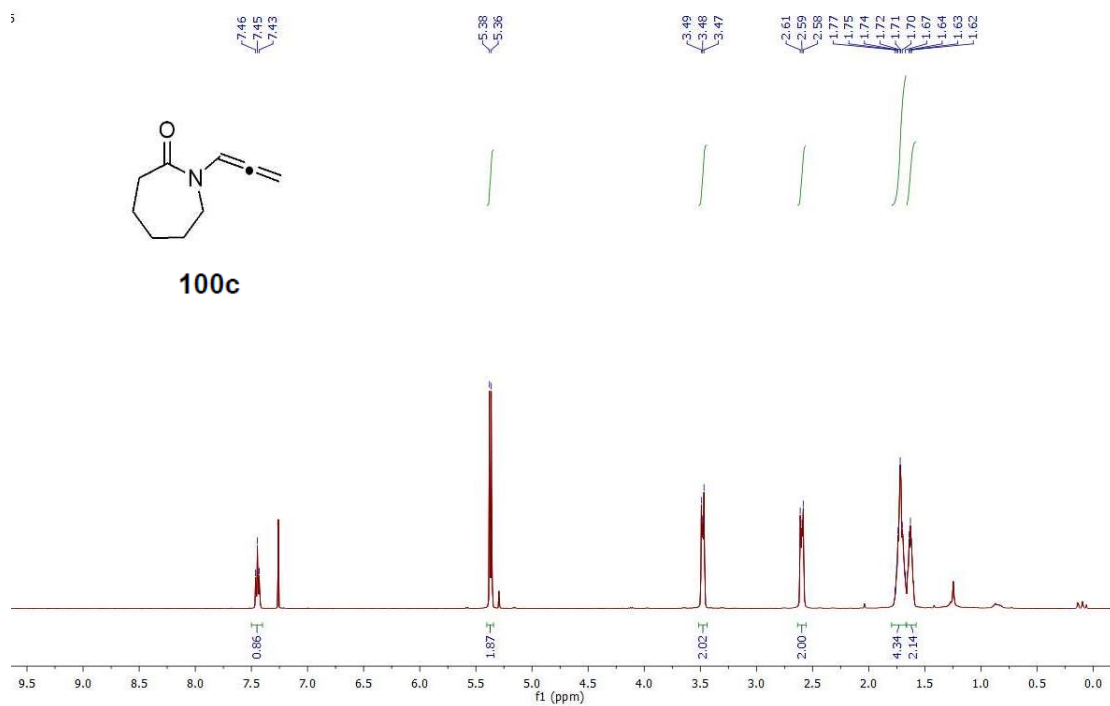


242, 30%, colorless oil. $^1\text{H NMR}$ (401 MHz, CDCl_3) δ 5.75 (brs, 1H), 4.85 (t, $J = 7.5$ Hz, 1H), 2.58 – 2.52 (m, 2H), 2.30 (m, 1H), 2.07 (m, 4H), 1.76 (m, 1H), 1.65 (m, 2H), 1.25 (m, 1H), 0.96 (dd, $J = 6.2, 2.3$ Hz, 3H). $^{13}\text{C NMR}$ (101 MHz, CDCl_3) δ 177.40, 177.34, 134.64, 134.62, 125.58, 124.33, 84.01, 83.67, 33.62, 33.42, 30.59, 30.51, 29.15, 28.93, 28.53, 28.33, 26.90, 26.78, 23.58, 23.43, 21.79, 21.65.

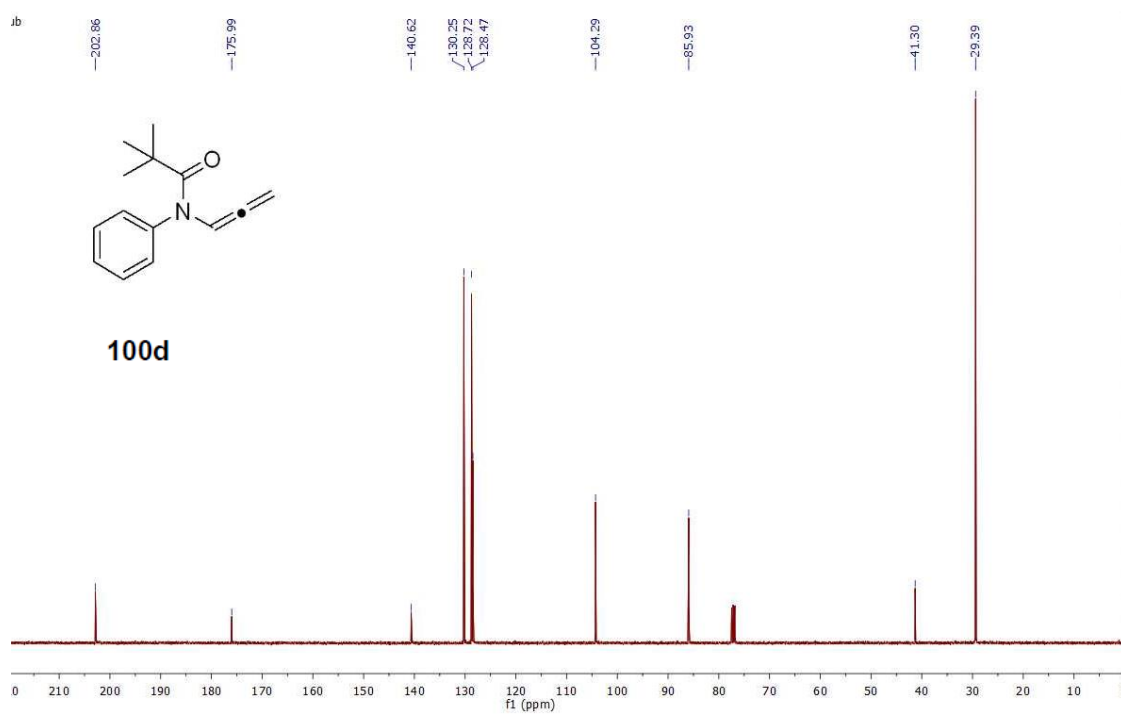
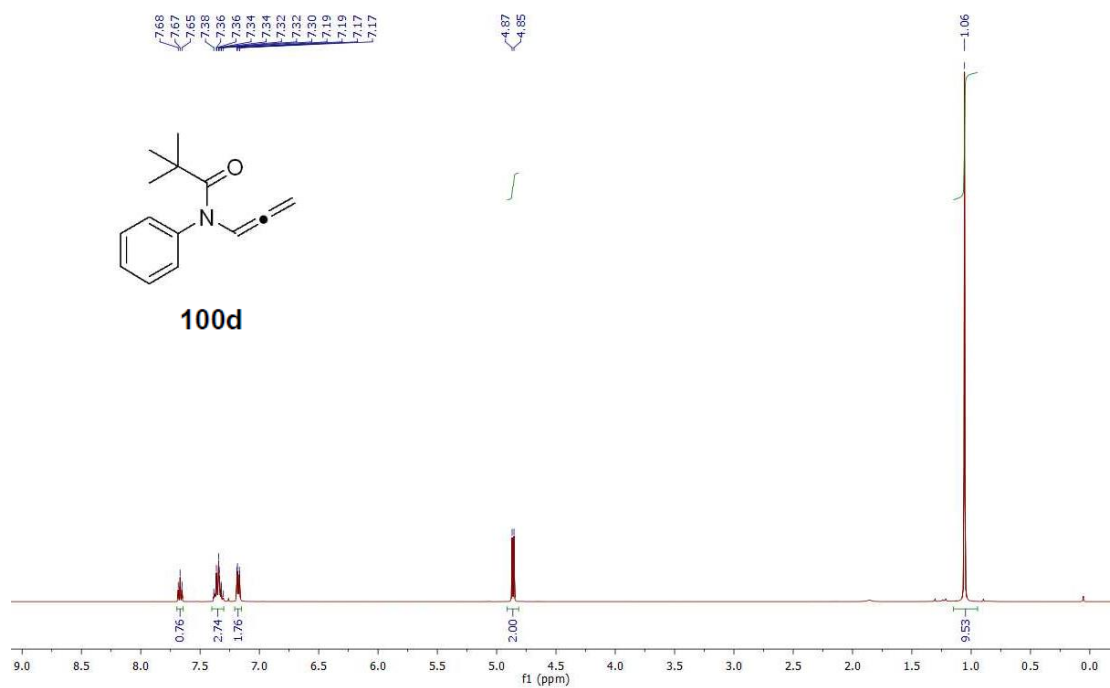
Reference

- ¹ L.-L. Wei, J. A. Mulder, H. Xiong, C. A. Zifcick, C. J. Douglas, R. P. Hsung, *Tetrahedron*, **2001**, *57*, 459 – 466.
- ² I. Fenandez, M. I. Monterde, J. Plumet, *Tetrahedron Lett.* **2005**, *46*, 6029 – 6031.
- ³ S. Oishi, K. Hatano, A. Tsubouchi and T. Takeda, *Chem. Commun.* **2011**, *47*, 11639 – 11640.
- ⁴ M. Nillson Bjoern, M. Vargas Hugo, Ringdahl Bjoern, Hacksell Uli, *J. of Med. Chem.* **1992**, *35*, 285 – 294.
- ⁵ M. K. Smith, B. H. Northrop, *Chem. Mater.* **2014**, *26*, 3781 – 3795.
- ⁶ Characterization of **1a** give similar data with literature: L. Rout, A. M. Harned, *Chem. Eur. J.* **2009**, *15*, 12926 – 12928.
- ⁷ B. Patzke, A. Stanger, *Organometallics*, **1996**, *15*, 2633 – 2639.
- ⁸ *SMART & SAINT Software Reference Manuals*, version 5.051 (Windows NT Version), Bruker Analytical X-ray Instruments Inc.: Madison, Wi, **1998**.
- ⁹ G. M. Sheldrick, *SADABS, program for empirical absorption correction*, University of Göttingen, Germany, **1996**.
- ¹⁰ A. Altomare, M.C. Burla, M. Camalli, G.L. Cascarano, C. Giacovazzo, A. Guagliardi, A.G.G. Moliterni, G. Polidori, R. Spagna, *J. Appl. Cryst.*, **1999**, *32*, 115 – 119.
- ¹¹ G.M. Sheldrick, *SHELXTL plus (Windows NT Version) Structure Determination Package*, Version 5.1. Bruker Analytical X-ray Instruments Inc.: Madison, WI, USA, **1998**.
- ¹² M. Mestri, M. Graetzel, *Ber. Bunsenges. Phys., Chem.* **1977**, *81*, 504-507.
- ¹³ S. Zhou, H. Liao, M. Liu, G. Feng, Fu, L. Baolin, M. Cheng, Y. Zhao, P. Gong, *Bioorg. Med. Chem.*, **2014**, *22*, 6438-6452.
- ¹⁴ D. Yadav, N. Singh, T. Kim, K. Wu, Y. Jae N.-J. Park, J.-O. Baeg, *Green Chem.*, **2019**, *21*, 2677-2685
- ¹⁵ F. Zhao, Z. Chen, K. Xie, R. Yang, Y.-B. Jiang, *Chin. Chem. Lett.*, **2016**, *27*, 109-113.
- ¹⁶ M. Hu, J. Li, S.Q. Yao, *Org. Lett.*, **2008**, *10*, 5529-5531.
- ¹⁷ D. Schweinfurth, K.I. Hardcastle, U.H.F. Bunz, *Chem. Commun.*, **2008**, 2203-2205.
- ¹⁸ F. Sebest, L. Casarrubios, H.S. Rzepa, A.J.P. White, S. Diez-González, *Green Chem.*, **2018**, *20*, 4023-4035.
- ¹⁹ H.C. Bertrand, M. Schaap, L. Baird, N.D. Georgakopoulos, A. Fowkes, C. Thiollier, H. Kachi, A.T. Dinkova-Kostova, G. Wells, *J. Med. Chem.*, **2015**, *58*, 7186-7194.
- ²⁰ D. Al-Smadi, T.R. Enugala, T. Norberg, J. Kihlberg, M. Widersten *Synlett*, **2018**, *29*, 1187-1190.
- ²¹ M. Ezawa, H. Togo, *Eur. J. Org. Chem.*, **2017**, 2379-2384.
- ²² H. Ji, H. Li, P.Martasek, L.J. Roman, T.L. Poulos, R.B. Silverman, *J. Med. Chem.*, **2009**, *52*, 779-797.
- ²³ B.M. Ruff, S.E. O'Connor, *Tetrahedron Lett.*, **2012**, *53*, 1071-1074.
- ²⁴ E. Reimann, C. Ettmayr, *Monatshefte für Chemie*, **2004**, *135*, 1289-1295.
- ²⁵ M. Rohmann, *Archiv der Pharmazie*, **1961**, *294*, 538-549.
- ²⁶ J.-C.; Xu, H.; Yu, F.; Zhang, F. *Tetrahedron Lett.* **2017**, *58*, 674-678.
- ²⁷ J. Wu, X. Chen, Y. Xie, Y. Guo, Q. Zhang, G.-J. Deng, *J. Org. Chem.* **2017**, *82*, 5743-5750.
- ²⁸ Y. Gao, C. Hu, J.-P.Wana, C. Wen, *Tetrahedron Lett.* **2016**, *57*, 4854-4857.
- ²⁹ X. Li, M. Chen, X. Xie, N. Sun, S. Li, Y. Liu, *Org. Lett.* **2015**, *17*, 2984-2987.
- ³⁰ *SMART & SAINT Software Reference Manuals*, version 5.051 (Windows NT Version), Bruker Analytical X-ray Instruments Inc.: Madison, Wi, **1998**.
- ³¹ G. M. Sheldrick, *SADABS-2008/1 - Bruker AXS Area Detector Scaling and Absorption Correction*, Bruker AXS: Madison, Wisconsin, USA, **2008**.
- ³² M.C. Burla, R. Caliandro, B. Carrozzini, G.L. Cascarano, C. Cuocci, C. Giacovazzo, M. Mallamo, A. Mazzone, G. Polidori, *J. Appl. Cryst.* **2015**, *48*, 306-309.
- ³³ G. M. Sheldrick, *Acta Cryst C* **71**, **2015**, 3-8.
- ³⁴ C. F. Macrae, I. J. Bruno, J. A. Chisholm, P. R. Edgington, P. McCabe, E. Pidcock, L. Rodriguez-Monge, R. Taylor, J. van de Streek, P. A. Wood, *J. Appl. Cryst.*, **2008**, *41*, 466-470
- ³⁵ M. Liu, P. Yang, M. K. Karunananda, Y. Wang, P. Liu, K. M. Engle, *J. Am. Chem. Soc.* **2018**, *140*, 5805-5813.

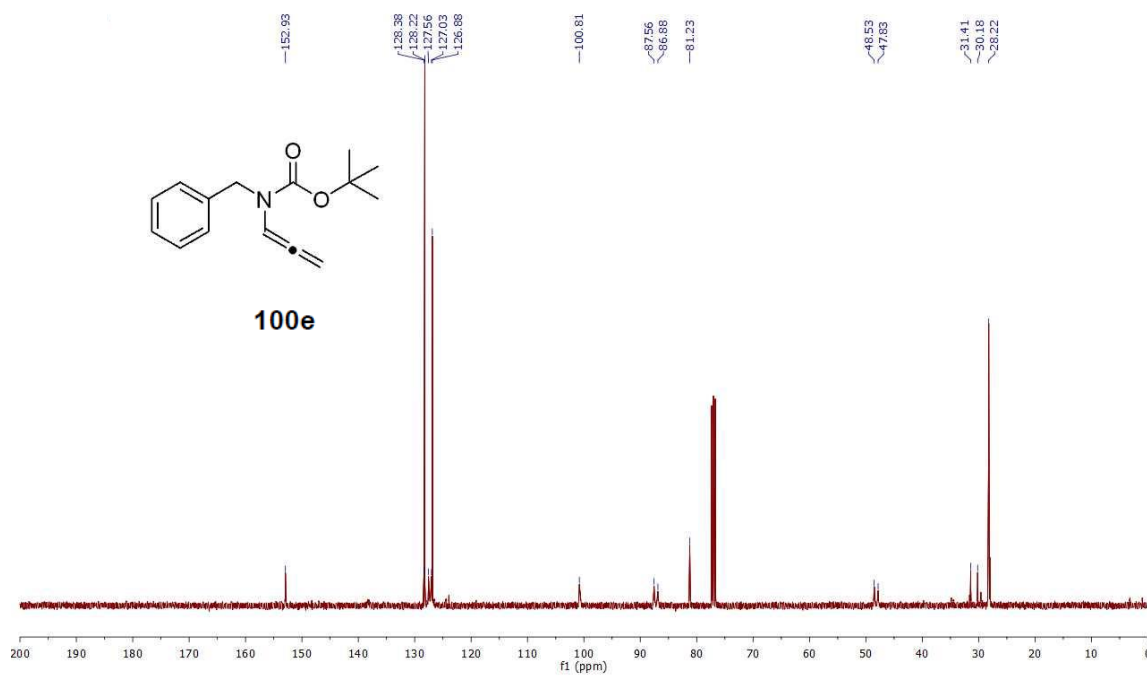
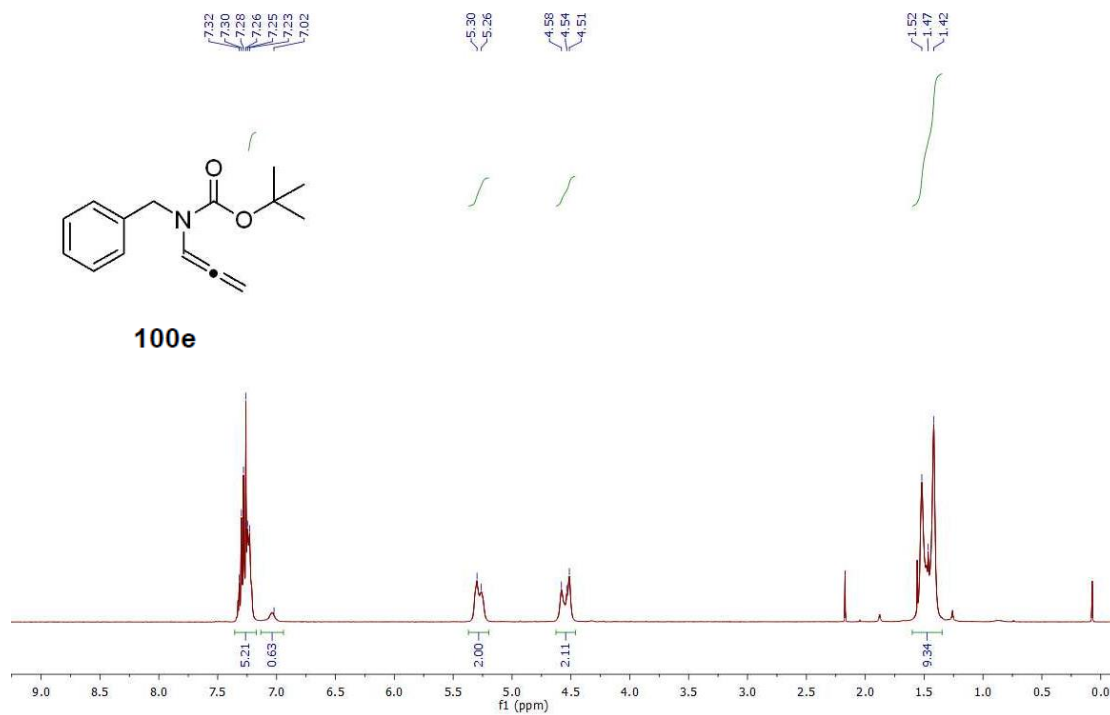
Spectra of Selected Compounds



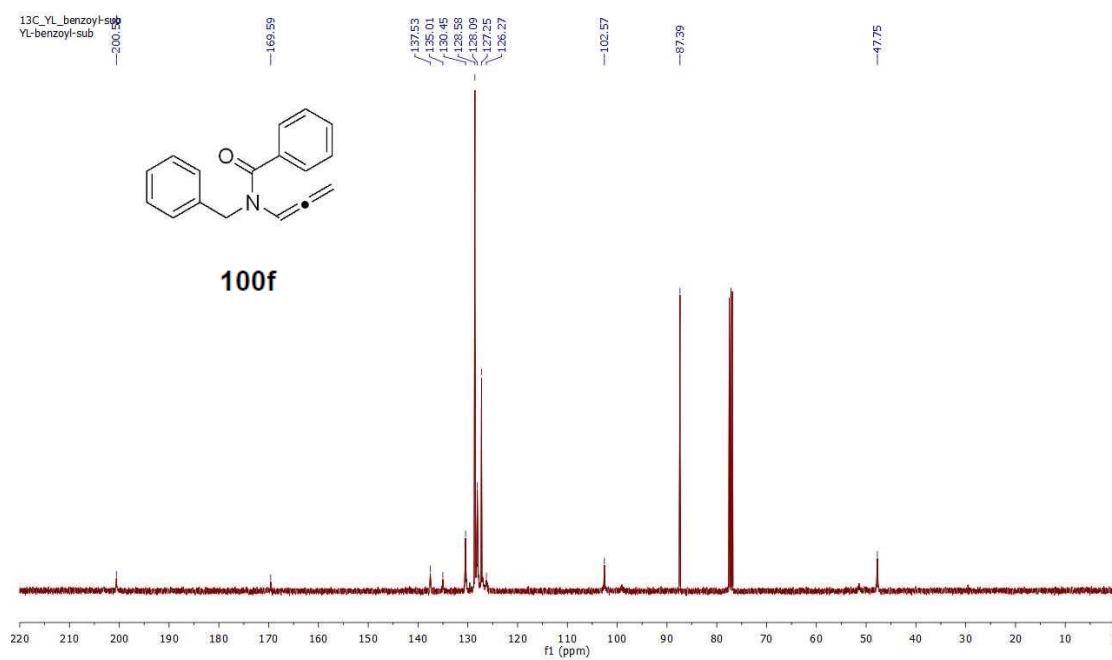
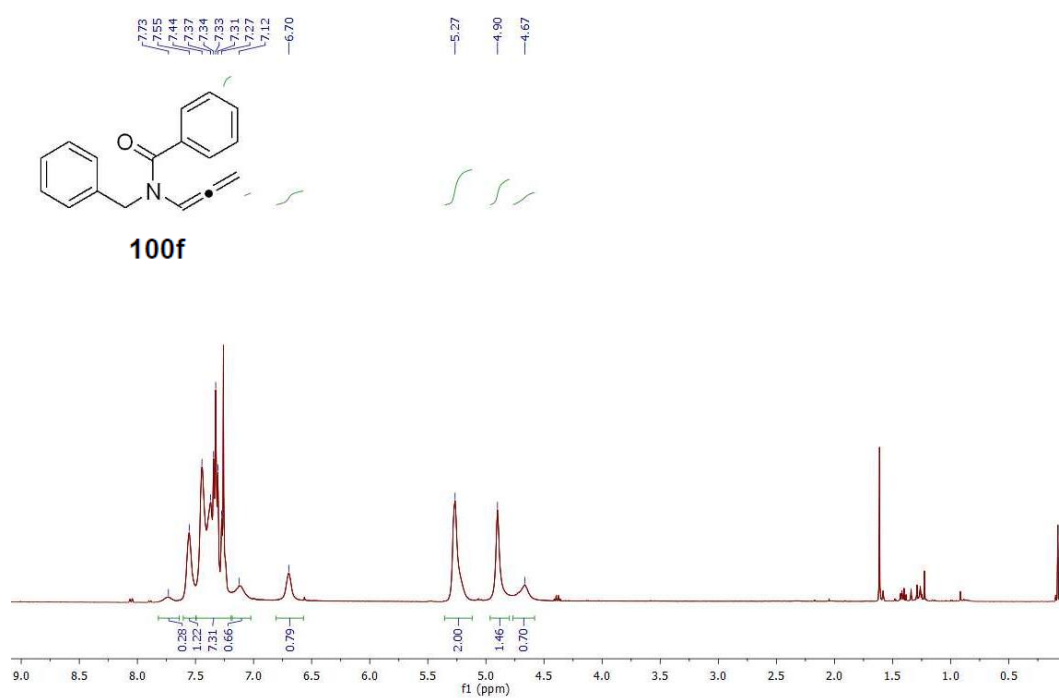
Spectra of Selected Compounds



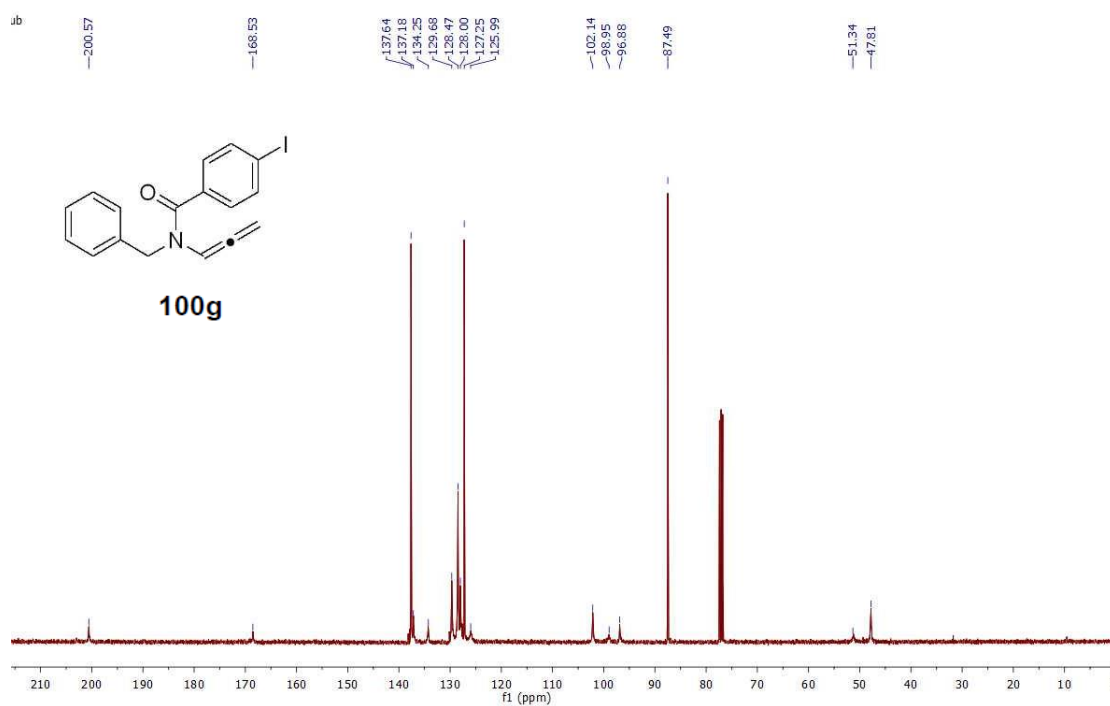
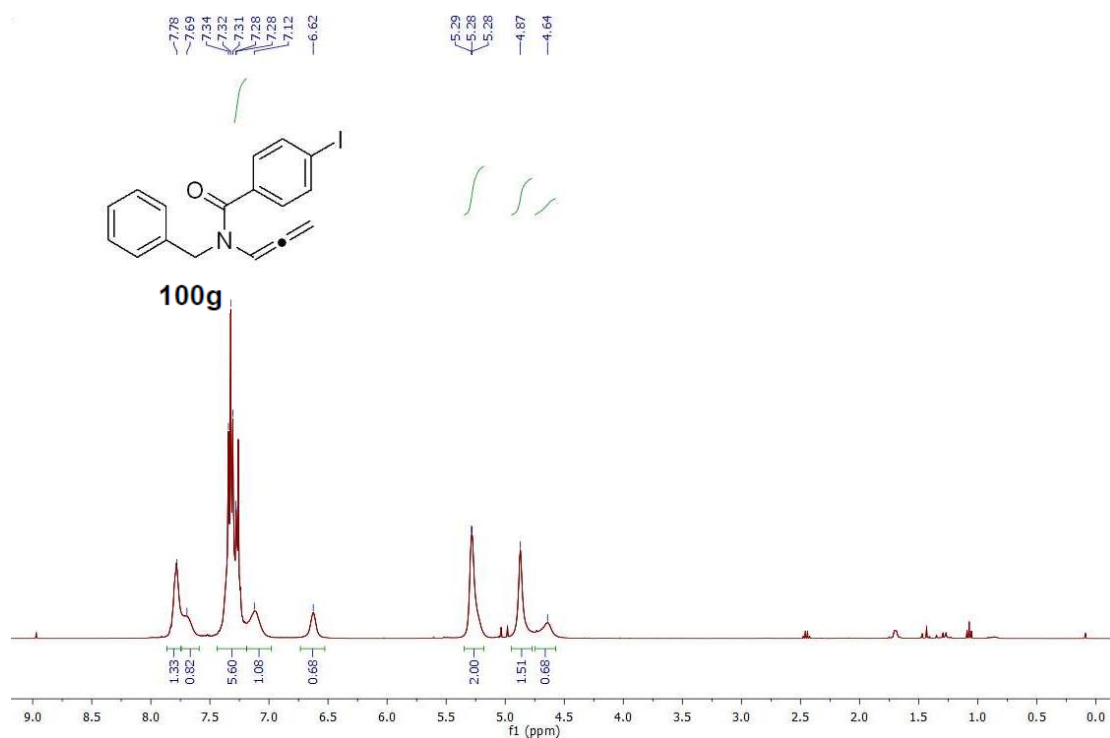
Spectra of Selected Compounds



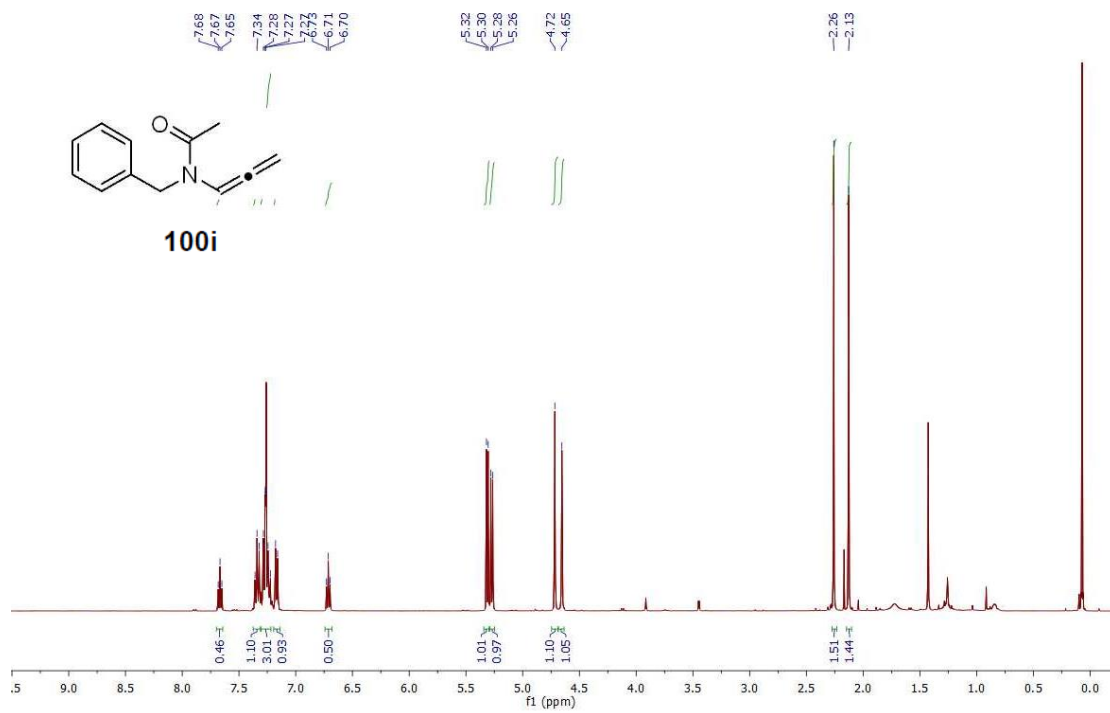
Spectra of Selected Compounds



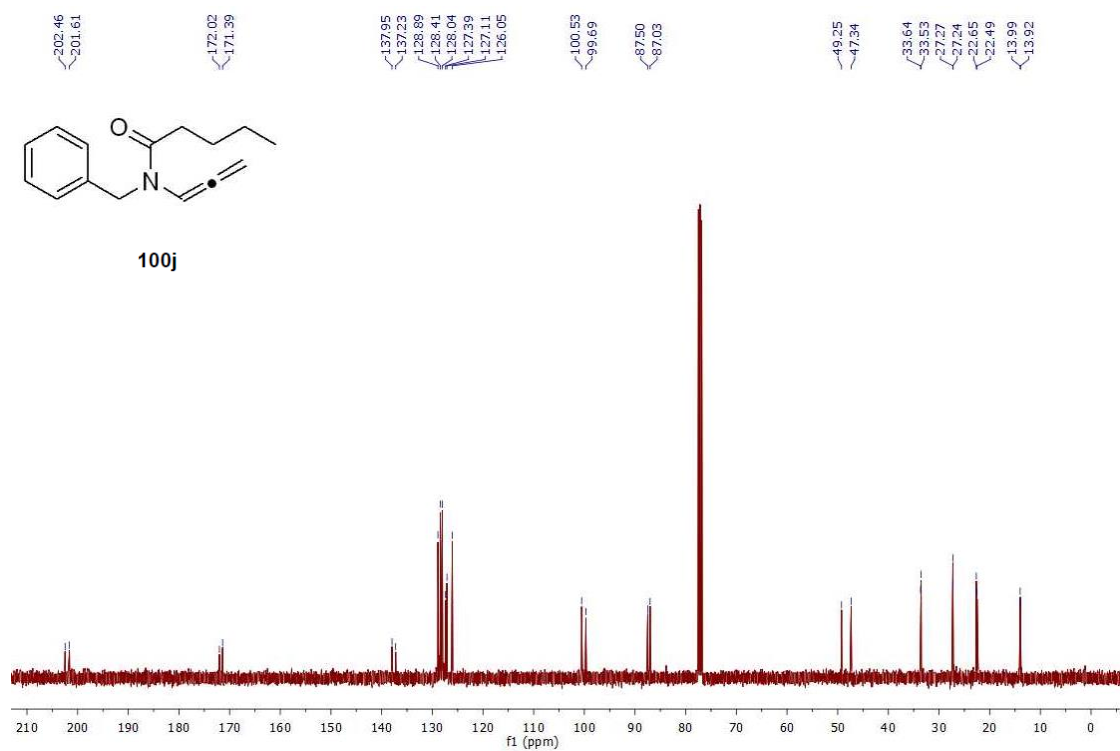
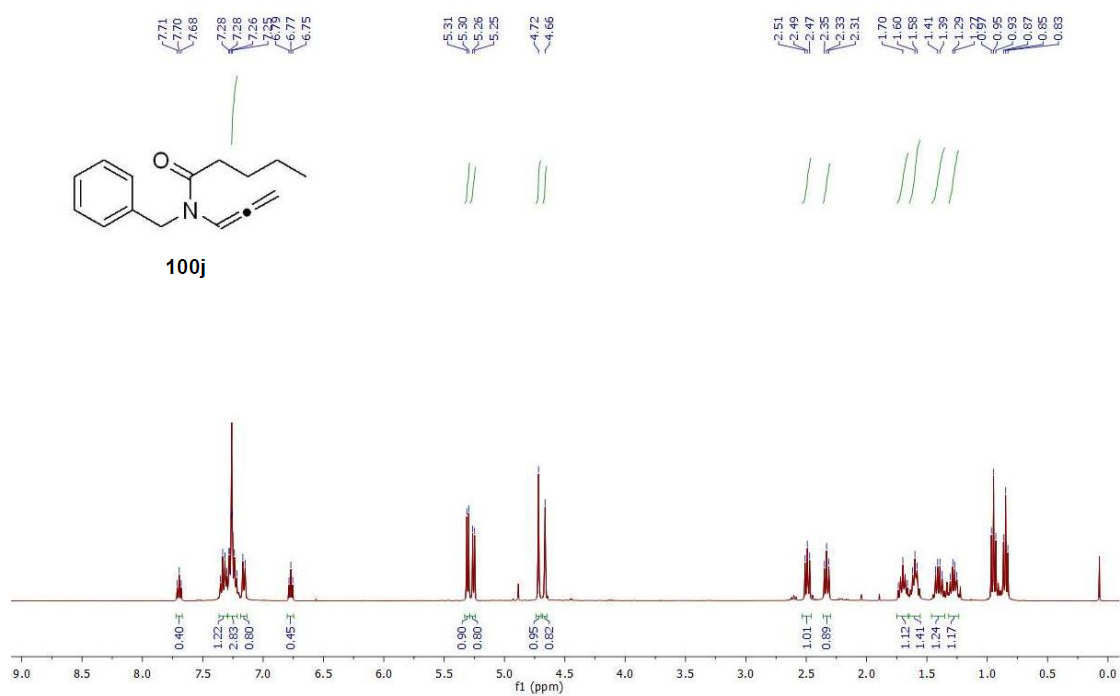
Spectra of Selected Compounds



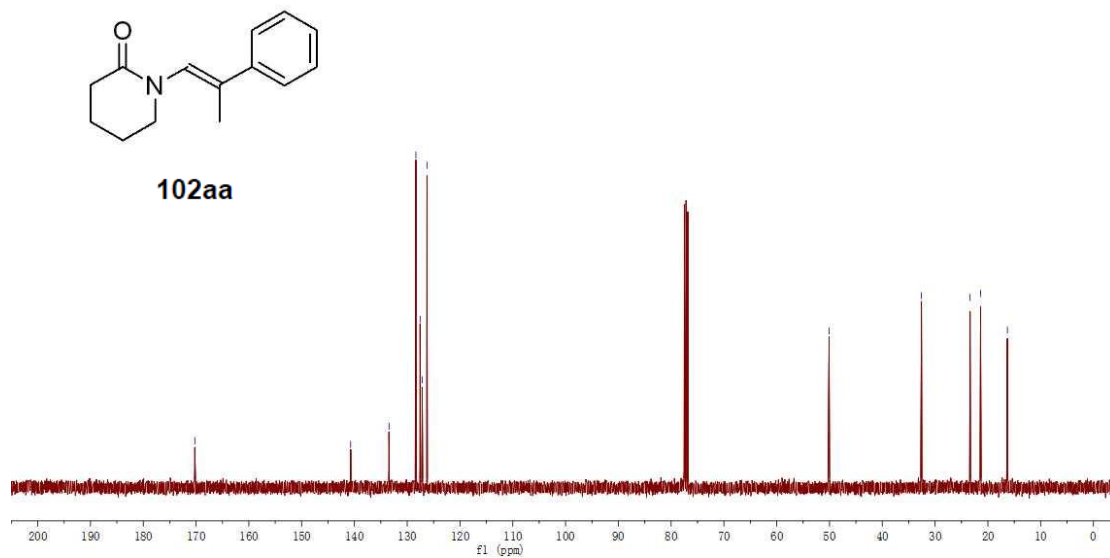
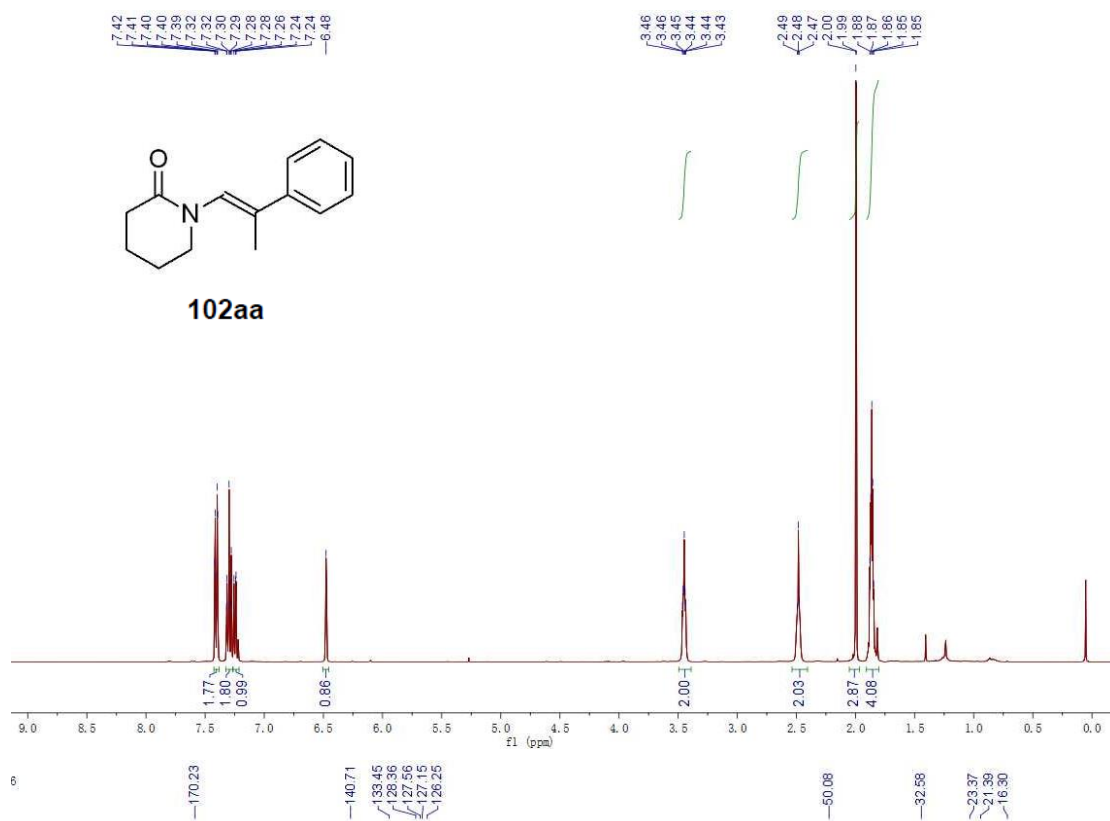
Spectra of Selected Compounds



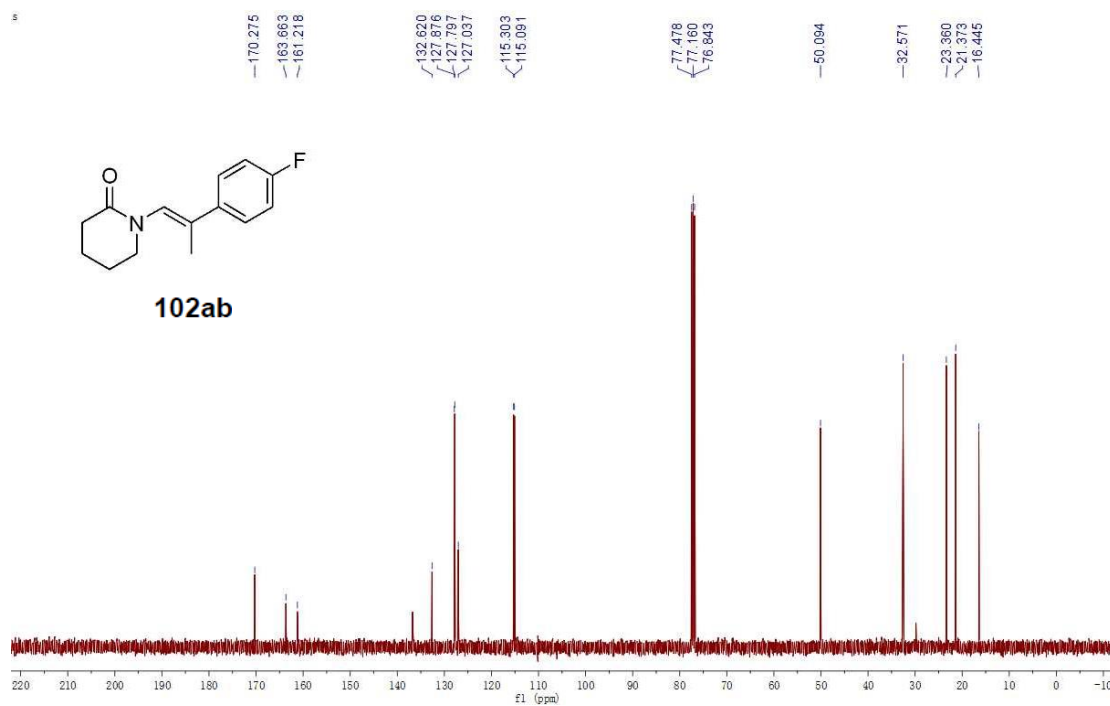
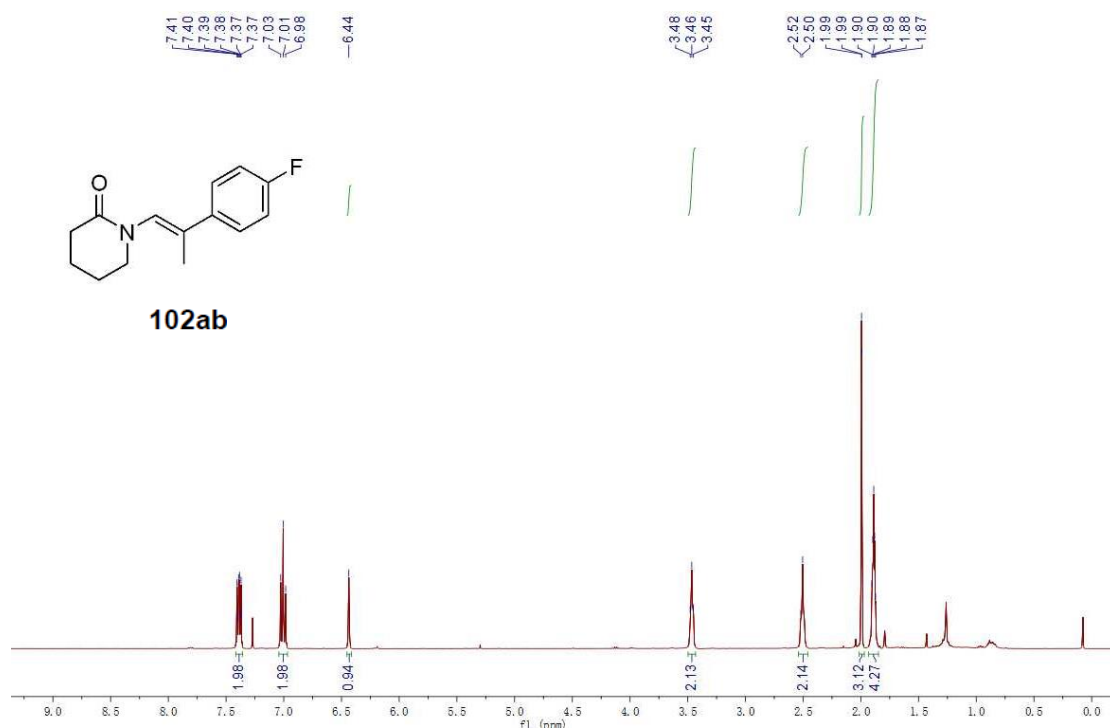
Spectra of Selected Compounds



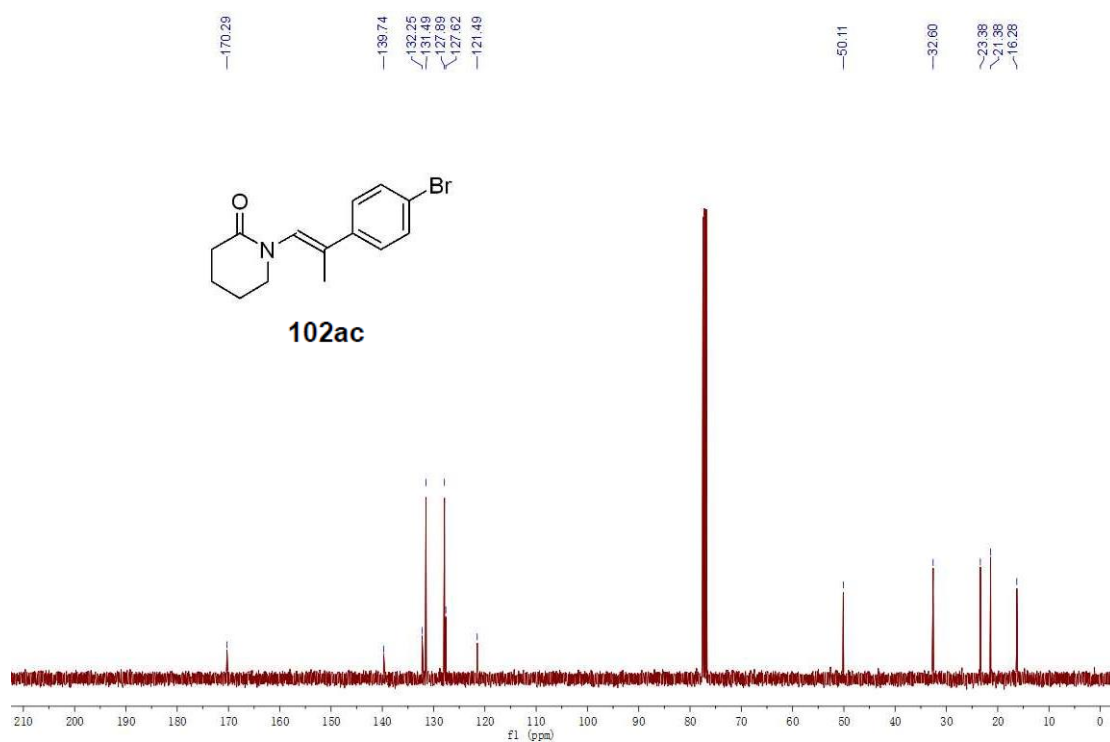
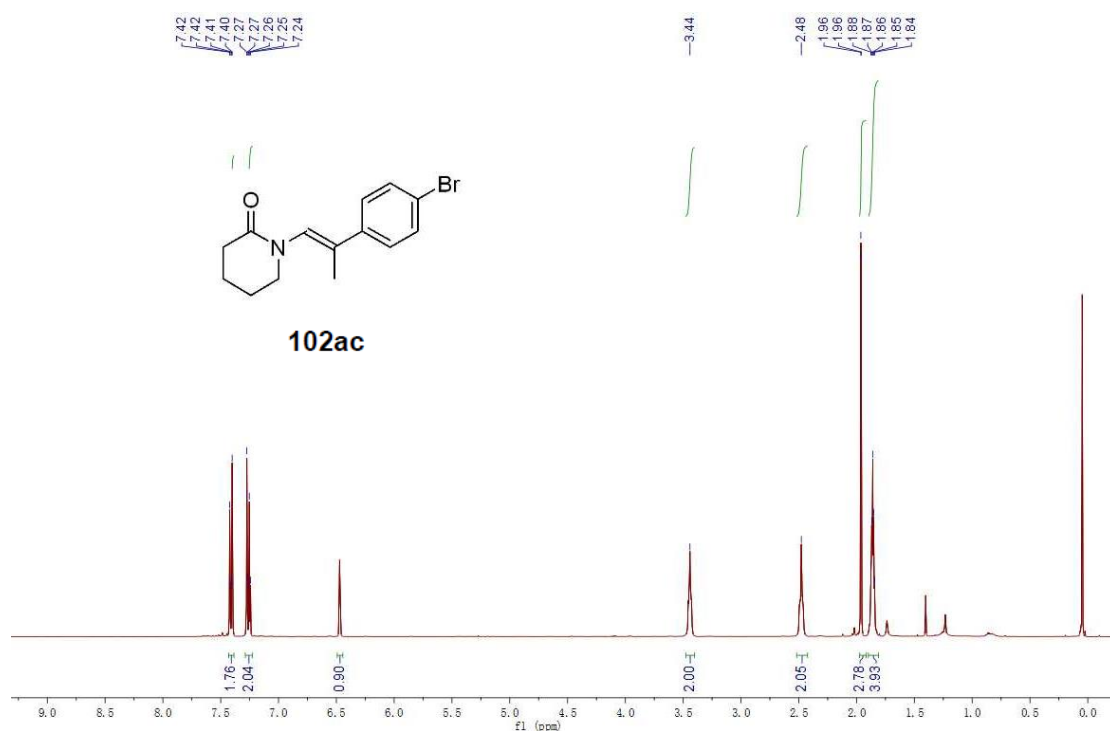
Spectra of Selected Compounds



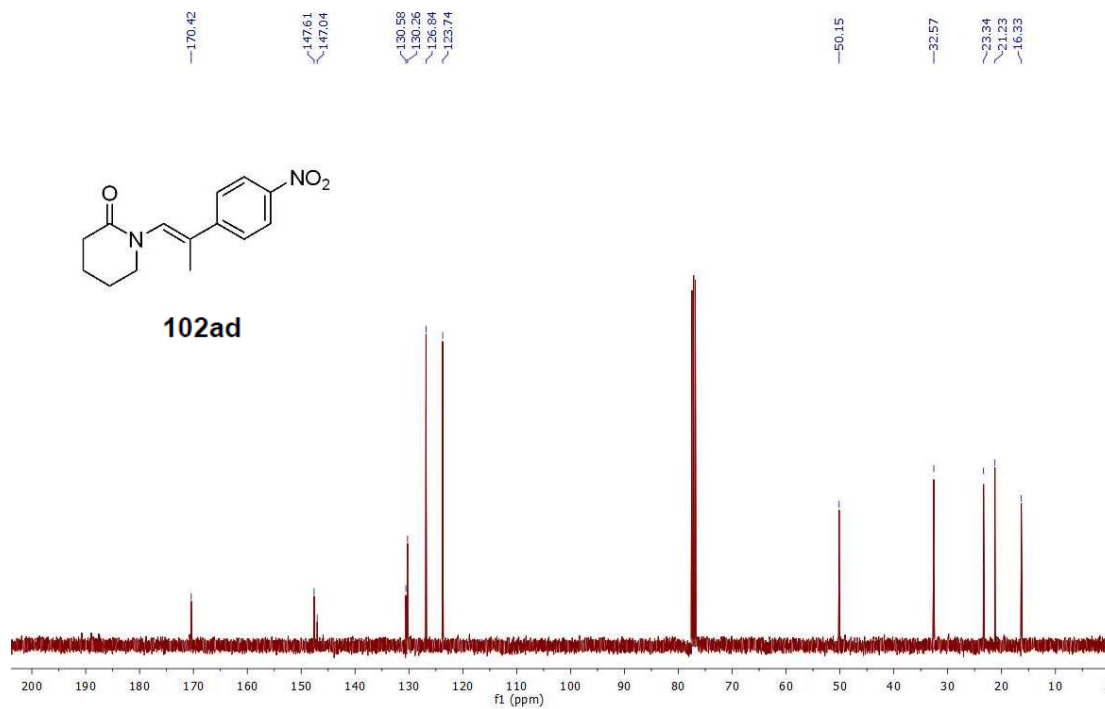
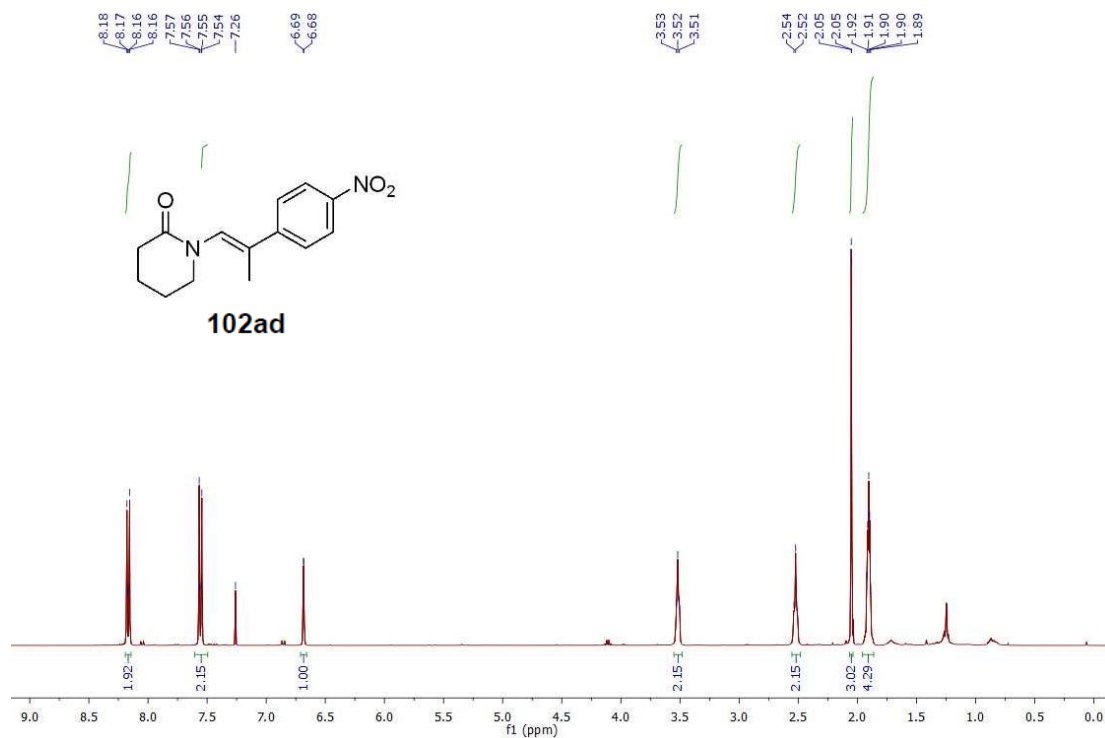
Spectra of Selected Compounds



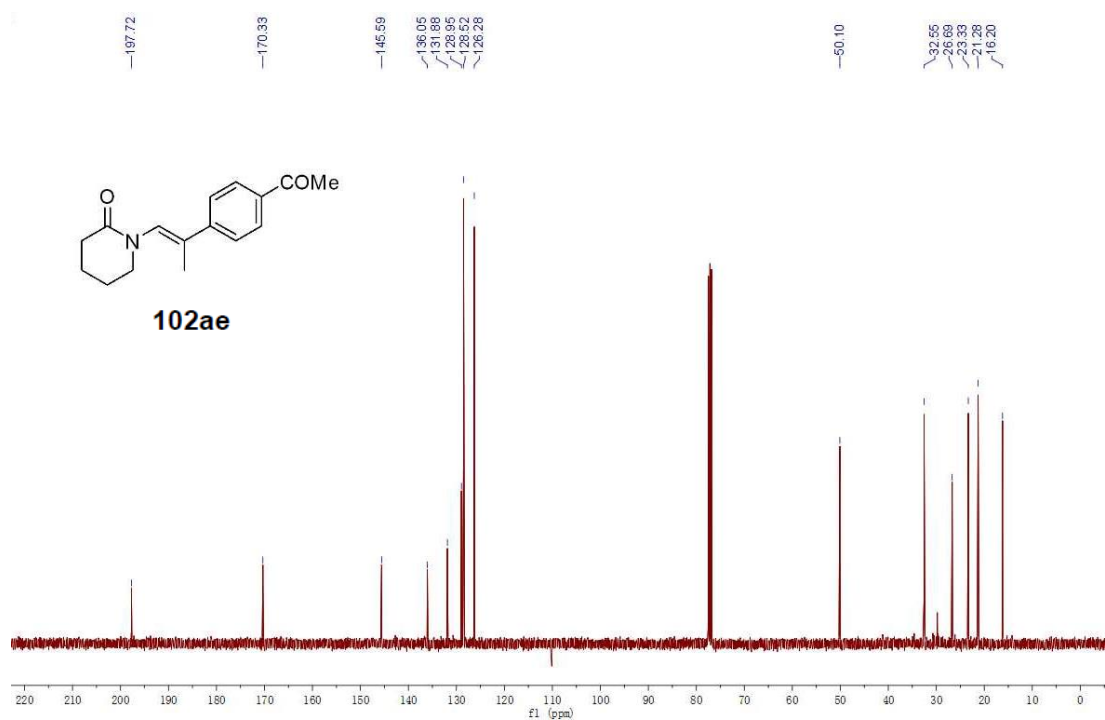
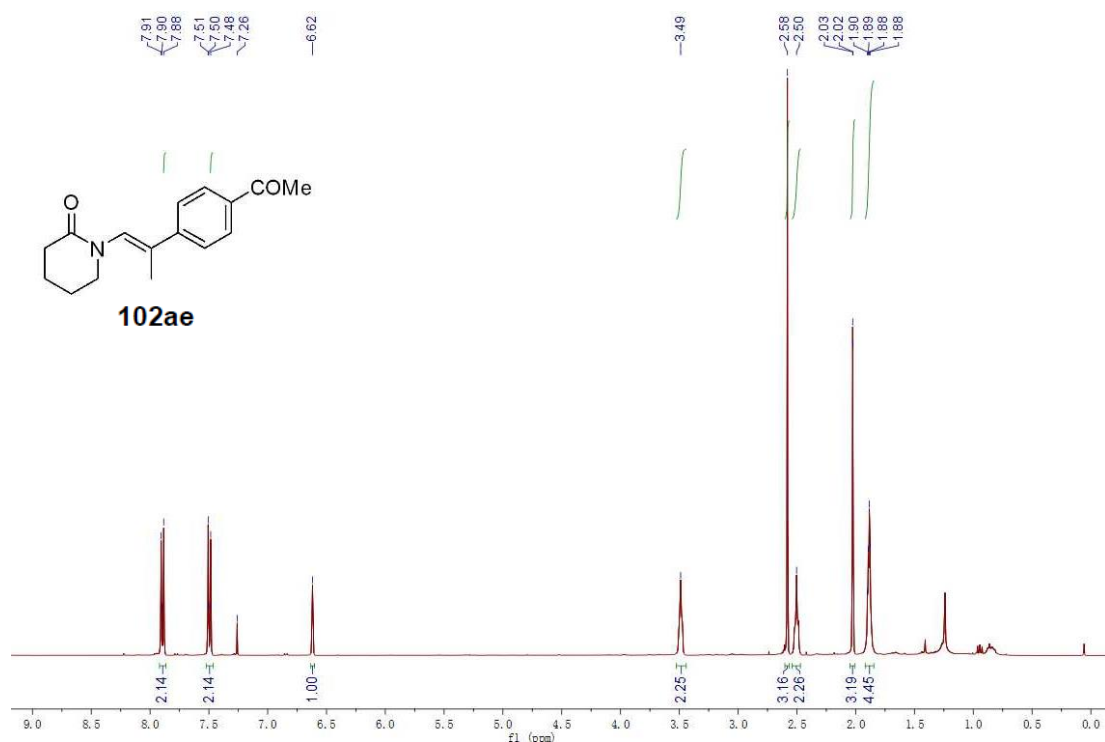
Spectra of Selected Compounds



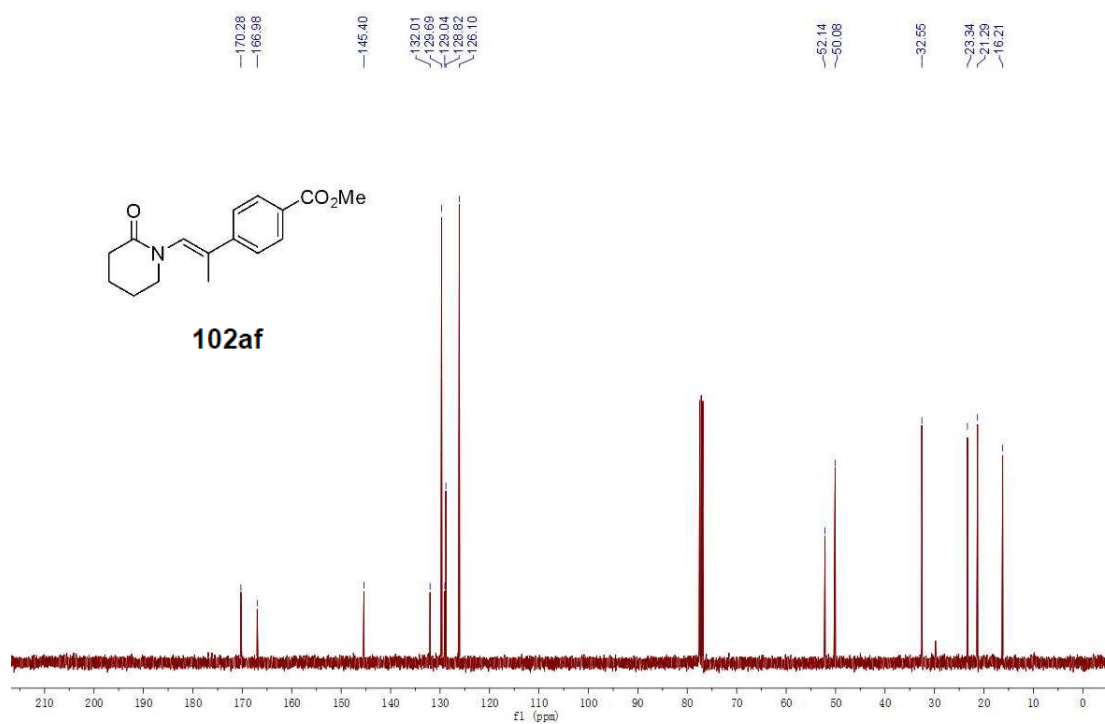
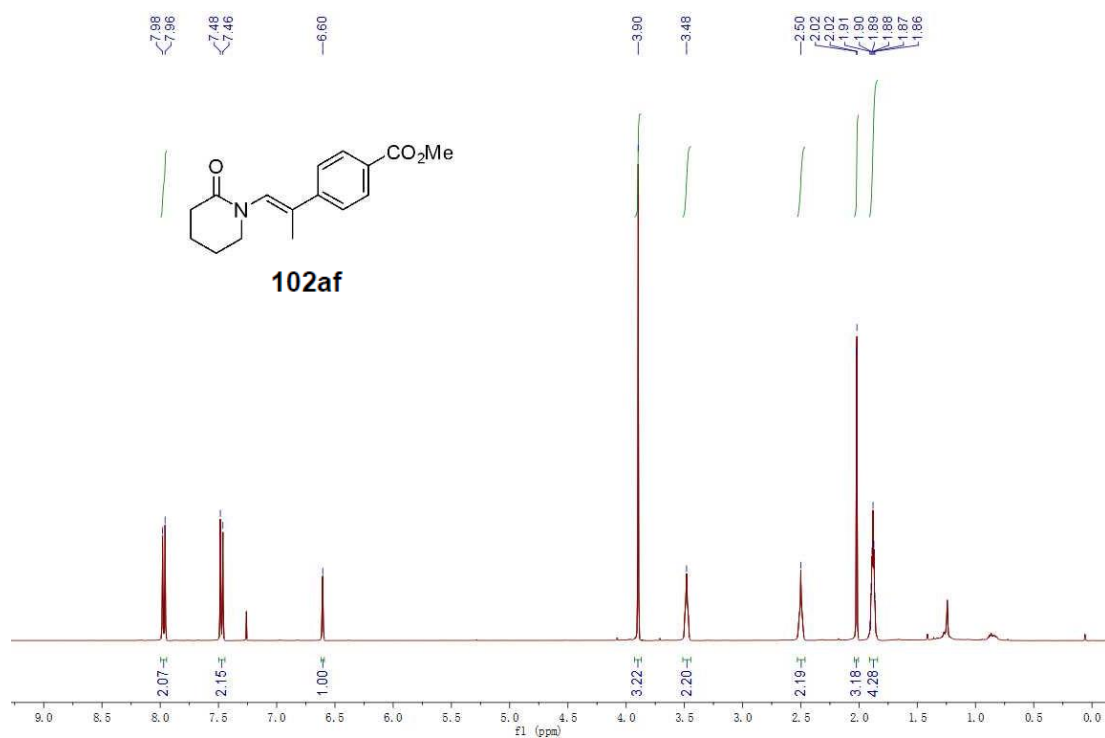
Spectra of Selected Compounds



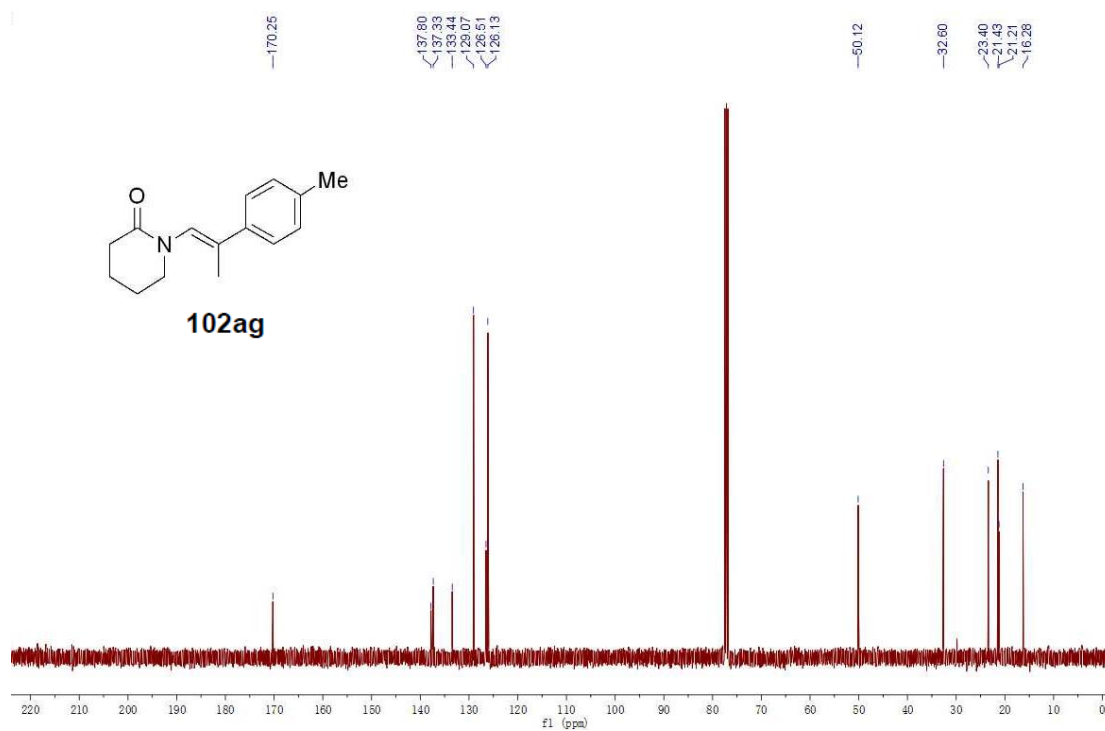
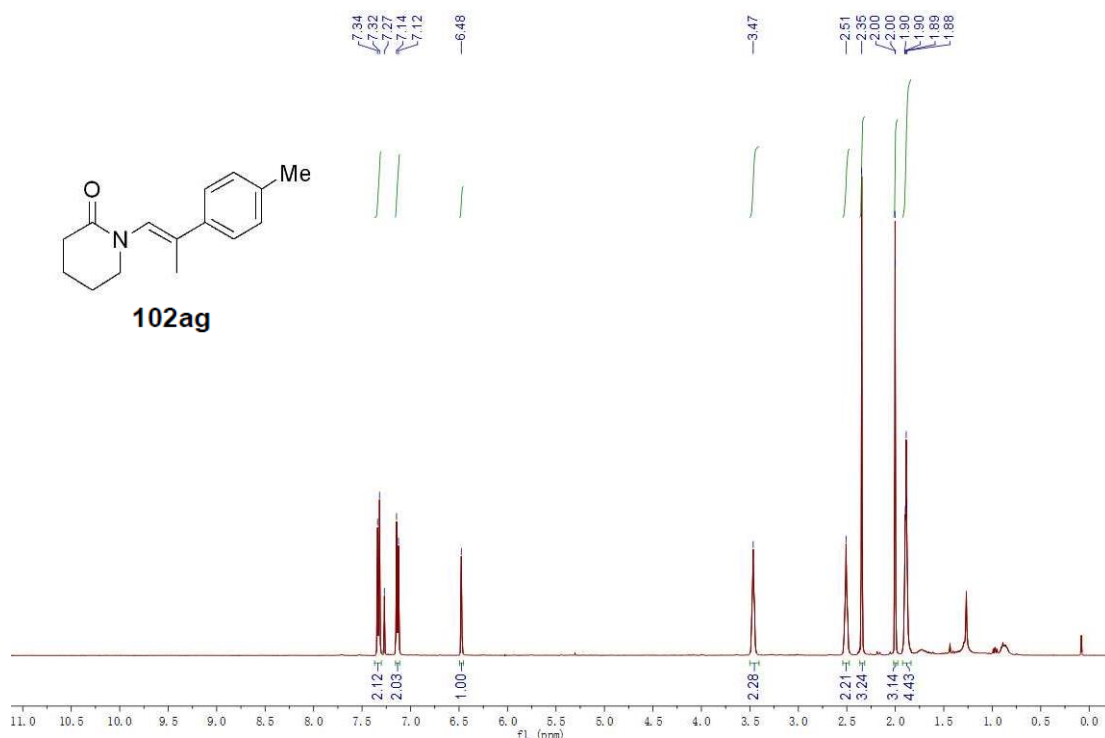
Spectra of Selected Compounds



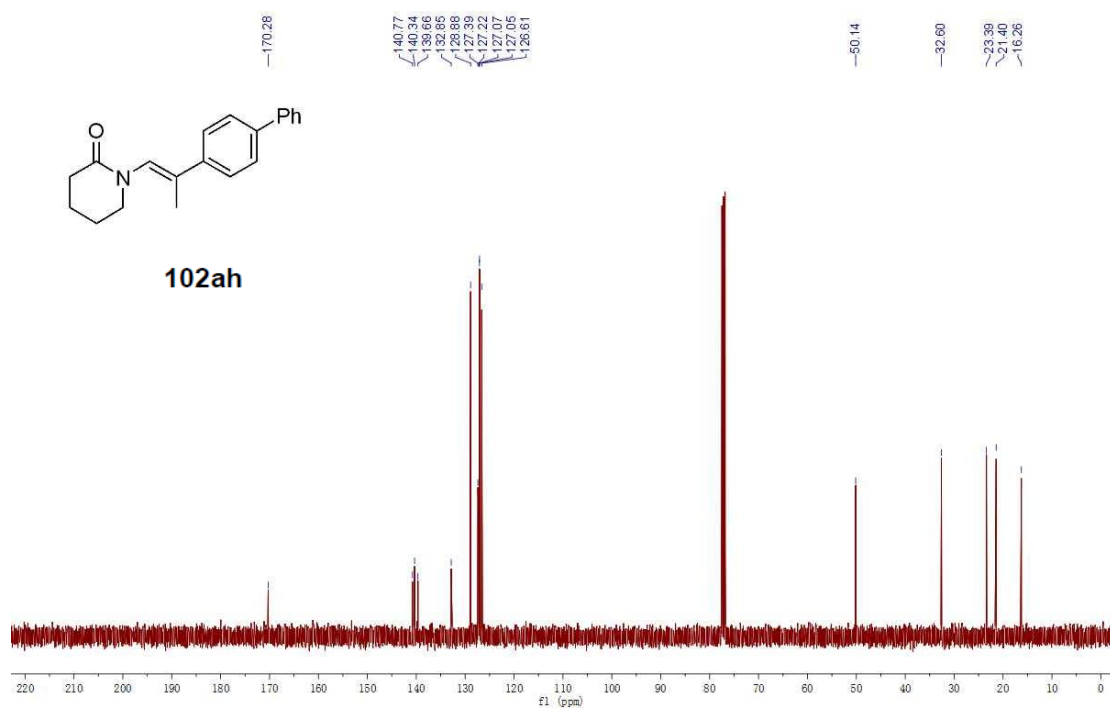
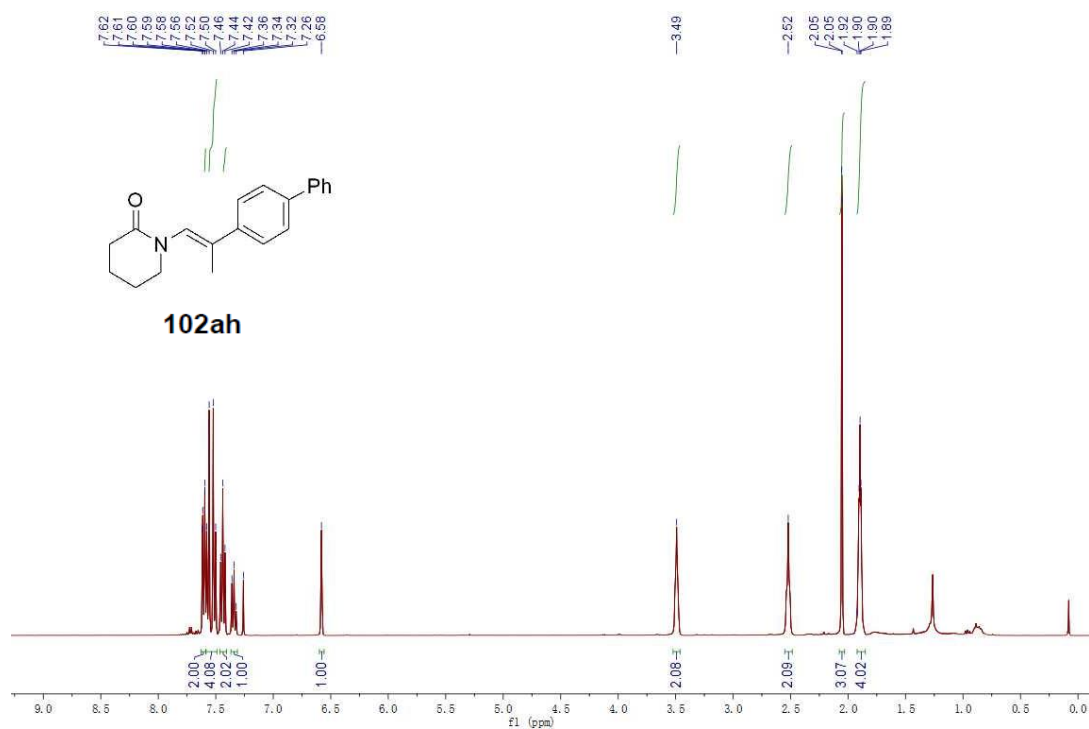
Spectra of Selected Compounds



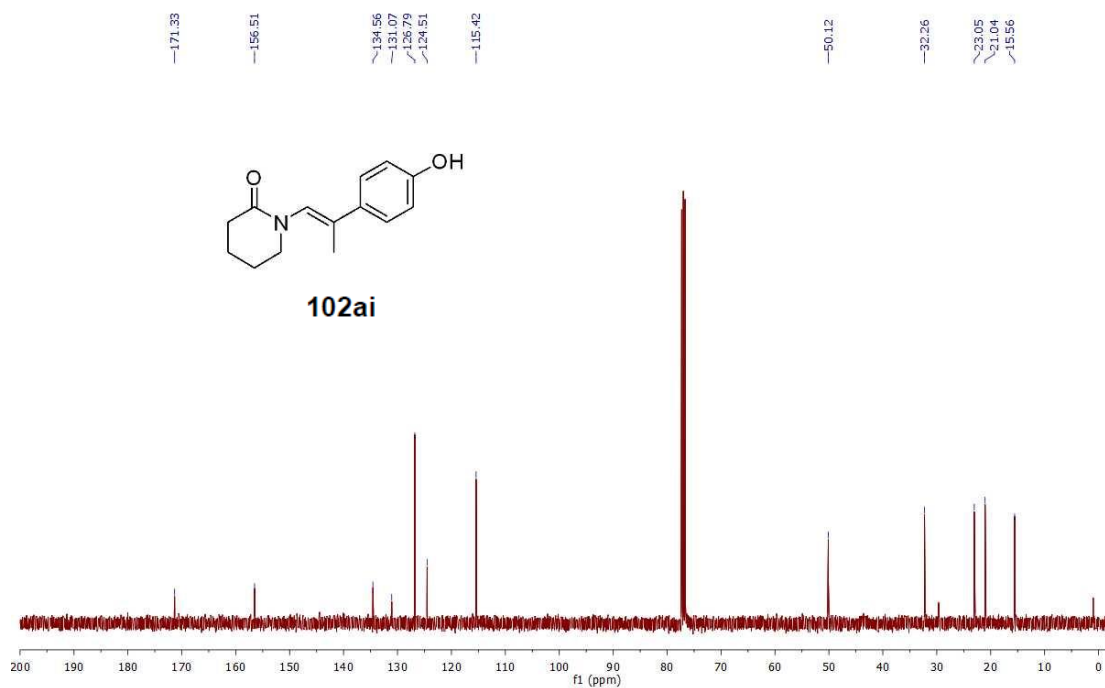
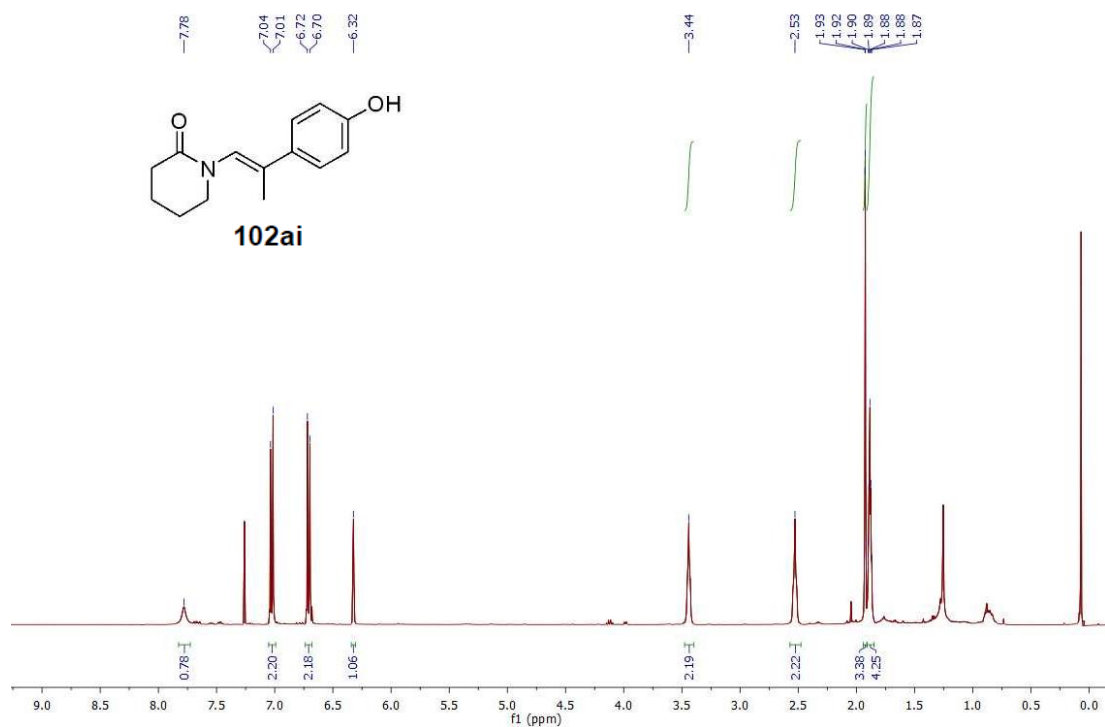
Spectra of Selected Compounds



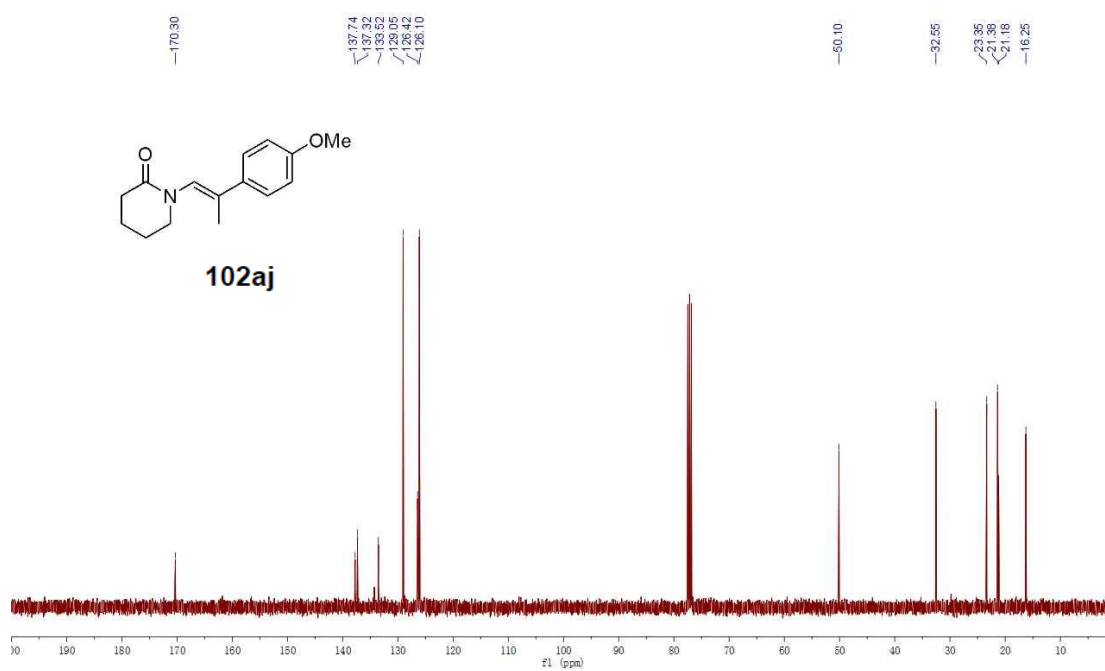
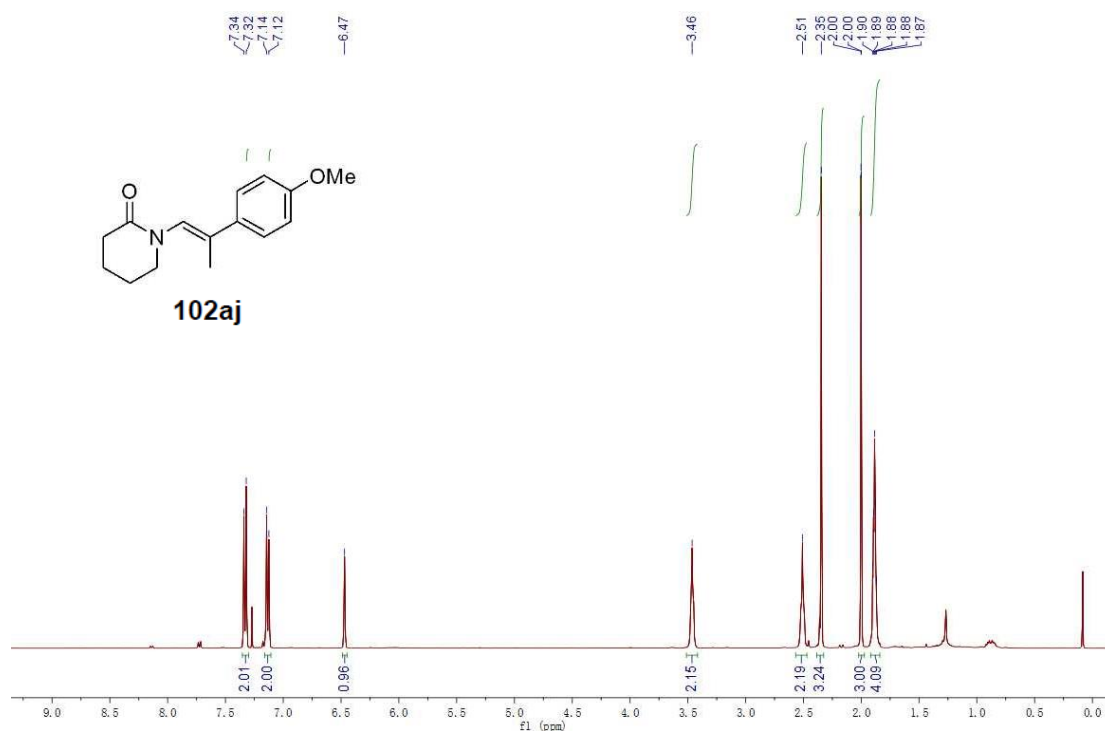
Spectra of Selected Compounds



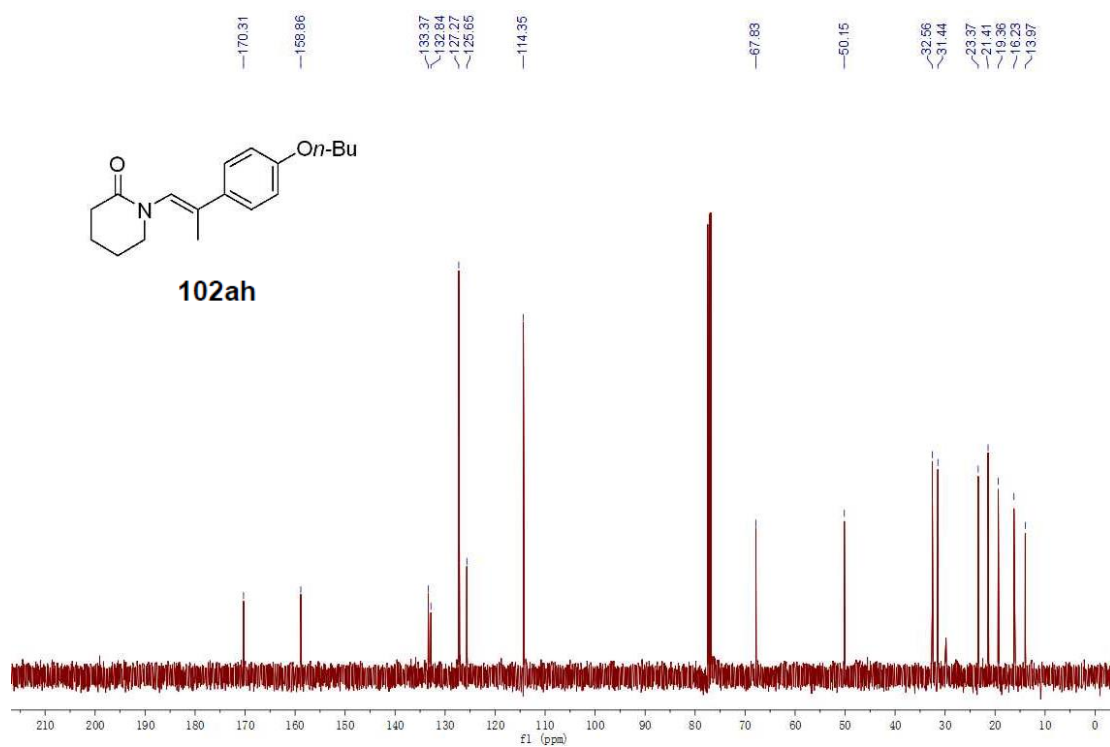
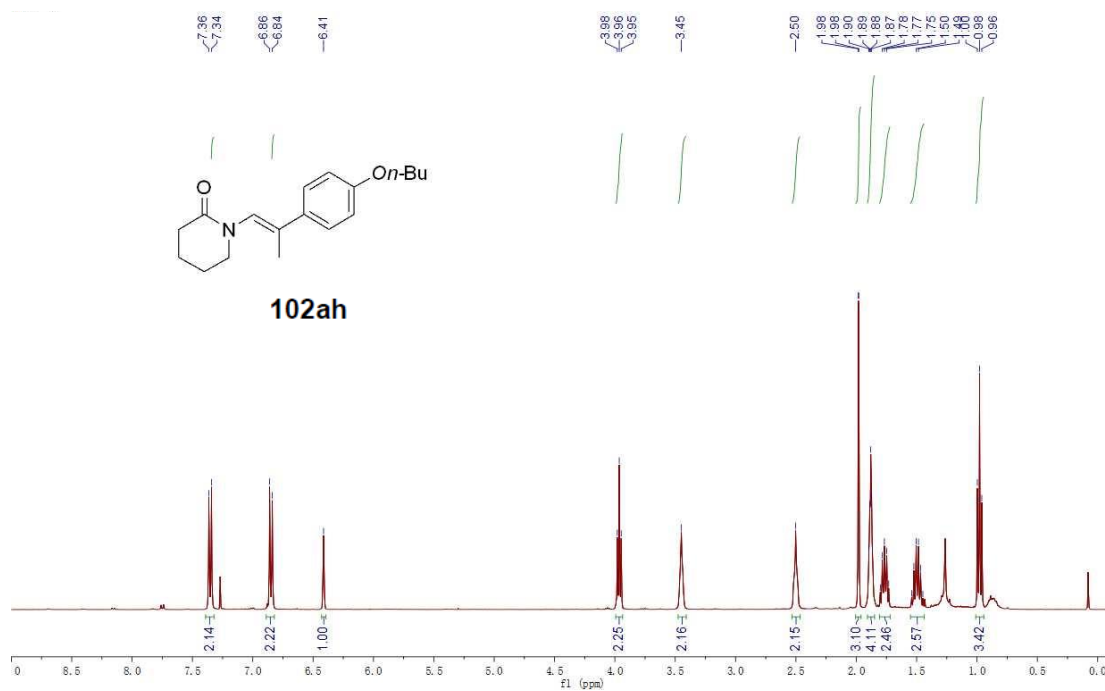
Spectra of Selected Compounds



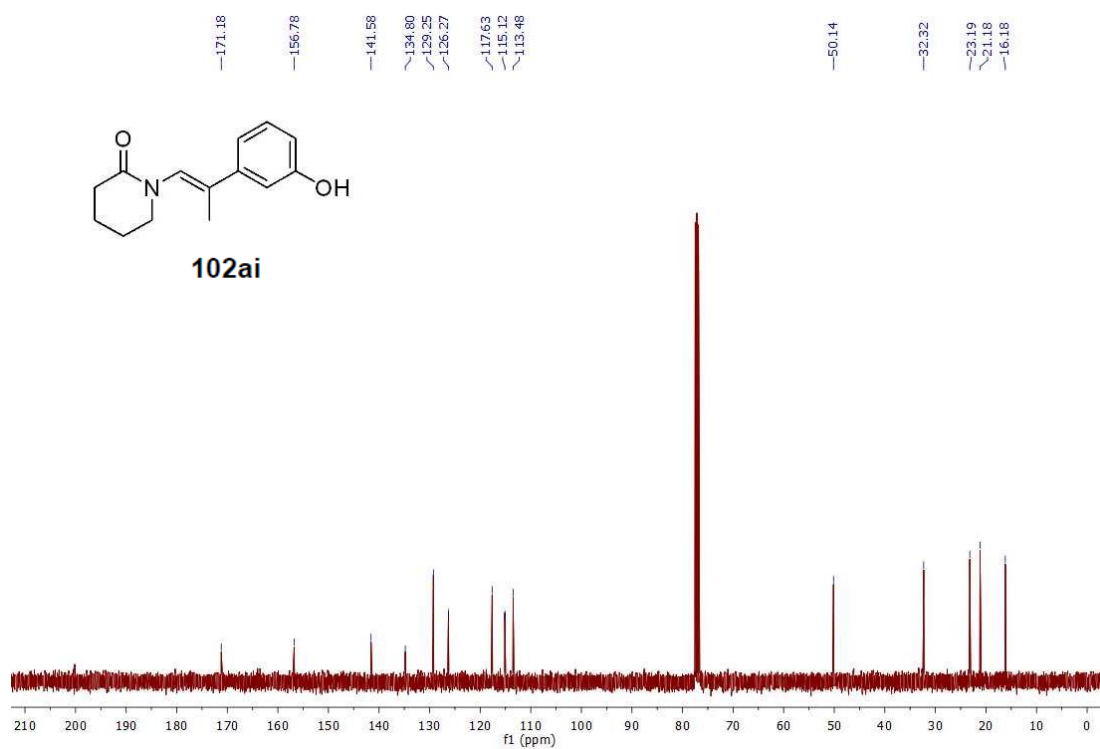
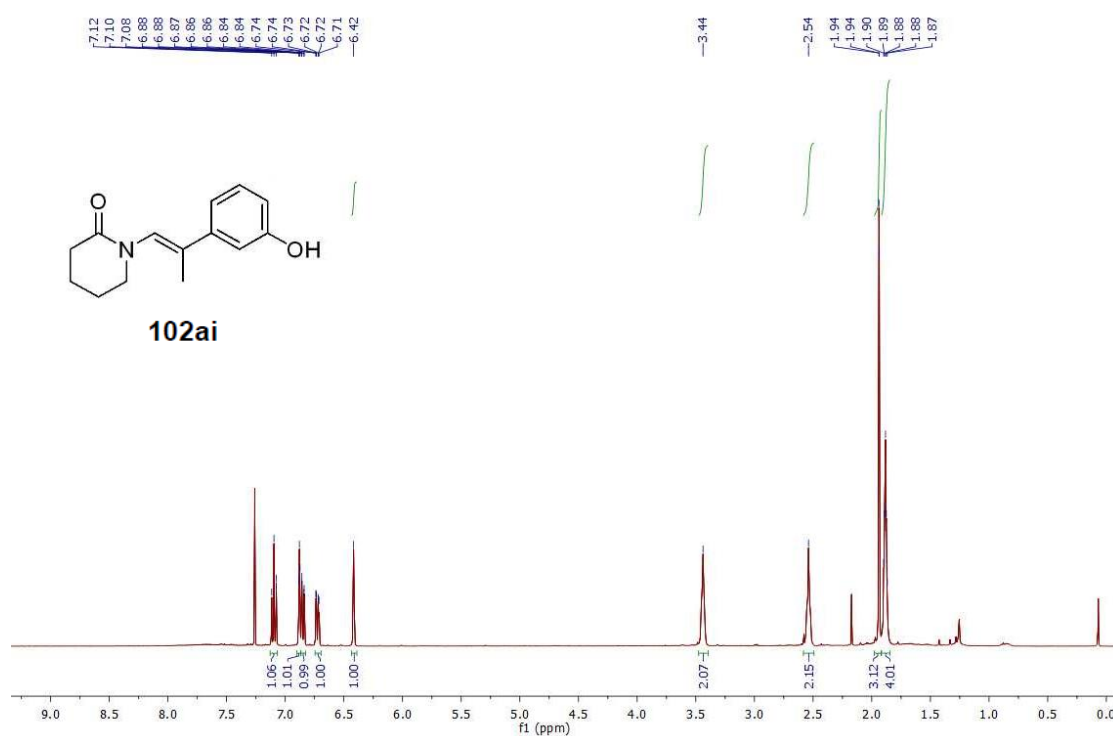
Spectra of Selected Compounds



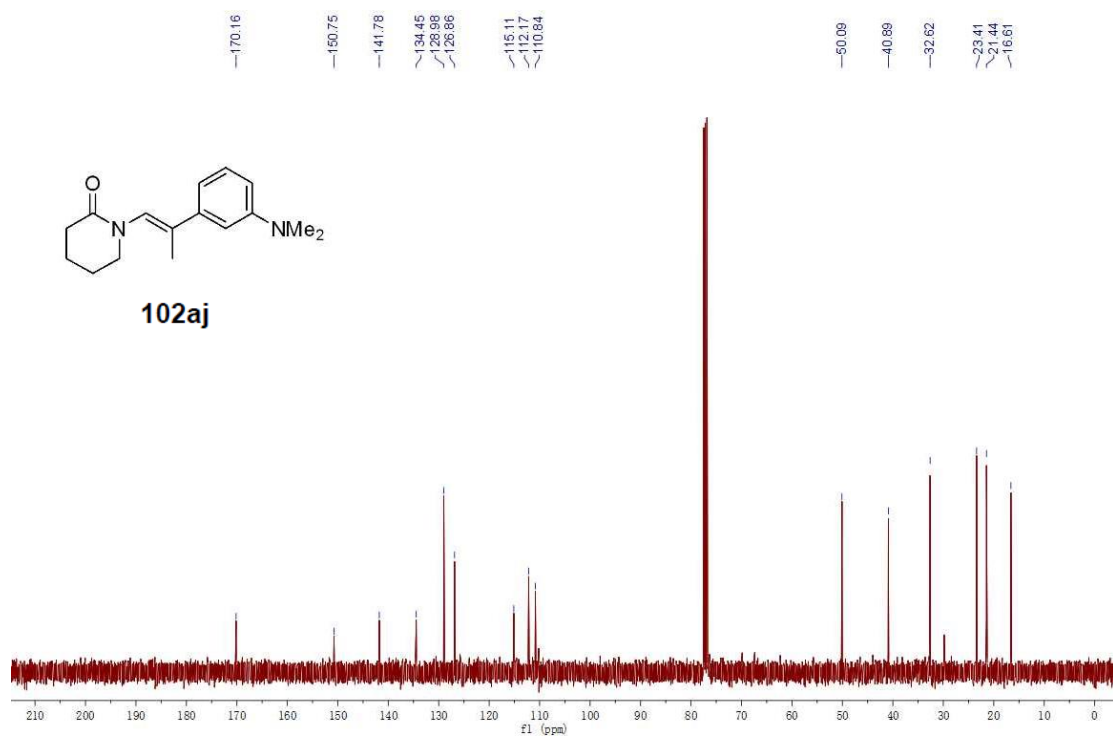
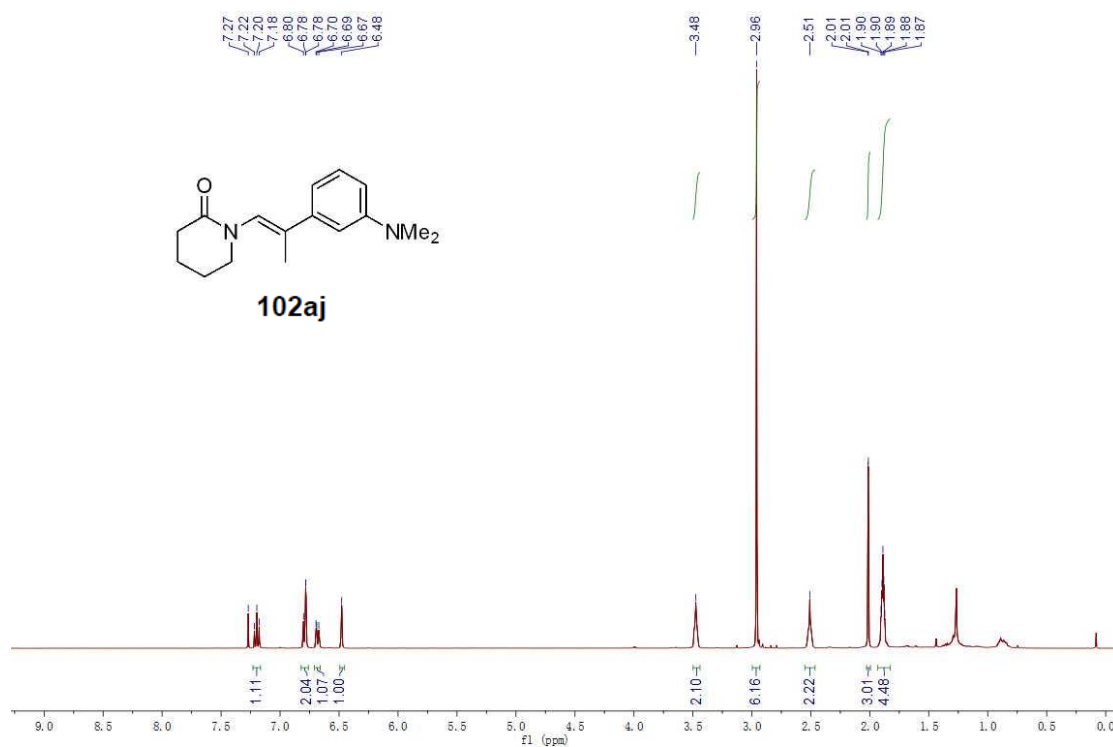
Spectra of Selected Compounds



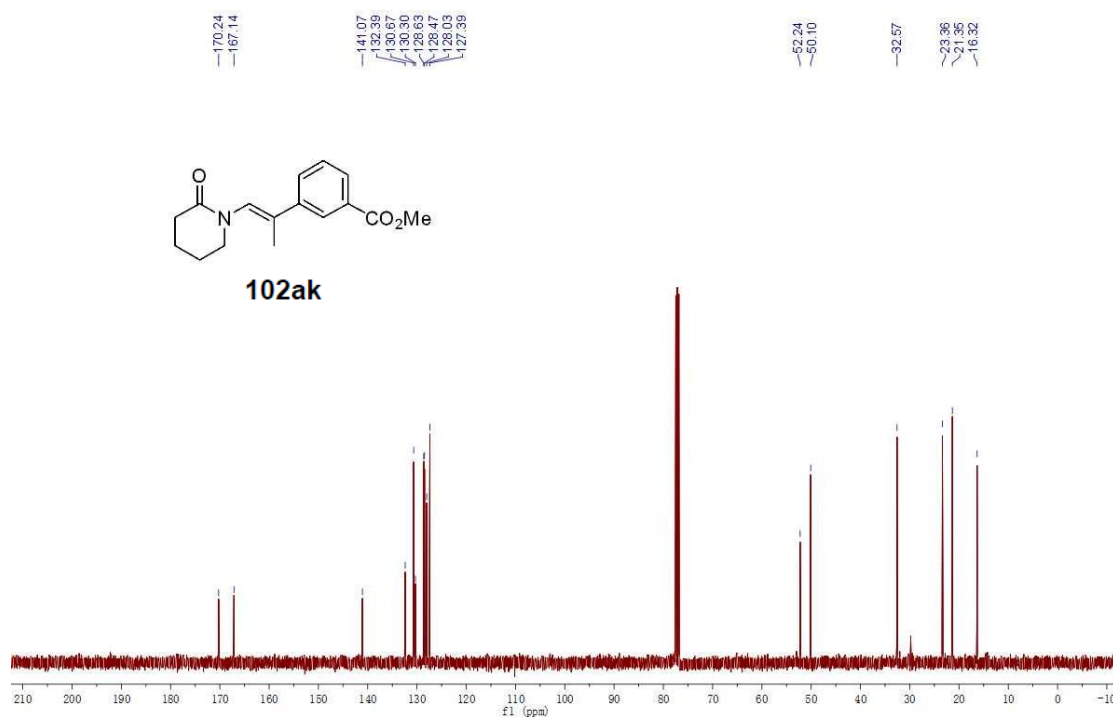
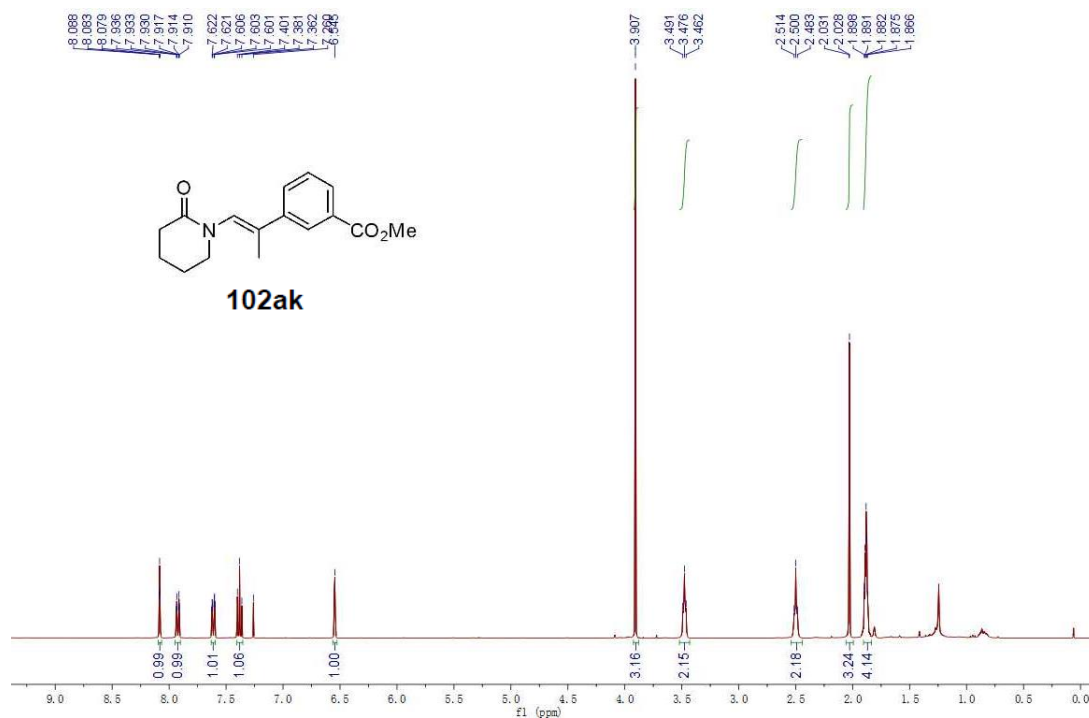
Spectra of Selected Compounds



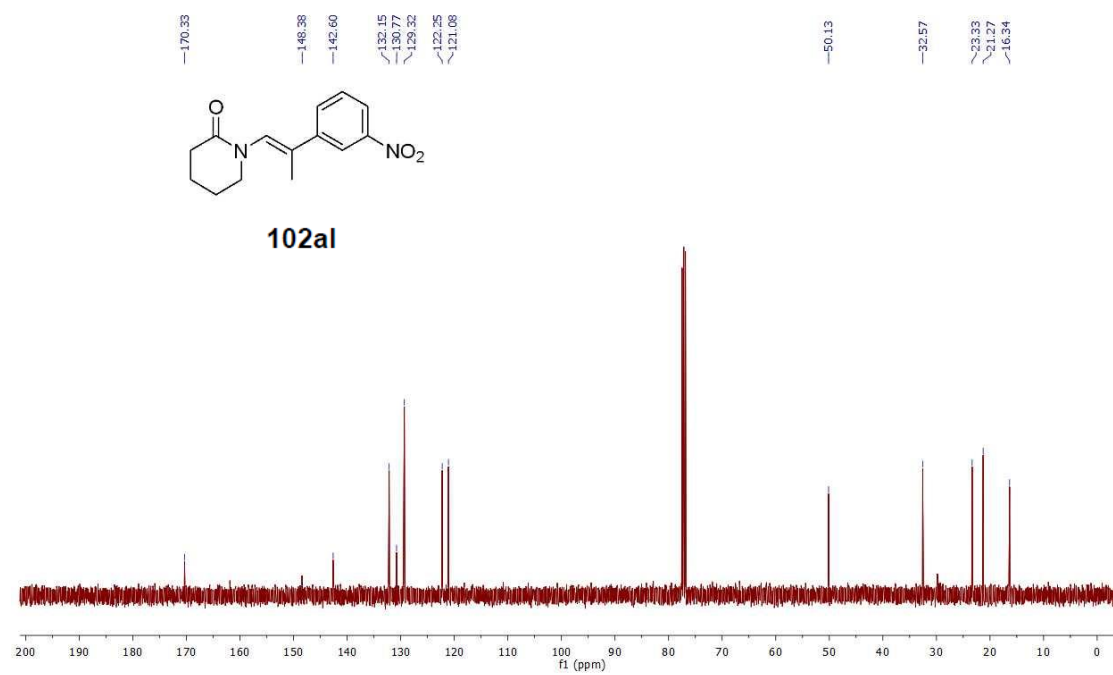
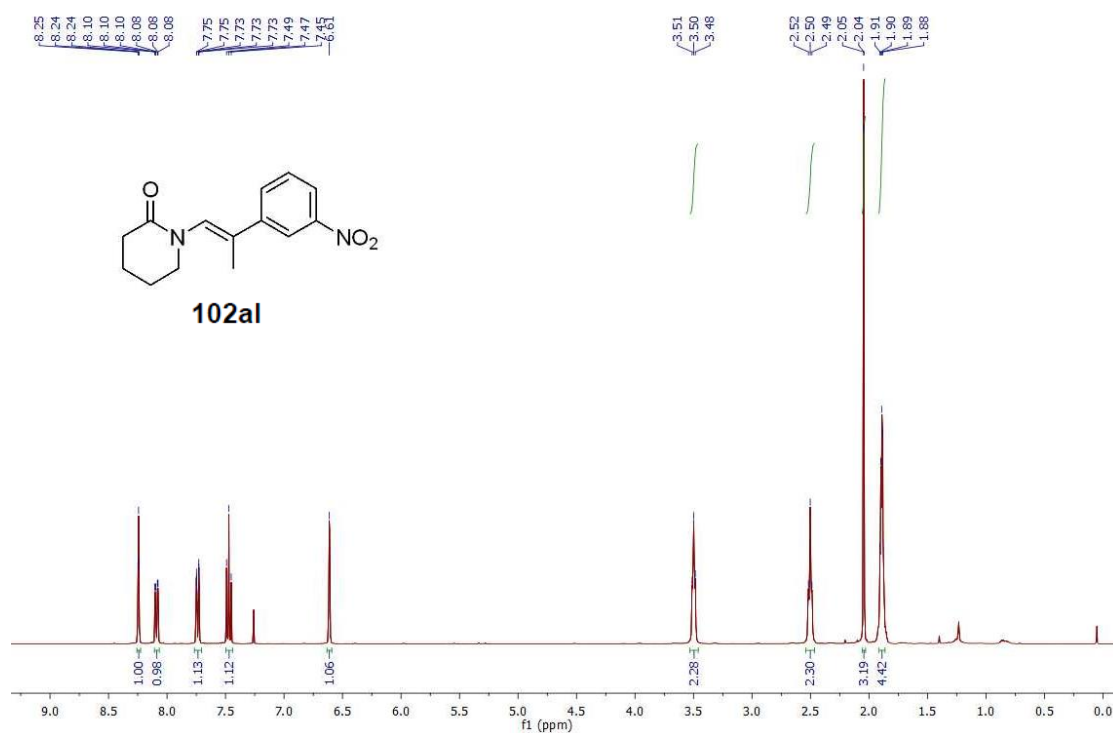
Spectra of Selected Compounds



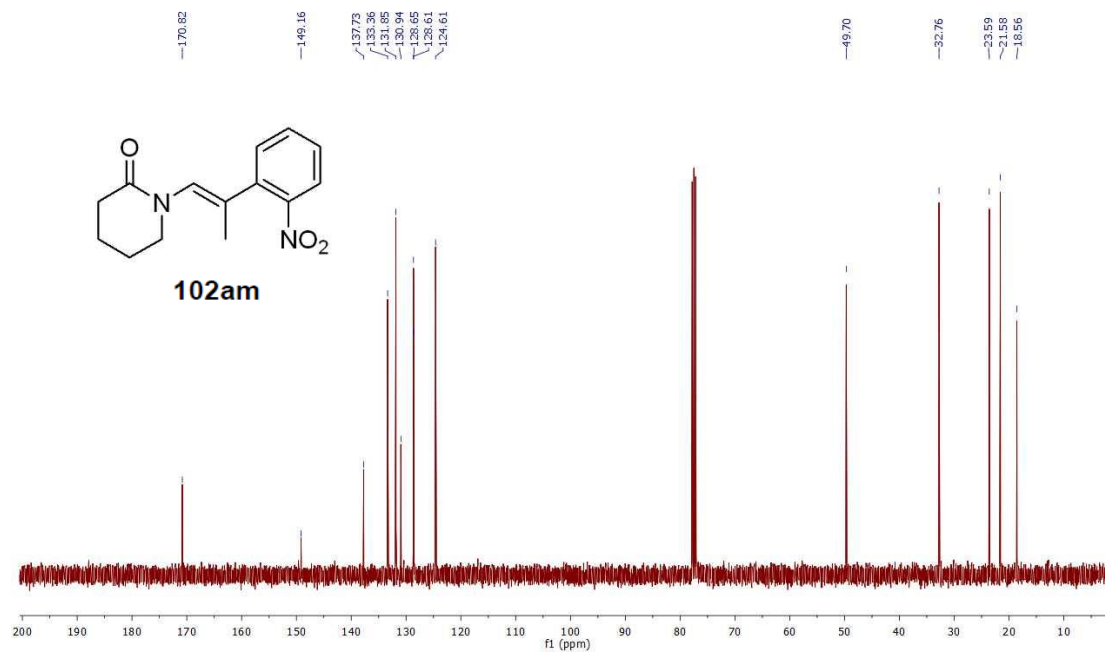
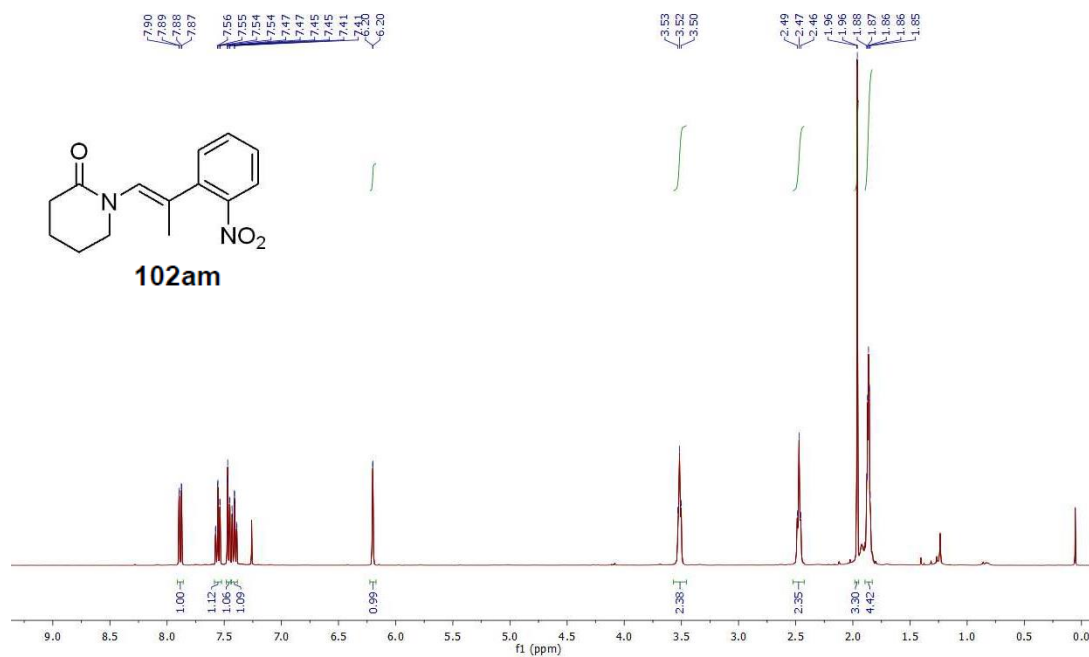
Spectra of Selected Compounds



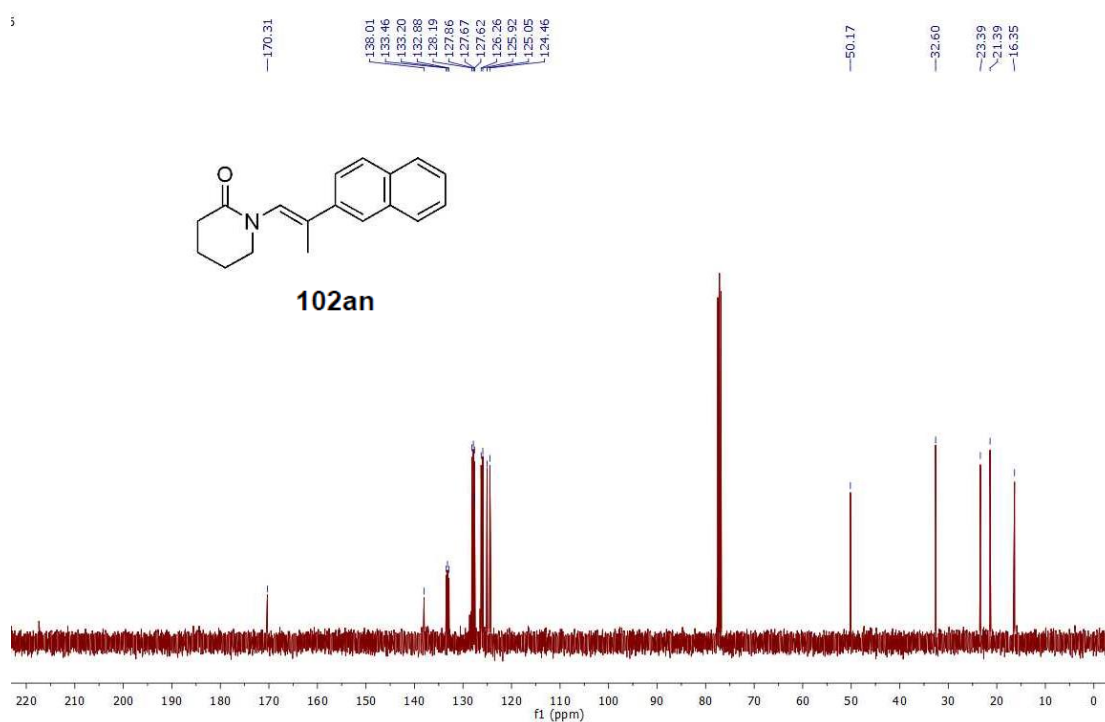
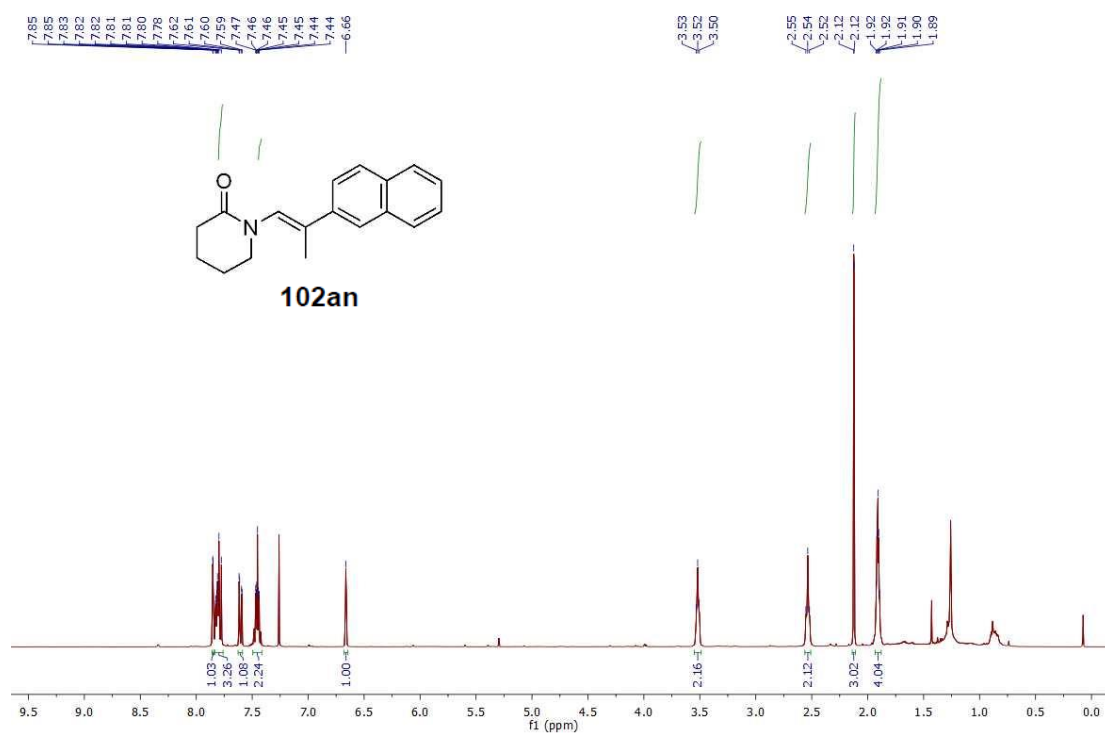
Spectra of Selected Compounds



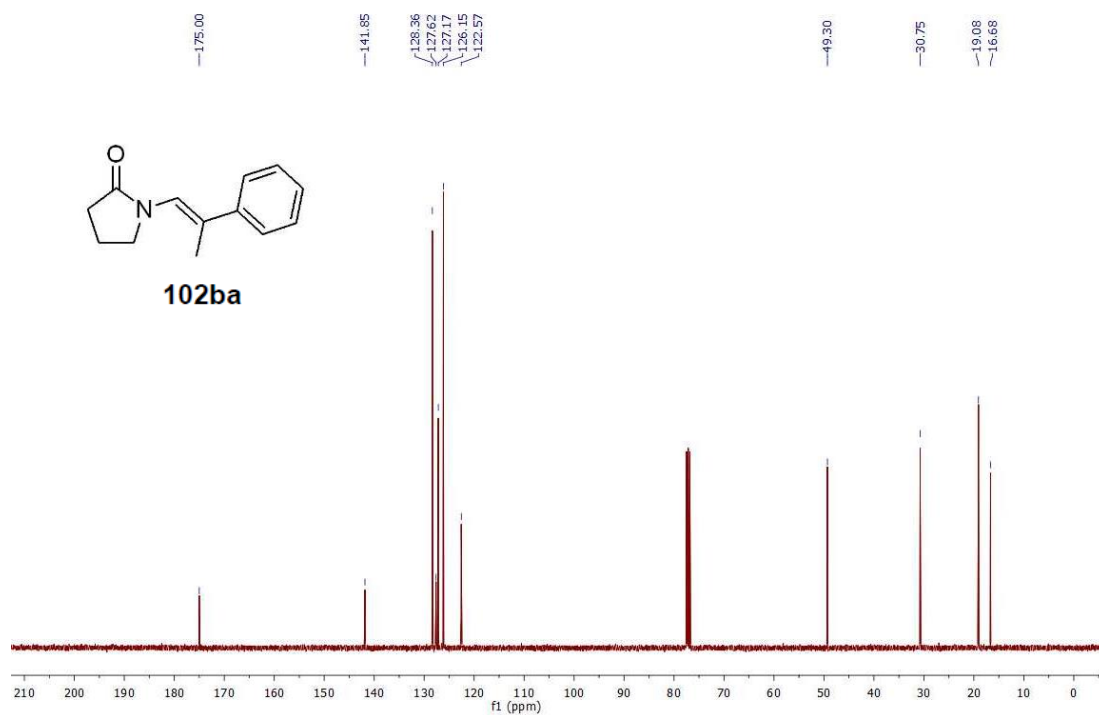
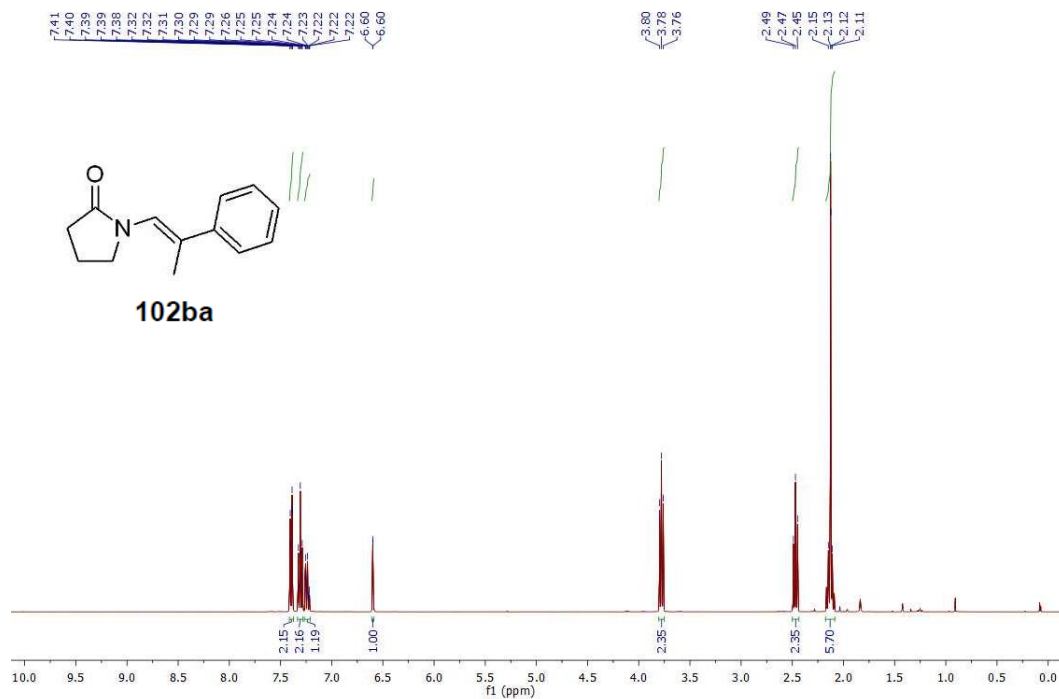
Spectra of Selected Compounds



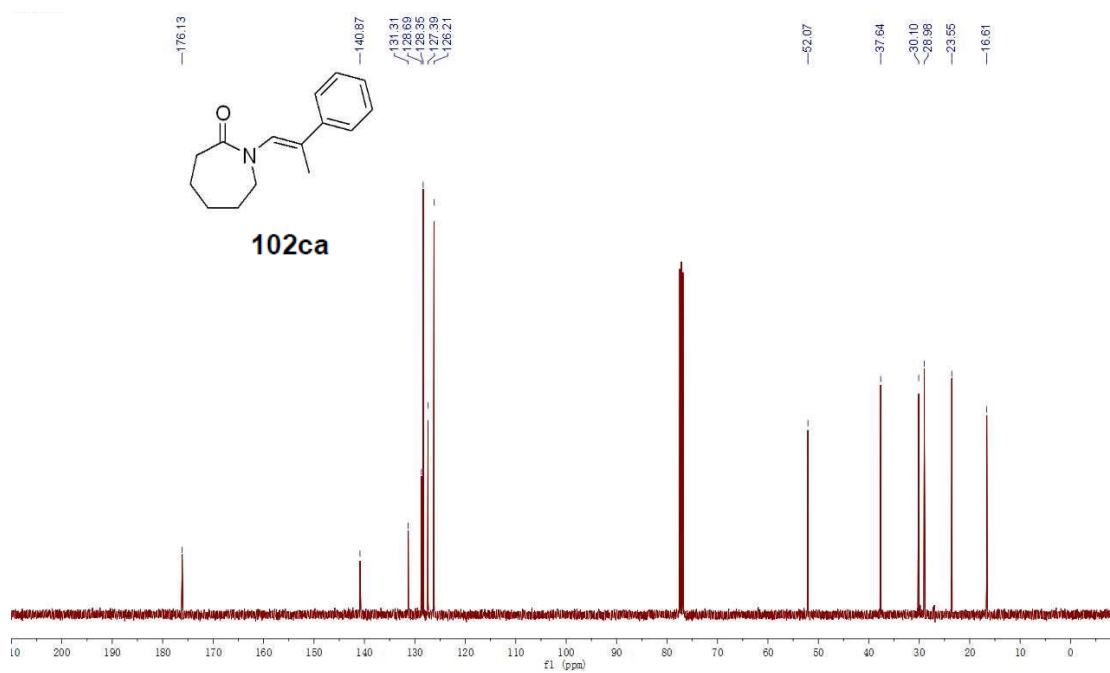
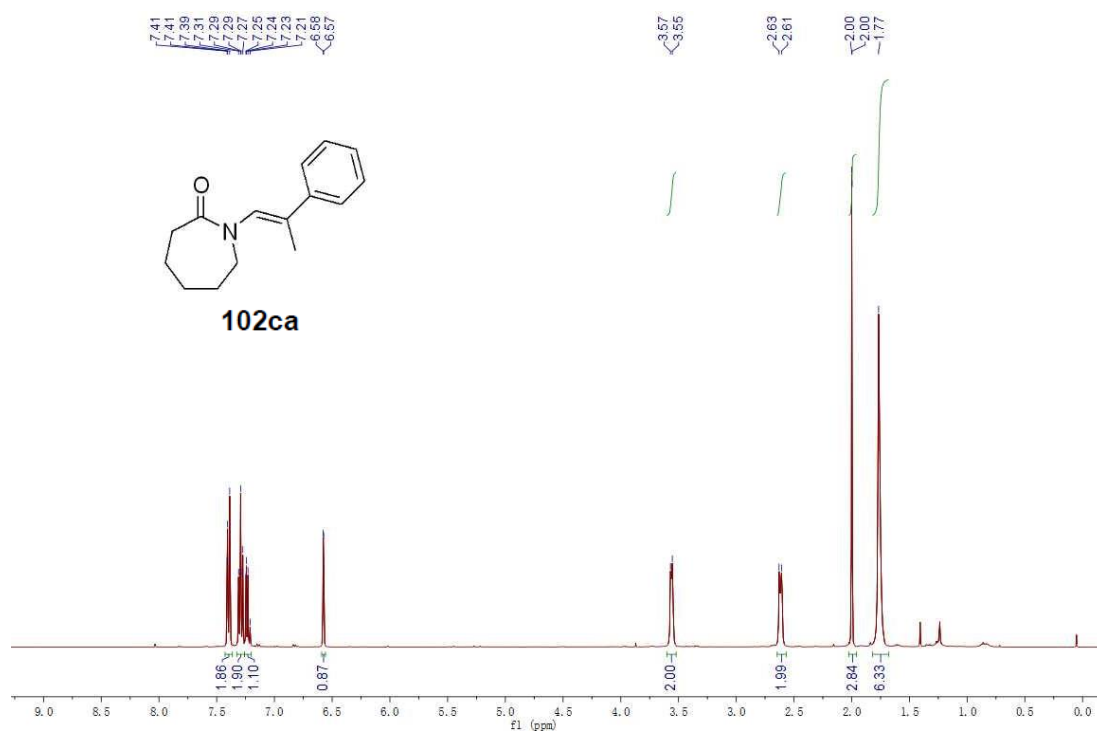
Spectra of Selected Compounds



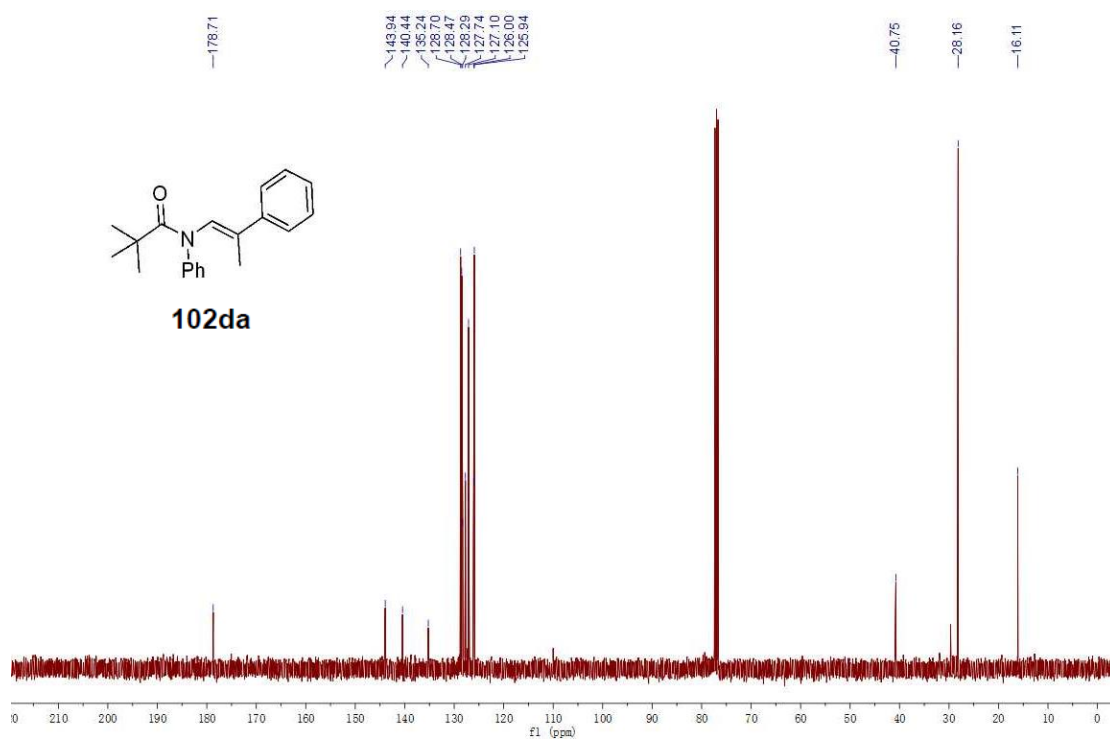
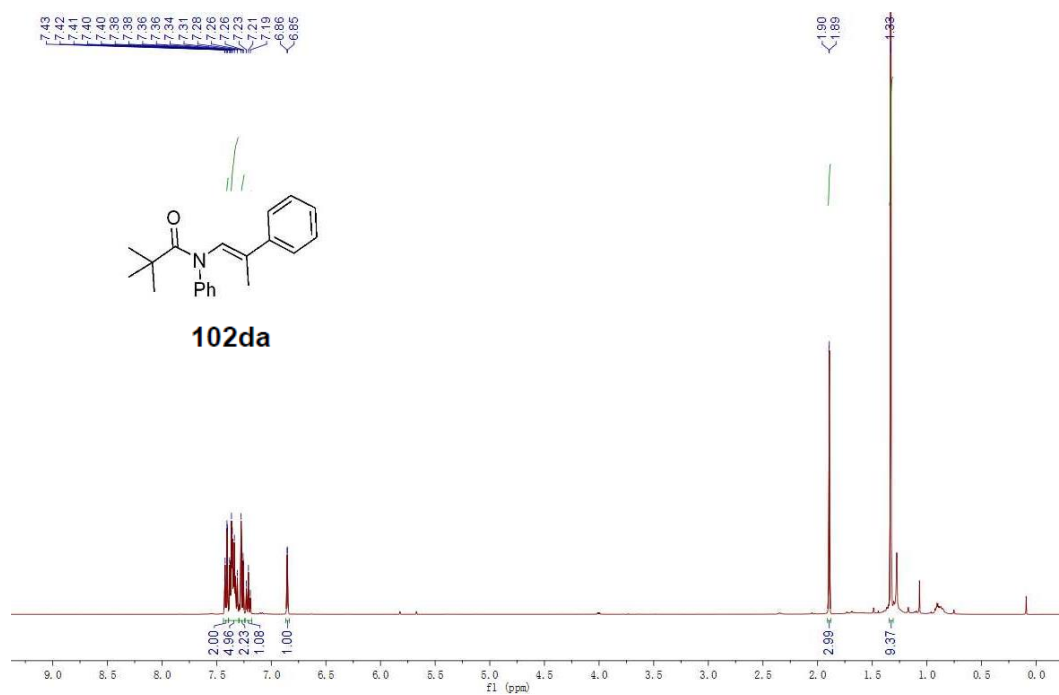
Spectra of Selected Compounds



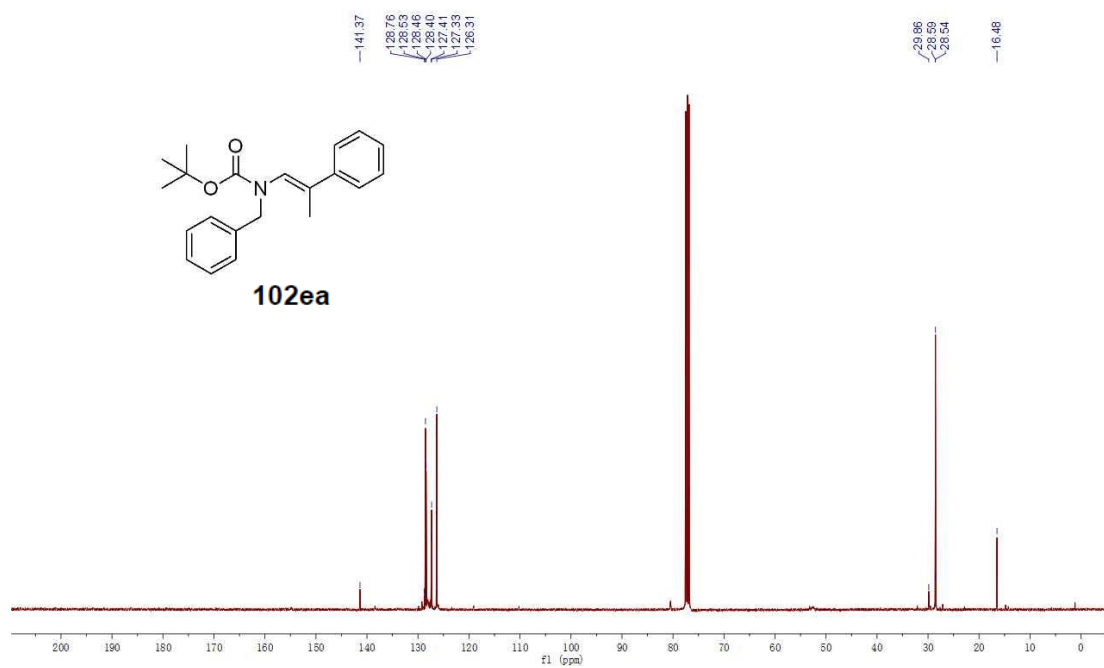
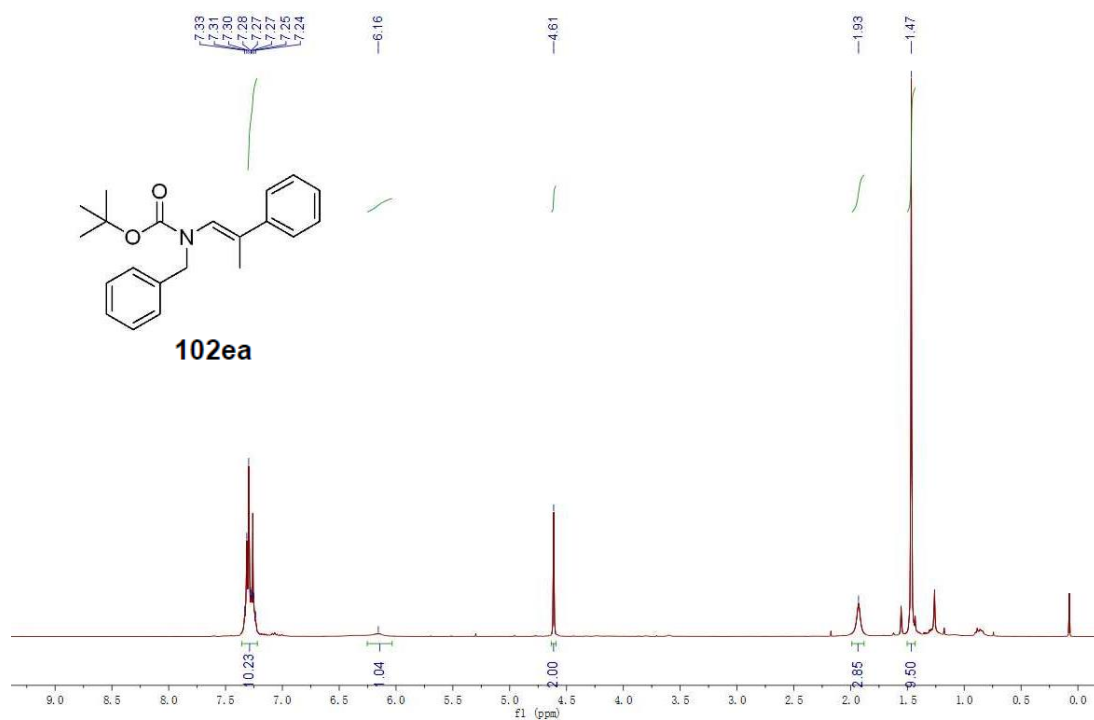
Spectra of Selected Compounds



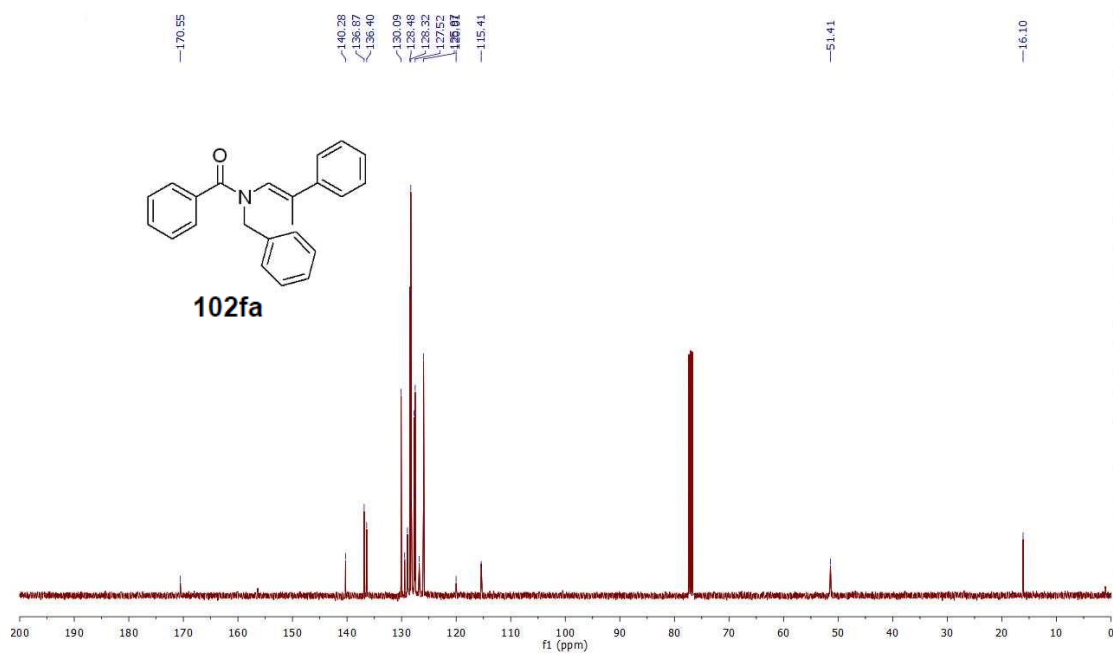
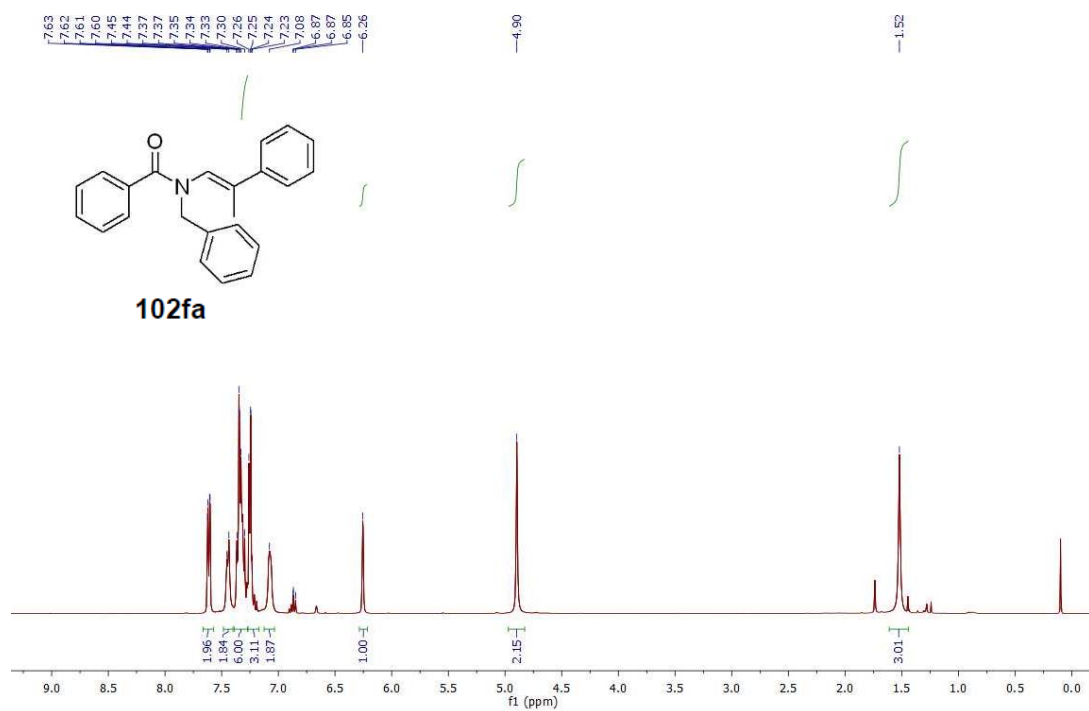
Spectra of Selected Compounds



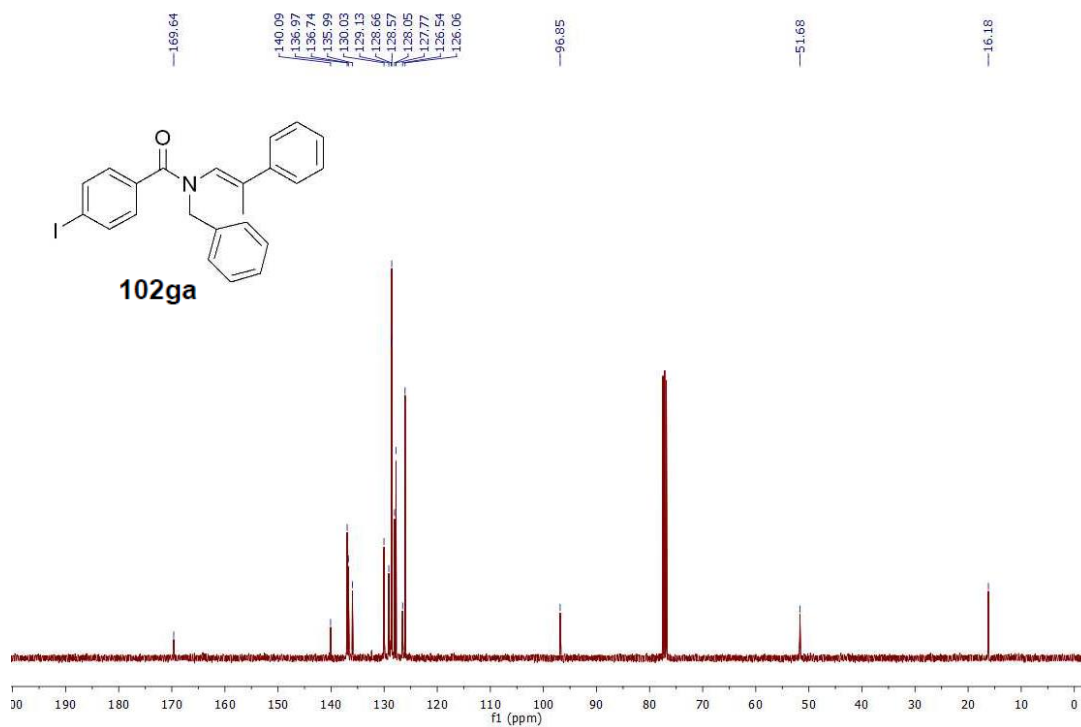
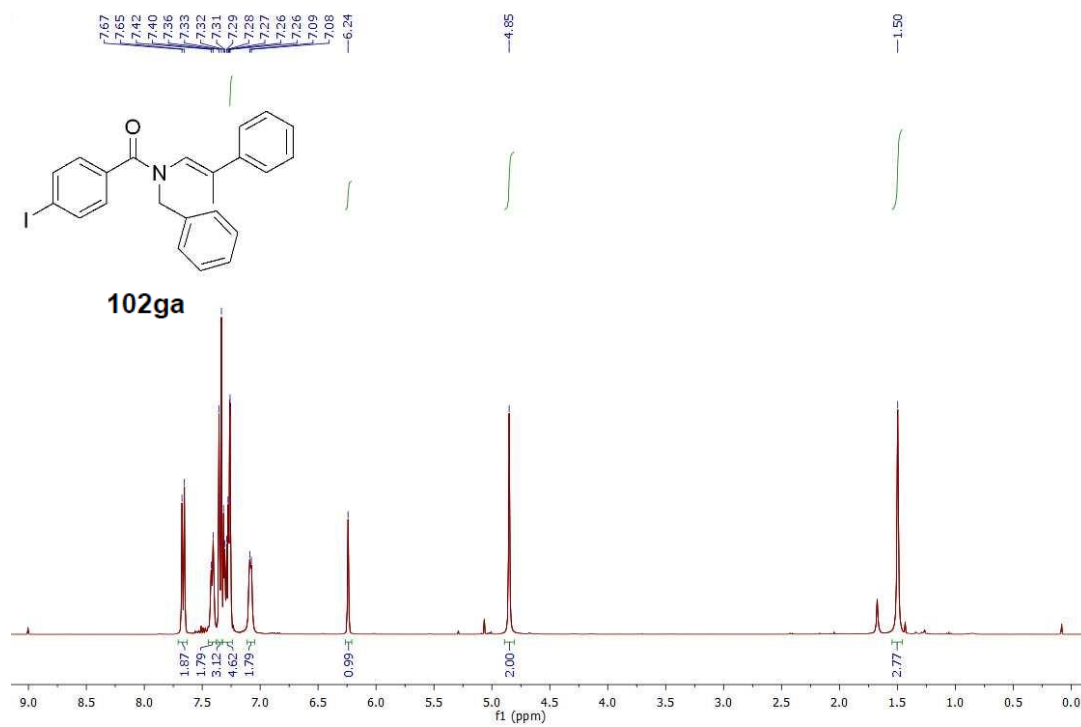
Spectra of Selected Compounds



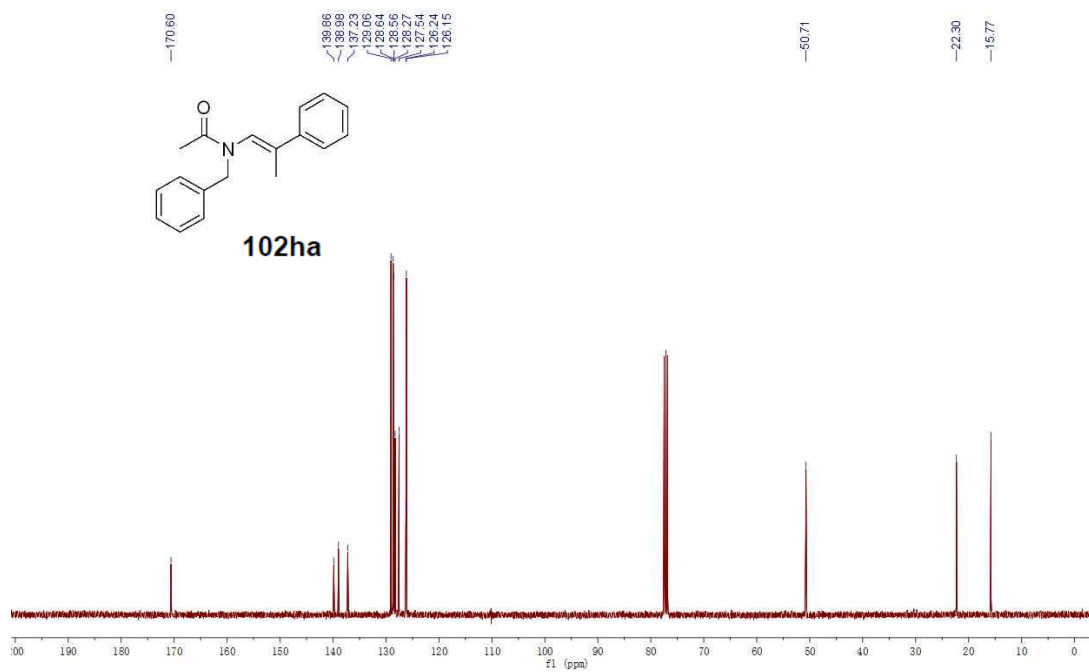
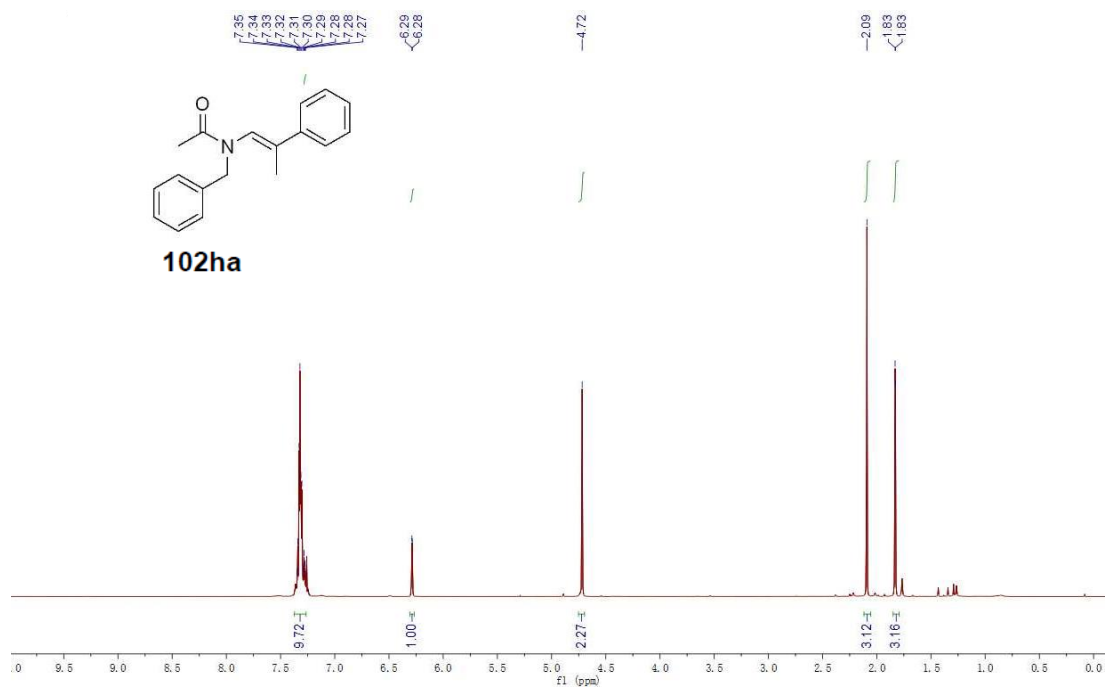
Spectra of Selected Compounds



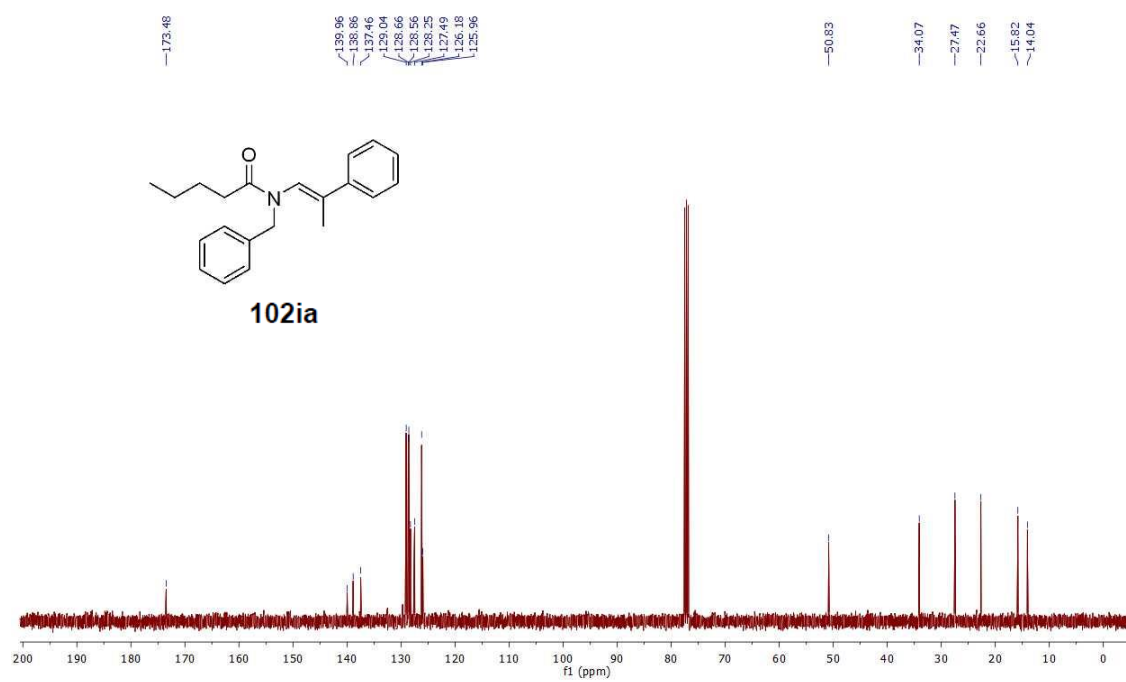
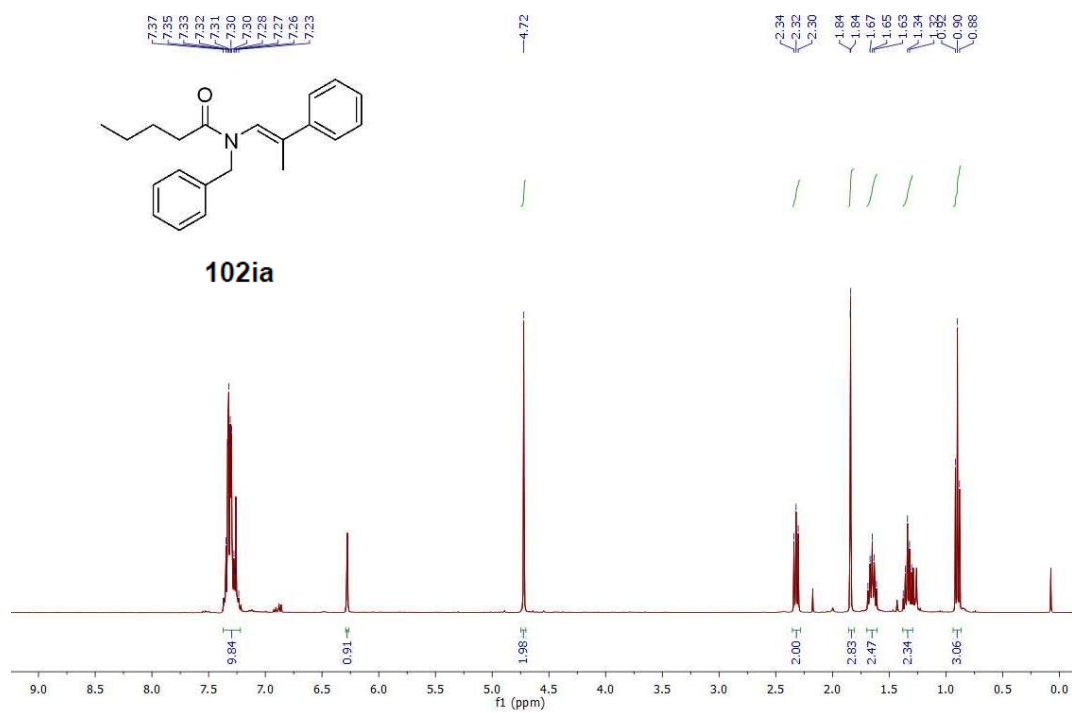
Spectra of Selected Compounds



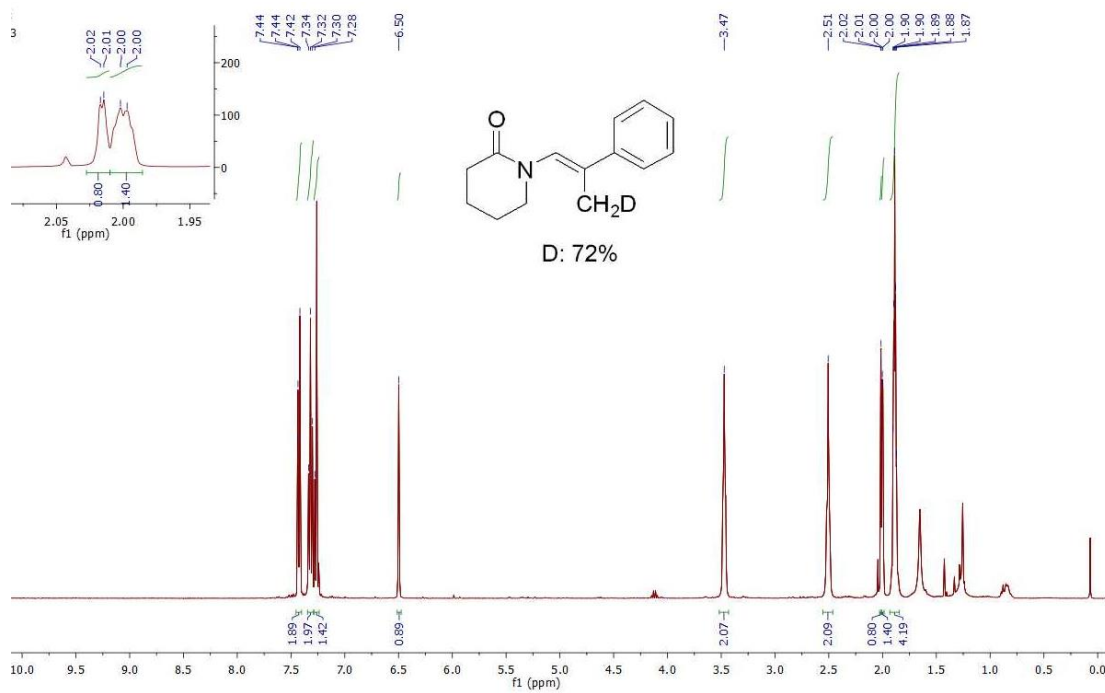
Spectra of Selected Compounds



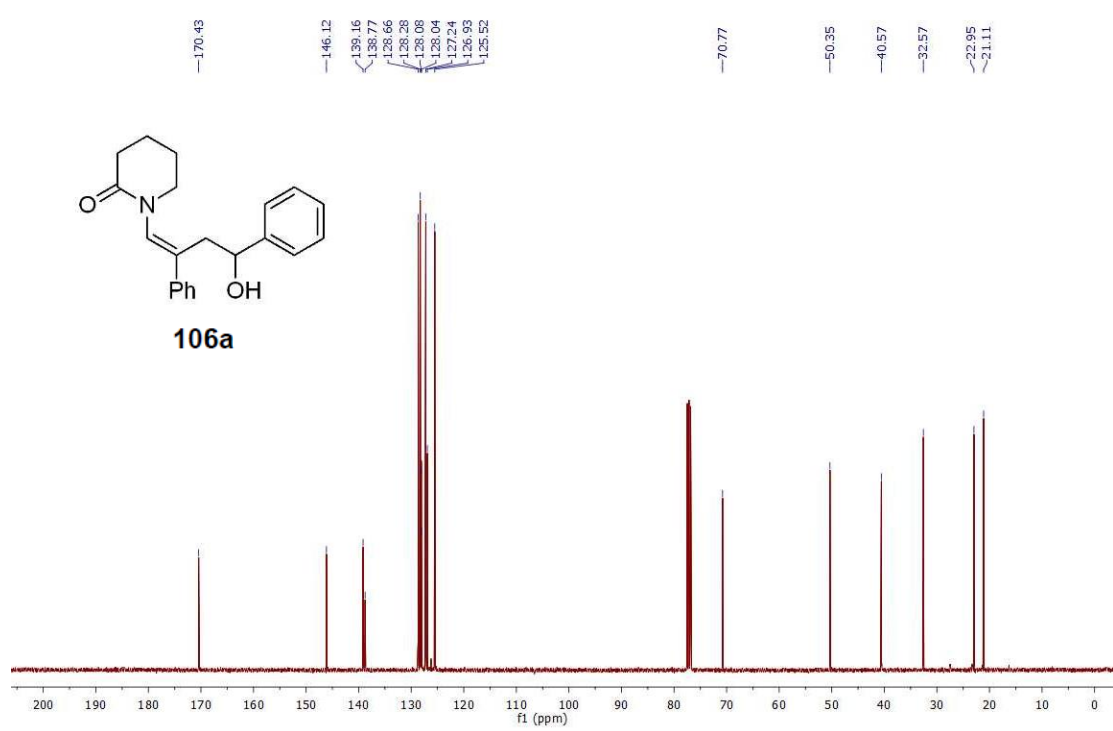
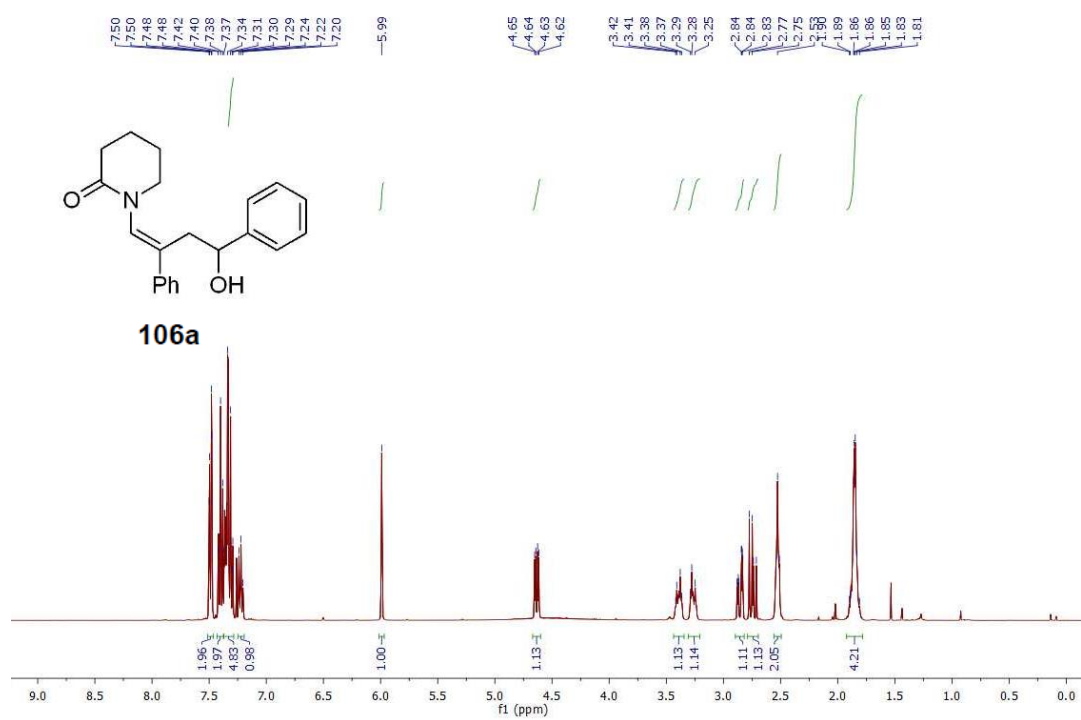
Spectra of Selected Compounds



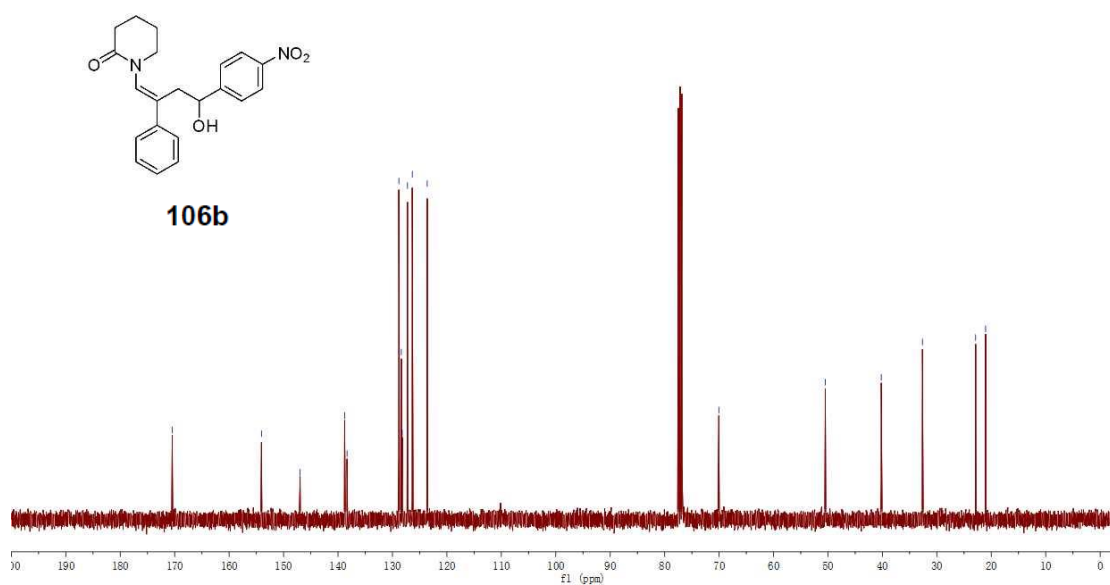
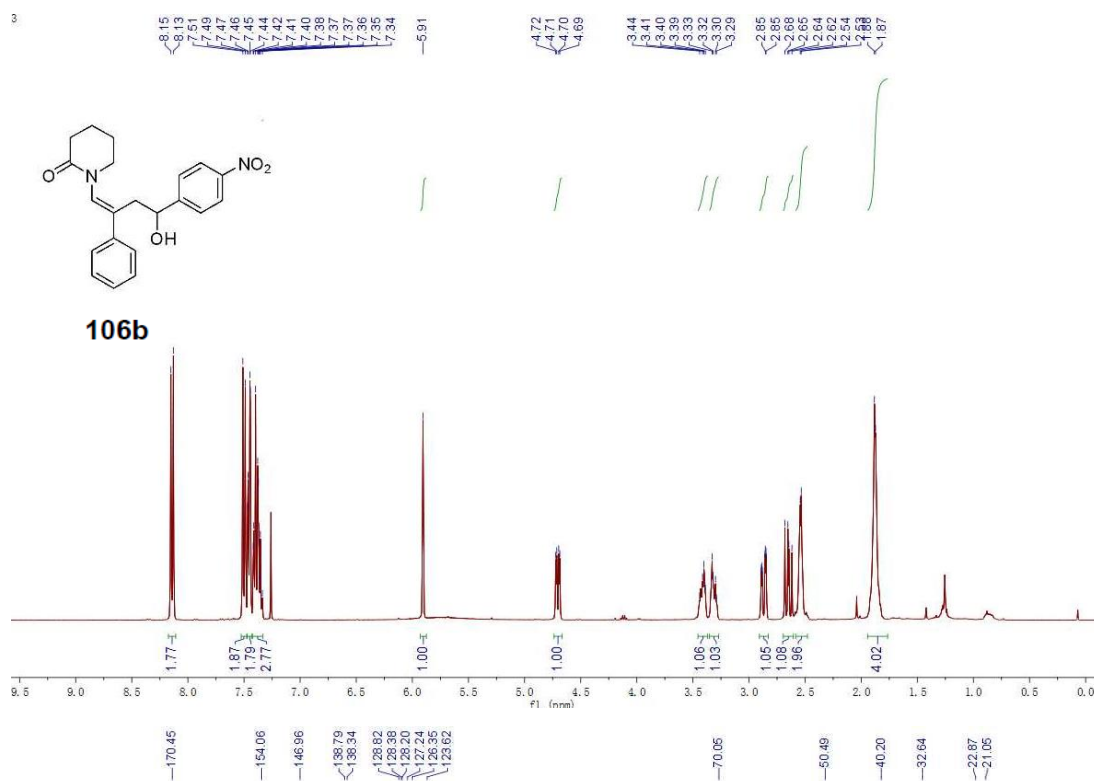
Spectra of Selected Compounds



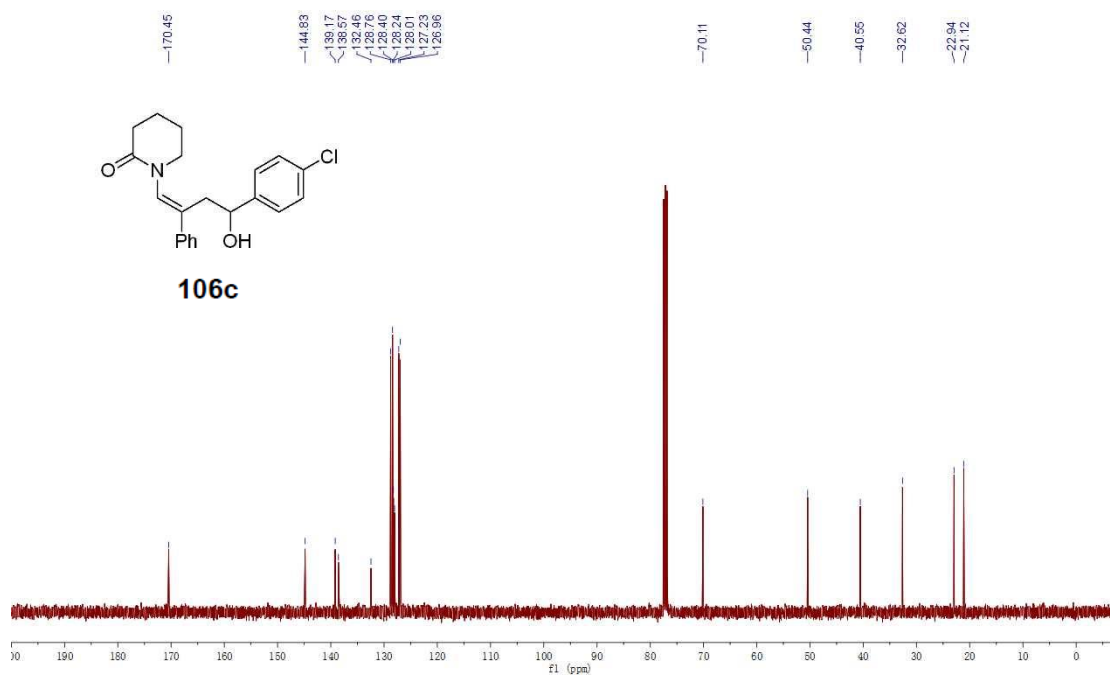
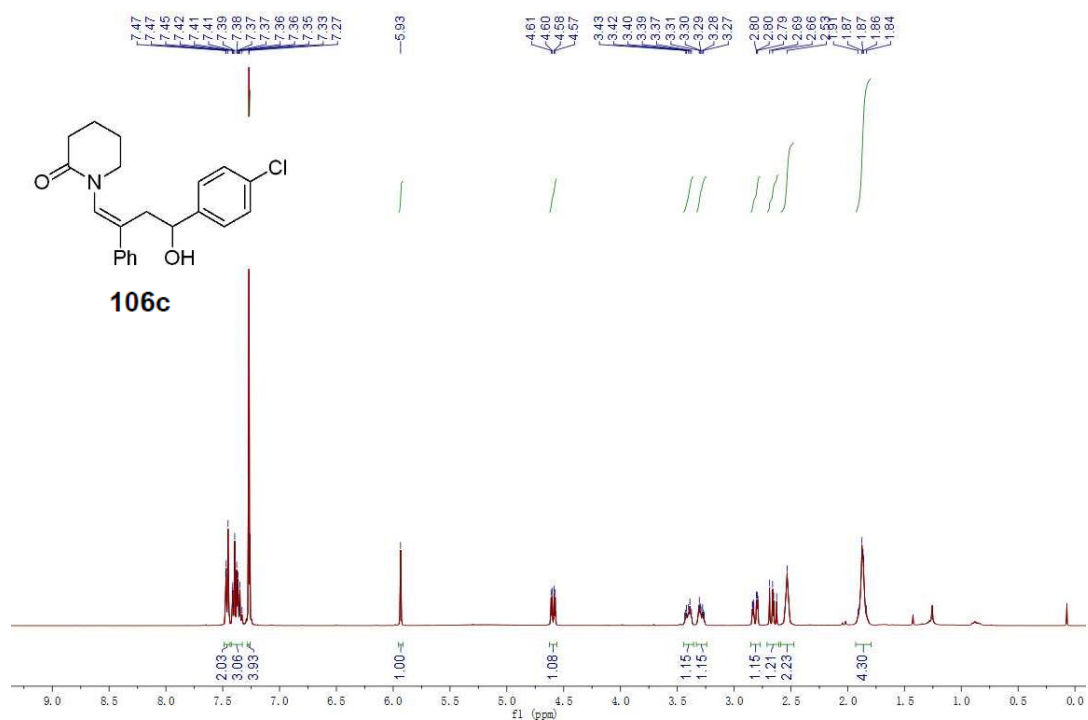
Spectra of Selected Compounds



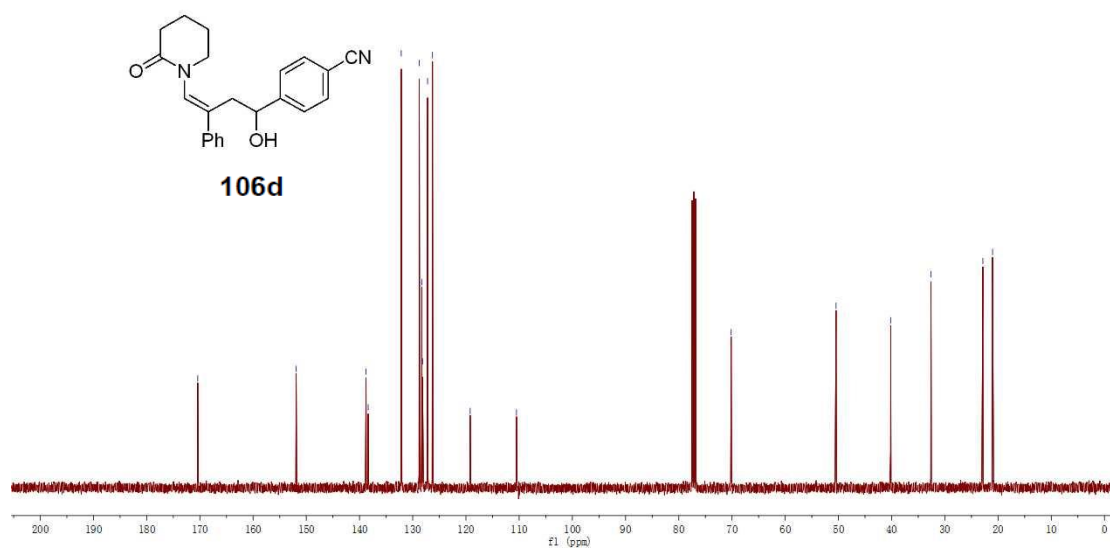
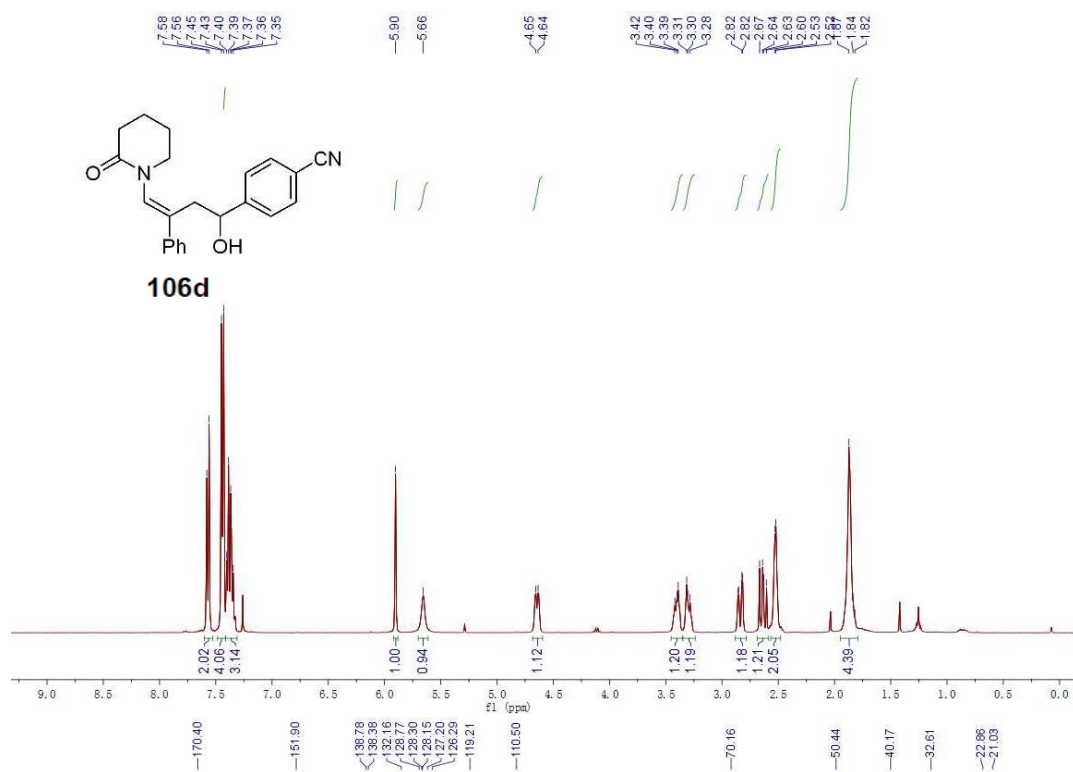
Spectra of Selected Compounds



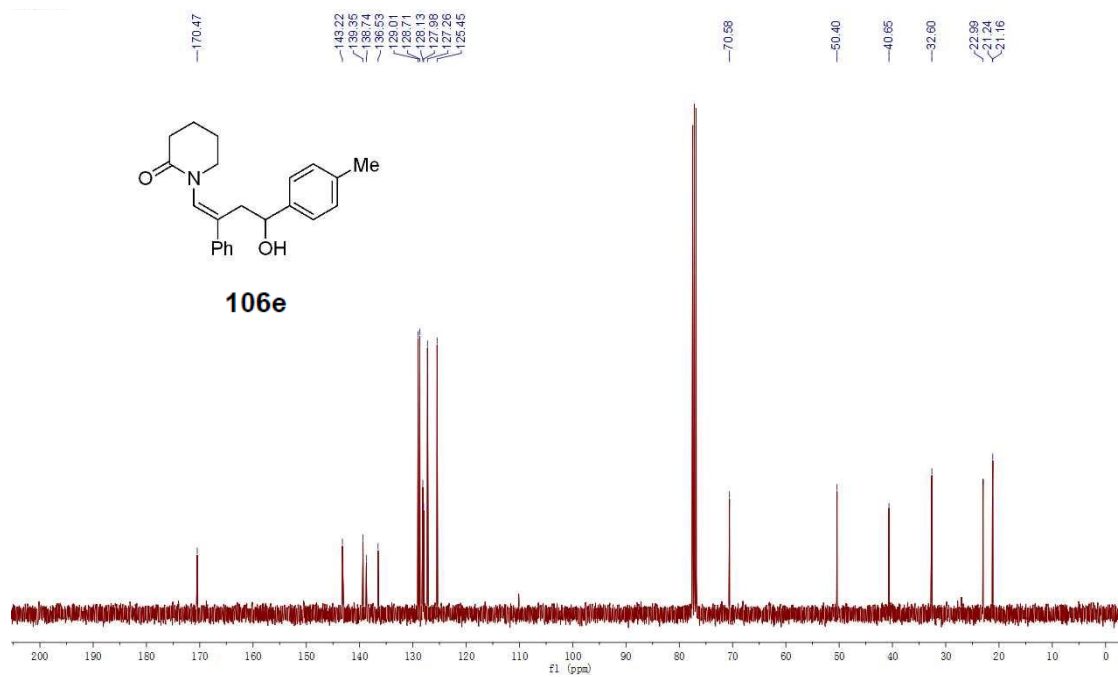
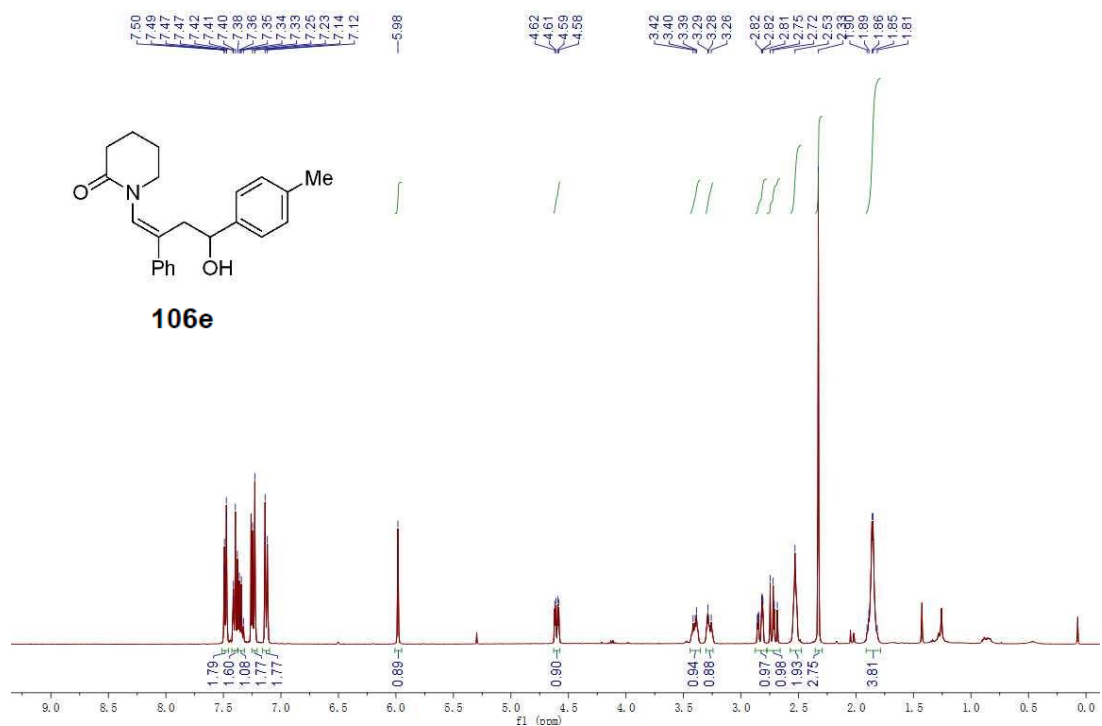
Spectra of Selected Compounds



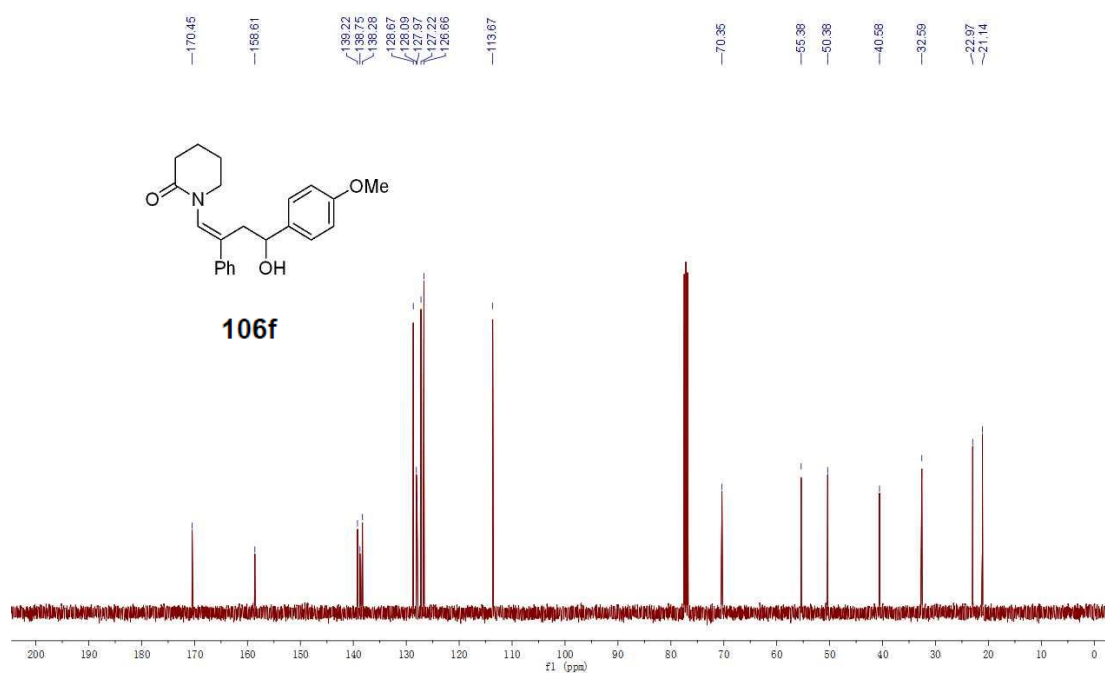
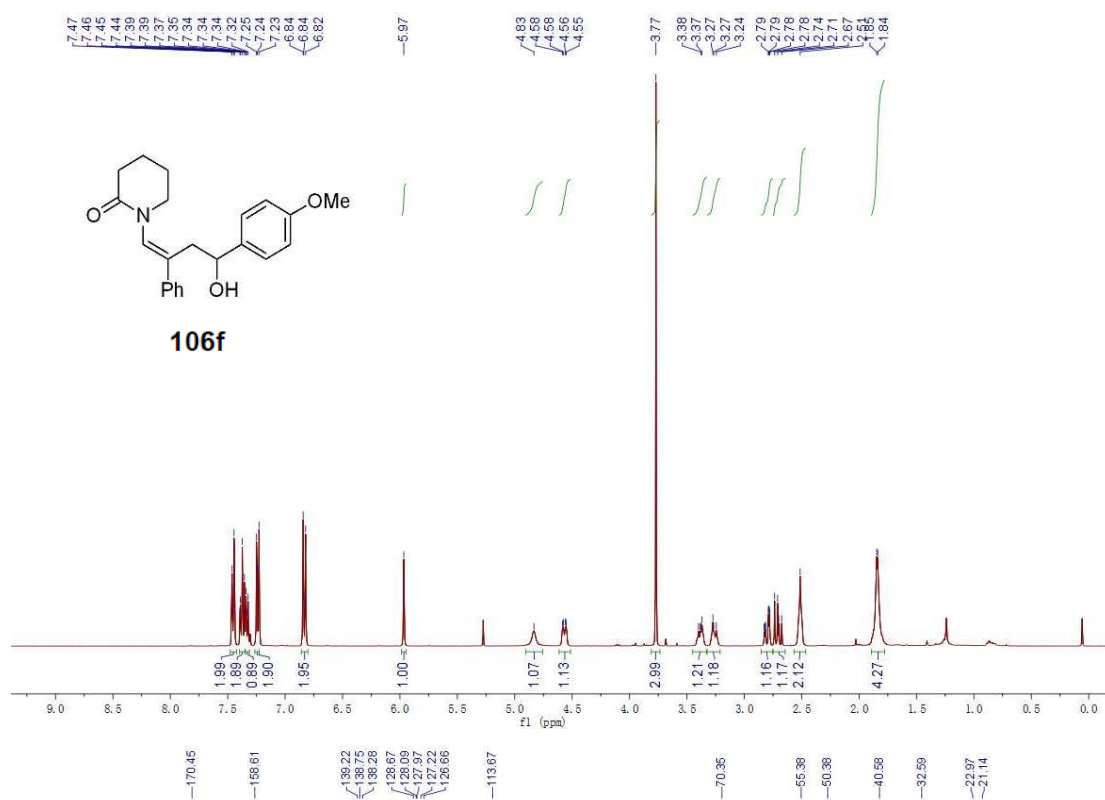
Spectra of Selected Compounds



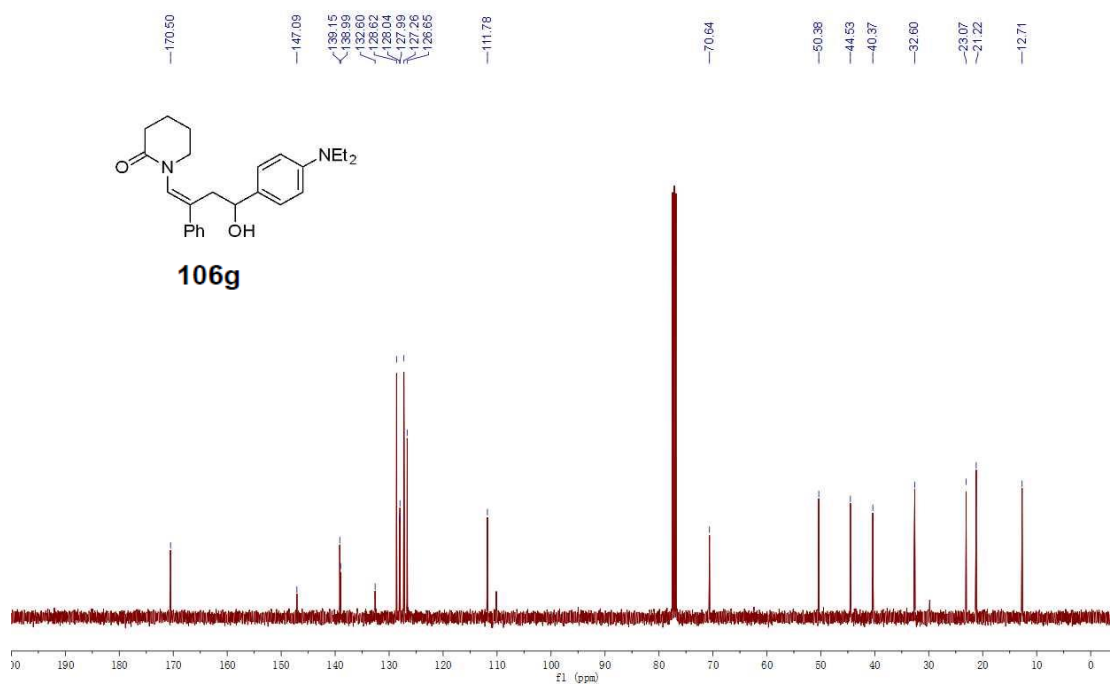
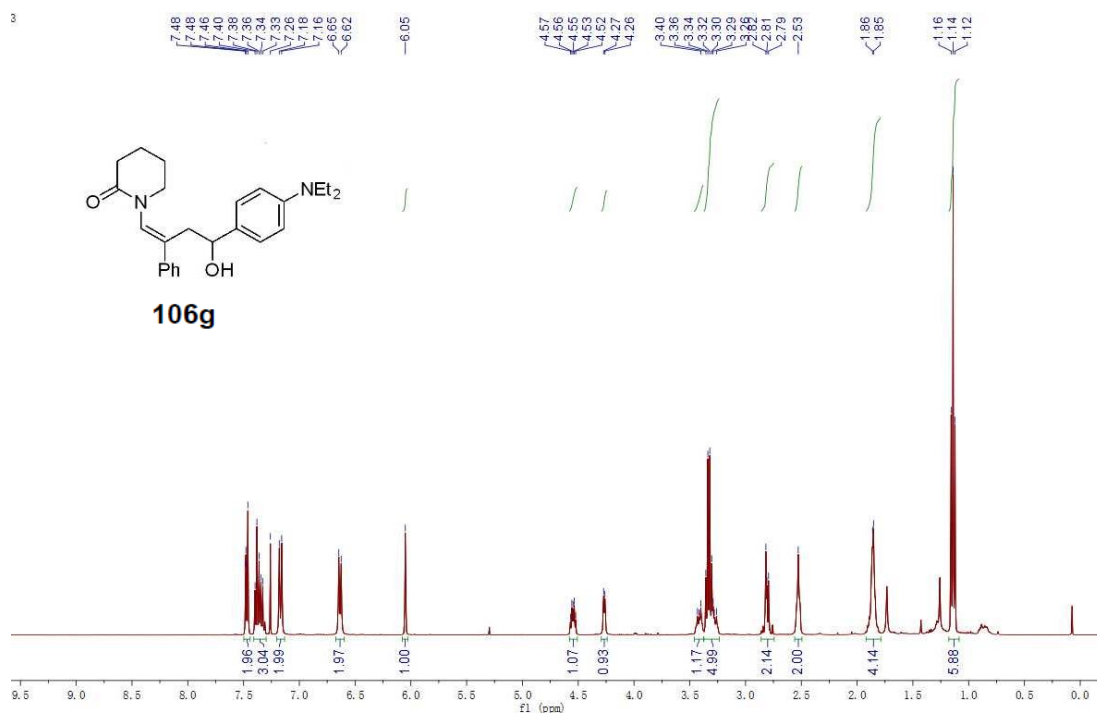
Spectra of Selected Compounds



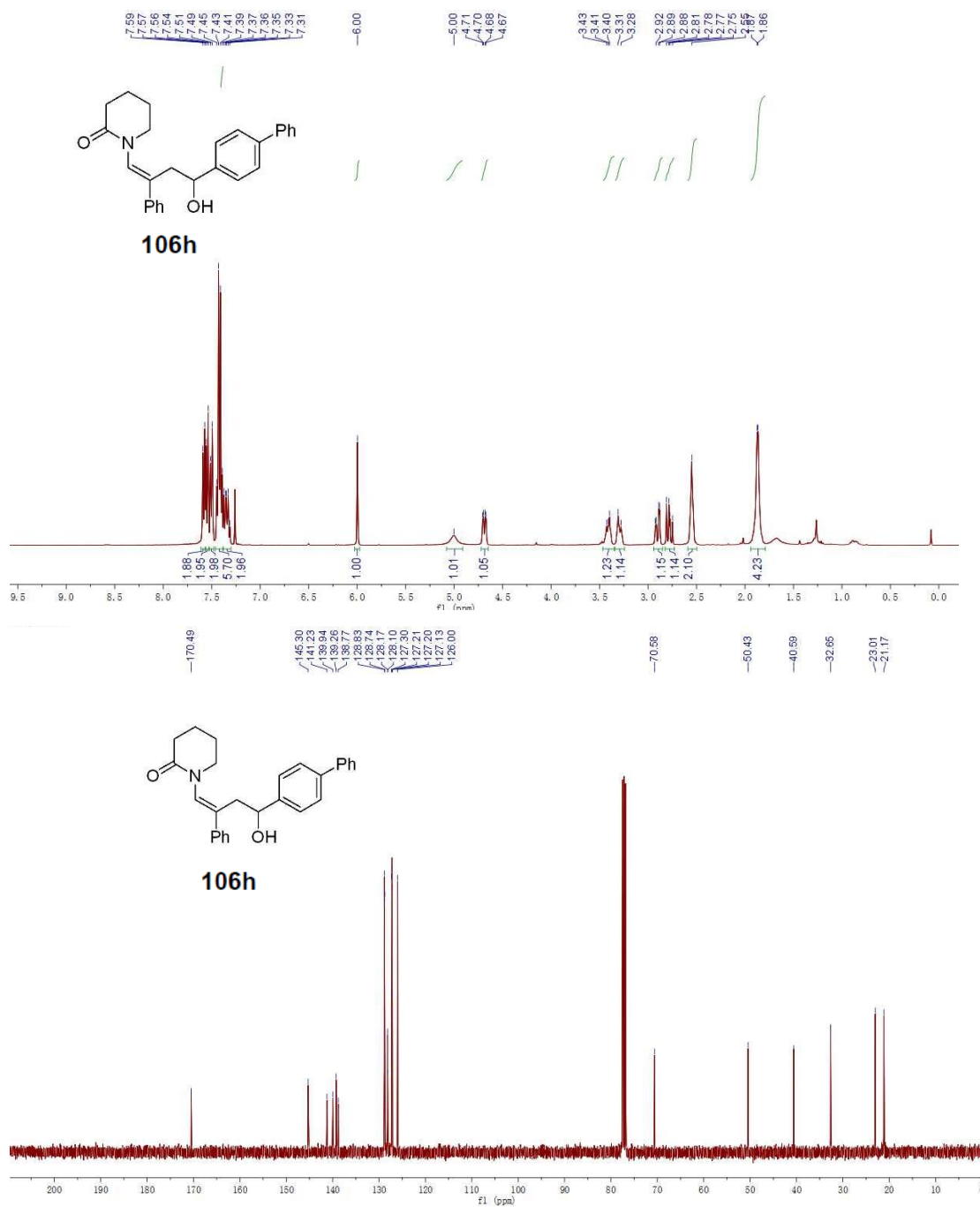
Spectra of Selected Compounds



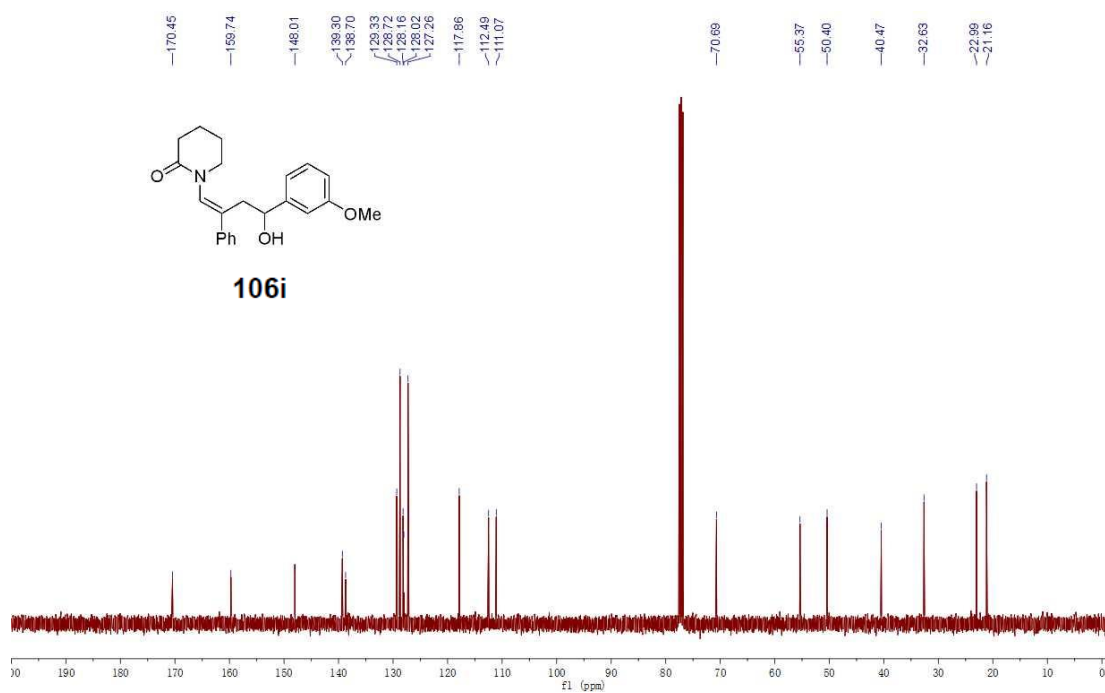
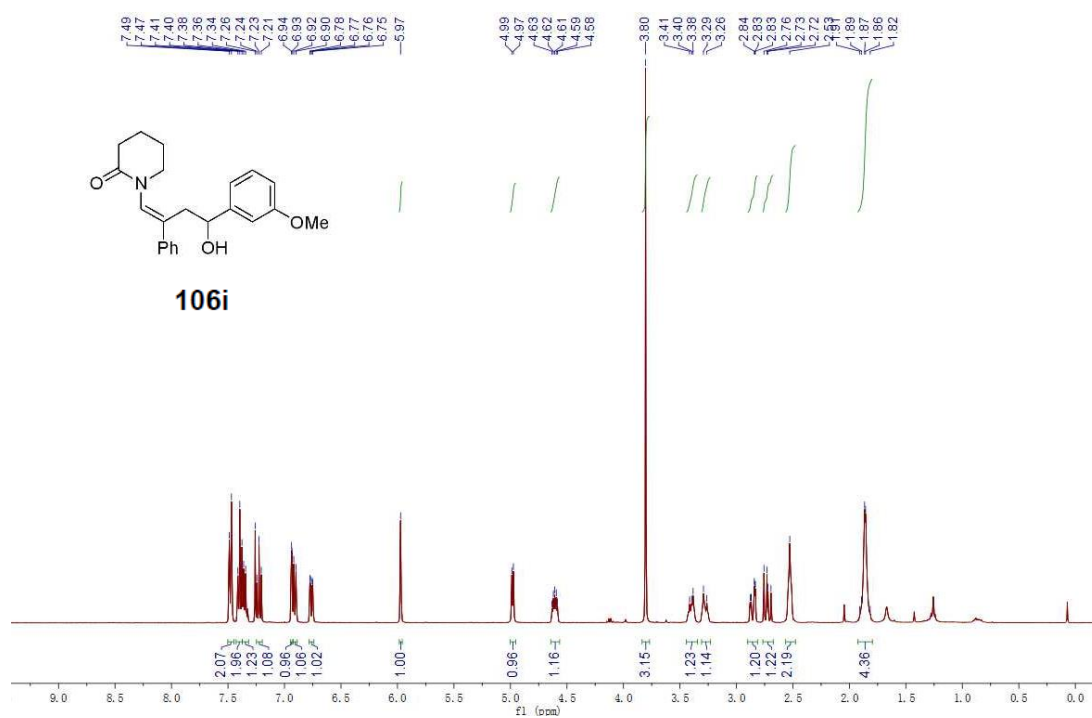
Spectra of Selected Compounds



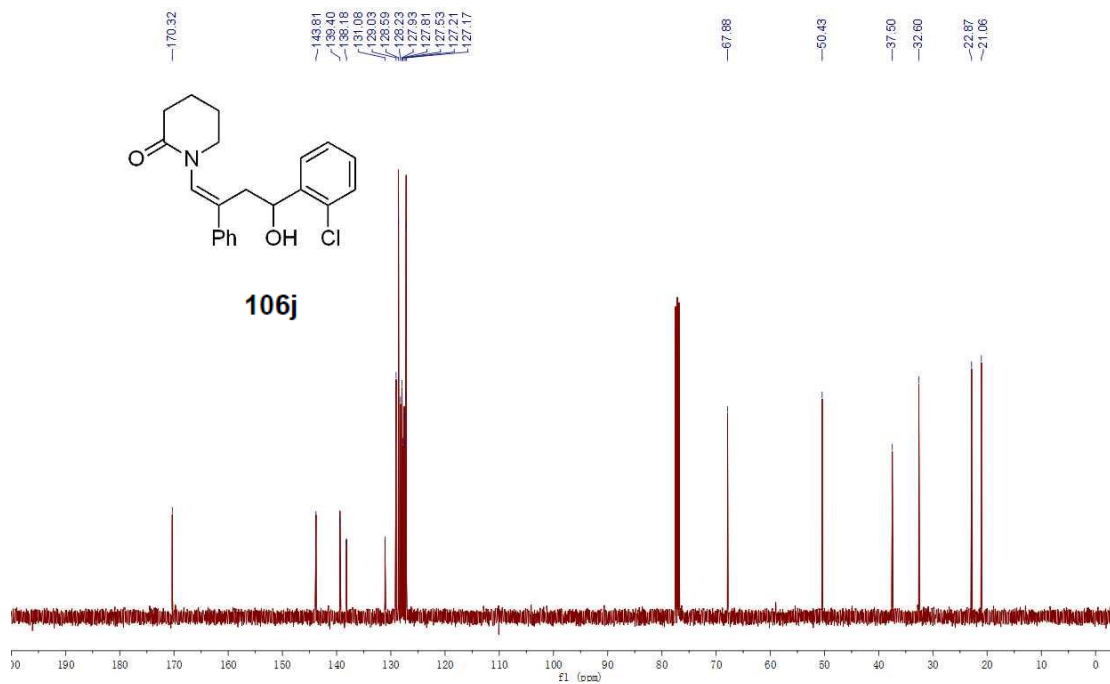
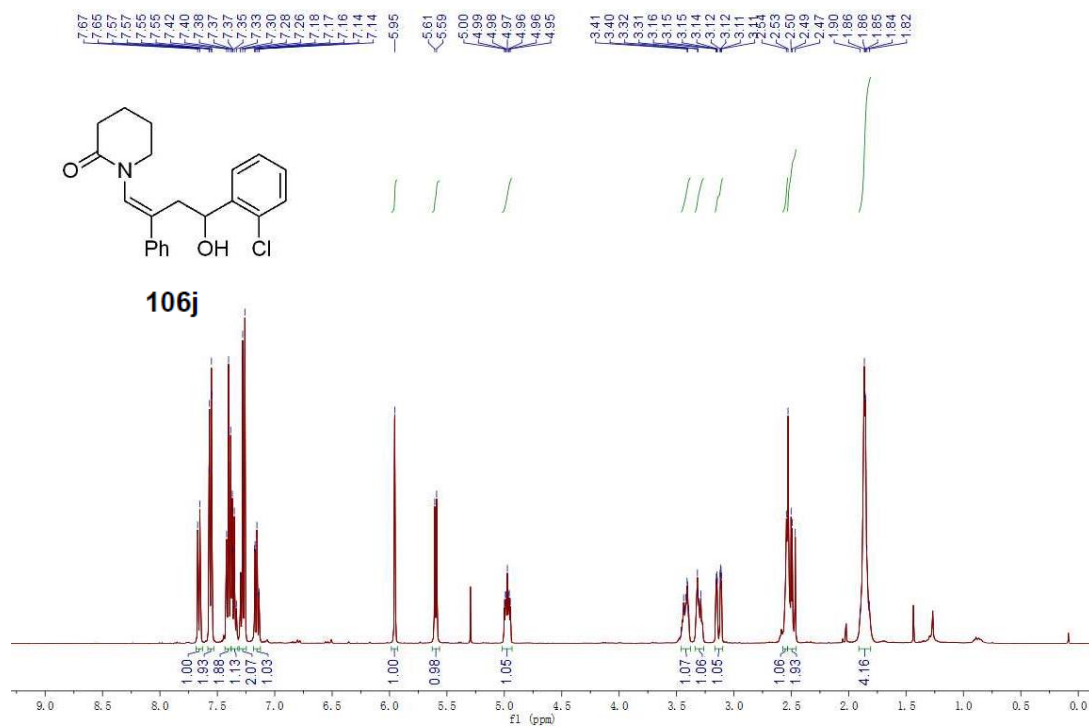
Spectra of Selected Compounds



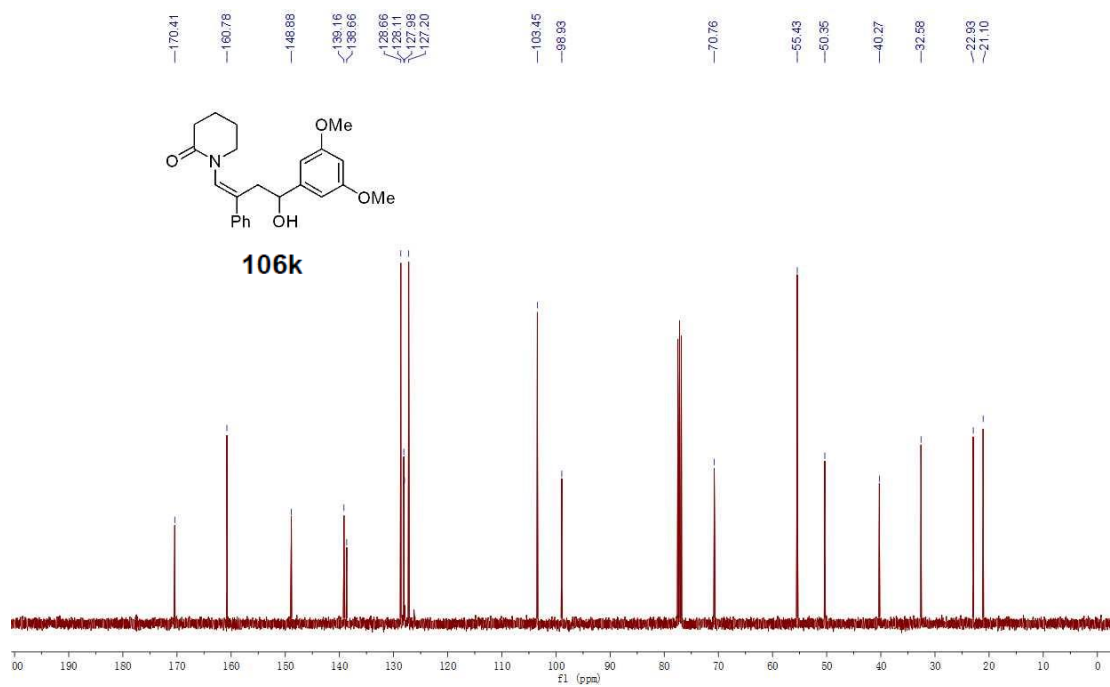
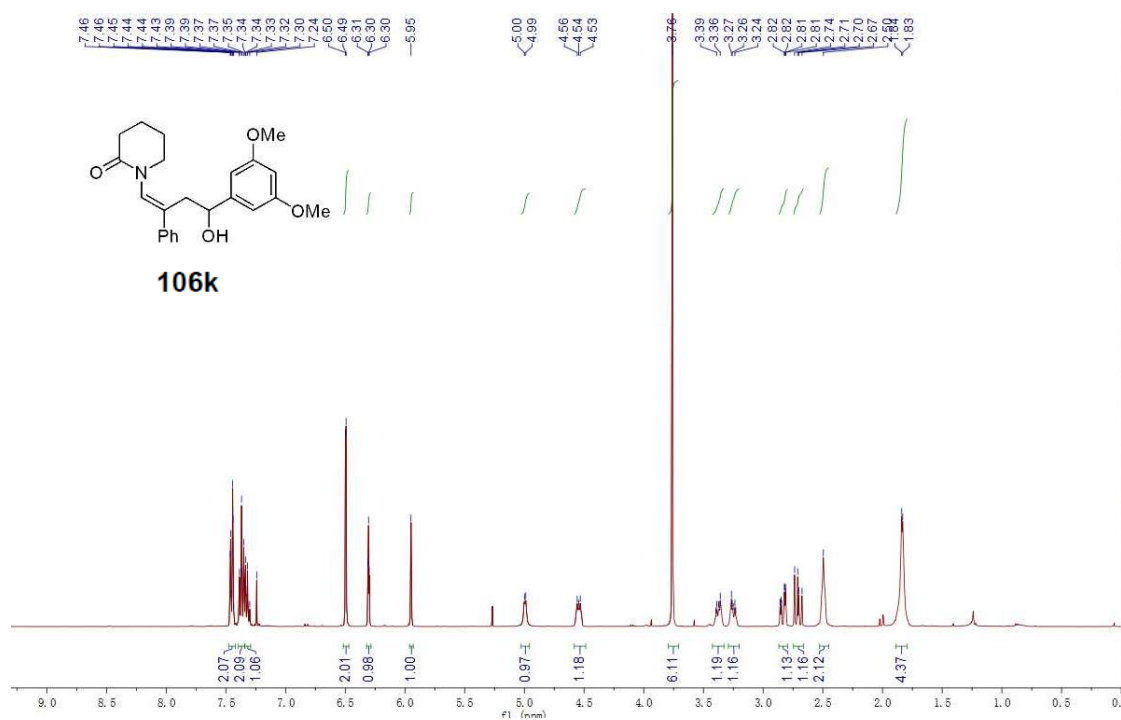
Spectra of Selected Compounds



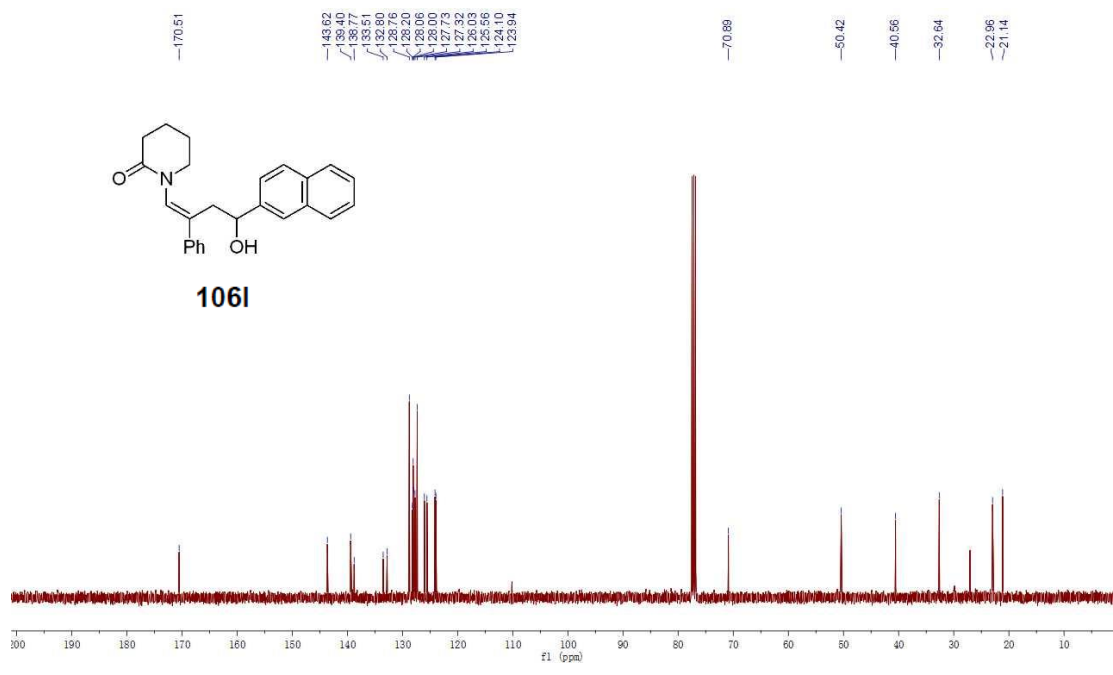
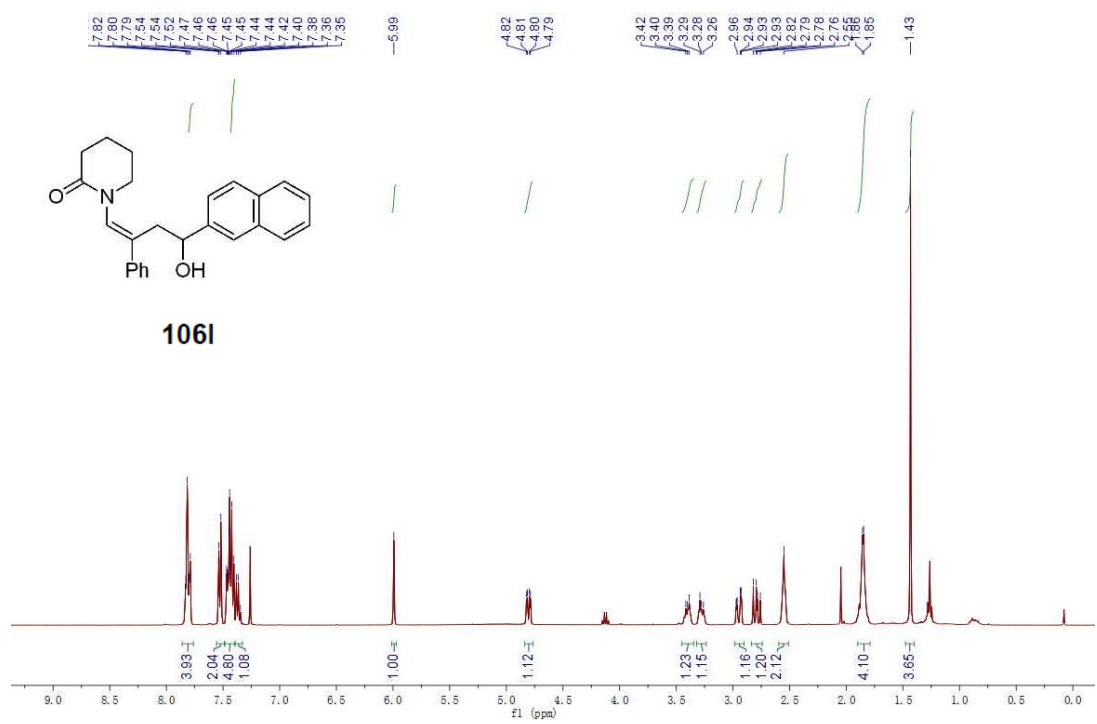
Spectra of Selected Compounds



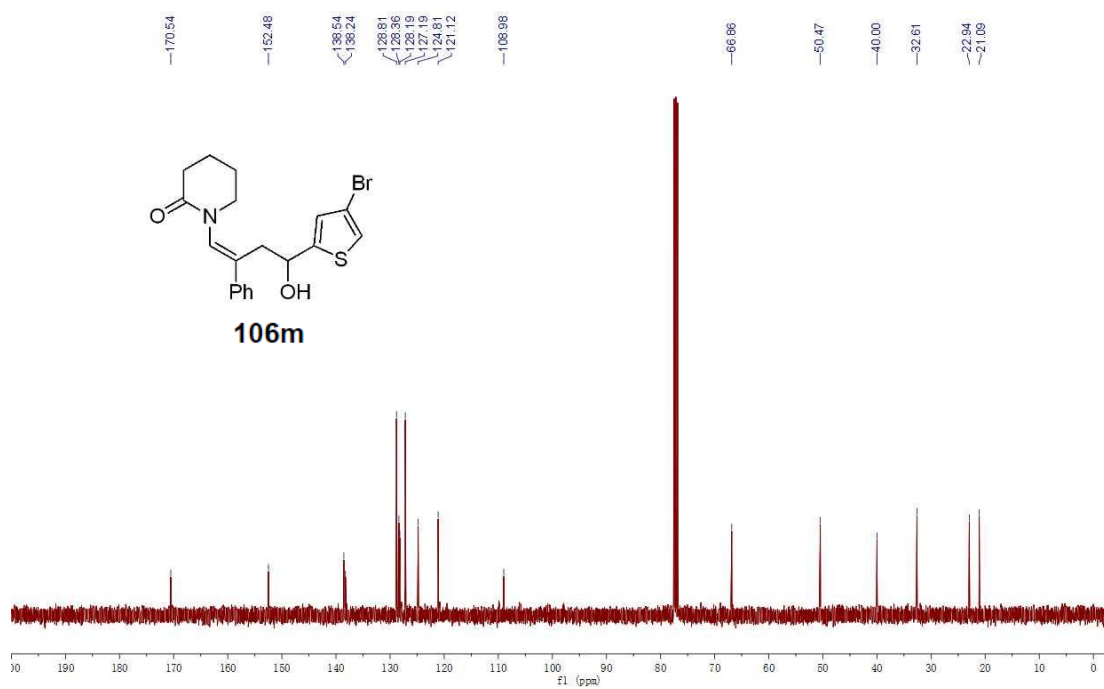
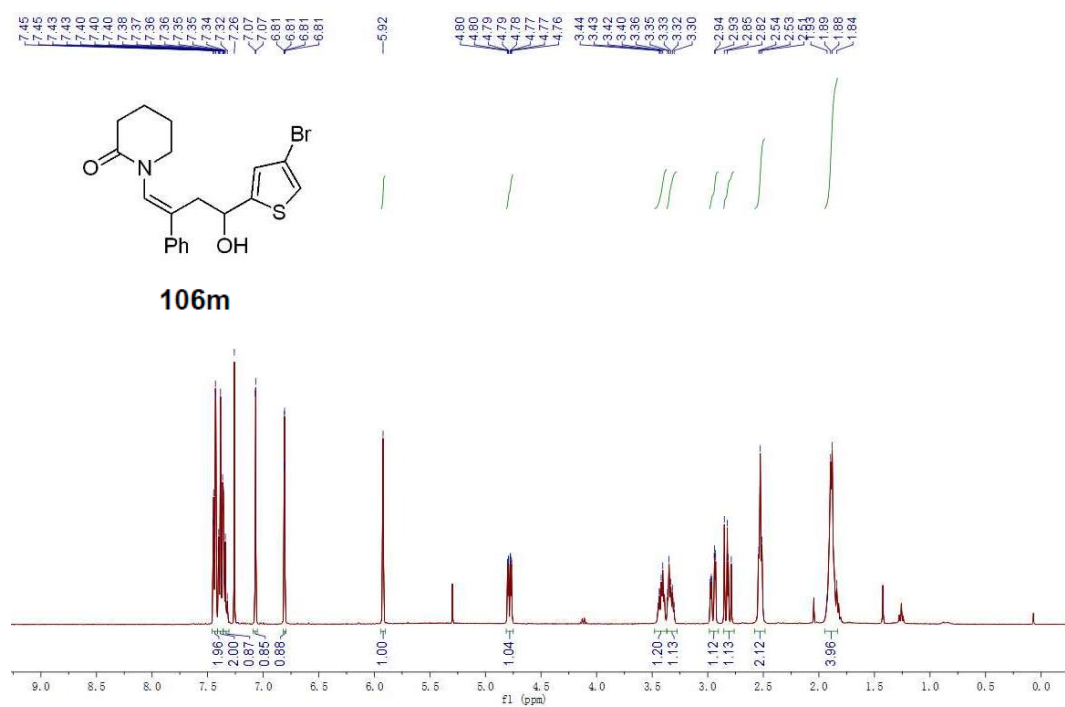
Spectra of Selected Compounds



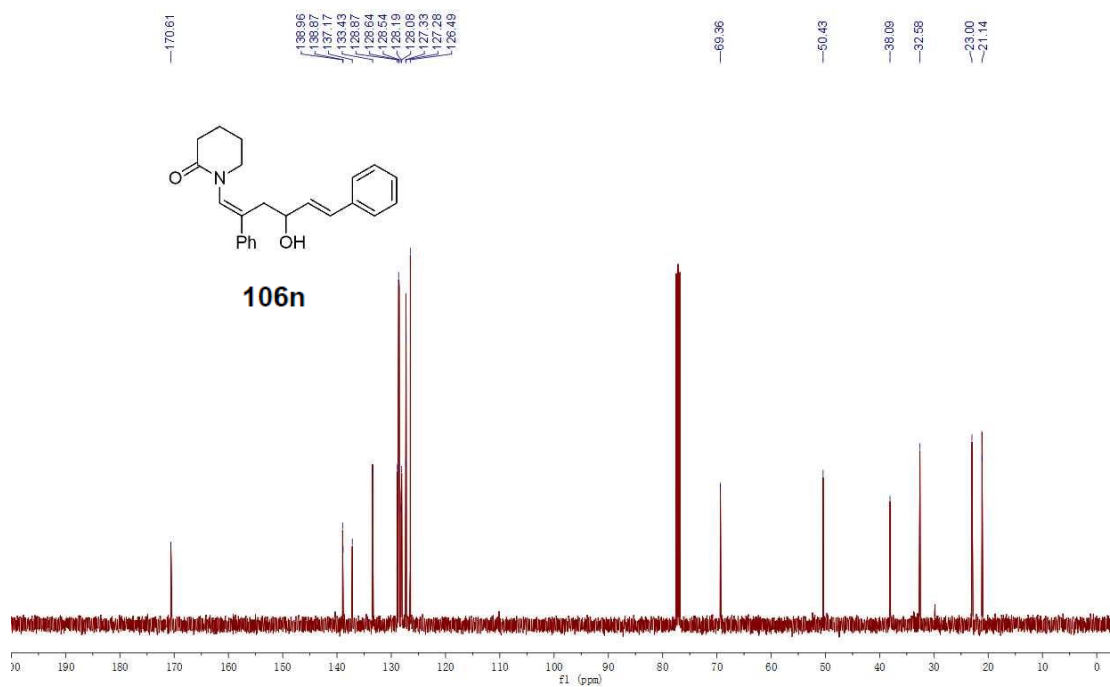
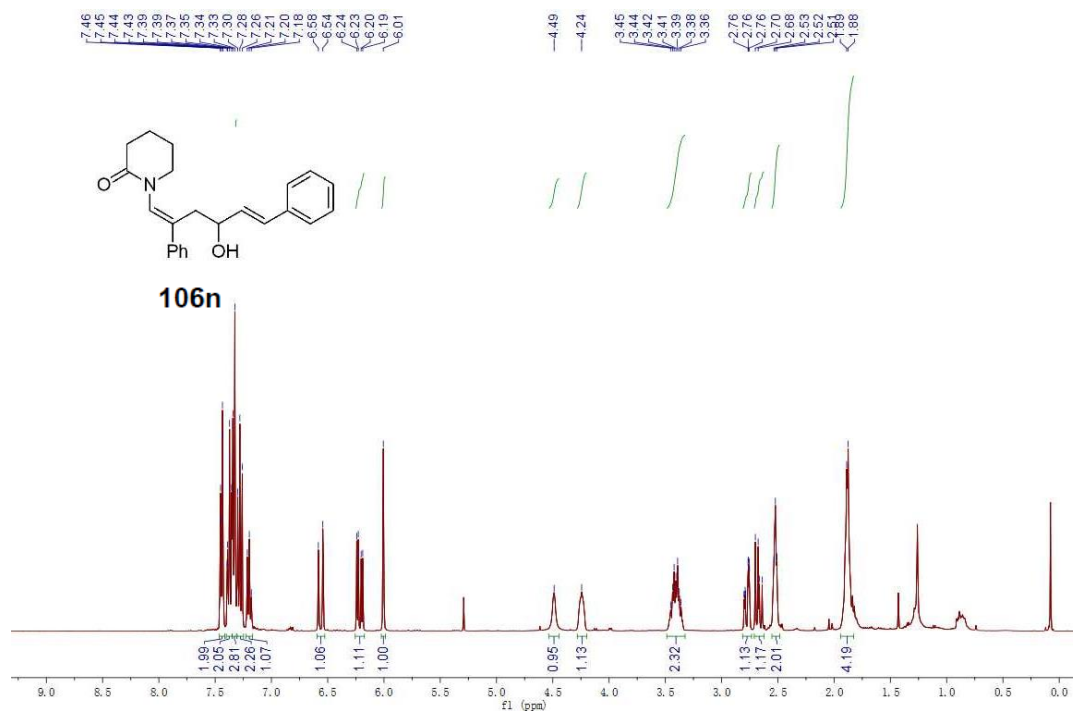
Spectra of Selected Compounds



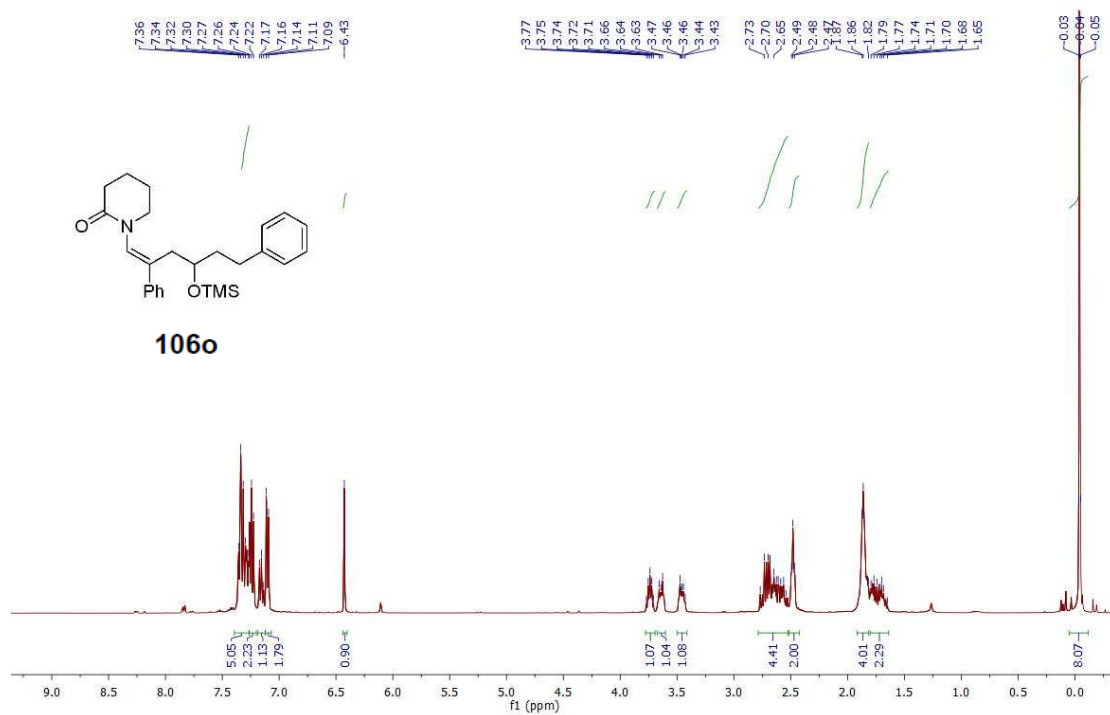
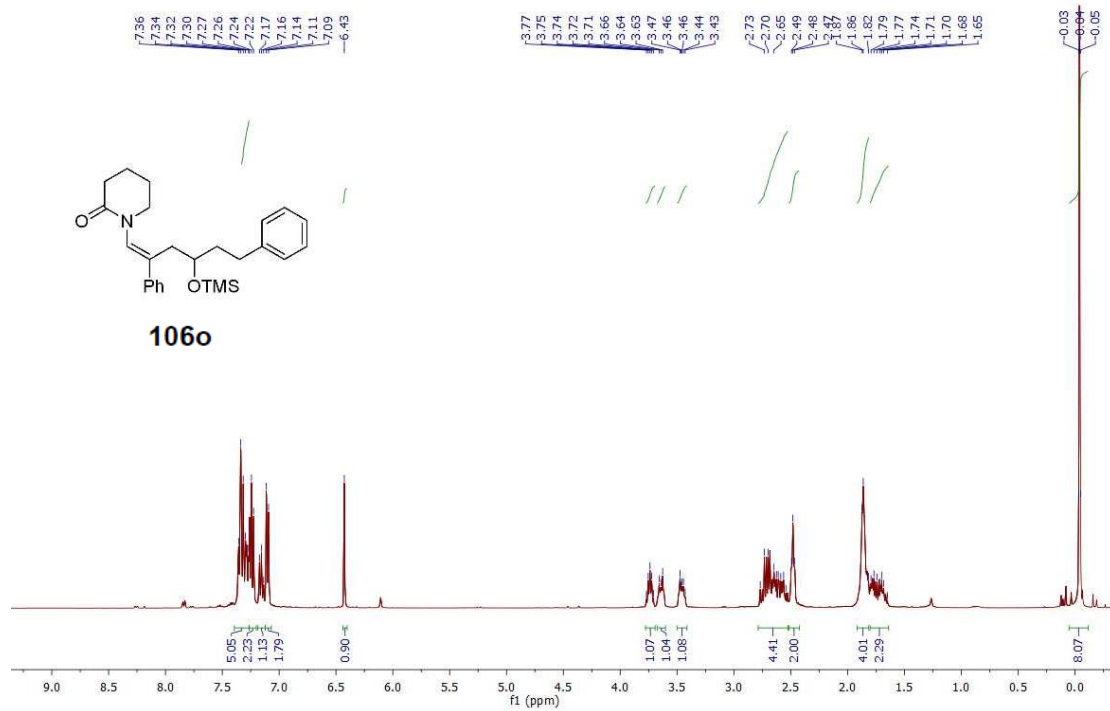
Spectra of Selected Compounds



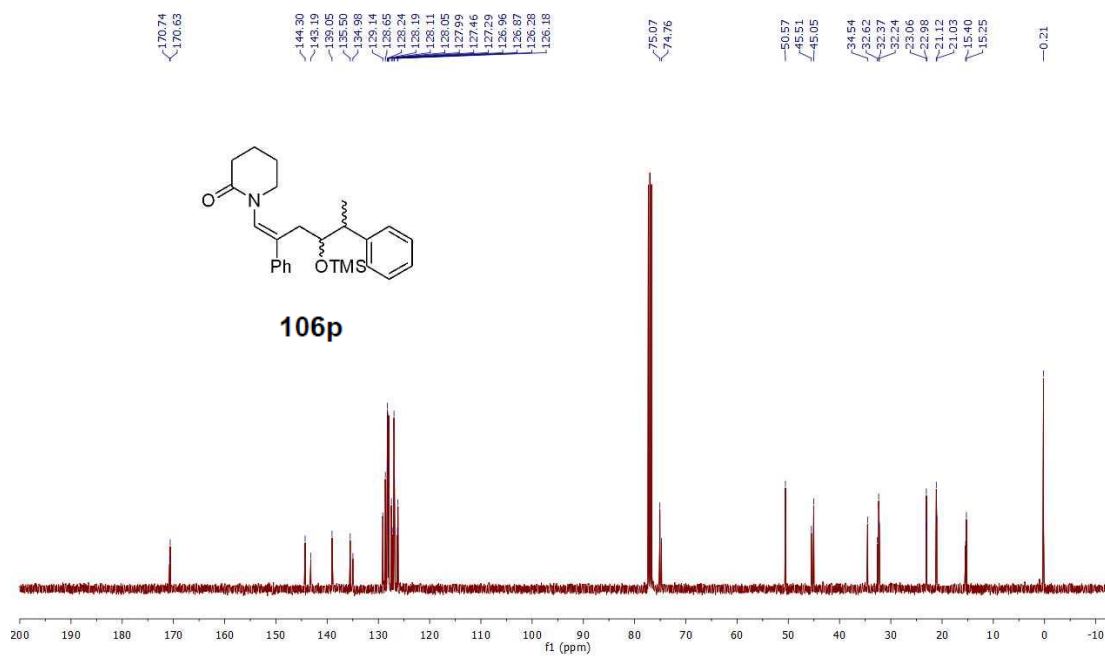
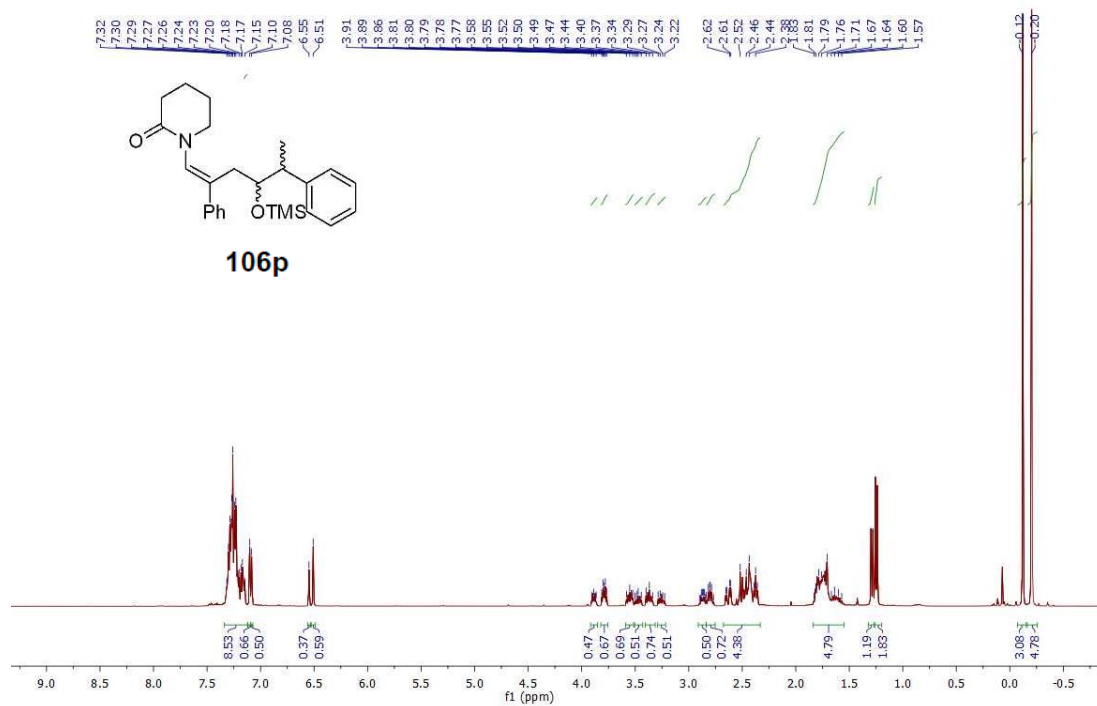
Spectra of Selected Compounds



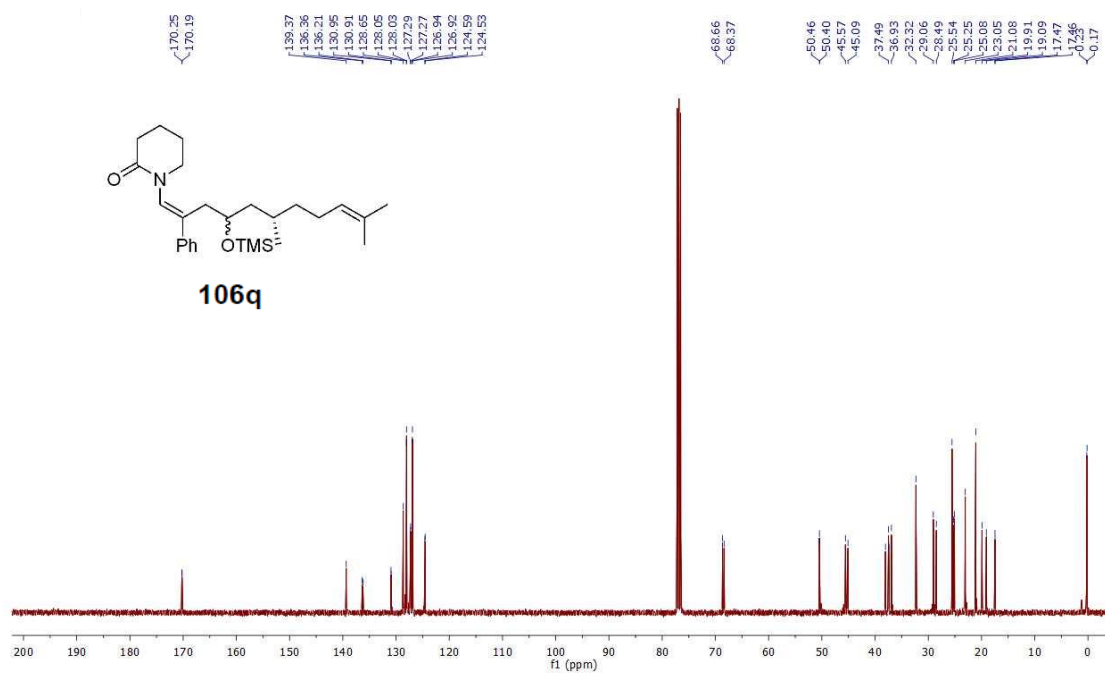
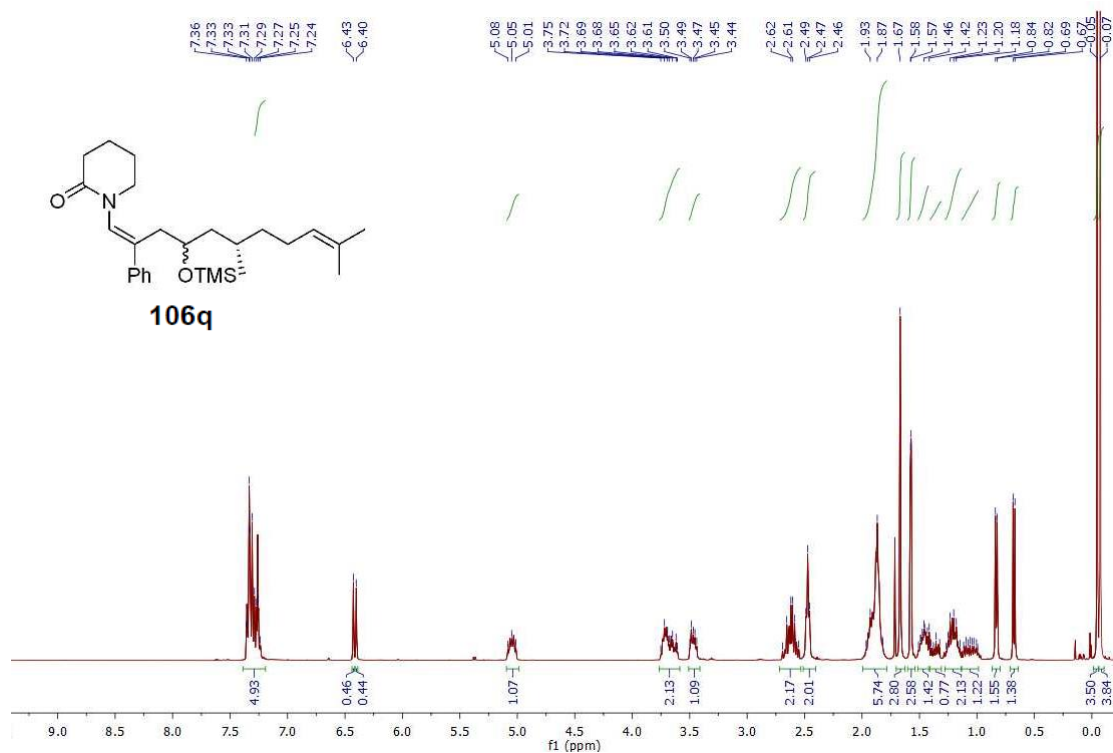
Spectra of Selected Compounds



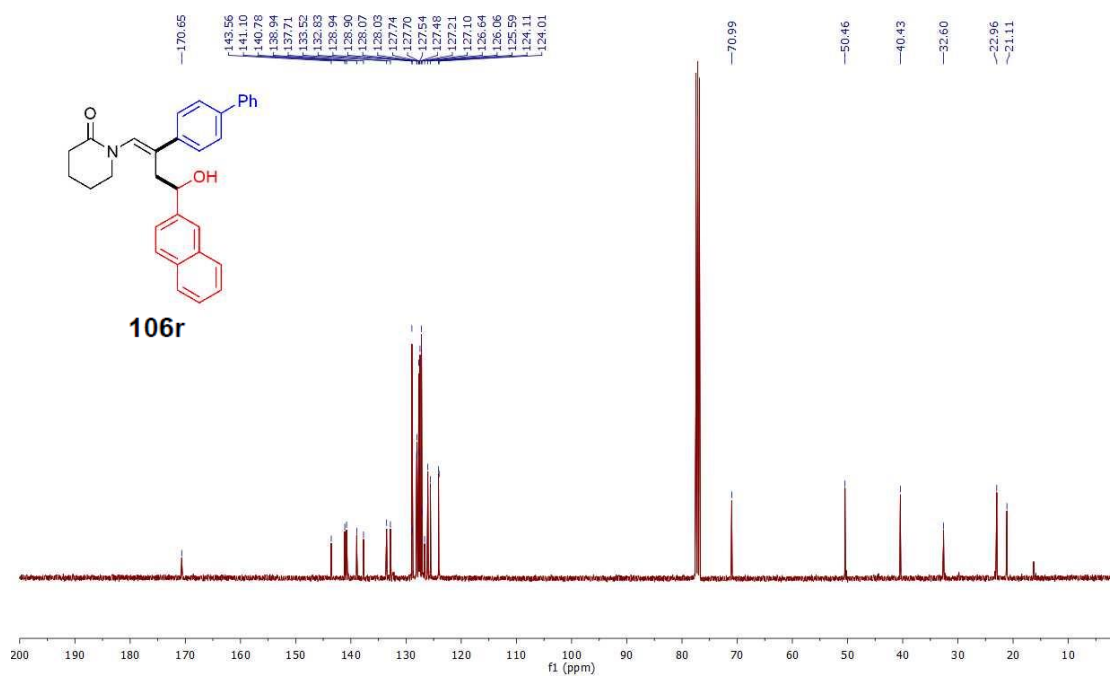
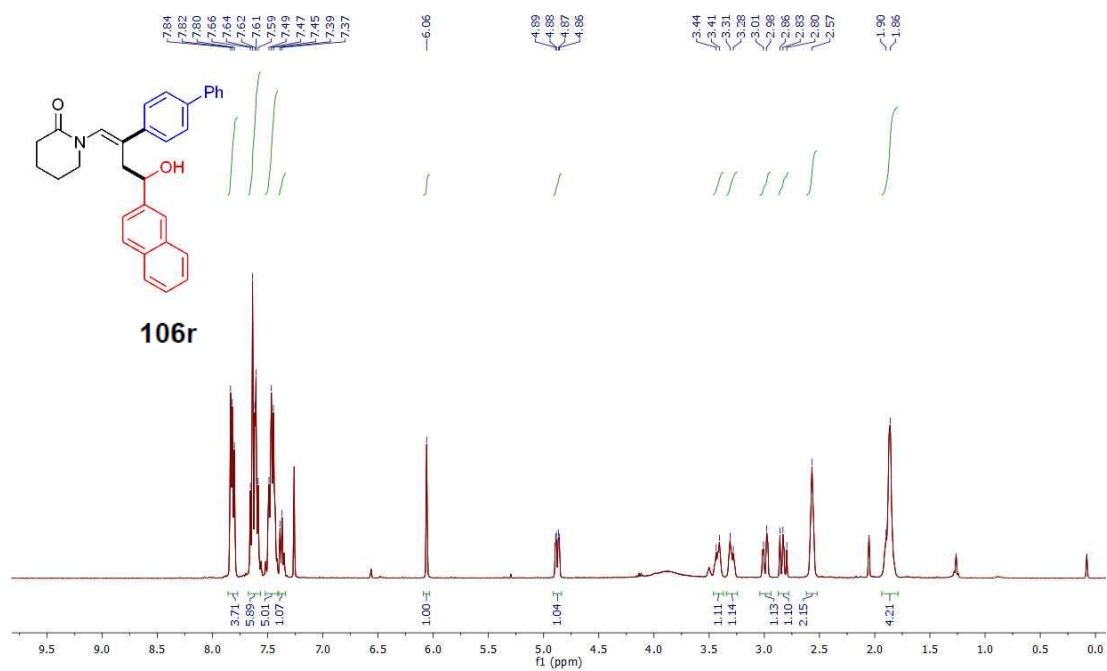
Spectra of Selected Compounds



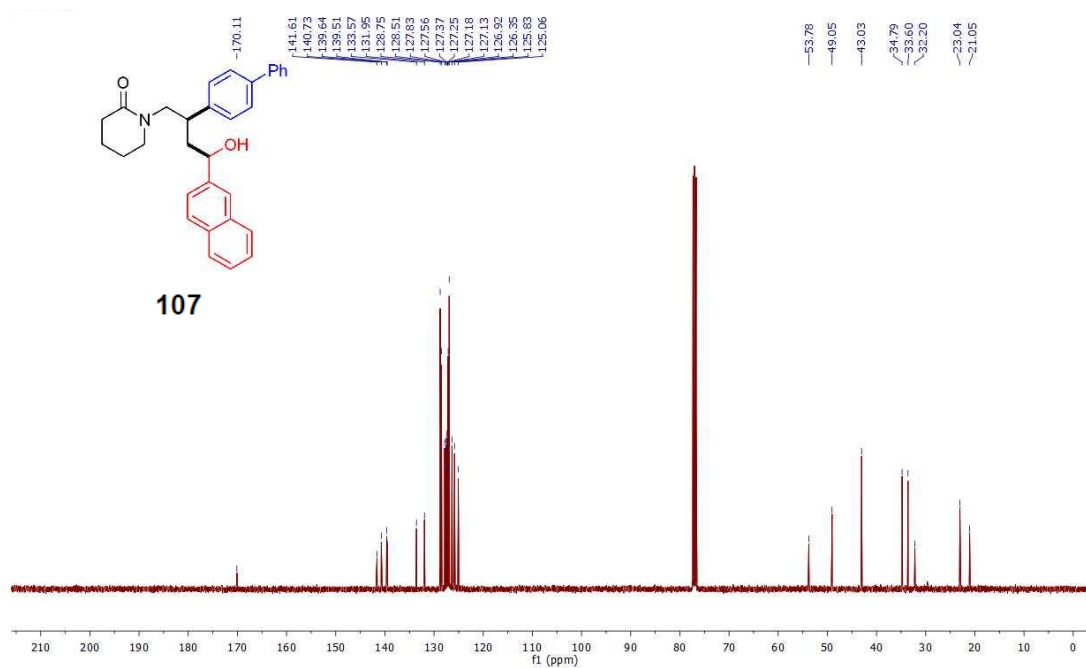
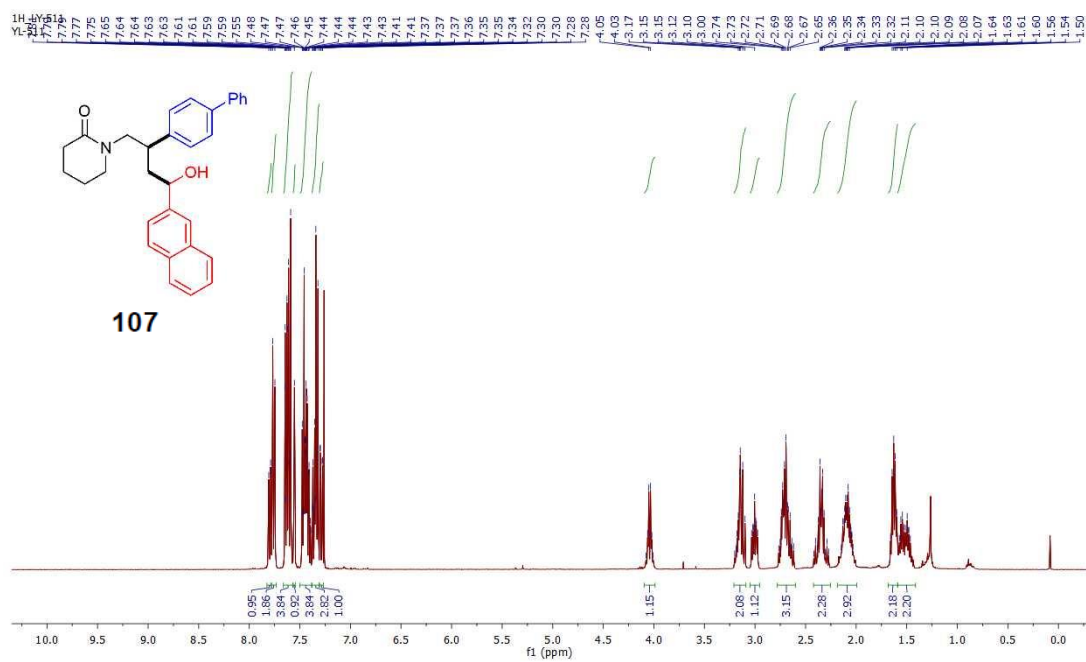
Spectra of Selected Compounds



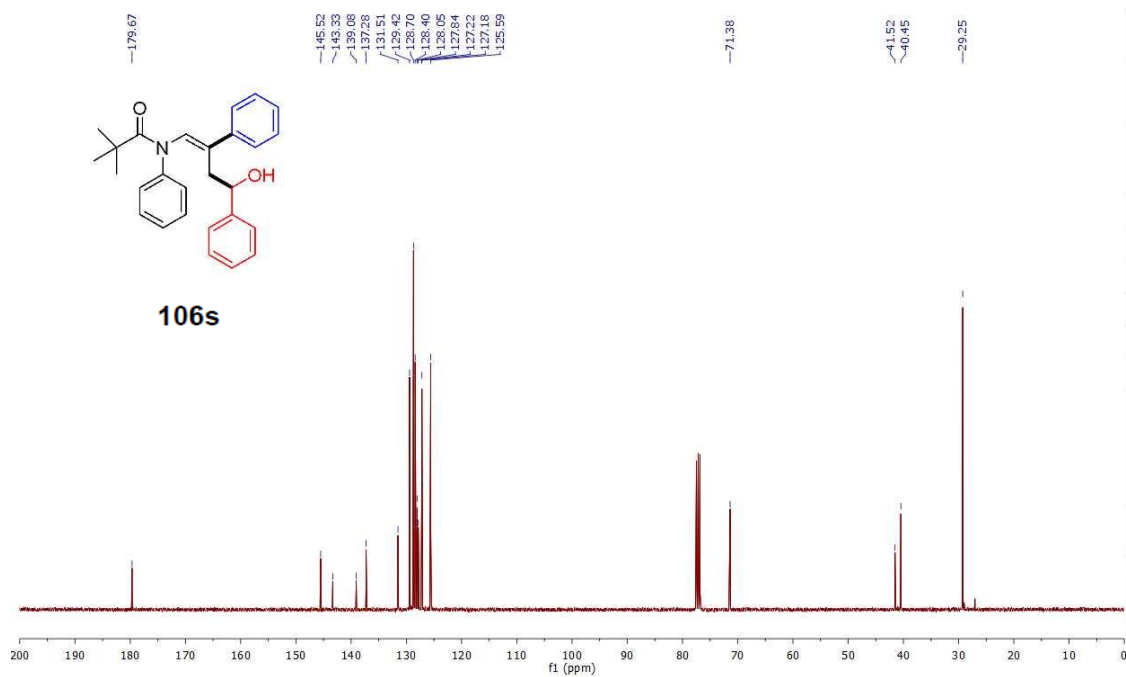
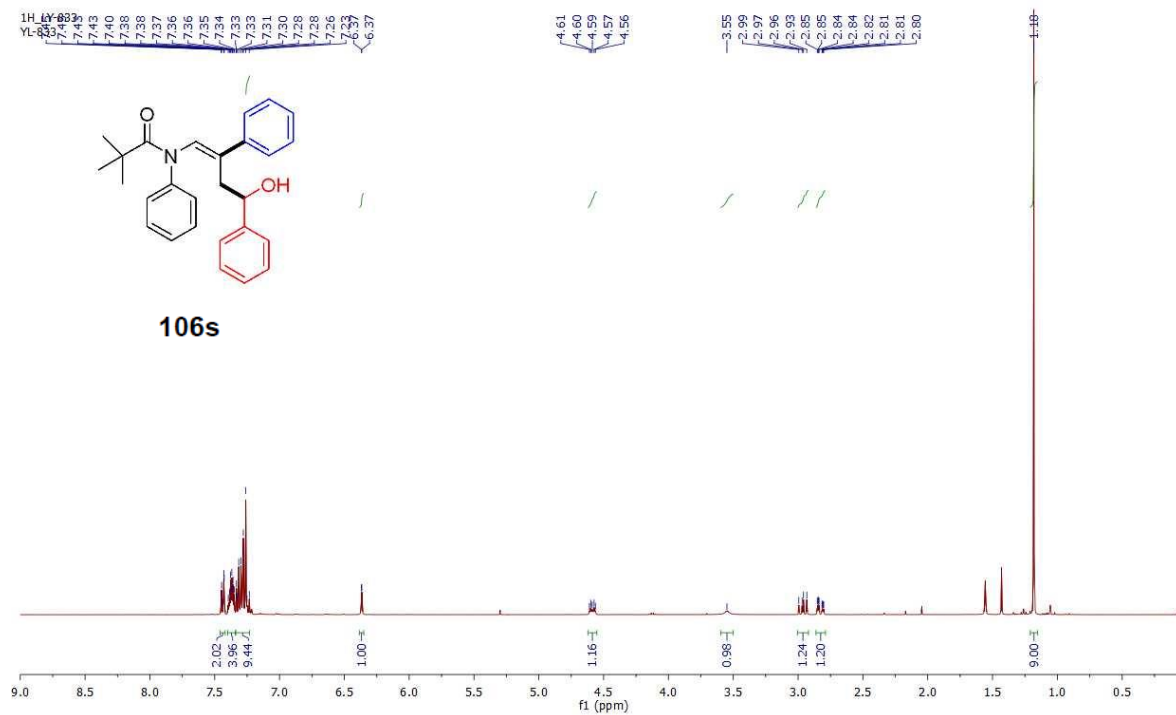
Spectra of Selected Compounds



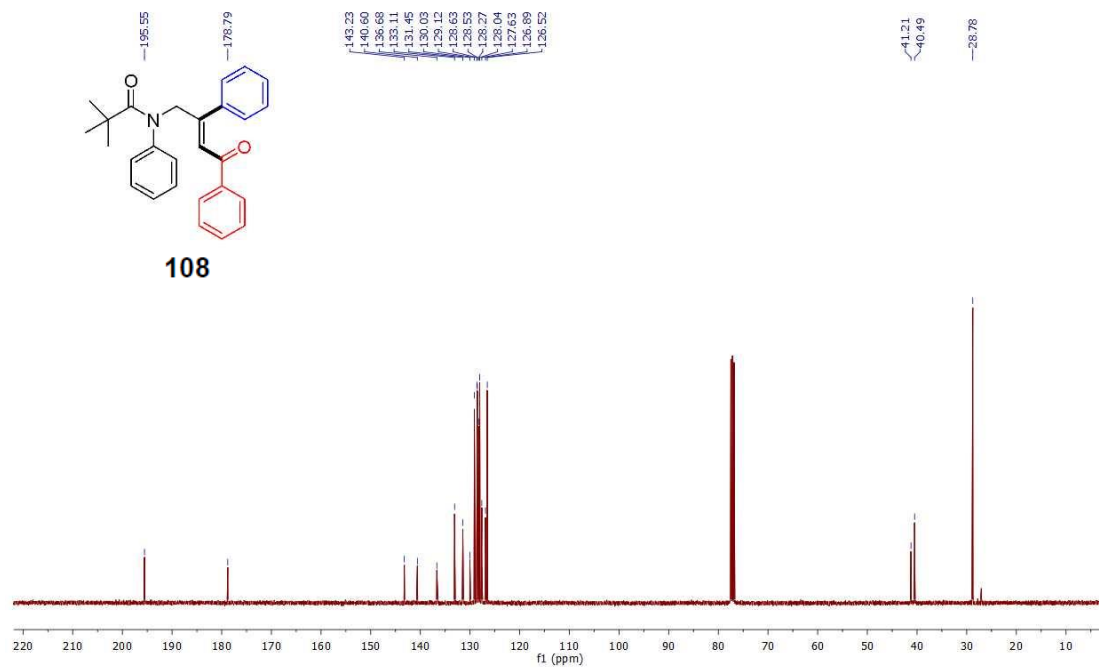
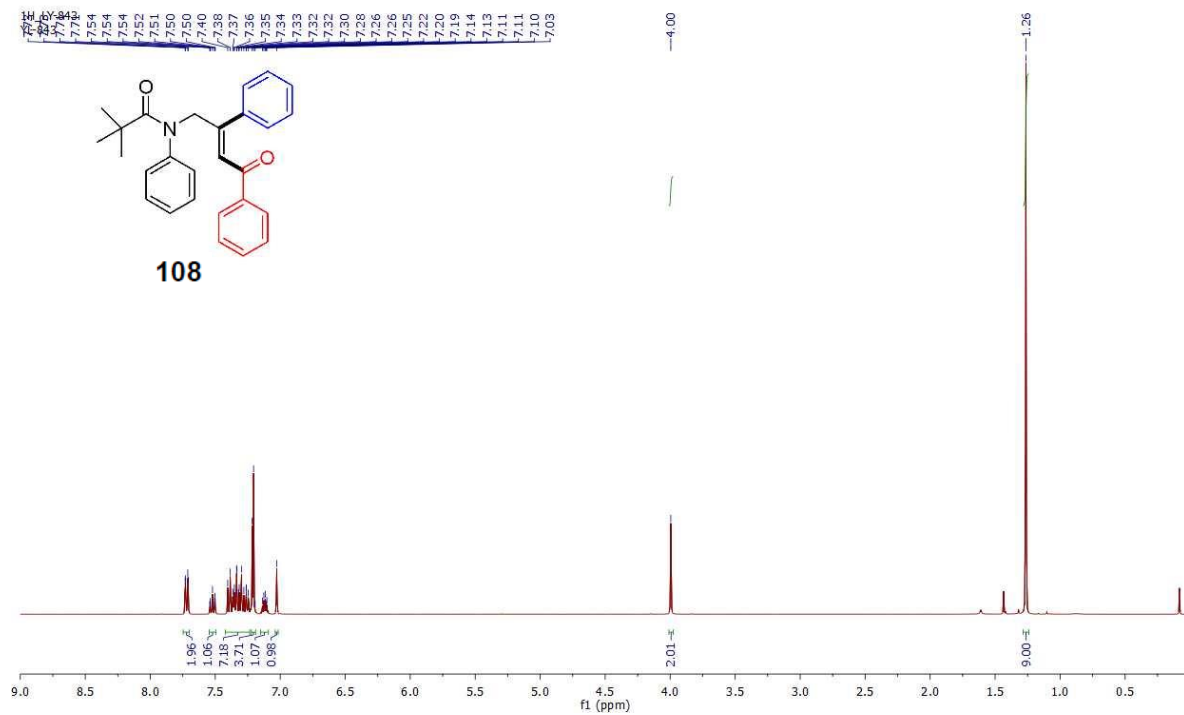
Spectra of Selected Compounds



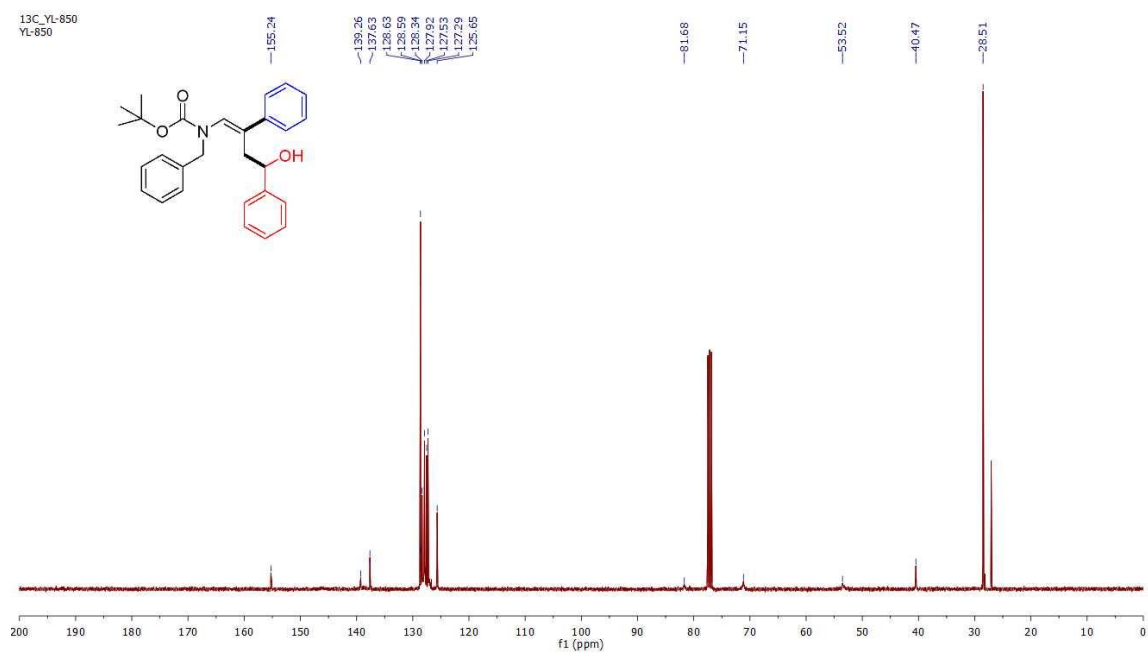
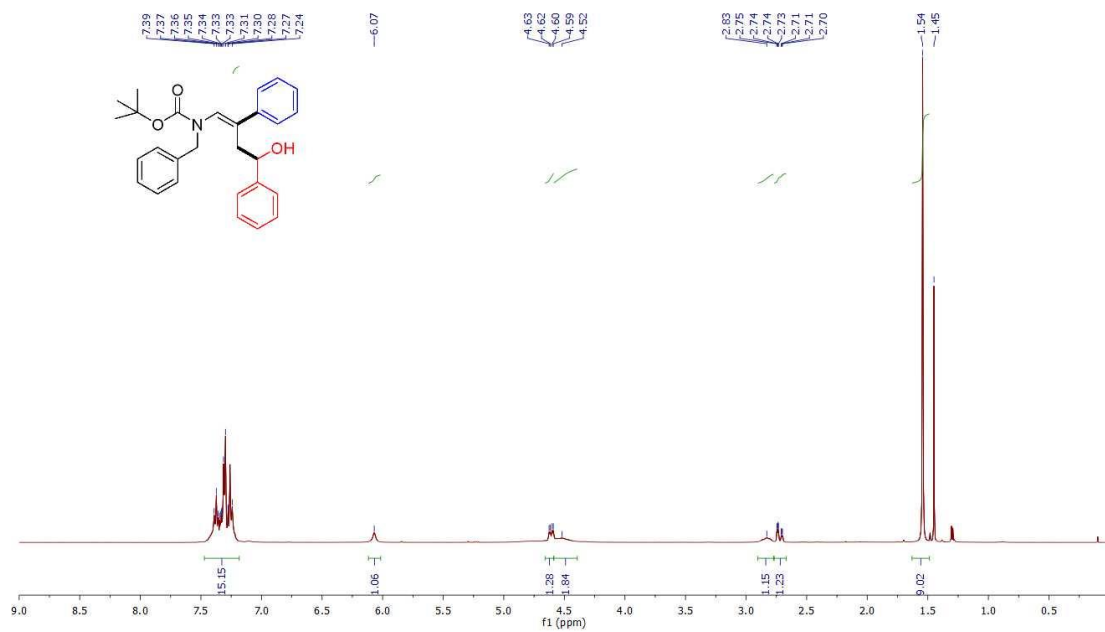
Spectra of Selected Compounds



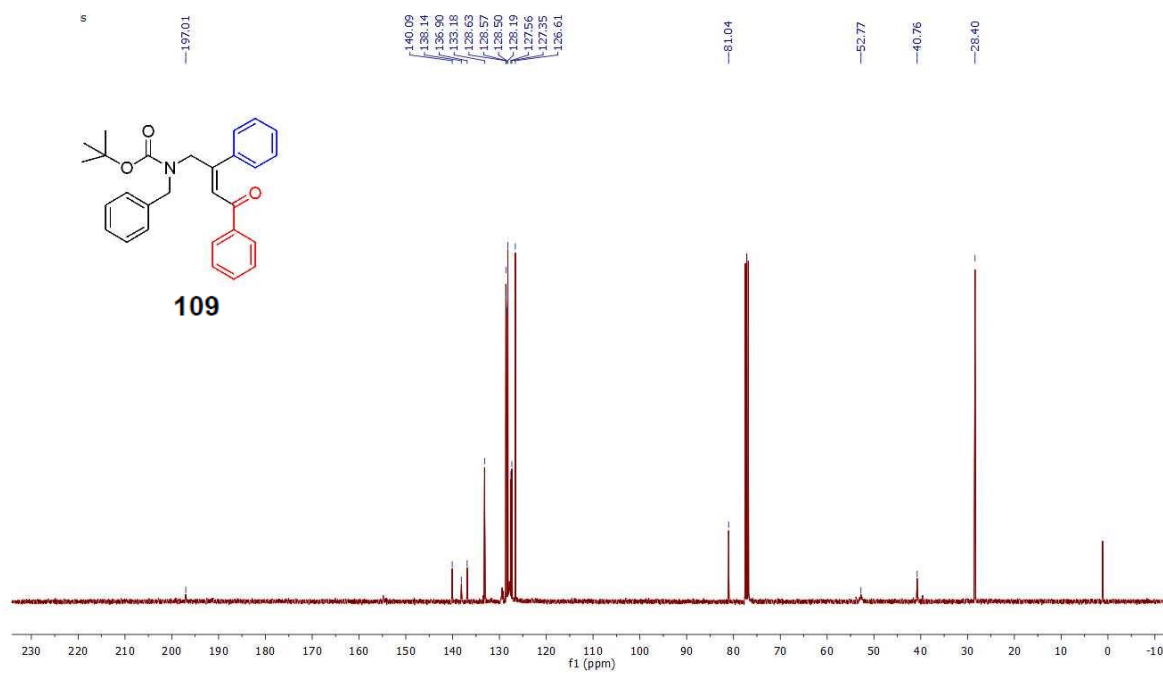
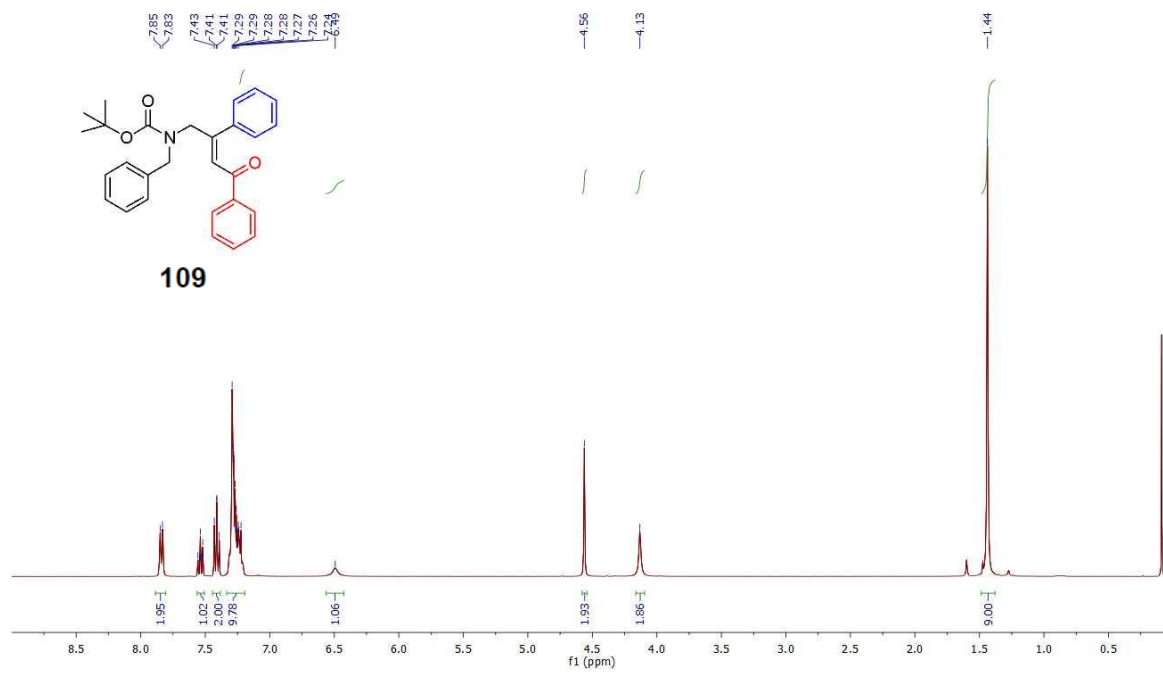
Spectra of Selected Compounds



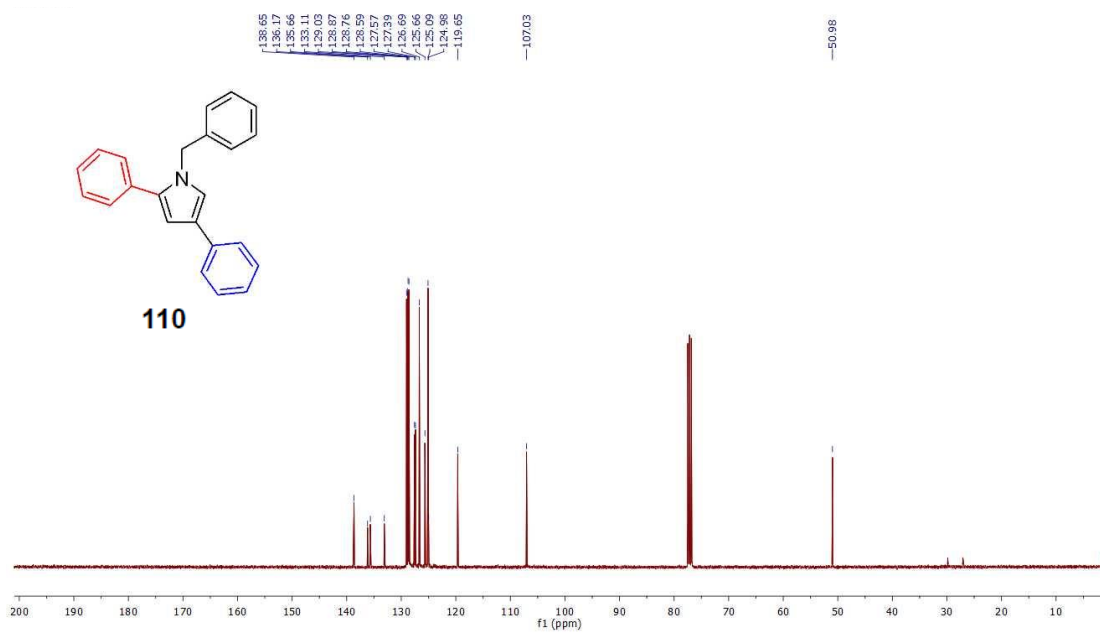
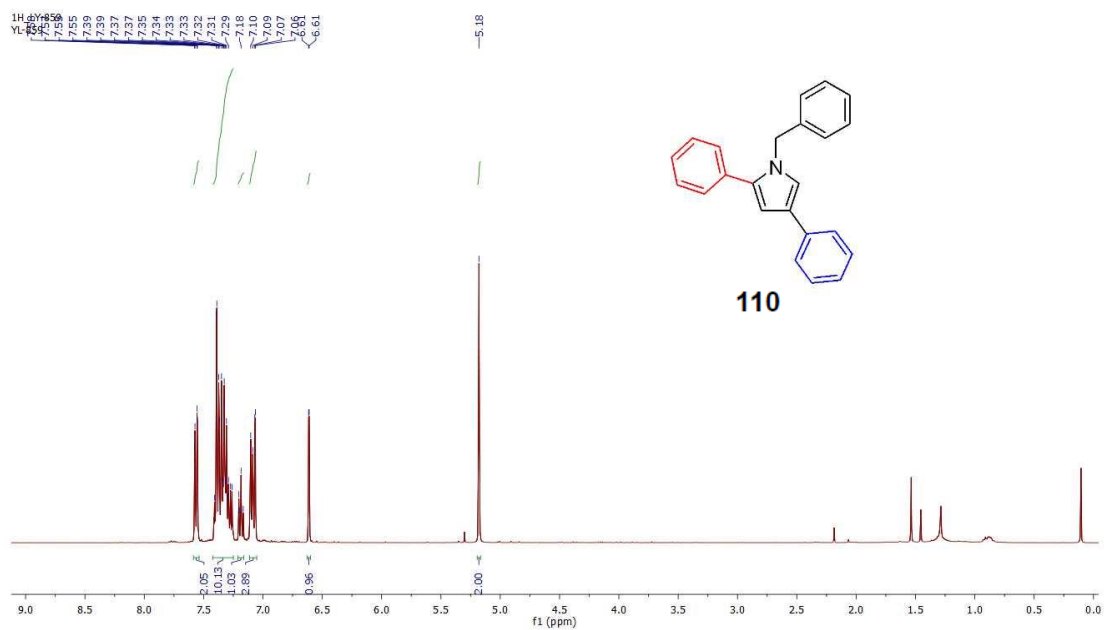
Spectra of Selected Compounds



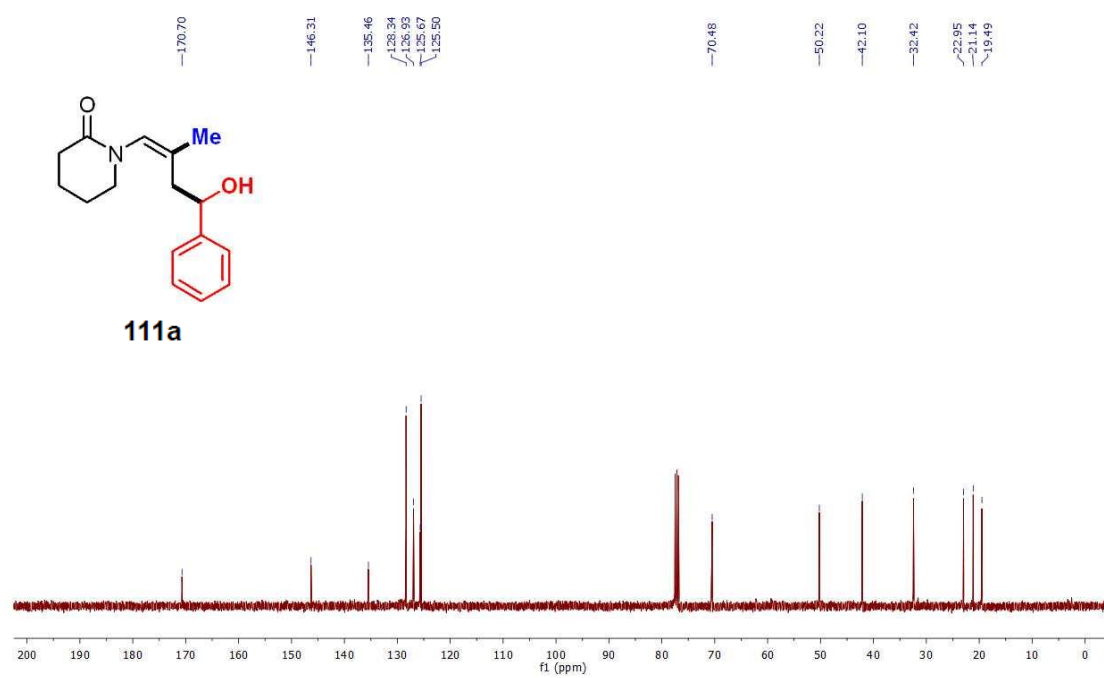
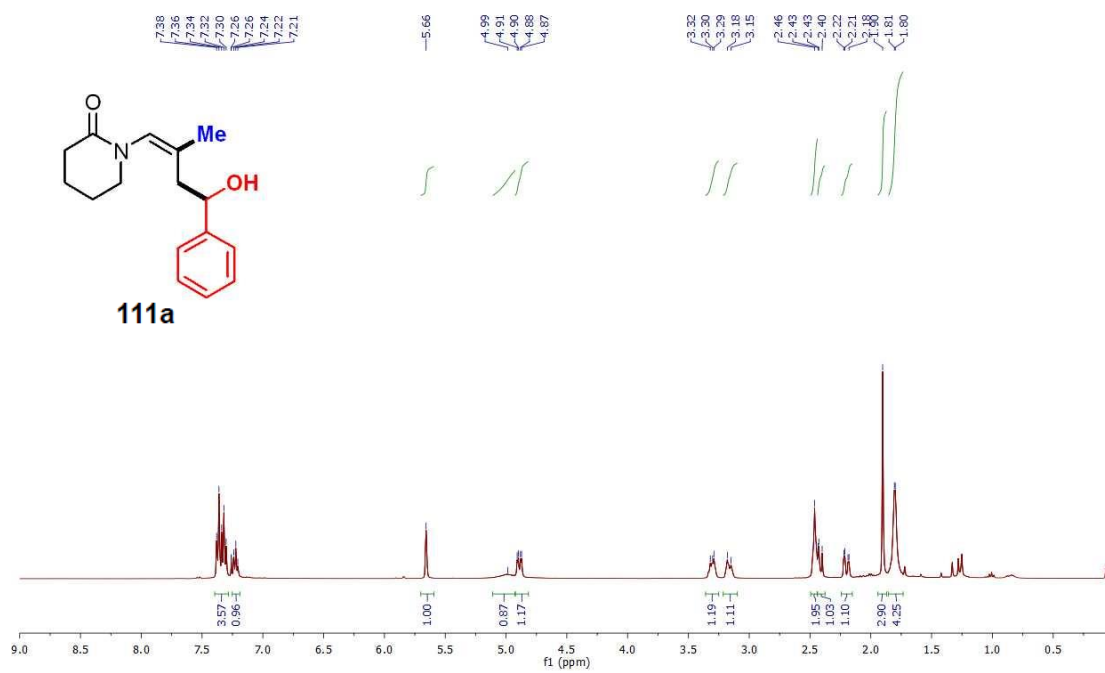
Spectra of Selected Compounds



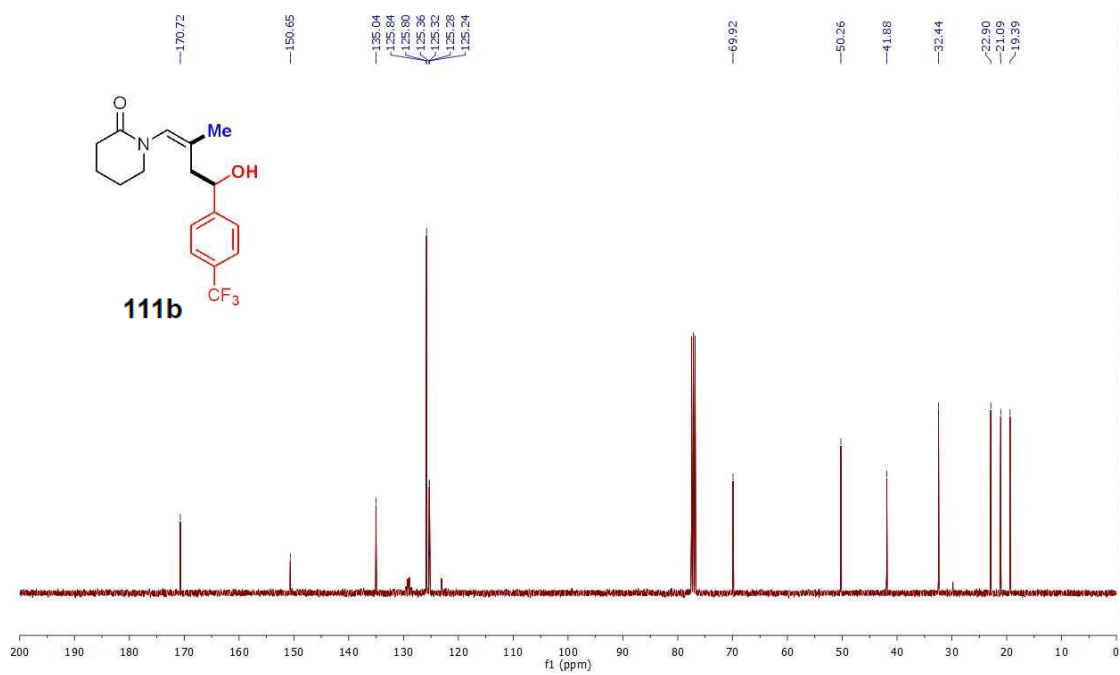
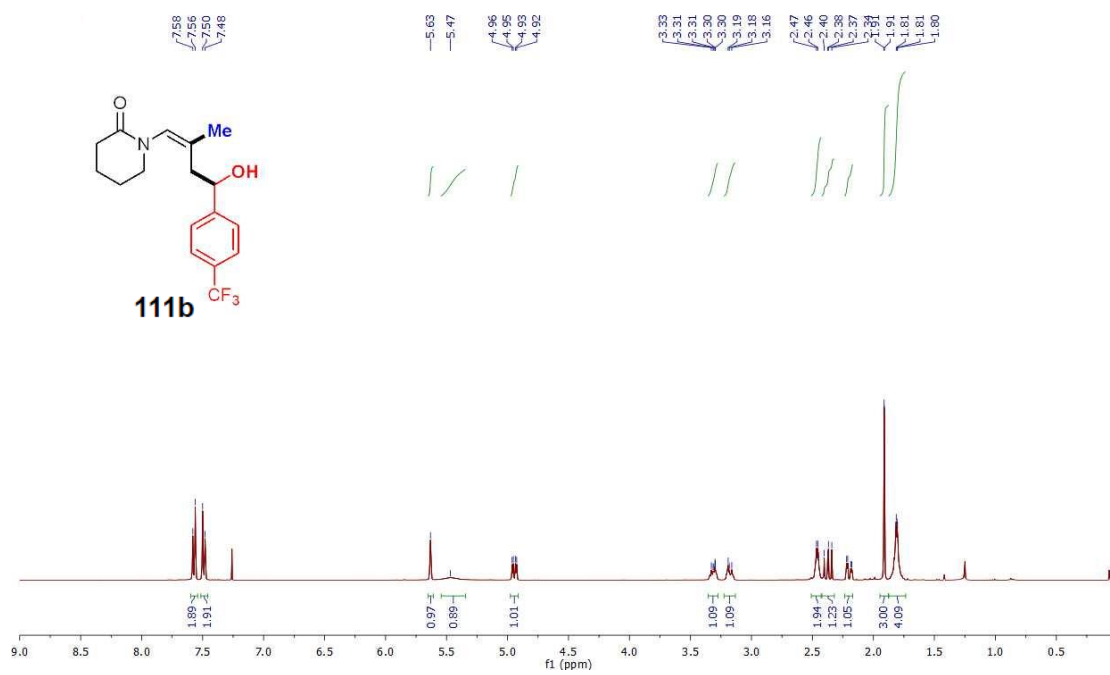
Spectra of Selected Compounds



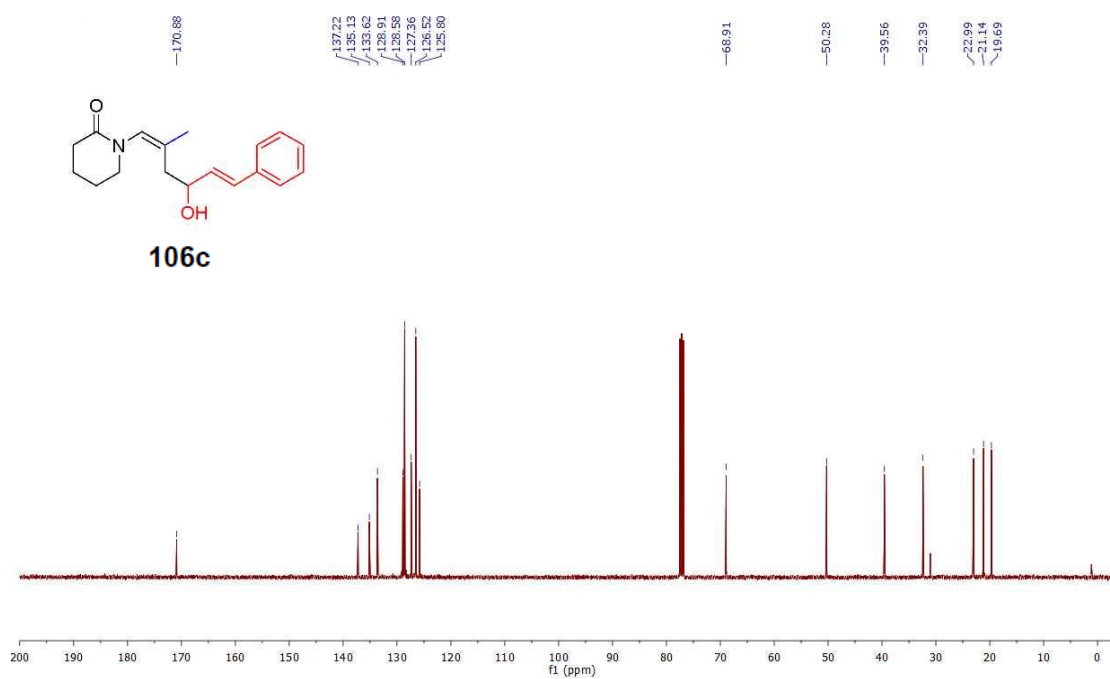
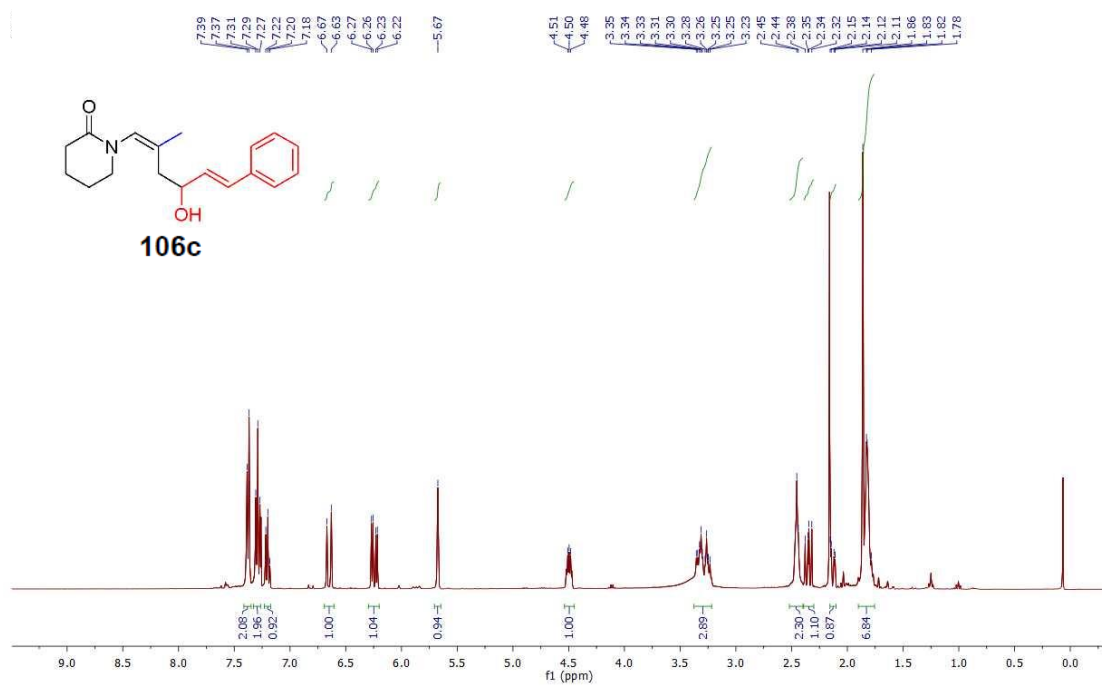
Spectra of Selected Compounds



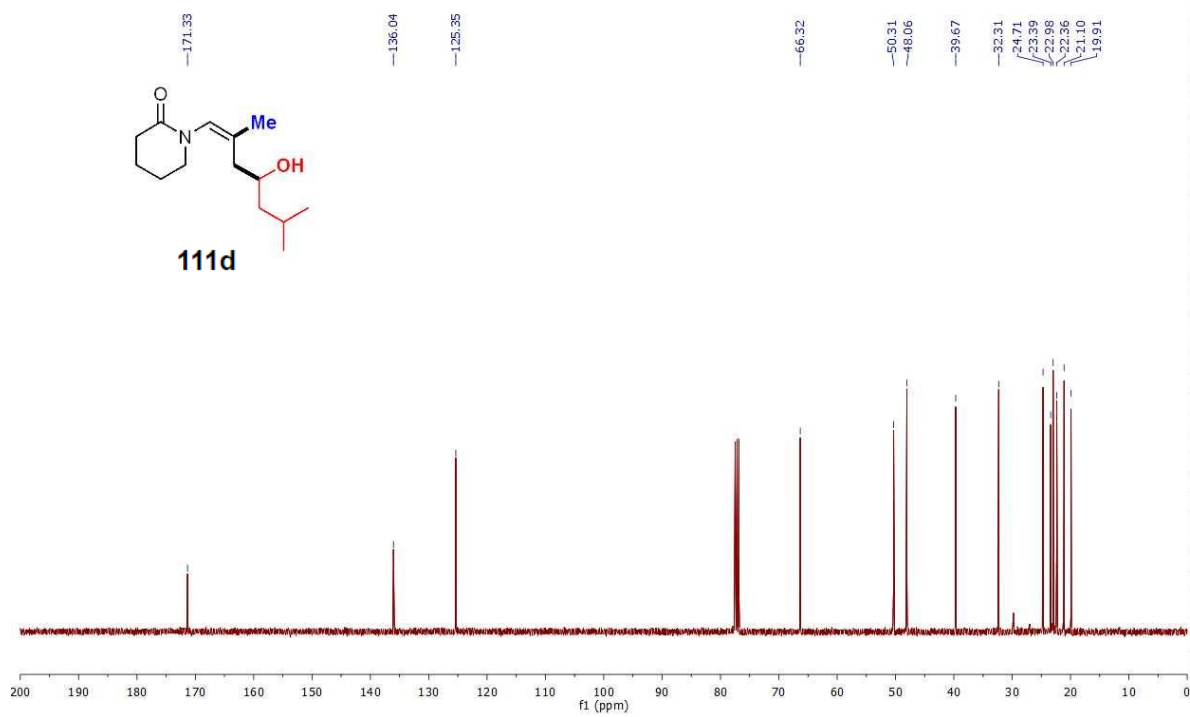
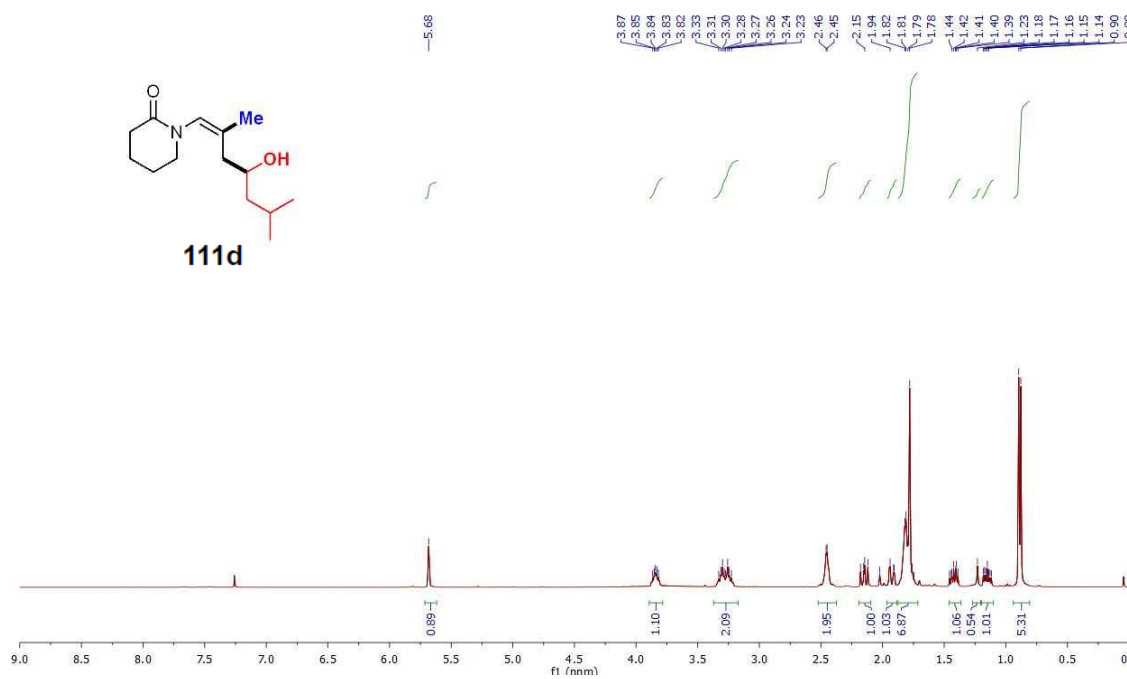
Spectra of Selected Compounds



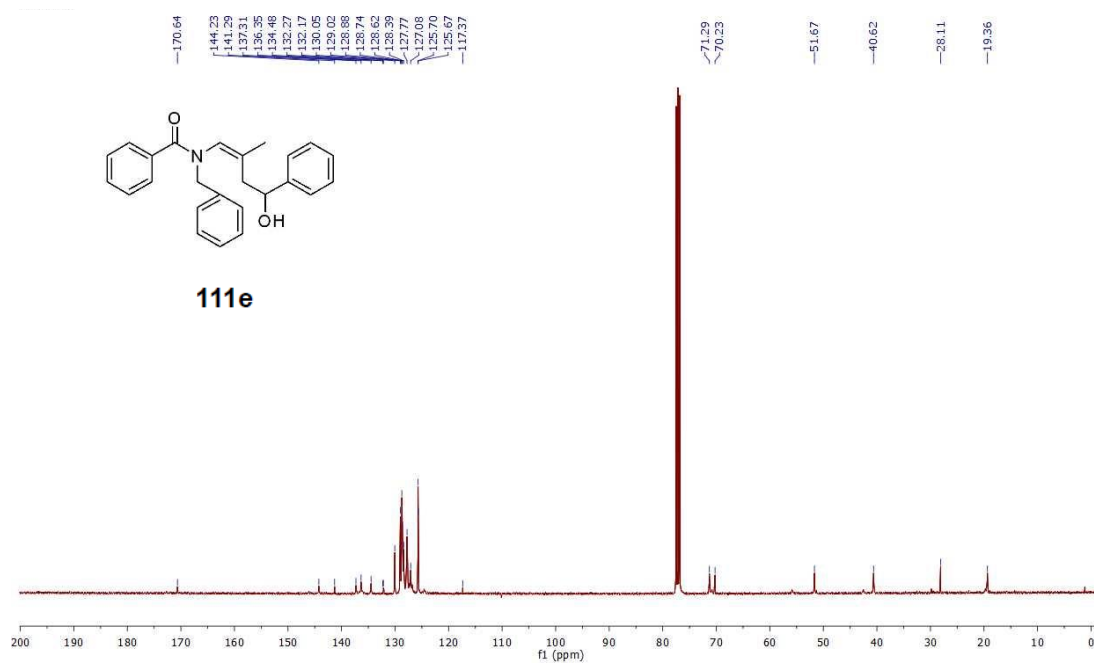
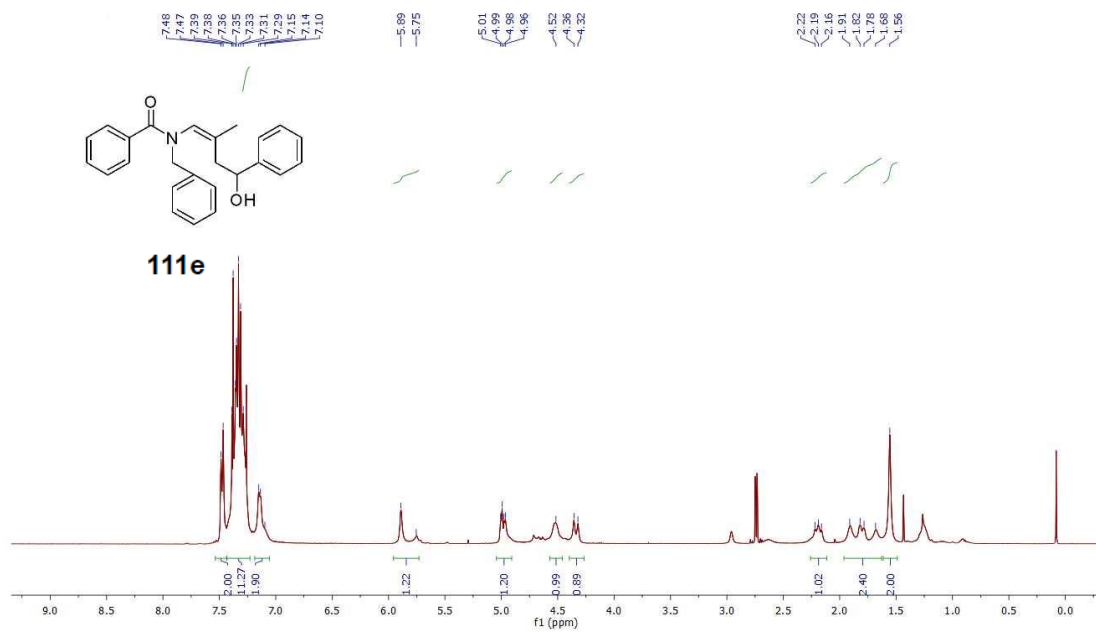
Spectra of Selected Compounds



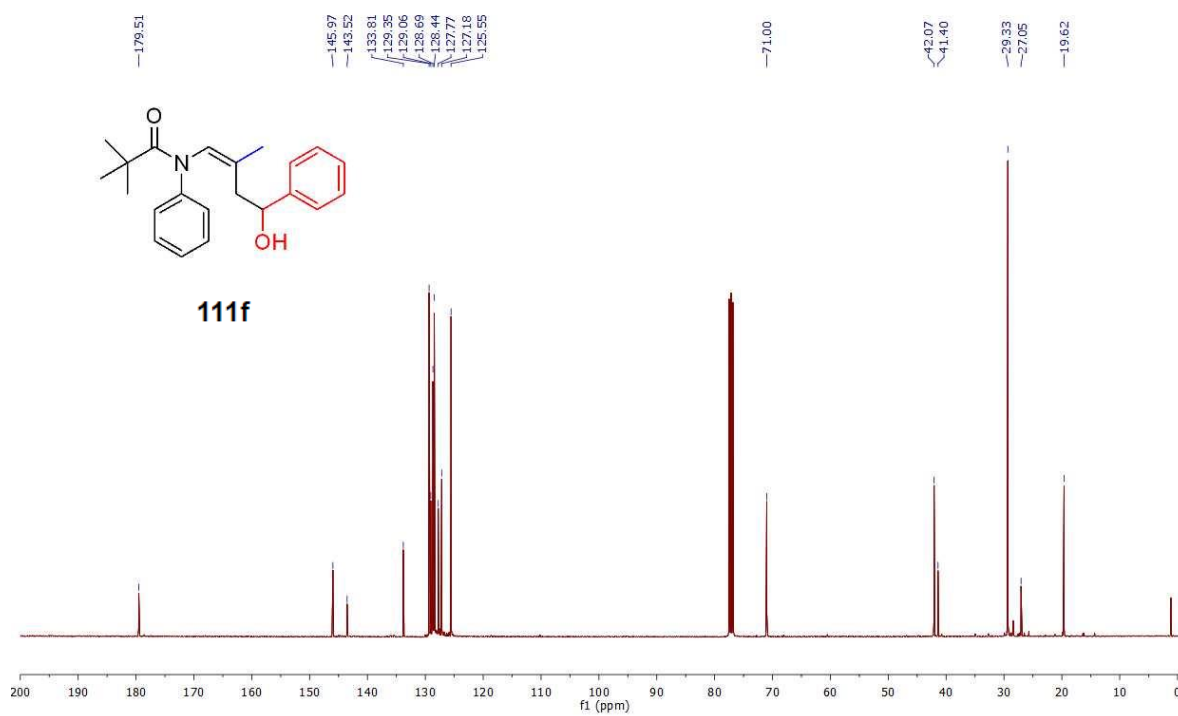
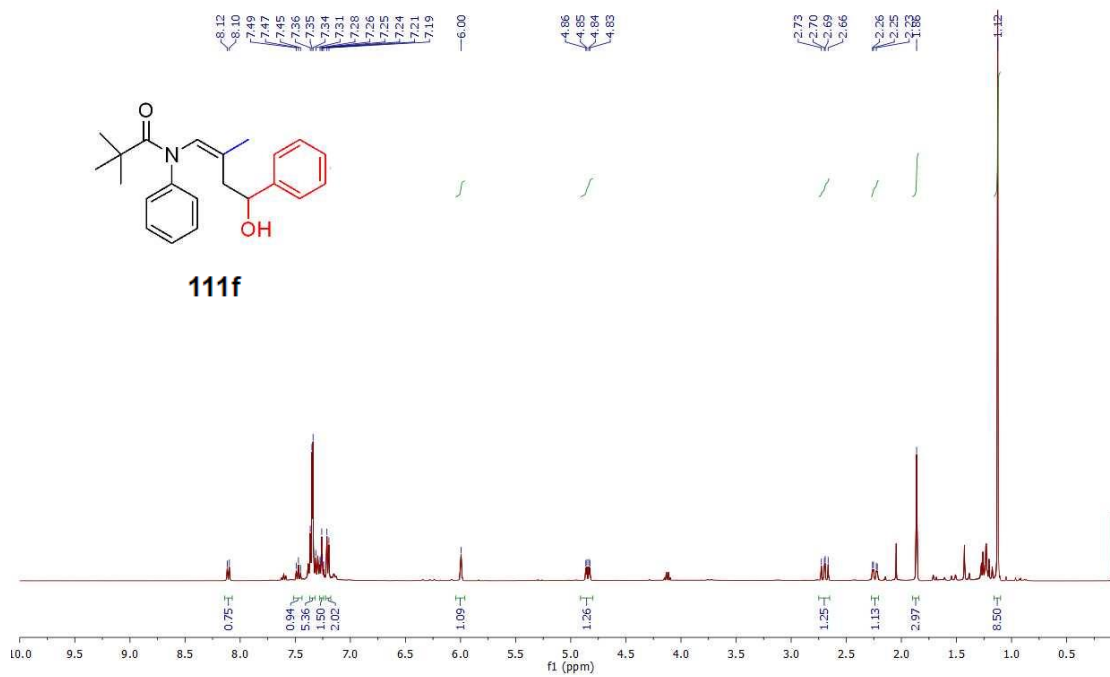
Spectra of Selected Compounds



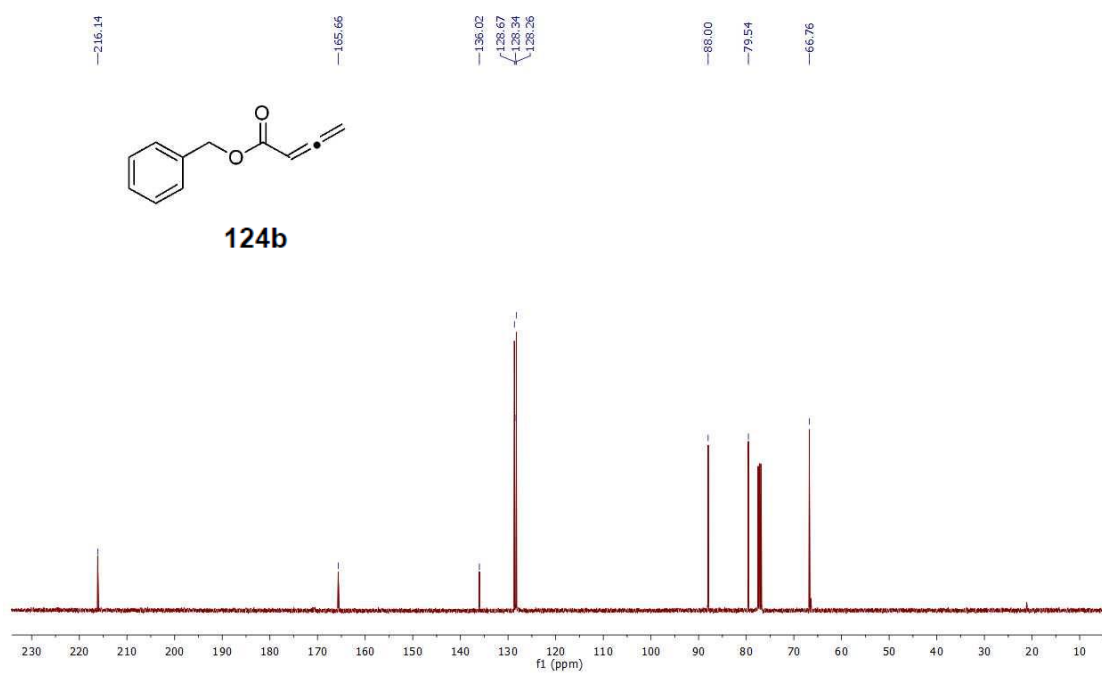
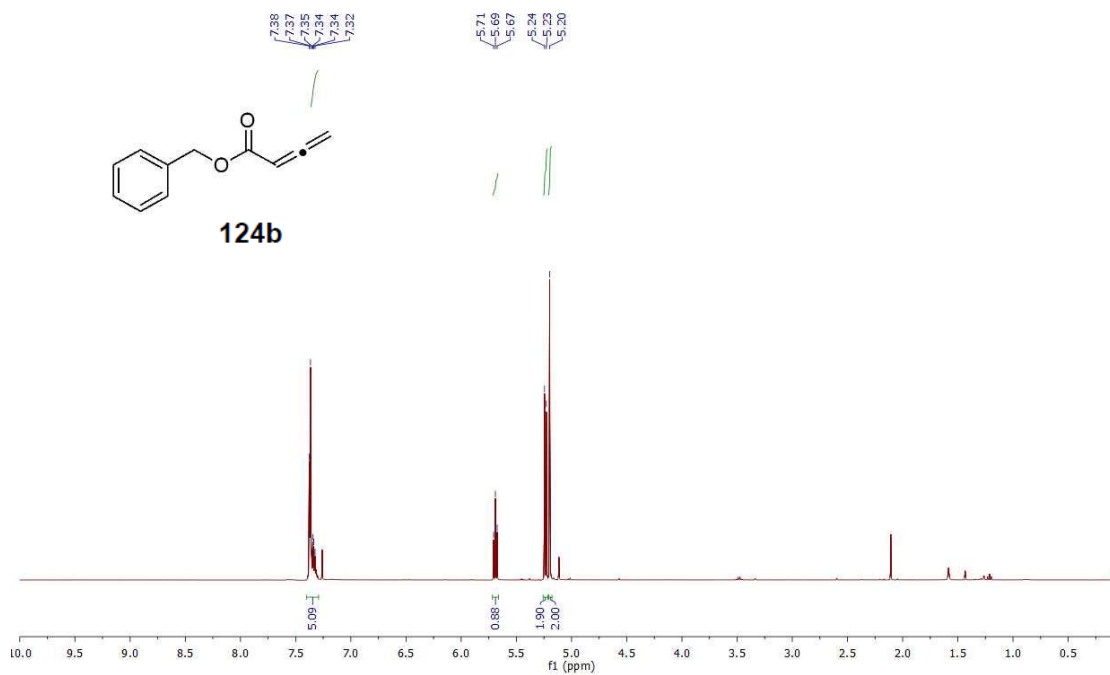
Spectra of Selected Compounds



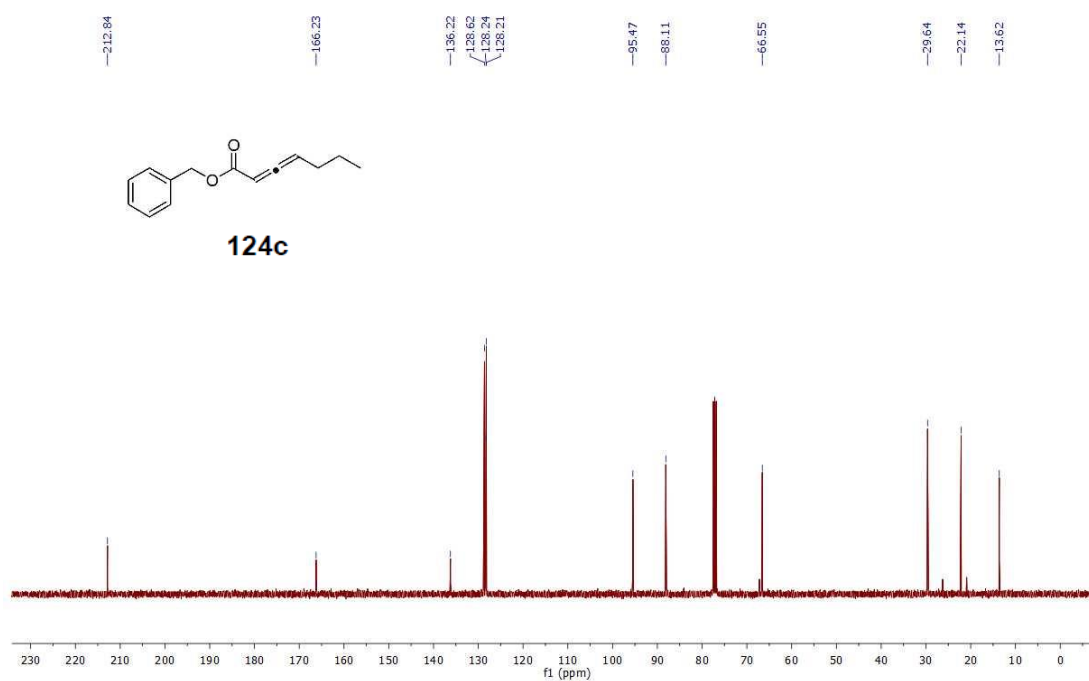
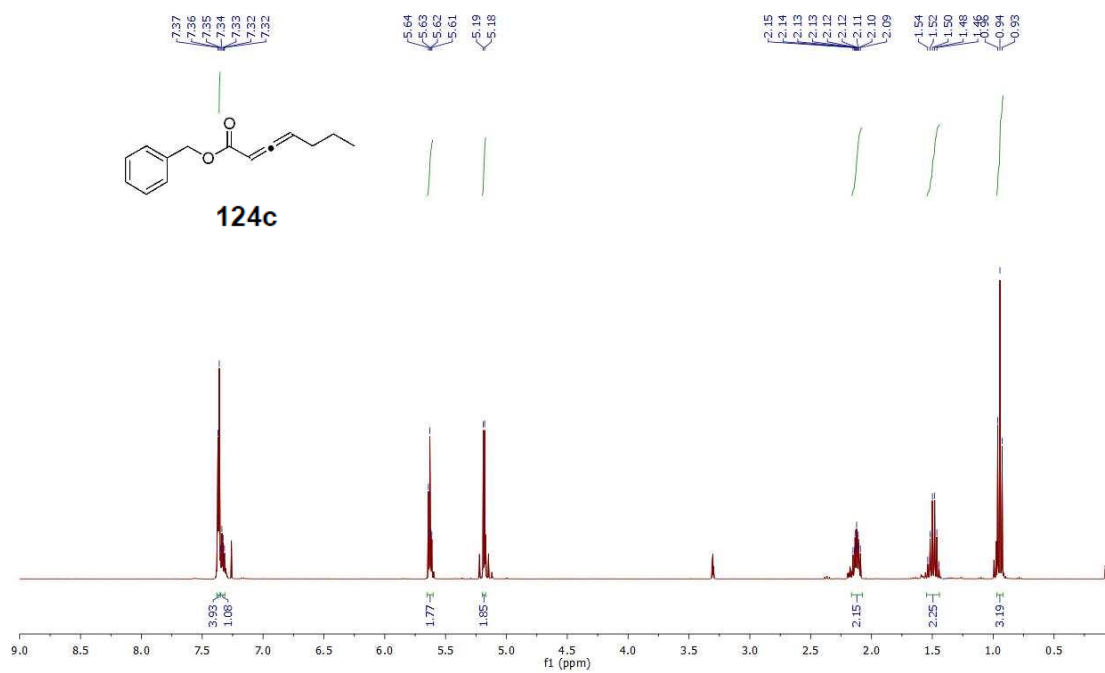
Spectra of Selected Compounds



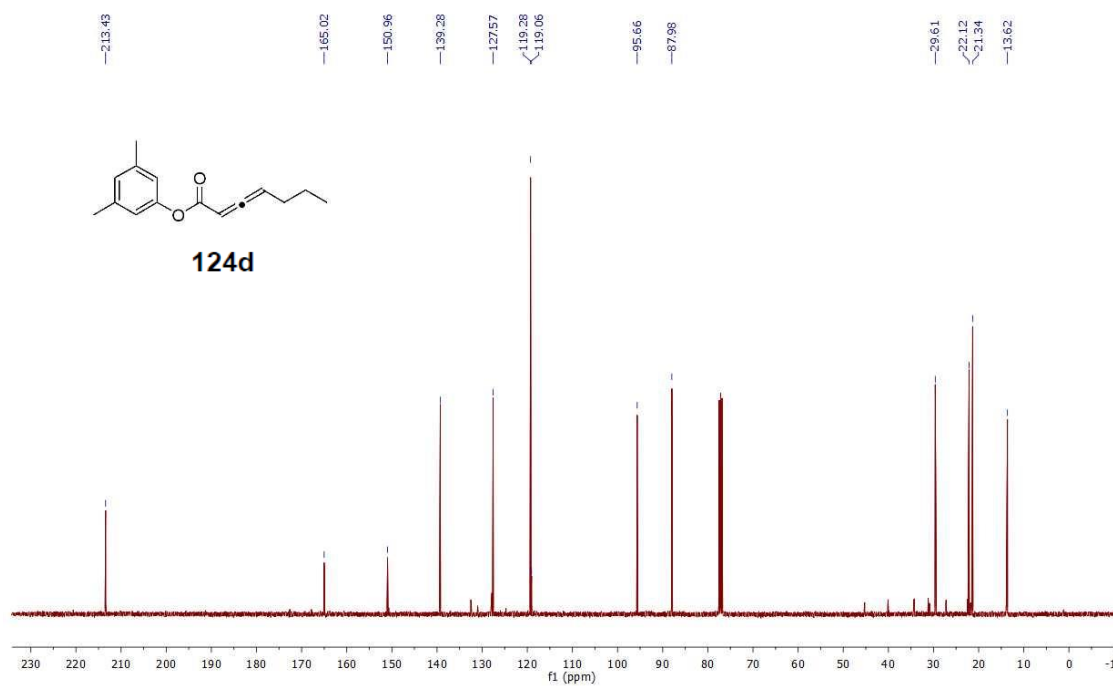
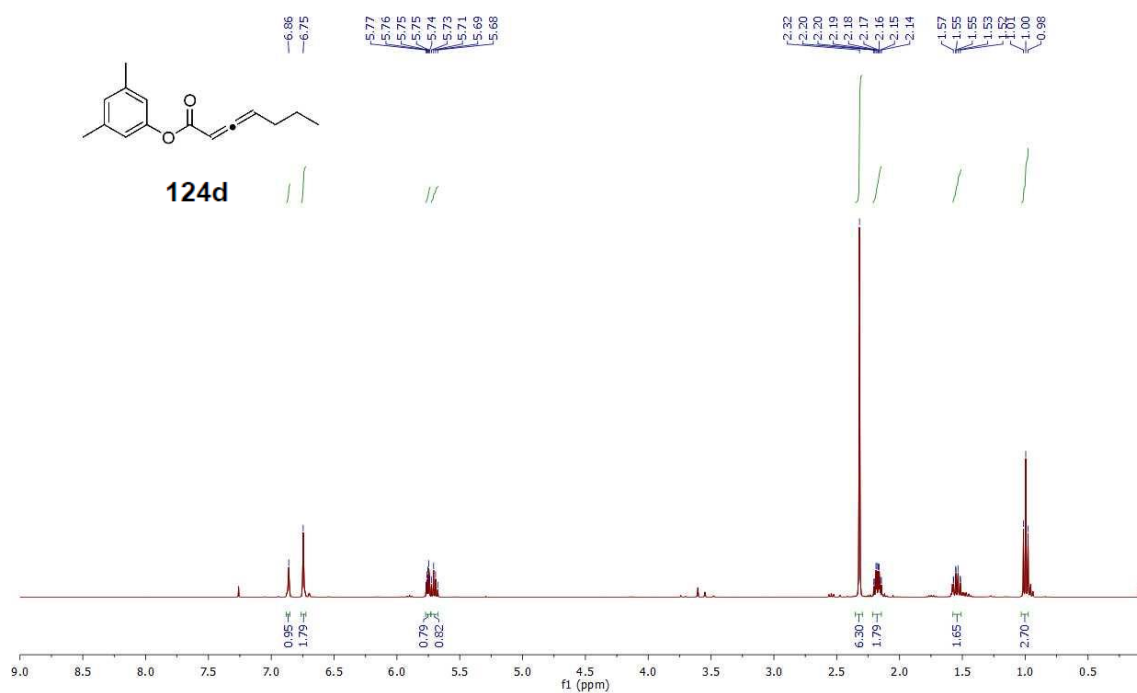
Spectra of Selected Compounds



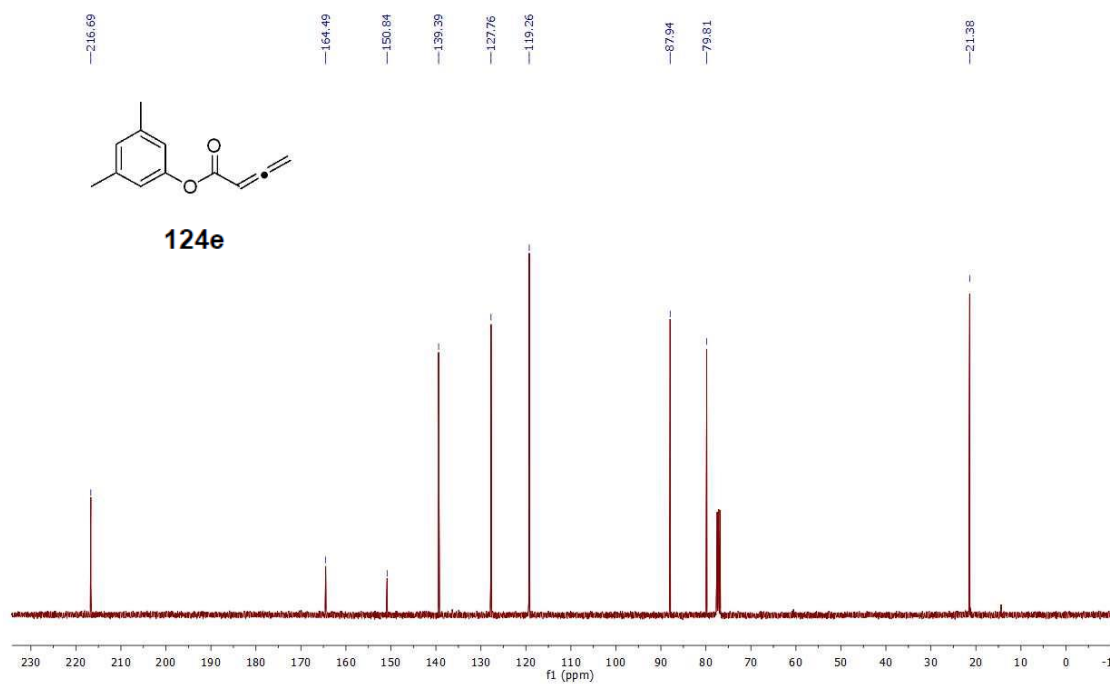
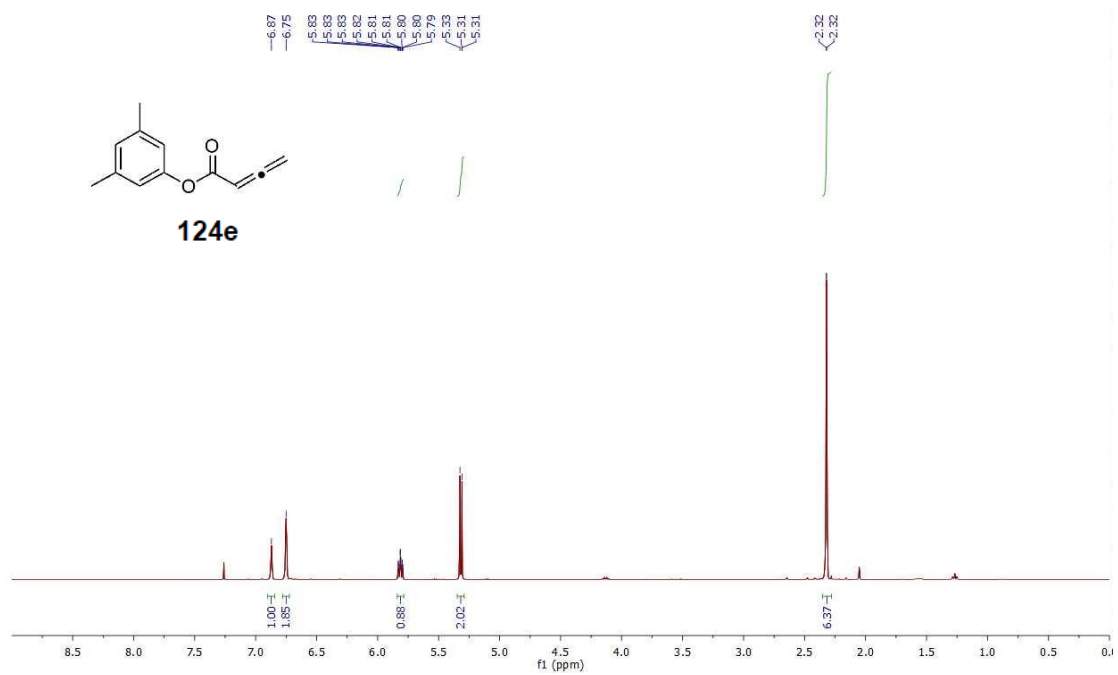
Spectra of Selected Compounds



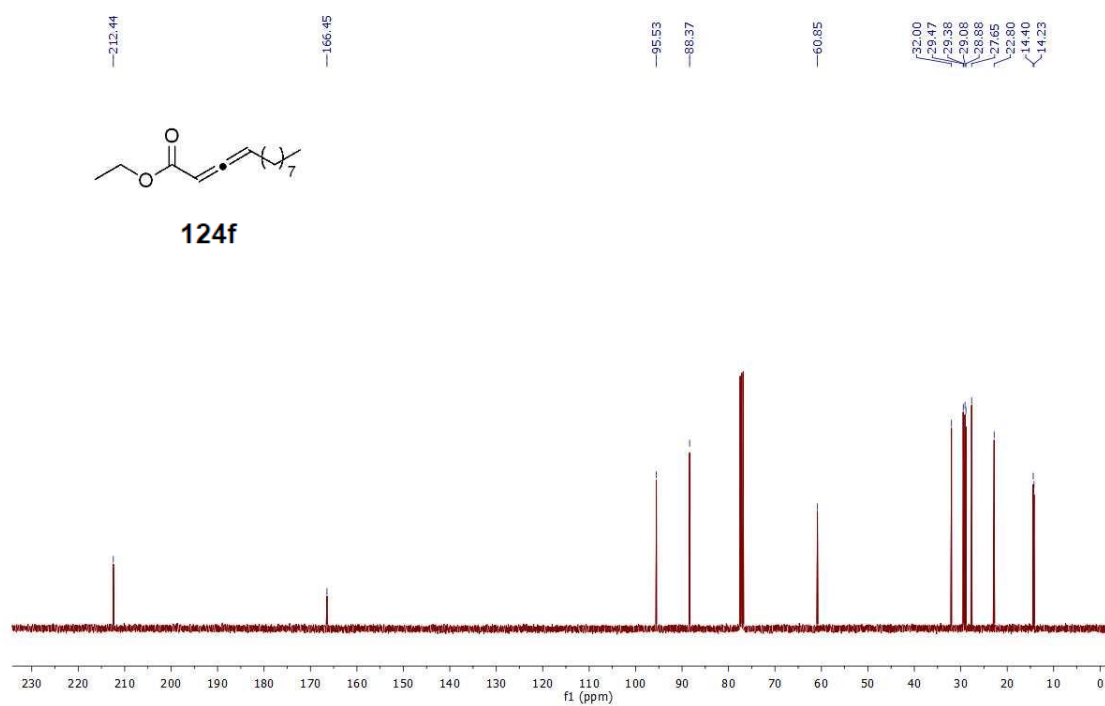
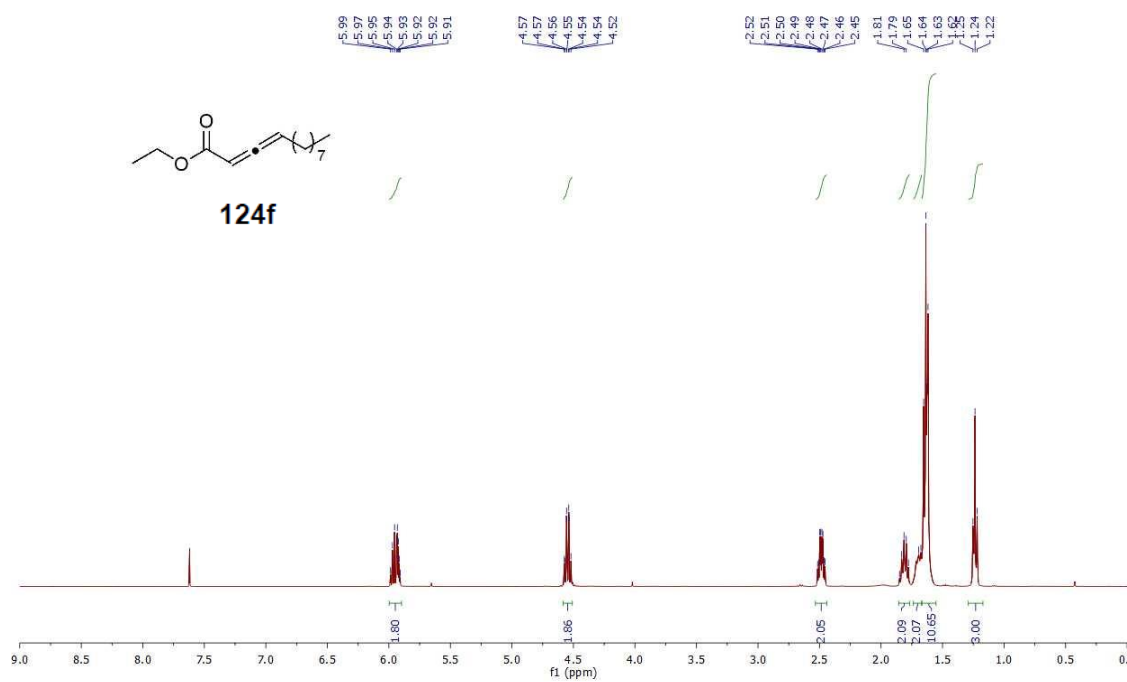
Spectra of Selected Compounds



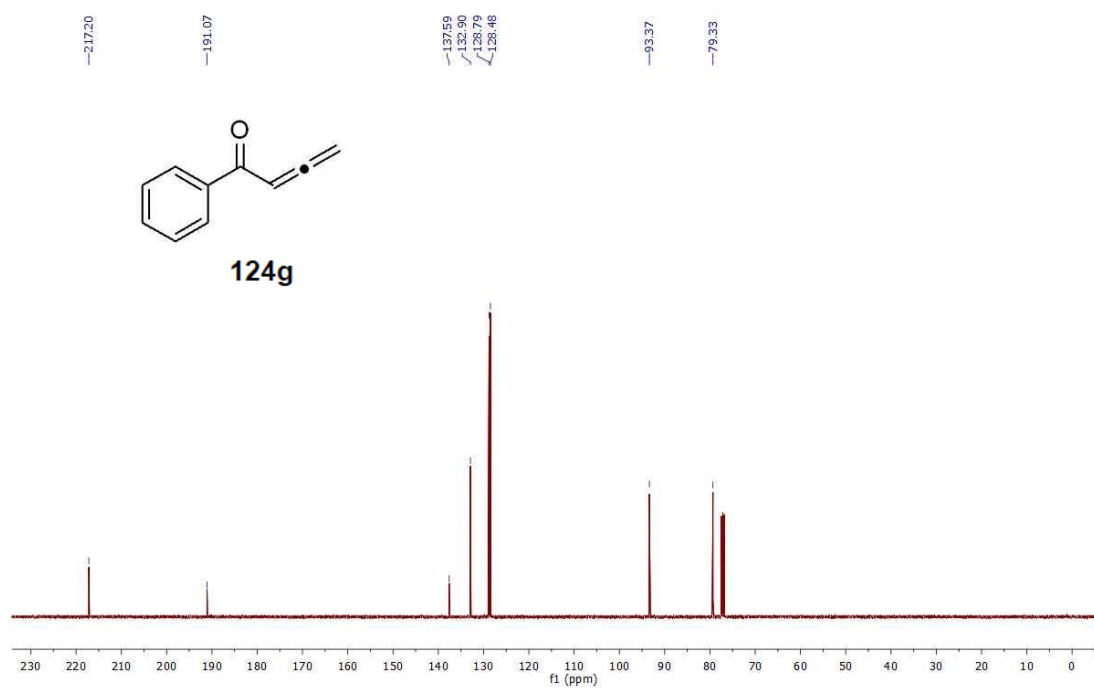
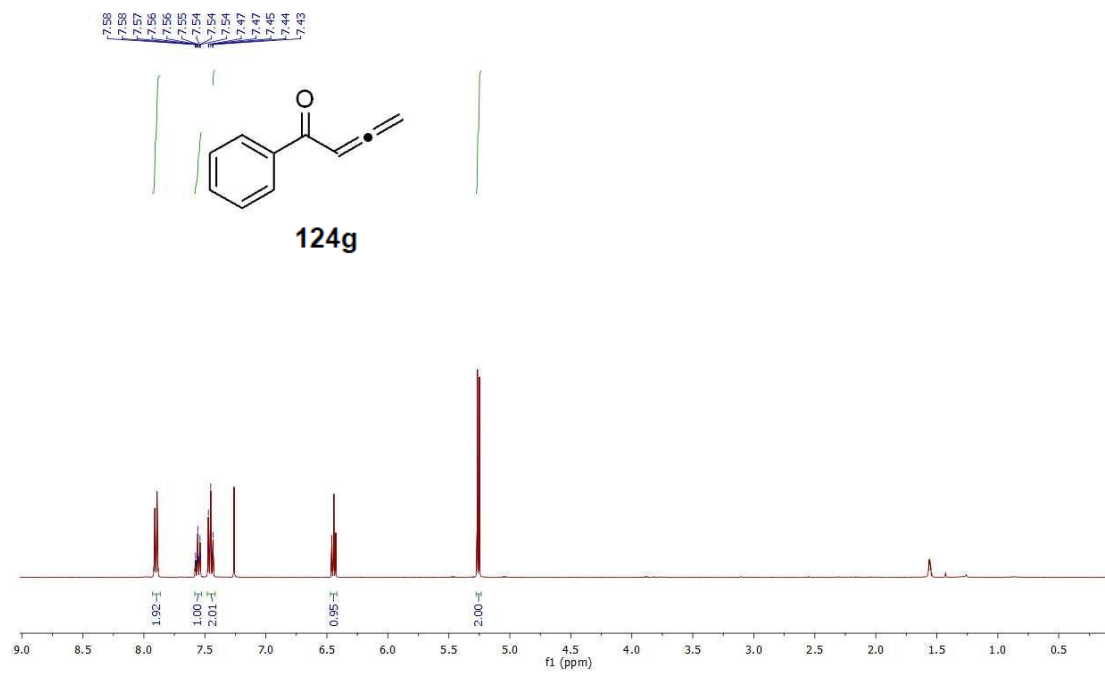
Spectra of Selected Compounds



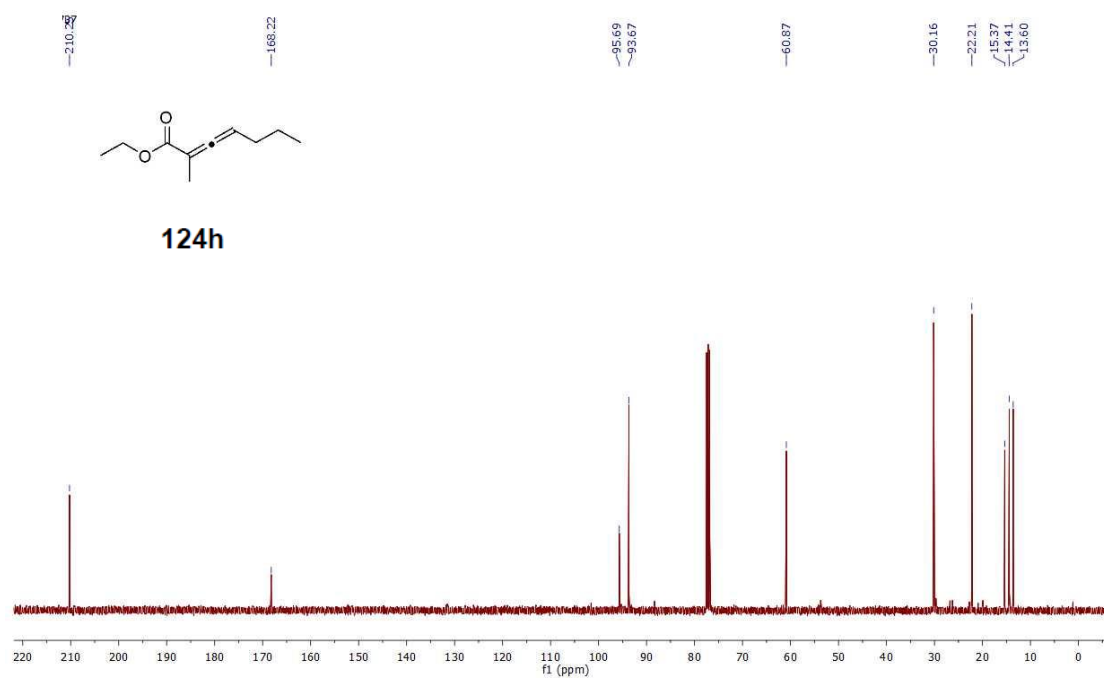
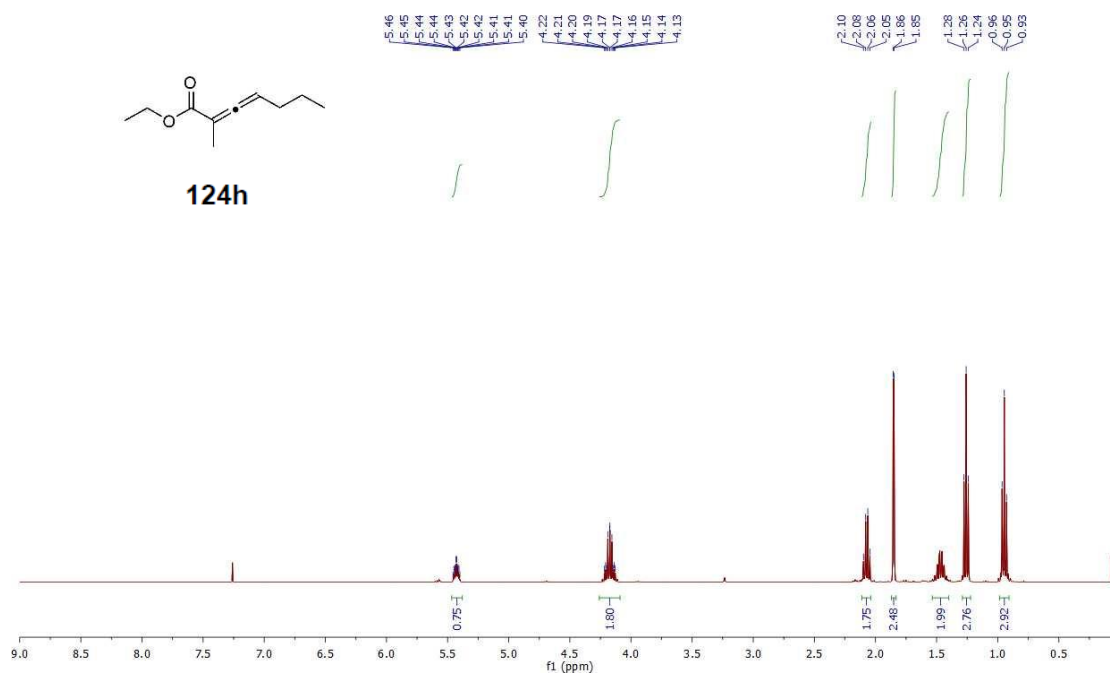
Spectra of Selected Compounds



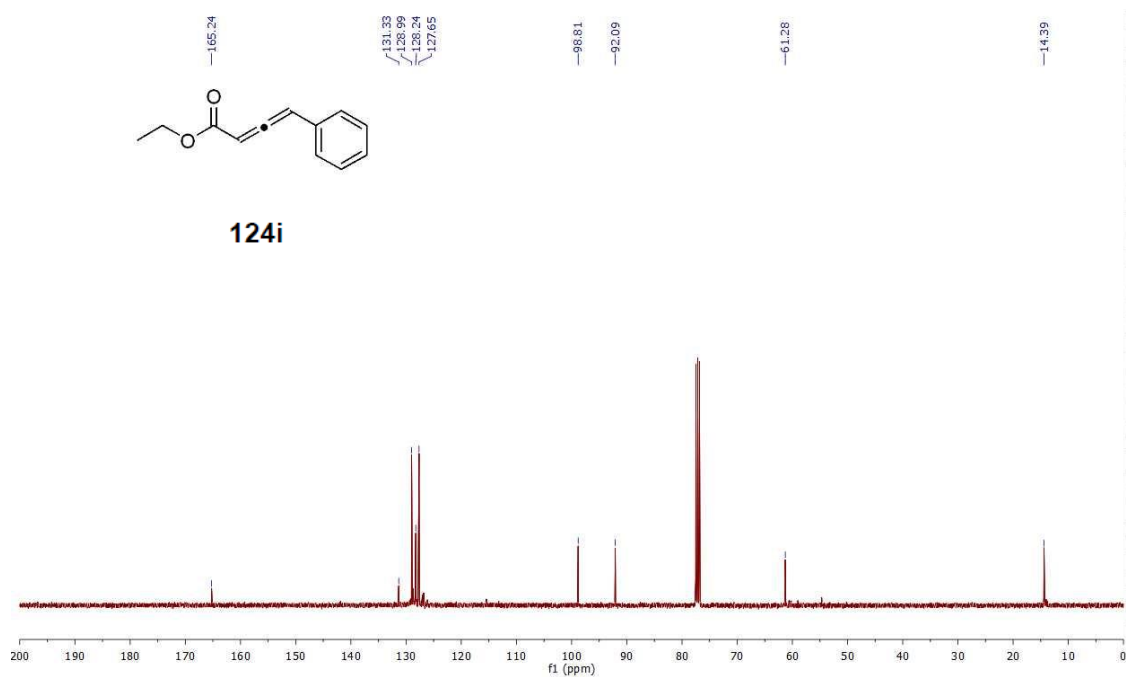
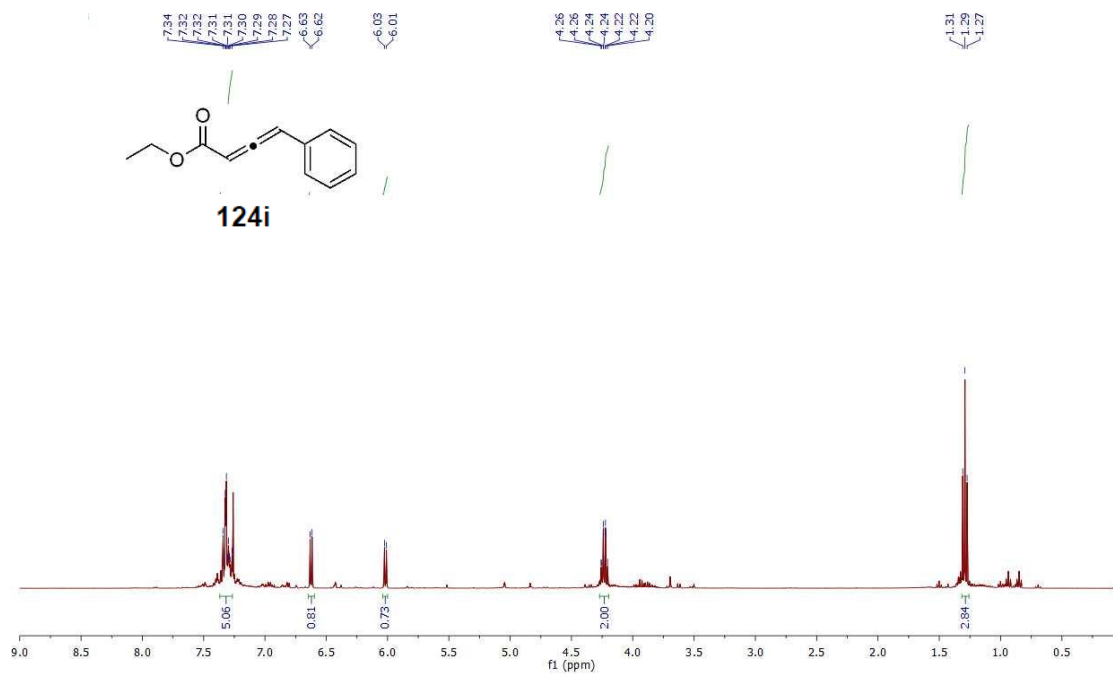
Spectra of Selected Compounds



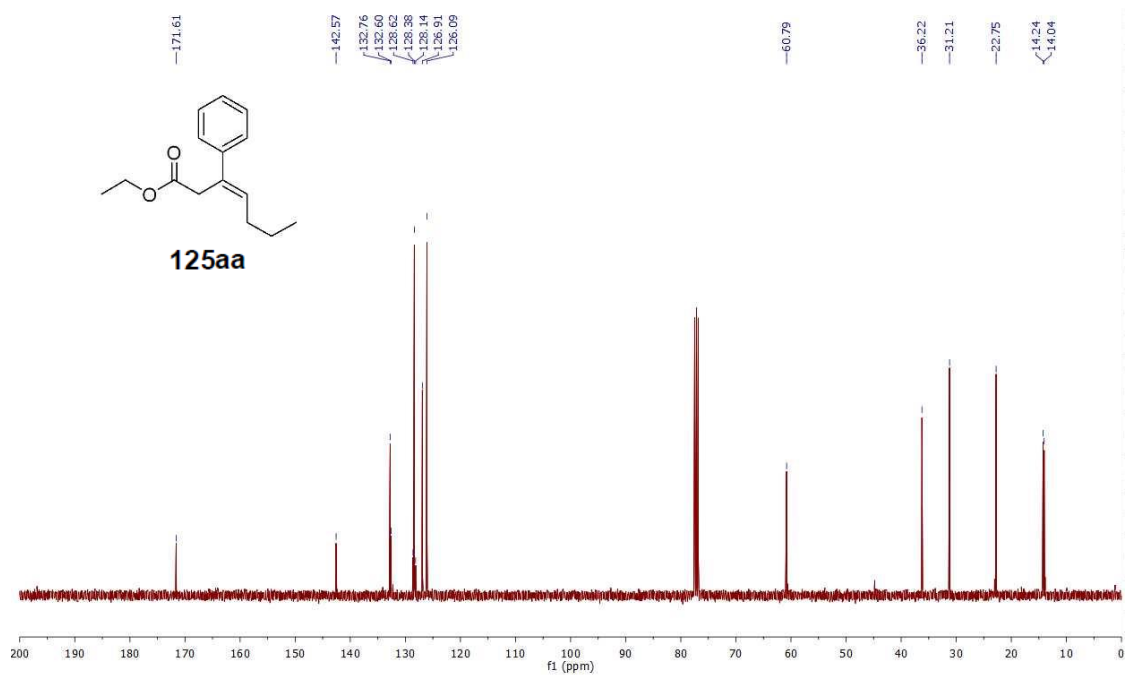
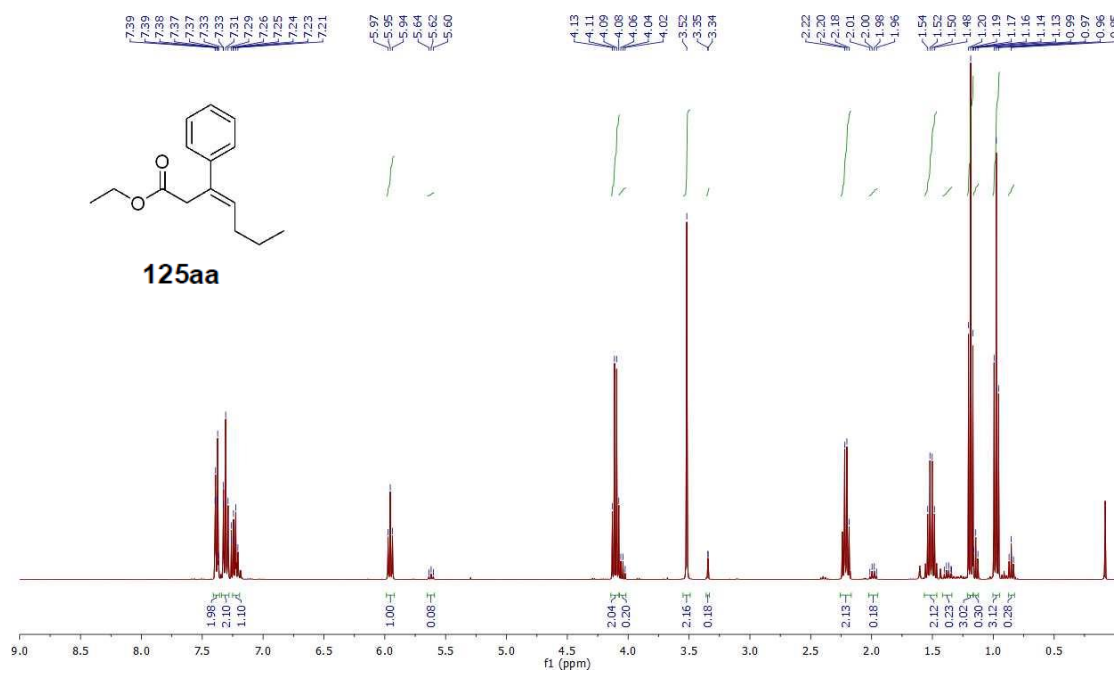
Spectra of Selected Compounds



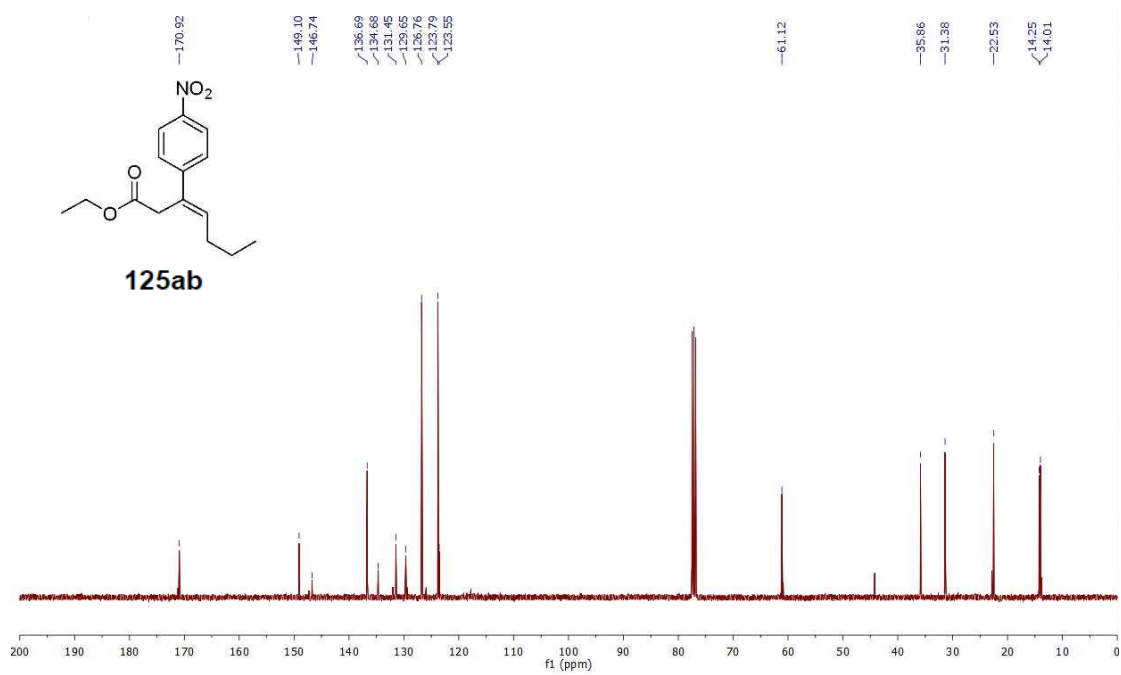
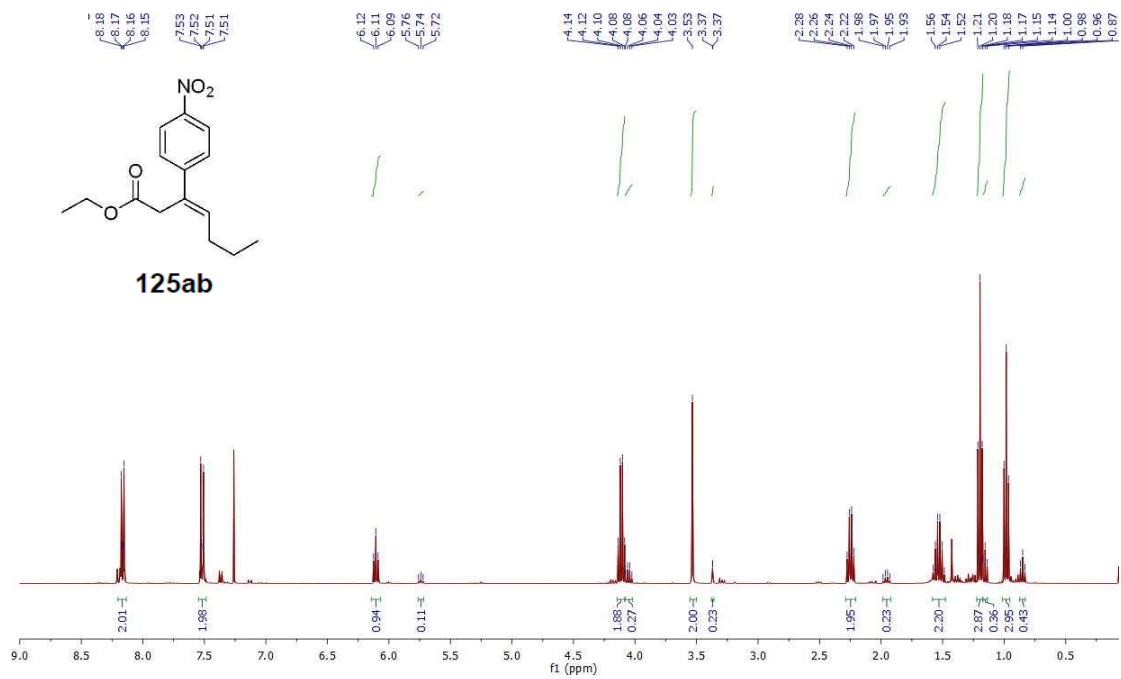
Spectra of Selected Compounds



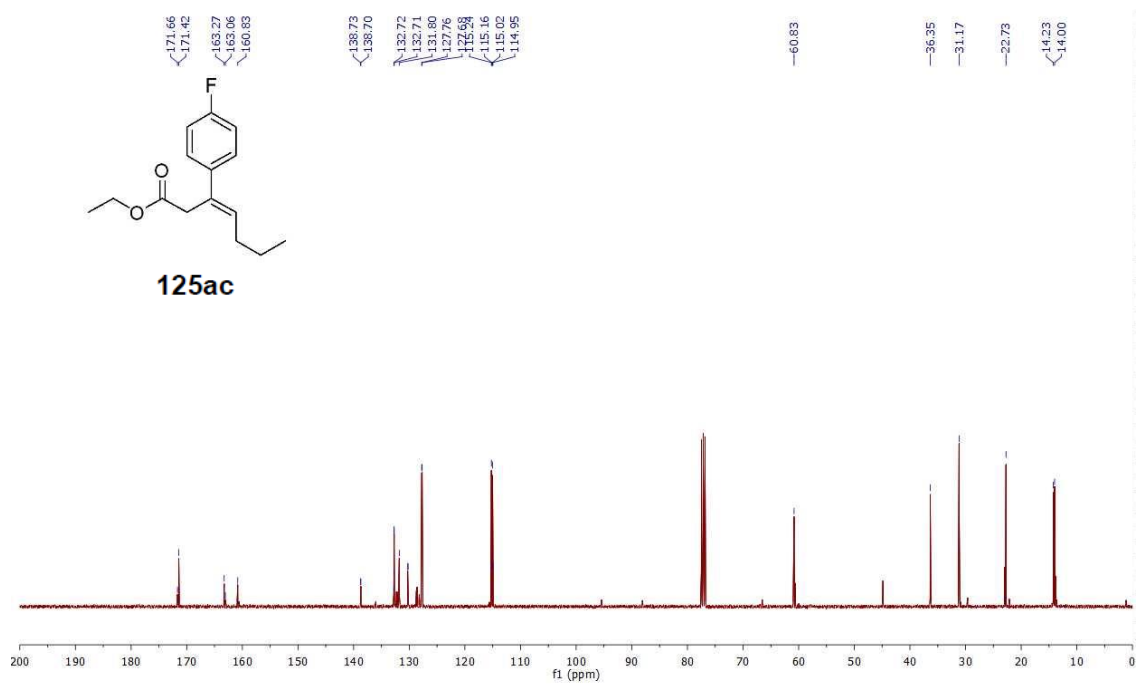
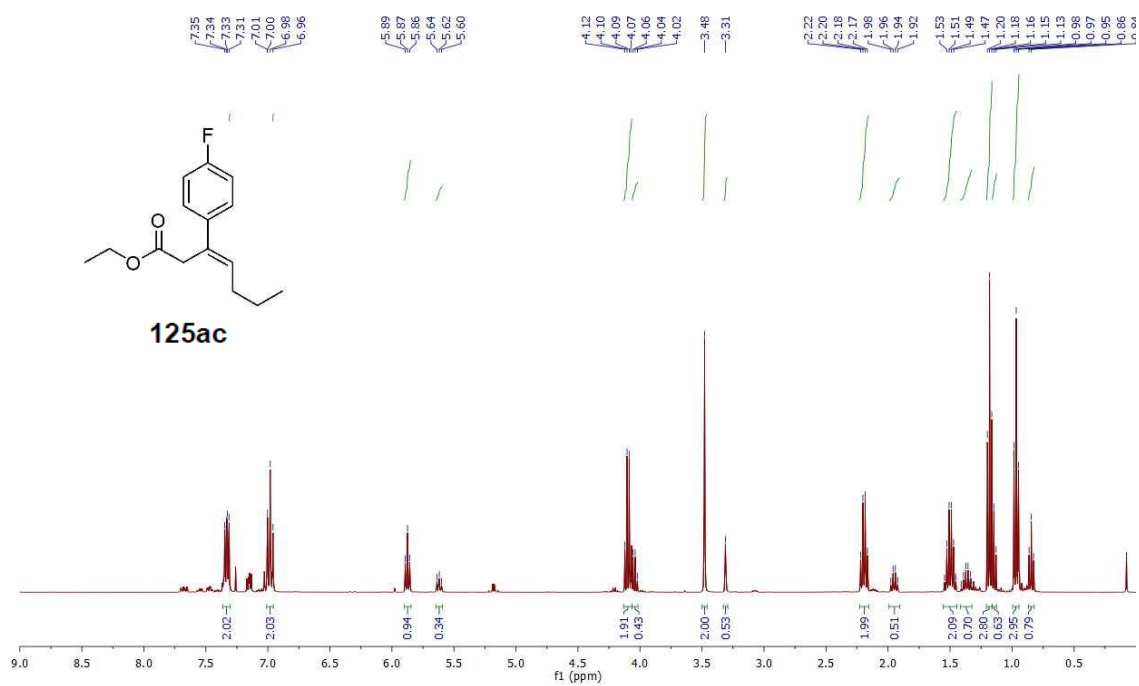
Spectra of Selected Compounds



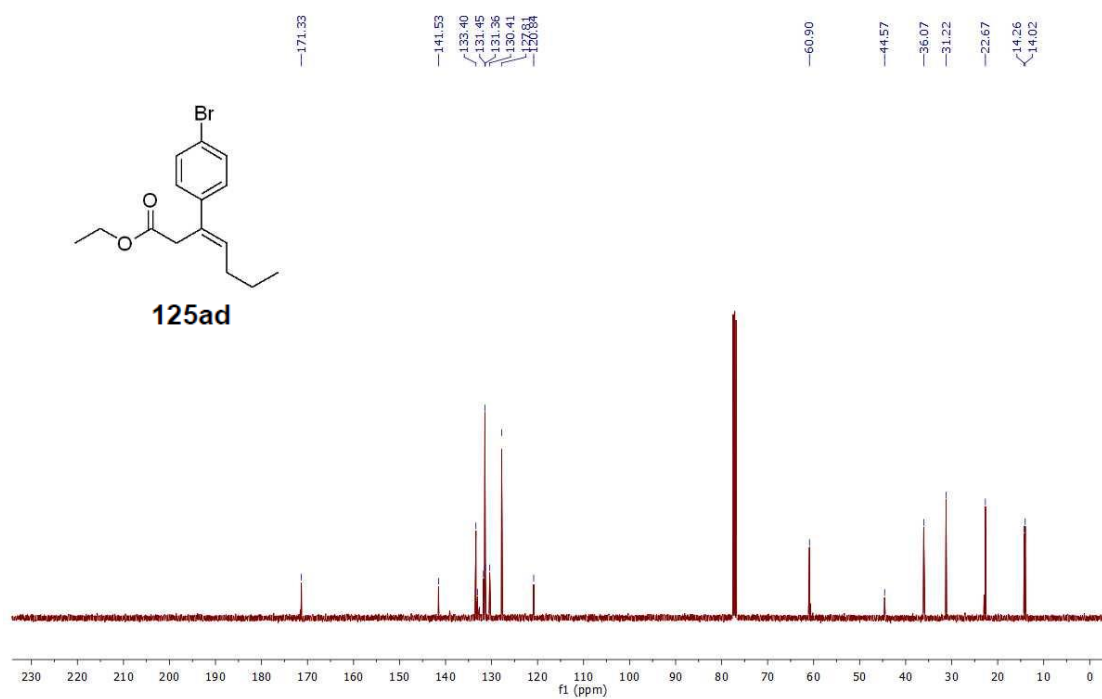
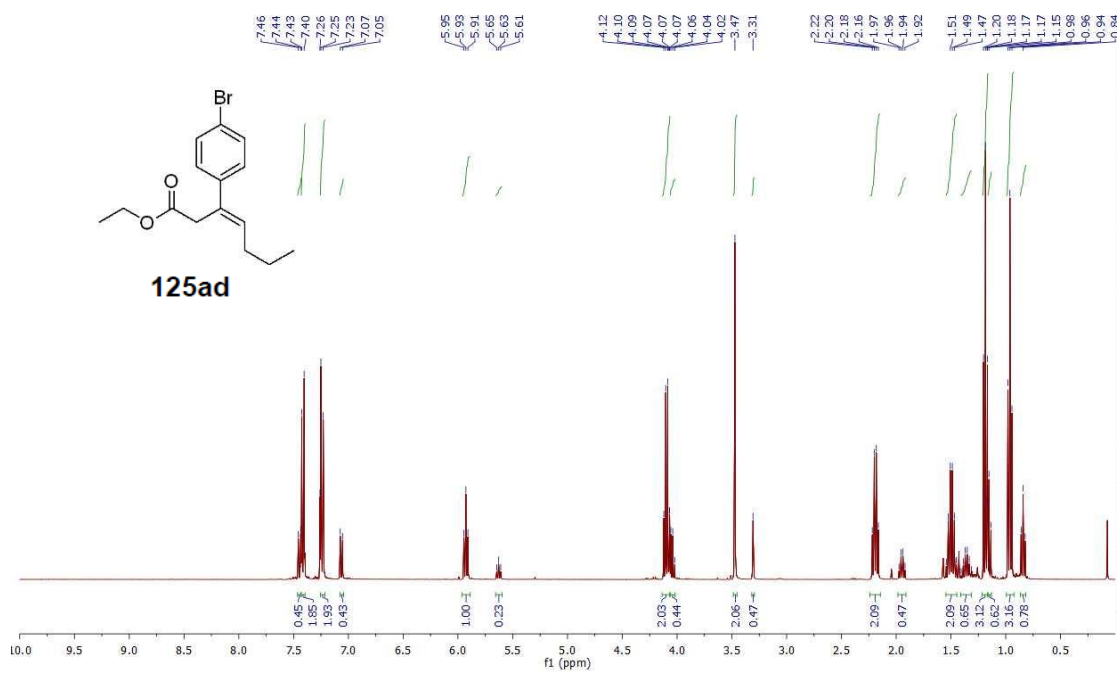
Spectra of Selected Compounds



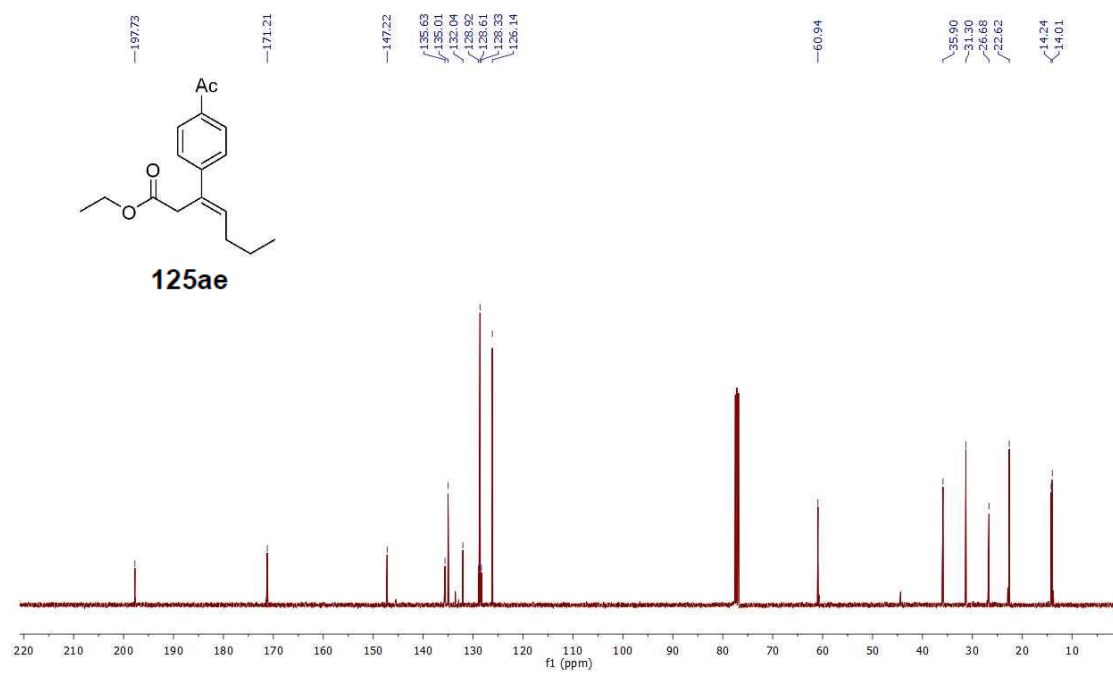
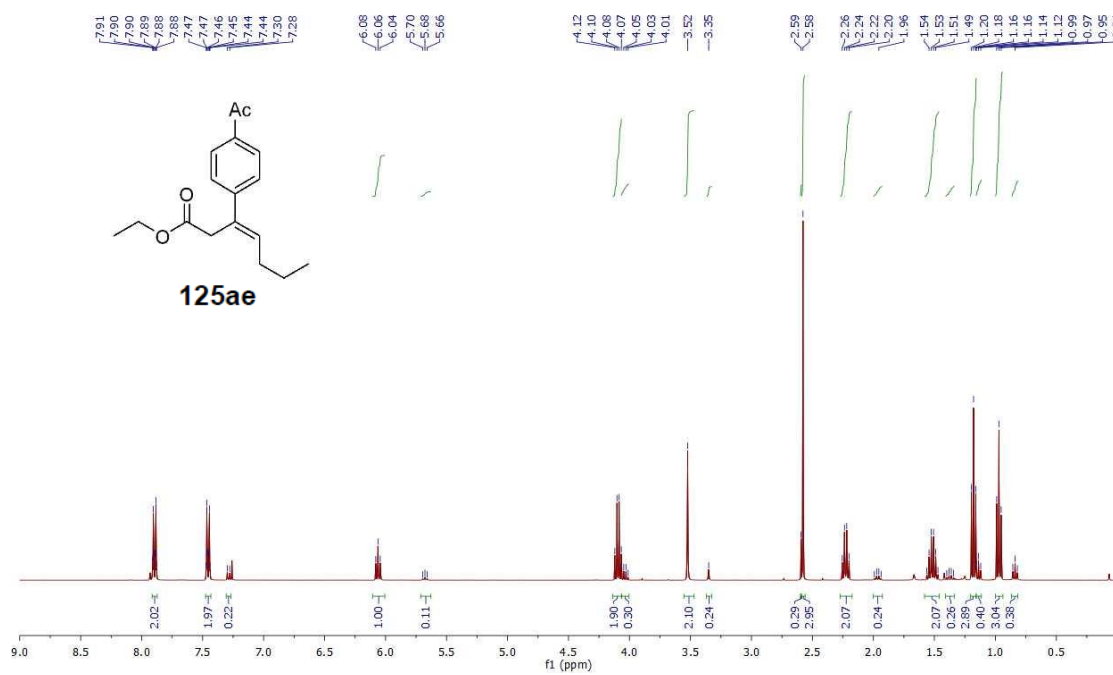
Spectra of Selected Compounds



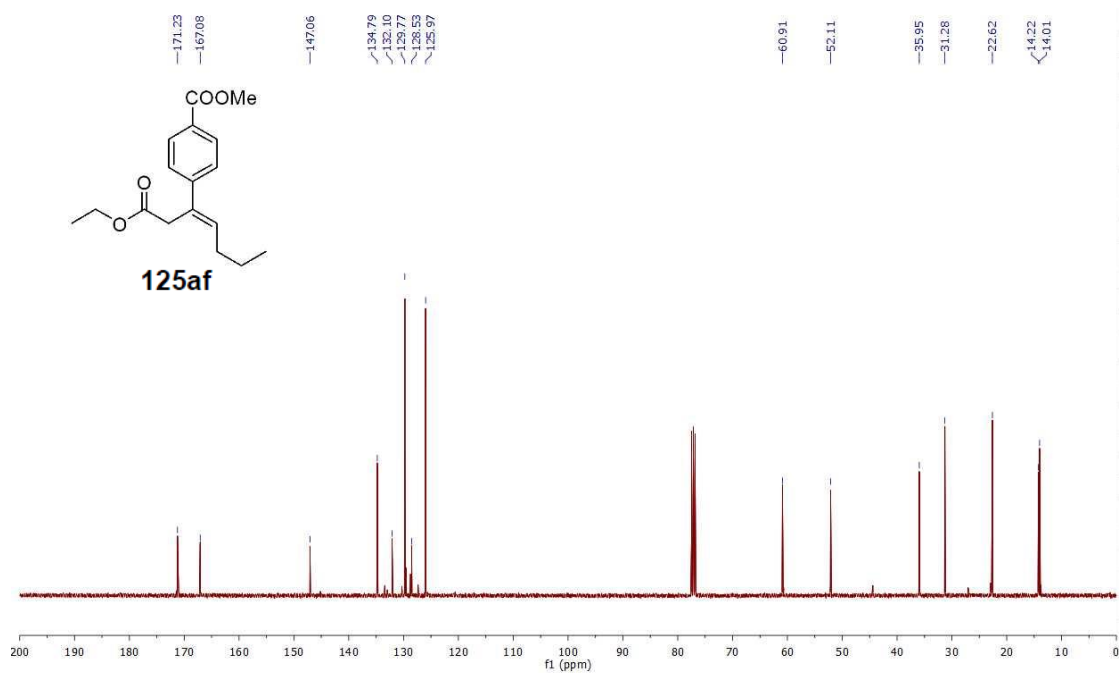
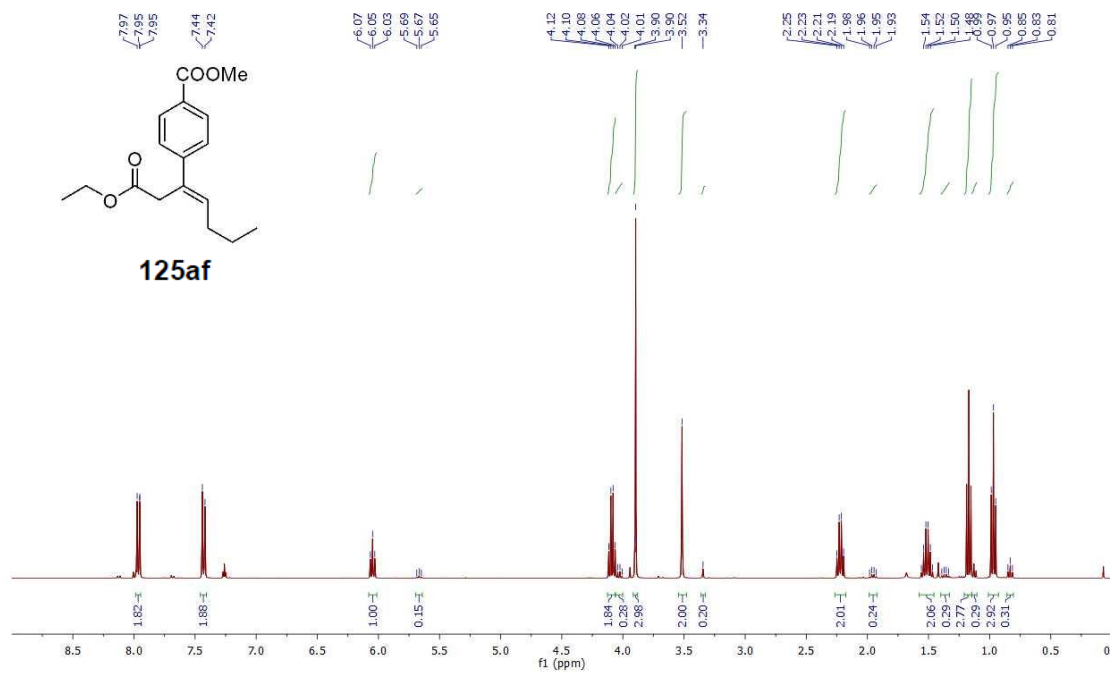
Spectra of Selected Compounds



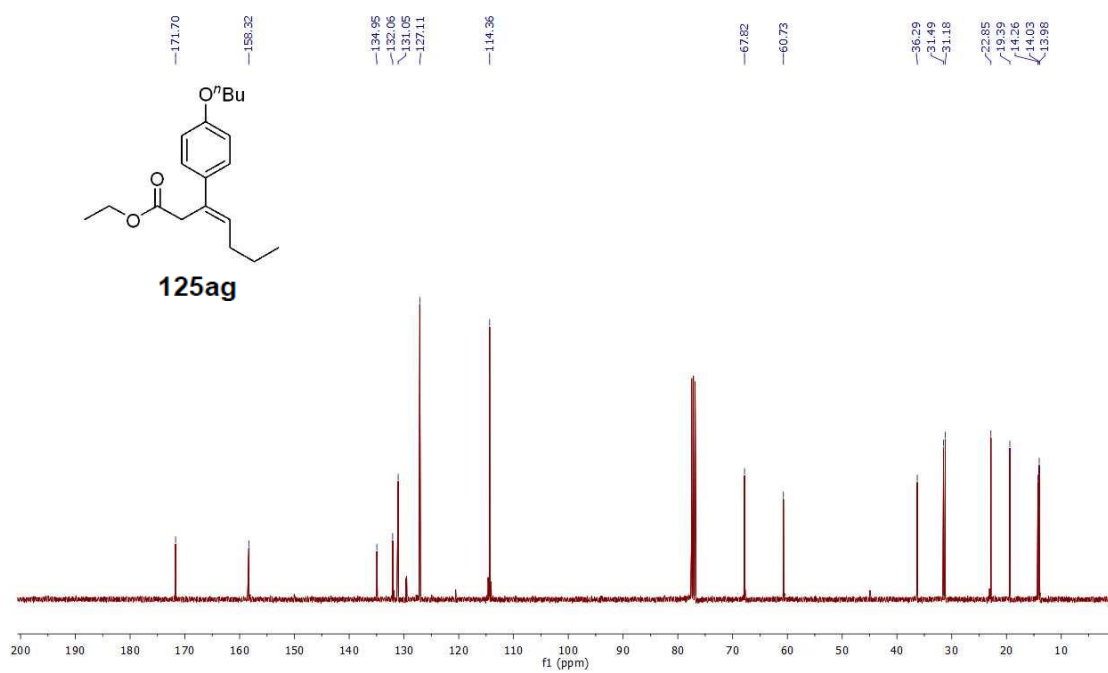
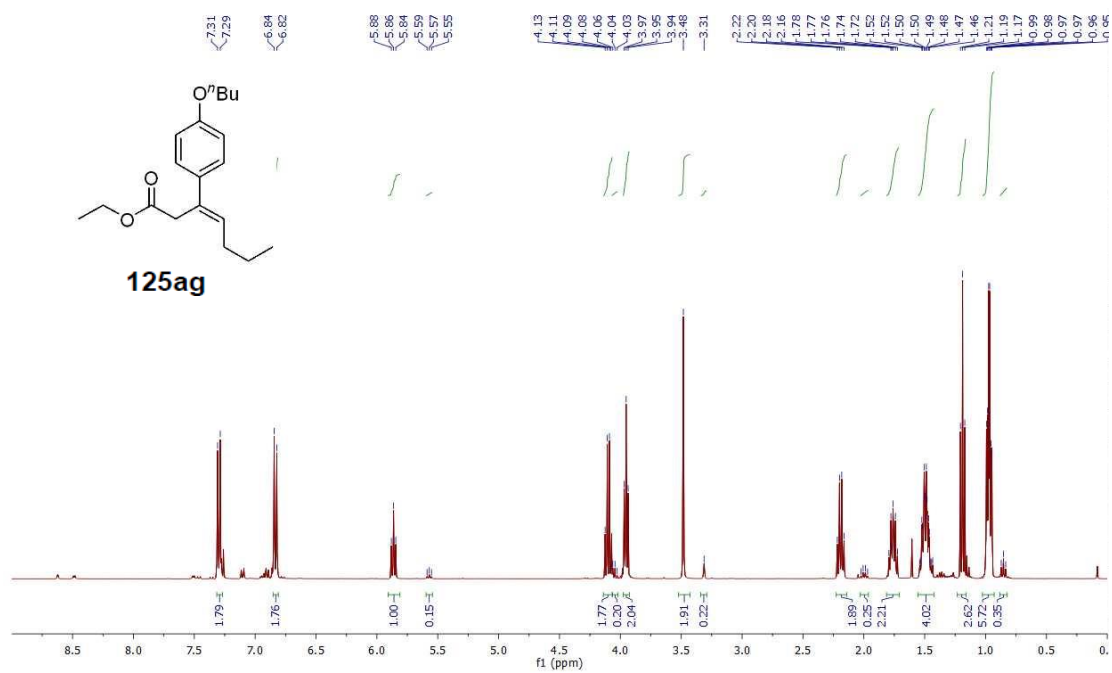
Spectra of Selected Compounds



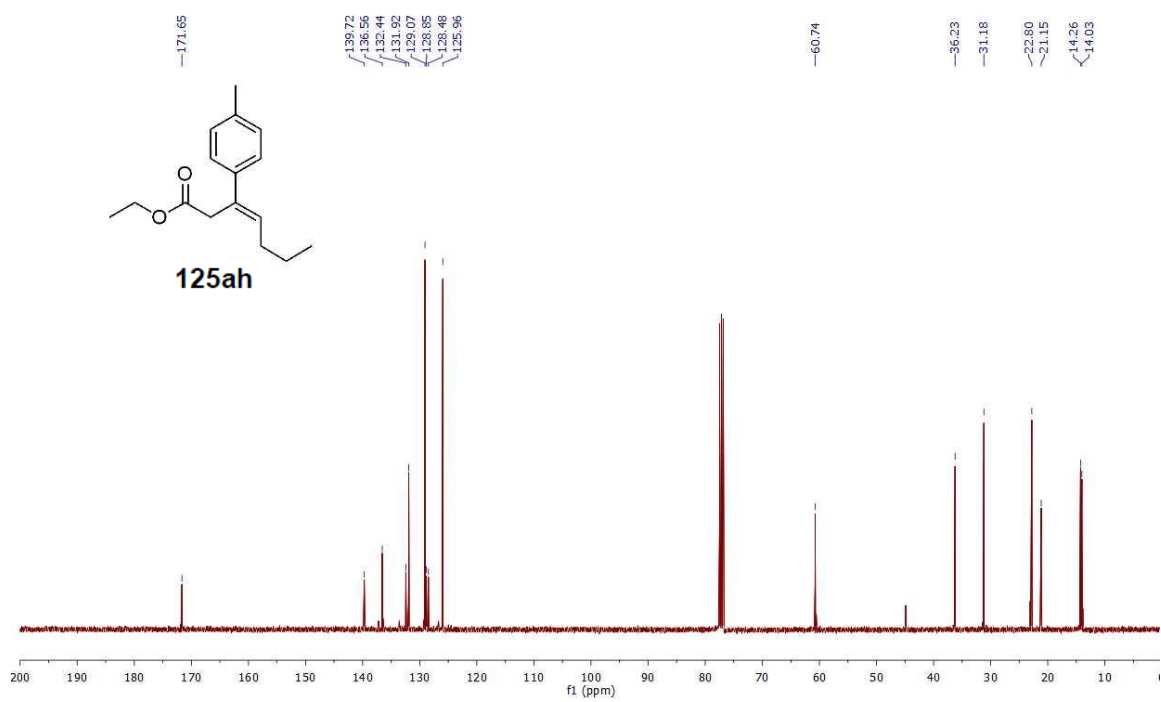
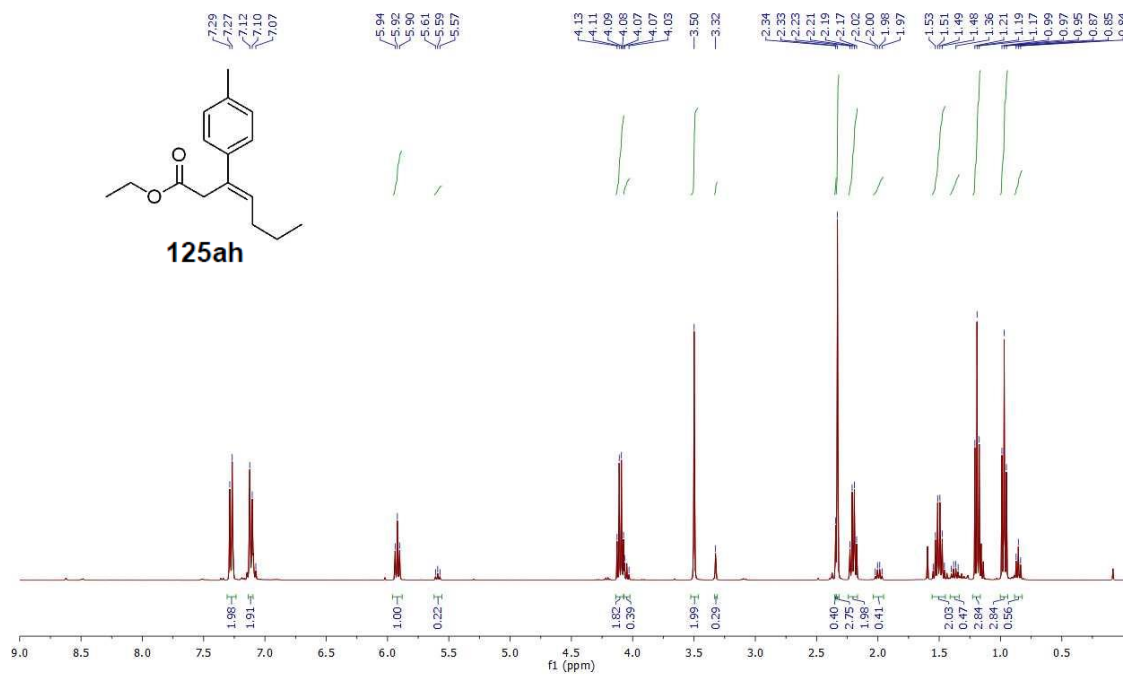
Spectra of Selected Compounds



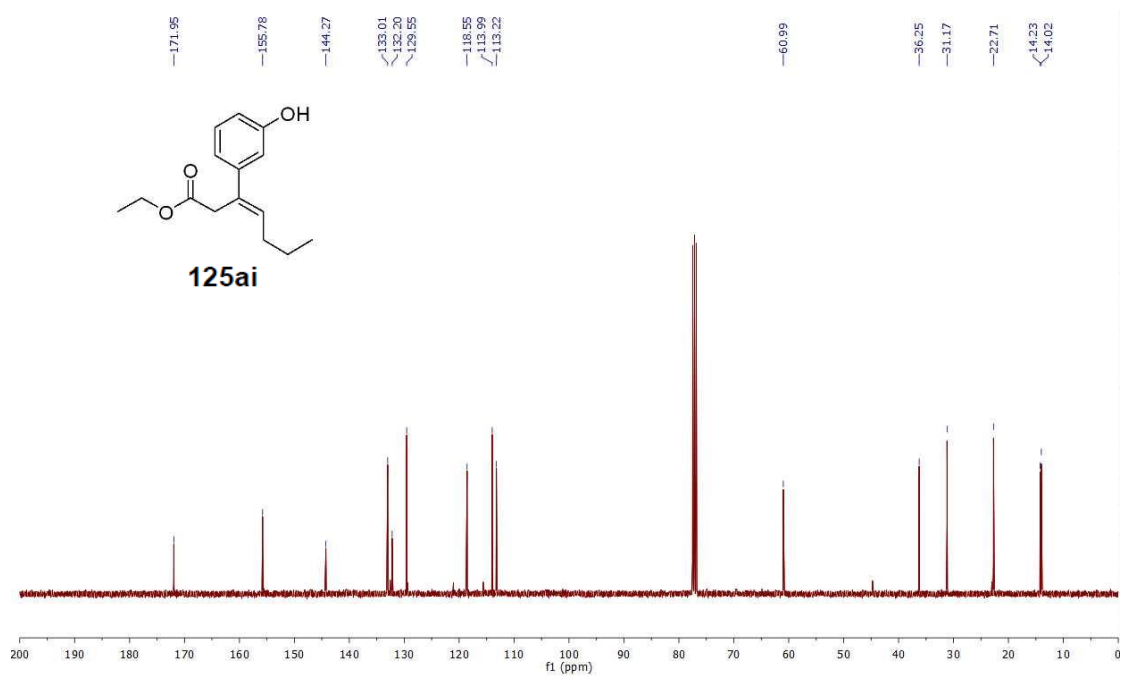
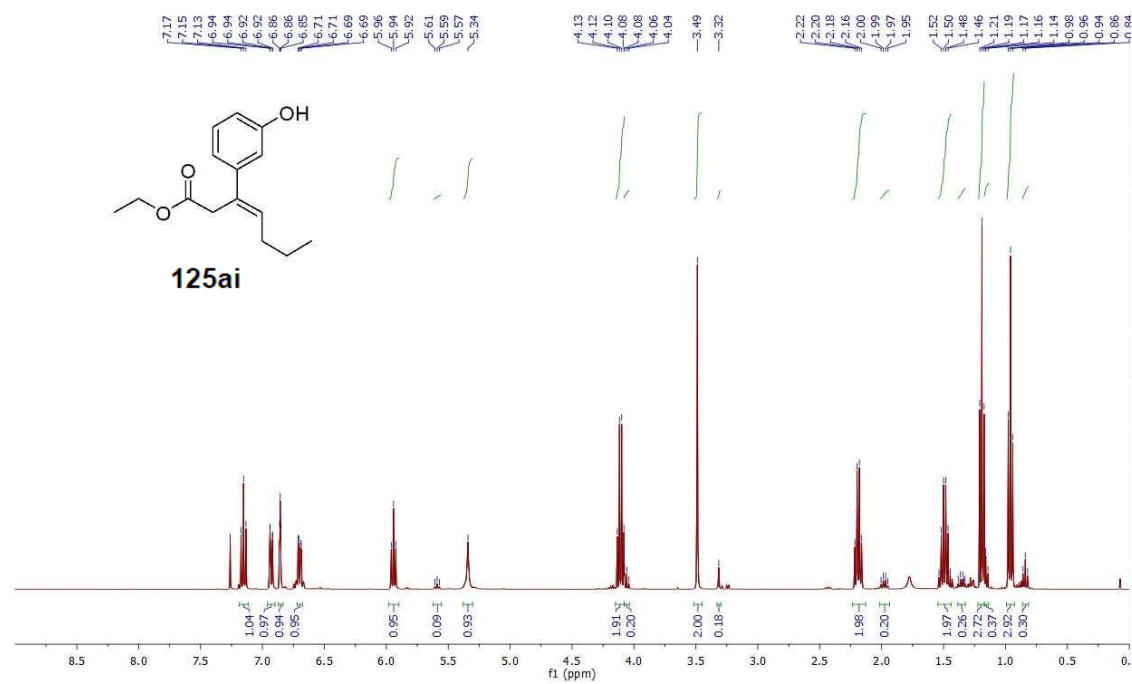
Spectra of Selected Compounds



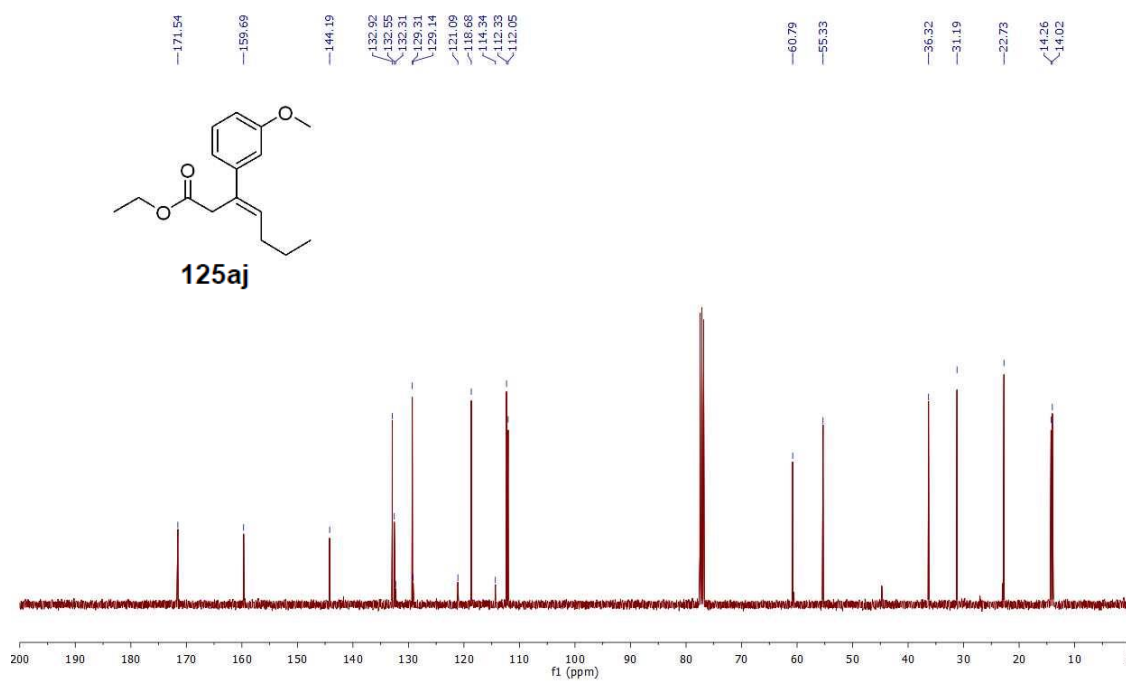
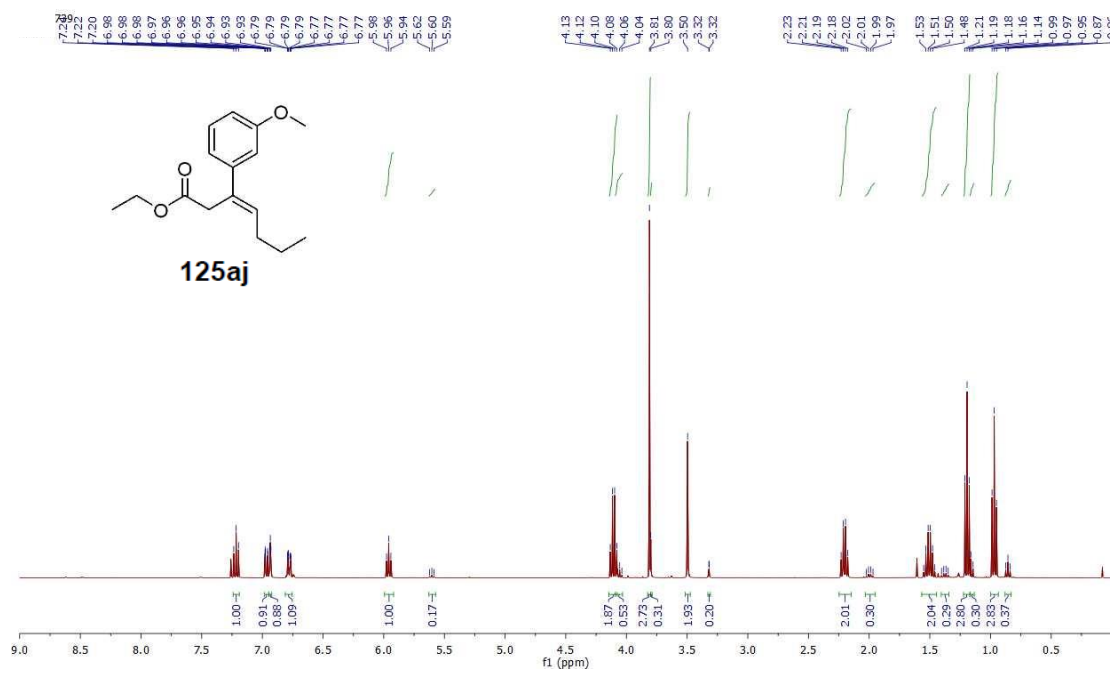
Spectra of Selected Compounds



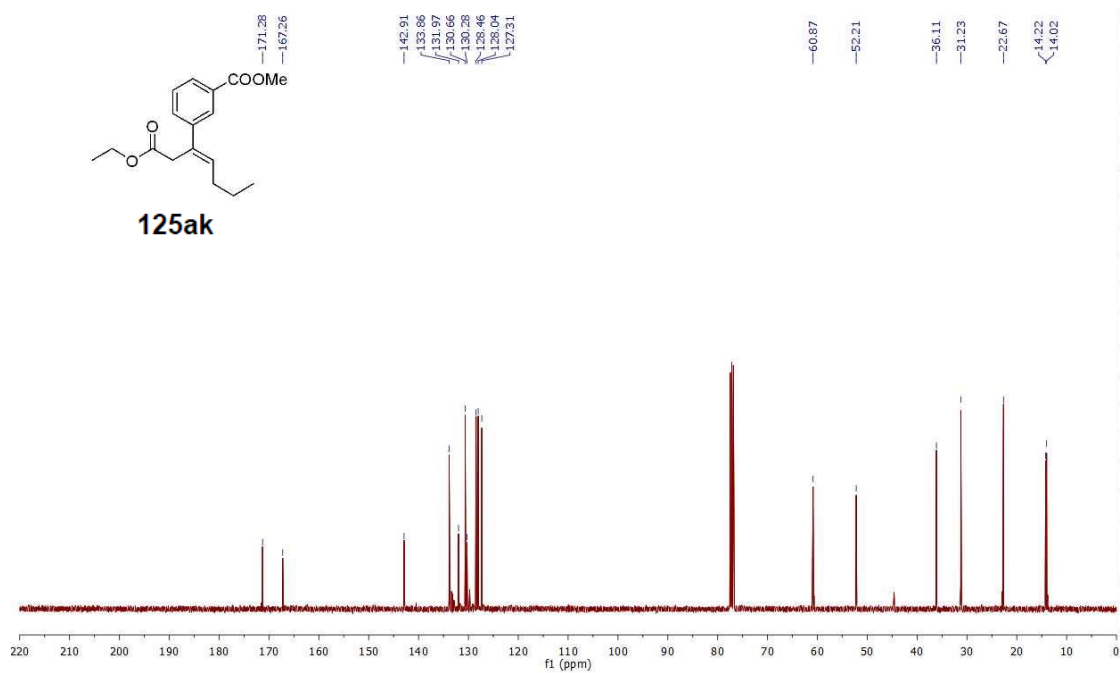
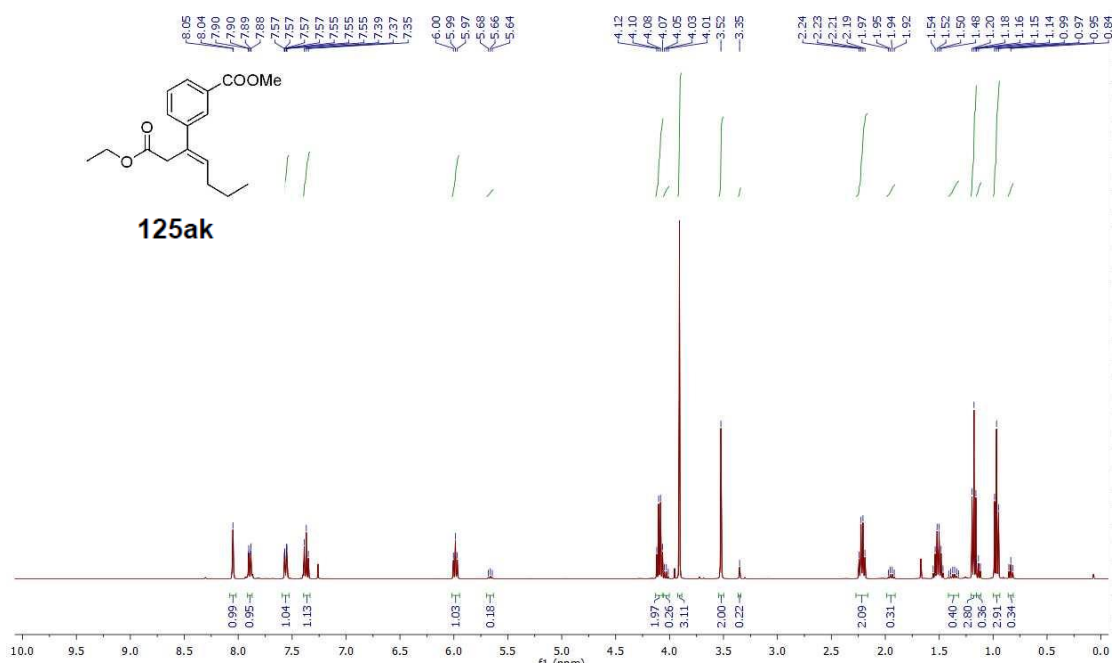
Spectra of Selected Compounds



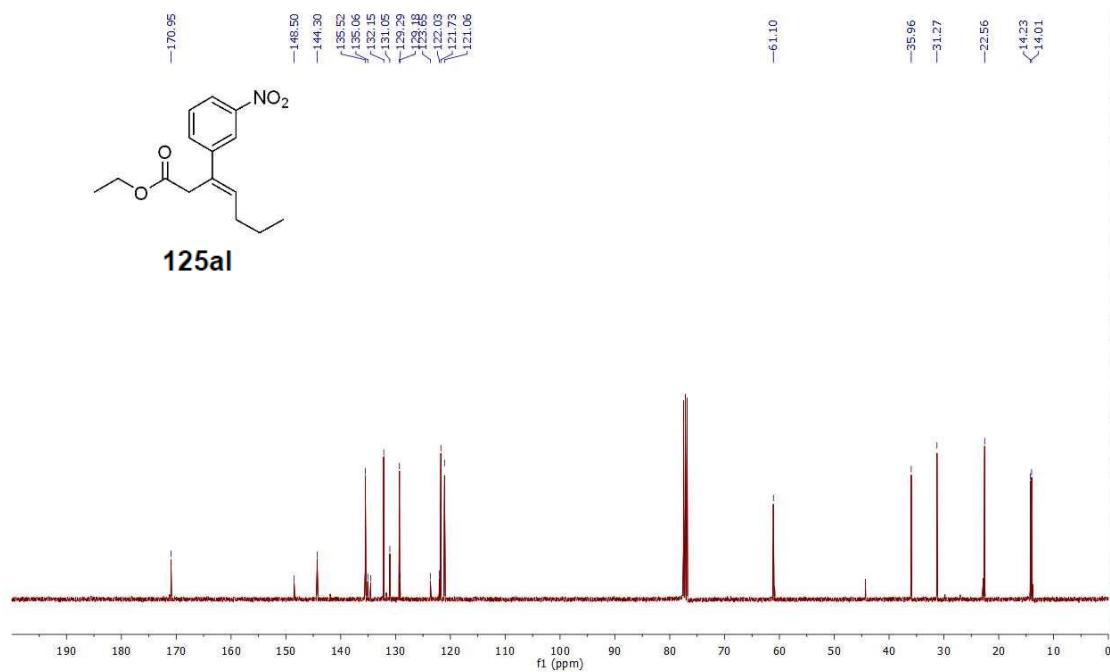
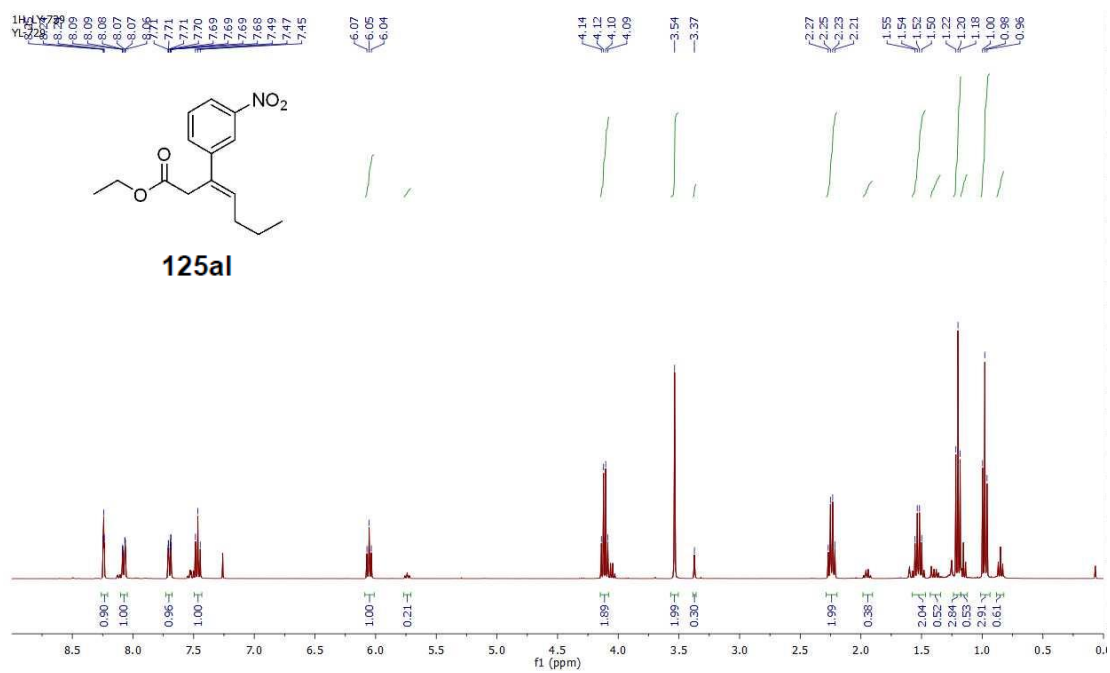
Spectra of Selected Compounds



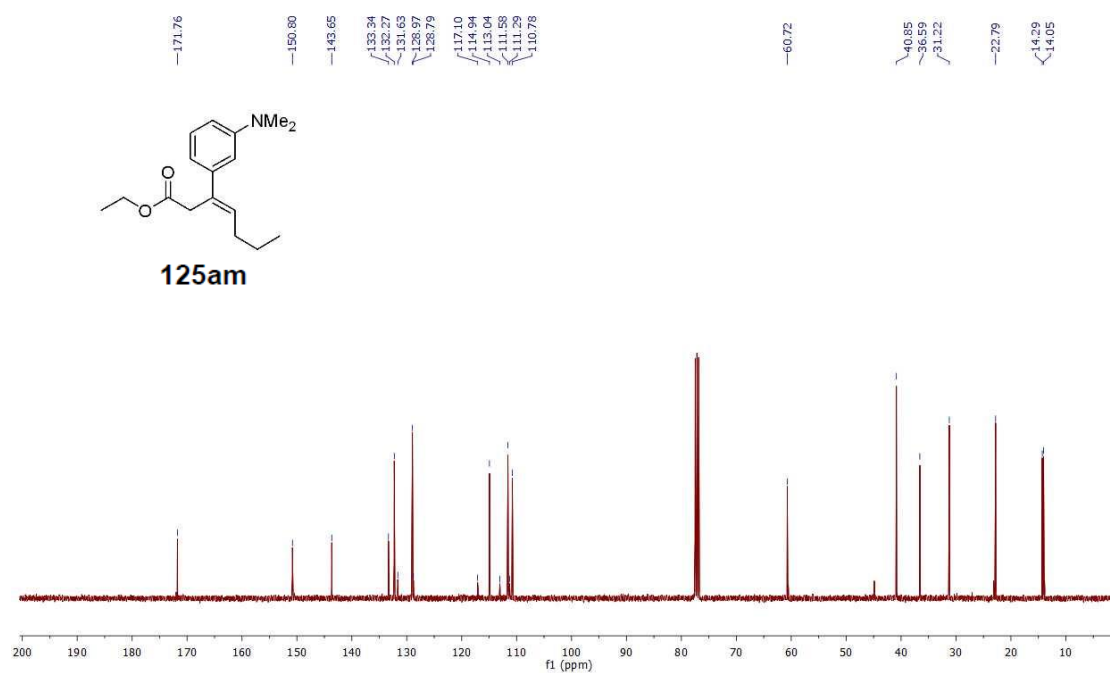
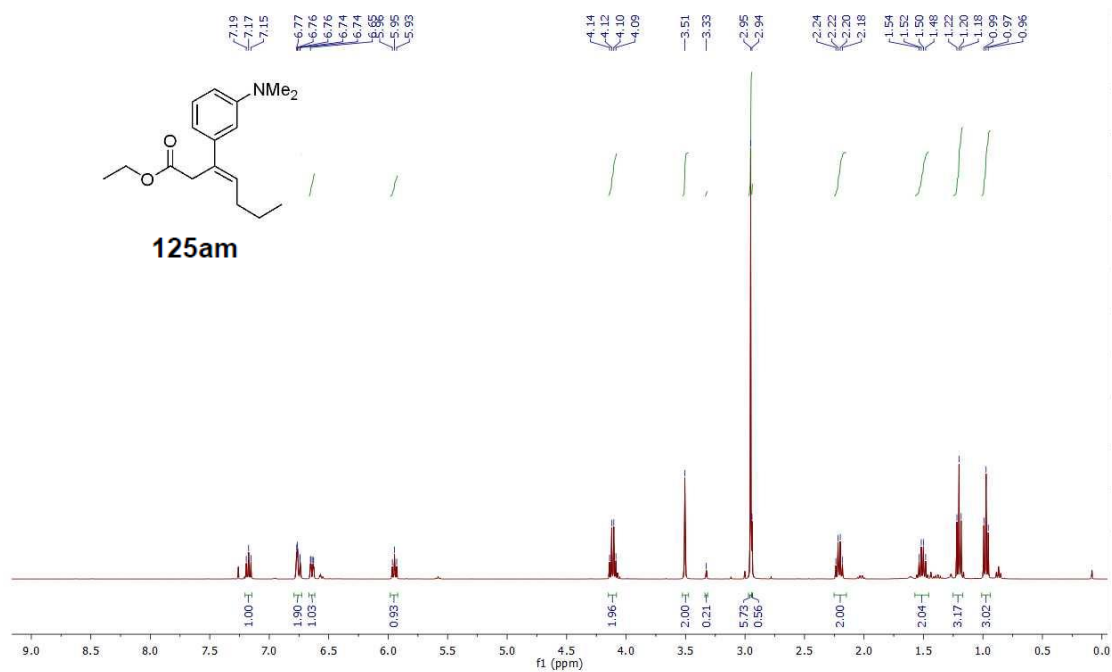
Spectra of Selected Compounds



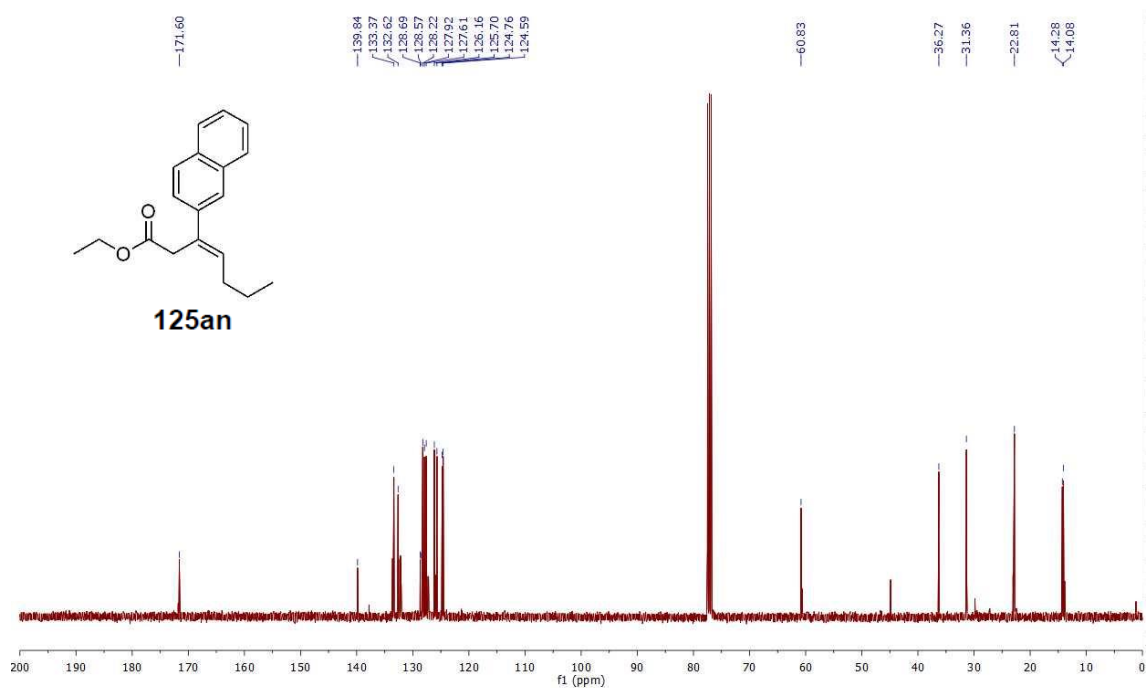
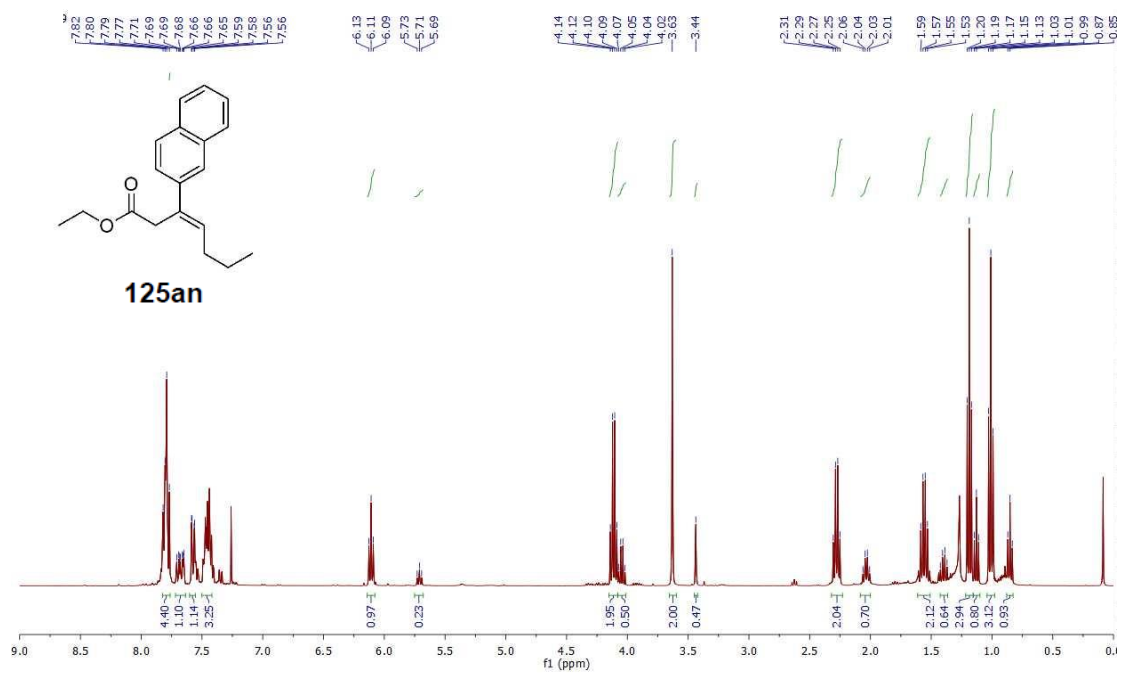
Spectra of Selected Compounds



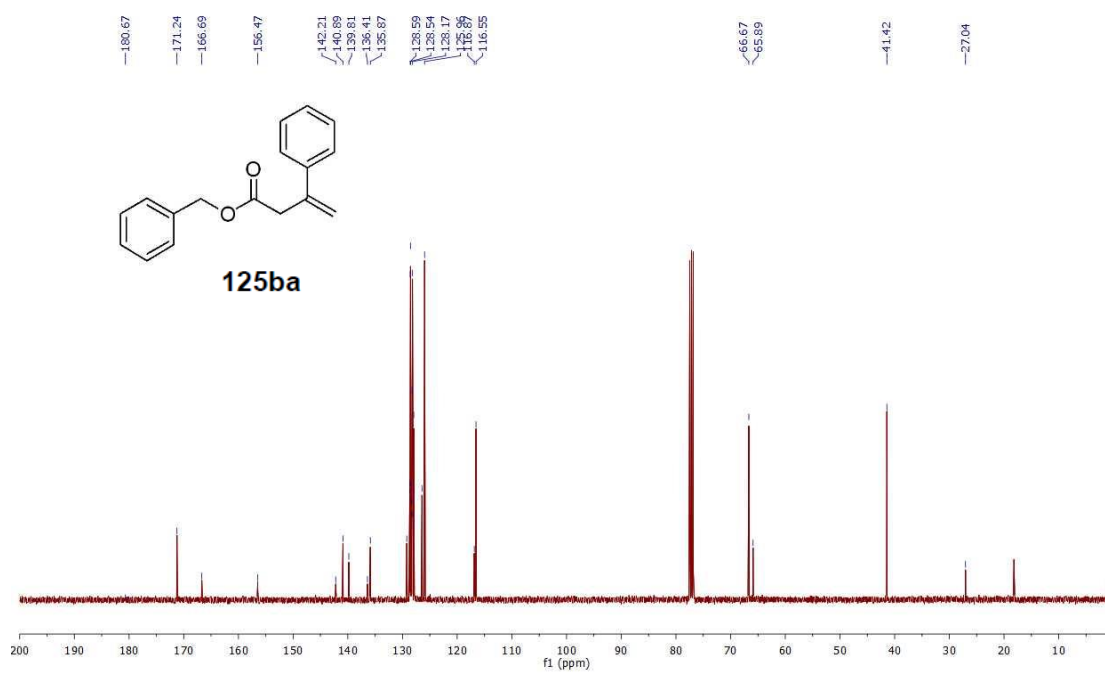
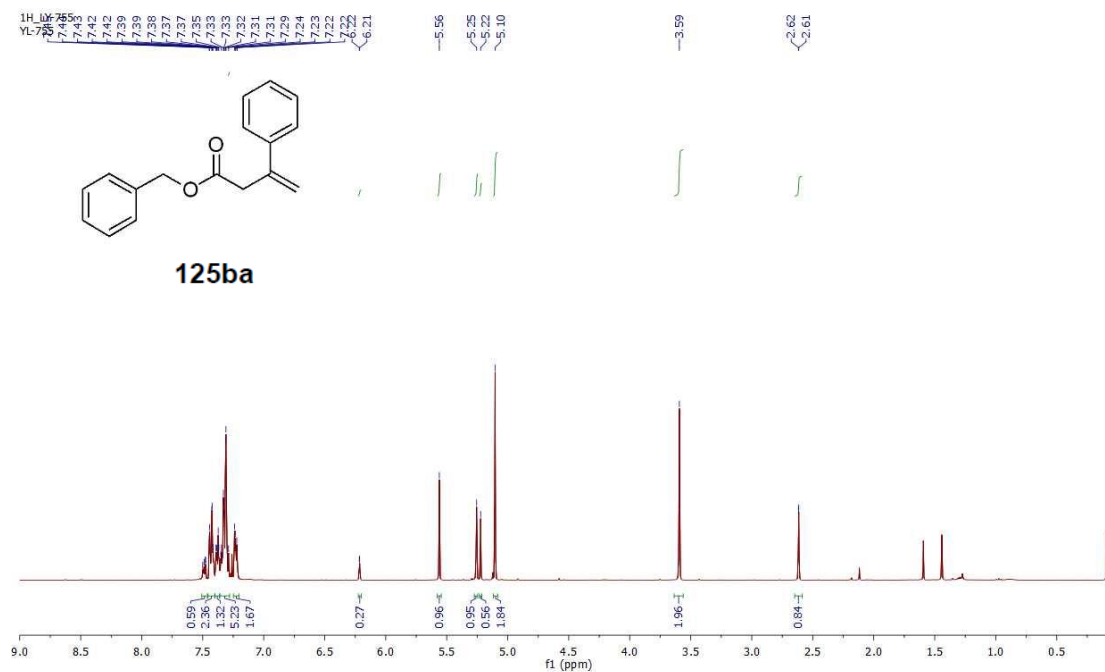
Spectra of Selected Compounds



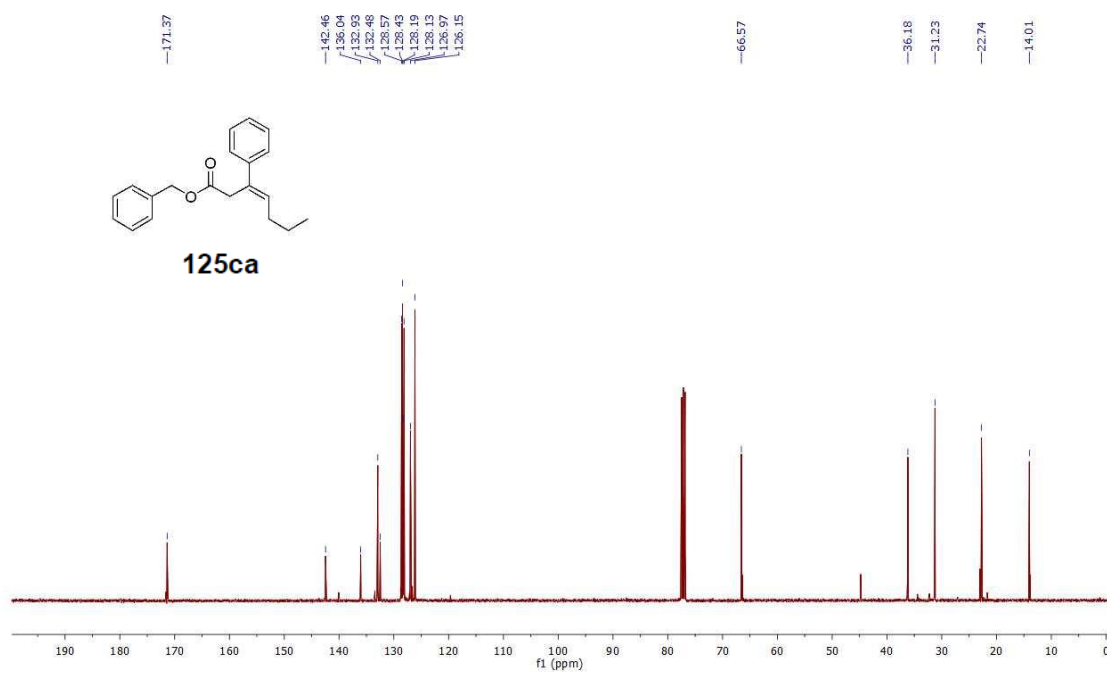
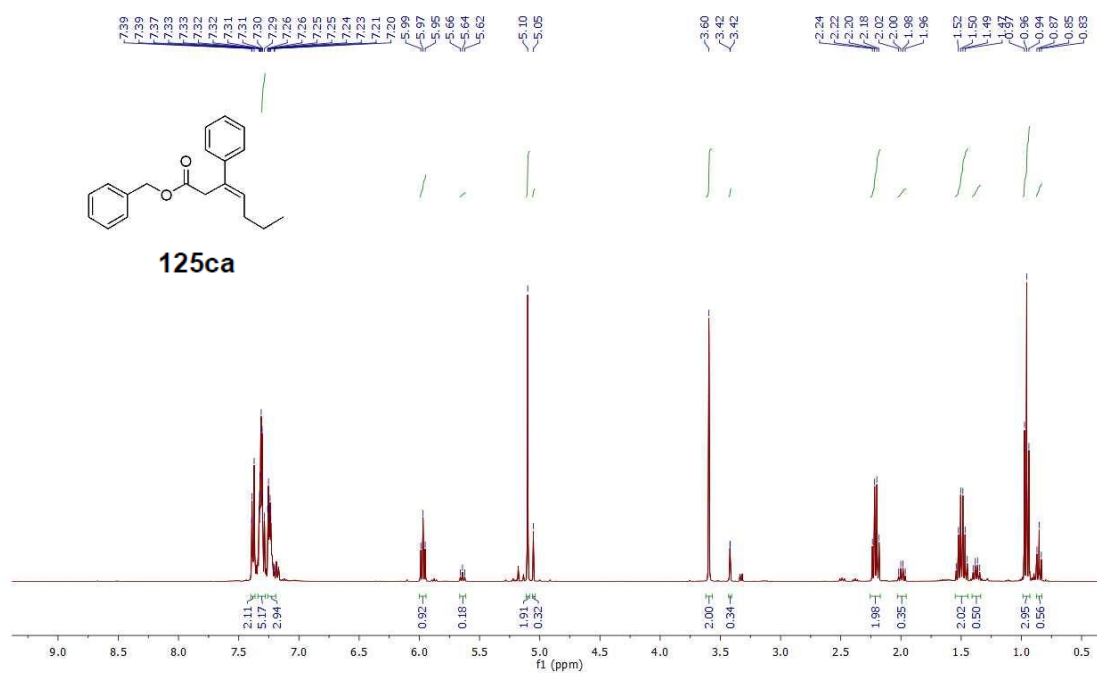
Spectra of Selected Compounds



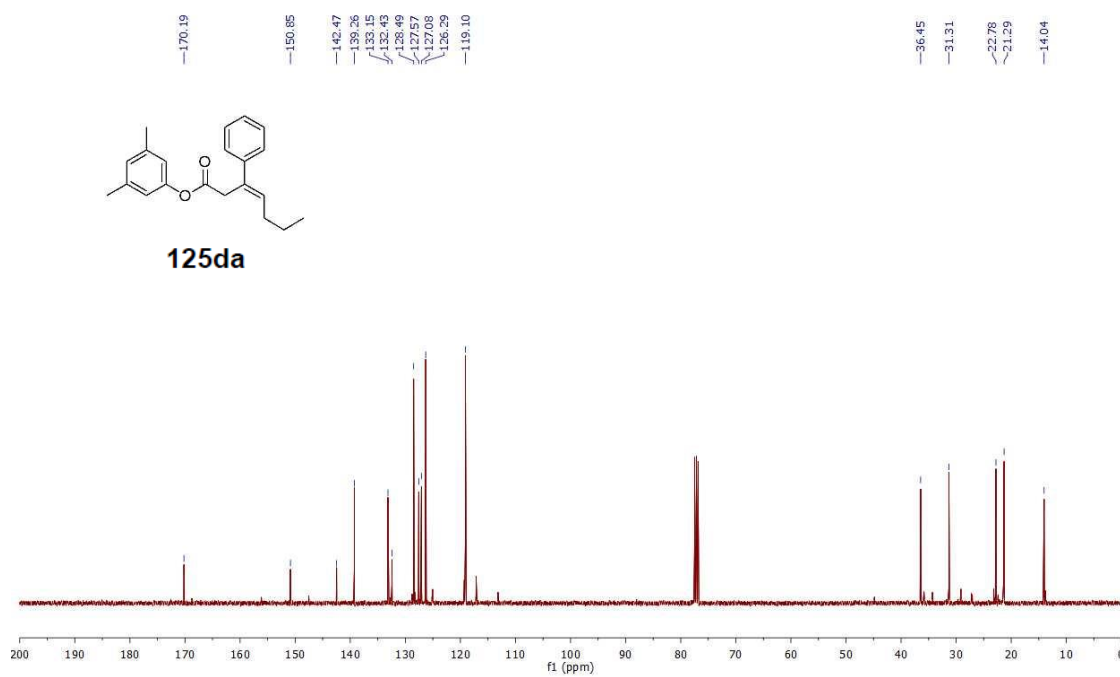
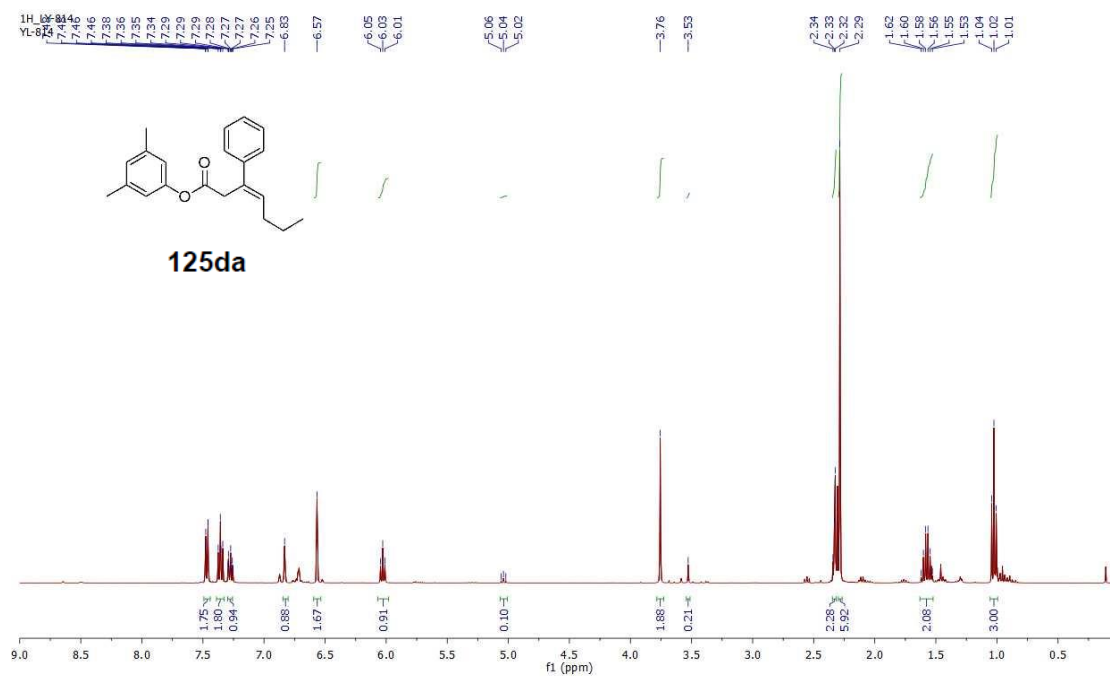
Spectra of Selected Compounds



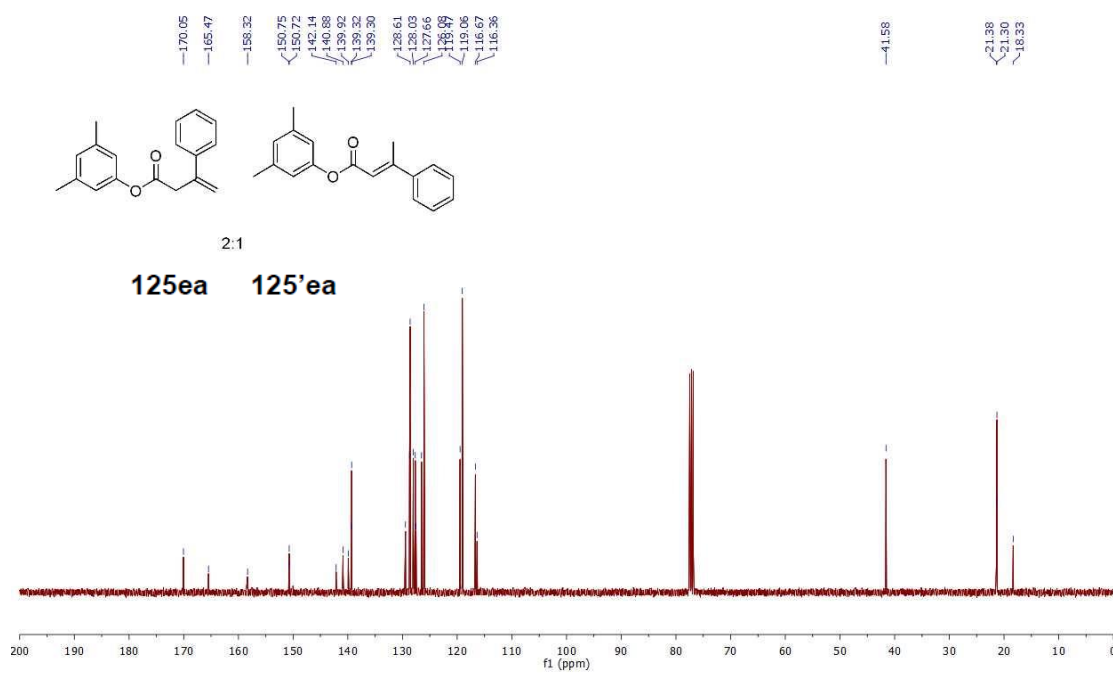
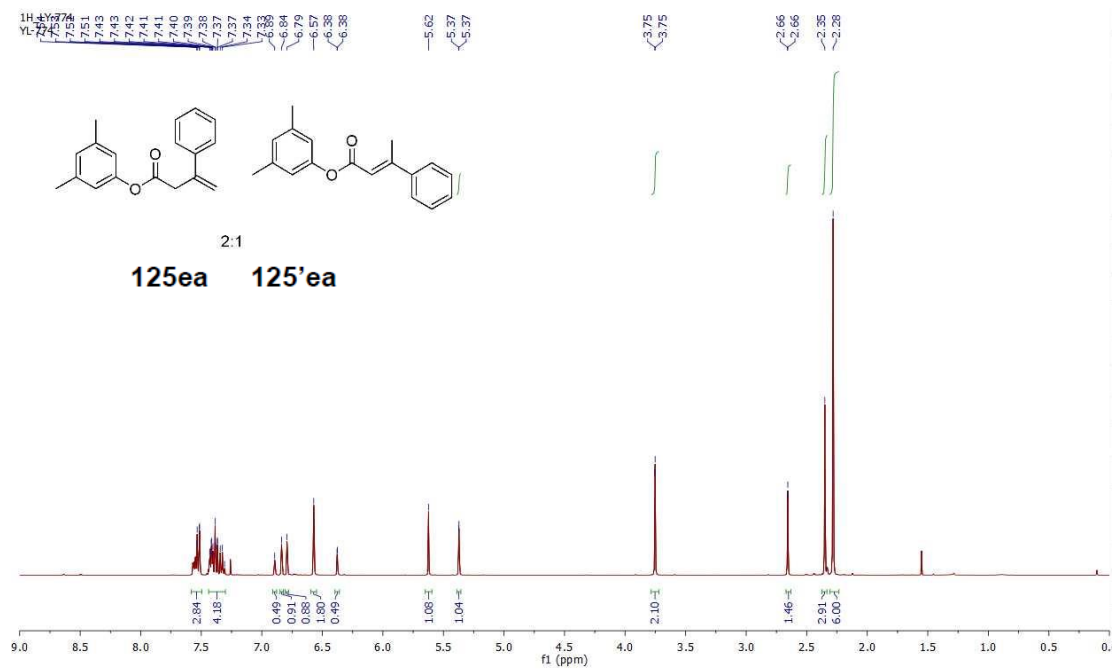
Spectra of Selected Compounds



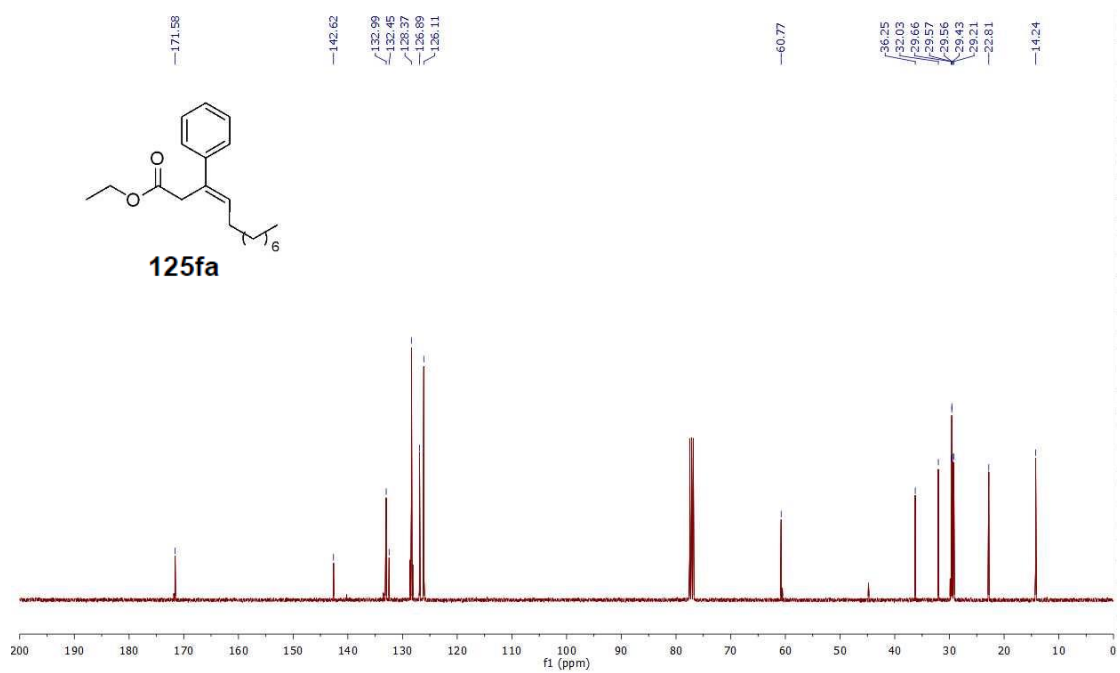
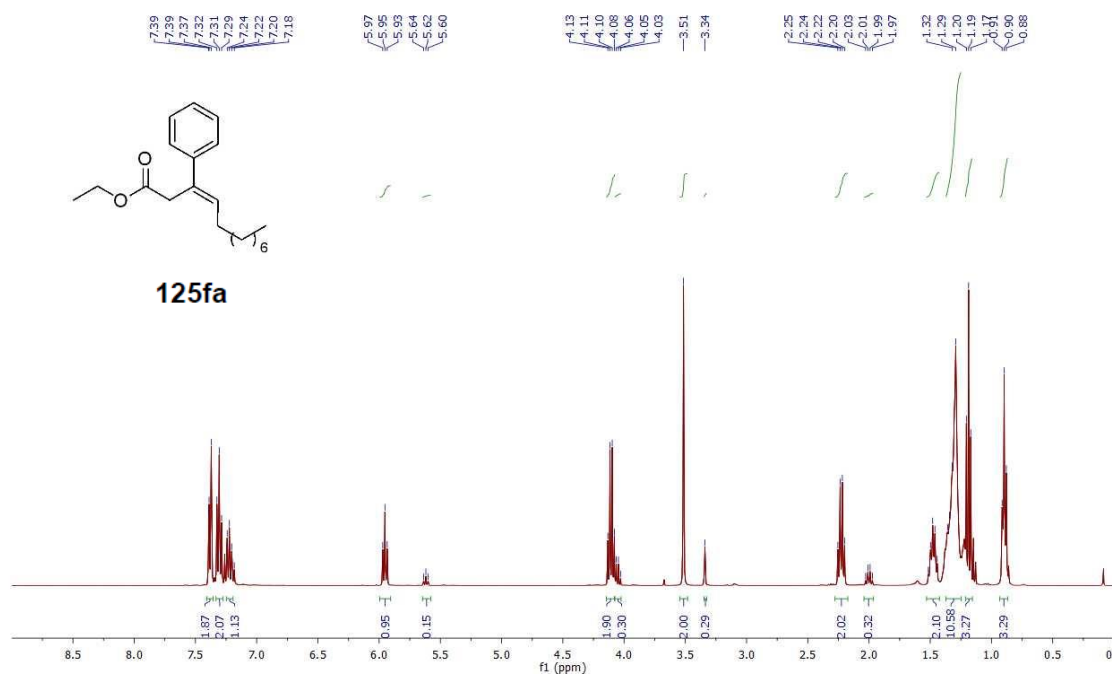
Spectra of Selected Compounds



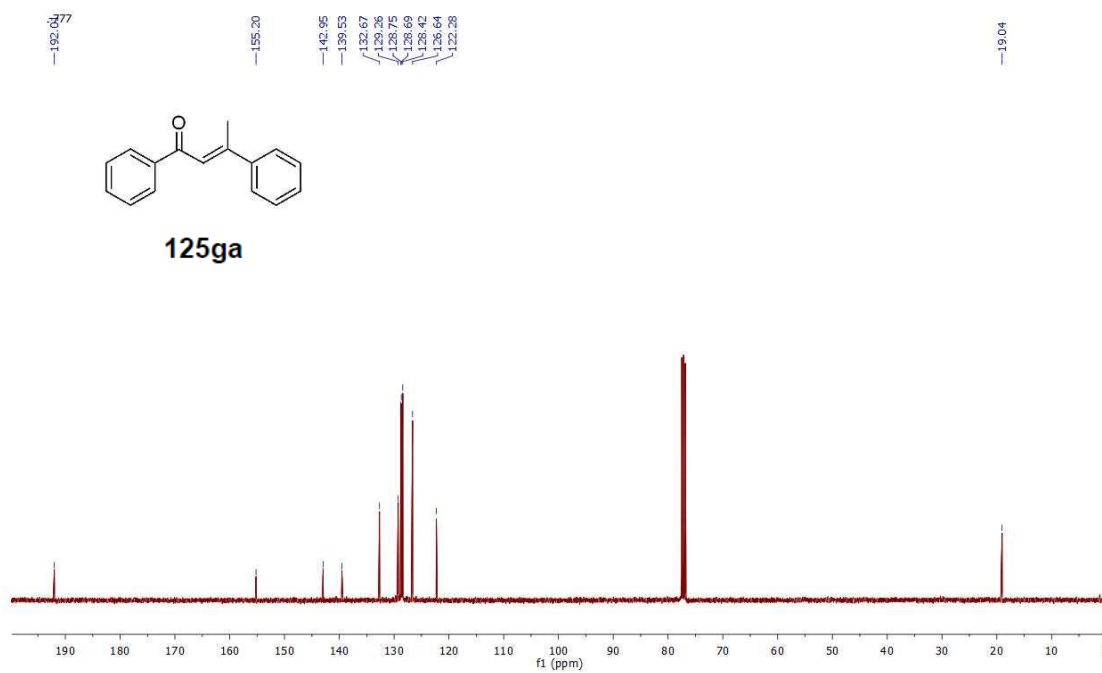
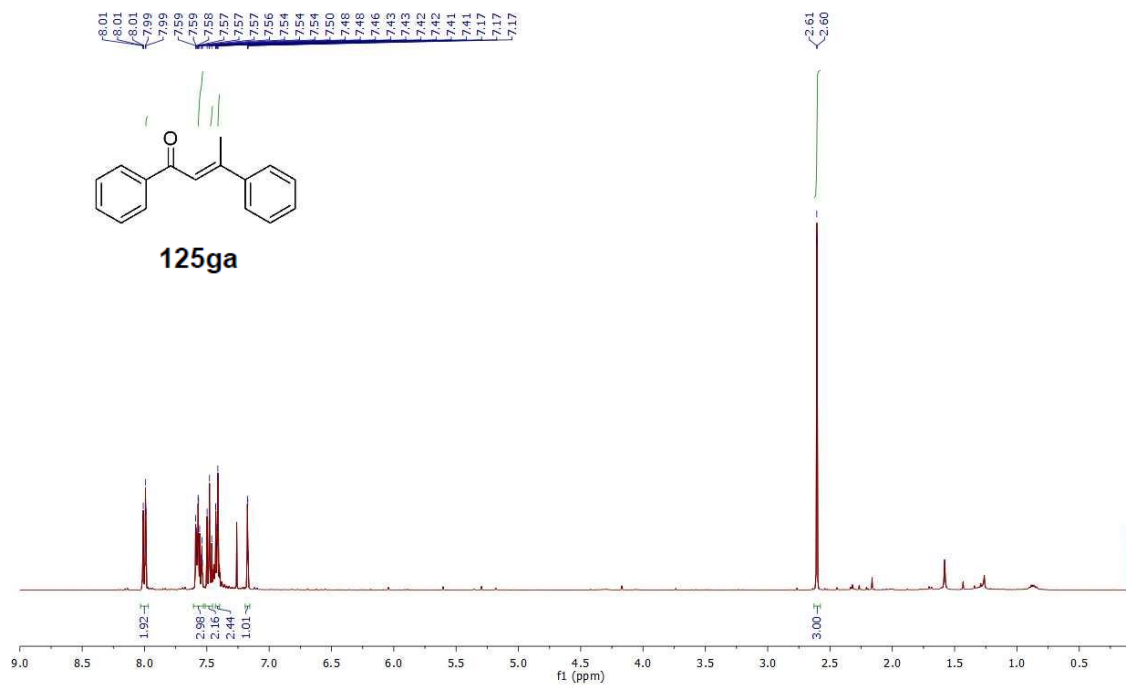
Spectra of Selected Compounds



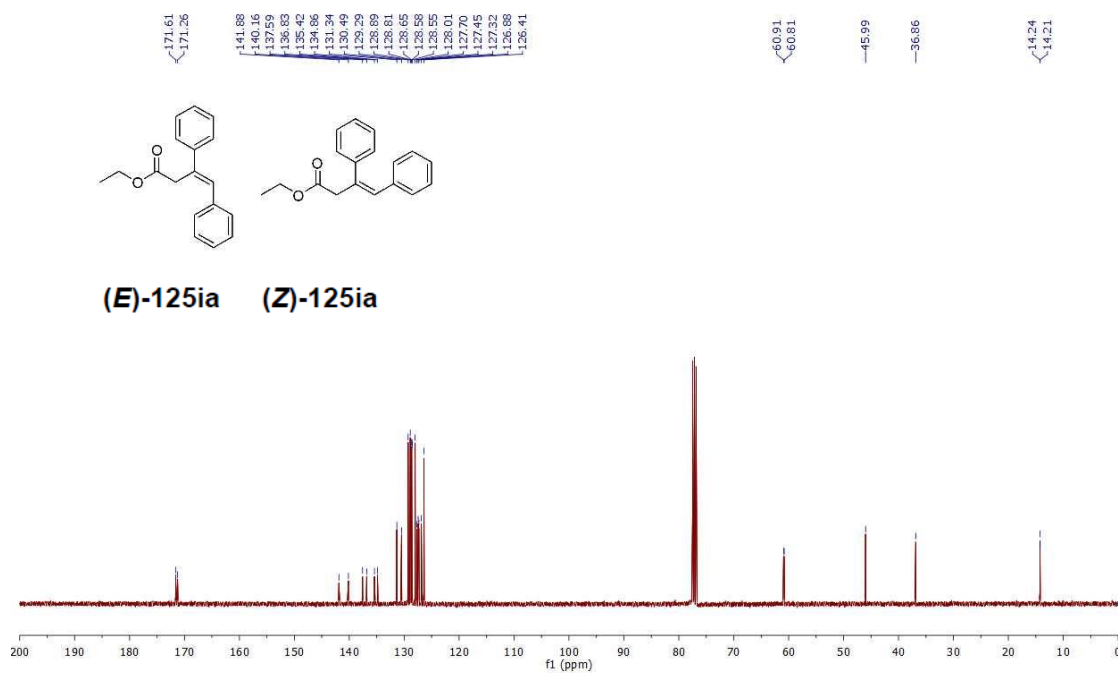
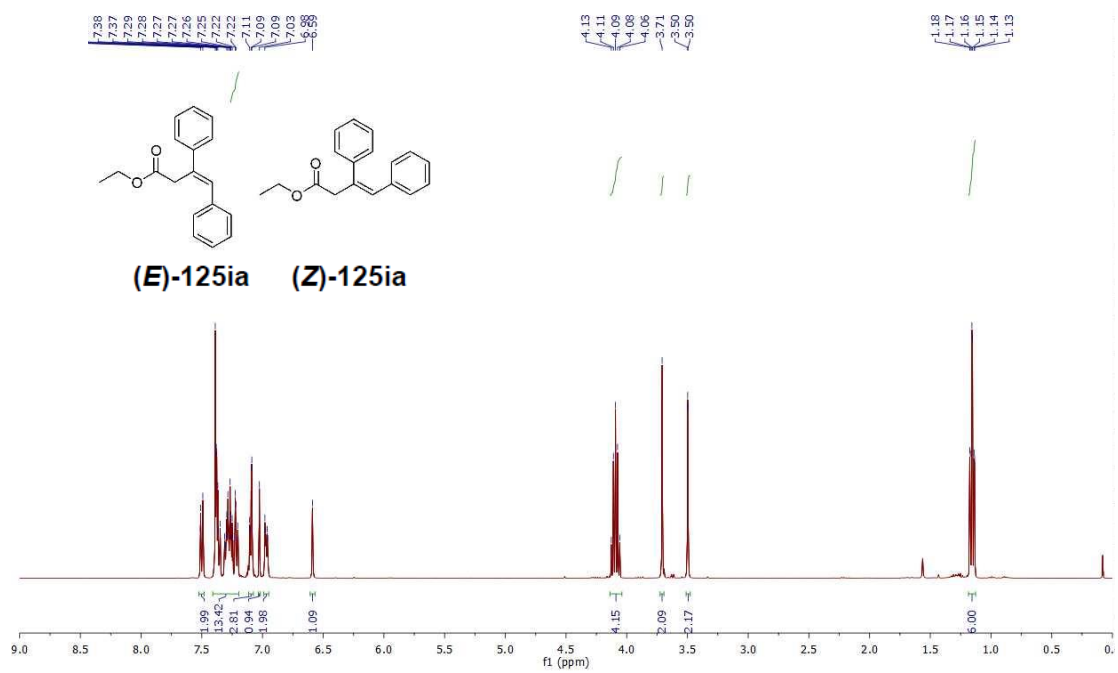
Spectra of Selected Compounds



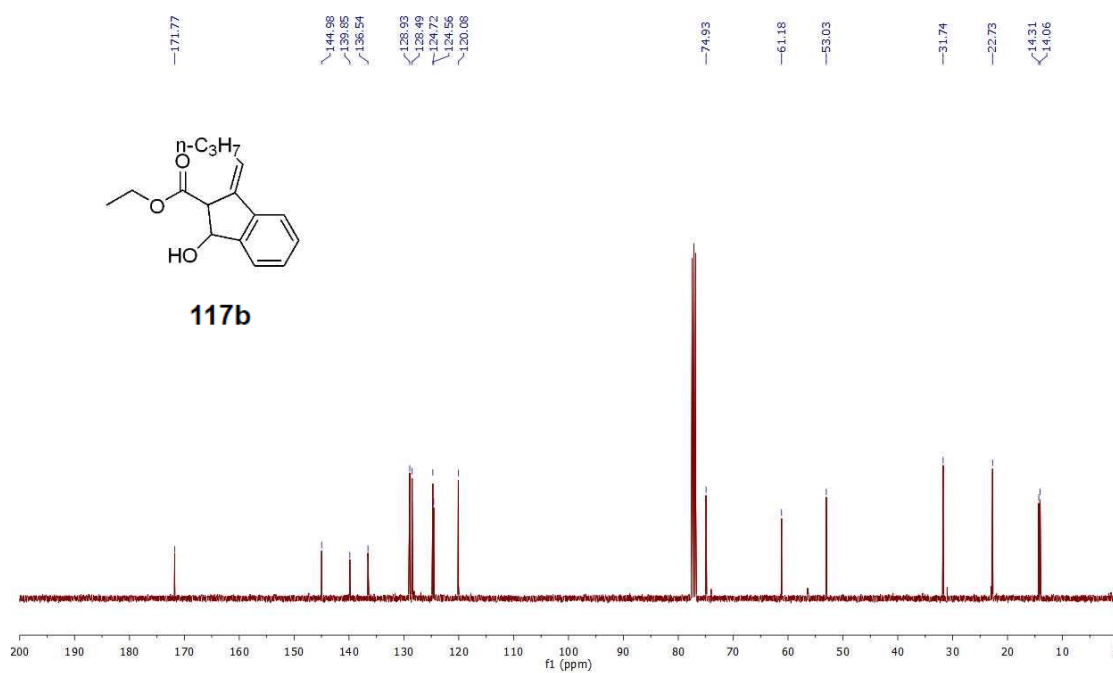
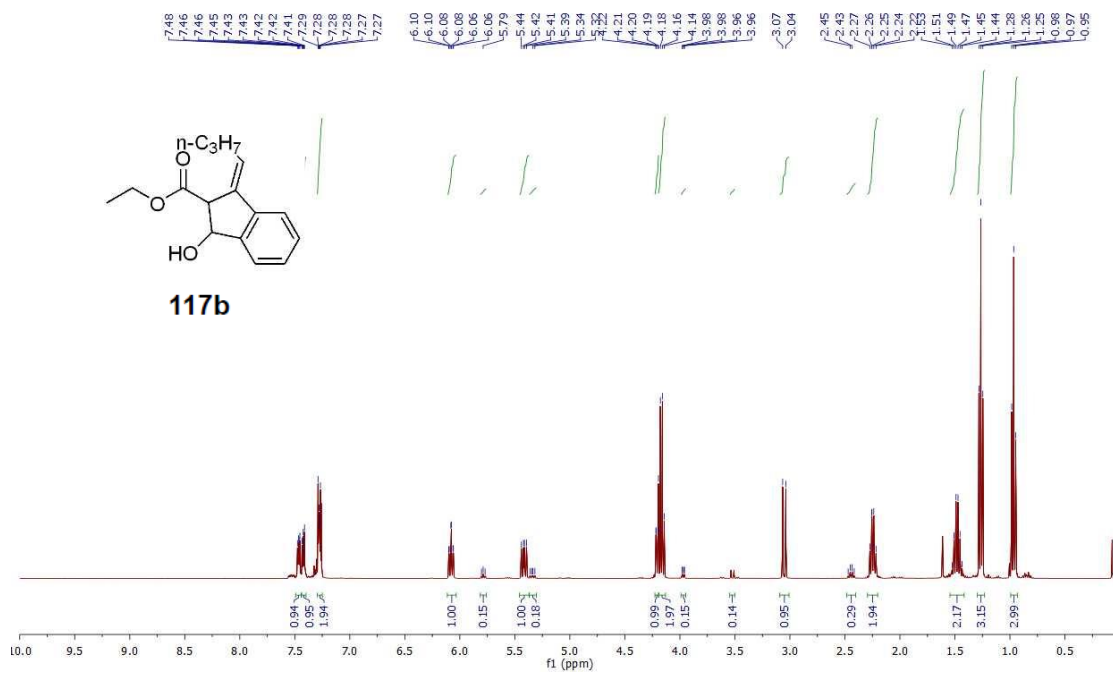
Spectra of Selected Compounds



Spectra of Selected Compounds



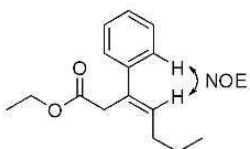
Spectra of Selected Compounds



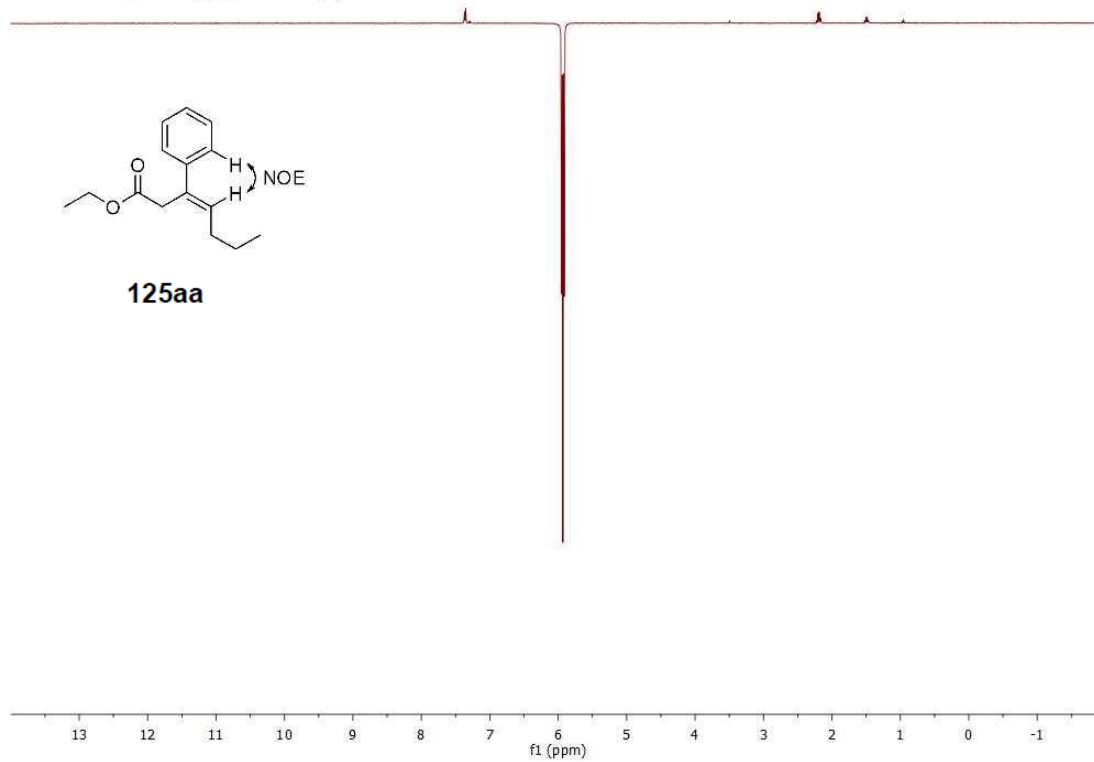
Spectra of Selected Compounds

NOE_YL_Allenoate
YL NOe1

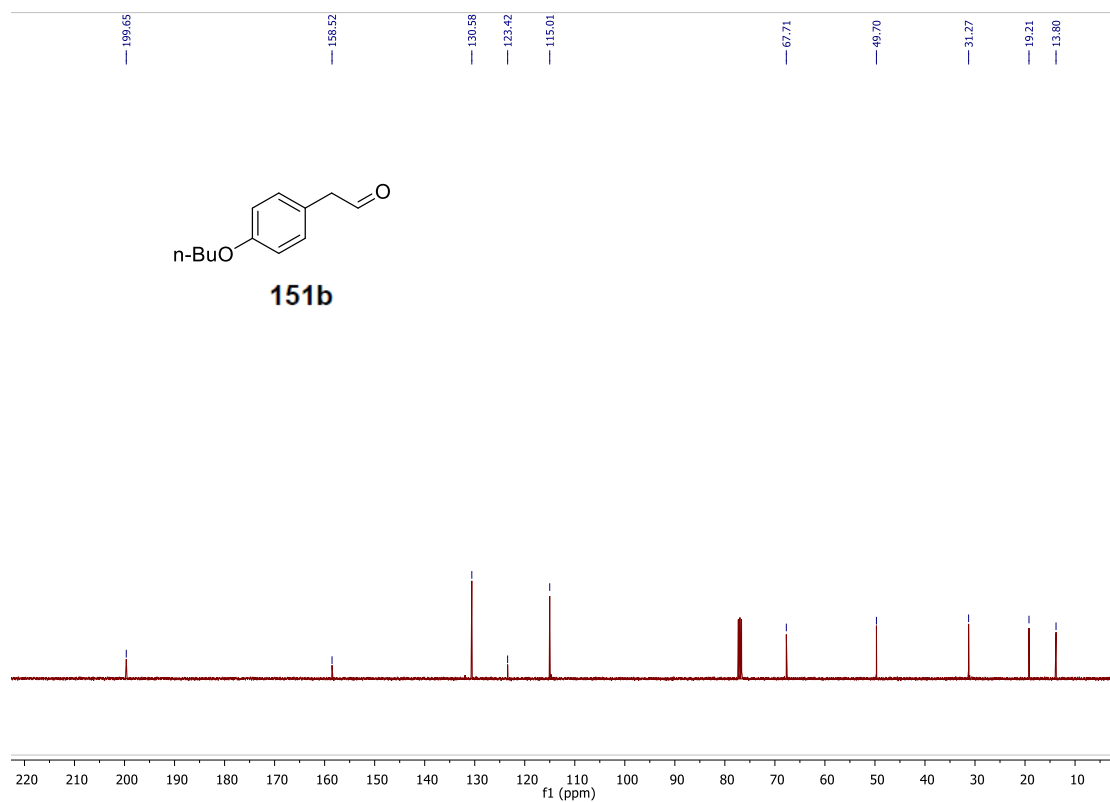
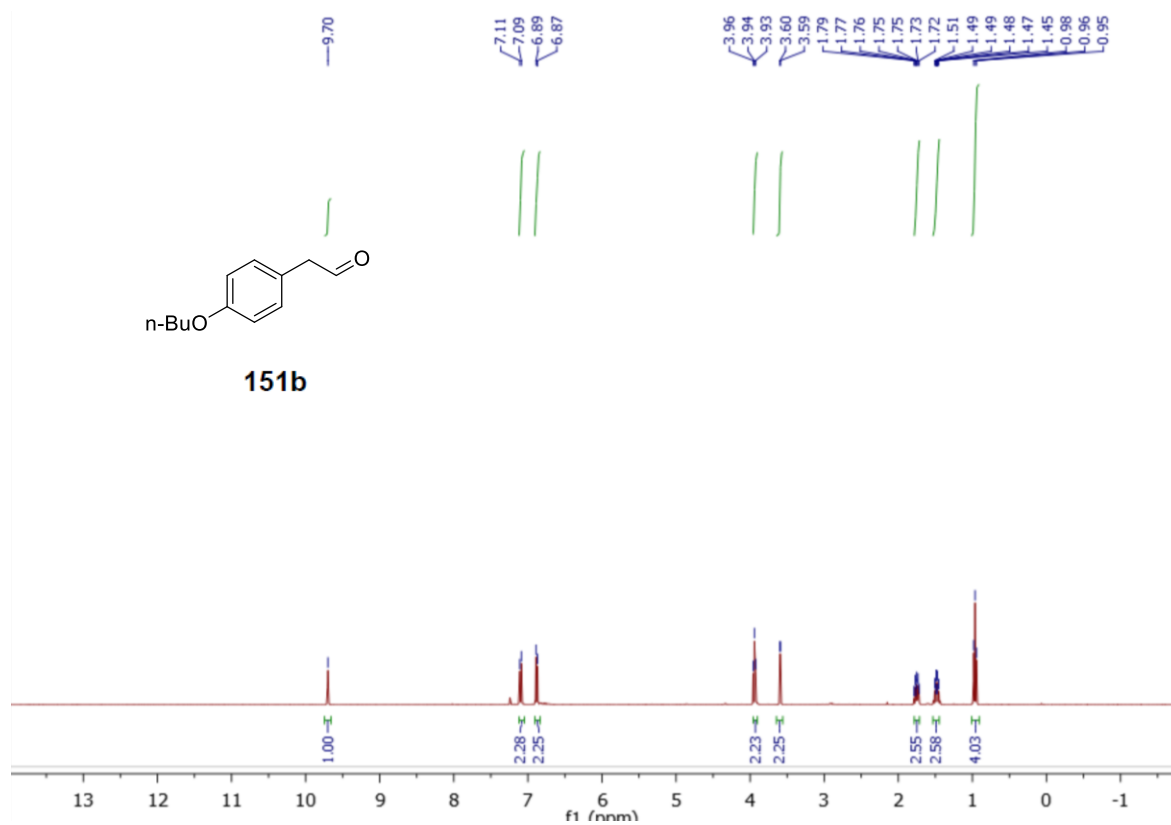
Selective band center: 5.93 (ppm); width: 50.9 (Hz)



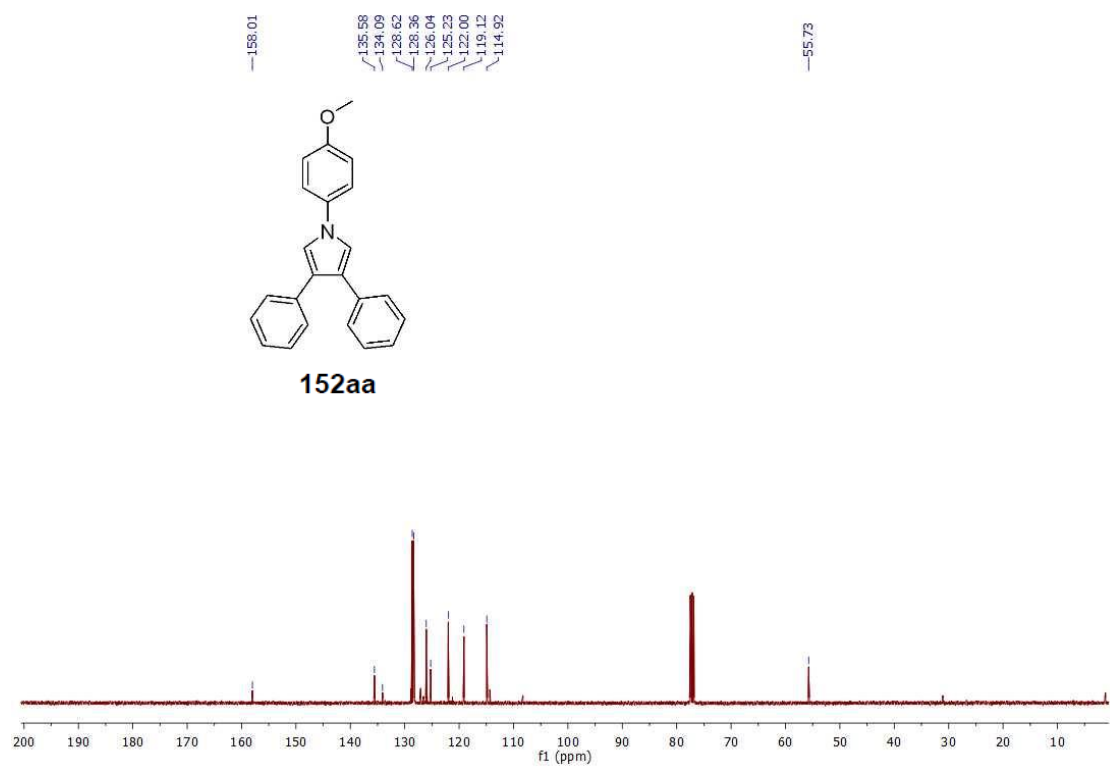
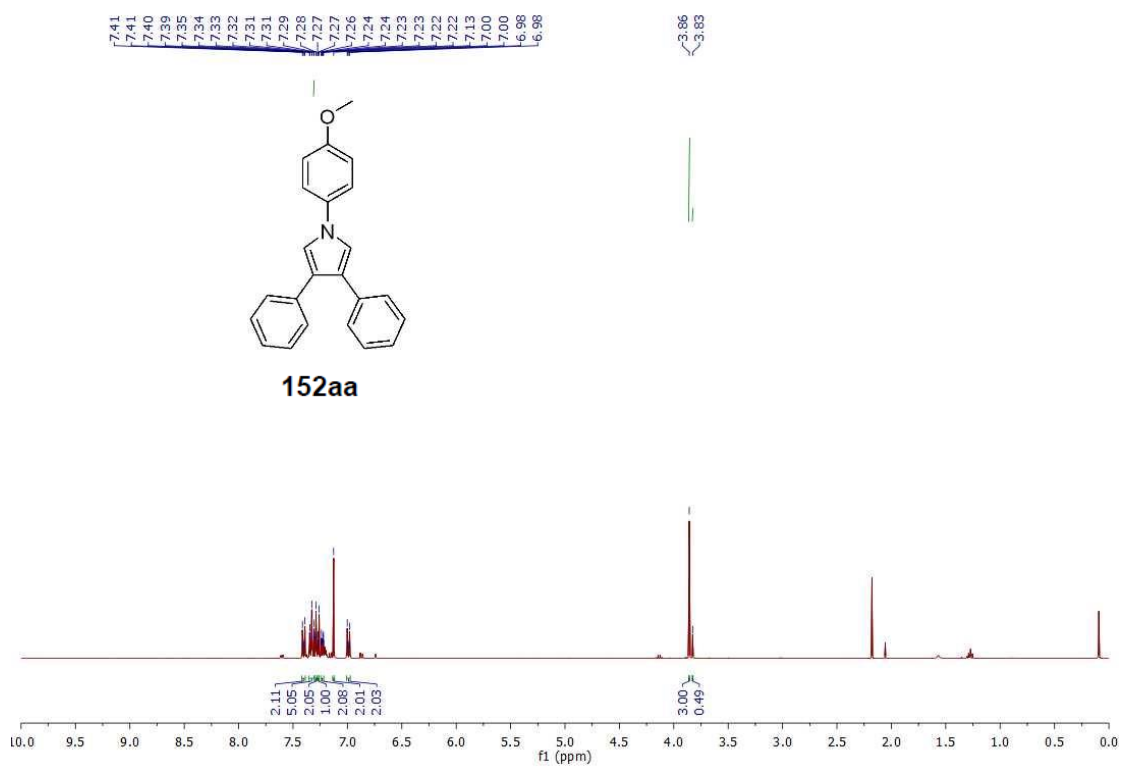
125aa

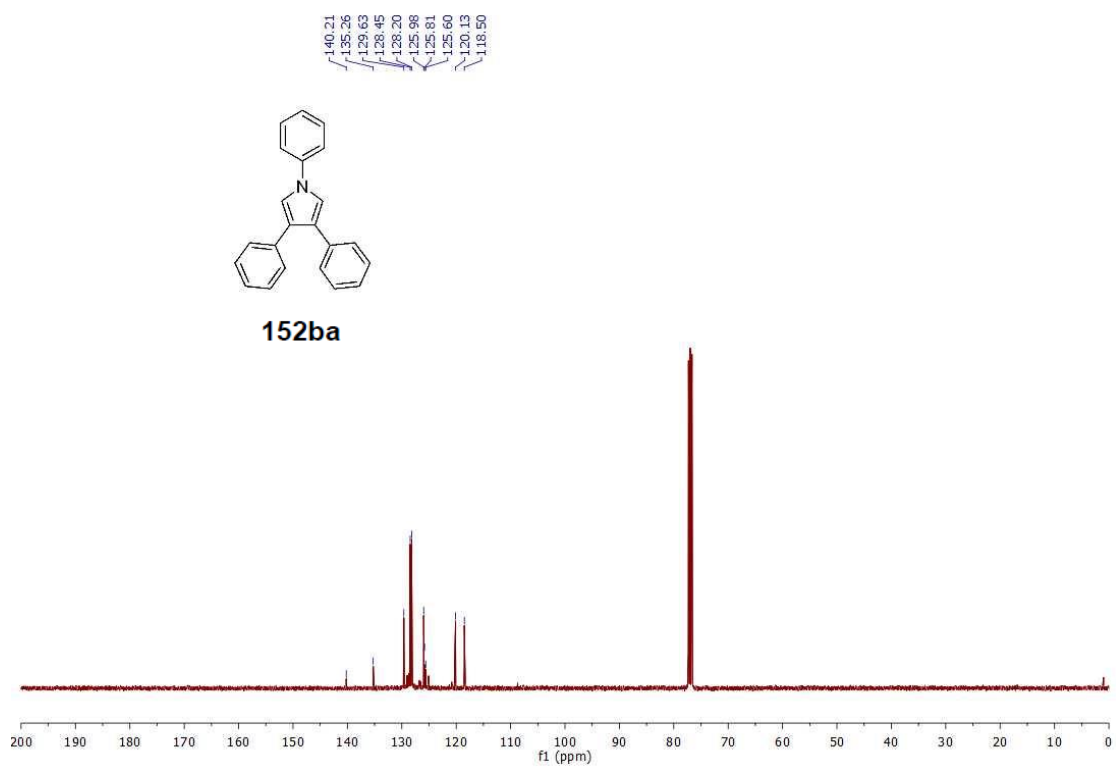
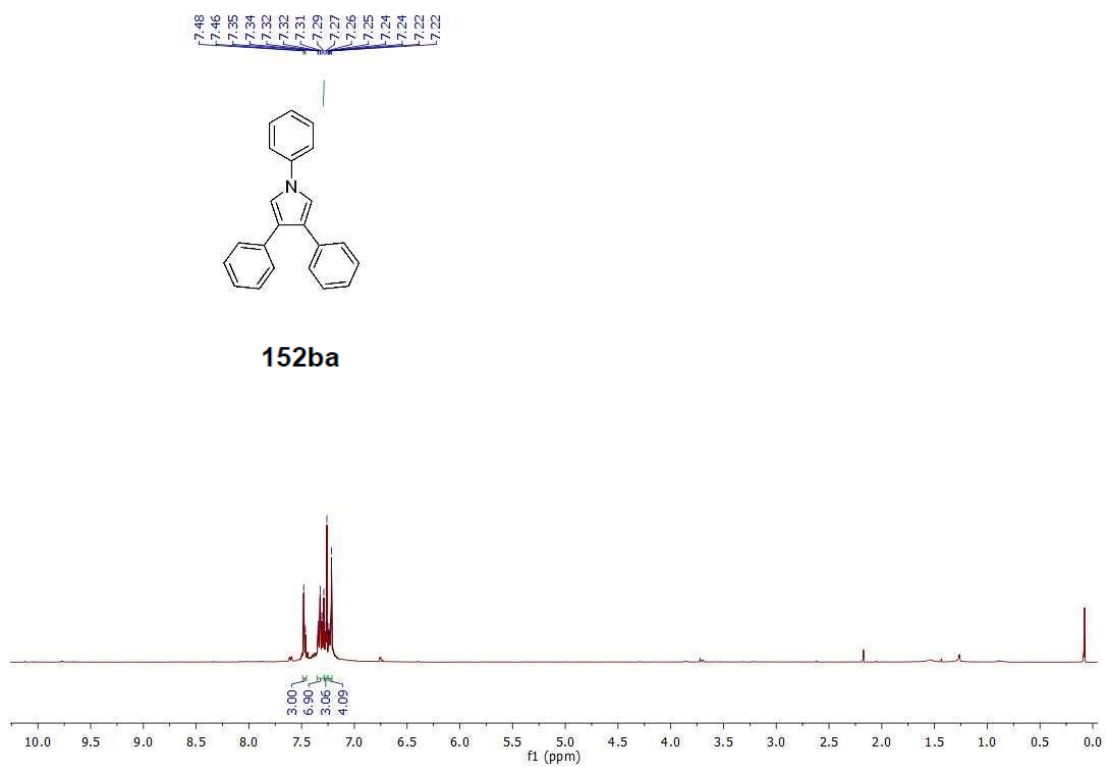


Spectra of Selected Compounds

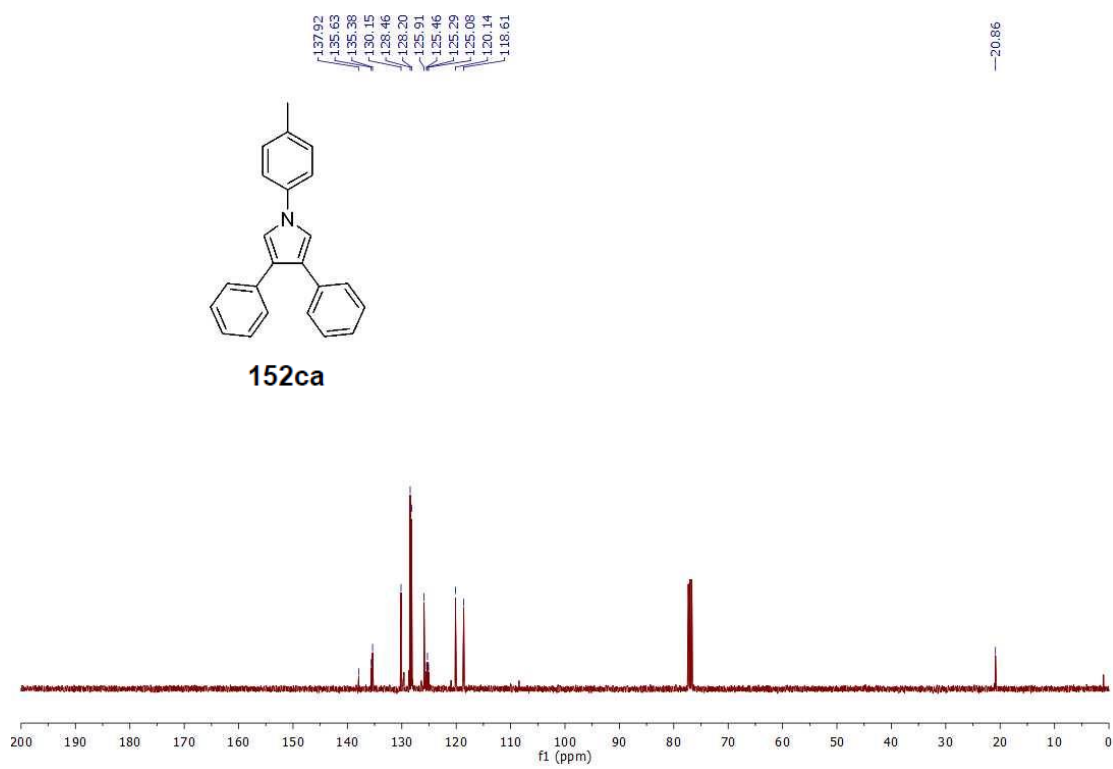
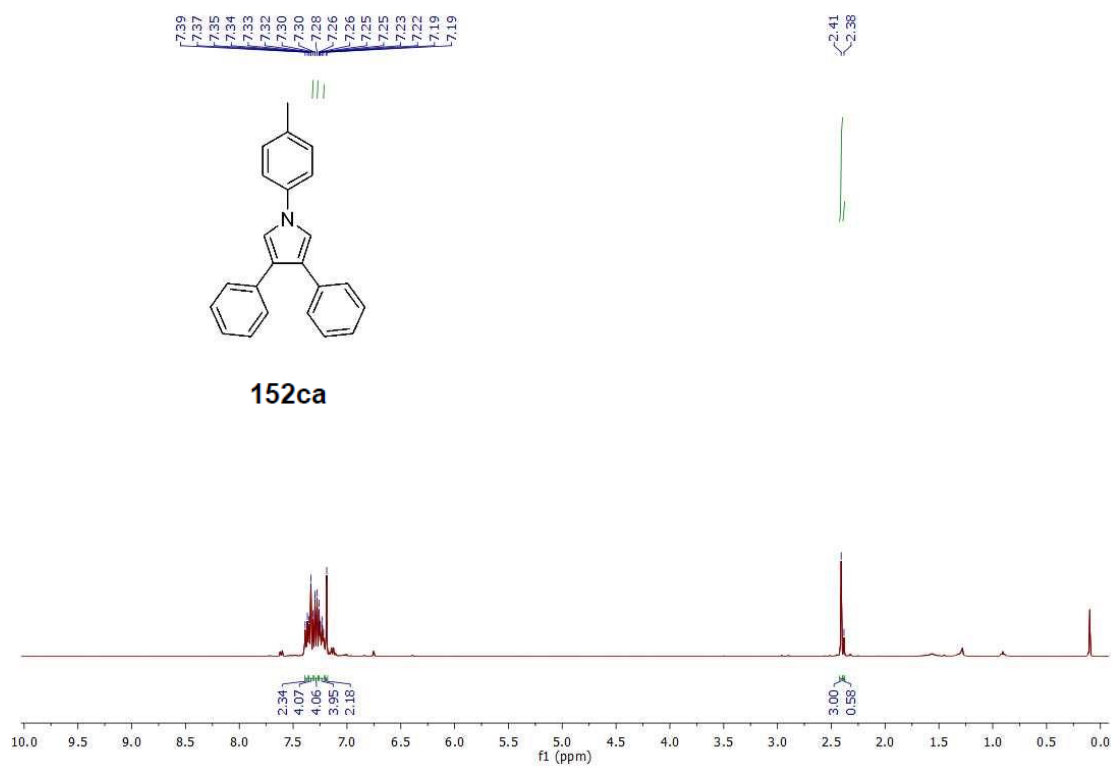


Spectra of Selected Compounds



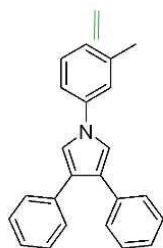


Spectra of Selected Compounds



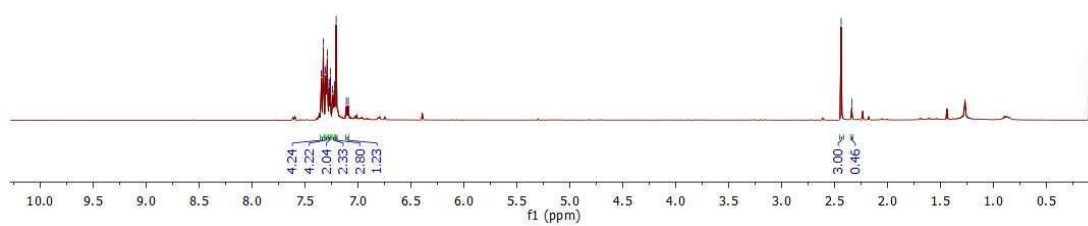
Spectra of Selected Compounds

7.35
7.33
7.31
7.29
7.27
7.26
7.24
7.22
7.21
7.11
7.09

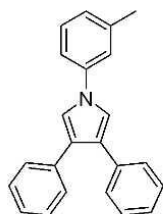


152da

2.44
2.34

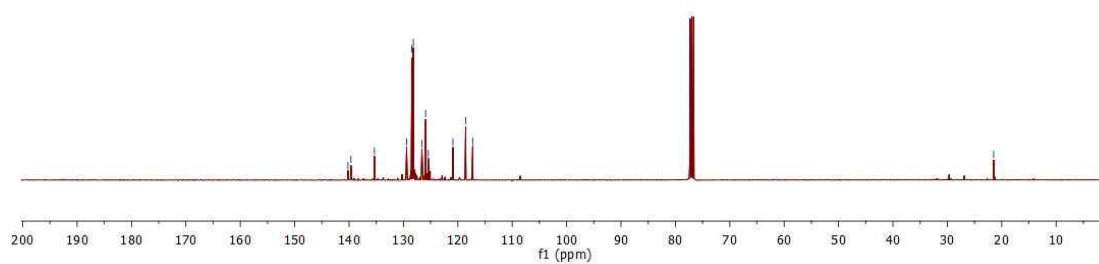


140.19
139.65
135.34
129.42
128.45
128.18
126.61
125.93
120.90
118.57
117.27

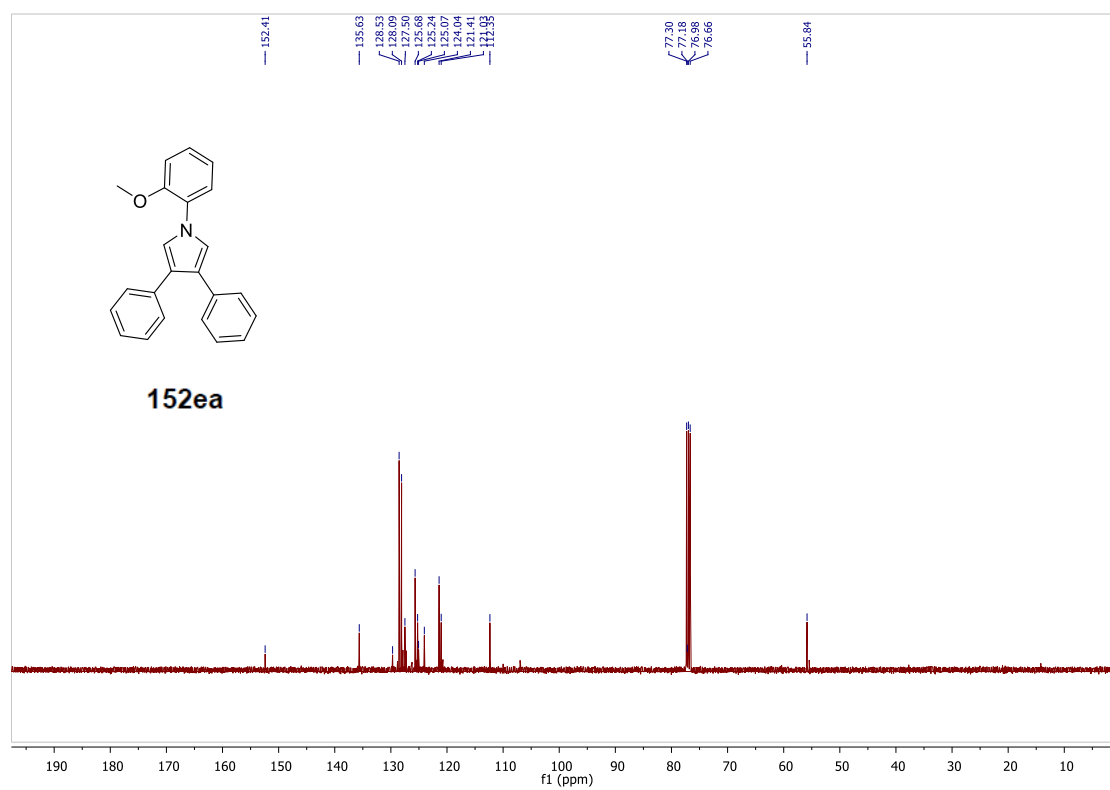
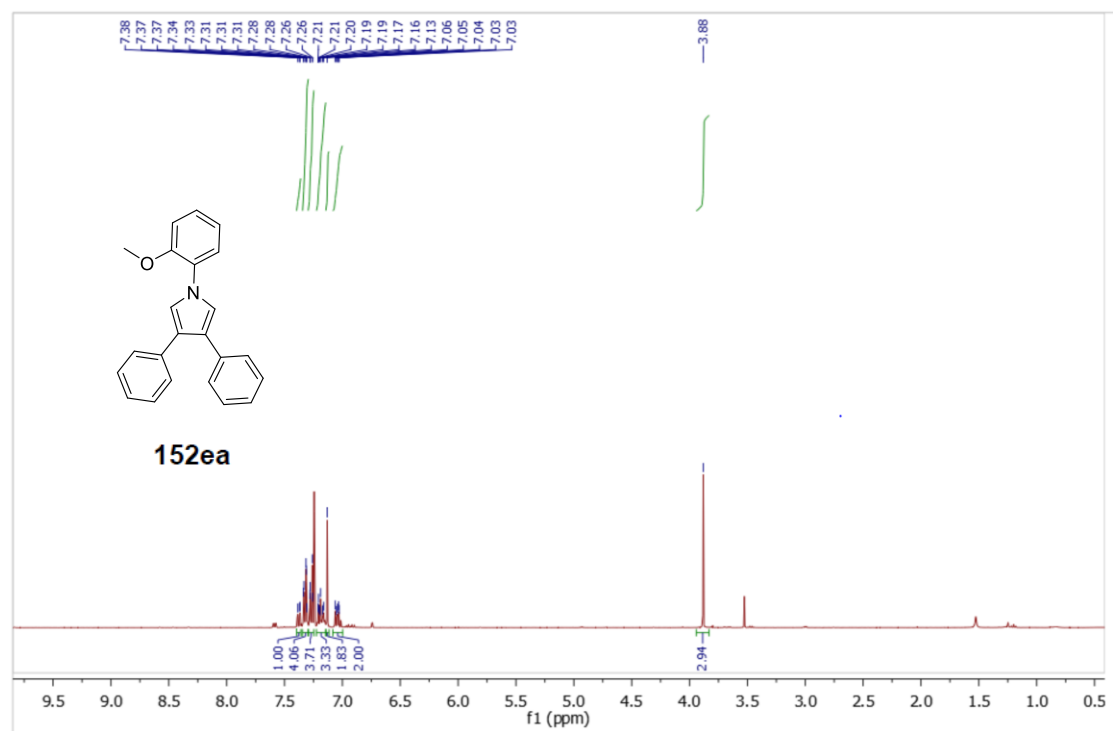


152da

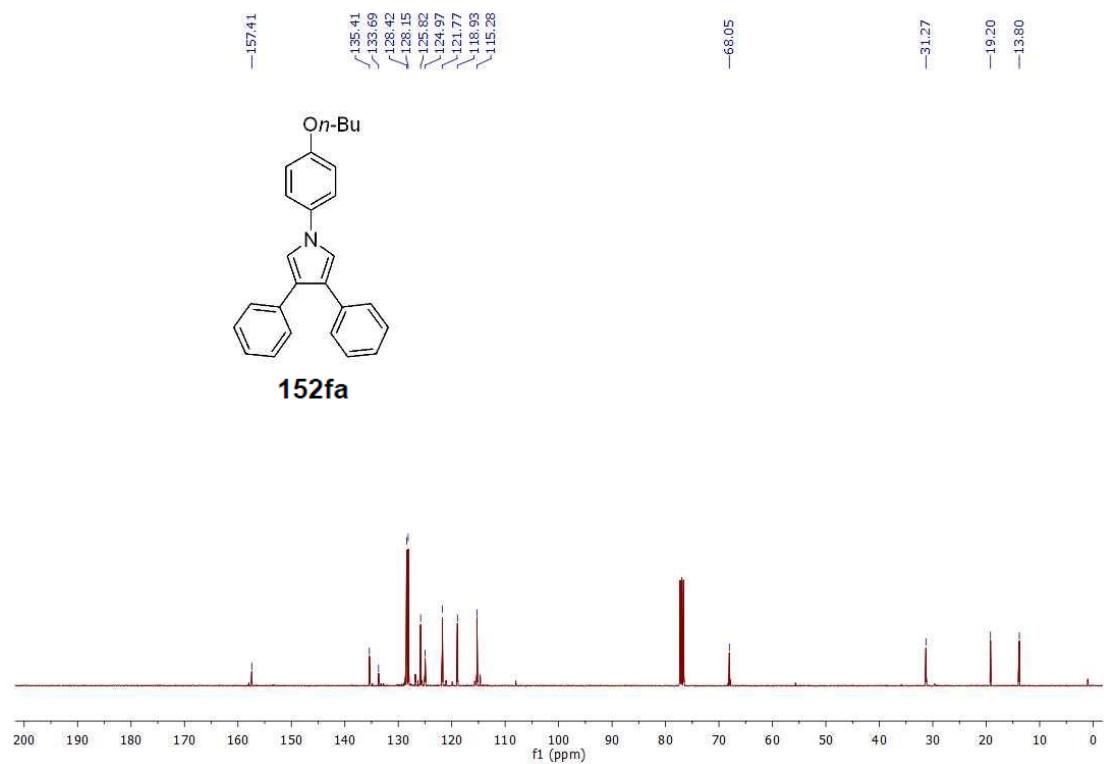
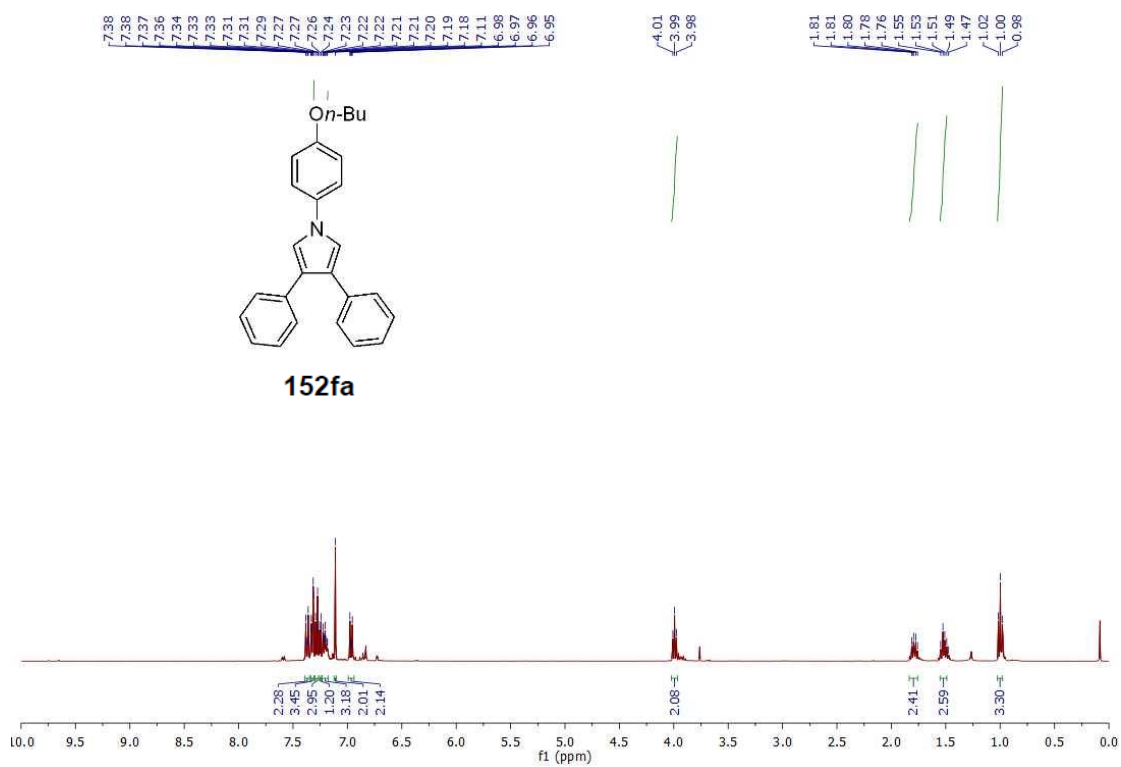
21.49



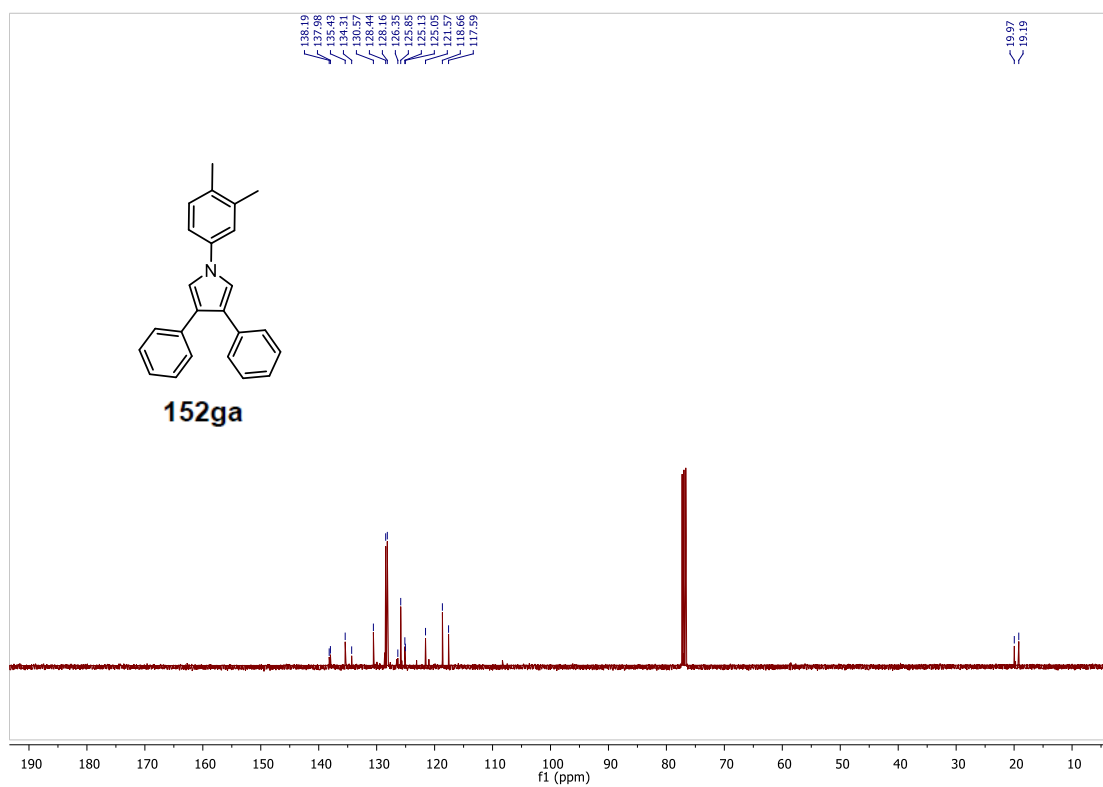
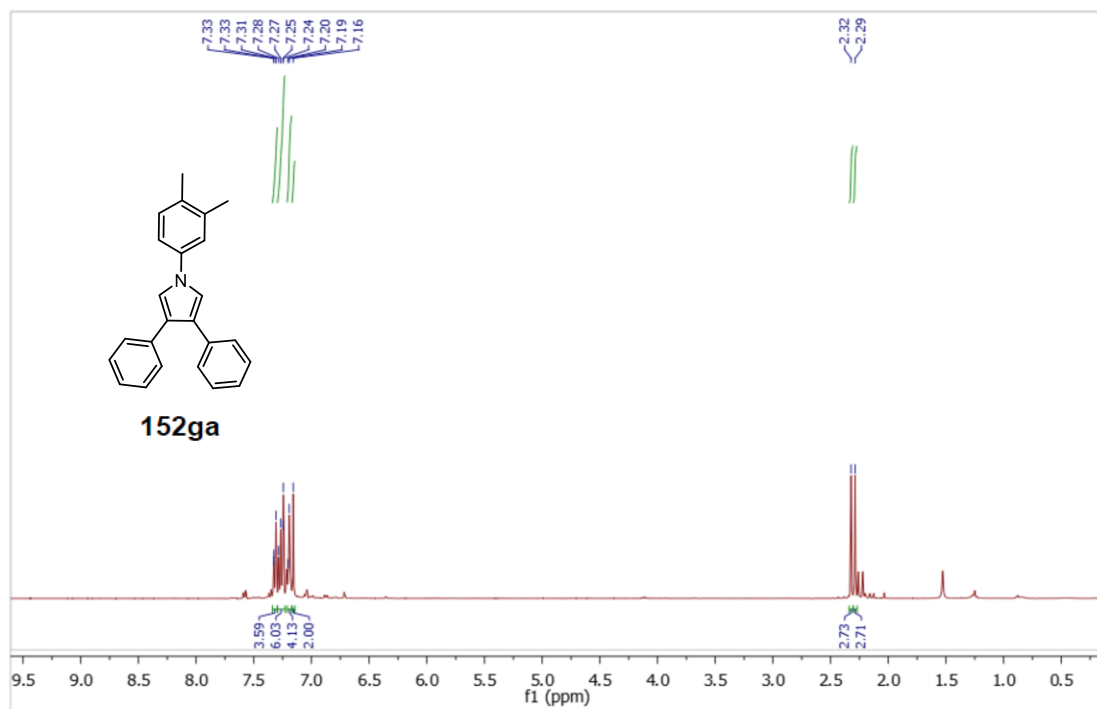
Spectra of Selected Compounds



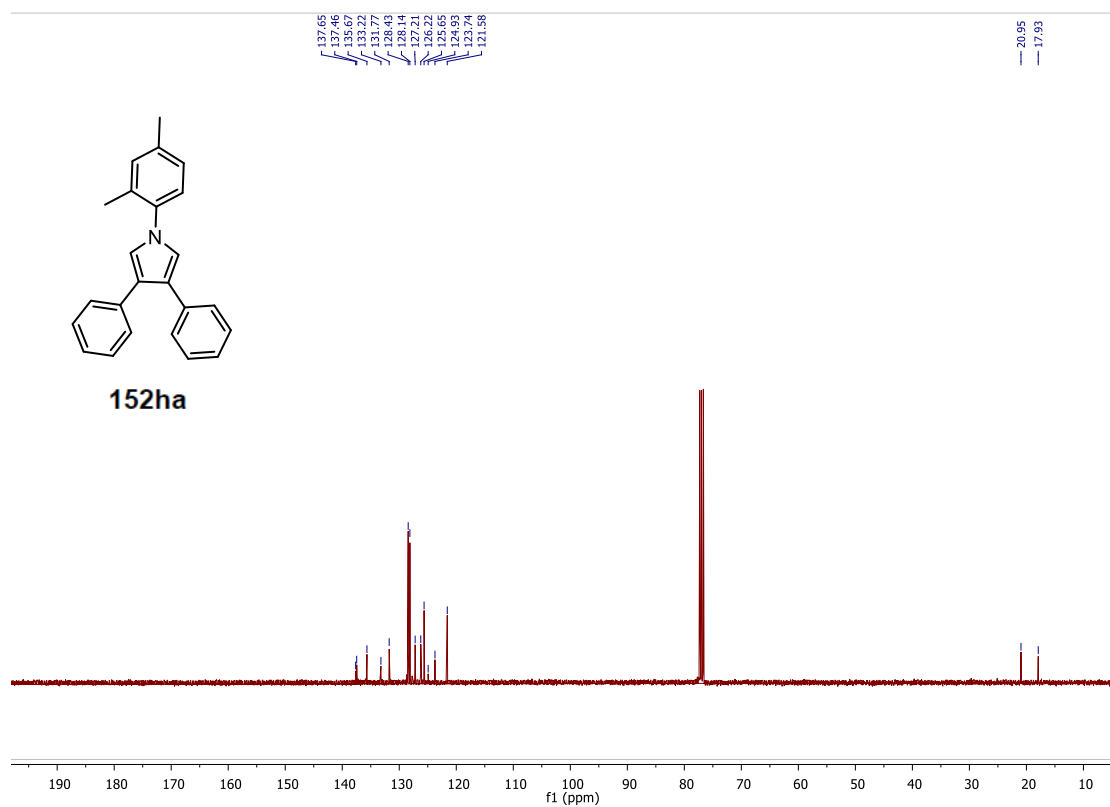
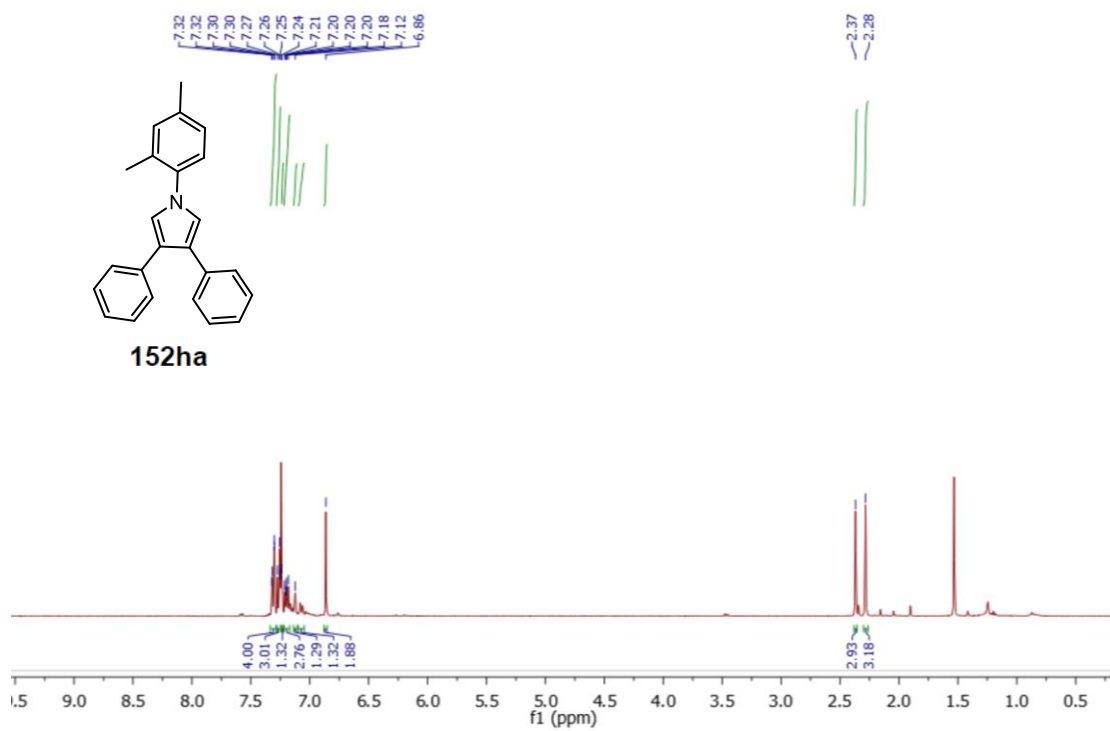
Spectra of Selected Compounds

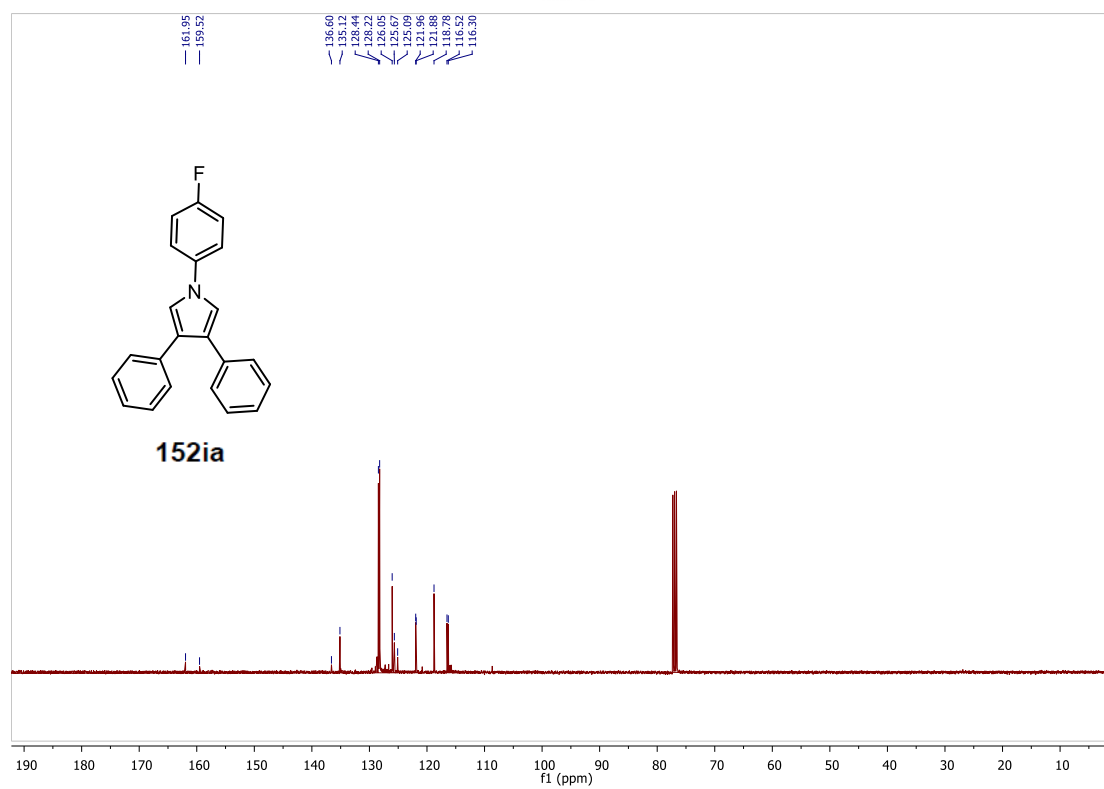
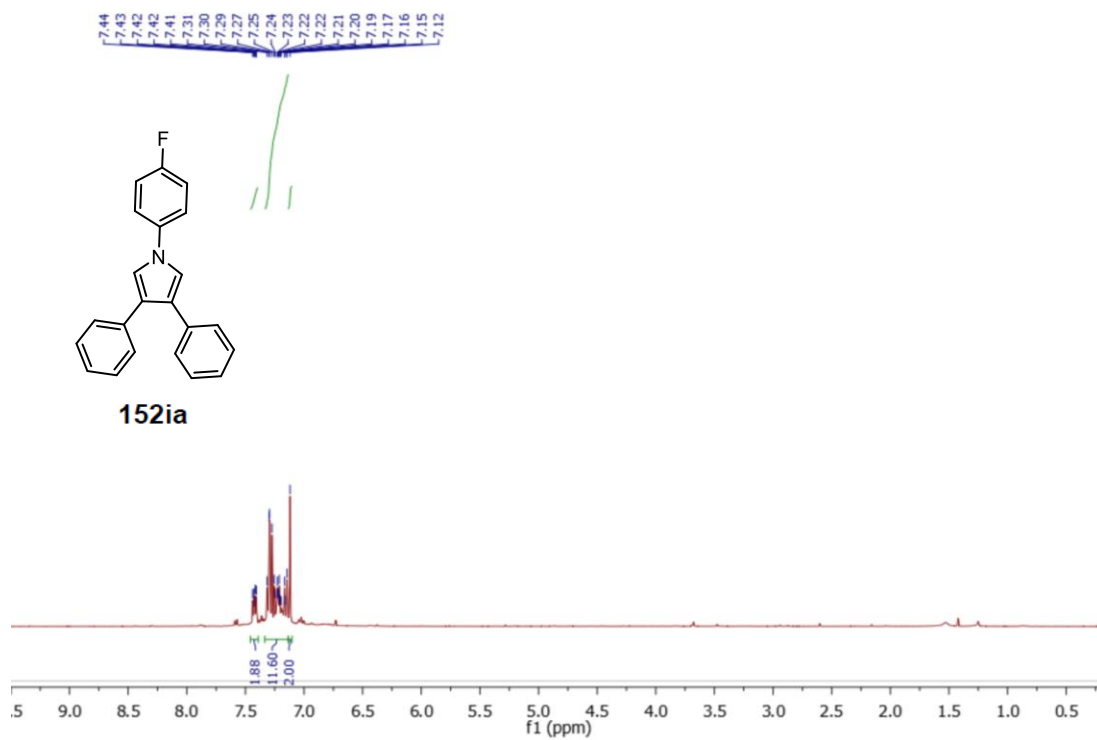


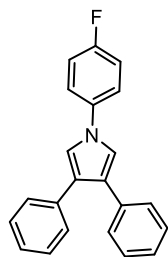
Spectra of Selected Compounds



Spectra of Selected Compounds

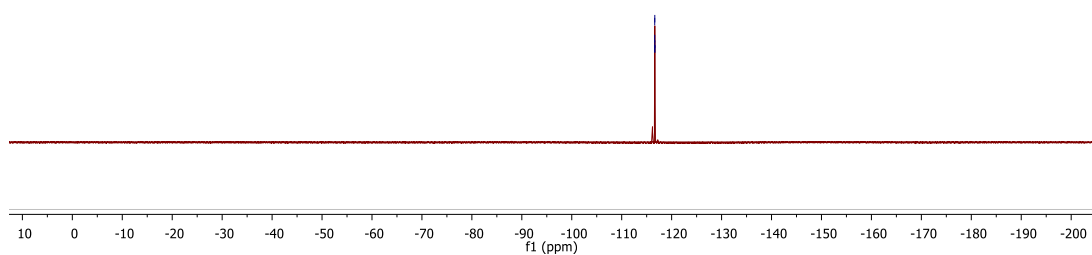


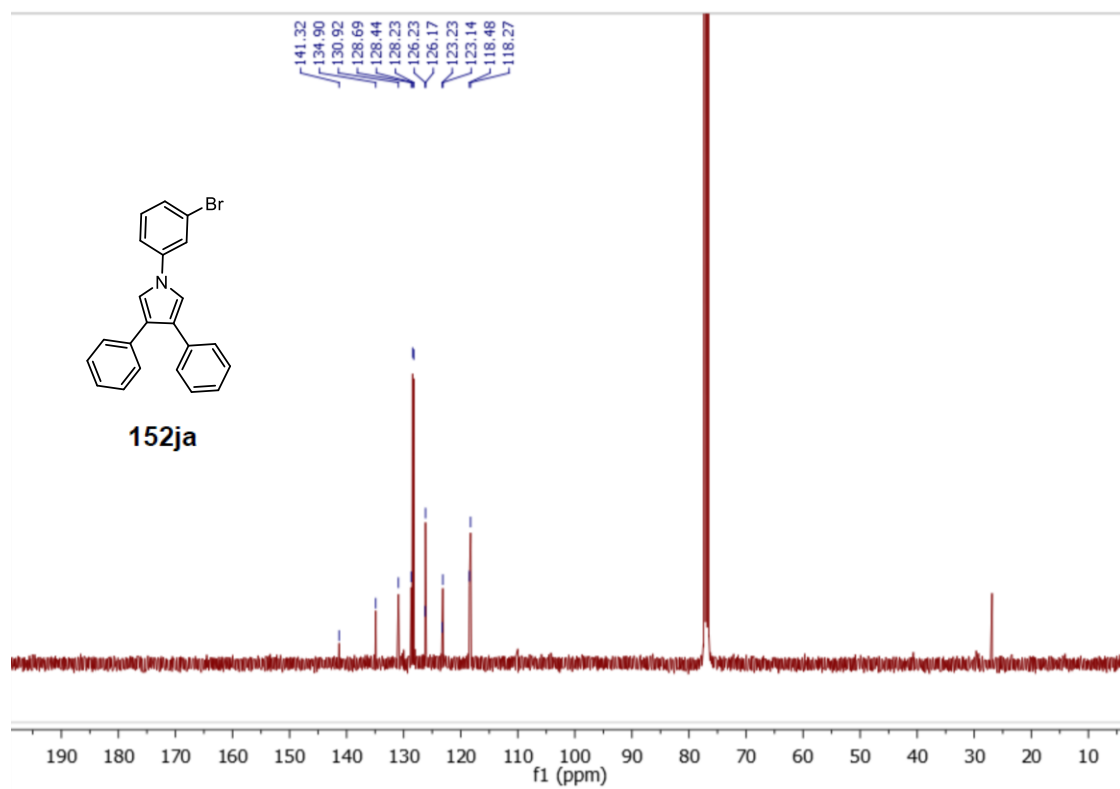
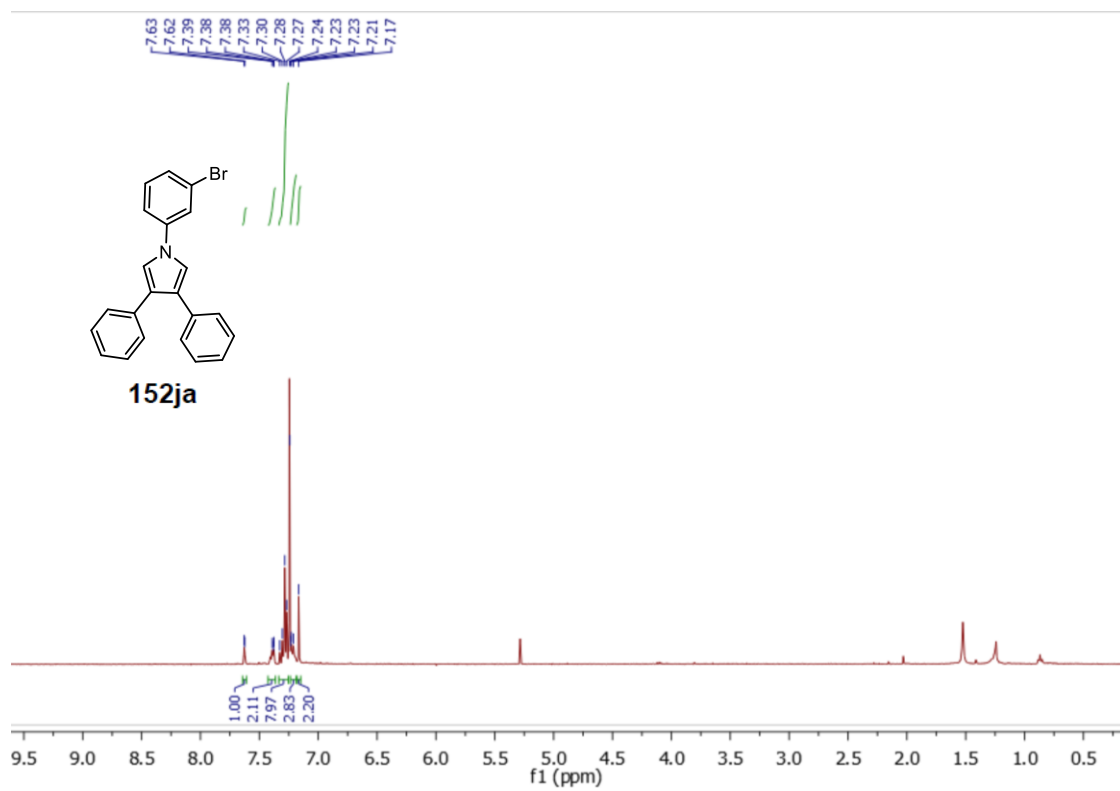


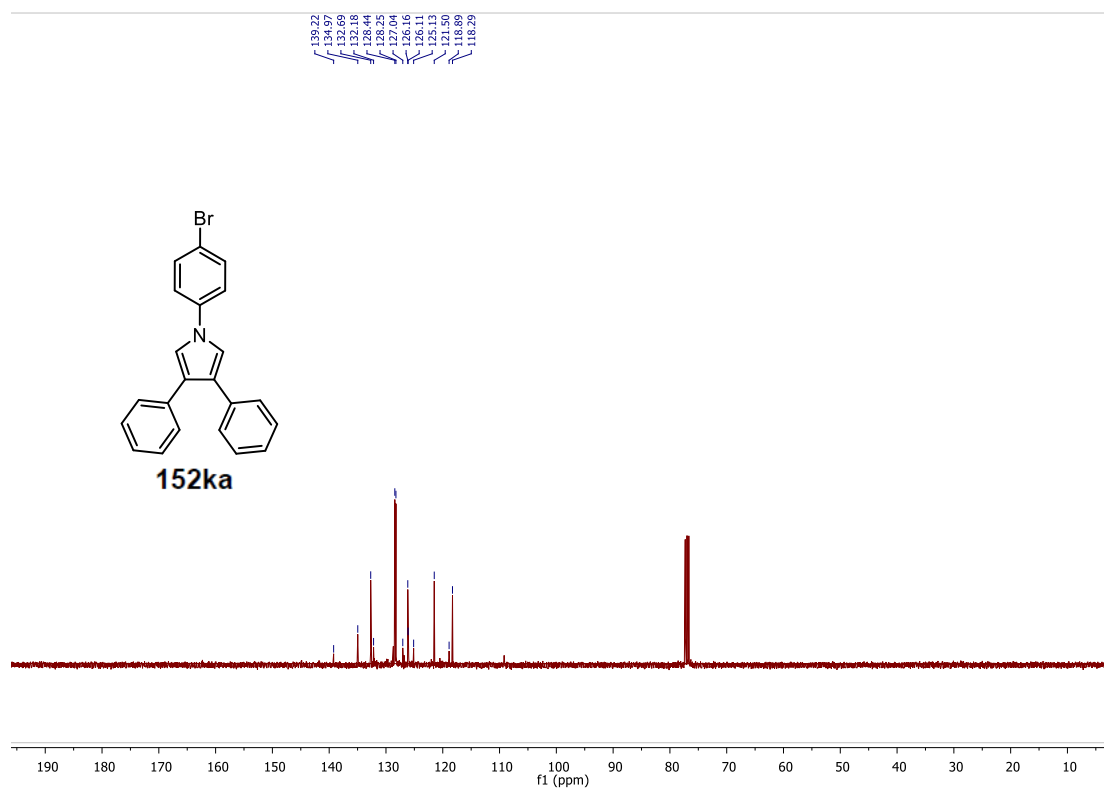
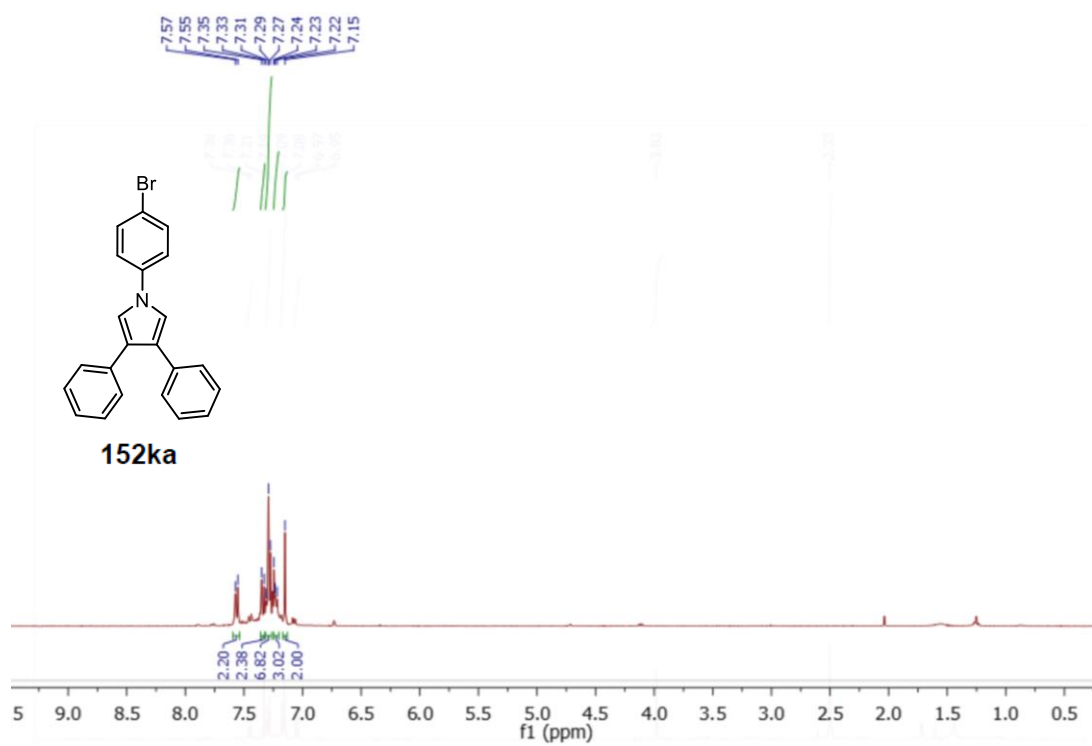


152ia

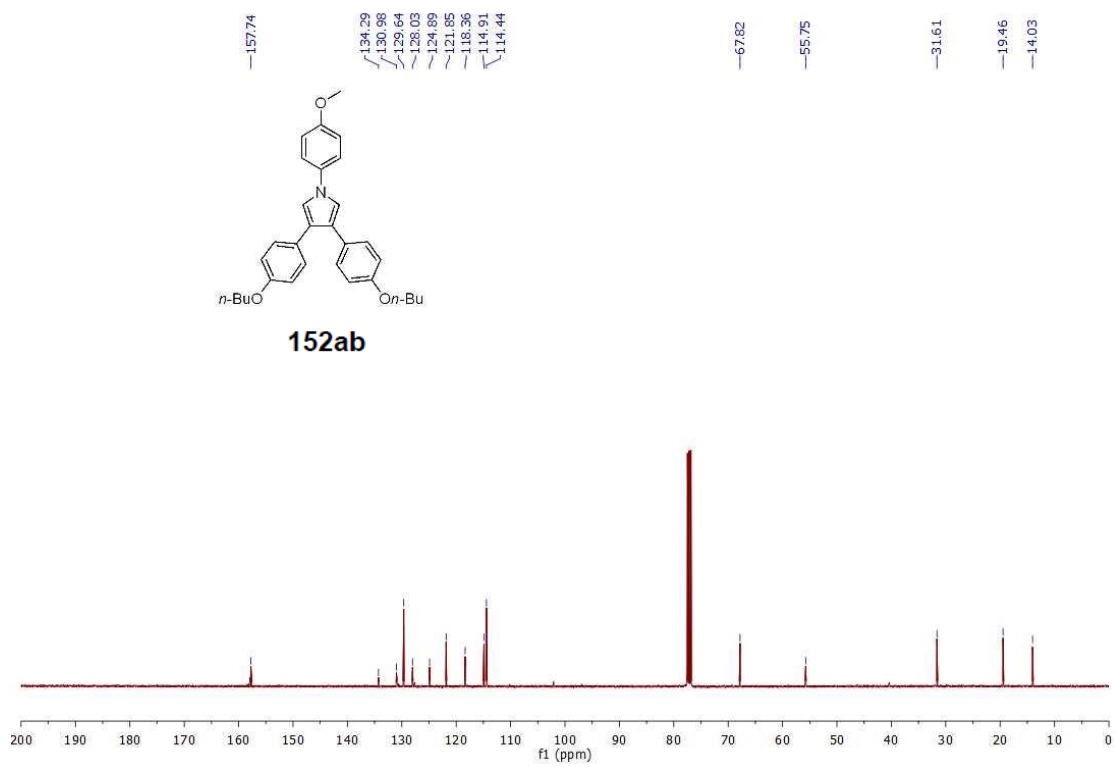
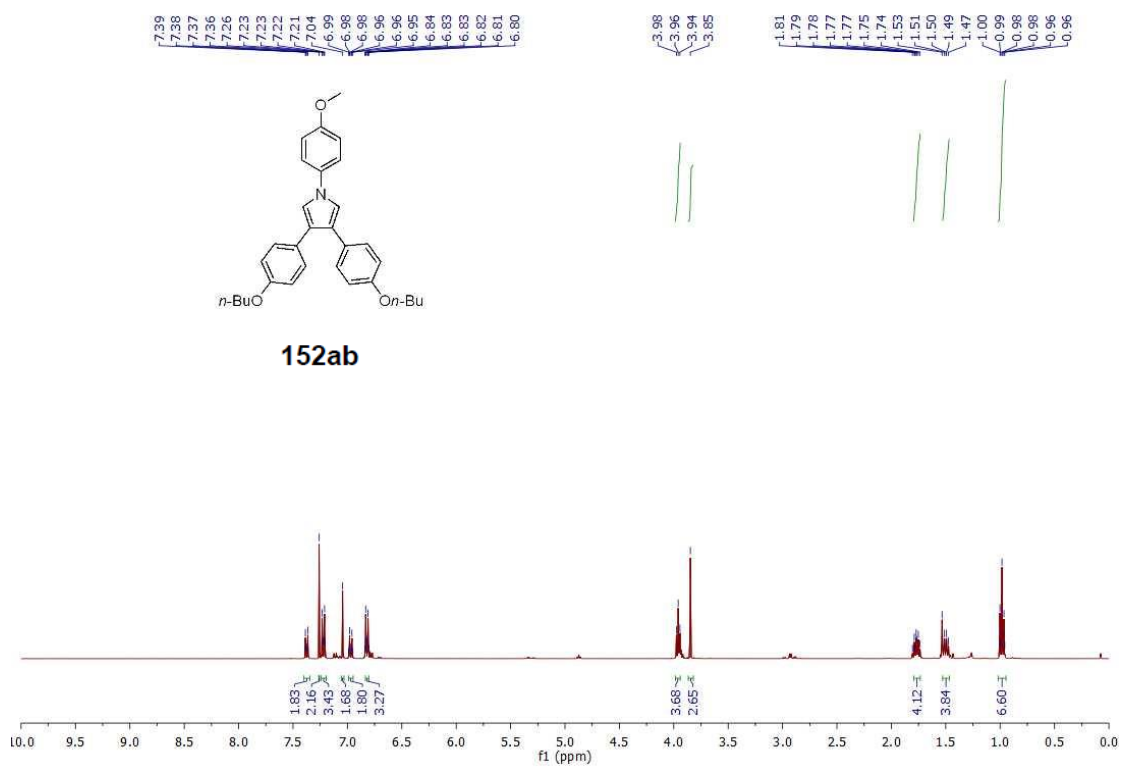
-116.59
-116.60
-116.61
-116.62
-116.65



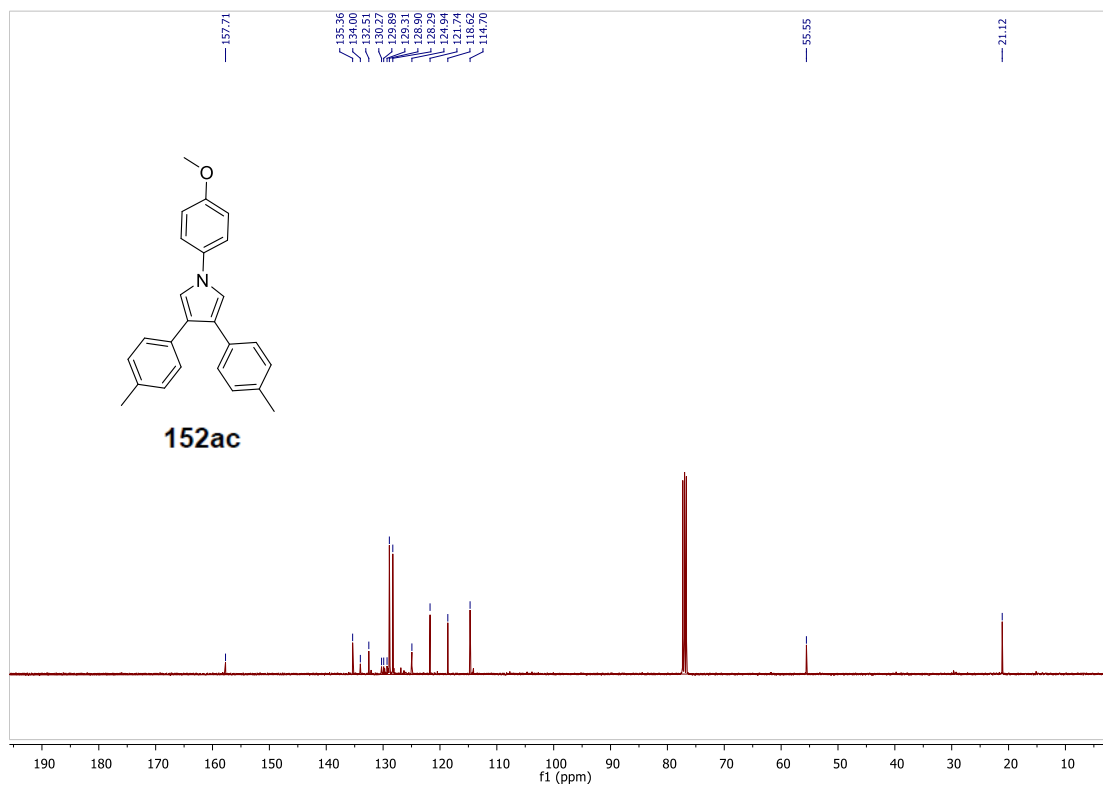
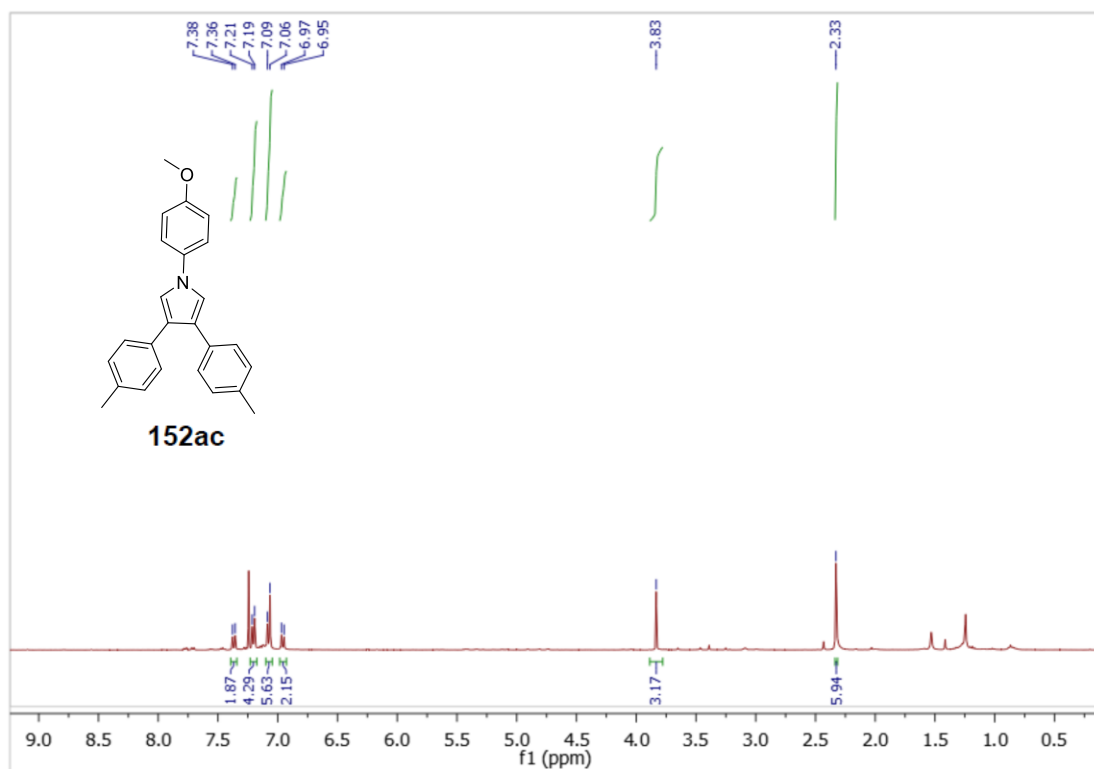




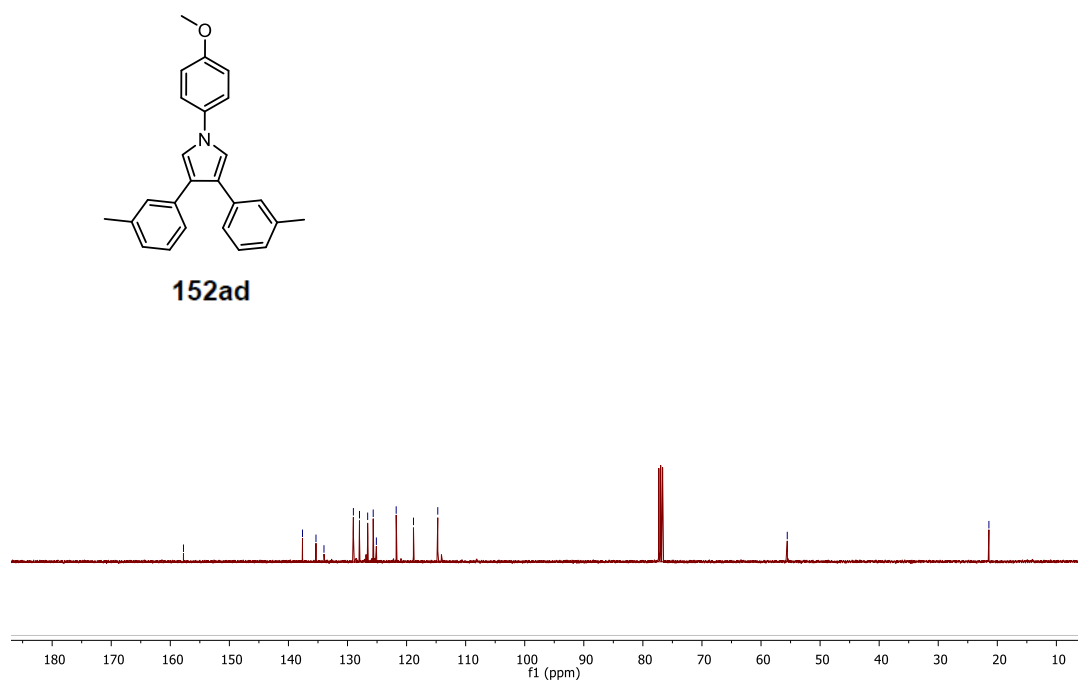
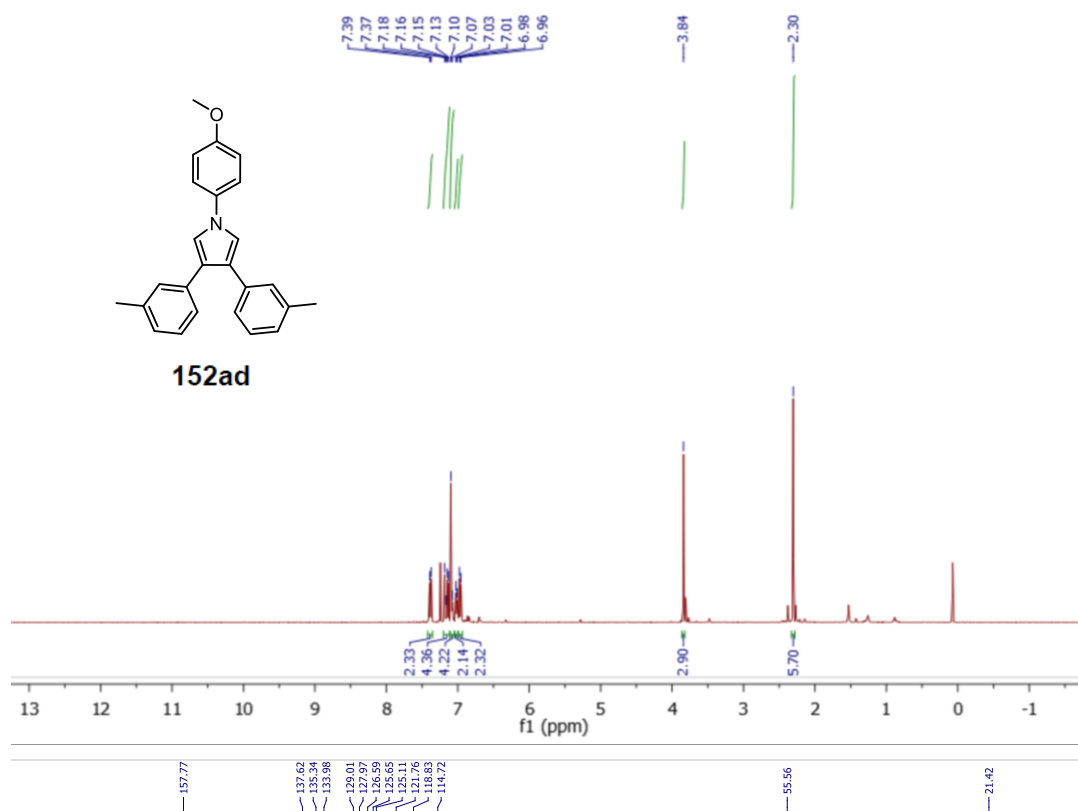
Spectra of Selected Compounds



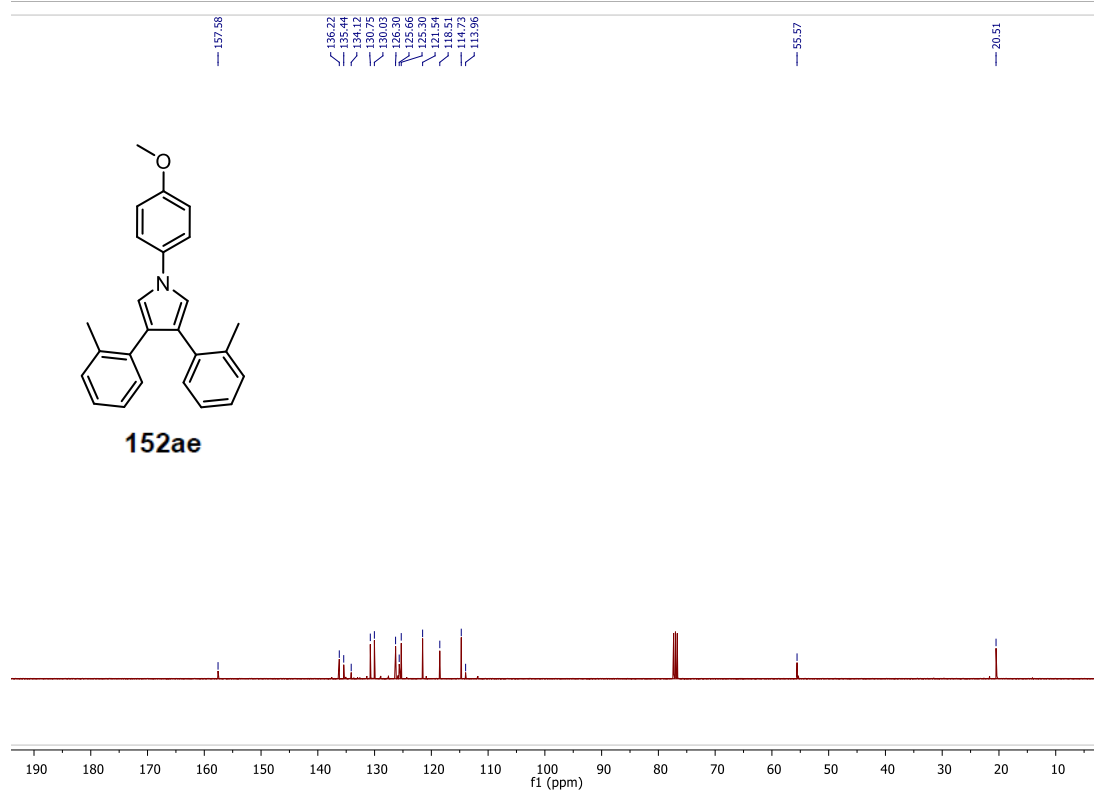
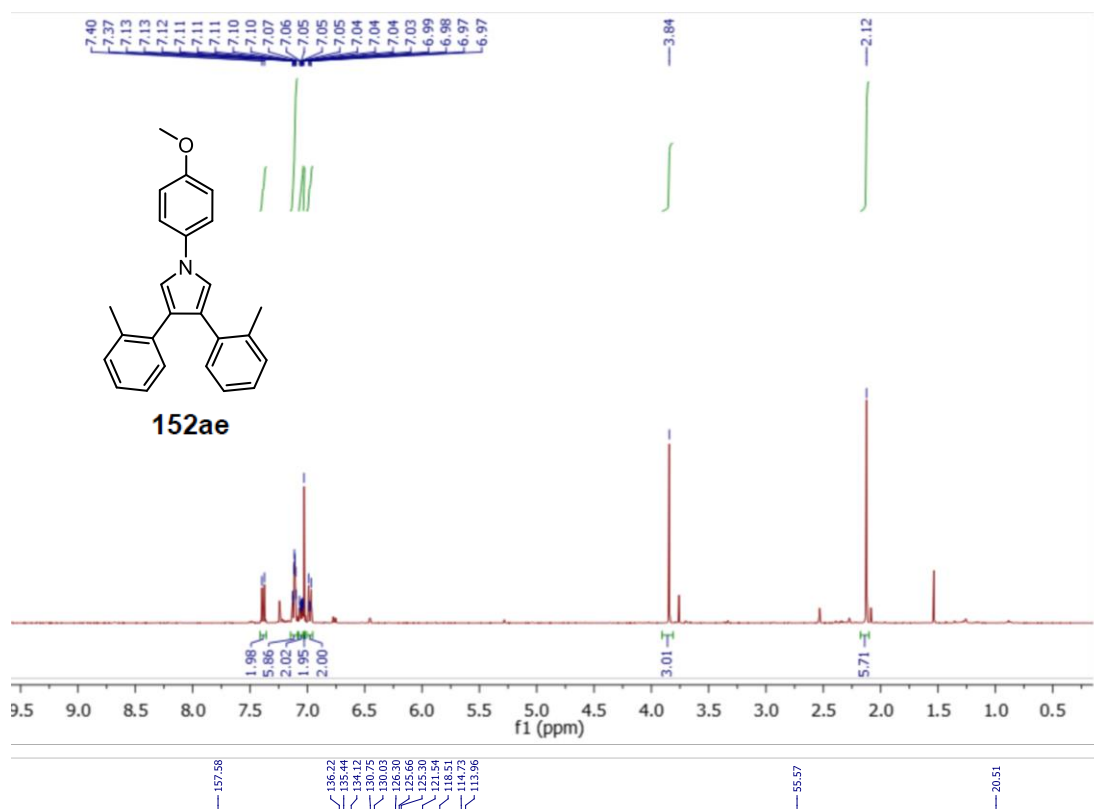
Spectra of Selected Compounds

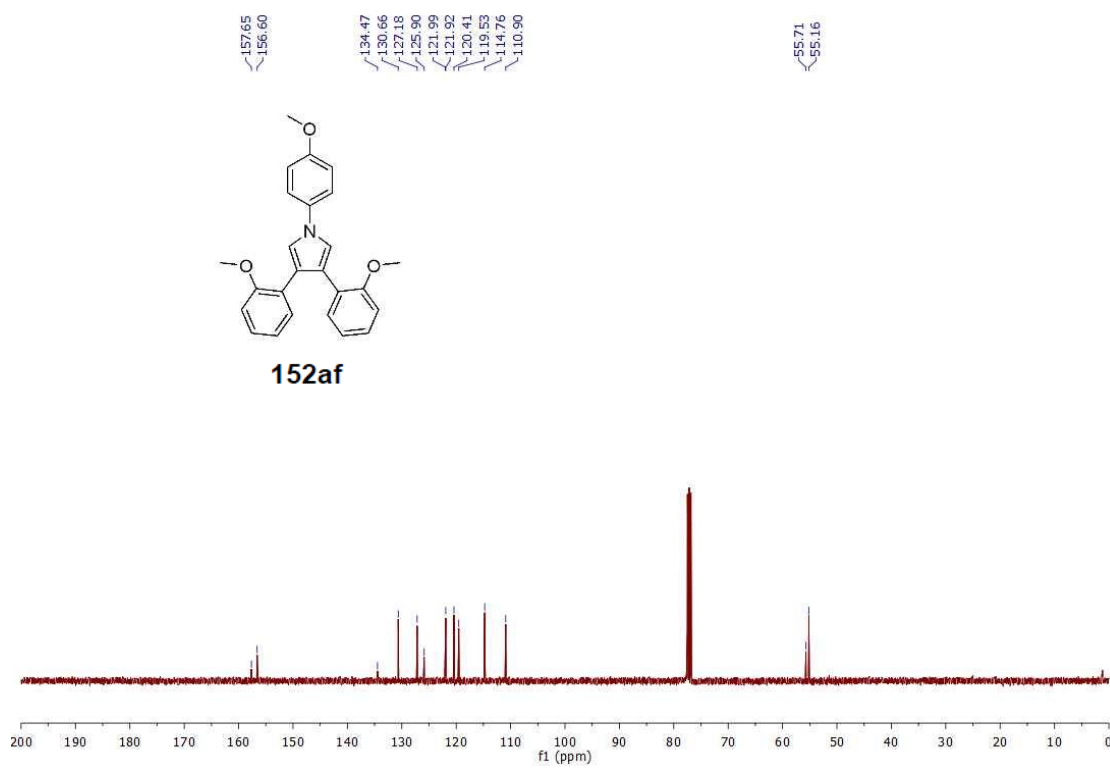
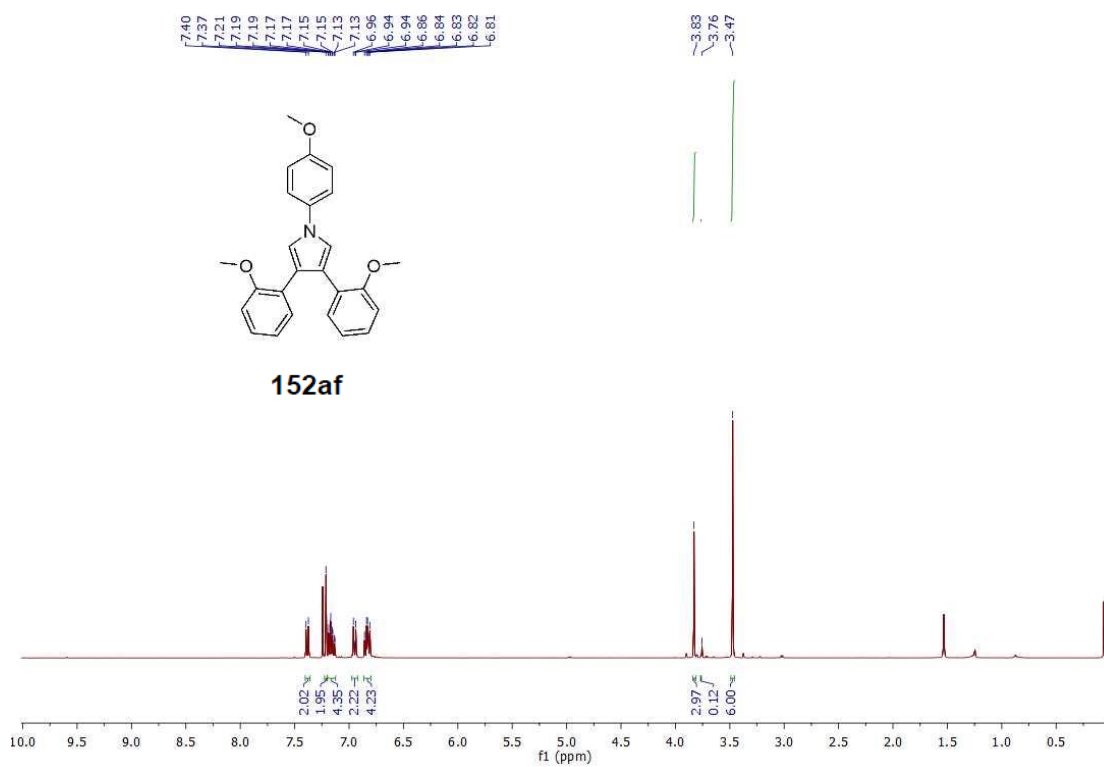


Spectra of Selected Compounds

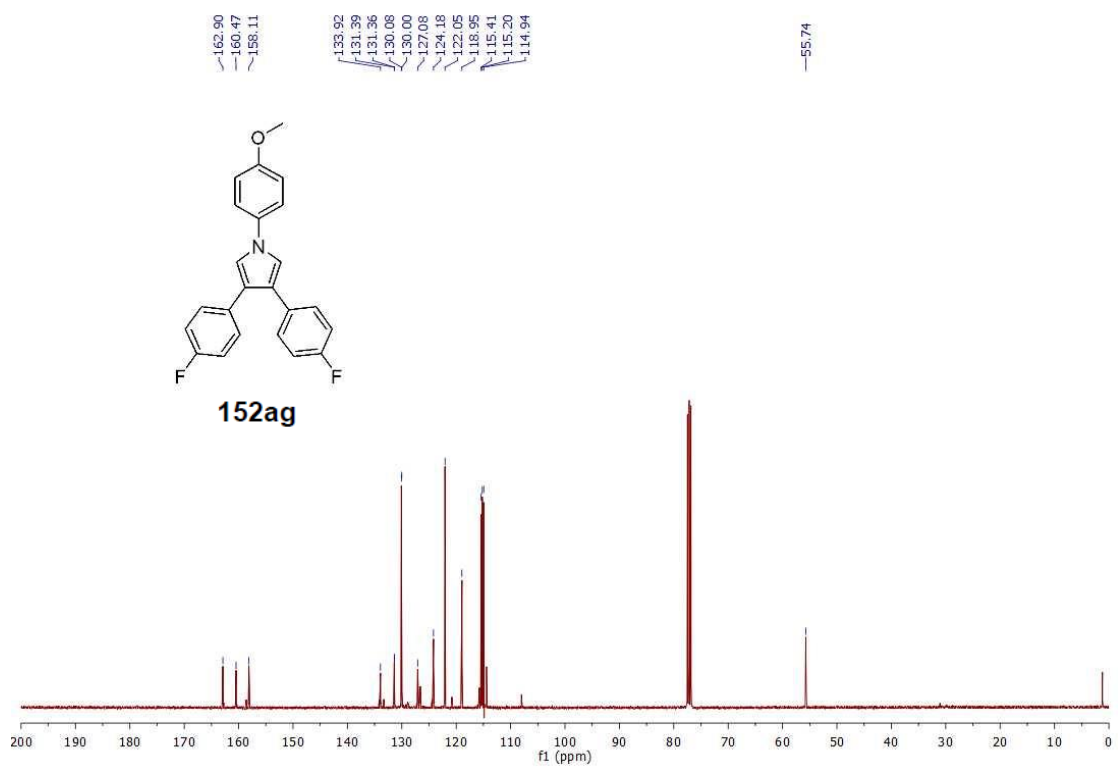
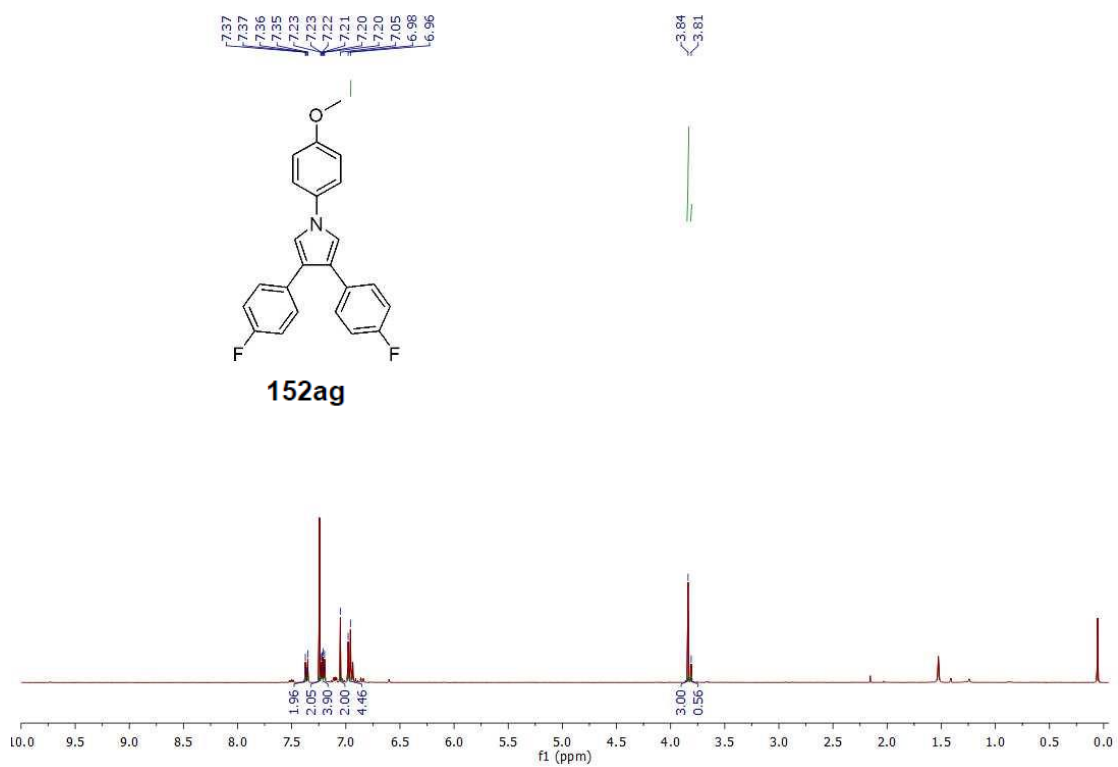


Spectra of Selected Compounds

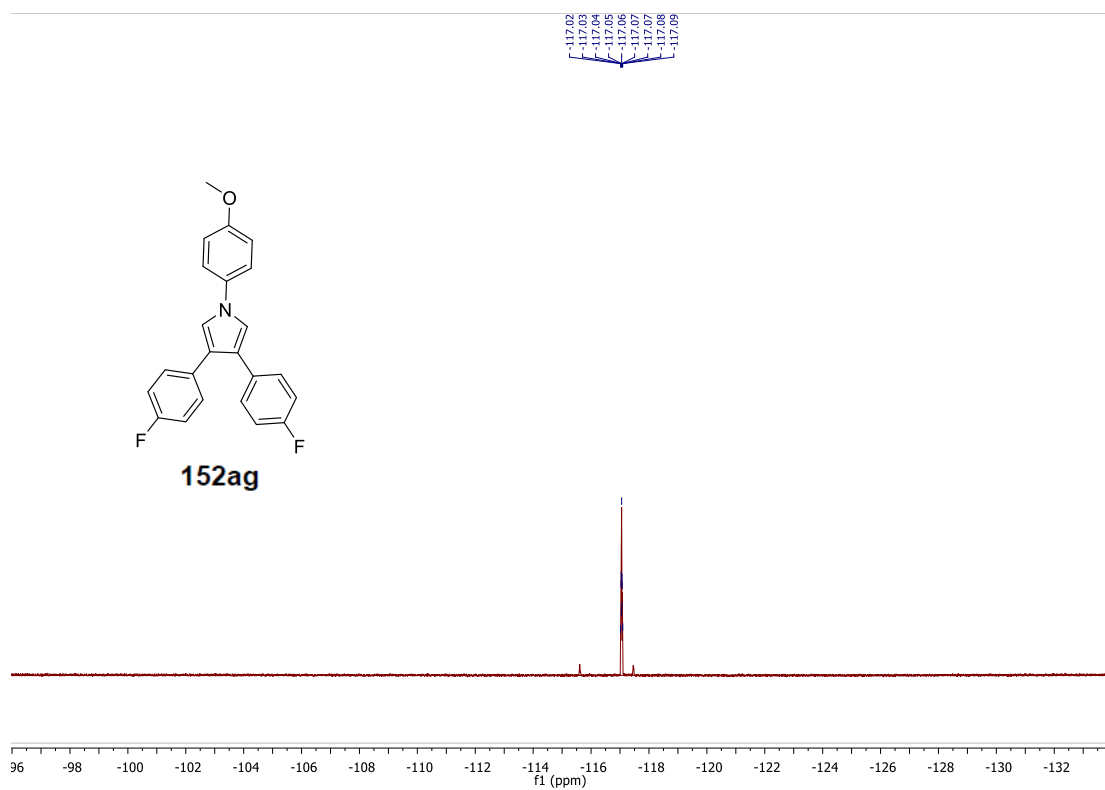




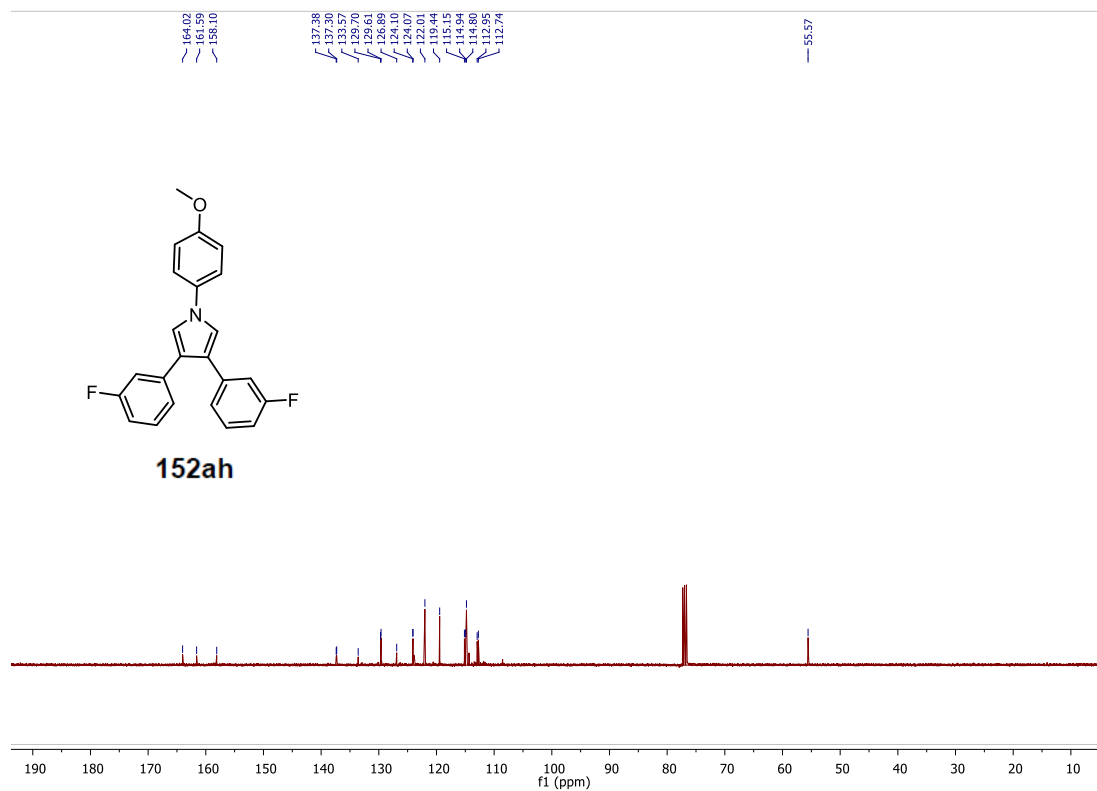
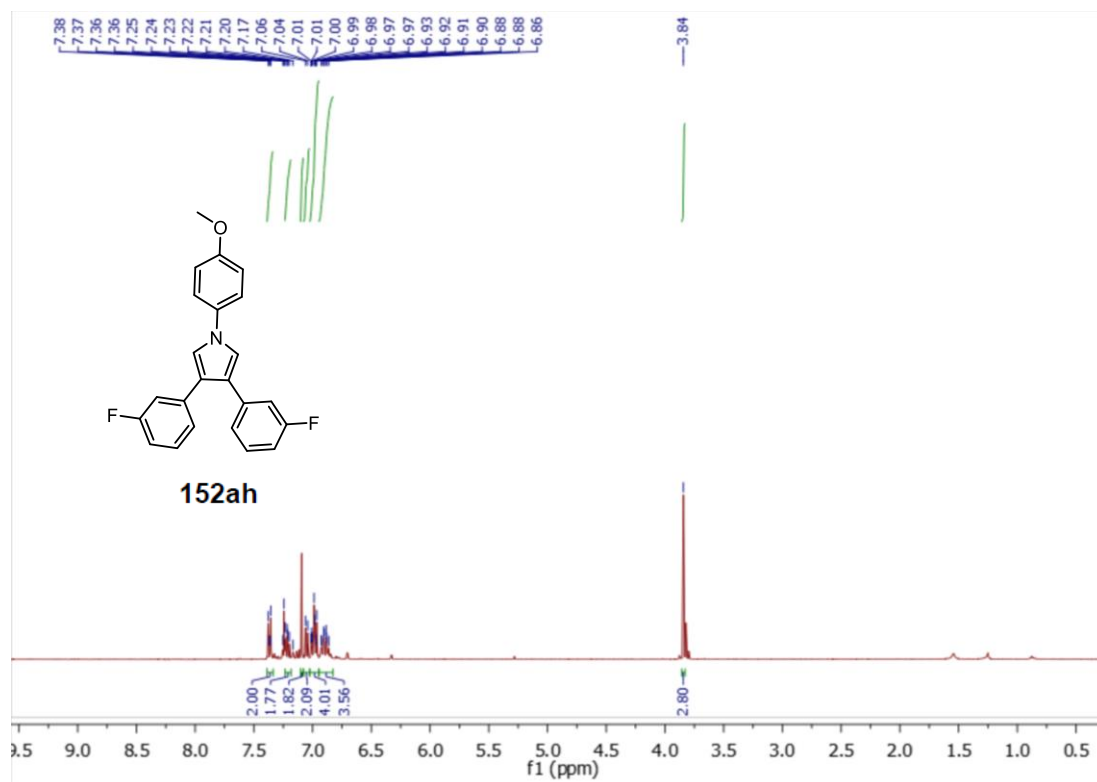
Spectra of Selected Compounds



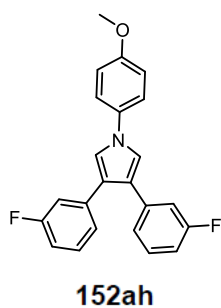
Spectra of Selected Compounds



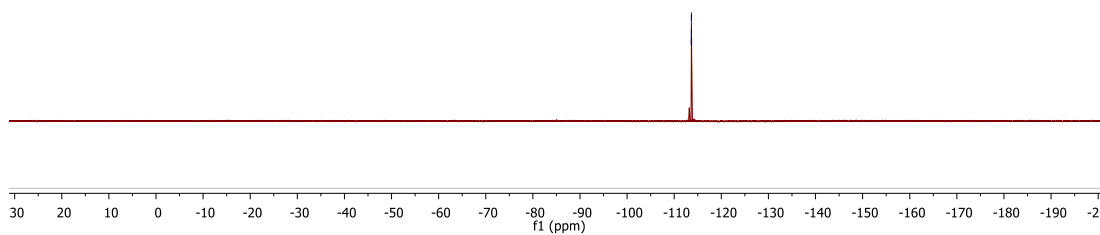
Spectra of Selected Compounds



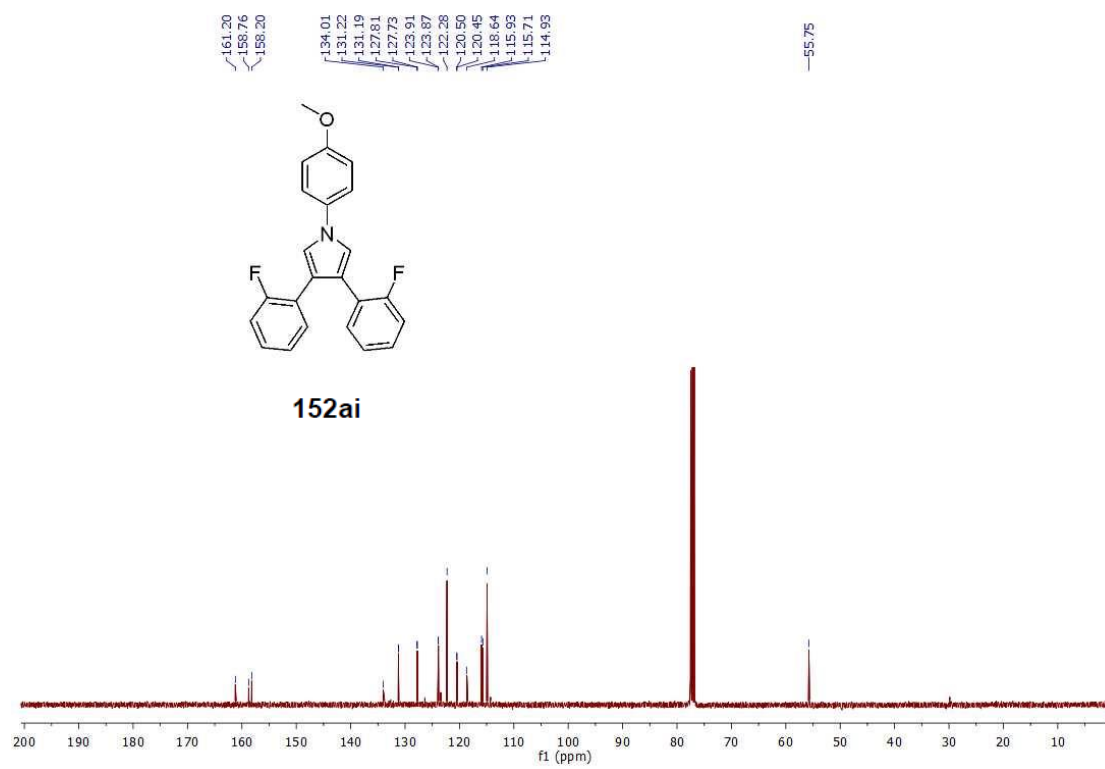
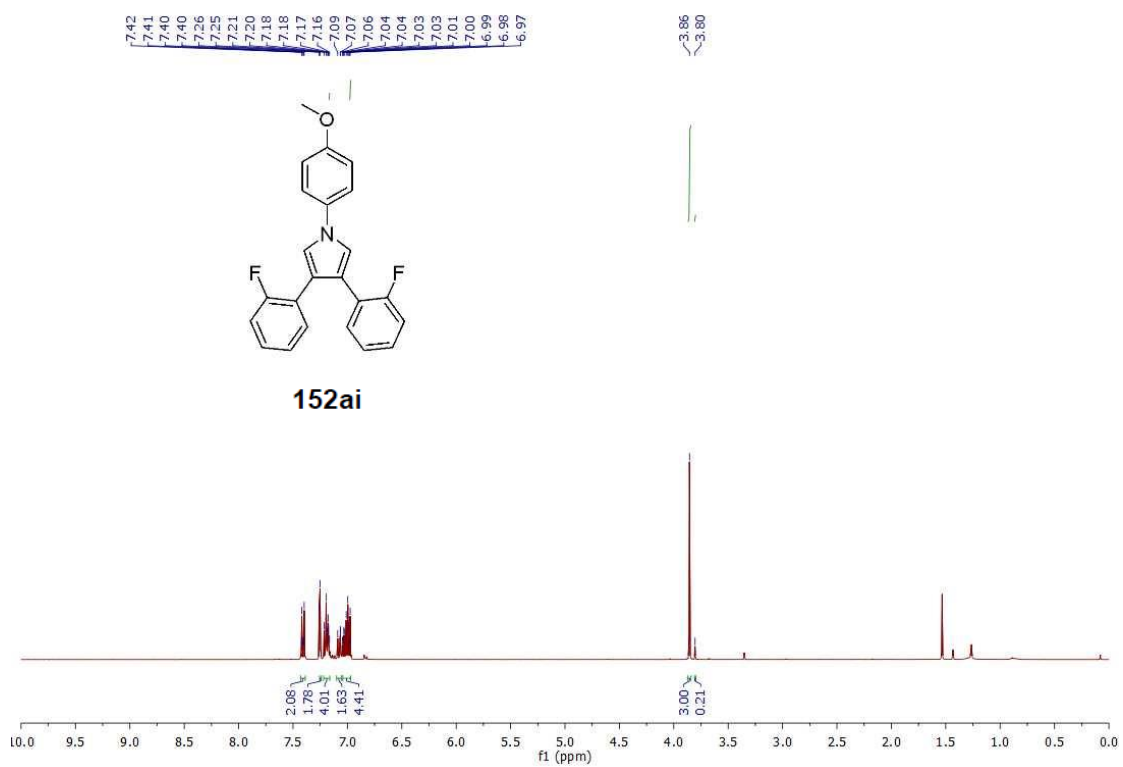
Spectra of Selected Compounds



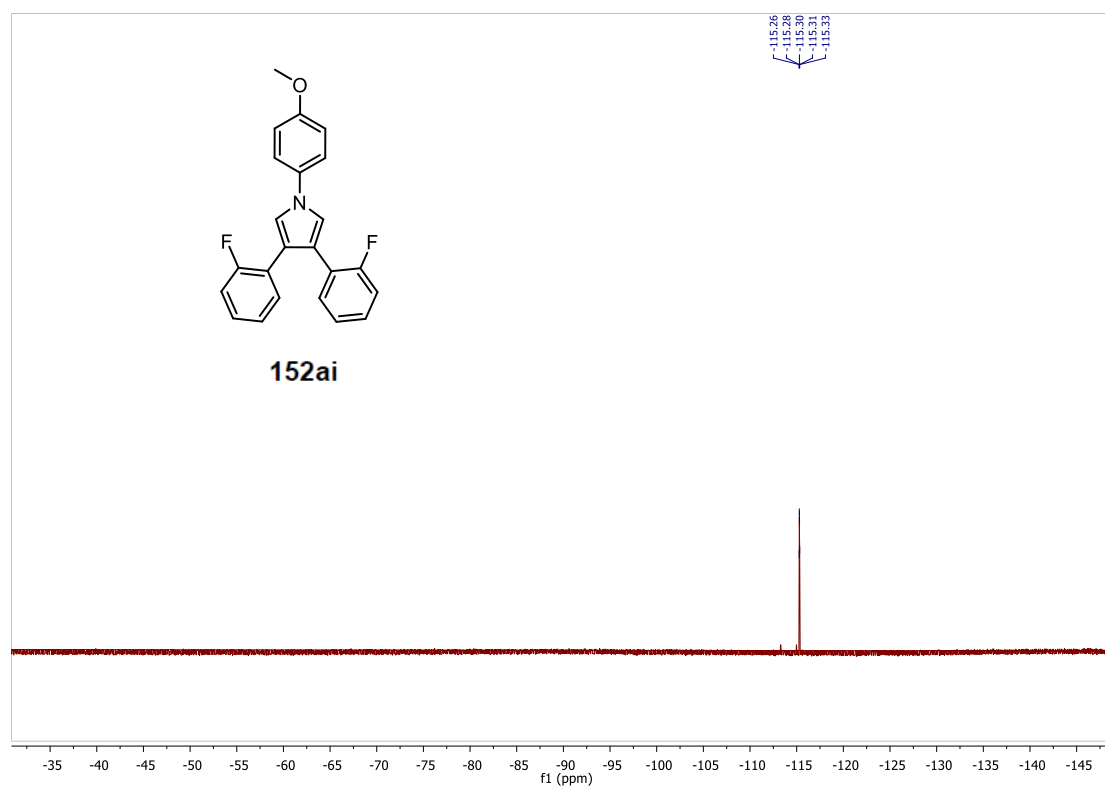
-113.62
-113.64
-113.65
-113.67
-113.69



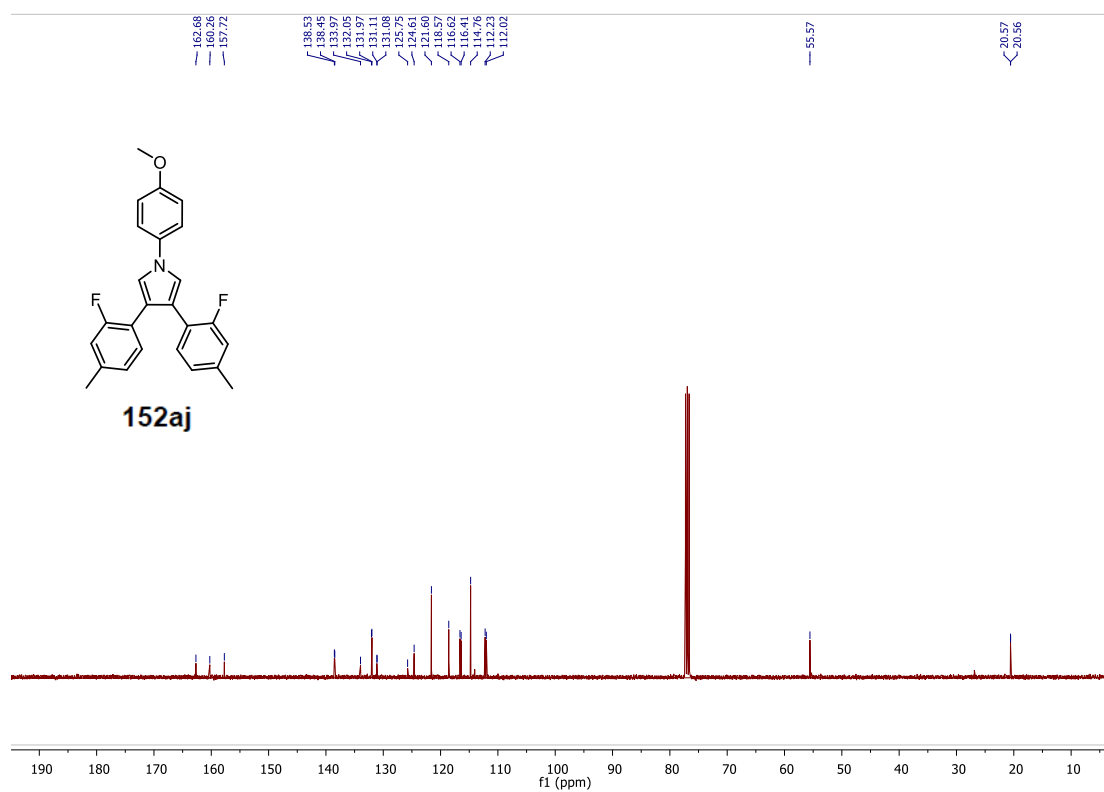
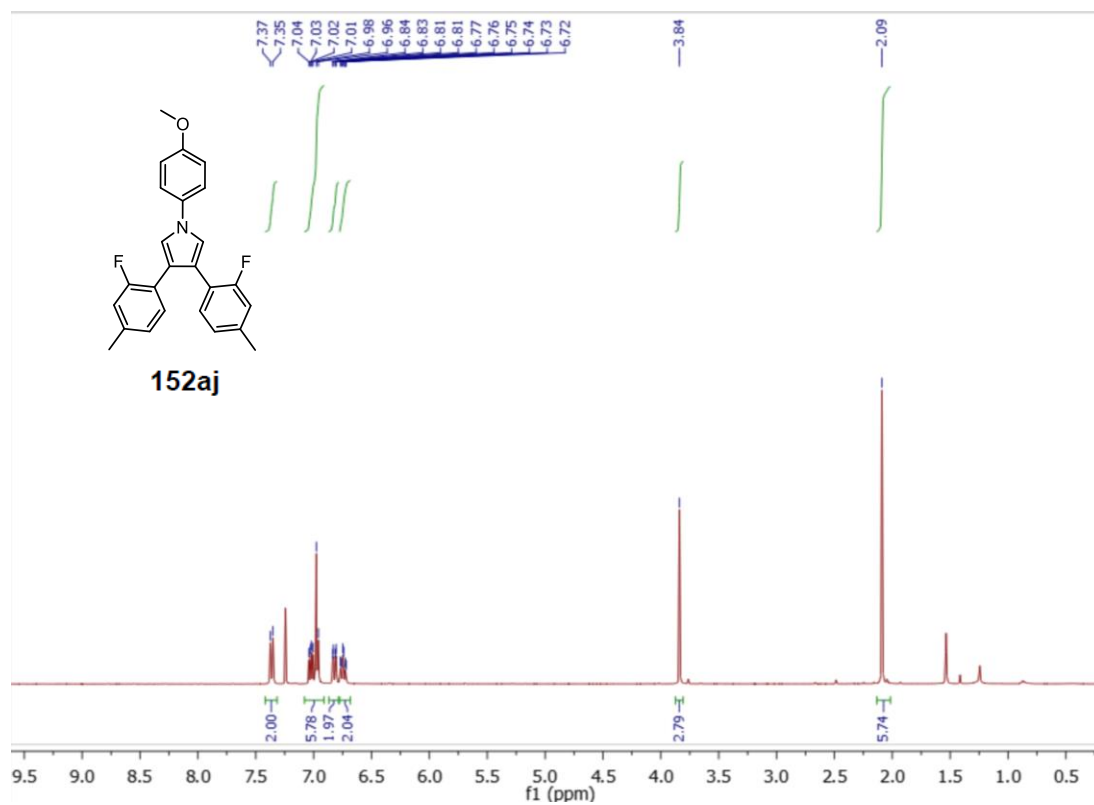
Spectra of Selected Compounds



Spectra of Selected Compounds

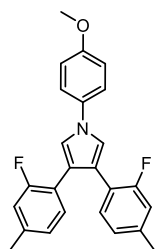


Spectra of Selected Compounds

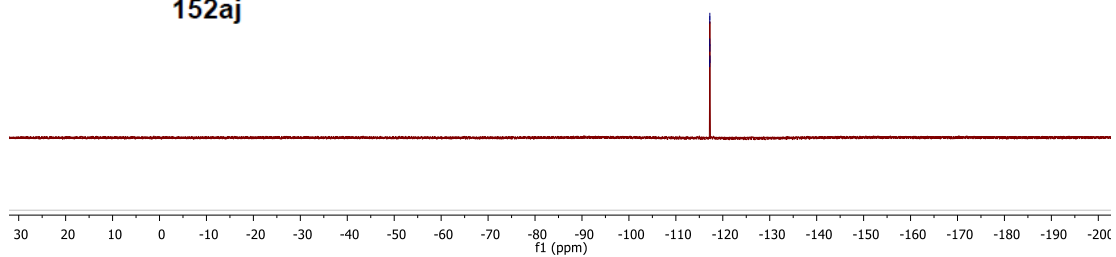


Spectra of Selected Compounds

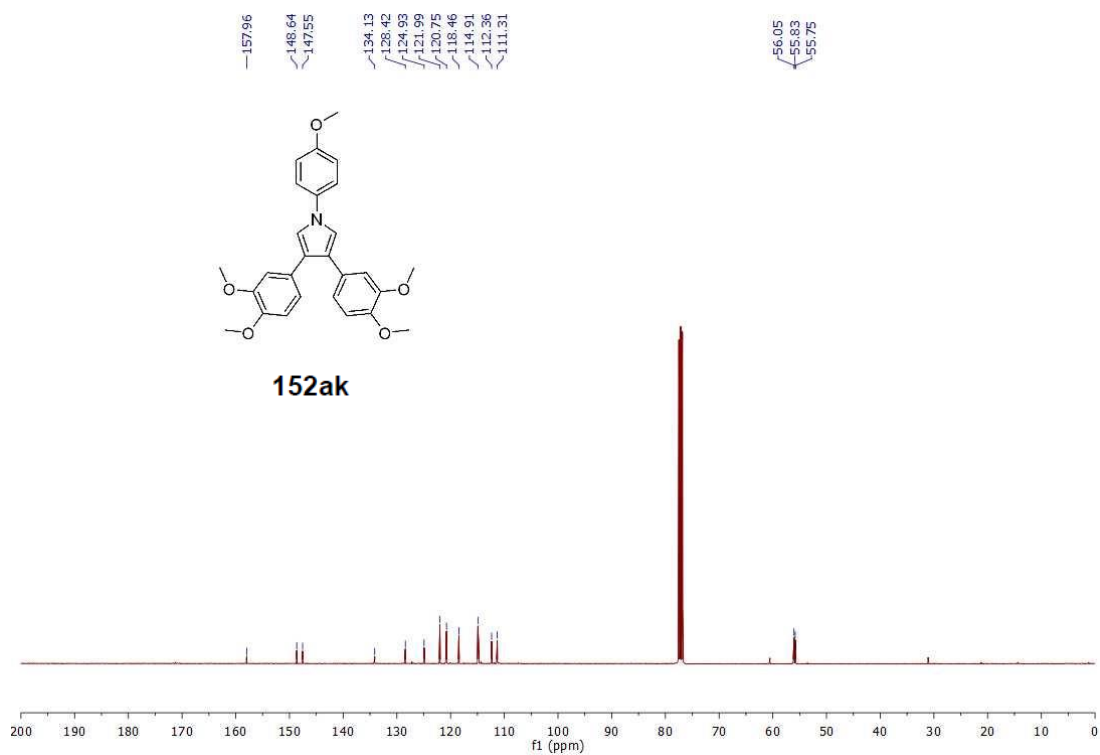
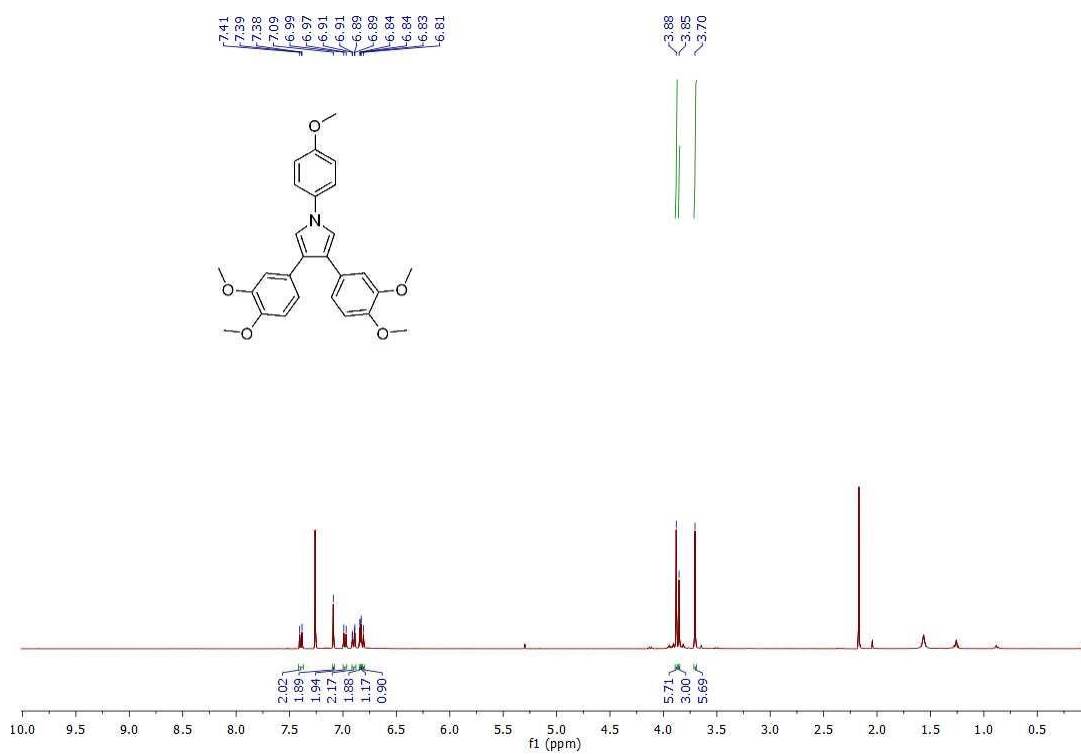
-117.26
-117.23
-117.24
-117.25



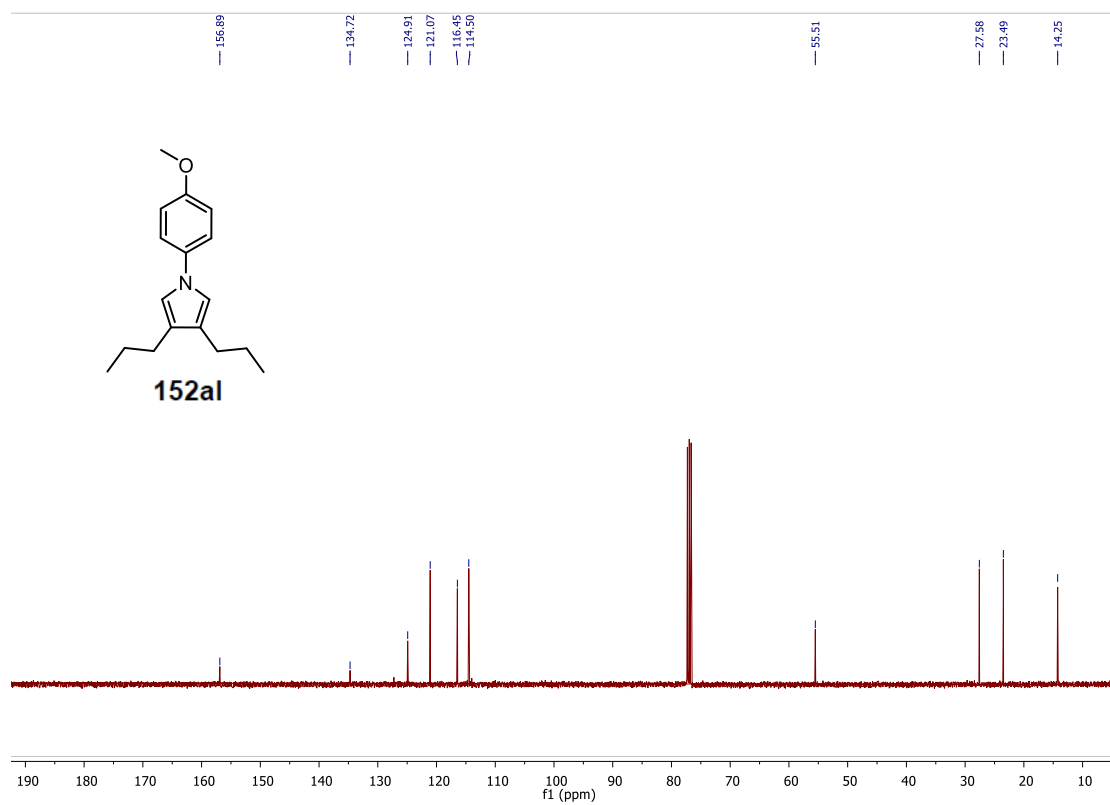
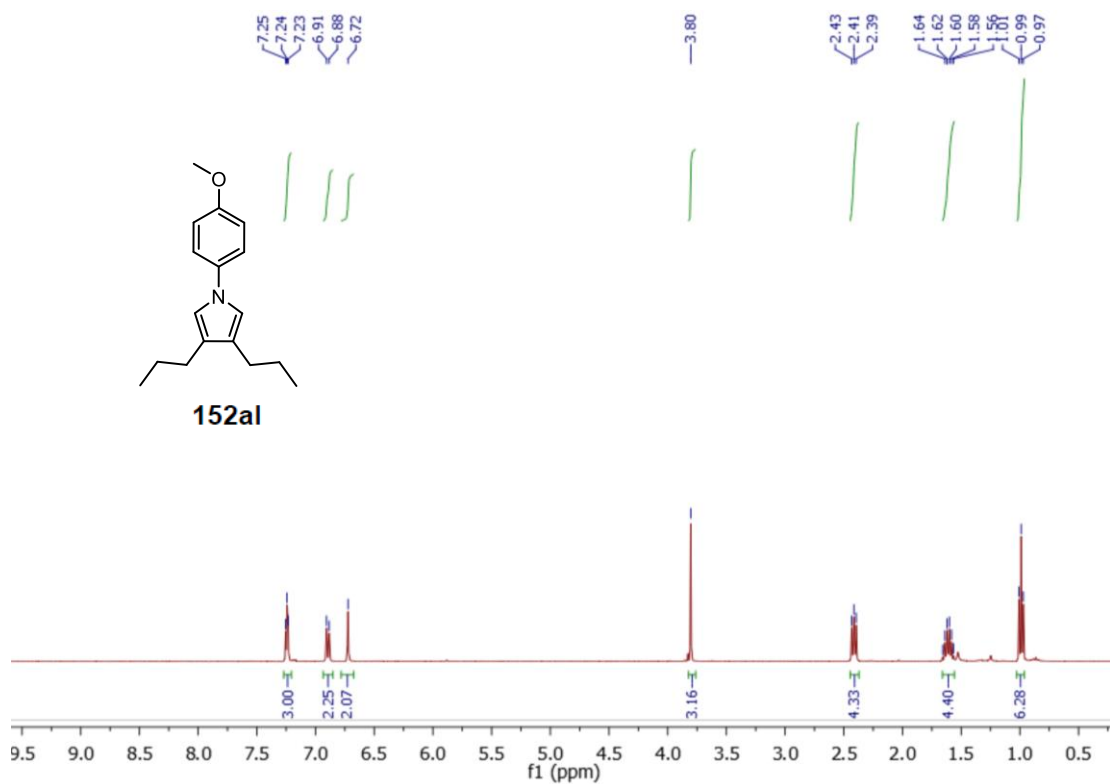
152aj



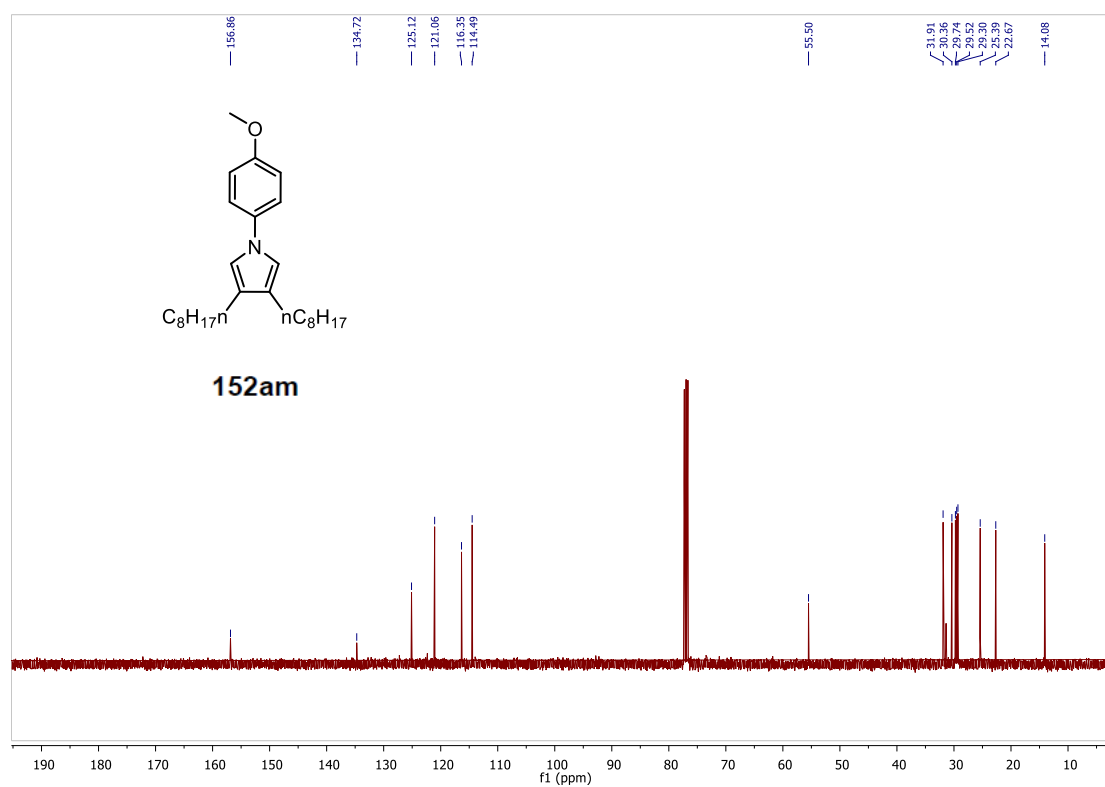
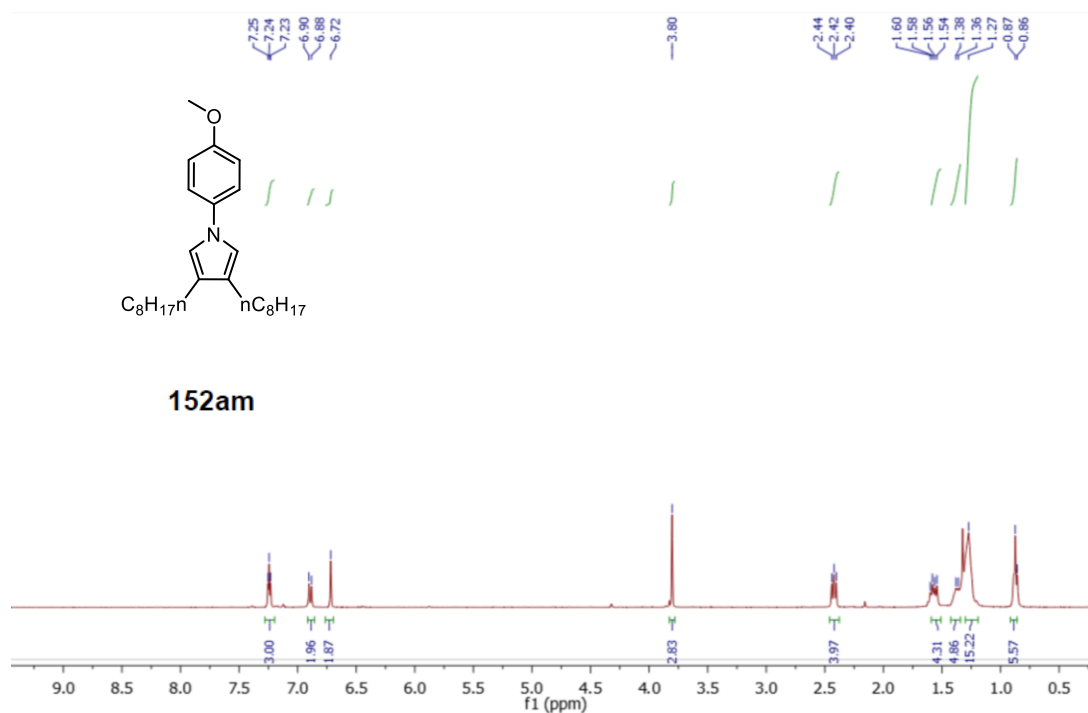
Spectra of Selected Compounds



Spectra of Selected Compounds

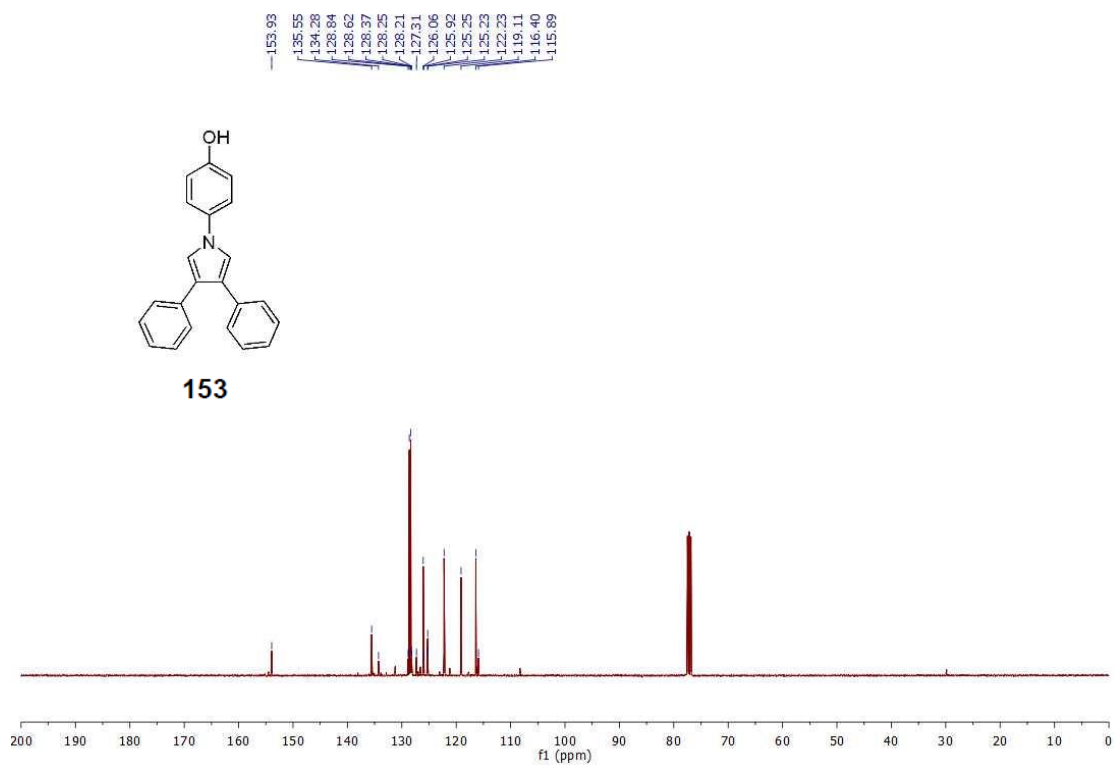
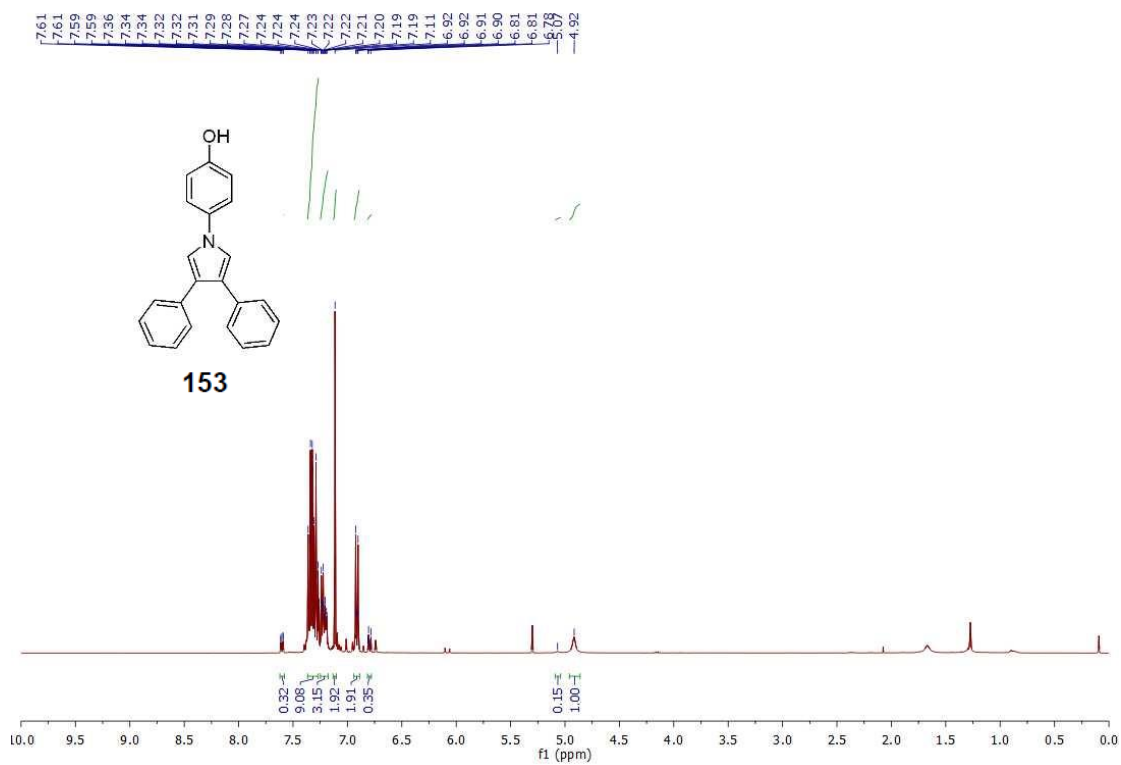


Spectra of Selected Compounds

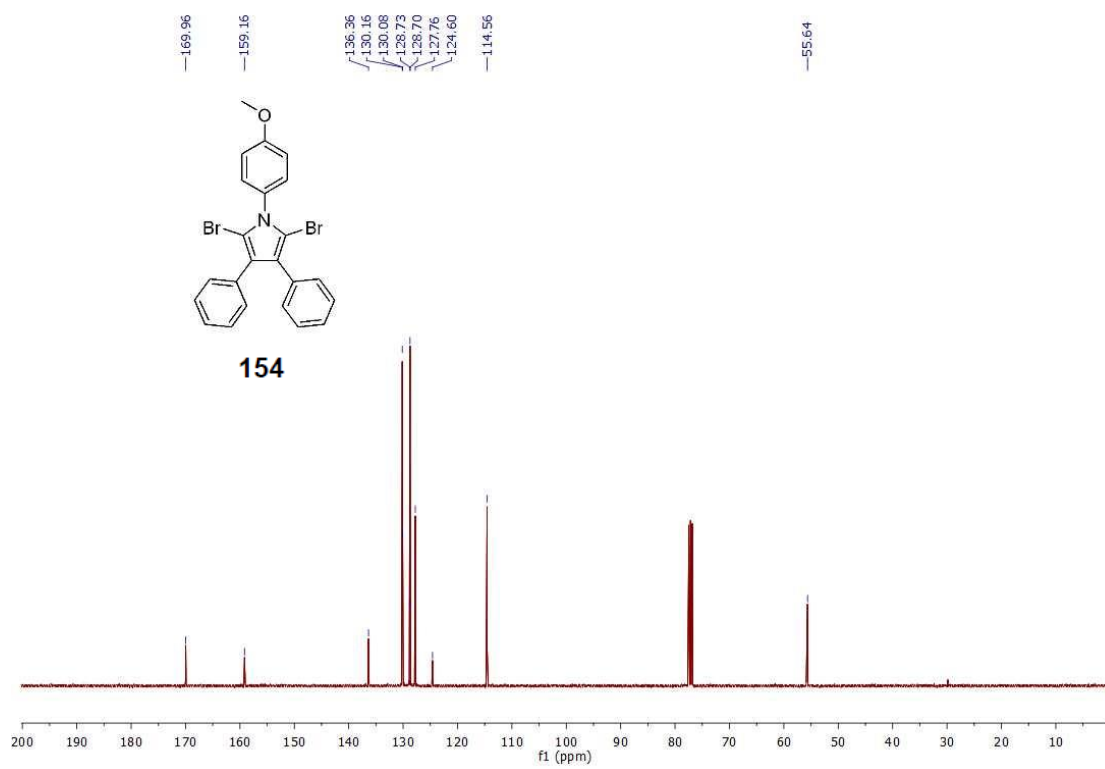
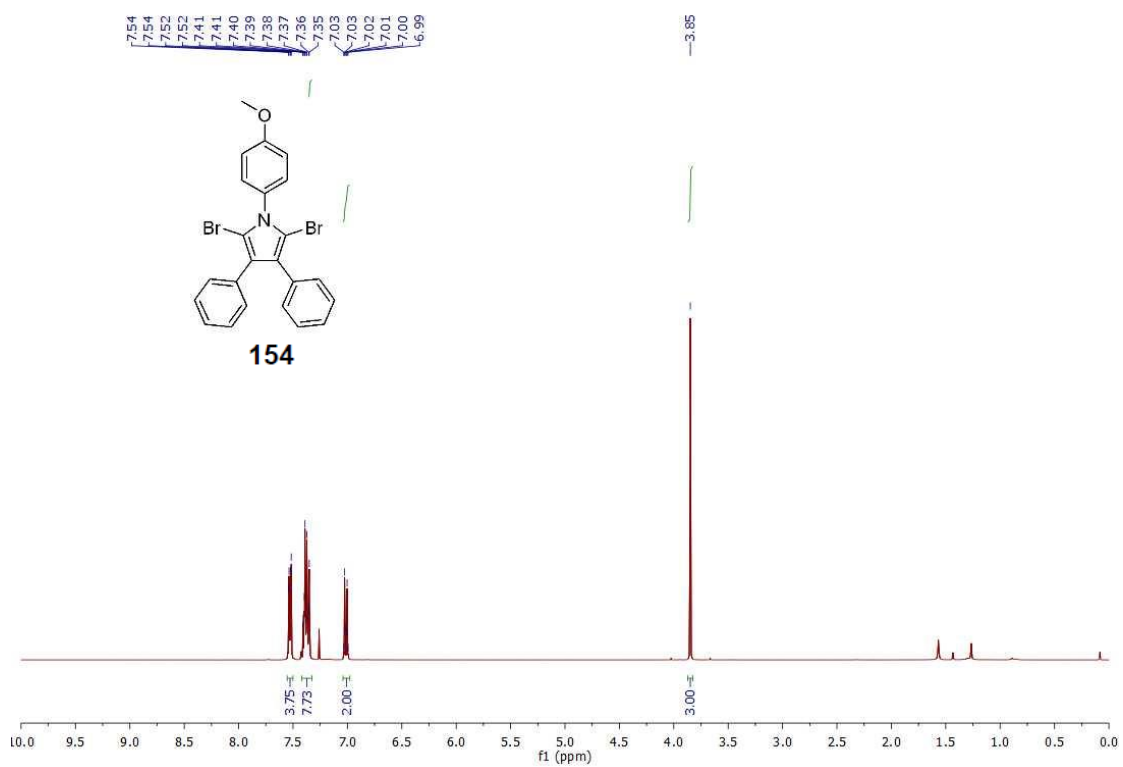


153

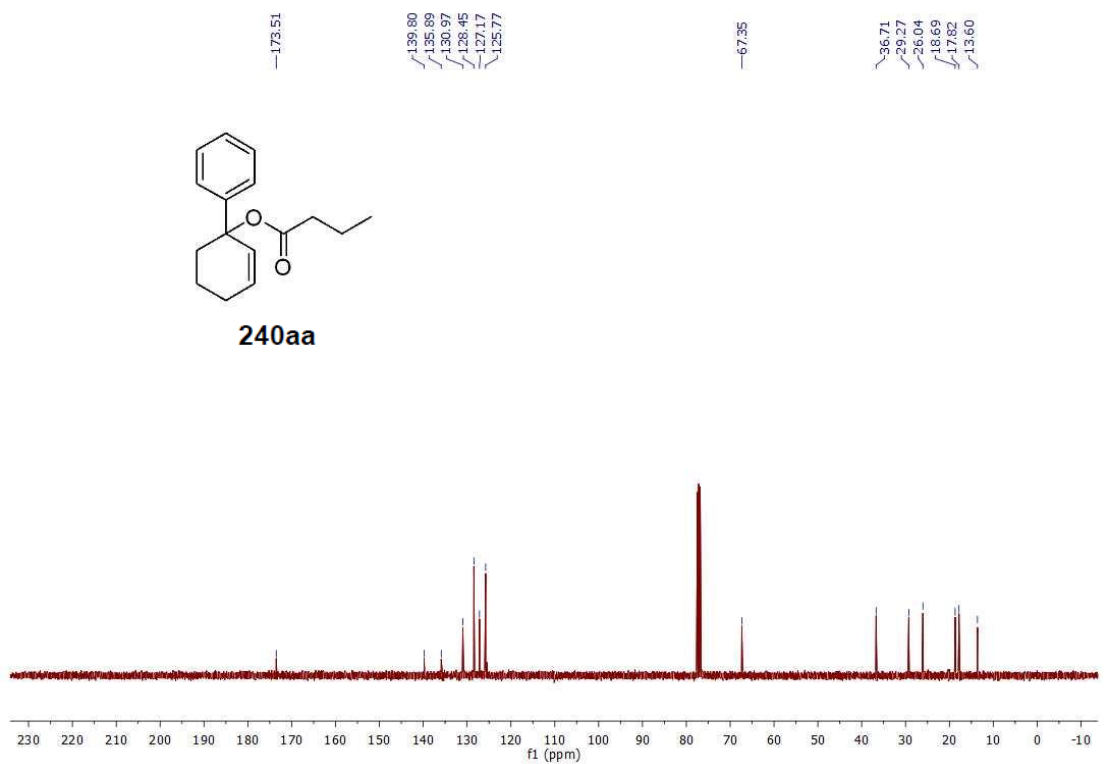
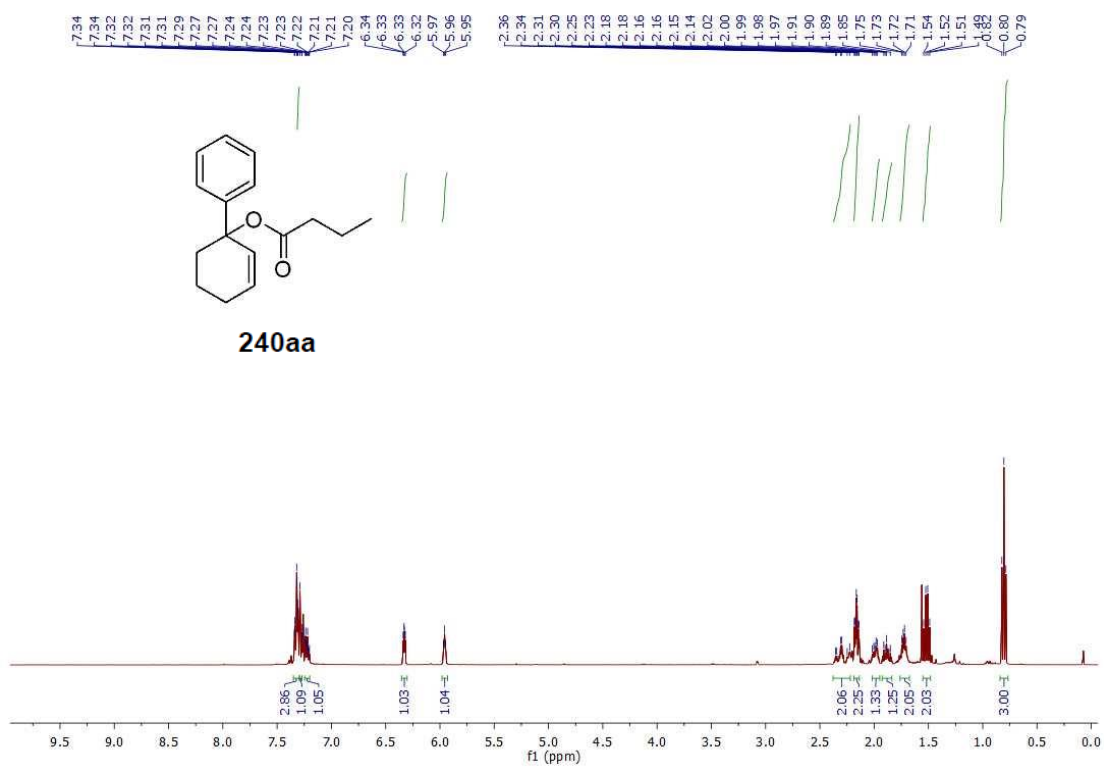
Spectra of Selected Compounds



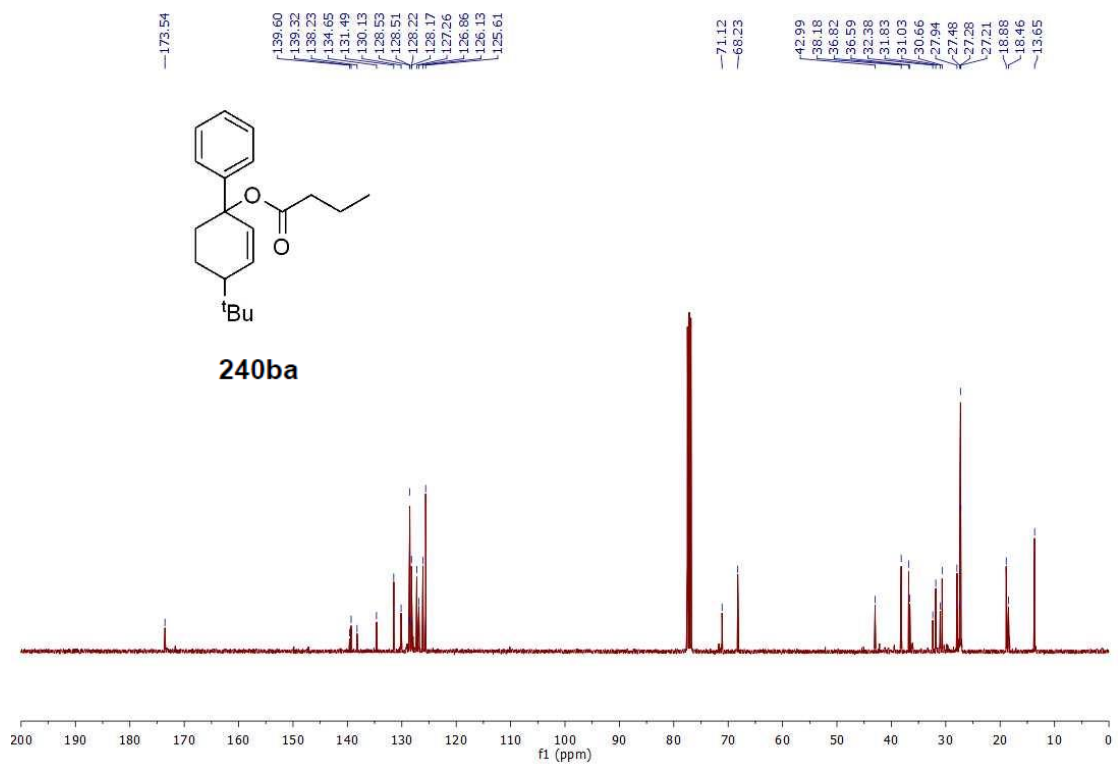
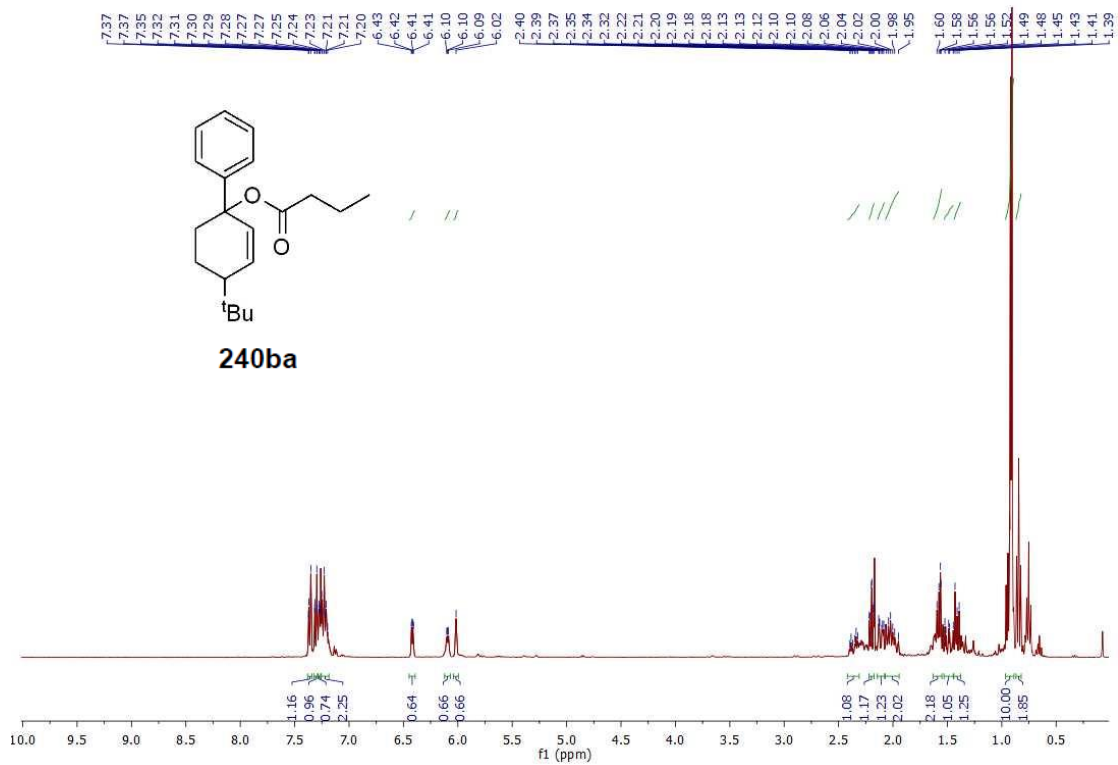
Spectra of Selected Compounds



Spectra of Selected Compounds



Spectra of Selected Compounds



Spectra of Selected Compounds

